Recent environmental change at Signy Island, maritime Antarctic: quantitative lake-sediment studies as a basis for reconstructing catchment ice-cover

Thesis submitted for the degree of
Doctor of Philosophy
University of London

Philippa Elizabeth Noon

Department of Geography
University College London

September 1997

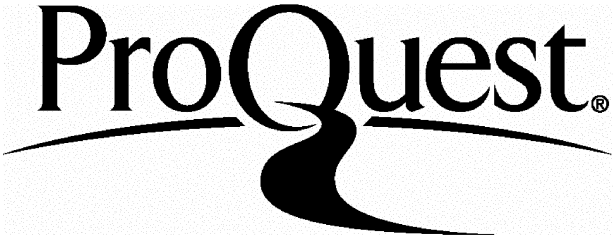

ABSTRACT

A quantitative reconstruction of recent environmental change at Signy Island (60°43'S, 45°38'W), maritime Antarctic, is performed using a model based on physical sediment characteristics.

20th Century climatic warming is the probable cause for recent deglaciation on Signy Island. Proxies in lake-sediments can be used to model the rates and directions of environmental change. Previous studies have made this link qualitatively. Here, a *quantitative* link is made between climate and lake-sediment response.

The island's 17 freshwater lakes display different characteristics within a small geographical area. Multiple cores from each basin yielded 209 surface-sediment (0-1 cm) samples which were analyzed for their lithology, particle-size and mineral magnetism. Ordination and classification identify relationships between the sediment variables and the environmental factors responsible for within- and between-lake variability. Variance partitioning using a minimum adequate model of 14 significant environmental variables provides insights into the balance of limnological and catchment factors affecting overall sediment character and its component fractions. A portion of unexplained variance suggests that other unmeasured variables also play a role in determining sediment character.

Catchment ice-cover is selected for reconstruction on the basis of its gradient length. An inverse regression model is constructed using four variables: % dry weight, % Loss On Ignition, mean particle-size and HARD%. Two methods of reconstruction - Partial Least Squares (PLS) Regression and analogue matching (MAT) are tested with various training-sets. Cross-validated prediction errors are *ca.*13%, comparing favourably with historical (1968 AD) records. Calibration is performed at four sites using optimal models to reconstruct ice-cover. The model is a sensitive proxy for erosion. Reconstructions are compared with temperature records and affirm that climatic warming is the most likely cause for observed ice-retreat. Based on simple measures, the model could see application in similar locations in the Antarctic, Arctic and Alpine regions.

DECLARATION

ACKNOWLEDGMENTS

It is indeed true that "a journey of a thousand miles begins with a single step" and in the same way, as my Thesis took its course it might well have touched a thousand lives. My thanks to all who have given help in one way or another.

For **Chapter 1**, I am indebted to my supervisors - Rick Battarbee, Viv Jones and Cynan Ellis-Evans - for their inspirational vision and motivating supervision over the last four years. This NERC/CASE Studentship was funded by the Natural Environment Research Council (Grant GT4/93/27G) and research facilities were provided by my host institutes - the Environmental Change Research Centre and the British Antarctic Survey. I also thank Peter Harding of Silsoe College, for pointing my nose in the right direction.

For **Chapter 2**, I nod to Barry Heywood for his contributions to freshwater studies at Signy Island. Martin Davey provided useful anecdotal information and Dominic Hodgson reviewed preliminary chapters and curbed my verbosity.

For **Chapter 3**, Martin Kernan for provision of a digitizing protocol and diminishing the agonies of ARC/INFO. Paul Cooper and Sarah King assisted me with Laserscan and ARC/INFO at the British Antarctic Survey. Joan Rae and Pete Bucktrout, British Antarctic Survey, supplied ice-retreat photographs of Signy Island.

For **Chapter 4**, I shake the cold, wet hands of the staff and visiting scientists at the British Antarctic Survey station on Signy Island who assisted me with fieldwork over the summers of 1993/94 and 1994/95. A unique experience, duplicated, which opened my eyes to the poles of human behaviour and has left me with memories that will last a lifetime.

For **Chapter 5**, the staff and postgraduates of the Department of Geography, University College London. Janet Hope for tolerating my occasionally remiss laboratory manner. Cath Pyke, Guy Baker and Nick Mann for drawing office advice and forgiving my limitless appetite for lemon puff biscuits. The unseen support of the computing staff should also be mentioned. Thankyous to Dave Allison, Paul Schooling and Angus Beare.

For **Chapter 6**, Sandra Bond and Vaughan Williamson, the Institute of Archaeology, University of London, trained and assisted me with particle-sizing. Adrian Chappell and Simeon Mellalieu offered additional advice. My day's grist at Malvern Instruments was lightened by the staff in the Applications Department and my sincere thanks to Maurice Wedd, Director of Malvern Instruments, for permission to use the Mastersizer.

For **Chapter 7**, I am indebted to Frank Oldfield and Jan Bloemendal for their meticulous scrutiny of my data and draft chapters. My thanks also are due to Bob Jude, Environmental Magnetism Laboratory, University of Liverpool, for technical assistance and mathematical wizardry.

For **Chapters 8 and 9**, my heartfelt gratitude to John Birks for his unending generosity of spirit and ready response to numerical queries. Funding for a weeks' visit to the Botanical Institute, University of Bergen, was awarded by the University of London Central Research Fund Grant. Sylvia Peglar fed me salmon and rømme and extended warm hospitality and good conversation. Much of the numerical software used in this Thesis was developed by Steve Juggins and has proved to be indispensable. The cost of radiometric dating a sediment core was met by the University College Graduate School Fund and the Department of Geography, University College London. Peter Appleby conducted the analyses with scrupulous precision.

For **Chapter 10**, I conclude by thanking members of my family and faithful friends who have survived these years also. Above anyone I dedicate this Thesis to Pam, devoted sister and constant friend. Her selfless succour is a model to us all.

TABLE OF CONTENTS

Chapter 4: Sampling strategy

Chapter 7: Surface-sediment mineral magnetic characteristics

LIST OF TABLES

LIST OF FIGURES

LIST OF APPENDICES

CHAPTER 1: INTRODUCTION

1.1 Background

Global warming studies predict that warming will be more pronounced in polar regions (Houghton, Jenkins & Ephraum, 1990) and an understanding of global climatic changes can be addressed by studying past climatic changes using a combination of General Circulation Model (GCM) simulations and validatory, quantitative reconstructions from a variety of palaeoclimate proxies. Palaeolimnology offers one such source of proxy data. Lake-sediment studies in high-latitude regions offer a promising means of high-resolution reconstructions of recent and Holocene environmental changes in a area where other long-term monitoring data and other palaeoclimatic indicators are absent or restricted (Smol, 1988; Hardy & Bradley, 1996; Smol & Douglas, 1996). These ecosystems are simple and perturbations are amplified by strong seasonality. The absence of direct human impacts maximises the possibility of monitoring environmental changes and identifying and modelling cause-effect relationships more readily than at lower, more populated latitudes.

Study sites on ecotones are of particular interest in studies of environmental change because of their sensitivity to climatic changes over time (Pienitz & Smol, 1993) and the maritime Antarctic offers a reference location for environmental reconstructions (Berglund, 1986). The region, defined by its climatic regime (Holdgate, 1964), broadly extends from the western Antarctic Peninsula Region to outlying islands at latitudes lying within the Antarctic Convergence (to *ca.*60°S), and includes lakes found on Alexander Island, James Ross Island, the South Shetland Islands and South Orkney Islands (Figure 1.1). Lakes on the sub-Antarctic islands of South Georgia, Marion Island, Îles Crozet and Kerguelen and Macquarie Island have evolved under more moderate climatic regimes. Lakes on the margins of Antarctica differ significantly from polar lakes of the Continent. Strong seasonality imposes a significant stress on these ecosystems through large fluctuations in temperature, day length and snow-cover (Heywood, 1977). By contrast, lakes on the Antarctic Continent are often perennially ice-covered (Doran, Wharton & Berry-Lyons, 1994) and/or highly saline (Matsumoto, 1993), and are to some extent more sheltered and temporally stable systems where the solar flux is the principal environmental control (McKay *et al.*, 1985). Stresses in these lakes are more persistent and many have attained a long-term equilibrium state for hundreds and even thousands of years. By contrast, the period of lake development in

Figure 1.1 Location of lake-sediment studies in Antarctica

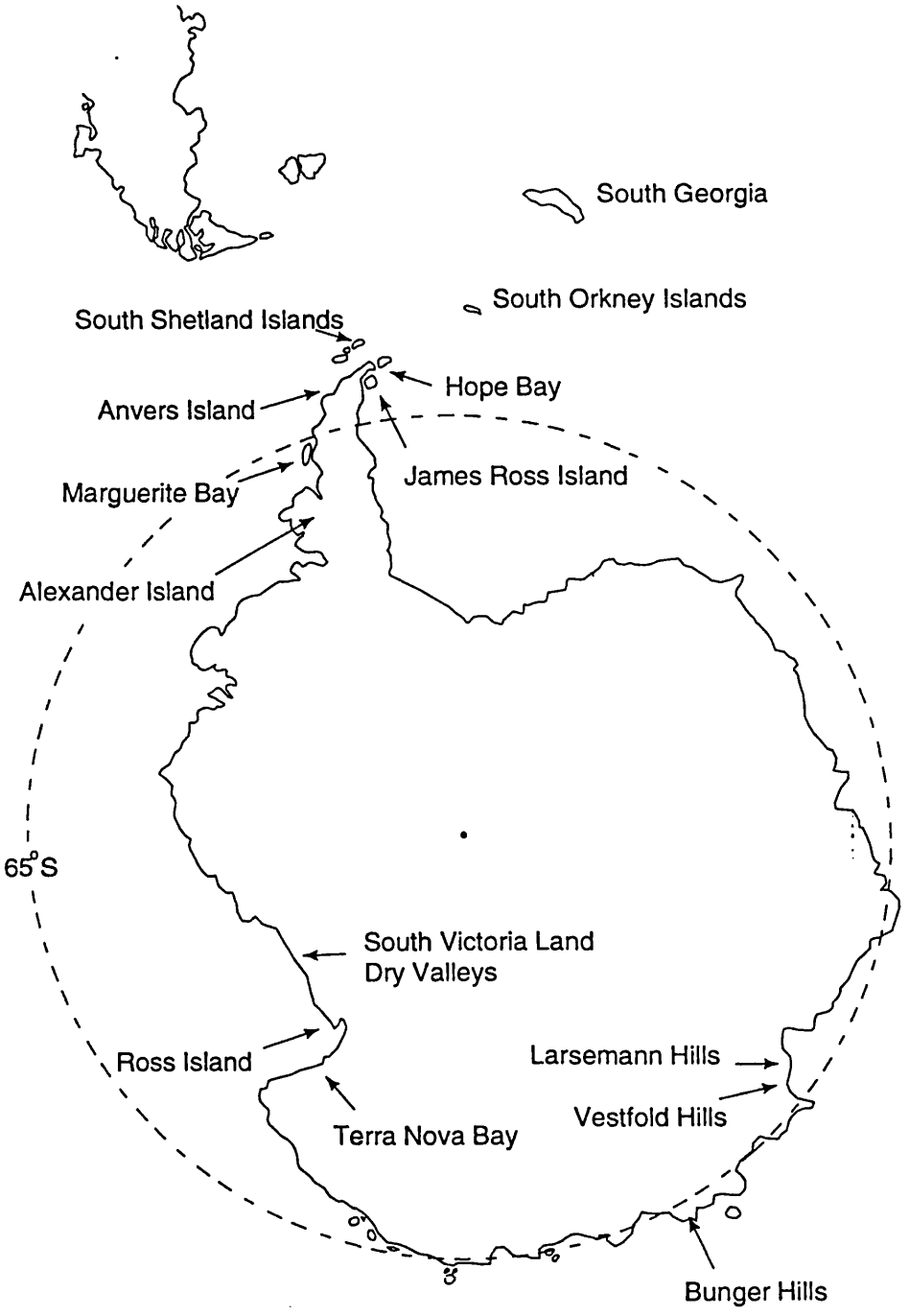

the maritime Antarctic is largely restricted to the last 10,000 years.

Lake-sediment studies in the maritime Antarctic emerged from studies of limnology and commenced in earnest in the late 1980s, the result of efforts of various national scientific programmes. Successive studies have highlighted the importance of climate in determining lake environments and their sediment characteristics. Methods of reconstruction have become increasingly sophisticated and the use of multiple proxies, coupled with intensive statistical techniques (e.g. Björck *et al.*, 1993, 1996), has become the standard technique. There has been a tendency however, to rely on biostratigraphical techniques at the expense of other proxies (Table 1.1) and for data to be interpreted in a qualitative way. Despite these limitations, palaeolimnological studies are providing a synthesis of long-term regional climatic changes, revealing new information concerning regional and local deglaciation after the Last Glacial Maximum (Mäusbacher, Müller & Schmidt, 1989; Birnie, 1990; Björck *et al.*, 1991a, 1991b; Ingólfsson *et al.*, 1992; Jones, 1993; Wasell, 1993b; Wilson, 1993; Zale, 1994), Holocene climate fluctuations (Birnie, 1990; Schmidt, Mäusbacher & Müller, 1990; Björck *et al.*, 1991a; Ingólfsson *et al.*, 1992; Björck *et al.*, 1993; Jones, 1993; Wilson, 1993; Björck *et al.*, 1996) and sea-level changes (Mäusbacher, Müller & Schmidt, 1989; Wasell & Håkanson, 1993). Little attention however, has been paid to the study of the most recent period of climate history (i.e. the last 100 years). Lake-sediment studies conducted over recent timescales have several advantages (Battarbee, 1991) including the ability to validate reconstructions of past environment using instrumental records and, unlike many other climate proxies in the region (e.g. ice cores), lake-sediments are sensitive to environmental changes at the catchment scale.

1.2 Recent climatic change in the maritime Antarctic

The most recent period of climate history has been highly unusual and possibly unique as a result of anthropogenic modification. The Antarctic Peninsula Region, Maritime- and Sub-Antarctic have experienced a long-term warming trend over the 20th Century of a greater magnitude than that reported for the Continent (Peel, 1992; Jones *et al.*, 1993c). In the South Orkney Islands, distinct warm and cold events have occurred on a sub-decadal timescale and since the 1950s, mean annual air temperatures at Signy and Laurie Islands have almost entirely been above -5°C (Smith, 1990) and the trend is continuing upwards. Higher temperatures are the probable cause for a regional deglaciation phenomenon. This has been of substantial magnitude at Signy Island and

Location	*Authors*	*Density*	*Dry weight*	*Organic matter*	*Lithology*	*Particle size*	*Mineral magnetism*	*Mineralogy/ chemistry*	*Tephra*	*Diatoms*	*Pollen/ spores*	*Moss remains*	*Dating*
King George Island, South Shetland Islands	Mäusbacher, Müller & Schmidt 1989			✓	✓	✓		✓		✓			^{14}C
King George Island, South Shetland Islands	Schmidt, Mäusbacher & Müller 1990				✓								^{14}C
Peninsula Region	Zale & Karlén 1989	✓X-ray	✓	✓	✓								^{14}C
Maiviken area, South Georgia	Birnie 1990	✓	✓	✓	✓	✓	*X* only	✓		✓	✓	✓	^{14}C
Midge Lake, Byers Peninsula, Livingston Island	Björck *et al.* 1991a			✓	✓					✓	✓	✓	
Antarctic Peninsula	Björck *et al.* 1991c				✓		✓	✓					^{14}C
Skua Lake, Horseshoe Island	Wasell & Håkanson 1992		✓	✓	✓			✓		✓			^{14}C
Lake Åsa, Byers Peninsula, Livingston Island	Björck *et al.* 1993			✓	✓	✓	*X* only	✓	✓	✓	✓	✓	^{14}C ^{210}Pb ^{137}Cs
Sombre Lake, Signy Island	Jones 1993	✓	✓	✓	✓					✓			^{14}C
Sombre and Heywood Lakes, Signy Island	Wilson 1993*	✓*	✓*	✓*	✓*		✓		✓?	✓*			^{14}C
Sombre, Heywood, Moss lakes, Signy Island	Jones & Juggins 1995	✓	✓	✓	✓					✓			^{137}Cs ^{210}Pb
James Ross Island, Antarctic Peninsula	Björck *et al.* 1996			✓	✓	✓	✓	✓	✓	✓			^{14}C
Signy and Livingston Islands	Dyson 1996						*X* only	✓	✓				

* data from Jones (1993)

Table 1.1 Methods used to reconstruct Holocene climate records using lake sediment records from the Peninsula Region, Maritime and Sub-Antarctic (in order of publication)

is paralleled by changes observed on South Georgia (Timmis, 1992; Gordon & Timmis, 1992). Results from lake-sediment studies suggest that this warming phenomenon is recorded in the sediments as enhanced sediment accumulation rates and inwash horizons (Birnie, 1990; Jones, 1993; Appleby, Jones & Ellis-Evans, 1995). The hypothesis that higher temperatures are causing widespread deglaciation which is impacting upon the lake-catchment systems and their sediment records is perfectly credible but needs to be tested using suitable proxies and methods. Calibration against known climate history could provide validated inference models which could then be applied to earlier time periods.

1.3 Lake-sediments and glacier variations

Climate has a pervasive influence on lake development and two scale-dependent temporal components may be distinguished: interannual variability (*scatter*) and longer lived processes (*trends*) (Smol, Walker & Leavitt, 1991). Against a background of longer-term evolutionary changes, shorter-lived climatic events and recent human impacts can cause limnological perturbations which contribute to overall lake development (ontogeny), deflecting or reinforcing longer-term trends. In high-latitude regions, variations in the extent and activity of glaciers is of particular relevance to lake development. Glacier size and dynamics are controlled by climatic parameters (e.g. mean summer air temperature, precipitation, radiation) and records of glacier variation are often used to infer climatic change over geologic and historic time. Continuous records from lake sediments downstream from glaciers contain one of the most important sources of information concerning glacier fluctuations (Karlén, 1981; Leonard, 1985; Karlén & Matthews, 1992) in the form of variations in particle-size, sediment thickness and organic/minerogenic content (Nesje, 1994) and palaeomagnetic characteristics (Karlén & Matthews, 1992). Glaciolacustrine sediments are sensitive to both small- and large-scale glacier and climatic variations over the Holocene timescale and their temporal continuity is a major advantage in recording Holocene glacier variations especially where for example, moraine records are incomplete (Ingólfsson *et al.*, 1992).

Glacial and non-glacial (control) lakes display contrasting sediment characteristics (Karlén 1981). In lakes fed by glacial meltwater, periods of increasing glacial activity can leave an imprint on the sediment record in the form of increased minerogenic and decreased organic contents. Sediments receiving glacial meltwater inflow display frequent fluctuations in the inorganic content, in contrast to other non-glacial lakes

which exhibit relatively constant inorganic content (Karlén, 1981). Glacier activity in the catchment is indicated by high sediment accumulation rates (Leonard, 1985). Under certain conditions, the presence of laminated sediments or varves (Lemmen, 1988) can be interpreted in terms of glacier presence in the catchment, although more accurately they represent levels of glacier activity above a certain threshold. The minerogenic content of glacial lake sediments tends to increase in association with the proportion of glaciated catchment and the levels of glacial activity and peaks in mineral input coincide with glacial maxima or with the initial retreat from glacial maxima (Leonard, 1997) where recently exposed glacial material is subject to paraglacial effects (Church & Ryder, 1972).

Sediments from non-glacial lakes are much more homogenous (Karlén, 1981) and glacial varves are absent. Lower sedimentation rates during periods of reduced ice extent (Leonard, 1985) mean that the proportion of allochthonous mineral material declines, allowing relative increases in organic content. In typical glacial landscapes, the organic component of the lake sediments mainly derives from autochthonous production within the lake, with minimal inputs derived from the inwash of soil organic matter from rudimentary soils of stable, glacier-free areas. Productivity is encouraged by increased nutrients as the catchments stabilise and develop under more favourable conditions (Mackereth, 1966). Peaks in organic matter therefore correspond with intervals when glaciers are absent from the catchment or are reduced in size. Consequently, lakes most likely to contain a sedimentary record of Holocene glacier variations are those that drain catchments in which the glacierized area has varied widely and which are low enough in altitude to possess sufficiently high biological production (Karlén, 1981).

Various factors complicate the ability to model climate directly through glacial activity. For instance, climatic warming does not always imply glacial retreat as rising temperatures may lead to increased precipitation and increased accumulation of glacier ice, leading to advance (Domack *et al.*, 1991). Confusingly, an advancing glacier with a positive mass balance can have low discharges and thus, lower potential to release sub-glacial materials. Therefore, maximum ice stands may actually represent relatively stable periods. A retreating glacier with a negative mass balance and high discharge can also increase the sedimentation rate as newly exposed glacial deposits are subject to fluvial reworking (Leonard, 1985).

1.4 Study framework for a quantitative environmental reconstruction

This study is concerned with lakes and lake-sediments adjacent to a small glacier and explores the extent to which past glacial extent and climate can be reconstructed from physical attributes in the lake-sediment record using quantitative methods. The rationale for the approach taken is as follows:

(i) Antarctic lakes are simple ecosystems which are responsive to extrinsic factors. They are therefore ideal sites for the modelling of cause-effect relationships. Their sediments hold a valuable archive of palaeoenvironmental information which is accessible through physical, chemical and biological indicators. Lake-sediment studies over the last 100 years mostly relate to short-term changes, such as recent climatic change, and its effects on glacier activity and extent (Leonard, 1997). Signy Island, situated in the maritime Antarctic, is the selected study location for testing these hypotheses of recent climatic change, glacier-activity and lake-sediment response. Its suite of glacial lakes covers long environmental gradients (Heywood, Dartnall & Priddle, 1980) and includes glacial and non-glacial (control) lakes (Karlén, 1981) for comparative purposes. Supporting documentary and observational evidence of contemporary and past environmental conditions are available for the validation of model results through the science programme of the British Antarctic Survey, which supports a permanent scientific station there.

(ii) The classic paper by Imbrie & Kipp (1971) spawned a revolution in the study of past environments and climate and over the past two decades the development of intensive computer-based techniques has encouraged the application of powerful multivariate techniques to test palaeoecological hypotheses (Birks, 1993). Many of these methods have developed from other disciplines (Birks & Gordon, 1985) and most of the required protocols, inferential techniques, and quality assurance/control guidelines developed for acidification studies (Smol, 1990) can be transferred to palaeolimnological studies of climatic change (Smol, Walker & Leavitt, 1991). The benefits of using multiple proxies and numerical techniques has been demonstrated in Holocene lake-sediment studies at Livingston Island (Björck *et al.*, 1996) suggesting that a similar approach could be used successfully at Signy Island. Birks (1995) provides a detailed proforma for environmental reconstructions which forms the basis of the methodology used in this Thesis.

(iii) Regional studies in the maritime Antarctic have tended to depend on fossil data, at the neglect of physical and chemical parameters. Diatoms have been used with success

to reconstruct lake nutrient-histories at Signy Island (Jones & Juggins, 1995) using a combined diatom-water chemistry training-set from maritime Antarctic lakes on Signy and Livingston Islands (Jones, Juggins & Ellis-Evans, 1993). Diatom-based reconstructions have several inherent problems (Fritz, 1990) and there are difficulties in establishing direct species-temperature relationships in freshwater ecosystems, especially in polar and sub-polar latitudes where diatoms for example, are not especially responsive to temperature (Smol, 1988). Researchers are presently extending methodologies to reconstruct past temperatures (Vyvermann & Sabbe, 1995; Pienitz *et al.*, 1995) but fossil data are prone to the 'no-analogue' problem in glacial periods and species-diversity can be low in contemporary maritime and continental Antarctic freshwater environments (Jones, 1996). Clearly, current numerical methods have the potential to make the quantitative link to climate or more specifically, temperature, and some of the problems associated with biological data could be solved by using other non-biological proxies.

1.5 Non-biological climate proxies

Non-biological climate proxies in the sediments need to be directly or indirectly responsive to climate (Smol, Walker & Leavitt, 1991). Instead of using bulk sediments (e.g. Mackereth, 1966), an improved sediment characterization is required to observe changes in different allochthonous and autochthonous sediment fractions (Engstrom & Wright, 1984) enabling a link to be made between sediment proxies and the processes responsible for their formation. These proxies also need to be simple so that they can be potentially applied to other lake-sediment records outside the locality. Quantitative variables are sought for the best possible reconstruction (Birks, 1995). The complementary physical determinands used in this study are:

(1) Lithology (density, water content, organic content, biogenic silica, clastic content)
Density, water content and organic content are conventionally measured in lake-sediment studies (Table 1.1). These however, provide limited information on sediment origin so a chemical extraction technique is used in addition to determine the allogenic and endogenic components and their relative contributions to the sediment matrix.

(2) Particle-size

Particle-size shares natural relationships with sediment lithology (Håkanson & Jansson, 1983). At Signy Island, sediment particle-size has been assessed qualitatively (Heywood, Dartnall & Priddle, 1980) and characterisation has been limited to individual cores using the semi-quantitative Troels-Smith scheme (Jones, 1993; Jones in Wilson, 1993).

Observed clay inwash horizons in sediment records from Signy Island, are seen to relate to abrupt changes in the dynamics of sediment transport and deposition (Appleby, Jones & Ellis-Evans, 1995). Particle-size is therefore regarded as a useful palaeoclimate proxy in these environmental systems (e.g. Björck *et al.*, 1993).

(3) Mineral magnetism

Mineral magnetic measurements have been made on two sediment sequences on Signy Island (Wilson, 1993) contributing towards a qualitative environmental reconstruction over the Holocene. Changes in mineral magnetic behaviour seem to relate to changes in allochthonous sediment flux but possible post-depositional modification has been largely overlooked. In the light of recent findings in Arctic lakes (Snowball, 1993b) this aspect of the mineral magnetic behaviour requires further investigation. This more detailed exploration, with reference to the other non-biological proxies, should provide a holistic environmental interpretation considering both intrinsic and extrinsic processes affecting the lake sediment record.

1.6 Project aims and outline

The key research aims are:

(1) To *test hypotheses* of climate, glacier activity and lake-sediment response in a climatically-sensitive area which has experienced climatic change and glacial retreat of known magnitude over recent timescales.

(2) To extend established methodologies for *quantitative environmental reconstruction* in a novel way using *non-biological proxies* in the lake sediments, thus avoiding problems associated with fossil data in glacial lakes and extending the potential for non-biological data to be used to achieve climate reconstructions.

(3) To produce a *validated climate-inference model* which is simple and repeatable and has potential for application (a) outside the reference area and (b) over longer timescales.

The project outline is summarised in Figure 1.2 and has four stages:

Stage I. Data collection and exploratory data analysis

Modern sediment and contemporary environmental data are collated for each lake catchment. Numerical analysis techniques are used with the combined lakes and catchment environment data (Chapter 3) to find the principal environmental gradients

Figure 1.2 Project outline

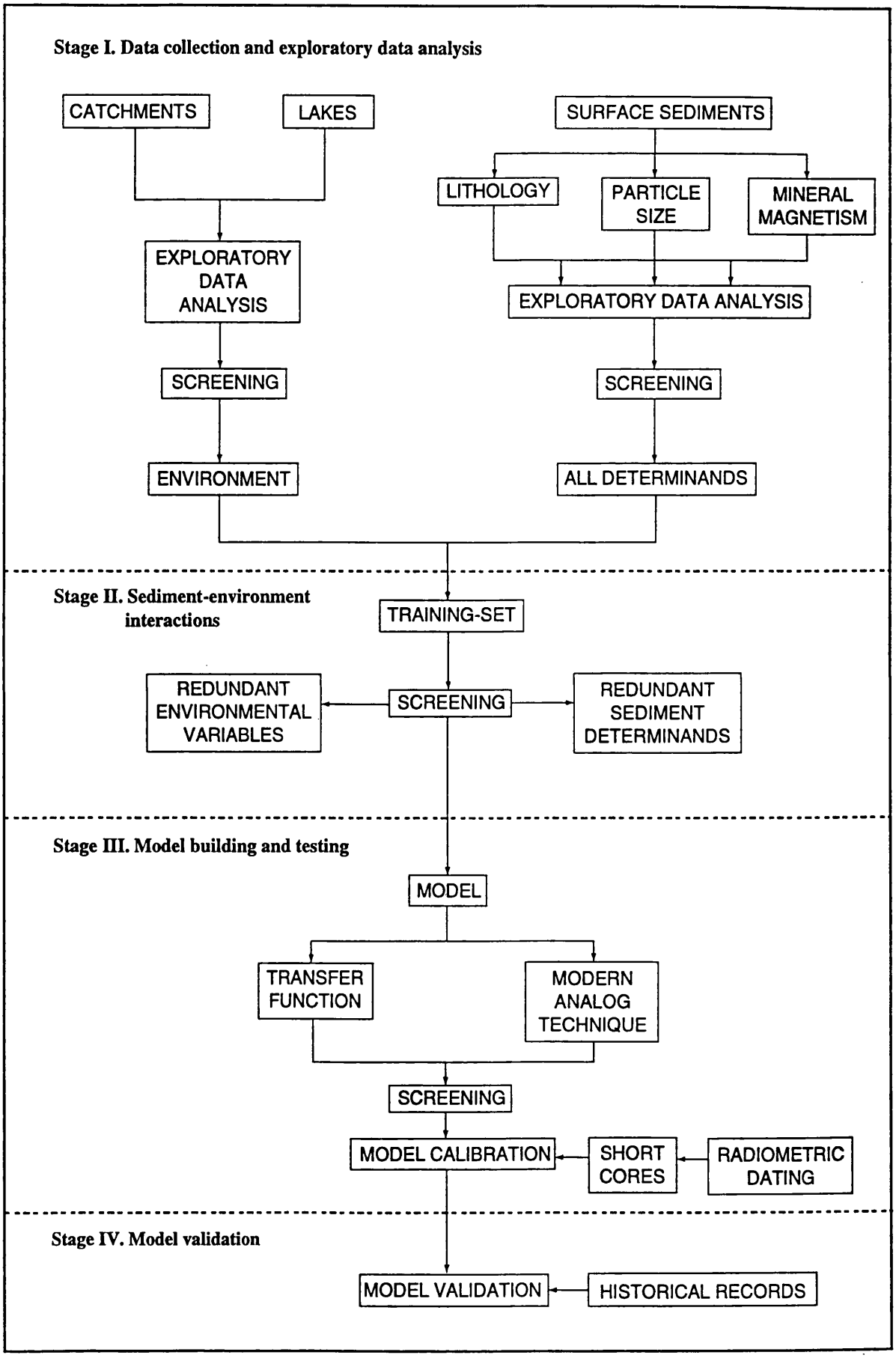

determining present-day lake characteristics. Multiple surface-sediment samples are collected (Chapter 4) and measured for their lithology (Chapter 5), particle-size (Chapter 6) and mineral magnetic characteristics (Chapter 7). Exploratory data analysis and screening for outliers is undertaken on the respective data-type (Chapters 5, 6 and 7) and then for all sediment variables combined in one summary data-set (Chapter 8), so providing an integrated characterization of the modern lake-sediments.

Stage II. Sediment-environment interactions

A training-set of modern sediment-environment interactions is formed by combining the screened data-sets from Stage I (Chapter 8). Direct ordination techniques are used to explore interactions between the sediments and the environment and the major environmental predictors are isolated from other redundant environmental variables. A climatically-relevant variable is selected for reconstruction using inverse multiple regression techniques (Chapter 9). The sediment data-set is screened for redundant variables against this single environmental predictor to find a parsimonious model of statistically-significant sediment variables to achieve the reconstruction.

Stage III. Model building and testing

Two methods of environmental reconstruction are conducted using the parsimonious model from Stage II: a transfer function approach and a modern analog approach (Chapter 9). The results and efficiencies of each method are assessed and the best models are applied ('calibrated') to fossil core data from contrasting sites using a series of matching sediment determinands. These cores are supported with radioisotope chronologies so that the magnitude and response-times to environmental perturbations between each site can be assessed.

Stage IV. Model validation

The models are validated using historical records of catchment conditions and climate (temperature) over the 20th Century to test model sensitivities to known climatic events and the representativity of results from different lake-catchment systems on Signy Island. Model predictions are referenced to the findings of previous palaeolimnological studies and discussion focuses on the potential for model application over longer timescales and in areas outside the maritime Antarctic (Chapter 10).

CHAPTER 2: STUDY LOCATION - SIGNY ISLAND, MARITIME ANTARCTIC

2.1 Introduction

Signy Island, maritime Antarctic (60°43'S, 45°38'W), is readily accessible through the operations of the British Antarctic Survey's terrestrial and freshwater life sciences programme. Its location, physiography and climate render it highly sensitive to environmental change (Smith, 1990). In this Chapter, Signy Island is located in a geographical context and its geology, physiography, climate, soils and vegetation are briefly outlined. The series of 17 freshwater lakes on the Island, all of contrasting character, are described with reference to their morphology, ecology and catchment characteristics. Signy Island has been subject to two significant environmental change phenomena over recent timescales: climatic warming and seal-related eutrophication of catchments and lakes associated with the destruction of terrestrial vegetation. Both phenomena are likely to have impacted on the lakes and analysis in subsequent chapters explores these processes through the recent sedimentary record.

2.2 Geographical description of Signy Island

2.2.1 Location

Signy Island is one of the South Orkney Group of Islands, found on the southern limb of the Scotia Ridge about 750 miles east of Cape Horn and 350 miles east-north-east of the tip of the Antarctic Peninsula. The Group is composed of four major islands and a number of smaller islets (Figure 2.1), the most distant of which are the Inaccessible Islands, lying 20 miles west of Coronation Island. Signy Island lies due south of Coronation Island and is separated by Normanna Strait, a stretch of water approximately 1.6 km wide at its narrowest point. The nearest land to the South Orkneys is Clarence Island, the eastern-most member of the South Shetland Islands, 220 miles to the south-west.

The South Orkneys are critically located between South America and the Antarctic Continent, bridging the continental divide. They are also within the limits of the Antarctic Convergence, an important component of the regional weather system. Weather conditions are strongly influenced by vagaries of the Weddell Sea current and its associated winter pack-ice. This isolated oceanic setting, compounded by a restricted areal extent and comparatively low altitude, make Signy Island exceptionally sensitive

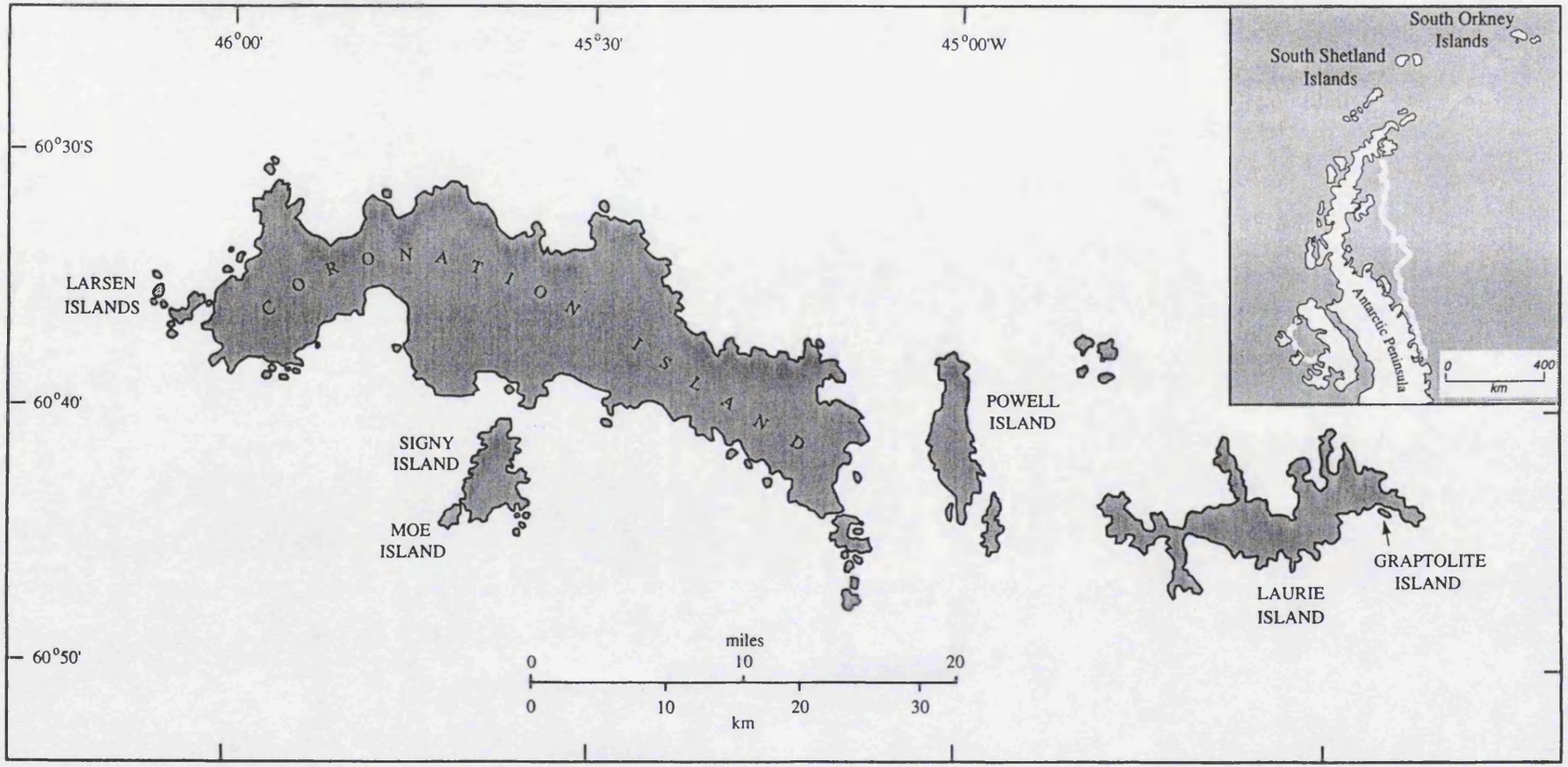

Thomson (1968)

Figure 2.1 Geographical location of Signy Island, South Orkney Islands

to environmental perturbations and for this reason Smith (1990) described Signy Island as a "paradigm of biological and environmental change in Antarctic terrestrial ecosystems". Signy Island has been home to a permanent British Antarctic Survey station since 1947. Their scientific research programme has led to the collection of an extensive database of environmental information which has invaluable potential for ecological hypothesis testing. Most records start in the period immediately antecedent to a mid-Twentieth Century warming trend in the climate, hence baseline conditions have been recorded in instrumental and documentary records, providing the opportunity to assess the rates and magnitude of environmental change.

2.2.2 Geology

The geology is part of the Precambrian 'Basement Complex' (Thomson, 1968), consisting of intensely folded regionally metamorphosed sediments, predominantly garnetiferous quartz-mica-schists in association with foliated amphibolites and marbles (Matthews & Maling, 1967). Post-metamorphic igneous activity is not indicated. The rocks are lithologically and petrologically comparable with those of the Elephant and Clarence Islands group, but differ from the Basement Complex of the Antarctic Peninsula, where orthogneisses have been noted. Faults play an important part in the structure of Signy Island (Matthews & Maling, 1967).

2.2.3 Physiography and glaciation

Signy Island is small and roughly triangular in outline, covering an area of about 20 km^2 (Figure 2.2). It extends approximately 10 km north to south and 5 km along the southern coast. It is mountainous with an ice-cap, temperate glaciers and rugged topography. Tioga Hill, near the centre of the island, is the highest point at 279 metres a.s.l.. Elsewhere separate summits reach to 220-270 metres. Summits are generally flat or convex and near the centre of the island they are connected by shallow, glaciated cols. The main upland forms a plateau dominated by the ice-cap and the principal summits protrude as nunataks. The plateau edges are sharply bounded and steep slopes formed by cirque glacial erosion surround the high ground. The east and west coasts are marked by small cirques separated by frost-shattered spurs. Most of these have floors at 10-50 metres a.s.l.. although some have floors below sea-level which were drowned following eustatic sea-level rise at the end of the Last Glaciation. The lowland is well-defined and most extensively developed on the east coast and in the extreme south-east rising to no more than 40 m a.s.l. except for a few hillocks reaching a maximum of 72 metres. The

Figure 2.2 Map of Signy Island

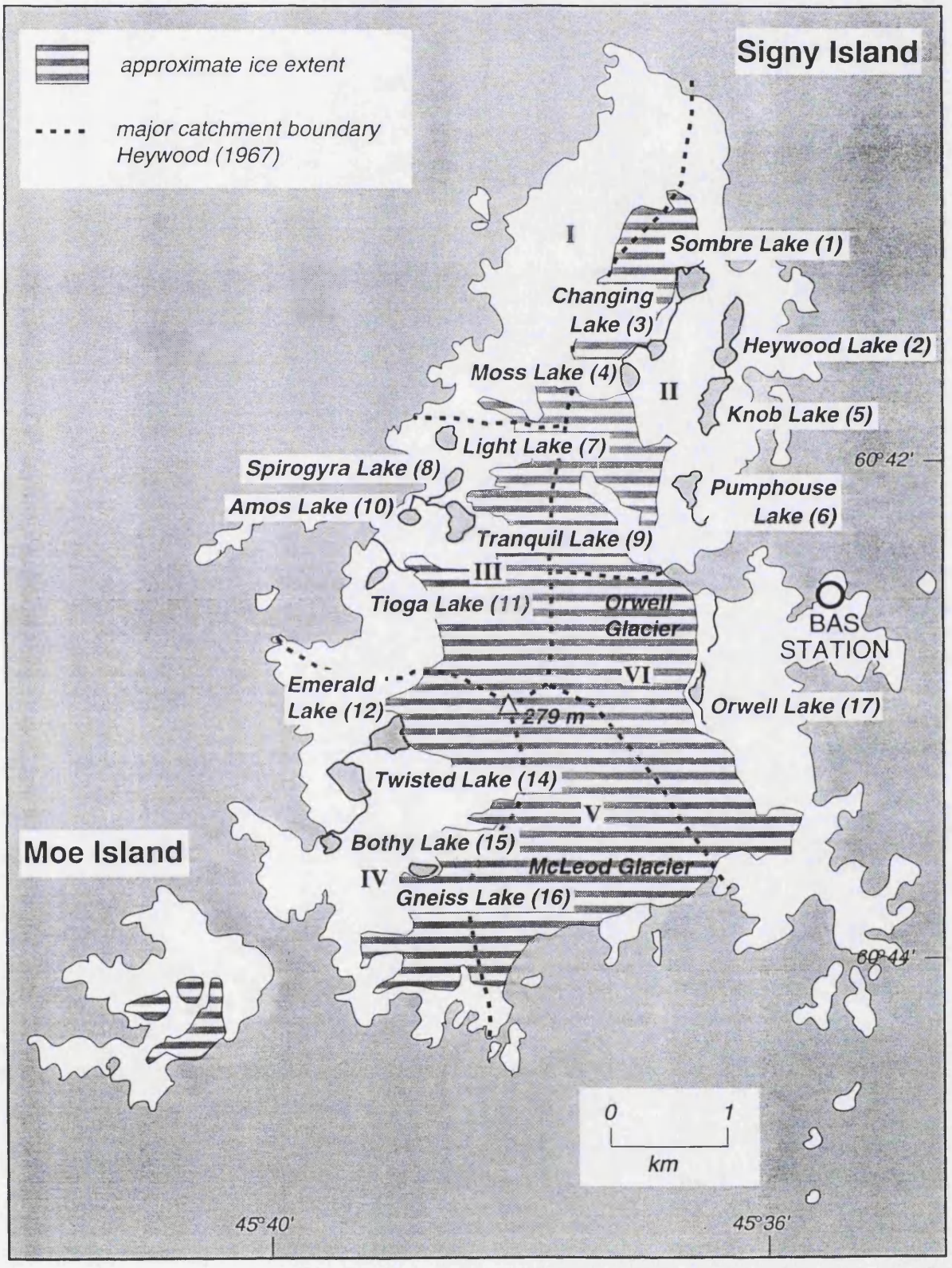

eastern lowland is covered with glacial diamicton or frost-shattered debris. This belt is narrow and discontinuous along the west and south-west coasts and sometimes absent. The north west has gently-sloping topography covered with diamicton.

About a third of the land-cover is permanent snow and ice. The ice-cap is subdivided into a series of small drainage basins but has only two major outlet glaciers: the McLeod and the Orwell (Heywood, 1967). The McLeod Glacier drains southwards from the central plateau forming an ice cliff over 2 km long in Clowes Bay. The Orwell Glacier is a valley glacier which calves into a shallow tidal bay on the east side of the Island. Active glacial geomorphology has led to alterations in several lake areas and catchment ice-coverage over recent decades (Smith, 1990) and new lakes (the Khyber Lakes) have been formed at the receding ice margins of the McLeod Glacier.

2.2.4 Climate and recent climate history

Signy Island lies in the maritime climatic zone of Antarctica (Holdgate, 1964) and has a typically Antarctic climate which is actually more harsh than the more southerly South Shetland Islands due to the effects of cold air from the Weddell Sea. The Southern Hemisphere climate has a larger interannual variability relative to the Northern Hemisphere (Trenberth, 1984) which is amplified by regional and local factors. Seasonal variability is high, dependent on the proximity of the Weddell Sea ice pack. Mean annual air temperatures for 1991 were sub-zero (-4°C) and monthly mean temperatures ranged from +2.8°C to -11.7°C. Annual precipitation ranges from 350-770 mm. Considerable accumulations of snow occur during the winter, mostly as drifts. Mean monthly temperatures exceeds 0°C for typically two months each summer resulting in complete seasonal snow-pack melt.

Instrumental temperature records from Signy and neighbouring Orcadas Station on Laurie Island display a warming trend over the last 50 to 100 years, similar to that of South Georgia (Gordon & Timmis, 1992) and also evidenced in regional ice-core records (Jones *et al.*, 1993). Five year running-means of mean annual summer air temperatures for Signy and Laurie Islands reveal distinct cold and warm events (Figure 2.3). Deposition of recent moraines on Signy Island (dated lichenometrically) coincide with cold spells of the early 1910s, early 1920s to mid 1930s, and late 1940s. Since 1951, a dramatic increase in mean summer air temperatures has occurred (Smith, 1990) and the trend is continuing upwards. The 35% observed loss of snow and ice between

Figure 2.3 Summer (December-February) air temperatures for Laurie Island (continuous lines) and Signy Island (dashed lines), South Orkney Islands, expressed as (a) annual means and (b) 5-year running means (Smith, 1990)

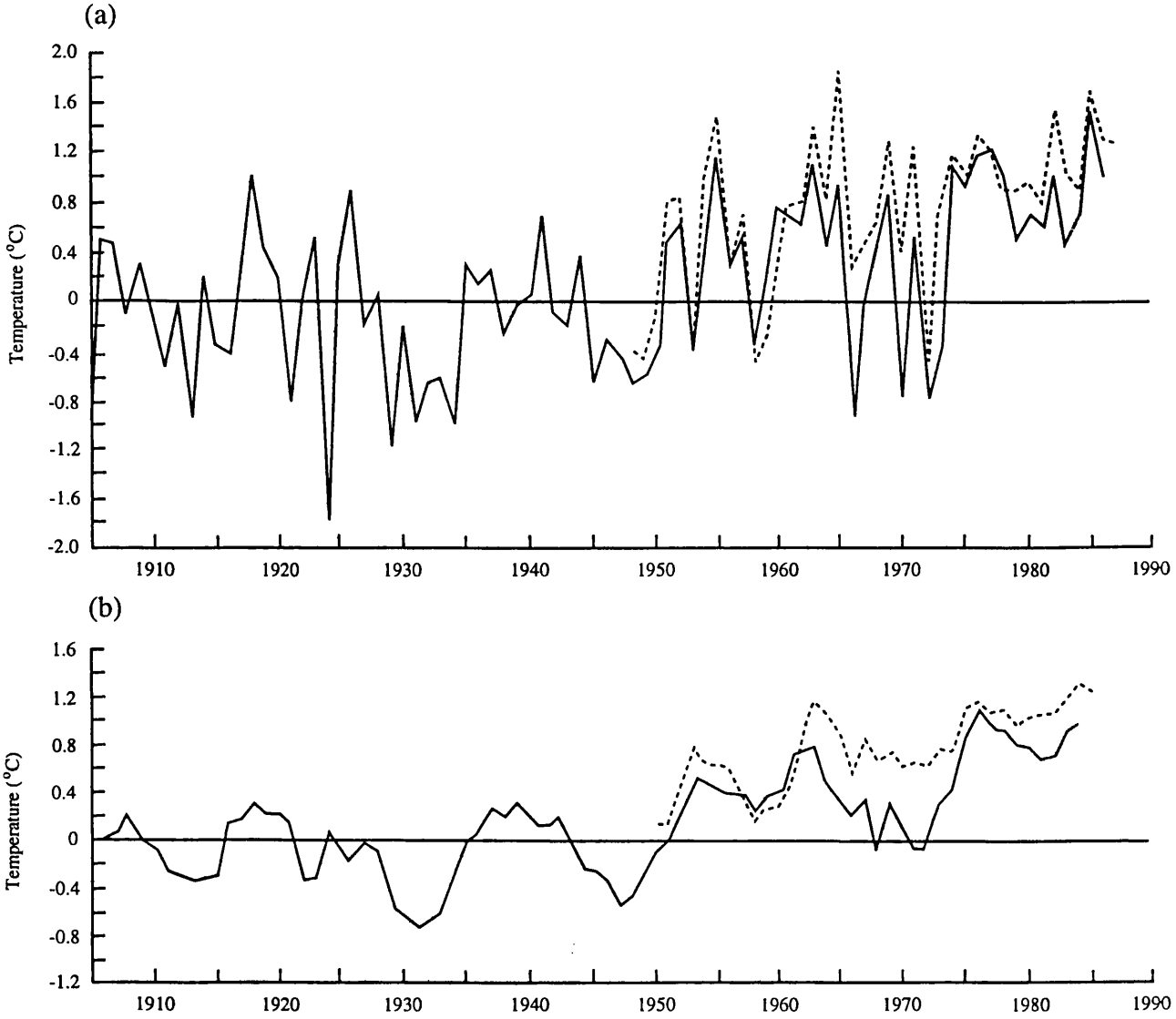

1949-1989 (section 2.2.8.1) suggests the transgression of a critical glacio-climatic threshold. The effects of increasing temperature might be amplified at ground level where climate is presently less harsh than air temperatures suggest (Davey, Pickup & Block, 1992).

2.2.5 Soils

Soils have been described by Holdgate *et al.* (1967). Physicochemical weathering phenomena are dominant in maritime Antarctic climates including leaching and freeze-thaw cycles. Permafrost is present below an active layer of 0.3-0.7 metres (Chambers, 1966). In summer months, ground temperatures fluctuate about 0°C but there are very few freeze-thaw cycles, i.e. only one freeze-thaw cycle in any one 24 hour period (Davey, Pickup & Block, 1992). The winter freeze is the major freezing event and snow depths cause considerable spatial variations in minimum winter ground temperatures. Frost-shattering and solifluction have produced a fine mineral soil in places but cryoturbation prevents the formation of soil horizons producing lithoskeletal, youthful soils. Patterned ground is widespread including frost-sorted soil polygons up to 1.5 metres in diameter. Soils of recently deglaciated terrain have very alkaline reactions. Areas frequented by seals undergo heavy nitrogen enrichment, acidification and physical disruption. A reducing mud of excrement mixed with moribund vegetation and mineral material develops around seal wallows (Collins, Baker & Tilbrook, 1975) containing exceedingly high nitrogen and phosphorus levels. Large populations of bacteria, yeasts and fungi are found in the soils (Baker, 1970), essential precursors for colonisation by macrovegetation.

2.2.6 Terrestrial vegetation

Terrestrial macroscopic flora and fauna are restricted to taxa which are preadapted to metabolising at low temperatures and tolerant of frequent and rapid freeze-thaw and hydration-dehydration cycles. Isolated from potential sources of immigrant propagules and faced with severe environmental stresses, vegetation is restricted to stress-tolerant types of lichens, mosses, algae, hepaticas, fungi, bacteria and two types of flowering plant (*Colobanthus quitensis* and *Deschampsia antarctica*). Vegetation successions are simple with very few stages because of low species-diversity, the absence of higher organisms and a lack of complex interactions. Under favourable conditions, a mosaic of large and diverse vegetation communities can develop within a decade or two of deglaciation, comprising of species best adapted to local site conditions (substrate

texture, nutrient status and hydrological regime). Colonisation of soil polygons results in some striking vegetation patterns. There are two significant mat-forming algae: *Prasiola crispa*, an opportunistic species associated with areas of disturbance and nitrogen enrichment caused by seals or penguins (Smith, 1988), and *Phormidium sp.*, the most successful of the fellfield algae in its resistance to desiccation and sustained growth at low irradiances (Davey, 1988), i.e. under seasonal snow-cover. Extensive stands of bryophyte carpet, moss hummocks and moss turf formations (Priddle, 1985) occur in the north-west sector of the Island and the deepest accumulations, up to 2 metres thick, have basal radiocarbon dates of 5500 *corr.*^{14}C years BP[1] (Fenton, 1980), indicating continuous *in situ* and prolonged growth through the Holocene.

Vegetation composition tends to remain static unless perturbed from its equilibrium state; when disturbed, these systems display little resilience and respond rapidly and often irreversibly (section 2.2.8.2). Field-cloche experiments have shown that a mean increase of *ca.*3°C in summer can have a dramatic effect on the rate of development of *in situ* propagules and continued climatic warming could promote significant vegetational change. The ameliorating summer climate over the past 25 years has probably been responsible for an increase in stands of Antarctic hair grass (*Deschampsia antarctica*) on Signy Island (Smith, 1990). Lynch Island, 1.5 km distant, is the most likely source of propagules which already had extensive swards. There is no evidence however, for an increase in the status or improved seed viability of the other native vascular plant, the Antarctic pearlwort (*Colobanthus quitensis*), or for the growth of alien plants from accidentally-introduced propagules.

2.2.7 Drainage

Six main catchment areas are recognised on Signy Island (Heywood, 1967; Figure 2.2). Drainage systems have fluctuated in response to changing ice-cover and features continue to evolve in this geomorphologically active landscape. Relict geomorphological features attest to shifting stream-courses and raised lake levels in relation to advanced ice-fronts. Drainage is largely by chaotic overland flow and very few stream-courses occupy permanent positions. Hawes (1989) categorized the island streams into three types according to channel-form and flow characteristics: (i) meltwater runnels (ii) larger streams and (iii) lake outflows and glacial streams. Snow-cover in the maritime

[1] Corrected for marine reservoir effect, typically 1200-1300 yrs (Björck *et al.*, 1991b)

Antarctic is an important source of water for streamflow and stream discharges are high in spring and summer coincident with the major period of melt, coupled with peak sediment transportation (Hawes, 1989) Discharge steadily declines over the course of the summer as meltwater sources are exhausted. This is essentially similar to that of Arctic streams (Harper, 1981) where the permafrost table permits minimal basin storage and promotes rapid runoff. Flow velocities determine vegetation zonation in the streams, characteristically a semi-aquatic margin consisting of a perennial cyanobacterial-diatom mat and a flowing channel with a similar perennial mat that becomes overgrown by annual filamentous chlorophytes during the summer (Davey, 1993). Throughout the summer the lowlands remain extensively waterlogged and perennial lakes occupy topographic depressions (section 2.3); other areas in contrast, such as scree slopes, drain very quickly and are often arid.

2.2.8 Recent environmental change

In a 1990 publication, Smith described two major environmental perturbations which were radically affecting the environment of Signy Island. These are a recent and rapid deglaciation of the Island's ice-cover (section 2.2.3), probably in response to a 20th Century warming trend in climate (section 2.2.4), and disturbance of lowland lake-catchment systems by fur seals. These are outlined below:

2.2.8.1 Climate warming and deglaciation

Climate fluctuations have affected glacier activity on Signy Island over the Holocene. Relict moss peat and lichen thalli have been exposed at various locations as ice-margins have retreated and, supported by radiocarbon dates, provide important information on former glacial extent in the past (Smith, 1990). During cold climate events the ice fields expanded, overwhelming the vegetation, but rarely removing it. There have been three or four periods of Neoglacial advance over the past *ca.*1500 years, with several minor glacier fluctuations between about 1250 and 1600 AD. These coincide with early events of the Northern Hemisphere Little Ice Age and possibly two during the Southern Hemisphere Little Ice Age of *ca.*1700-1850 AD (Smith, 1990). Periods of increased warming and cooling are fairly consistent with those reported in the Antarctic Peninsula Region (Björck *et al.*, 1991a; Björck *et al.*, 1993) and South Georgia (Wasell, 1993) using lake sediment records. This relatively thin mantle of low density ice is very sensitive to minor fluctuations in austral summer (December to February) temperature and Smith (1990) predicted that an increase in mean summer air temperature of <1°C

could significantly alter the balance between accumulation and ablation. Comparison of the island's ice-cover based on ground surveys in 1949 and 1989 reveal a 35% reduction over the 40 years. Between the mid-1960s and mid-1980s ice margins have receded by over 100 metres in many places and the thickness of the island's glaciers reduced by 7-8 metres. Modelling of ice dynamics is ongoing (M. Gardiner, *pers.comm.*) but in the interim an additional means of predicting the causal mechanisms for glacier variations and predicting the rate of future changes is through climate proxies in the freshwater lakes.

Since the period of major deglaciation and lake inception, *ca.*6500-6000 ^{14}C years BP, sedimentation in the lakes has fluctuated over time with changing catchment conditions (Appleby, Jones & Ellis-Evans, 1995); changing erosion rates are therefore a useful surrogate for glacier activity and climate. Apart from a period of rapid sedimentation *ca.*3000-1000 ^{14}C yrs BP (V. Jones, *pers.comm.*), the greatest departures from equilibrium behaviour in sedimentation have occurred since the 19th Century, but most importantly since the mid-20th Century. Since the 1950s there has been a major increase in the sedimentation rate in Sombre and Heywood Lakes, which was especially high in the early 1960s. Mean sedimentation rates since the mid-1970s have remained at 2-3 times the pre-1955 level. Mineral magnetic measurements (Wilson, 1993) also evidence changing allochthonous sediment inputs in response to increased erosion and the period is matched by changing diatom assemblages (Jones, 1993). Parallel changes in sedimentation, mineralogy and ecology in separate lakes suggest an island-wide response to forcing mechanisms.

2.2.8.2 Fur seal-related eutrophication

Fur seals (*Arctocephalus gazella*) pose a significant threat to terrestrial and freshwater ecosystem stability on Signy Island. These marine mammals were close to extinction in the 19th Century but the cessation of commercial sealing activities in the early 20th Century, the implementation of conservation measures, a dramatic reduction in the predatory whale population in the Southern Ocean and an increase in their principal food source - krill - has led to an exponential population increase in recent decades (Figure 2.4). The massive annual immigration to Signy Island each summer represents an overspill of young (2-5 years) males from sub-Antarctic South Georgia, 900 km to the north-east. Census figures witness a mean annual increase of 725% for the years 1982-1988. Fur seals have visited Signy Island in the past (Hodgson & Johnson, 1997) but

Figure 2.4 Increase in the number of fur seals on Signy Island (1956 - 1995)

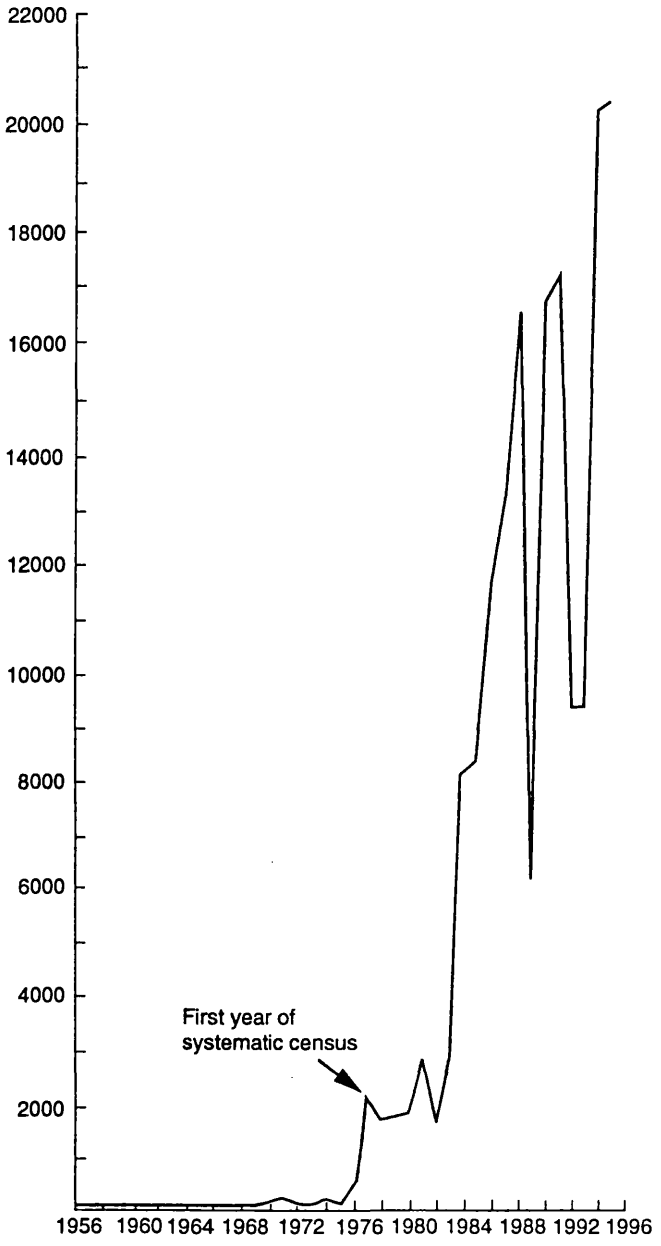

All censuses since 1977 made around 24 February
Source: British Antarctic Survey

were probably never as abundant and past population levels are difficult to quantify. In contrast, elephant seal populations have remained fairly static on Signy Island since records started (Ellis-Evans, 1990) tending to frequent the same wallows every year and only affecting lakes in Three Lakes Valley (Heywood, Knob, Pumphouse) and Amos and Bothy Lakes.

Seals have caused sudden and catastrophic ecological transformation (Smith, 1988) and have impacted heavily on the terrestrial environment. Highly mobile on land, their trampling has destroyed the delicate moss and lichen communities and defecation causes nutrient-enrichment leading to vegetation compositional changes. Every year population pressure has driven more fur seals further inland and upslope into pristine areas; several bird colonies have been abandoned and elephant seals have been displaced from traditional wallows. Ellis-Evans (1990) produced convincing evidence for seal-related nutrient increases in Heywood Lake since the time of the major population increase (post-1984) and trophic reconstructions from fossil diatom assemblages in Sombre and Heywood Lakes evidence enhanced nutrient status driving increased lake productivity (Jones, 1993; Jones, Juggins & Ellis-Evans, 1995). Fur seal-related eutrophication of Sombre Lake was thought to be minimal in 1989 (Oppenheim & Ellis-Evans, 1989) but signs of change were noted by Jones (1993) from surface-sediment diatom counts from samples collected in 1991. The gravity of the problem has led to the instatement of an exclusion policy from Lynch Island, a Specially Protected Area, and critical locations on Signy Island (Light, Spirogyra and Tranquil Lakes) using seal-proof fencing at coastal access points. Some have argued that seals may themselves be a function of changing regional climate (Guinet, Jouventin & Georges, 1994).

2.3 The freshwater lakes of Signy Island

2.3.1 Overview

There are 17 freshwater lakes on Signy Island (Figure 2.2). The original numerical identification system was superseded with names approved by the Antarctic Place Names Committee (Ellis-Evans, 1983), with the exception of one lake - Lake 13 - which had virtually disappeared by the early 1980s. The lakes are situated in different major catchment systems (Heywood, 1967); individual catchments though, are small and tend to be isolated from each other. On the east side of the Island, Sombre, Changing and Moss Lakes form a cascade system in Paternoster Valley. Heywood, Knob and Pumphouse Lakes are on the coastal strip of Three Lakes Valley and Orwell Lake is

juxtaposed to the Orwell Glacier. On the west side of the island there are two major catchment systems: to the west, the group including Light, Spirogyra, Tranquil and Amos Lakes; to the south-west the Cummings Ampitheatre group of Emerald, Lake 13, Twisted, Bothy and Gneiss Lakes. Tioga lake is isolated between these two systems.

The suite of lakes provides a unique laboratory for the study of many processes, for they lie within a small area and are geologically similar but are influenced by different gradients of other environmental factors. These subtle differences suggest a sensitivity to the surrounding environment, making them useful for testing hypotheses of lake ontogeny, glacier activity and climate. The outcome of 25 years of freshwater ecological studies by the British Antarctic Survey has led to a large volume of information on the present-day limnology, chemistry and ecology of the lakes (Heywood, 1967; Heywood, 1968; Heywood, Dartnall & Priddle, 1980; Ellis-Evans, 1990; Ellis-Evans & Lemon, 1989; Hawes, 1988; Jones, Juggins & Ellis-Evans, 1993; Light & Heywood, 1973; Oppenheim, 1990; Oppenheim & Ellis-Evans, 1989; Oppenheim & Greenwood, 1990; Oppenheim & Paterson, 1990) providing abundant data for environmental modelling.

2.3.2 Site descriptions

The original site descriptions were collated from various sources by Heywood, Dartnall & Priddle (1979). These have been appended and updated in the following sections using more recent references and field observations.

2.3.2.1 Sombre Lake

Sombre Lake (Figure 2.5) has been in existence since *ca.*6500 ^{14}C years BP (Wilson, 1993) and is the most studied of the Signy lakes, with detailed documentation of its limnology, flora and fauna (Jones, 1993; Wilson, 1993; Oppenheim, 1990; Oppenheim & Ellis-Evans, 1989; Oppenheim & Paterson, 1989; Oppenheim & Greenwood, 1990). Physico-chemical conditions in the lake are actively monitored and other projects concerning lake flora, fauna and catchment geochemistry are ongoing. This oligotrophic lake is the lowest of three in a Paternoster sequence; its inflow comes from Changing Lake above. Basin morphometry is relatively simple and the largest accumulations of sediment are located at the deepest point in the zone of winter anoxia. The steep west and north-west sides of the basin consist of unstable scree which is vegetation free (Light, 1976). Boulders are common in shallow waters, especially near the outflow and partial moss-cover has been noted here (Heywood, Dartnall & Priddle, 1979). The

Figure 2.5 Sombre Lake

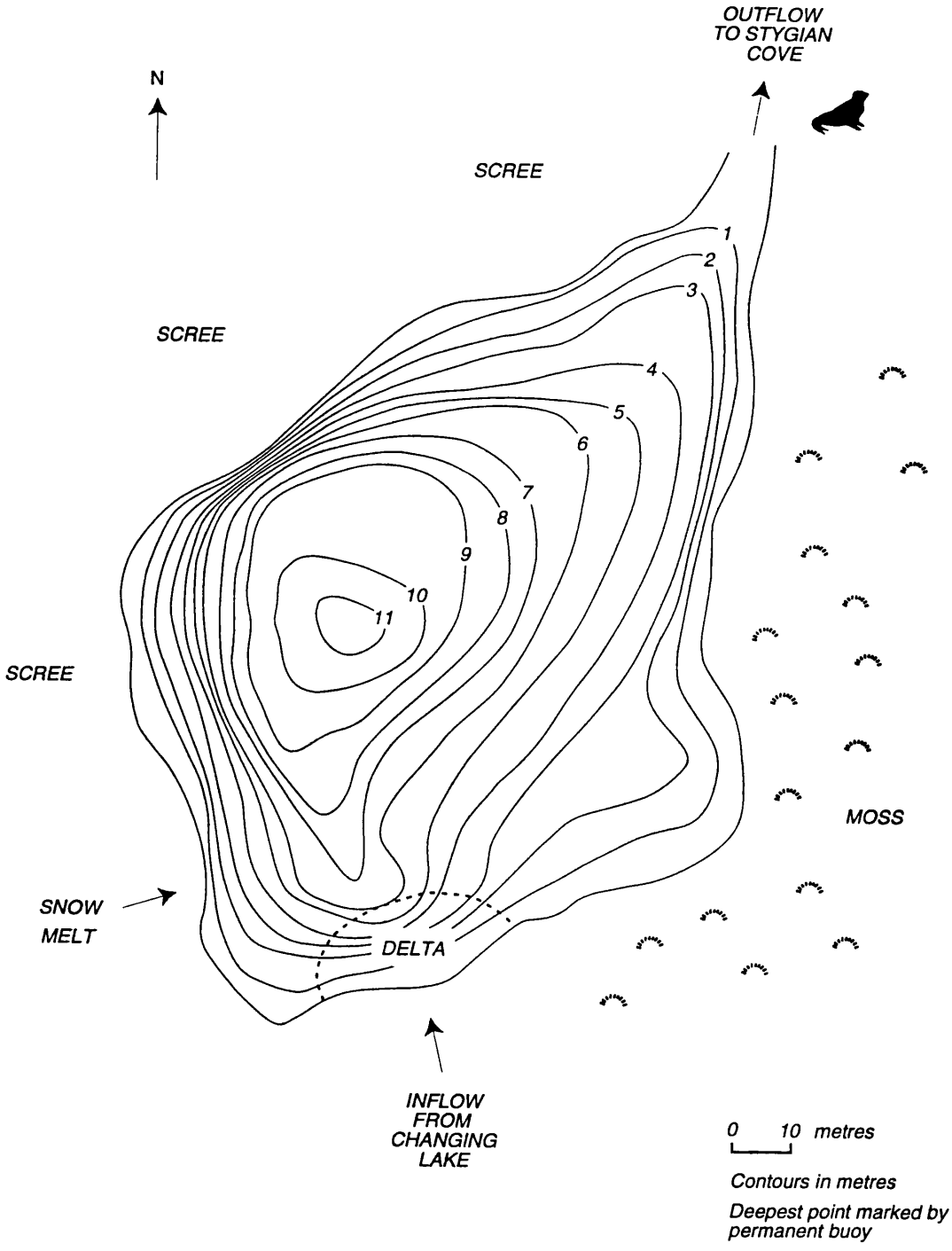

shallow shelf along the south-east shore is composed of coarse, poorly stratified sediment with little organic debris. With increasing water depth, sediments become more cohesive with greater amounts of organic detritus (Oppenheim & Ellis-Evans, 1989).

A long sediment-sequence from this lake has been analyzed for its diatom flora (Jones, 1993) and mineral magnetic characteristics (Wilson, 1993) with supporting ^{14}C (Jones, 1993) and ^{210}Pb radiometric dates (Appleby, Jones & Ellis-Evans, 1995). Although the lake has been influenced by migratory fur seals over time (Hodgson & Johnson, 1997) it is less frequented than others in the lowland coastal strip and actual disturbance has been minimal; shifts in diatom assemblages however, in response to changing water chemistry, have been detected (Jones, 1993). The catchment has experienced a significant loss of its permanent snow and ice cover over the past 20 years exposing new areas of unstable sediments. At higher altitudes the catchment is vegetated by fellfield communities and scree and boulder-fields are colonised by lichens; the lowlands around the lake are principally vegetated by hydrophillic mosses.

2.3.2.2 Heywood Lake

Heywood Lake (Figure 2.6) is one of two morphologically-similar water bodies (cf. Knob Lake, section 2.3.5) on the eastern coastal strip developed in a pre-glacial valley/plain (Three Lakes Valley). Moss fragments in basal sediments were AMS-radiocarbon dated to 5890±60 ^{14}C years BP. This is the largest of the Signy lakes. Linear in form, it has two major basins of differing areas separated by a shallow neck. The principal inflow drains from Knob Lake above. The sub-lacustrine shelf is well-developed except along the southern shoreline and boulders are common in the littoral margins. Ridges, knolls and troughs form a complex pattern in its bathymetry, complicating patterns of soft sediment deposition (Heywood, Dartnall & Priddle, 1979). The eutrophic waters support a dense summer phytoplankton population and this, combined with wind stress, promotes a highly turbid environment. Phytobenthos is poorly developed due to shading effects. Under winter ice, the lake becomes anoxic and the water column clears. A core taken near the deepest point was analyzed for diatoms (V. Jones, *pers.comm.*) and mineral magnetic characteristics (Wilson, 1993). Calculations of sediment accumulation rates (see Appendix D) from ^{210}Pb chronologies (Appleby, Jones & Ellis-Evans, 1995) latterly suggest accelerated deposition, perhaps in response to recent climatic change, and possible inwash horizons occur at 5.75 cm and 9.25 cm. Sandy lenses interspersed with horizons rich in moss fragments might also relate to

Figure 2.6 Heywood Lake

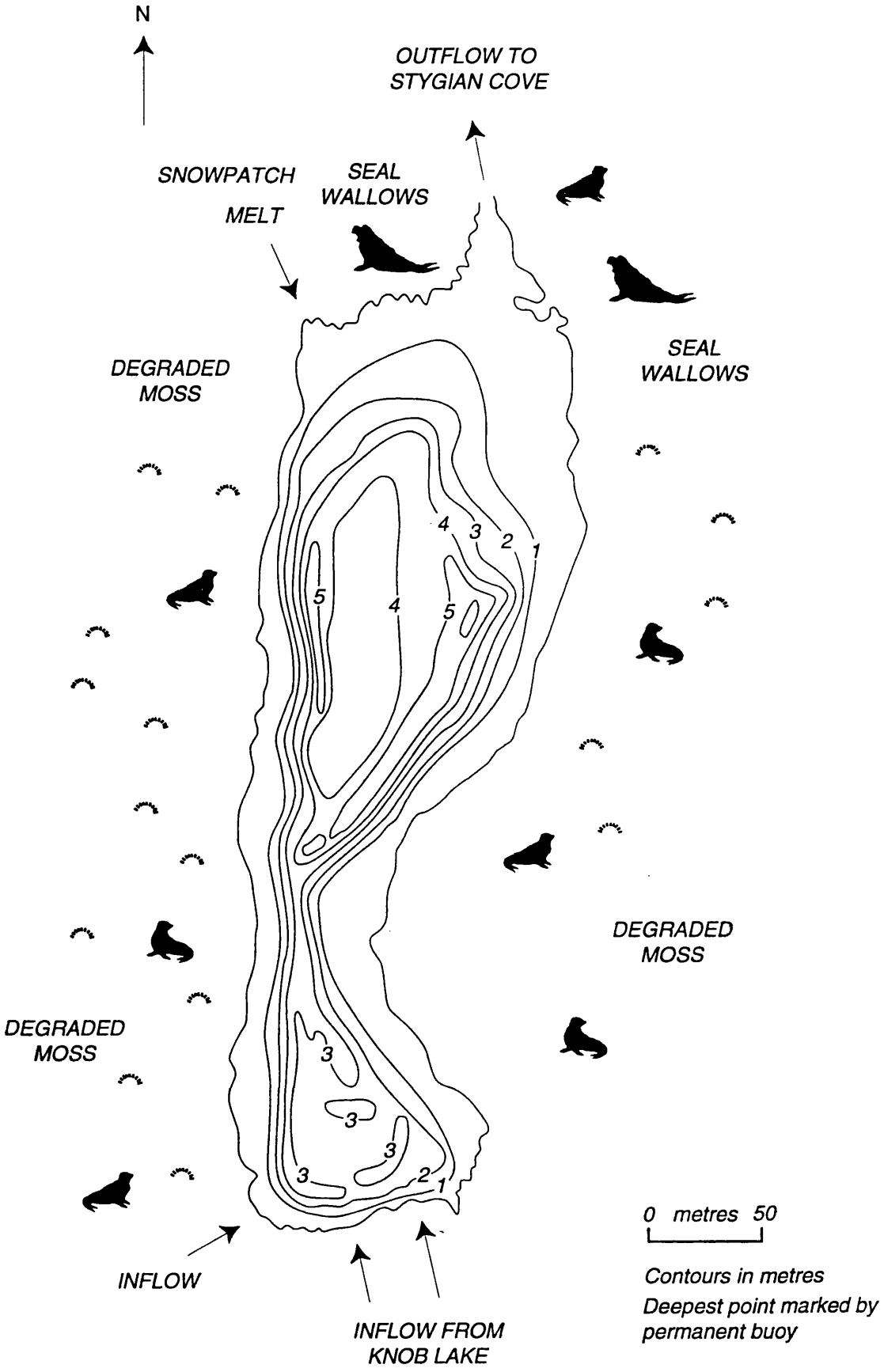

inwash events (Wilson, 1993). Until recently, the catchment was largely vegetated with 'luxuriant stands of moss' (Heywood, 1967). Only 4 metres above sea level it is readily accessible to seals and extensive trampling by both fur-seals and elephant seals has wrought destruction on catchment vegetation and further nutrient-enrichment of its waters (Ellis-Evans, 1990).

2.3.2.3 Changing Lake

Changing Lake (Figure 2.7) is a proglacial, oligotrophic lake, the middle member in the Paternoster Valley sequence. It is small and triangular in outline, surrounded on three sides by a wide sub-lacustrine shelf colonised by algal felts. A steep-sided terminal moraine separates it from Moss Lake above. The deepest point lies in the centre of the basin. The trough is covered with a layer of well-consolidated, yellow-grey coloured sediment and low bank features cut across the basin (Heywood *et al.*, 1979). The lake is part ice-dammed by a glacial advance which occurred as late as 1948 (Light, 1976) and a raised beach 10-12 metres above present lake level and a relict streamcourse visible in topography to the east show the pathway for outflow in the past over the ridge into Three Lakes Valley. Recession of the eastern edge of the Spindrift Col ice-field in the late 1970s has reduced the western shoreline to a less significant bank of permanent snow and ice and released the outflow stream from its enclosed 'ice tunnel' since the mid-1980s. The two inflow streams enter at the west and south margins; a small delta is forming at the principal inflow from Moss Lake which also collects melt from the retreating snowfield of Spindrift Col. Subterranean drainage from Moss Lake enters the lake via the terminal moraine at depths of 5-6 metres. Dominant diatom taxa represent a mixture of species found in both oligotrophic and mesotrophic lakes (Oppenheim, 1990), reflecting the transitional evolutionary status of this lake-catchment system. Wind exposure is relatively high, encouraging resuspension and decreasing light transmission. The catchment is composed almost entirely of scree and permanent ice and snow with lichen vegetation. Resident lake fauna include *Alona*, *Eucypris* (Ostracoda) and enchytraeid (Annelida) and in summer the lake is frequented by a large number of bachelor skuas (*Catharacta lonnbergi*). It is too remote for seal access.

2.3.2.4 Moss Lake

Moss Lake (Figure 2.8) is the first in the Paternoster Valley sequence and occupies a cirque basin at the head of the valley underneath Jane Peak (204 metres). It is topographically-sheltered from most winds. The lake is tear-shaped and is complicated

Figure 2.7 Changing Lake

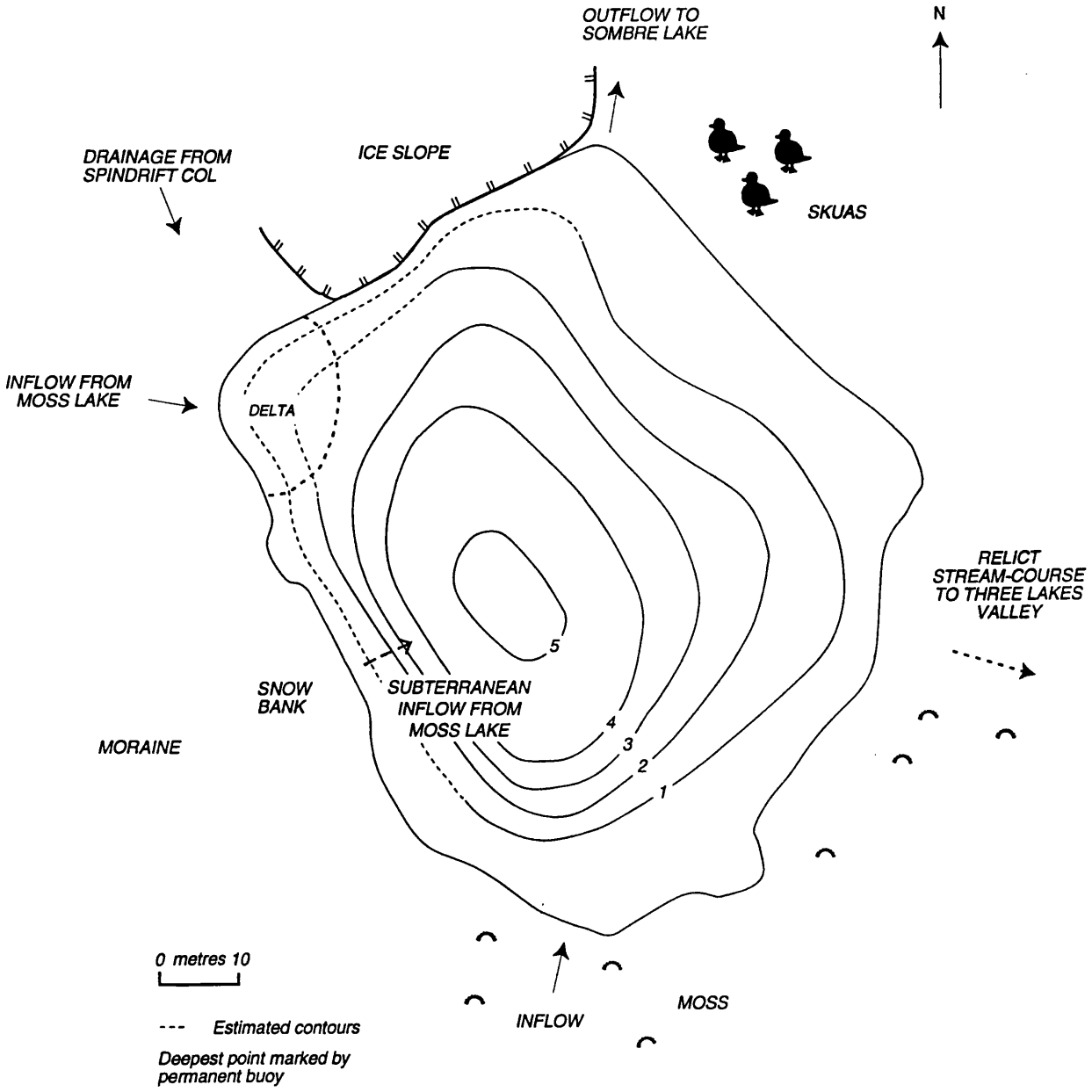

Figure 6.8 Moss Lake

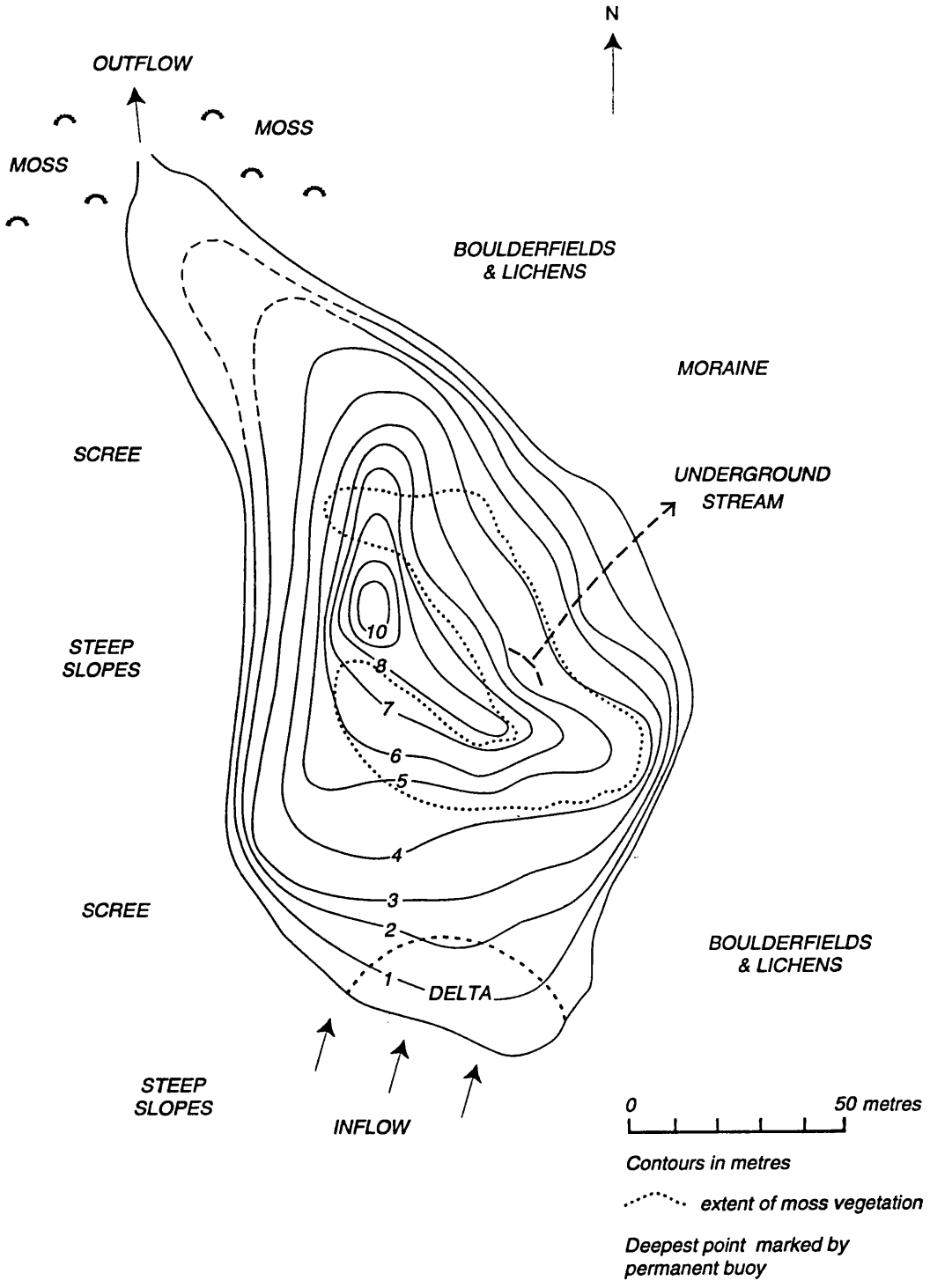

by an unusual drainage system (Light, 1976) as lake waters are lost in late winter by subterranean drainage through the damming moraine, causing the water level to drop by as much as three metres. This loss represents about 75% of its total volume (Light, 1976). Scour by winter ice-cover therefore affects a large zone inhibiting perennial vegetation growth above the 5 metre isobath. The deepest point is central and the slopes are steep, especially on the western margin which follows the topography of the cirque back-wall. The littoral shelf is most developed near the outflow. Deep-water sediments are fine glacial silts including moss fragments (Light & Heywood, 1973); littoral sediments are more coarse especially near the inflow, which is developing a small delta. The lake is ultra-oligotrophic and supports a rich freshwater moss community with roughly 40% coverage below the 5 metre isobath (Light & Heywood, 1973). Lake fauna include *Alona*, the ostracods *Cypridopsis frigogena* and *Eucypris sp.* and the enchytraeid. Sessile rotifers are abundant on the moss. A long sediment-sequence has been dated radiometrically. Aquatic moss remains in basal (94-98 cm) sediments were dated by AMS radiocarbon dating to 2620±55 *14*C yrs BP (V. Jones, *pers.comm.*). The ^{210}Pb chronology was disrupted by a dense sediment layer at 6 cm (*ca.* 1958 AD) posing dating difficulties below this level (Appleby, Jones & Ellis-Evans, 1995) and a second dated sequence was similarly truncated (P. Appleby, *pers.comm.*). This inwash event is probably associated with a catastrophic breaching of an ice-dammed lake on Jane Peak Ridge. The catchment is characterized by steep topography, permanent snowfields, moss and lichen-covered boulder-fields and scree. The lake is remote from the coast and few birds nest in the catchment. Priddle & Heywood (1980) proposed that this lake represents the final stage of a maritime Antarctic lake not in receipt of nutrient enrichment.

2.3.2.5 Knob Lake

Knob Lake (Figure 2.9) is the second lake occupying Three Lakes Valley and shares many similarities with Heywood Lake. It has been modified by heavy silting (Heywood, 1967) and the sublacustrine shelf is extensive and rocky. The trough has three small, steep-sided basins aligned along the eastern side of the lake. The bottom of the trough is covered with a well-consolidated gyttya. The small island at the southern end is a residual knob of resistant rock, inspiring the lake's name. Multiple inflow streams feed the lake from the south and north-west. A single outflow drains towards Heywood Lake. Summer waters are turbid due to high suspended sediment loads and phytoplankton productivity, supported by enhanced nutrient levels. Wind exposure is also high

Figure 2.9 Knob Lake

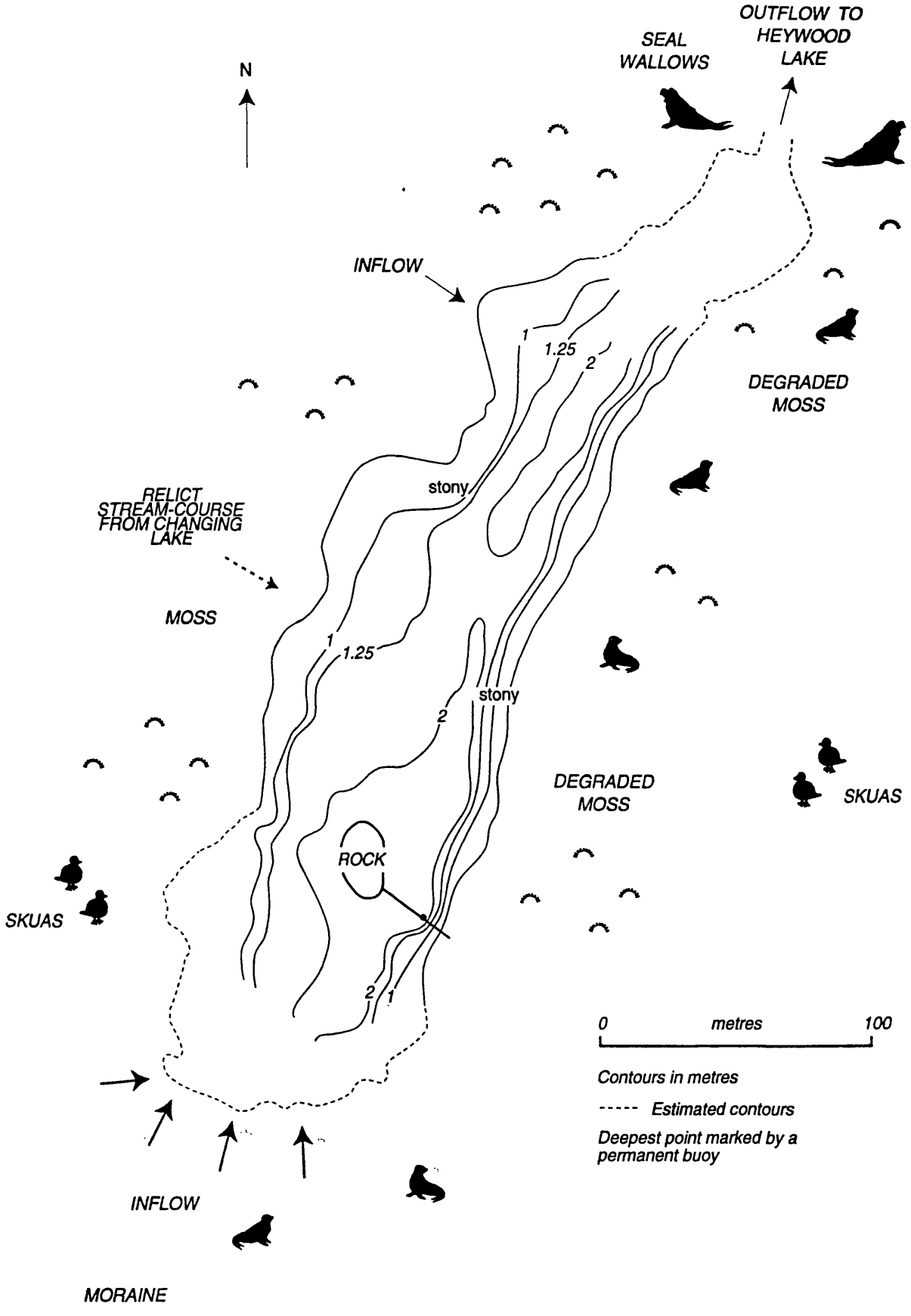

encouraging resuspension. The shallow littoral zone supports dense growths of filamentous algae and heavy diatom colonisation where chlorophytes are less prolific. Lake fauna include both *Branchinecta* and *Alona*. The catchment is moss-covered but low-lying areas have suffered from seal trampling. This damage is greatest on either side of the outflow where elephant seals have created haul-points and wallows. Fur seals also bathe in the lake and are common around the eastern shore. Several pairs of skuas nest within the catchment boundaries. Catchment topography supports the hypothesis for a significant inflow of water in the past from ice-dammed Changing Lake, cutting-through the ridge dividing Three Lakes Valley from Paternoster Valley (section 2.3.2.3). This relict streamcourse supports well-established lichen and moss vegetation and is remote from seal disturbance.

2.3.2.6 Pumphouse Lake

Pumphouse Lake (Figure 2.10) is a sub-circular shaped ice-scour basin (Heywood, Dartnall & Priddle, 1979). It is encircled by a rocky sublacustrine shelf of 1-2 metres depth. A shallow dam built by Norwegian whalers in the 1910s-1920s extends the shelf area near the outflow such that the artificial dam merges with the natural shore. This forms an ideal habitat for heavy growth of *Phormidium* algae in summer. The bathymetry is complicated by boulders, and a central rock mound surrounded by a horseshoe-shaped trough acts as a trap for fine sediments. The western shelf is boulder-strewn (Heywood, 1967). Marble debris litters the eastern shelf, probably part of an underlying marble outcrop which continues aerially a few metres distant at the 'Marble Knolls', a collection of distinctive marble hillocks. The lake is oligotrophic and the trough is colonised in summer by *Tribonema*, *Tolypothrix* and other chlorophytes. Light & Heywood (1973) also noted the presence of freshwater moss. *Alona*, the enchytraeid and the gastrotrich are present. Several small streams are influent around the west and north shores, draining the sheer ice-slope beneath Jane Peak (204 metres) and percolating through an area of waterlogged moss and boulders of mixed lithologies. The moss cover was previously 'luxuriant' (Heywood, 1967) and extended to the eastern shoreline however, these have been subject to heavy disturbance by fur seals and are severely degraded. The remains of the whaler's pumphouse is found on the east shore of the lake. The effect of past water abstraction on the lake is unknown.

2.3.2.7 Light Lake

Light Lake (Figure 2.11) is sub-circular in outline, of either ice-scour or kettle-hole

Figure 2.10 Pumphouse Lake

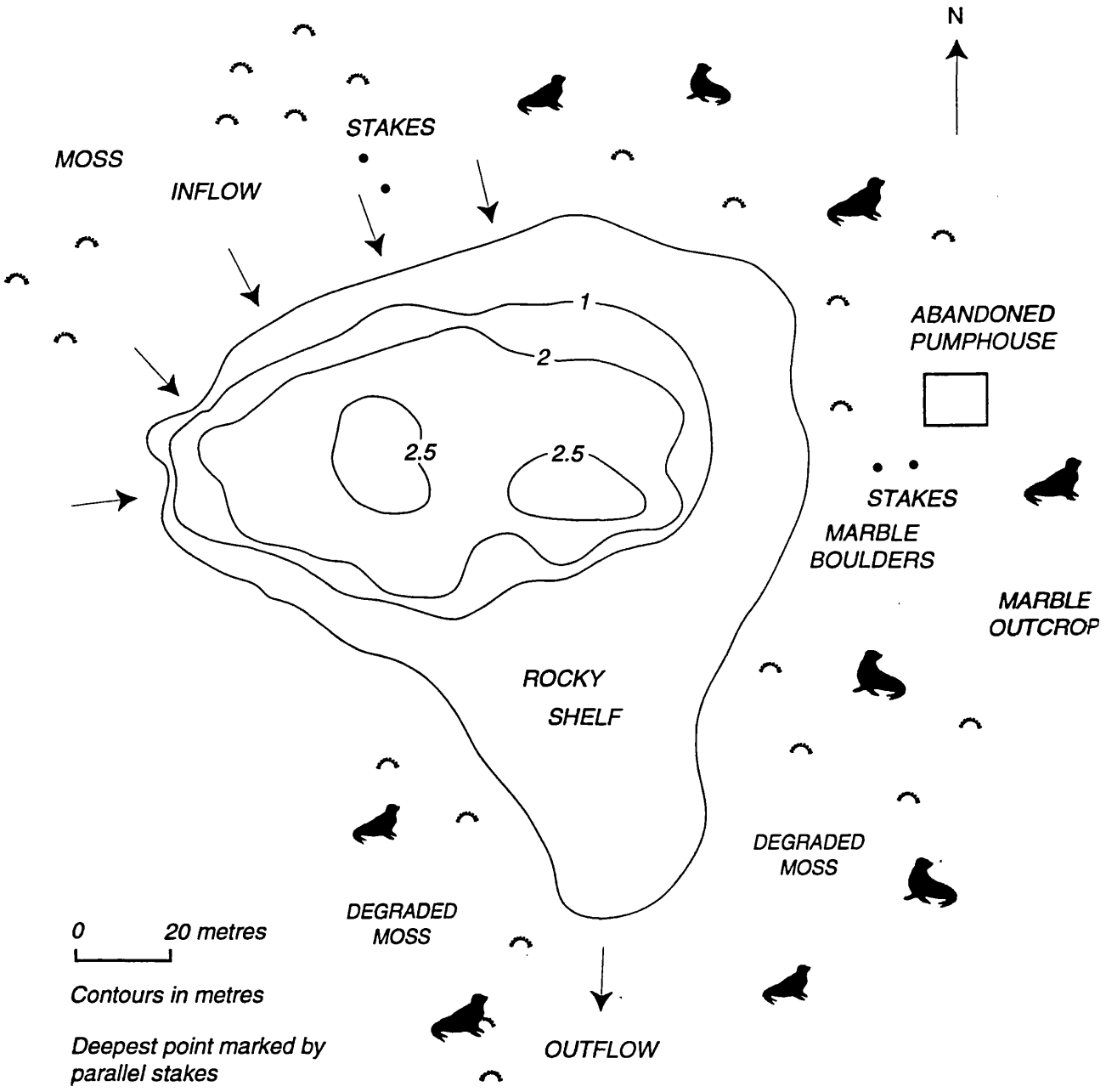

Figure 2.11 Light Lake

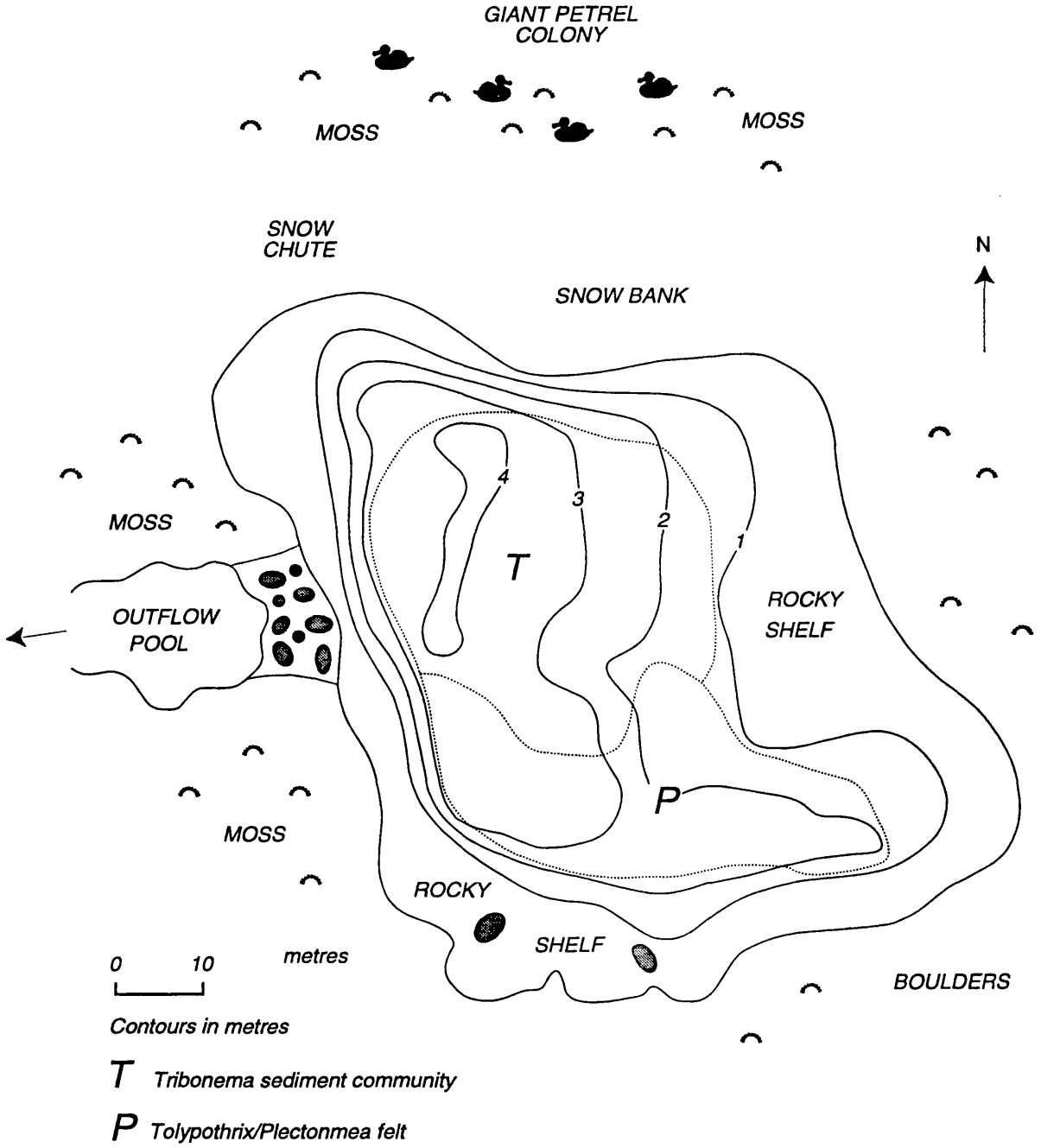

origin (Heywood, Dartnall & Priddle, 1979). Retreat of a permanent snow bank on the eastern and northern margins has enlarged the area of the sub-lacustrine shelf and increased the lake depth (Heywood, 1967). The central basin is roughly 5 metres deep and lies close to the outflow. Where the shelf is absent, slopes are steep with large boulders, including marble lithologies. Sediment grades from coarse silts and fine sands in the littoral zone to fine silts in the basin. Lake waters are clear but sometimes become clouded by a short-lived summer phytoplankton bloom. The lake is also highly exposed to prevailing westerly winds. Habitat zonation is distinctive in the trough: the southern half of the lake supports a *Tolypothrix-Plectonema* community and the northern part is dominated by summer *Tribonema* with associated *Fragilaria*, grazed by *Alona* and abundant rotifers. The shelf supports an epilithic felt community. Oddly, *Branchinecta* are absent from the main lake but are found in the shallow outflow pool instead. Meltwater inputs are seemingly small in volume compared to the other lakes. There are no glacial meltwater streams and all inputs are from melting snowbanks. Melt from the north drains through rich moss stands of Thulla Ridge which are loaded with nutrients from a long-established colony of giant petrels (*Macronectes giganteus*). Small volumes of meltwater input and the presence of the petrels are probably responsible for the slightly enhanced nutrient status of this lake. Lichens dominate the vegetation in the remainder of the catchment which is characterized by frost-shattered boulder-fields and scree slopes.

2.3.2.8 Spirogyra Lake

This small, shallow lake (Figure 2.12) occupies an irregularity in the glacial drift and attains a maximum depth of 2.3 metres and a mean depth of only 0.85 metres (Heywood, Dartnall & Priddle, 1979). A shallow rocky shelf zone follows most of the shoreline which is frozen in winter. In summer it supports *Phormidium* algae (Hawes, 1988). The flat, central trough is sufficiently deep to escape freezing and is covered with fine silty sediment but it does not support perennial vegetation owing to winter anoxia, which is most pronounced in this lake due to its small size and low volume (Hawes, 1988). Dense growths of *Spirogyra* form throughout the lake in summer (Hawes, 1988). Several streams enter the lake from the north and one from the east, fed by permanent snowfields. A well-defined alluvial fan has been deposited at the northern end and clumps of *Zygnema* algae are washed-in from the fan. The southern end is more rocky and the outflow channel is well-defined, merging with the outflow from Tranquil Lake and forming a large shallow pool in summer. Both *Branchinecta* and *Alona* are present

Figure 2.12 Spirogyra Lake

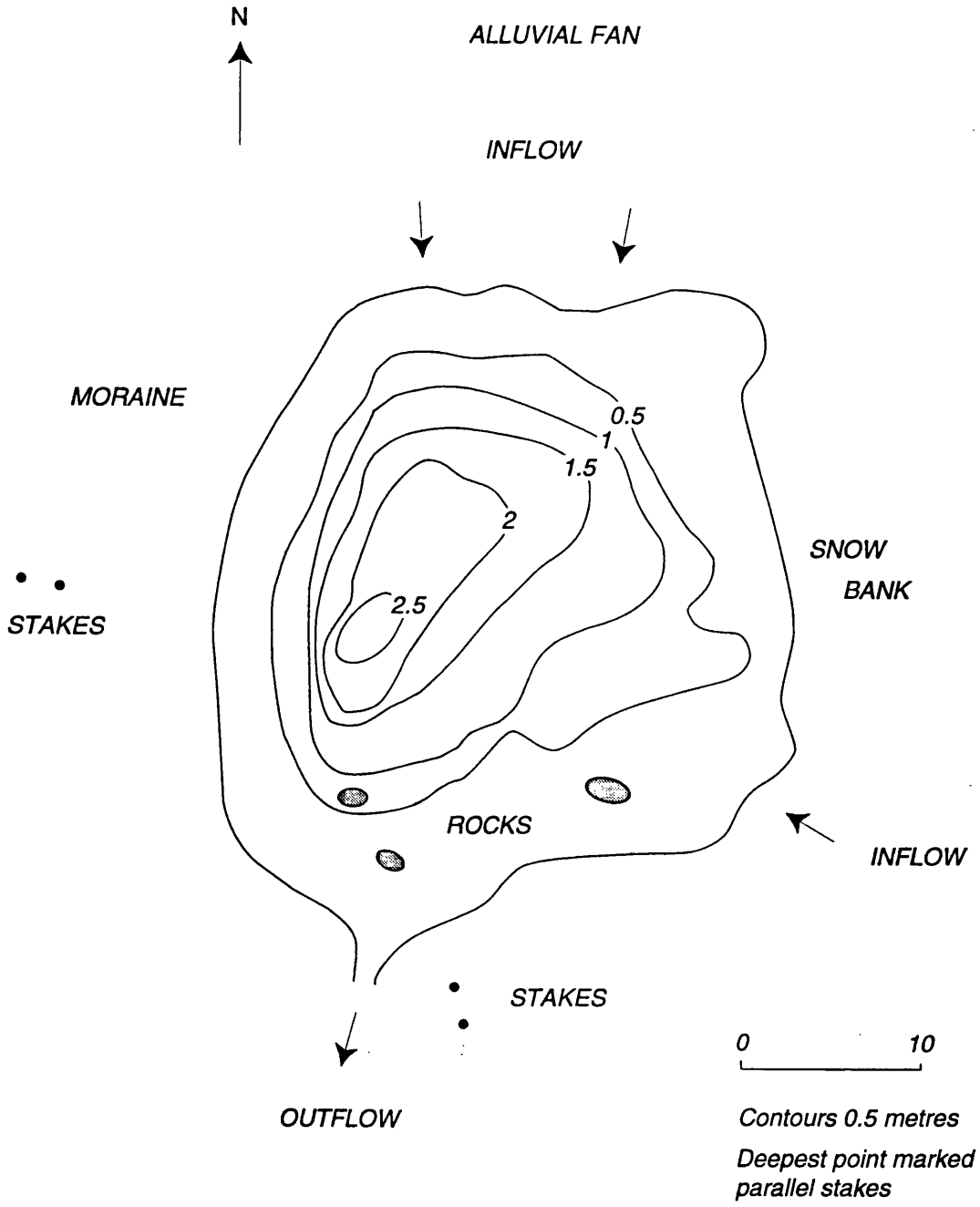

in Spirogyra Lake. The catchment includes permanent snowfields and extensive areas of scree and unconsolidated glacial till. Vegetation cover is poorly developed with isolated clumps of moss and lichen. The only sources of biotic enrichment are a few giant petrels and terns (*Sterna vittata*) nesting in the vicinity. Fur seals have not yet influenced the lake or its catchment and an exclusion policy should prevent any disturbance.

2.3.2.9 Tranquil Lake

Tranquil Lake (Figure 2.13) is a large, oligotrophic, glacier-fed lake on the west coast of the Island. It occupies a cirque basin and has three sub-basins. The two largest sub-basins - located north and south - are directly in alignment with the two principal meltwater inflows and are probably the focus for inwashed sediment. A third sub-basin is found close to the outflow, linked by a 3 metre deep linear trough to the southern basin. A central bank of consolidated sediment separates the north and south sub-basins. The sub-lacustrine shelf is best-developed on the northern and southern margins and there are several large, emergent boulders. Sediments in deep water are firm and silty (Heywood, Dartnall & Priddle, 1979). A short sediment sequence from the northern sub-basin has been dated radiometrically (Appleby, Jones & Ellis-Evans, 1995) and the rate of sedimentation is much slower than either Sombre or Heywood Lakes (Appendix C). Suspended sediment concentrations in summer reduce light transmission but *Tribonema* and *Fragilaria* survive in deeper waters. At shallower depths *Tolypothrix* and the aquatic mosses *Calliergon* and *Pohlia* are recorded, heavily colonised by epiphytic algae and rotifers. Other lake fauna include *Alona*, a gastrotrich and nematodes. The two meltwater streams drain different zones of the catchment: the northern inflow drains the glaciated backslope and the southern inflow drains an area of rock and scree. The catchment is sparsely vegetated. Fur seals have had little effect to date and an exclusion policy should ensure its pristine status in the future.

2.3.2.10 Amos Lake

Amos Lake (Figure 2.14) occupies an irregular ice-scour basin (Heywood, Dartnall & Priddle, 1979). The sublacustrine shelf is extensive and the trough has several parallel ridges and furrows. There is a steep slope at the base of the cliff on the east side. Silty sediment is fine but firm, with an organic rich layer overlying a mineral mud (Heywood, 1967). The lake water is highly turbid in the summer and high levels of phytoplankton grow in response to high nutrient levels. Suspended materials and wind turbulence

Figure 2.13 Tranquil Lake

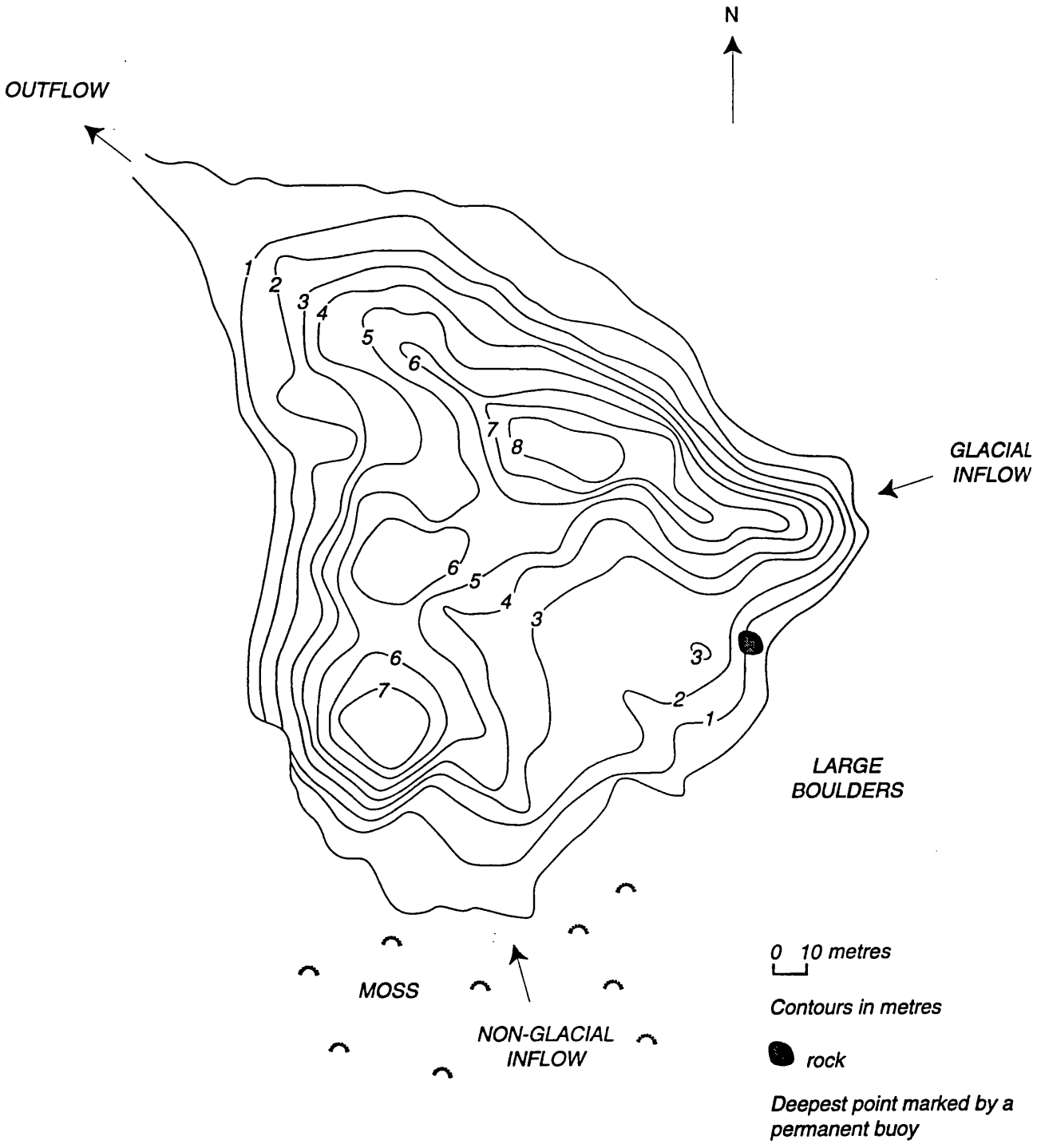

Figure 2.14 Amos Lake

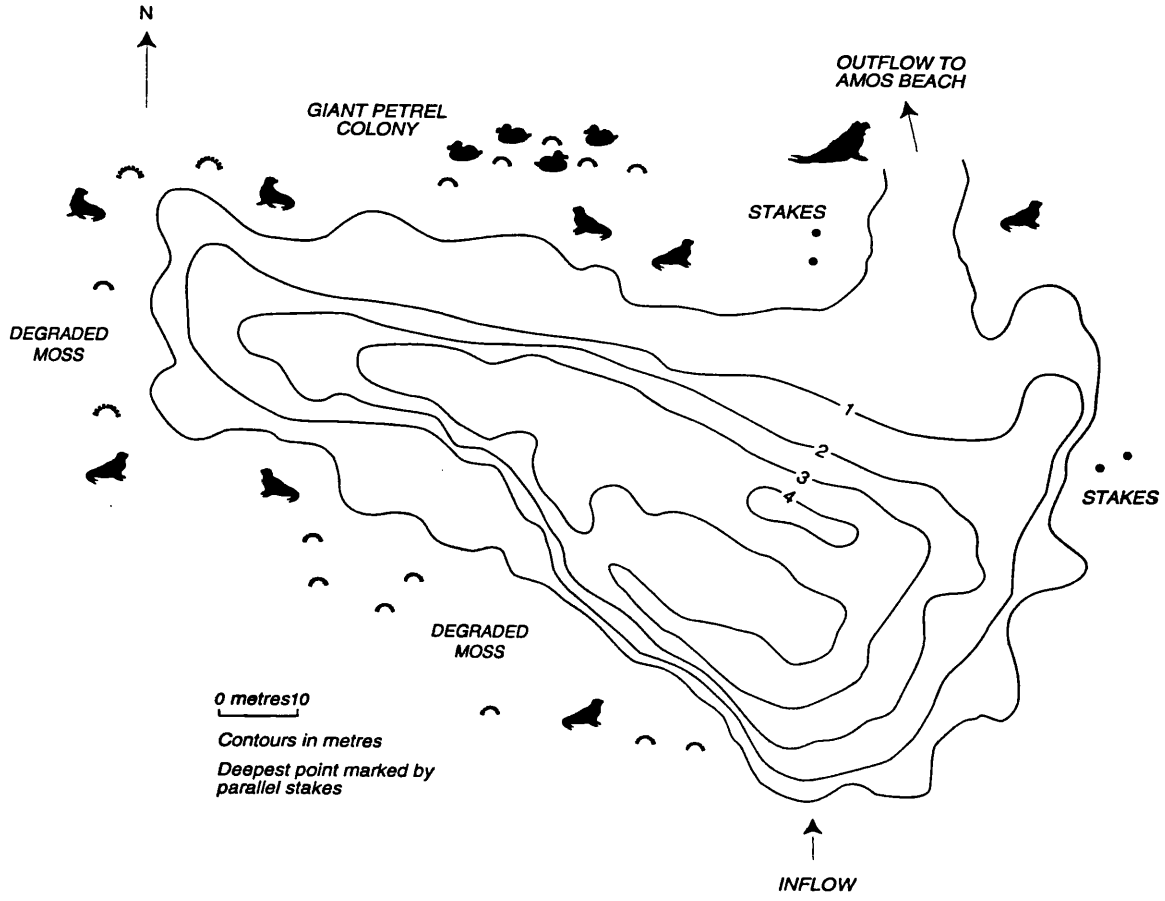

Figure 2.15 Tioga Lake

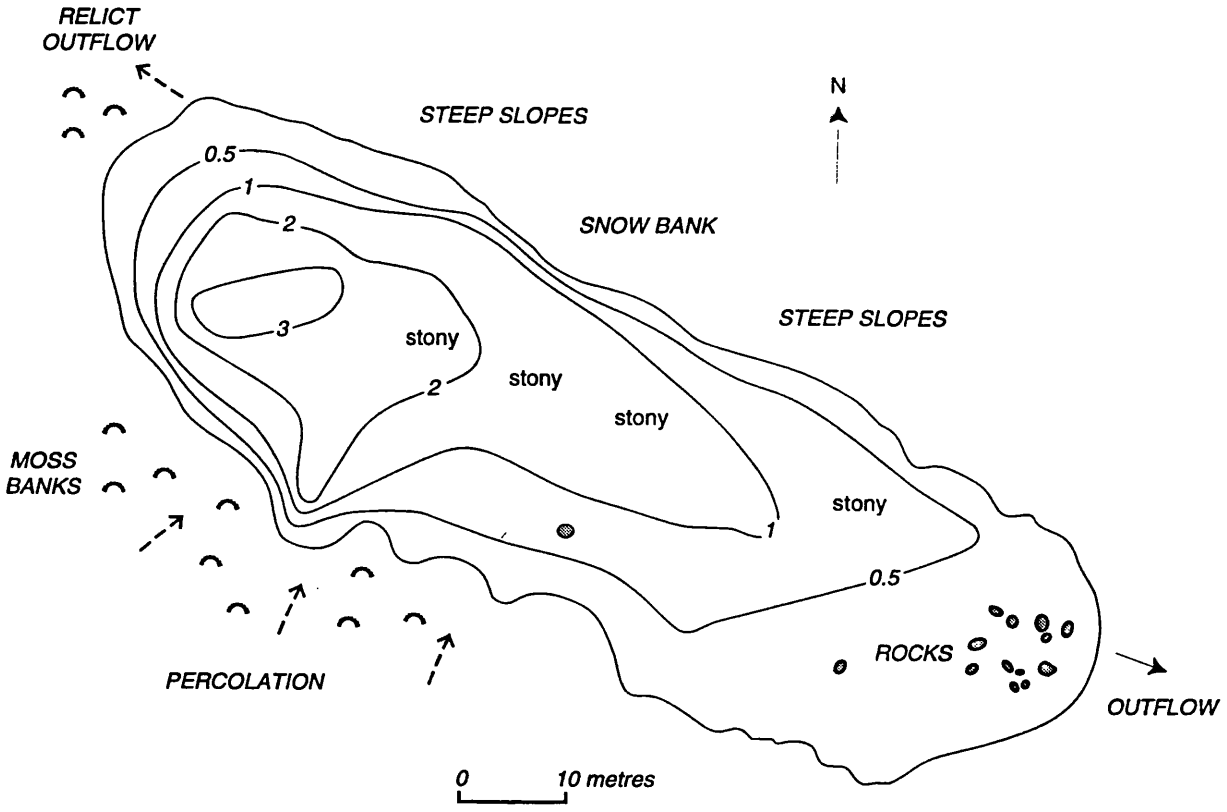

promote further turbidity, precluding the development of phytobenthos. Lake closure in April/May causes organics to sediment from the water column (Ellis-Evans & Lemon, 1989) and decomposition under anoxic conditions is absolute. The lake supports *Branchinecta*, two species of copepod and one species of rotifer. One principal inflow drains a shallow pool (Amos Pool) to the south-east of the lake. Elephant seals and large numbers of fur seals are found in all accessible areas in summer and seal haul-points restrict the growth of shelf algae except in the south-west margin. A decline in elephant seal numbers in the catchment may be in response to increasing numbers of fur seals and competition for space (Heywood, 1967). Giant petrels nest on a ridge to the north of the lake. Seal excreta, moulted fur and glacial debris and scree have combined to form a rudimentary fine, stable soil in this catchment. Most water entering the lake drains over this ground which supports little vegetation, mostly the alga *Prasiola crispa.*

2.3.2.11 Tioga Lake

Tioga Lake (Figure 2.15) has an unusual form, dammed by moraine at both ends. The deep spot is centred in a single basin to the south where the slopes plunge steeply to depths of 2-3 metres. The sub-lacustrine shelf is only developed near the outflow. Margins are rocky and boulders are common at depth. The floor is covered by a thin layer of sediment with emergent boulders. The lake water is oligotrophic and fairly clear however, topographic shading occurs in this sheltered valley all year. A perennial epilithic felt of blue-green algae exists in the lake and filamentous green algae are found in bottom waters in late summer. *Branchinecta* are abundant on the bottom and the lake has a distinctive rotifer fauna (Heywood, Dartnall & Priddle, 1979). Lake inflow is unusual and ill-defined, predominantly by seepage from areas of waterlogged moss to the east and south and from a snowbank to the north and west. This snowbank has receded in recent years and is no longer in contact with the lake water by mid-summer. The local topography suggests that the outflow was formerly from the opposite end of the basin and that the lake was ice-dammed to the north by a lobe of ice in the shallow valley. The ice-front has since retreated into Erratics Valley and lake water levels are too low to re-activate this relict outflow.

2.3.2.12 Emerald Lake

Emerald Lake (Figure 2.16) is found in the third major catchment system in the south-west sector of the Island (Figure 2.2). This proglacial, cirque lake receives large volumes of suspended sediment-inwash in the summer from two principal inflows, one from the

Figure 2.16 Emerald Lake

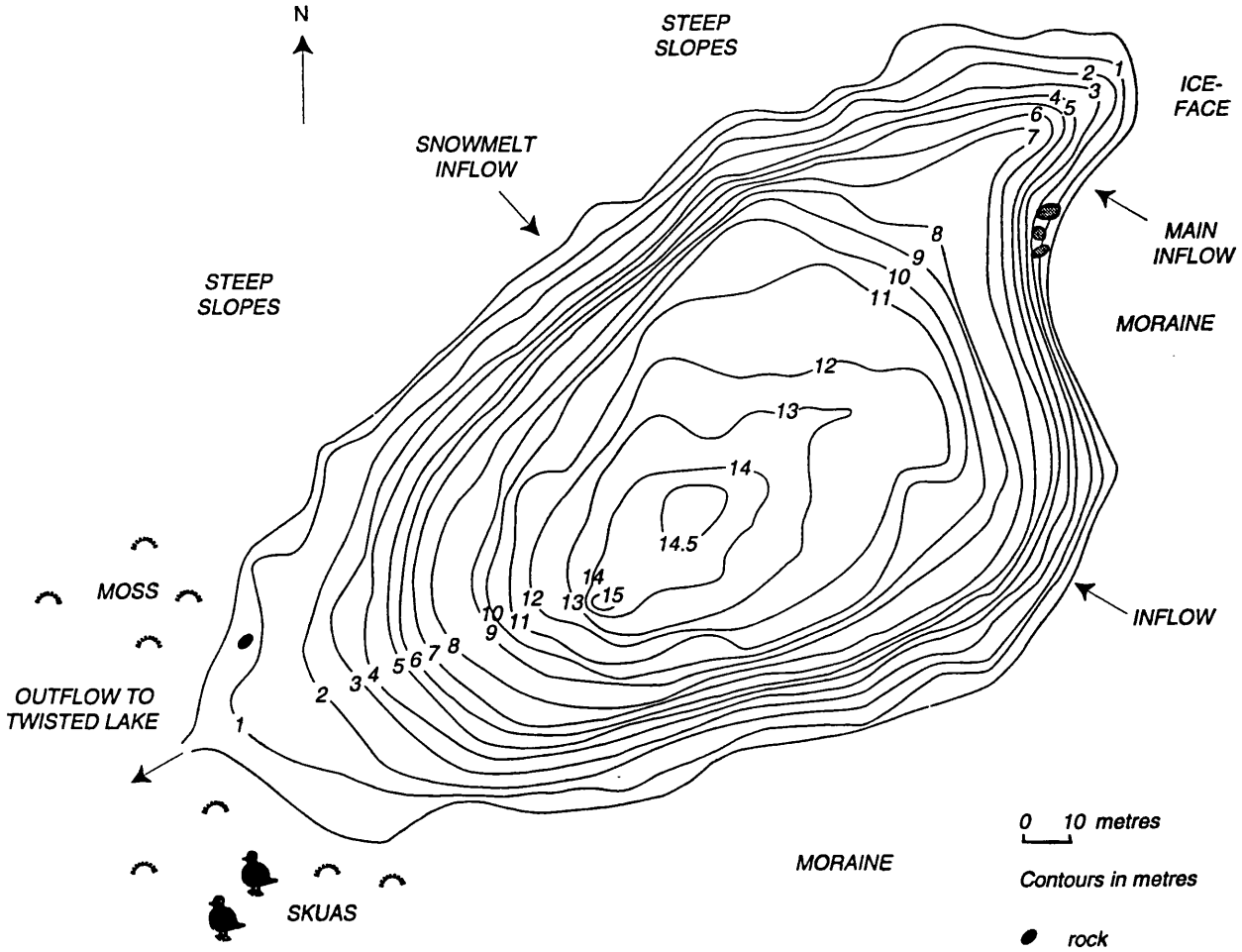

Figure 2.17 Lake 13

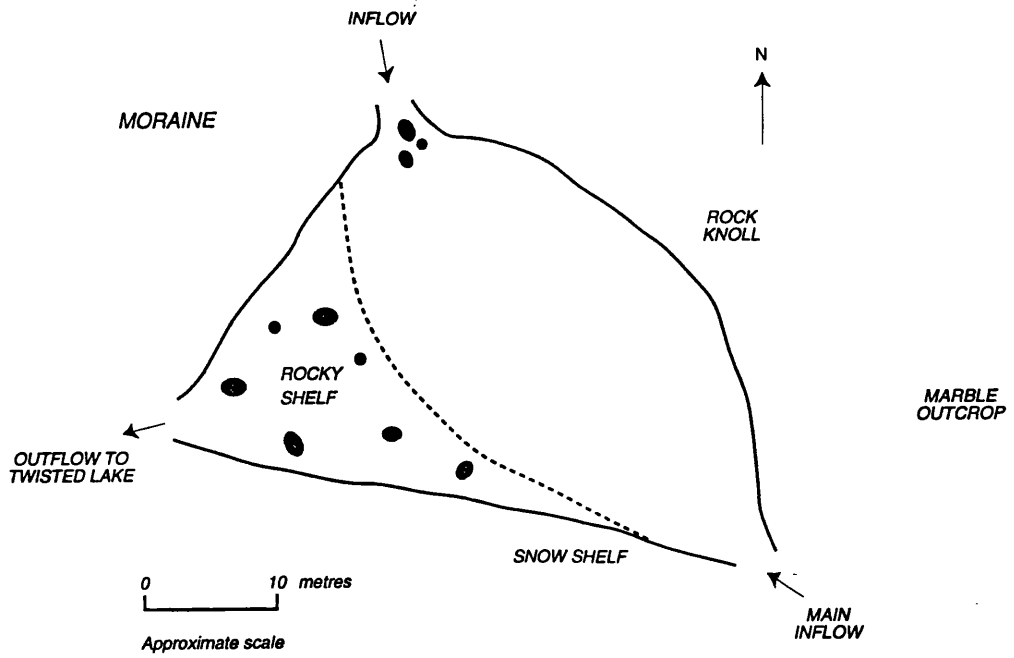

north-east via the terminal moraine and the second from the south-east, having made a more circuitous route around the moraine. The shelf is well-developed near the outflow and delta formation is leading to basin shallowing near the inflow. The basin otherwise is steep-sided with a single, extensive trough covered with a thick layer of sediment (Heywood, Dartnall & Priddle, 1979). This is the deepest of the Signy Lakes (maximum depth 15 metres). Shading effects caused by catchment topography create a strong light climate gradient between the summer and winter. The high suspended sediment load additionally restricts light transmission, affecting lake biotic activity. Habitat zones for algae are depth related: *Mougeotia* is abundant in shallow water in summer, isolated stands of the freshwater moss *Calliergon sarmentosum* occur between 3 and 7 metres, and a patchy cover of *Tolypothrix-Plectonema* extends to 9-10 metres depth. *Alona*, nematodes, a gastrotrich and two species of sessile rotifer have been recorded. The lake environs are of moraine and scree, colonised by mostly by lichens with a few mosses in wetter sites. A few birds nest in this area, notably a pair of skuas on the outflow moraine. The outflow stream drains into Twisted Lake.

2.3.2.13 Lake 13

Lake 13 (Figure 2.17) is an ephemeral pond occupying an irregularity in the glacial drift near Emerald Lake. It is very small and shallow, with a mean depth of less than 1 metre and in winter it freezes to the bottom. The basin is covered with fine glacial silts with a few emergent rocks. The lake was previously more extensive but heavy silting has reduced its size considerably. The lake is fed from a stream flowing from the ice-field above Emerald Lake and vagaries in meltwater discharge mean that the lake sometimes drains completely. The lake is too shallow to define a distinction between shelf and basin communities. In summer it fills with filamentous chlorophytes especially *Mougeotia*. Two copepods and one rotifer are recorded here. A marble outcrop occurs nearby and several marble boulders are found amongst the scree around the lake. The outflow drains towards the eastern shore of Twisted Lake across an area of saturated ground colonised by *Phormidium* felt and mosses.

2.3.2.14 Twisted Lake

Twisted Lake (Figure 2.18) occupies a glacially-deepened hollow in glacial drift. Its bathymetry is irregular with several sub-basins, the deepest of which reaches depths of 4-5 metres. The sublacustrine shelf dominates the bathymetry and is very extensive towards the outflow. The sides slope steeply on the north, west and south-west

Figure 2.18 Twisted Lake

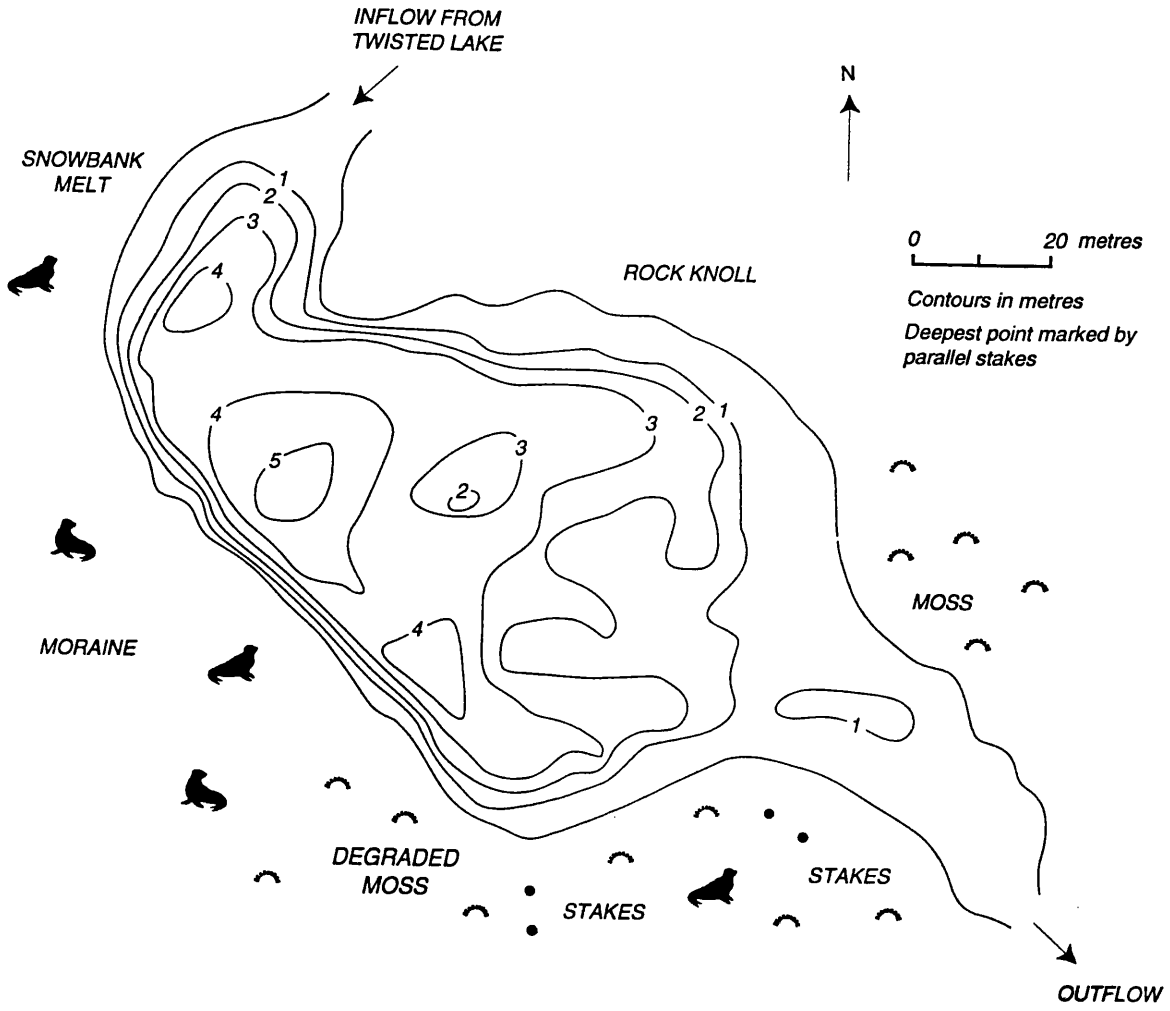

Figure 2.19 Bothy Lake

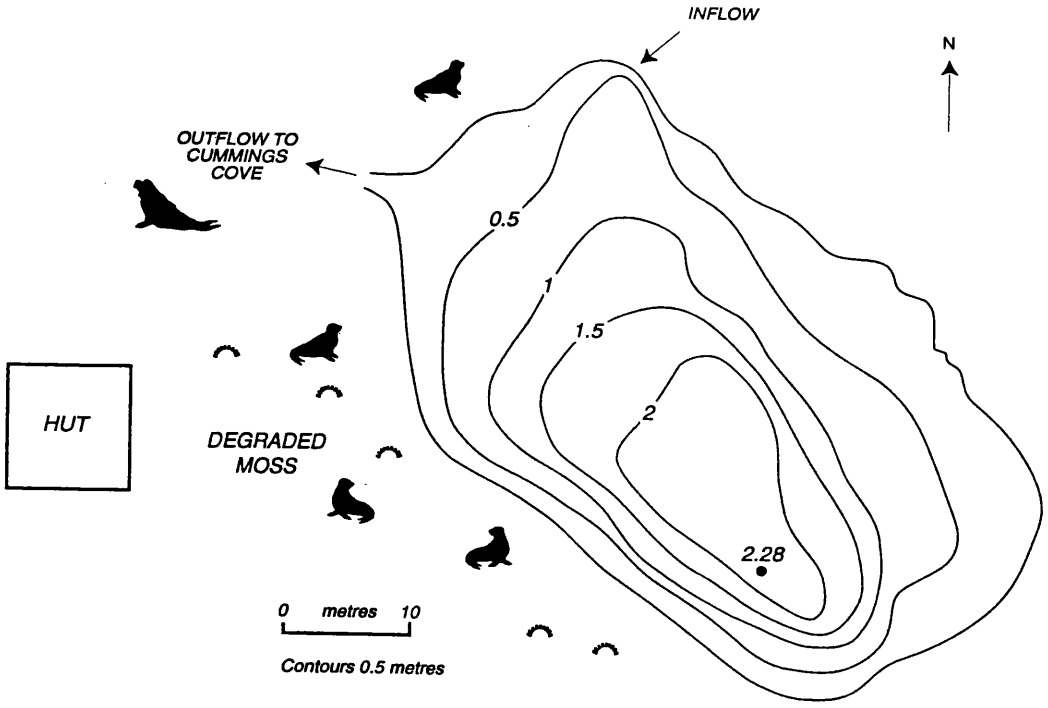

shorelines where the lake is bounded by a terminal moraine. This is a paternoster type lake (Hutchinson, 1957) and the main inflow is from Emerald Lake above. A second stream from Lake 13 enters the lake on the east shore near the outflow. A snowbank is found along the north-west margin of the lake which persists through the summer. Suspended sediment loads are relatively high and exposure to wind turbulence encourages resuspension. Benthic flora include *Tribonema* and Light and Heywood (1973) record the freshwater mosses *Amblystegium sp.*, *Pohlia nutans*, and *Calliergon sarmentosum*. *Alona*, *Cypridopsis* and the gastrotrich are present in the lake. The area to the north and west of the lake is characterized by freely-draining, frost-shattered rocks colonised by lichens; moss vegetation dominates the more waterlogged areas to the south and east. Fur seals bathe in the lake and frequent the shores. Damage to the moss swards has been heavy to the south near the outflow but so far minimal on the eastern side.

2.3.2.15 Bothy Lake

This small lake occupies an irregularity in the moraine close to the coastline. The basin is shallow, simple and lacks an obvious shelf (Figure 2.19). The inflow and outflow are very close to each other and damming may have contributed to this strange arrangement (Heywood, Dartnall & Priddle, 1979). The principal inflow is from Twisted Lake although the lake is in receipt of meltwaters from the entire Cummings Amphitheatre catchment. Its small volume relative to these combined inputs means a very short water retention time. In winter the ice freezes close to the lake bottom, and seepage through the moraine causes the water level to fall and the ice to sag, promoting much ice scour of the margins and basin. Algal growth is therefore restricted to the summer when *Spirogyra* and *Mougeotia* rapidly colonise its nutrient-enriched waters. *Branchinecta* and the copepods are also found here. Elephant and fur seals bathe in the lake and heavily populate the immediate environs during the summer.

2.3.2.16 Gneiss Lake

Gneiss Lake (Figure 2.20) is unique amongst the Signy lakes in that until recently it had a perennial ice-cover and it rarely opened. This closed environment bears similarities to perennially ice-covered lakes on the Antarctic Continent and is atypical of contemporary maritime Antarctic lakes. The lake is remote and at high altitude relative to the others on the Island. It is prone to wind exposure from prevailing westerlies. It has formed in a moraine-dammed valley in an area of different bedrock - the Gneiss Hills. The basin is simple and the deepest point is central to the basin. Soft sediments have been

Figure 2.20 Gneiss Lake

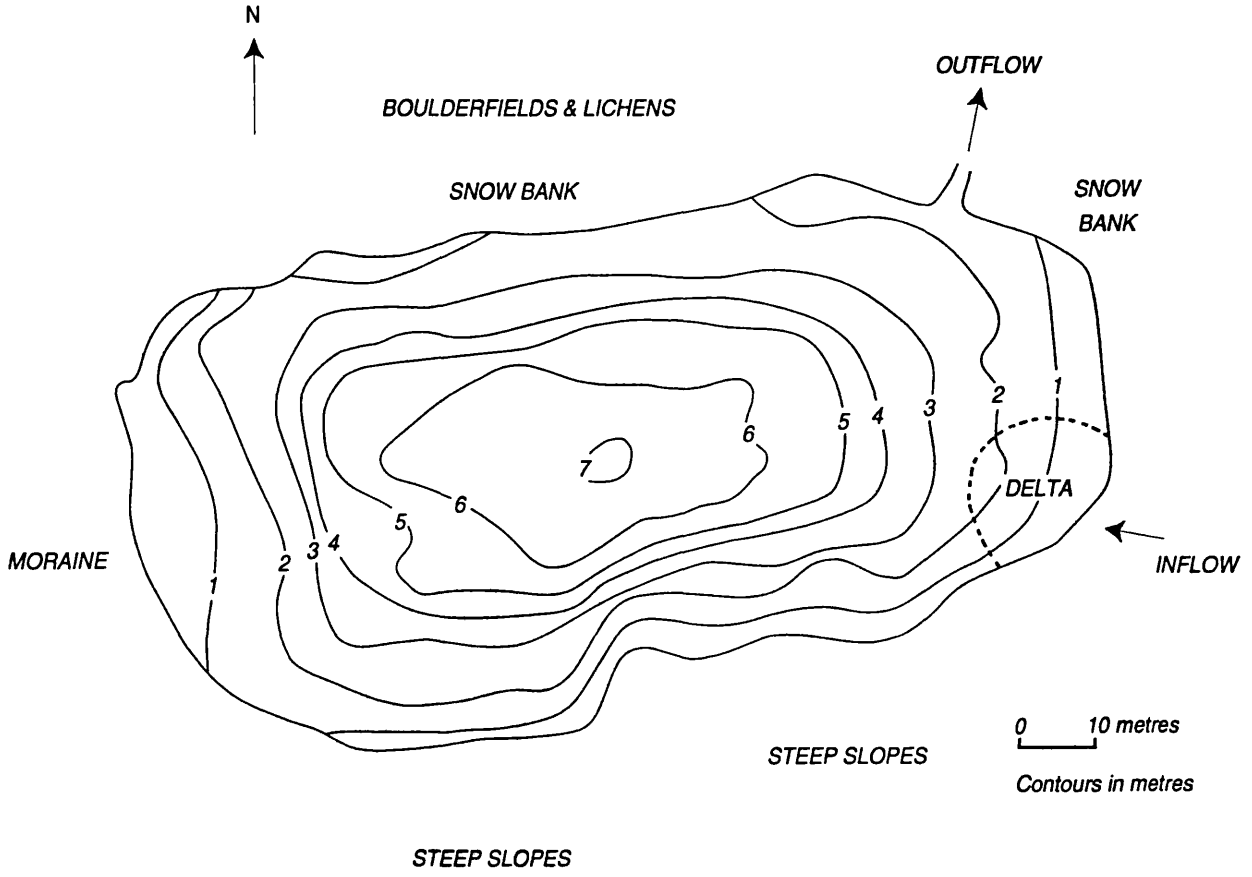

Figure 2.21 Orwell Lake

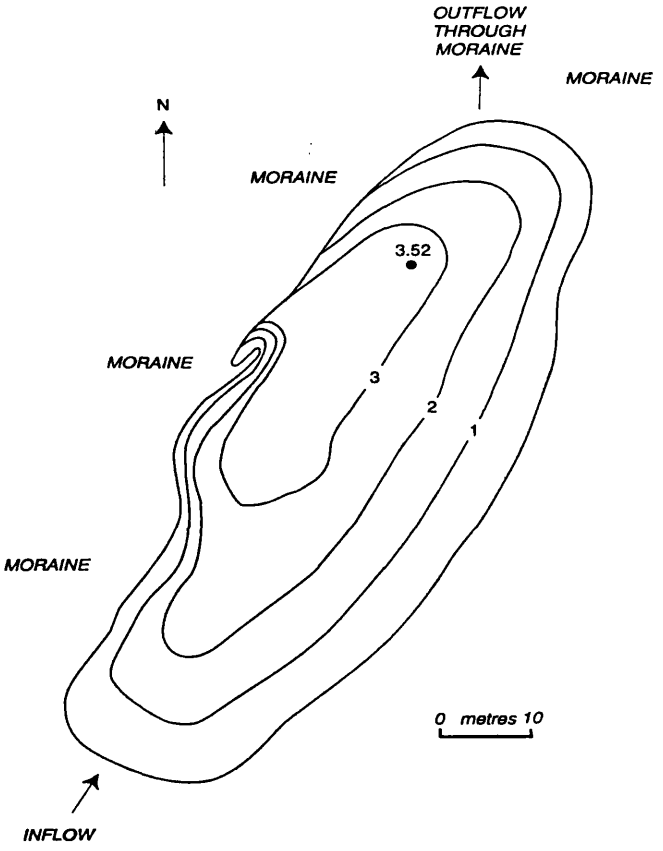

collected from this basin (V. Jones, *pers.comm.*) but the sequence has not been dated with any accuracy. Meltwater inflow is from adjacent snowbanks, especially to the east at the head of a small valley. The inflow and outflow are closely positioned and a delta of coarse sediments is beginning to form near the inflow. Much fine sediment probably by-passes the main basin, leaving the outflow before sedimenting. A significant loss of snow-cover has occurred in the catchment over the last 20 years (J.C. Ellis-Evans, *pers comm.*), causing the mobilisation of recently uncovered sediments to the lake. Subterranean drainage through the moraine which forms the eastern shoreline causes the lake water level to drop in winter and the ice-cover to crack and sag. *Tribonema* and *Fragilaria* have been collected from here, in common with the other lakes. Subtle differences in physico-chemical status and its geographical isolation have been responsible for some unusual species including the centric diatom *Melosira* (Heywood, Dartnall & Priddle, 1979) and a large population of a small form of *Pseudoboeckella poppei* (Heywood, 1970). *Alona* is also present. Catchment vegetation is sparse and dominated by lichens. It is extremely remote from fur seals and few birds nest in the area.

2.3.2.17 Orwell Lake

Orwell Lake (Figure 2.21), formerly 'Moraine Valley Lake', has formed by the damming of a melt stream by the lateral moraine of the Orwell Glacier. A small lake was noted here in 1960 (Harrison, 1960) but it had disappeared by 1962. The present lake formed in the summer of 1972-73 although its presence continues to be unstable. Drainage appears to relate to shifts in the Orwell Glacier on the other side of the moraine and the water level fluctuates over the summer, sometimes leaving the basin dry. The basin is simple and the slopes grade gently towards the deep spot which is very close to the moraine, indicating basin subsidence. There is no shelf. The principal inflow stream is from the head of Moraine Valley; other inflow sources originate from melting snowpatches from the surrounding hills and ablation of the Orwell Glacier. The sediment load is high and coarse sediments dominate the basin floor. High suspended sediment concentrations, shading effects and lake instability restrict lake biota to summer blooms of *Zygnema*, *Phormidium* and *Lyngba* in shallow waters. *Branchinecta* have been recorded here (Heywood, Dartnall & Priddle, 1979). The catchment is predominantly ice-covered and ice-free areas are characterized by scree and boulders colonised by lichens.

2.4 Summary

(1) Signy Island is critically located between the Antarctic Continent and South America. Its position within the Antarctic Convergence and the strong influence of winter pack-ice from the Weddell Sea means that its climate is colder than expected for its latitude. Of fairly uniform geology, the island is glaciated and has a permanent ice-cap. Glacial activity has shaped the landscape, resulting in several glacially-overdeepened troughs, some of which support perennial freshwater lakes. Glacial geomorphological processes continue to be active and ice-retreat over the past forty years, in response to climate warming, has exposed new areas of terrain. Areas free from permanent snow and ice are vegetated by a variety of algae, mosses and lichens. Some of these vegetation stands have been in continued existence for centuries.

(2) The 17 officially-recognised lakes display contrasting morphological features and are influenced by various combinations of abiotic and biotic factors. There is much available information concerning aspects of their present-day limnology. Contrasting lakes conform to Karlén's (1981) suggestion of glacial versus non-control lakes for the comparative study of glacier variations and their effect on the sedimentary record. Palaeolimological studies have tried to link catchment processes to sedimentary responses but so far this has only been effected in a qualitative way.

CHAPTER 3: CONTEMPORARY ENVIRONMENT DATA

3.1 Introduction

An accurate interpretation of the sediment record depends on a thorough understanding of contemporary environmental processes in a study lake and lakes spanning large environment gradients, such as the Signy lakes, are ideal for reconstructions (Pienitz, Smol & Birks, 1995). The collation of relevant quantitative environmental variables is an essential prerequisite for a quantitative reconstruction (Birks, 1995) and the data-set should include climatically-relevant variables which are potentially reconstructible, matching the temporal resolution of the sediment samples. In this Chapter, a large data-set (n=44) of lake physico-chemical, morphometric and catchment compositional variables is collated from literature and archive sources and field observations. This data-set is of comparable size to those of other palaeoclimate reconstructions (Pienitz, Smol & Birks, 1995). Classification and indirect ordination methods are used to explore the major environmental gradients affecting the lakes and the underlying causes for between lake-variability. A new lakes classification based on this improved data-set is compared with previous classification schemes (Heywood, Dartnall & Priddle, 1980; Priddle & Belcher, 1982; Oppenheim, 1990; Jones, Juggins & Ellis-Evans, 1993). An awareness of contemporary environmental factors provides a background for the interpretation of surface-sediment characteristics (Chapters 5, 6, 7 and 8) in both indirect and direct gradient analysis. Eventually, a climatically-relevant variable is selected from this data-set for reconstruction in Chapter 9.

3.2 Data sources and temporal resolution

This study provides the opportunity to update and improve previous environmental data-sets to achieve the best possible quantitative environmental reconstruction for Signy Island. The calibration dataset of Jones, Juggins & Ellis-Evans (1995), essentially that of Heywood, Dartnall & Priddle (1980) forms the basis of the environment data-set. Some variables required updating; others were quantified for the first time. Environmental variables were selected on the basis of being able to provide an estimate for every lake under consideration (n=17) or for the majority of sites so that missing values could be replaced by the mean. The BAS science programme entails the routine monitoring of lake water chemistry and publications and unpublished archive information were used as additional data sources.

Figure 3.1 Summary of lake and catchment environment data (44 variables)

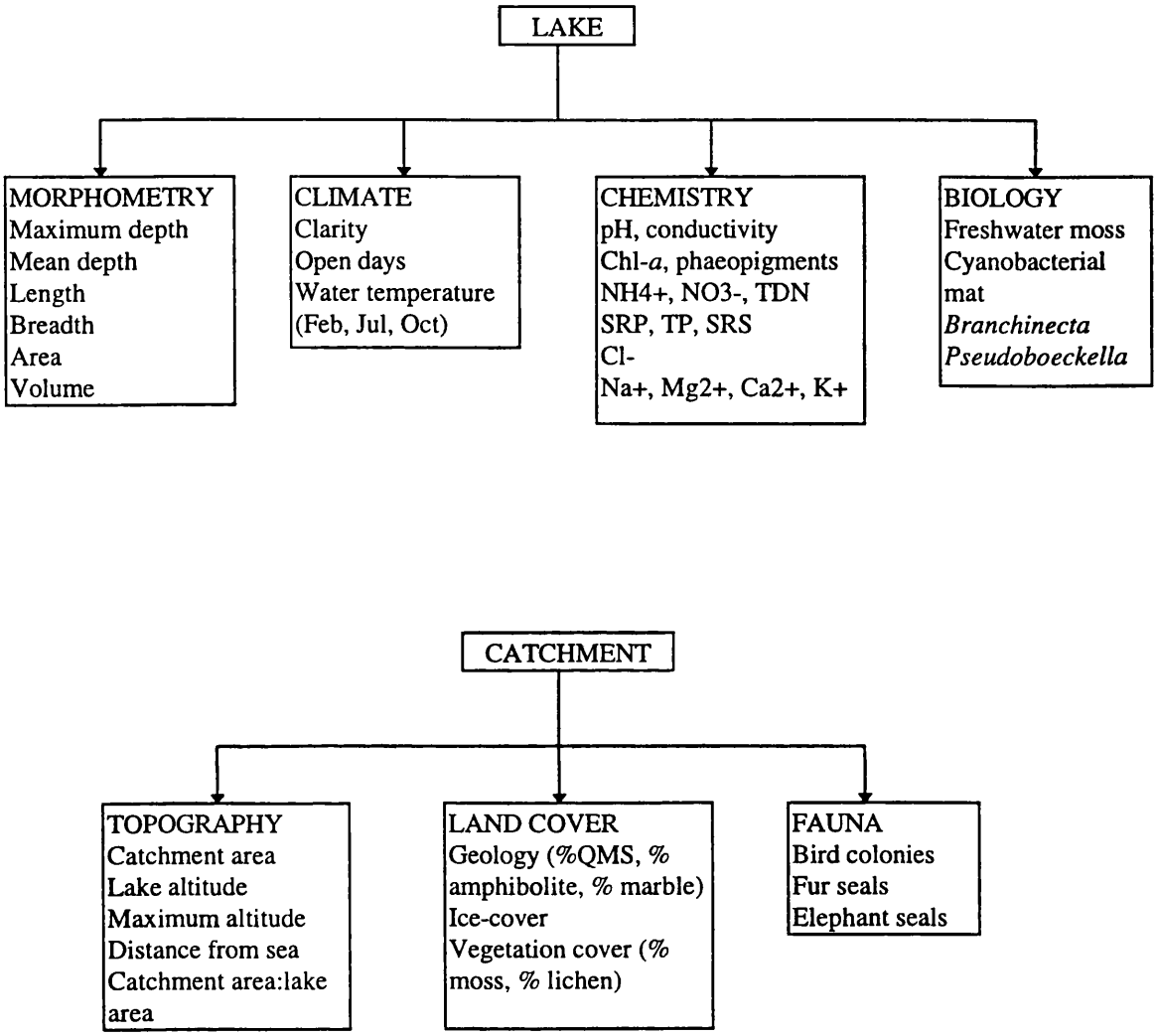

Environmental data were selected to match the temporal resolution of the surface-sediment samples (Chapter 4). Jones, Juggins and Ellis-Evans (1995) chose a 1989-1991 summer average in their diatom-chlorophyll-*a* transfer function for the maritime Antarctic to match surface-sediment (0-1 cm) samples collected in a 1991 fieldwork season. Sediment samples for this study were collected in the 1993/94 and 1994/95 austral summers, therefore 1993 was adopted as the baseline year. Recent sediment accumulation rates calculated from radiometric dating (Appleby, Jones & Ellis-Evans, 1995) suggest that the upper 0-1 cm of surface sediment is equal to approximately 5-10 years of sediment accumulation. Environmental data are therefore calculated as mean values of the 5 years preceding and including the 1993 control year (i.e. 1989/90-1993/94) unless stated otherwise to account for the rate of sediment accumulation and mixing of surface layers. Environmental variables can be broadly divided into sub-sets (Figure 3.1) relating to the lake environment (morphology, climate, chemistry, flora and fauna) and catchment environment (topography, geology, permanent ice-cover, vegetation, fauna).

3.3 Data handling and storage

Lake sites are listed in original numerical order (1-17), not alphabetically, in line with the original lakes classification (Ellis-Evans, 1983). Data handling was performed using Quattro Pro (Borland International, 1991) and a Paradox Relational Database (Borland International, 1988). Data was converted using the CHEMOUT script (S. Juggins, unpublished) to Cornell Condensed format for use with the numerical analysis software (CANOCO, CALIBRATE). Data was expanded to full format using EXPAND (H.J.B. Birks, unpublished) for use with the cluster analysis program CLUSTER (H.J.B. Birks, unpublished).

3.4 Lake environment data

3.4.1 Lake morphometry

Lake morphometry affects lake climate (Ragotzkie, 1978) and sedimentation processes (Håkanson & Jansson, 1983). Littoral-profundal zones in these lakes are markedly different and depth zonation is evident in benthic communities (Oppenheim & Ellis-Evans, 1990). Morphometry was summarised by Heywood, Dartnall & Priddle (1980) for each lake using 4 variables (area, length, breadth, maximum depth). Jones, Juggins & Ellis-Evans (1995) appended mean depth to this list to account for the strong effects of the littoral and mid-depth zones on biological activity. Much of this information

originally derives from Heywood (1967). Since the 1970s, improved survey of the lake bathymetries, coupled with environmental change, has meant that some lakes have undergone significant cartographic changes, for example the increased area of Changing Lake with recession of the ice-shelf covering the inflow and outflow (section 2.3.2.3), the increased recorded maximum depth in Heywood Lake (section 2.3.2.2), and the silting-up and decreased area and volume of Lake 13 (section 2.3.2.13). Updated estimates of lake morphometry, including lake volume, collated by McInnes (1996) are used in this Thesis. Lake area calculations are derived from digitized catchments (section 3.5.3). Core sample depths (Chapter 5) are used in subsequent analysis with the sediment data. Morphometric variables for the 17 lakes are listed in Table 3.1.

Table 3.1 Summary of lake morphometric data

lake	*maximum depth (m)*	*mean depth (m)*	*length (m)*	*breadth (m)*	*lake area (ha)*	*volume (m^3x10^3)*
1 Sombre	10.8	5.0	250	150	2.13	132.60
2 Heywood	6.0	2.0	427	137	4.22	96.20
3 Changing	5.4	2.4	95	80	0.51	21.81
4 Moss	10.2	3.4	235	125	1.32	51.36
5 Knob	3.5	1.1	410	100	3.26	26.00
6 Pumphouse	2.8	1.1	166	155	1.26	15.48
7 Light	4.4	1.7	110	80	0.49	9.09
8 Spirogyra	2.5	0.9	75	60	0.29	2.85
9 Tranquil	8.8	3.4	210	150	2.14	74.50
10 Amos	4.1	1.7	90	50	0.58	8.0
11 Tioga	3.1	3.61	114	40	2.14	16.42*
12 Emerald	14.6	5.6	190	140	1.68	157.95
13 Lake 13	2.0	0.5*	40	20	0.08	0.4*
14 Twisted	5.4	2.0	270	160	2.28	64.60
15 Bothy	2.3	0.9	57	32	0.23	1.53
16 Gneiss	7.0	3.2	105	40	0.38	26.76
17 Orwell	3.5	1.8	90	30	0.21	4.86*
mean	5.67	2.37	172.59	91.12	1.25	41.79
median	4.4	2.0	114.0	80.0	0.58	21.81
S.D.	3.55	1.46	115.72	51.18	1.21	48.1

* estimated

Maximum depth has a large range, at a minimum of 1.5 metres in Lake 13 to 15 metres in Emerald Lake. The population-distribution is slightly left-skewed with a tendency towards shallow basin depths (mean=5.67 m; median=4.4 m; S.D.=3.55 m).

Mean depth ranges from 0.5 m to 5.6 metres. The distribution is near-normal (mean=2.37; median=2.0 m; S.D.=1.46 m). Shallow littoral zones (1-3 metres) are clearly an important feature of lake morphometry.

The minimum basin length is 40 metres (Lake 13) and the maximum is 427 metres (Heywood Lake). The population distribution is left-skewed (mean=172.59 m; median=114 m; S.D.=115.72 m).

Breadth ranges from 20 metres (Lake 13) to 160 metres (Twisted). The population distribution is left-skewed (mean=91.12 m; median=80 m; S.D.=51.18 m).

Lake area covers a large range from 0.08 hectares (Lake 13) to 4.22 hectares (Heywood Lake). The population distribution is strongly left-skewed (mean=1.25 ha; median=0.58 ha; S.D.=1.21 ha) and most lakes are small.

The smallest lake volume is 0.4 m^3x10^3 (Lake 13) and the range extends to a maximum of 157.95 m^3x10^3 (Emerald Lake). This distribution is highly left-skewed (mean=41.79; median=21.81; S.D.=48.1 m^3x10^3).

The maximum sample depth is 15 metres in Emerald Lake and a minimum of 0.9 metres in Tioga Lake. The distribution is approximately normal (mean=5.85 m, median=5 m). The majority of samples are therefore well within the photic limits of each lake basin but also below the effects of winter ice-scour.

3.4.2 Lake climate

Lake climate is summarised by measures of water clarity, water temperature and lake ice-cover (Table 3.2).

3.4.2.1 Clarity

Clarity affects light transmission and is a surrogate for the levels of phytoplankton production and organic and inorganic suspended materials in the water column. It is

Table 3.2 Summary of lake climate data

Lake	*Clarity*	*Open days per annum*	*February water temperature (°C)*	*July water temperature (°C)*	*October water temperature (°C)*
1 Sombre	1	88	4.6	1.08	0.96
2 Heywood	0	99	4.6	0.55	0.45
3 Changing	1	63	3.2	1.06	0.68
4 Moss	1	55.8	4.5*	1.2	1.29
5 Knob	0	71	4.3	0.31	0.1
6 Pumphouse	1	68.7	4.7	0.65	0.36
7 Light	0	59.7	3.1	0.72	0.35
8 Spirogyra	1	67.5	3.9	0.11	0.23
9 Tranquil	1	70.5	4.5*	0.7	0.7
10 Amos	0	90	6.9	0.52	0.32
11 Tioga	1	64.3	5.6	0.13	0.3
12 Emerald	0	73	3.8	0.71	0.75
13 Lake 13	0	72	4.5*	0.56*	0.5*
14 Twisted	0*	71.3	5.5	0.47	0.63
15 Bothy	0*	83	6.6	0.08	0.06
16 Gneiss	1*	28	2.11	0.1	0.33
17 Orwell	0	68.5	4.5*	0.56*	0.5*
mean	0.47	70.19	4.52	0.56	0.50
median	0	70.50	4.50	0.56	0.45
S.D.	0.52	15.64	1.19	0.35	0.31

* replacement for missing value

recorded as a binary code (1/0) based on secchi depth readings (J.C.Ellis-Evans, *pers.comm.*) where a value of 1 indicates clear and 0 represents turbid waters. Missing values for Twisted, Bothy and Gneiss Lakes were replaced with observations at the time of sampling for surface-sediments (Chapter 4).

Clarity divides the dataset into two groups: eight clearwater lakes (Sombre, Changing, Moss, Pumphouse, Spirogyra, Tranquil, Tioga and Gneiss Lakes) and nine turbid lakes with considerable organic and/or inorganic suspended materials (Heywood, Knob, Light, Amos, Emerald, Lake 13, Twisted, Bothy, Orwell). Tranquil Lake is a border-line case which requires re-assessment since observed suspended sediment-concentrations are high

in summer due to appreciable volumes of inwashed allochthonous minerogenic material from the glaciated backslope above the lake.

3.4.2.2 Water temperature

Water temperature profiles are routinely recorded for all the lakes at three critical times each year: high summer (February), midwinter (July) and late winter (October). A high number of values are missing for profundal temperature therefore only the surface water temperature (0-20 cm) is used as the best reasonable estimate of the lake's thermal climate. Its value is calculated as the mean of 4 years prior to actual sediment sampling (i.e. 1990-1993 inclusive) and results are summarised in Table 3.2. In summer, lake waters are fully mixed and there is no thermal stratification (Heywood, Dartnall & Priddle, 1980); surface water temperature should therefore provide a reasonable approximation of whole lake temperature. February water temperature data are missing for Moss, Tranquil, Lake 13, Orwell Lakes; July and October temperature data are missing for Lake 13 and Orwell Lake only. These values were replaced by mean values of from the remaining lakes. Winter surface-temperatures are probably a slight underestimate of the whole-volume water temperature because of slight bottom warming (Hawes, 1983) and heat conduction from the lake surface (Heywood, 1967) means that surface-waters are probably cooler than profundal ones. These processes are a function of lake morphometry and the duration of lake ice-cover and are likely to vary between lakes on an interannual basis. Water temperature readings (February, July and October) range between 0.06-6.9°C. Winter (July and October) water temperatures share very similar distribution statistics (mean=0.56-0.5.0; median=0.56-0.45; S.D.=0.35-0.31°C). February (high summer) temperatures display more variation between lakes ranging from 2.11°C (Gneiss Lake), a probable underestimate, to 6.9°C (Amos Lake) (mean=4.52; median=4.5; std=1.19°C) where bottom heating is encouraged by the low albedo of effluent heavy waters (Hawes, 1983). The greater variability of summer temperatures probably reflects morphometric controls (area, volume, depth), exposure and the duration of the open water period.

3.4.2.3 Lake ice-cover (open days)

Lake ice-cover is the most obvious manifestation of external climate control. It strongly affects water circulation and stratification, patterns of sedimentation, the development of winter lake anoxia (Hawes, 1988), water chemistry (Ellis-Evans, 1990) and lake biology. Snow-cover is the main factor separating these lakes from Continental

counterparts (Heywood, 1977), further reducing winter light levels and suppressing biological activity (Ellis-Evans, 1990). Ice-cover was not used explicitly in previous classifications of the Signy Lakes (Heywood, Dartnall & Priddle, 1980; Jones, Juggins & Ellis-Evans, 1993) although archive records of lake ice-cover - the Signy Island Lake Ice Diaries - are held at BAS, recording over 20 years of freeze-over and melt-out dates. Since the mid-1980s there has been an obvious trend towards longer periods of open water with the thaw commencing roughly a month earlier (mid-to late December) than melt-out in the mid-1970s (mid-January). In all years, dates for melt-out on the west coast lakes lag behind those of the east owing to local site-effects (topography and insolation). Closure in the 1970s tended to be in March but by the 1990s was occurring in early to mid-April. Once frozen-over the ice-cover remains until spring. Occasional mid-winter breaks are known to occur with meltwater flooding the ice-surface and some activity occurs near the outflow, especially at Knob, Heywood and Sombre lakes. These breaks could be responsible for a degree of lake mixing during the winter.

Dates for melt-out are more reliably reported than the inception of freeze-over therefore a value was derived for the duration of lake 'open days' per annum instead of the period of closure. The average duration of open water per annum was calculated for the austral summers of 1989/90 to 1992/93 inclusive and results are summarised in Table 3.2. Freezing is largely controlled by air temperature and once initiated, the onset of freezing is assumed to be rapid and absolute (Ragotzkie, 1978). Restricted geographical and altitudinal ranges implies that the lakes freeze-in within a few days of each other thus, where dates are missing it is reasonable to draw-upon nearest neighbour analogue lakes of similar morphometry (especially area and depth) and altitude. The timing of melt-out is much more variable and relates to several morphometric and external climate controls (cf. Ragotzkie, 1978). 1992 was an anomalously cold year with a short summer but was still included in calculations as part of the inherent natural variability of the local climate. Records are scant for Gneiss Lake, the most remote site. Since the mid-1980s it has been breaking open for approximately a month (N.Rose, *pers.comm.*) thus a value of 28 days was adopted for this study. Unfortunately it was not possible to make a valid estimate of snow-cover above the ice for each lake.

The shortest period of open-water is recorded for Gneiss Lake (28 days) and the maximum is for Heywood Lake (99 days). The distribution is near-normal (mean=70.19 days; median=70.5 days; S.D.=15.64 days). This consistency shows an apparent

uniformity of lake response to climate independent of morphological and site differences.

3.4.3 Lake water chemistry

The Antarctic terrestrial environment is nutrient-poor due to limited nutrient sources in unweathered materials and sparse vegetation development. Meltwaters draining recently deglaciated catchments contain little dissolved material and the volume of spring and summer meltwater, coupled with high precipitation, has a strong diluting effect on lake-water chemistry. Most inland lakes are oligotrophic and lakes with the highest nutrient concentrations are therefore found in the most highly vegetated and animal-influenced catchments close to the coast (Grobbelaar, 1975; Priddle & Heywood, 1980; Hawes, 1983; Kieffer & Copes, 1983; Ellis-Evans, 1990). Differences in lake-water chemistry between the Signy Lakes have been used as the basis for a lake classification scheme (Heywood, Dartnall & Priddle, 1980).

Water-chemistry data (15 variables) were taken from Jones, Juggins & Ellis-Evans (1993) and Jones & Juggins (1995). Their 1990-92 averages were updated to include 1993 summer data from BAS records (J.C. Ellis-Evans, *pers.comm.*). Winter conductivity values were used when summer values were unavailable as conductivity changes little throughout the year. Other missing values were replaced with the column mean. Data are summarised in Table 3.3.

Conductivity is at a minimum of 30 μS cm^{-1} in Orwell Lake and a maximum of 233 μS cm^{-1} in Bothy Lake. The population is normally-distributed (mean=95.53; median=92; S.D.=47.99 μS cm^{-1}).

Chlorophyll-*a* (Chl-*a*) ranges from 1.24 μg l^{-1} in Bothy Lake to 10.06 μg l^{-1} in Heywood Lake. The distribution is left-skewed (mean=3.86; median=3.02; S.D.=2.82 μg l^{-1}). Most lakes tend to have low measures of phytoplankton productivity.

Phaeopigments range from 0.42 μg l^{-1} in Bothy Lake to 6.6 μg l^{-1} in Knob Lake (mean=2.31; median=1.74; S.D.=1.82 μg l^{-1}).

Ammonium ranges from 1.79 μg l^{-1} in Tranquil Lake to 214.4 μg l^{-1} in Amos Lake. Amos Lake forces the population to be highly left-skewed (mean=35; median=16.33;

Lake	*pH*	*Cond.*	*Chl-a*	*Phae.*	NH_4+	NO_3^-	*TDN*	*SRP*	Cl^-	*TP*	Na^+	K^+	$Mg2^+$	Ca^{2+}	*SRS*
		µS cm^{-1}	µg l^{-1}	µg l^{-1}	µg l^{-1}	µg l^{-1}	µg l^{-1}	µg l^{-1}	mg l^{-1}	mg l^{-1}	mg l^{-1}	mg l^{-1}	mg l^{-1}	mg l^{-1}	µg l^{-1}
1 Sombre	6.82	78	3.99	1.74	12.95	181.88	272.50	2.64	25.80	9.00	24.90	1.0	4.6	3.8	169.18
2 Heywood	6.87	134	10.06	5.19	56.14	326.95	614.70	32.10	42.30	122.10	33.20	1.5	5.9	4.0	201.14
3 Changing	6.79	94	2.43	0.58	8.45	146.45	223.20	3.51	25.30	10.80	23.00	1.0	4.2	3.4	236.60
4 Moss	6.75	40	1.85	0.77	5.65	110.95	204.00	2.34	23.20	7.80	12.60	1.2	1.4	2.2	136.96
5 Knob	7.29	62	8.70	6.60	16.33	123.36	328.70	0.89	18.70	33.70	22.80	1.4	3.1	4.1	168.36
6 Pumphouse	6.86	86	3.02	1.13	7.05	63.55	174.90	3.50	18.40	9.40	13.80	1.2	2.5	4.2	83.66
7 Light	6.81	121	9.21	3.57	11.24	33.46	145.90	1.37	44.10	27.60	29.60	2.3	4.7	4.9	122.87
8 Spirogyra	7.37	60	1.51	1.23	17.36	116.19	209.60	0.34	19.40	11.00	28.80	2.2	4.7	6.2	149.54
9 Tranquil	6.89	52	1.53	1.15	1.79	80.65	146.40	0.29	16.70	5.00	16.30	1.0	2.7	3.1	88.81
10 Amos	8.81	120	4.11	4.28	214.40	520.64	1150.50	205.36	33.90	252.50	36.00	3.4	20.3	9.7	88.81
11 Tioga	7.41	134	4.29	4.06	53.28	105.69	421.80	28.04	20.90	73.90	30.00	1.8	6.1	5.2	127.225
12 Emerald	6.61	67	1.33	0.54	10.33	97.32	187.70	3.21	23.40	7.60	12.30	1.2	2.1	2.4	76.25
13 Lake 13	7.03*	96*	3.86*	2.31*	35.00*	179.97*	86.38	21.68*	7.44	14.18	22.96*	1.6*	5.0*	4.4*	135.51*
14 Twisted	6.8	92	2.43	1.01	2.54	65.56	150.20	2.62	28.70	9.50	17.30	1.5	3.4	4.2	56.18
15 Bothy	6.75	233	1.24	0.42	94.84	570.68	864.70	54.49	44.20	180.60	20.80	1.7	4.1	4.7	191.52
16 Gneiss	6.74	125	2.12	2.31*	22.47	219.68	275.20	2.88	18.30	37.04	22.96*	1.6*	5.0*	4.4*	135.51*
17 Orwell	6.87	30	3.86*	2.31*	25.2	116.44	148.83	3.27	9.83	10.69	22.96*	1.6*	5.0*	4.4*	135.51*
mean	7.03	95.53	3.86	2.31	35.00	179.96	329.72	21.678	24.739	48.38	22.96	1.6	4.99	4.43	135.51
median	6.86	92.0	3.02	1.74	16.33	116.44	209.6	3.21	23.2	11.0	22.96	1.5	4.6	4.2	135.51
S.D.	0.51	47.99	2.82	1.82	52.22	153.99	288.65	49.696	10.94	71.23	7.04	0.6	4.16	1.67	18.19

TDN Total Dissolved Nitrogen; SRP Soluble Reactive Phosphorous; TP Total Phosphorous; SRS = Soluble Reactive Silicate

* Replacement for missing value

Table 3.3 Summary of lake-water chemistry data

S.D.=52.22 μg l^{-1}).

Nitrate ranges from 33.437 μg l^{-1} in Light Lake to 570.68 μg l^{-1} in Bothy Lake. The population distribution is near-normal (mean=179.96; median=116.44; S.D.=153.99), slightly left-skewed due to the high values for Amos and Bothy lakes.

Total dissolved nitrogen (TDN) has an extremely wide range from 86.38 μg l^{-1} in Lake 13 to 1150.5 μg l^{-1}in Amos Lake. The population is left-skewed (mean=329.72; median=209.6; S.D.=288.65 μg l^{-1}).

Total phosphorous (TP) ranges from 5 in Tranquil Lake to 252.5 mg l^{-1} in Amos Lake (mean=48.38; median=11; S.D.=71.23).

Soluble reactive phosphorous (SRP) has a wide range from 0.29 μg l^{-1} in Tranquil Lake to 205.36 μg l^{-1} in Amos Lake. The population is strongly left-skewed (mean=21.68; median=3.21; S.D.=49.7 μg l^{-1}) due to Amos Lake.

Soluble reactive silicate (SRS) is at a minimum of 56.18 μg l^{-1} in Twisted Lake and a maximum of 236.6 μg l^{-1} in Changing Lake. The population is normally-distributed (mean=135.51; median=135.51; S.D.=48.191 μg l^{-1}).

Chloride ion concentrations (Cl^-) range from 7.44 mg l^{-1} in Lake 13 to 44.2 mg l^{-1} in Light Lake with a normal distribution (mean=24.74; median=23.2; S.D.=10.94 mg l^{-1}).

Sodium ion concentrations (Na^+) range from 12.3 mg l^{-1} in Emerald Lake to 36 mg l^{-1} in Amos Lake (mean=22.96; median=22.96; S.D.=7.04 mg l^{-1}).

Potassium ion (K^+) concentrations range from 1 mg l^{-1} in Sombre and Tranquil Lakes to 3.4 mg l^{-1} in Amos Lake (mean=1.6; median=1.5; S.D.=0.6 mg l^{-1}).

Magnesium ion (Mg^{2+}) concentrations range from 1.4 mg l^{-1} in Moss Lake to 20.3 mgl^{-1} in Amos Lake (mean=2.99; median=4.6; S.D.=4.16 mg l^{-1}).

Calcium ion (Ca^{2+}) concentrations range from 2.2 mg l^{-1} in Moss Lake to 9.7 mg l^{-1} in Amos Lake (mean=4.43; median=4.2; S.D.=1.67).

3.4.4 Flora

There is no emergent vegetation due to seasonal ice-cover. The main phototrophs are cyanobacteria, phytoflagellates, chlorophytes and bacillariophyceae. Lake flora fulfils a dual role as both a predictor and response to the lake environment: macro-vegetation can affect flow velocities and patterns of sedimentation; conversely, substrate stability can affect vegetation distributions and benthic community structure (Oppenheim & Greenwood, 1990). Macro-vegetation (moss and cyanobacterial mat) is of principal interest to this study. Freshwater moss species found in these lakes include *Amblystegium* sp., *Calliergon sarmentosum*, *Drepanocladus* cf. *aduncus*, *Drepanocladus* sp., and *Pohlia nutans* (Light & Heywood, 1973), providing a variety of habitat niches for periphytic algal species (Priddle, 1985). Presence/absence data for freshwater mosses and cyanobacterial mats are derived from Heywood, Dartnall & Priddle (1979) and updated from field observations (Table 3.4).

Freshwater mosses are present in Moss, Tranquil, Emerald and Twisted Lakes. Observations made at the time of surface-sediment sampling confirm their presence in the first three lakes but not in Twisted Lake. Cyanobacterial mat is found in all the lakes except Heywood, Amos and Lake 13.

3.4.5 Fauna

Mollusca and fish are absent from these lakes and fauna are restricted to Protozoa, Turbellaria, Rotifera, Tardigrada, Nematoda, Gastrotricha, Annelida (Enchtracidae) and Arthropoda (Crustacea) (Heywood, Dartnall & Priddle, 1979). Two invertebrate indicator species, *Branchinecta gaini* (Anostraca) and *Pseudoboeckella poppei* (Copepoda)[1], are associated with their food sources, either well-developed cyanobacterial mat communities or organic-rich sediments. These species were included in a factor analysis to help define a lake classification scheme (Heywood, Dartnall & Priddle, 1980). High clastic inputs to the lakes can preclude the growth and development of mats. *Branchinecta* require 4-5 months of liquid water to complete its life cycle and can be used as a palaeoenvironmental indicator (Björck *et al.*, 1996). Both species therefore

[1] *Pseudoboeckella* has since been fused with the Genera *Boeckella* (Bayly, 1992)

give some prediction of the lake benthic environment and climate. Records for both species are derived from Heywood, Dartnall & Priddle (1979) and were updated from field observations. They are recorded as a binary code (Table 3.4).

Table 3.4 Summary of lake biological data

lake	*Moss*	*Mat*	*Branchinecta*	*Pseudoboeckella*
1 Sombre	0	1	1	1
2 Heywood	0	0	1	1
3 Changing	0	1	0	1
4 Moss	1	1	0	1
5 Knob	0	1	1	1
6 Pumphouse	0	1	0	1
7 Light	0	1	0	1
8 Spirogyra	0	1	1	1
9 Tranquil	1	1	0	1
10 Amos	0	0	1	1
11 Tioga	0	1	1	1
12 Emerald	1	1	0	1
13 Lake 13	0	0	1	0
14 Twisted	1	1	0	1
15 Bothy	0	1	1	1
16 Gneiss	0	1	0	1
17 Orwell	0	1	1	0

Pseudoboeckella are present in all the lakes except Lake 13 and Orwell Lake, which are probably too minerogenic and hydrologically unstable to support sufficient food sources.

Branchinecta are found in Sombre, Heywood, Knob, Spirogyra, Amos, Tioga, Lake 13, Bothy and Orwell lakes. Their absence from Changing, Moss, Pumphouse, Light, Tranquil, Emerald, Twisted and Gneiss is probably a function of food source availability, water temperatures and the short open-water season (cf. Björck *et al.*, 1996).

3.5 Catchment environment

3.5.1 Topography

Catchment topography affects the development of the drainage network, the presence of

permanent snow and ice, vegetation cover and other aspects of catchment development. It is summarised by the following variables: catchment area, catchment area to lake area ratio, and the maximum altitude in the catchment, lake altitude and distance from the sea (Table 3.5). Catchment area (hectares) and the catchment to lake area ratio were derived from digitized catchment boundaries within ARC/INFO (section 3.3.4). New catchment areas superseding those of Heywood, Dartnall & Priddle (1980) were mapped onto overlays of the 1:10,000 island map on the basis of contours. The match between these catchment area estimates is not perfect since boundary definition is subjective, especially in areas lacking distinct topography. The catchment to lake-area ratio was used by Hawes (1990) in his discussion of lake development and eutrophication and is a useful summary variable. Maximum altitude in the catchment was taken from the 1:10,000 island map of Signy Island as a surrogate measure for average slope in the catchment. Lake altitude is an expression of lake site and reflects latent physical controls such as altitude-temperature relationships and distance from the sea.

The major summits of the central ice-cap are captured by several lake catchments. Tioga Hill (279 m) is shared by the lakes in Cummings Amphitheatre (Emerald, Lake 13, Twisted, Bothy lakes). The mean maximum altitude for all 17 lakes is 233.41 metres, therefore most lakes are affected to some degree by the ice-cap. Maximum altitude is also a function of catchment size as smaller, discrete catchments (Light, Amos, Tioga) do not include the highest island elevations and meltstreams from the ice-cap largely by-pass these lake basins. The catchment with the smallest altitudinal range is Tioga Lake with a maximum altitude of 111 metres and lake altitude of 35 metres.

Lake baseline altitude (m.a.s.l.) ranges from a shared minimum of 4 metres (Heywood and Bothy Lakes) to a maximum of 150 metres (Gneiss Lake). The distribution is strongly left-skewed (mean=33.18 m; median=29 m; S.D.=34.05 m) and most lakes lie at relatively low altitude.

The minimum distance from the sea is only 15 metres (Bothy Lake); this lake is separated from the beach by a morainic bar which is readily transgressed by seals. The maximum distance from the sea - 800 metres - is for Moss Lake, at the head of Paternoster Valley (Figure 2.2). The mean distance from the sea is 382.44 metres, thus most lakes are sited inland away from immediate marine effects.

Table 3.5 Summary of lake-catchment site and biological data

Lake	*Catchment area* (*ha*)	*Lake altitude* (*m*)	*Maximum altitude* (*m*)	*Distance from sea* (*m*)	*Catchment area:lake area ratio*	*Bird colonies*	*Fur seals*	*Elephant seals*
1 Sombre	86.54	5	261	50	40.7	0	271	0
2 Heywood	53.68	4	204	200	12.7	0	549	16
3 Changing	44.12	35	204	700	87.0	0	0	0
4 Moss	22.01	48	204	800	16.7	0	0	0
5 Knob	35.94	8	204	200	11.02	1	145	10
6 Pumphouse	27.22	20	204	150	21.6	0	247	0
7 Light	0.60	35	204	200	11.9	1	0	0
8 Spirogyra	21.45	25	210	300	7.6	0	0	0
9 Tranquil	69.97	28	210	400	32.7	0	2	0
10 Amos	13.91	8	265	25	24.1	1	326	6
11 Tioga	3.38	35	261	200	15.9	0	0	0
12 Emerald	37.76	45	111	500	22.5	0	0	0
13 Lake 13	23.00	55	279	700	287.5	0	0	0
14 Twisted	79.60	30	279	300	34.9	0	30	0
15 Bothy	182.01	4	279	15	782.1	0	294	5
16 Gneiss	19.73	150	255	640	51.9	0	0	0
17 Orwell	73.28	29	279	620	354.5	0	0	0
mean	46.72	33.18	233.41	352.94	106.78	0.18	109.7	2.18
median	35.94	29.00	255.00	300.00	24.10	0.0	0	0
S.D.	43.64	34.05	44.97	258.87	200.46	0.39	167.1	4.59

Catchment areas range from 0.6 hectares for Light Lake, a very discrete catchment, to 181.88 hectares for Bothy Lake, which encompasses the entire Cummings Amphitheatre from the central ice-cap to the Gneiss Hills. The mean catchment size is 46.72 hectares (median=35.94; S.D.=43.64).

The catchment to lake area ratio is largest for Bothy Lake (782.1), i.e. a very small lake with the largest catchment, and smallest for Heywood and Spirogyra Lakes (7.6), i.e. large lakes in relatively small catchments. The distribution is highly left-skewed because of the Bothy catchment however, the mean for all lakes is 106.78 (median=24.1; S.D.=200.46).

3.5.2 Geology

Bedrock plays a role in determining characteristic lake water chemistries for certain

lakes (Heywood, Dartnall and Priddle, 1980). For instance, meltwaters draining marble and amphibolite lithologies are iron-rich with slightly enhanced pH. These authors used three categories of rock type for each catchment as a proportion of exposed rock in the catchment (i.e. inverse of catchment ice-cover): quartz-mica-schist (QMS), amphibolite and marble. Recent deglaciation has exposed new areas of terrain since the 1980 publication but lack of more recent maps and/or aerial photographs makes it difficult to estimate accurately these new exposures. Hence the 1980 data are recognised as areal under-estimates which are non-contemporaneous with respect to the other environment variables. Obvious mis-matches occur in catchments which have experienced extensive recent deglaciation, for example, Sombre, Changing and Moss Lakes. Gneiss Lake is the only lake in a distinctly different area of bedrock which has not been categorized.

Table 3.6 Summary of catchment land-cover data

Lake	*% quartz-mica-schist*	*% marble*	*% amphibolite*	*% permanant snow & ice*	*% moss*	*% lichen*
1 Sombre	12	1	1	19.55	2	9
2 Heywood	95	1	1	0.82	1	5
3 Changing	12	1	1	21.74	1	5
4 Moss	53	1	6	5.98	1	5
5 Knob	95	1	1	0.91	26	12
6 Pumphouse	53	6	1	31.95	12	26
7 Light	69	12	1	2.32	1	4
8 Spirogyra	69	1	1	4.92	1	4
9 Tranquil	5	1	1	32.27	1	5
10 Amos	90	0	5	0.99	1	4
11 Tioga	90	0	1	2.42	1	4
12 Emerald	5	0	1	52.83	1	4
13 Lake 13	10	5	1	69.6	0	0
14 Twisted	5	0	1	36.61	1	4
15 Bothy	69	0	1	25.61	1	4
16 Gneiss	9	0	6	6.55	1	4
17 Orwell	12	1	1	61.09	1	5
mean	44.29	1.82	1.82	22.13	3.12	6.12
median	53.0	1.00	1.00	19.55	1.00	4.00
S.D.	36.65	3.13	1.85	22.46	6.48	5.69

Bedrock as a percentage of ice-free catchment (Heywood, Dartnall & Priddle, 1980)
% permanent snow and ice calculated for 1993 AD in this study (section 3.5.3)

Quartz-mica-schist, the most common lithology, ranges from 5-95% of the catchment area with a mean of 44.29% (Table 3.5). Tranquil, Emerald, Twisted and Gneiss Lakes have the lowest exposures of this rock type (5-9%) which are likely underestimates. The most extensive exposures are obviously in the low-lying, deglaciated coastal areas with high values for Heywood and Knob Lakes (95%), Amos and Tioga (90%) and Light, Spirogyra and Bothy (69%).

Amphibolite occurs less commonly as small outcrops reaching a maximum of 6% in Moss and Gneiss Lake catchments and 5% in Amos Lake catchment (Table 3.6). It is recorded as a token fraction (1%) in all other catchments.

The most extensive exposure of marble bedrock is in Moss Lake catchment (12%). New outcrops have since been exposed following glacial retreat along Spindrift Ridge and a large marble outcrop above Changing Lake is the chosen location for a Global Positioning System reference station (J.C. Ellis-Evans, *pers.comm.*). Pumphouse lake catchment has 6% marble relating to the Marble Knolls to the east of the lake and Lake 13 had 5% in rocky bluffs nearby. All other lakes have negligible fractions (1%) except Amos, Tioga, Emerald, Twisted, Bothy and Gneiss which have none.

3.5.3 Catchment ice-cover

The most recent (1972) edition of the 1:10,000 map of Signy Island was compiled using aerial photographs from 1968. From this map and field observations, Heywood, Dartnall & Priddle (1980) determined the percentages of permanent snow- and ice-cover in each lake-catchment. However, significant ice-retreat has occurred since this mapping exercise (Smith, 1990; essentially derived from the late 1960s/early 1970s) and signs of continued decline were noted in the short time which elapsed between the first and second fieldwork seasons in this study. Therefore, revised values were necessary for this study.

Efforts to map the ice-cover using a planetable survey in Paternoster Valley in the second fieldwork season produced unsatisfactory results and left large areas of the Island unmapped. Mapping was therefore completed as a desk exercise in the UK. Every year ice limits in critical locations are photographed at the time of maximum summer melt-back (February-March). These are archived at the BAS. Photographs from 1993 were used to define new estimates of ice-cover. Approximate limits were drawn onto overlays

of the 1:10,000 map within predefined catchments. It was impossible to discern accurately between areas of permanent snow or ice so mapped 'ice' cover was an amalgamation of both cover-types. The new catchments and permanent snow- and ice-cover patches were digitized in the ARC/INFO Geographical Information System (Environmental Systems Research Institute Inc., 1989-92) to generate coverages composed of polygons and arcs representing the lakes, streams and the ice-patches within the confines of each catchment boundary. Area and perimeter fields in digitizer units were converted to the original grid coordinates of the 1:10,000 Signy map so that absolute areas of ice-cover in square metres could be derived. The ARC-EDIT Polygon Attribute File (PAT) lists the areas and perimeters of the polygons and from these a new catchment area (sum of all polygon areas) and values for ice-cover (sum of polygon areas labelled as 'ice') were calculated as a percentage of each catchment (Table 3.6).

Catchment ice-cover ranges from 0.86% in Heywood Lake catchment to 69.6% in Lake 13 catchment (Table 3.6). The group mean is 22.13% (median=19.55%; S.D.=22.46%); all catchments are affected to some degree by glaciation. Many catchments have ice-cover in excess of the minimum quoted by Karlén (1981) to discriminate a glacier response in lacustrine sediment-sequences.

Table 3.7 shows the comparison of 1993 versus 1980 estimates of catchment ice-cover and the dramatic decrease is obvious. The greatest losses have occurred in proglacial lake catchments (Changing, Emerald, Orwell) or where the catchments extend to high altitudes (Changing, Tranquil, Gneiss). Gneiss catchment has shown a -91.6% change in cover over *ca.* 25 years, closely followed by Sombre (-73.58%) and Changing catchments (-71.01%). Others experienced an approximate 50% decrease in the same time period. The smallest losses have been in Amos (-1%) and Knob (-9%) Lake catchments. In low-lying coastal areas the snow and/or ice-cover 20 years ago was probably already at its minimum, the residual cover remaining in sheltered accumulation hollows where insolation and wind effects are slight (cf.Watson, Davison & French, 1994). These residual patches are probably composed of snow and are ephemeral features subject to high inter-annual variability. Deviations in catchment boundary definitions (section 3.5.1) account for poor comparisons in some instances for example, the apparent increase in ice-cover for Pumphouse and Bothy catchments where new catchments encompass larger areas than before.

Table 3.7 Comparison of previous estimates of catchment permanent snow and ice-cover with estimates of 1993 ice-cover derived from photographic survey of ice-retreat margins

Lake	*Catchment area (ha)**	*% snow and ice***	*1993 catchment area (ha)*	*1993 % snow and ice*	*% areal change (1967-93)*
1 Sombre	48.00	74	86.54	19.55	-73.58
2 Heywood	41.00	1	53.68	0.82	-18.0
3 Changing	24.00	75	44.12	21.74	-71.01
4 Moss	9.00	10	22.01	5.98	-40.2
5 Knob	23.00	1	35.94	0.91	-9.0
6 Pumphouse	17.00	12	27.22	31.95	+166.25
7 Light	5.00	5	5.96	2.32	-53.6
8 Spirogyra	11.00	10	21.45	4.92	-50.8
9 Tranquil	36.00	74	69.97	32.27	-56.39
10 Amos	7.00	1	13.91	0.99	-1.0
11 Tioga	4.00	5	3.38	2.42	-51.6
12 Emerald	35.00	74	37.76	52.83	-28.61
13 Lake 13	NA	NA	2.30	69.6	NA
14 Twisted	64.00	74	79.60	36.61	-50.53
15 Bothy	108.00	13	182.01	25.61	+97.00
16 Gneiss	9.00	78	19.73	6.55	-91.6
17 Orwell	31.00	78	73.28	61.09	-21.68

* estimates from Heywood, Dartnall & Priddle (1979)
** revised estimates from Heywood (1967) in Heywood, Dartnall & Priddle (1980)

3.5.4 Vegetation cover

Vegetation is a function of catchment and soil development and geomorphic stability (Mackereth, 1966). Many exposed rock faces are colonised by lichens (Collins, Baker and Tilbrook, 1975) which are resistant to desiccation; moss vegetation by contrast, is hydrologically sensitive and typically inhabits areas of permanent moisture on level ground and gentle slopes (Smith, 1972). Vegetation plays a role in regulating nutrient inputs to the lakes (Hawes, 1983) and where nutrient inputs are excessively high or the vegetation damaged or removed the nutrient inwash into the lakes in the summer months is more pronounced (Ellis-Evans, 1990). Loss of moss cover may also relate to changing hydrological regimes due to climatic change (Collins, Baker & Tilbrook, 1975). Heywood, Dartnall & Priddle (1980) estimated the moss and lichen-cover in each

catchment which are the best available figures since no extensive mapping of vegetation cover has been completed more recently. Unfortunately, these estimates do not take into account the subsequent destructive activities of fur seals in the coastal lowlands (Smith, 1990; Ellis-Evans, 1990) and the potential colonisation of recently deglaciated terrain over the last decade. It was not possible to quantify soil type owing to lack of survey information.

Moss vegetation has a maximum ground coverage of 26% moss in Knob Lake catchment, 12% in Pumphouse Lake, and 2% in Sombre Lake catchment (Table 3.6). Other catchments recorded a token 1%, except Lake 13 which records zero.

Lichen vegetation has a maximum ground coverage of 26% in Pumphouse catchment, 12% in Knob Lake catchment and 4-5% in the remaining catchments except Lake 13 where an estimate cannot be made.

3.5.5 Fauna

3.5.5.1 Seals

Seals are an important vector for nutrient transfer from the marine to the terrestrial biome and the effects of recent population increases were described in section 2.2.8.2. A full characterisation of the contemporary environment requires their inclusion in the data-set to assess for their effects on the lakes and their catchments. The seal species of significance to the lakes are fur seals (*Arctocephalus gazella*) and elephant seals (*Mirounga leonina*). The original lakes' classification of Heywood, Dartnall & Priddle (1980) used an index of percentage seal pollution for each lake but they did not disclose how this figure was calculated. Therefore, updated, quantitative estimates for each lake catchment were re-calculated. For most years since 1977 a seal census has been undertaken at Signy Island in the third week of February when seal numbers are usually at their peak (Smith, 1988). Naturally, this peak does not always coincide exactly with the census day. A census by geographical sectors was started in 1985. These sectors tend to follow readily-defined topographic divisions which approximate to catchment boundaries. Sector counts were amalgamated as appropriate using *a priori* knowledge of their likely geographical ranges. The mean value for the summers of 1989-1993 (British Antarctic Survey, 1989-93) was used to estimate the number of fur and elephant seals per annum by catchment, rounded-up to the nearest individual. Results are summarised in Table 3.5. 1993 is a below average year, possibly due to weather

conditions, but is still included in calculations as part of the natural variability.

The population distribution is highly skewed (mean=110; median=0; S.D.=167) and catchments tend to have high counts or none at all, reflecting accessibility. Lowland lakes are most susceptible to visitations (Sombre, Heywood, Knob, Pumphouse, Amos, Bothy Lakes) and the maximum average summer population of 550 individuals is found in Heywood Lake. Twisted Lake, previously unaffected (cf. Heywood, Dartnall & Priddle, 1980), records 5 individuals resulting from recent increased population pressure on nearby beaches.

Elephant seals are only recorded in four catchments (Heywood, Knob, Amos, Bothy) and do not exceed 17 individuals per annum (Heywood Lake). The group mean for the 17 lakes is 2 elephant seals per annum (median=0; S.D.=5) supporting Ellis-Evans's (1990) observation that population size is relatively static.

3.5.5.2 Birds

Birds are an additional biological agent affecting the lake-catchments. Like seals, they cause eutrophication of lake waters. A substantial increase in the numbers of breeding penguins has occurred in the past 40 years (Croxall *et al.*, 1981) but their colonies are restricted to rocky coastal locations at distance from the lakes. The significant species of relevance to the lakes are giant petrels (*Macronectes giganteus*). Their colony above Light Lake for example, has probably resulted in the mesotrophic status of what otherwise would be an oligotrophic lake (Heywood, Dartnall & Priddle, 1980). These authors used an index of percentage bird pollution in their lake classification but it was not known how the index was calculated. For this study bird colonies are recorded as a binary code (Table 3.5). Skua (*Catharacta skua lönnbergi* (Matthews)) populations are at low densities over the entire island but are unlikely to contribute significant nutrient inputs to the lakes except perhaps the concentration of bachelor skuas at Changing Lake over the summer months (section 2.3.2.3).

Bird colonies are only present in Knob, Light and Amos lake catchments. The remainder are unpopulated by summer colonies. Hawes (1988) reported colonies of *Macronectes giganteus* in Spirogyra catchment but none were observed at the time of this study.

3.6 Relationships between environment variables

3.6.1 Correlations

A Pearson's product-moment correlation matrix for the 44 environmental variables from the 17 lakes was produced using CANOCO version 3.1 (ter Braak, 1990) to identify significant relationships between variables. The matrix is displayed in Table 3.8. The product-moment correlation has a value between -1.0 (perfect negative correlation) and 1.0 (perfect positive correlation). A value of zero indicates no correlation. The method assumes that both variables come from normally-distributed populations therefore the following variables were $\log_{10}$ transformed to reduce skewness: altitude, catchment area, quartz-mica-schist, % lichen, catchment to lake area ratio, mean depth, length, volume, conductivity, Chl-*a*, phaeopigments, ammonium, nitrate, total dissolved nitrogen, total phosphorous, soluble reactive phosphorous, soluble reactive silicate, chloride, major cations, water temperatures and seals. A two-tailed (non-directional) significance test was used to calculate the significance of the sample correlation coefficient (Ebdon, 1985). High multicollinearity between variables was anticipated therefore in the correlation matrix only highly significant cells ($p<0.001$, $r>0.606$, 15 d.f.) are shaded.

Excluding self-correlations, 67 relationships are positive and significant at $p<0.01$ ($r=0.606$); of these, 29 are positive and very significant, $p<0.001$ ($r>0.725$). The strongest positive correlations are between soluble reactive phosphorous and ammonium ($r=0.93$), lake area and length ($r=0.92$), calcium and potassium ($r=0.91$), calcium and magnesium ($r=0.89$), total phosphorous and total dissolved nitrogen ($r=0.89$) and mean depth and maximum depth ($r=0.89$). Thirteen relationships are negative and significant at $p<0.001$ ($r=-0.606$); of these, only 2 are highly negative at $p<0.001$ ($r=-0.725$) and include fur seals and altitude ($r=-0.83$) and fur seals and distance from the sea ($r=-0.75$). Many other relationships are significant at lower levels ($p<0.05$, $r=0.482$, 15 d.f.) in either direction.

3.6.2 Classification

Various schemes exist for the classification of lakes (Håkanson & Jansson, 1983). Classification of the Signy Lakes has been used to help explain ontogeny under a maritime Antarctic climate and the reasons for a high diversity of lake types in a restricted geographic area. At the simplest level, all the lakes can subjectively be termed glacial lakes, i.e. they have been formed by glacial action. Heywood (1967) adopted a morpho-genetic approach to classify the Signy Lakes according to Hutchinson's (1957)

Table 3.8 Pearson product-moment correlation matrix showing relationships between lake and catchment environment variables (n=44)

	Alt.	Max.alt	D.sea	Catch.area	% ice	% QMS	% amph	% marb	%moss	%lichen	catch:lake	Max.depth	Mean depth	Length	Breadth	Area	Volume	Open days	pH
Altitude	1.0000																		
Max.alt.	0.0038	1.0000																	
D.sea	0.7609	0.0911	1.0000																
Catch.area	-0.4291	0.5798	-0.0851	1.0000															
% ice	0.3828	0.5838	0.4007	0.3970	1.0000														
% QMS	0.1140	-0.6117	-0.5332	-0.3750	-0.6972	1.0000													
% amph.	-0.2956	0.0561	0.3002	-0.2864	-0.3681	0.0792	1.0000												
% marble	-0.3283	-0.1270	-0.0673	-0.4889	0.0257	0.1676	-0.2233	1.0000											
% moss	-0.0018	-0.2310	-0.2499	-0.0010	-0.2029	0.3372	-0.1552	0.0659	1.0000										
% lichen	0.1742	-0.2594	-0.3633	0.0901	-0.1688	0.2345	-0.1348	0.1464	0.6718	1.0000									
Catch:lake	0.2171	0.5112	0.1982	0.5518	0.6211	-0.3347	-0.1376	-0.1174	-0.2672	-0.3048	1.0000								
Max.depth	-0.3075	0.2646	0.2485	0.1573	0.0775	-0.4768	0.2157	-0.2561	-0.2093	-0.0333	-0.2784	1.0000							
Mean depth	-0.2262	-0.0005	0.1516	0.0173	-0.0218	-0.4202	0.1712	-0.3326	-0.2802	-0.4203	-0.2786	0.8858	1.0000						
Length	-0.4613	-0.1651	-0.1804	0.1742	-0.3161	0.0621	-0.0423	-0.1776	0.4434	0.4522	-0.5983	0.4784	0.3836	1.0000					
Breadth	-0.2262	0.0598	-0.1539	0.2585	-0.0366	-0.2040	-0.1683	-0.0010	0.1988	0.5040	-0.5172	0.5872	0.4212	0.8091	1.0000				
Area	-0.4613	-0.0049	-0.2486	0.3219	-0.2104	0.0708	-0.1882	-0.1792	0.4168	0.3315	-0.4476	0.3564	0.1895	0.9195	0.7377	1.0000			
Volume	-0.0615	0.0959	0.0165	0.2536	-0.0583	-0.3593	0.0047	-0.3042	-0.0067	0.1665	-0.4408	0.8549	0.7833	0.7987	0.8145	0.7212	1.0000		
Open days	-0.8759	0.1578	-0.5912	0.4038	0.0574	0.2714	-0.4318	-0.1331	0.0122	0.0623	0.0517	-0.0343	-0.1122	0.2242	0.2474	0.4501	0.1615	1.0000	
pH	-0.3016	-0.1241	-0.3948	-0.3611	-0.3554	0.4729	0.2978	-0.1626	0.0846	-0.0744	-0.2231	-0.3499	-0.2557	-0.1931	-0.3314	-0.1573	-0.3496	0.3093	1.0000
Cond.	-0.2034	-0.0611	-0.5012	-0.0580	-0.3062	0.3311	-0.0266	0.0880	-0.1634	-0.1565	0.1666	-0.3209	-0.2020	-0.2580	-0.2678	-0.1146	-0.2074	0.1661	0.1323
Chl-a	-0.3631	-0.3646	-0.3265	-0.3278	-0.3718	0.5017	-0.2047	0.4443	0.3864	0.1299	-0.3212	-0.2589	-0.2441	0.3754	0.0197	0.4530	0.0042	0.2942	0.1561

Shaded cells have a significance level of $p<0.001$ where $r=0.606$ for 15 degrees of freedom

Table 3.8 (contd.)

Phaeo.	-0.2903	-0.3964	-0.3426	-0.4075	-0.4656	0.5620	0.0208	0.1221	0.4577	0.0505	-0.3520	-0.3265	-0.2256	0.2921	-0.1922	0.3526	-0.0917	0.2066	0.4828
NH_4	-0.3851	-0.0142	-0.4143	-0.0799	-0.2206	0.5244	0.2079	-0.2134	-0.1427	-0.2833	0.2734	-0.4128	-0.2949	-0.3912	-0.6171	-0.2289	-0.4441	0.4144	0.6639
NO_3	-0.4006	0.2588	-0.2225	0.3610	-0.1455	0.2362	0.3108	-0.5268	-0.1512	-0.2488	0.4173	-0.1347	-0.1442	-0.2291	-0.4033	-0.0217	-0.1651	0.4083	0.3956
TDN	-0.5805	-0.1431	-0.5940	0.1046	-0.5753	0.6107	0.2681	-0.4280	0.0431	0.0285	-0.0150	-0.1412	-0.0426	0.0538	-0.1997	0.1226	-0.0545	0.4375	0.5446
TP	-0.4442	-0.1260	-0.5468	-0.0758	-0.4694	0.6425	0.2200	-0.1697	-0.2984	-0.1696	0.1068	-0.3821	-0.2753	-0.1502	-0.4310	-0.0169	-0.2984	0.3687	0.5601
SRP	-0.4079	0.0491	-0.4177	-0.0421	-0.1574	0.4414	0.2278	-0.2088	-0.2217	-0.2687	0.2345	-0.3215	-0.2416	-0.3174	-0.4147	-0.1555	-0.3178	0.5118	0.6866
SRS	-0.2481	-0.2963	0.0739	0.1342	-0.3032	0.3175	-0.0742	-0.0571	0.0670	-0.0865	0.2528	-0.2145	-0.1708	-0.1244	-0.3742	-0.0158	-0.2125	0.0731	-0.1401
Cl^-	-0.4766	-0.0856	-0.5745	0.0381	-0.5839	0.4532	0.0399	0.0841	-0.1394	0.0100	-0.2286	0.0966	0.0620	0.2435	0.2244	0.2604	0.2014	0.3537	0.0731
Na^+	-0.3167	-0.2842	-0.4085	-0.3227	-0.4755	0.4885	-0.0295	0.0749	-0.1252	-0.2941	-0.0867	-0.4874	-0.2978	-0.2217	-0.5010	-0.0942	-0.3680	0.2838	0.5794
K^+	-0.1306	-0.0284	-0.3807	-0.4742	-0.3457	0.5153	0.2956	0.1443	-0.1609	-0.3059	-0.1061	-0.4566	-0.4019	-0.4161	-0.5267	-0.3708	-0.5512	0.1380	0.7959
Mg^{2+}	-0.2695	0.0344	-0.3825	-0.2676	-0.2804	0.3336	0.3027	-0.1095	-0.2051	-0.2510	0.0001	-0.3275	-0.2021	-0.3134	-0.4428	-0.2214	-0.3372	0.3390	0.8730
Ca^{2+}	-0.2762	-0.0435	-0.5204	-0.3160	-0.3206	0.4709	0.1628	0.0246	-0.0533	-0.1181	-0.0327	-0.5944	-0.4640	-0.4209	-0.5065	-0.3421	-0.5785	0.2369	0.8615
Clarity	0.3014	-0.4141	0.1954	-0.1496	-0.2792	-0.1013	0.2185	-0.1394	-0.0926	0.2948	-0.2802	0.1792	0.3507	0.0144	0.1687	-0.1773	0.1496	-0.4331	-0.1399
Feb.WT	-0.6465	0.0755	-0.5537	0.2892	0.0368	0.3518	-0.1005	-0.2985	-0.0159	0.0151	-0.2128	-0.2718	-0.2143	-0.0370	-0.0251	0.0462	-0.1558	0.6823	0.5076
Jul.WT	-0.0201	0.0833	0.3226	0.0599	0.1574	-0.3040	0.0657	0.2123	-0.1294	0.1492	-0.1222	0.5544	0.4068	0.3040	0.5231	0.2098	0.4662	0.1304	-0.2454
Oct.WT	0.2243	0.1408	0.4963	0.1192	0.2065	-0.4832	0.2453	-0.1093	-0.3490	-0.0743	-0.1294	0.7377	0.6341	0.3257	0.5200	0.1805	0.6156	-0.0453	-0.3434
Pseud.	-0.2114	-0.2978	-0.4465	-0.0847	-0.7241	0.3174	0.1683	-0.1416	0.1521	0.3284	-0.6175	0.3097	0.3271	0.4653	0.4863	0.3435	0.4413	-0.0013	0.0569
Branch.	-0.5707	-0.0892	-0.4066	0.1313	-0.0716	0.4461	-0.2185	-0.2491	0.1114	-0.1567	0.2447	-0.4529	-0.3346	-0.1897	-0.4773	-0.0051	-0.3668	0.5558	0.4665
Moss	0.2589	0.1007	0.3248	0.2014	0.2493	-0.4655	0.1286	-0.2420	-0.1869	-0.1407	-0.2029	0.6571	0.4835	0.3958	0.5881	0.2849	0.5949	-0.0930	-0.2953
Mat	0.2372	-0.0799	0.0822	0.1220	-0.0356	-0.2165	-0.1405	-0.0269	0.1805	0.3371	-0.0604	0.2201	0.3219	0.1237	0.2062	-0.1478	0.1435	-0.5128	-0.5041
Birds	-0.2659	0.1007	-0.3894	-0.4403	-0.4401	0.4885	0.1405	0.3830	0.4577	0.0889	-0.3243	-0.2246	-0.2797	0.0902	-0.1347	0.0757	-0.2279	0.1029	0.5661
Fur	-0.8300	-0.0799	-0.7451	0.3866	-0.2725	0.4412	-0.0740	-0.1224	0.3596	0.4833	-0.0160	-0.1463	-0.2151	0.3599	0.2768	0.5067	0.1280	0.6990	0.2830
Elephant	-0.6601	-0.0799	-0.4428	0.1926	-0.4094	0.5826	-0.0175	-0.1993	0.3902	0.0984	-0.1091	-0.1958	-0.3062	0.3997	0.0276	0.6092	0.0675	0.5745	0.3109
	Altitude	*Max.alt*	*D.sea*	*Catch. area*	*% ice*	*% QMS*	*% amph.*	*% marble*	*% moss*	*% lichen*	*Catch: lake*	*Max. depth*	*Mean depth*	*Length*	*Breadth*	*Area*	*Volume*	*Open days*	*pH*

Table 3.8 (contd.)

pH	1.0000																	
Cond.	0.1323	1.0000																
Chl-a	0.1561	0.1621	1.0000															
Phaeo.	0.4828	0.1536	0.8601	1.0000														
NH_4	0.6639	0.5603	0.2088	0.4388	1.0000													
NO_3	0.3956	0.4673	-0.0613	0.1419	0.8017	1.0000												
TDN	0.5446	0.5709	0.1607	0.3615	0.7899	0.7739	1.0000											
TP	0.5601	0.7229	0.3351	0.5134	0.9060	0.7293	0.8963	1.0000										
SRP	0.6866	0.5913	0.1173	0.3098	0.9263	0.7586	0.7655	0.8672	1.0000									
SRS	-0.1401	0.1829	0.2798	0.1948	0.2483	0.4273	0.2826	0.2429	0.0511	1.0000								
Cl	0.0731	0.6050	0.2685	0.0938	0.2729	0.2419	0.6140	0.5551	0.3478	0.1211	1.0000							
Na^+	0.5794	0.4179	0.5652	0.6592	0.6593	0.3941	0.4898	0.6295	0.5102	0.4127	0.2801	1.0000						
K^+	0.7959	0.3291	0.2232	0.4150	0.6979	0.3029	0.4639	0.6378	0.6444	-0.1462	0.2866	0.6634	1.0000					
Mg^{2+}	0.8730	0.3602	0.2302	0.4594	0.8013	0.5596	0.6108	0.6956	0.8015	-0.0150	0.2236	0.7507	0.8253	1.0000				
Ca^{2+}	0.8615	0.3739	0.1813	0.4168	0.7235	0.3984	0.5201	0.6353	0.6687	-0.0743	0.1807	0.7371	0.9077	0.8894	1.0000			
Clarity	-0.1399	-0.1902	-0.4261	-0.3551	-0.3861	-0.2017	-0.1561	-0.3816	-0.3749	0.1358	-0.2215	-0.1860	-0.3716	-0.2579	-0.2132	1.0000		
Feb.WT	0.5076	0.2335	-0.0591	0.0741	0.5430	0.4240	0.5309	0.5034	0.6946	-0.2101	0.2296	0.1196	0.3343	0.4133	0.4195	-0.3117	1.0000	
Jul.WT	-0.2454	-0.4314	0.0104	-0.2843	-0.4560	-0.2680	-0.3357	-0.4909	-0.2730	0.0172	0.0179	-0.3487	-0.4251	-0.2269	-0.4828	0.1849	-0.1501	1.0000
Oct.WT	-0.3434	-0.5175	-0.2820	-0.4462	-0.5179	-0.2472	-0.3888	-0.5777	-0.3432	-0.1335	-0.1200	-0.4949	-0.5048	-0.3461	-0.6020	0.3270	-0.1470	0.8421
Pseud.	0.0569	0.3328	-0.0356	-0.0267	-0.1150	-0.0192	0.4360	0.1993	-0.0258	-0.0591	0.6850	-0.0382	-0.0091	-0.0460	-0.0127	0.3443	-0.0069	-0.0063
Branch.	0.4665	0.1495	0.3203	0.4959	0.6932	0.5708	0.4653	0.5089	0.5147	0.4339	-0.0712	0.6345	0.3704	0.4716	0.5063	-0.2917	0.4923	-0.3996
Moss	-0.2953	-0.4077	-0.4470	-0.4668	-0.5464	-0.3626	-0.3375	-0.4607	-0.3226	-0.5988	-0.0239	-0.7128	-0.3647	-0.4505	-0.5460	0.0327	0.0405	0.3498
Mat	-0.5041	-0.2864	-0.3770	-0.4392	-0.6220	-0.5397	-0.3112	-0.5021	-0.6980	-0.0683	-0.0472	-0.4865	-0.4442	-0.6318	-0.4394	0.4364	-0.3189	0.0150
	pH	*Cond.*	*Chl-a*	*Phaeo.*	NH_4	NO_3	*TDN*	*TP*	*SRP*	*SRS*	*Cl*	Na^+	K^+	Mg^{2+}	Ca^{2+}	*Clarity*	*Feb WT*	*Jul WT*

Oct WT	
0.6259	
0.1137	

Table 3.8 (contd.)

Birds	0.5661	0.1135	0.5964	0.6497	0.2846	-0.0204	0.2797	0.3858	0.2470	-0.0496	0.3135	0.4198	0.6033	0.4706	0.5007	-0.4364	0.0819	-0.0539	-0.3761
Fur	0.2830	0.4050	0.3445	0.3182	0.4409	0.5296	0.6564	0.5499	0.4909	0.1206	0.4825	0.2310	0.1274	0.3271	0.3035	-0.2597	0.5475	-0.0595	-0.2651
Elephant	0.3109	0.3328	0.6005	0.6529	0.5386	0.5688	0.6823	0.6892	0.4943	0.3528	0.4429	0.4238	0.2285	0.3320	0.2428	-0.4871	0.3279	-0.2378	-0.4026
	pH	*Cond.*	*Chl-a*	*Phaeo.*	NH_4	NO_x	*TDN*	*TP*	*SRP*	*SRS*	*Cl*	Na^+	K^+	Mg^{2+}	Ca^{2+}	*Clarity*	*Feb WT*	*Jul WT*	*Oct WT*

Pseud.	1.0000						
Branch.	-0.3443	1.0000					
Moss	0.2025	-0.5883	1.0000				
Mat	0.3099	-0.4364	0.2568	1.0000			
Birds	0.1690	0.1273	-0.2568	-0.1905	1.0000		
Elephant	0.2941	0.4037	-0.3104	-0.3564	0.2321	1.0000	
Fur	0.1887	0.4871	-0.2866	-0.5262	0.3854	0.7106	1.0000
	Pseud.	*Branch.*	*Moss*	*Mat*	*Birds*	*Elephant*	*Fur*

Shaded cells have a significance level of $p<0.001$ where $r=0.606$ for 15 degrees of freedom

scheme and in a similar way, a bipartite division can be recognised: (i) glacier-fed and non ice-contact and (ii) non-glacier fed (Figure 3.2). Differences in glaciolacustrine sedimentation (section 2.3.2) in each type has important implications for the resultant sediment types in each lake basin (Karlén, 1981).

A trophic classification has been achieved using water chemistry and/or algal (diatom) species assemblages (Heywood, 1968; Hawes, 1990; Oppenheim, 1990; Jones & Juggins, 1995). Three trophic states occur in these lakes: oligotrophic, mesotrophic and eutrophic (Figure 3.3) and lake groupings relate to the genetic lake classes above. The non-glacier-fed lakes are more nutrient-enriched and either mesotrophic or eutrophic; glacier-fed lakes are oligotrophic. Mesotrophic lakes occur for special reasons. Mesotrophy in Light Lake probably occurs because of a combination of moss stands and bird colonies in its catchment (Heywood, Dartnall & Priddle, 1980) and there are indications of a shift towards mesotrophy in Sombre Lake, possibly resulting from fur seal activities (Jones, 1993).

The new environment data-set presented here provides the opportunity to update the lakes' classification in a holistic way considering the lake and catchment environments together. Classification of the 17 sites using the 44 environment variables data-set was performed using the program CLUSTER Version 2.60 (H.J.B. Birks, unpublished) which uses agglomerative hierarchical techniques (van Tongeren, 1987). Classification was performed in Euclidean distance and the data-set was standardised to zero mean and unit variance. Five methods (nearest neighbour, furthest neighbour, weighted group average, group average and minimum variance cluster analysis) were chosen to assess relative performances. Performance, the goodness of fit between the original (dis)similarity matrix and the dendrogram, is assessed using the cophenetic correlation coefficient. For any sample pair it is the lowest dissimilarity (or highest similarity) required to join the samples in the dendrogram. Large values of this coefficient ($r \geq 0.8$) indicate that the dendrogram provides a reasonable summary of the observed (dis)similarities (Everitt & Dunn, 1991).

All cluster methods resolve the data into 5 or 6 groups which share similar memberships (Table 3.9) and cophenetic correlations are all high ($r > 0.8$) suggesting that groups are reflecting real patterns in the data. Heywood, Amos and Bothy Lakes are found in the

Figure 3.2 Genetic classification of Signy lakes

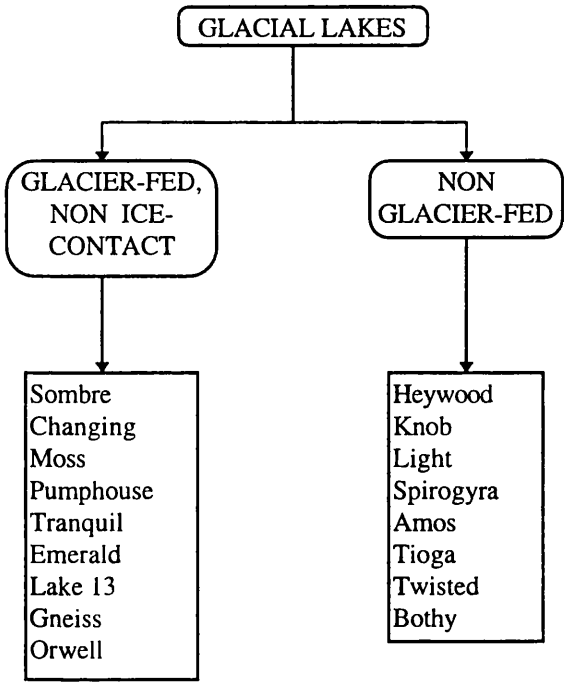

Figure 3.3 Trophic classification of Signy Lakes

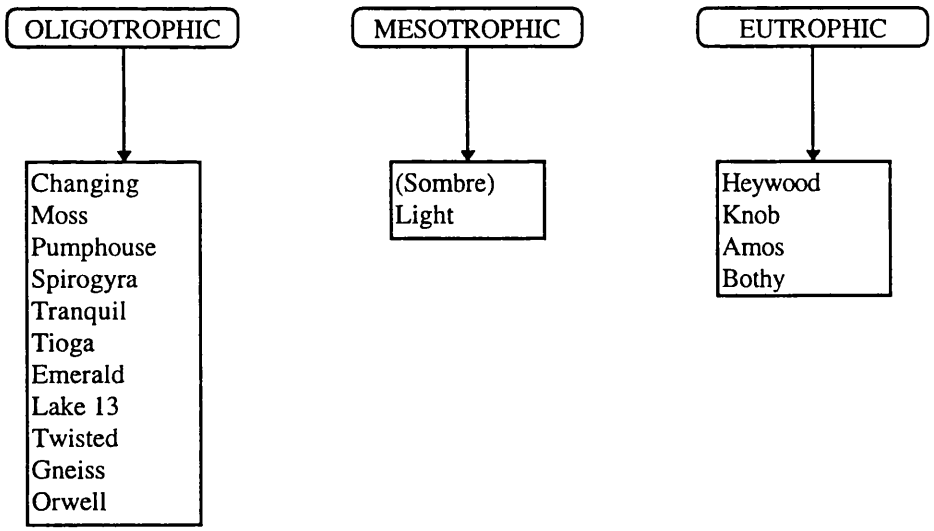

Table 3.9 Comparison of cluster groups of Signy environment data using 5 different hierarchical agglomerative cluster methods

Cluster group	*Nearest neighbour (single-link)*	*Furthest neighbour (complete link)*	*Weighted group average*	*Group average*	*Minimum variance (Ward's method)*
1	Bothy	Heywood, Amos, Bothy	Heywood, Amos, Bothy	Heywood, Amos, Bothy	Heywood, Amos, Bothy
2	Amos	Changing, Gneiss, Moss, Lake 13, Orwell	Changing, Gneiss, Moss, Lake 13, Orwell	Changing, Gneiss, Moss, Lake 13, Orwell	Changing, Gneiss, Moss, Lake 13, Orwell
3	Heywood	Tranquil, Twisted, Emerald	Light, Spirogyra, Tioga, Tranquil, Twisted, Emerald	Light, Spirogyra, Tioga, Tranquil, Twisted, Emerald	Light, Spirogyra, Tioga, Tranquil, Twisted, Emerald
4	Knob, Changing, Gneiss, Moss, Lake 13, Orwell	Light, Spirogyra, Tioga	Knob	Knob	Knob
5	Light, Spirogyra, Tranquil, Twisted, Emerald, Tioga	Knob	Sombre, Pumphouse	Pumphouse, Sombre	Sombre, Pumphouse
6	Pumphouse, Sombre	Sombre, Pumphouse	nil	nil	nil
cophenetic correlation	0.919353	0.889297	0.900074	0.900773	0.848380
delta one hat	0.334286	0.337707	0.170073	0.169533	2.50265
Gower's delta	4.320006E+07	-5.403029E+07	-4.029828E+06	3.166818E+06	-2.121857E+14

Shaded cells = adopted classification scheme

first group in 4 methods; Changing, Gneiss, Moss, Lake 13 and Orwell Lakes are found in the second group in 4 methods; Sombre and Pumphouse occur together in the last group. Knob Lake is clearly different from the others and occurs singly in 4 methods. Light, Spirogyra, Tranquil, Twisted, Emerald and Tioga Lakes are similar and tend to occur together. Group average cluster analysis was also used by Jones & Juggins (1995) with diatom-water chemistry data from Signy and Livingston Island lakes and for comparative purposes it is adopted here and used to classify the sites on the ordination

biplot (Figure 3.5).

Results of various qualitative and quantitative classifications of the Signy Lakes are summarised in Figure 3.4. Common groupings are evident along a trophic gradient. Oppenheim (1990) found 3 groups from a sub-set of 11 on the basis of diatom-assemblage composition which matches the three genetic-trophic categories (proglacial, oligotrophic, mesotrophic). The proglacial Khyber lakes were not sample in this study owing to scarcity of sediment. Priddle & Belcher's (1982) classification using algal ecology (chlorophytes and cyanophytes) identified Heywood, Tioga and Orwell Lakes as outliers with high leverage; once removed, further site groupings were found in the complement of lakes, bearing similarities to the genetic and trophic classifications. Heywood, Dartnall & Priddle's (1980) factor analysis of physico-chemico data found that nutrient status and lake morphology largely determined the characteristics of the lakes; maximum (mean) depth determined the winter lake environment but proximity to the sea and associated influences controlled the summer environment. Changing, Tioga, Lake 13, Gneiss and Orwell Lakes were seen to be very individual lakes with characteristics which could not be easily related to the others. Jones, Juggins & Ellis-Evans (1993) classification also included sites from Livingston Island hence resolved the Signy Lakes into two groups. One of these was further sub-divided into two: Group 3a (Sombre, Heywood, Changing, Moss, Knob, Light, Spirogyra, Tranquil, Bothy) and Group 3b (Tioga, Emerald, Twisted). Amos Lake was an outlier associating with lakes of high nutrient concentrations and/or conductivities. Lake 13 and Orwell Lakes were not included in their data-set. Redundancy analysis showed that diatom species abundance was predominantly related to nutrient and salinity gradients in the lakes.

Excluding the Livingston Island lakes and increasing the number of variables, this classification finds a better separation of sites, resolving 5 groups in cluster analysis. Heywood, Amos, Knob and Bothy Lakes are clearly strongly nutrient-enriched and have similar lake-catchments. The minor dissociation of Sombre and Pumphouse Lakes from the other oligotrophic lakes and intermediate position with more nutrient-enriched lakes perhaps reflects the recent influence of fur seals which populate their catchments over the summer. Orwell Lake is an outlier site in other classifications but this analysis places it in a proglacial group including Lake 13, Gneiss and Spirogyra Lakes.

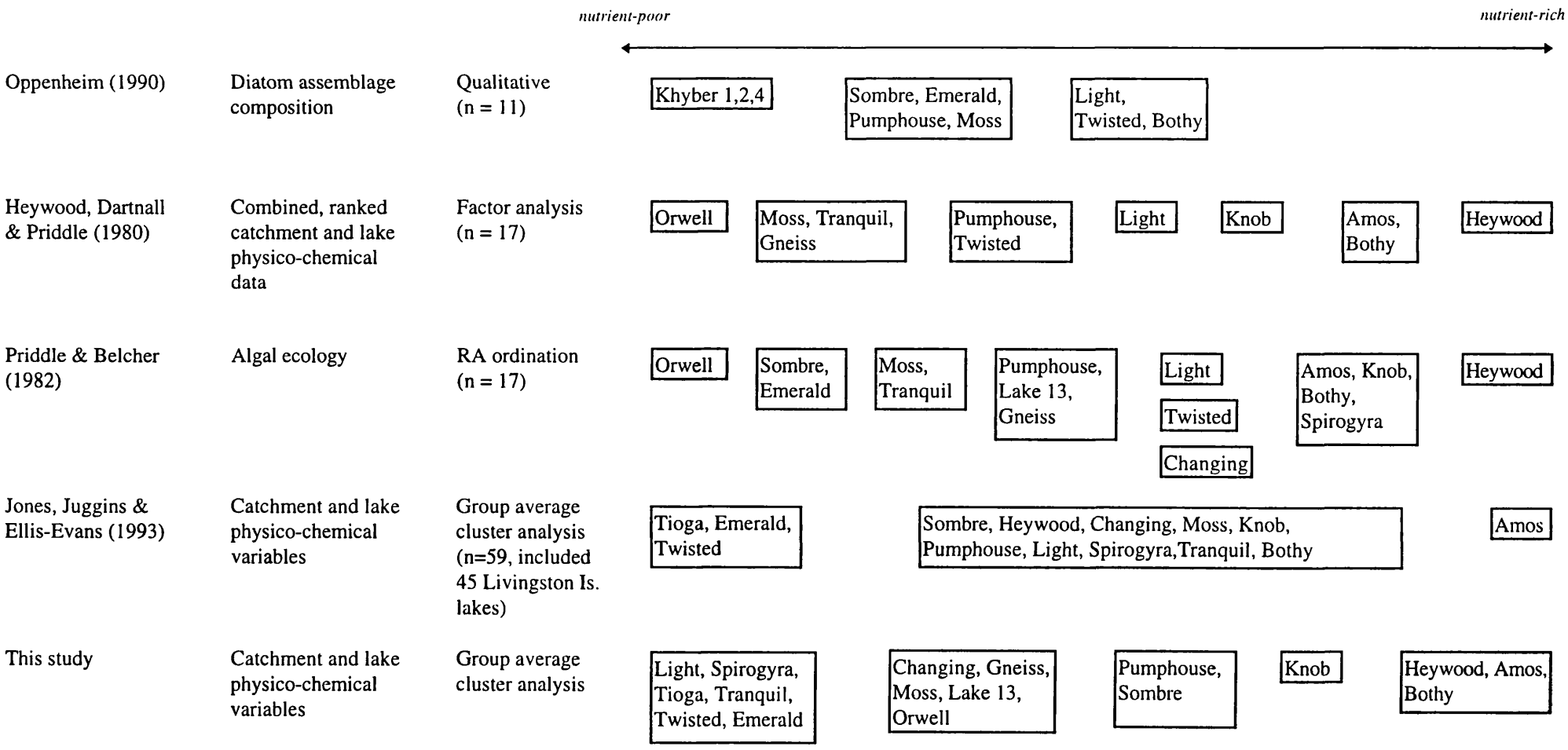

Figure 3.4 Various classifications of the Signy Lakes

3.6.3 Ordination

Ordination is a useful tool for studying relationships between group composition and the environment (Gauch, 1982; Jongman *et al.*, 1987). Principal components analysis (PCA) was used to explore and summarise the major patterns of variation within the environment data-set. Data analysis was performed in CANOCO (ter Braak, 1988, 1990). The correlation matrix was centred and standardized by species (the environmental variables) but not centred by samples (lakes). No transformation of species data was performed since data standardisation reduces the variables to means of zero and variances of one. This standardisation tends to inflate variables whose variance is small and reduces the influence of variables whose variance is large. This is undesirable but unavoidable since the original variables are expressed in different, incompatible units (Davis, 1973).

PCA was performed on the 17 lakes by 44 environmental variables data matrix. Eigenvalues and cumulative percentage variance accounted-for in the first four PCA axes are listed in Table 3.10. Eigenvalues in the PCA are fractions of the total variance in the sites data (percentage variance accounted for).

Table 3.10 Eigenvalues and cumulative variance accounted for in PCA of the 17 lakes and 44 environmental variables

PCA axes	*1*	*2*	*3*	*4*	*Total variance*
Eigenvalues	0.312	0.147	0.116	0.097	1.000
Cumulative % variance of species data	31.2	45.9	57.5	67.2	
Σ *unconstrained eigenvalues*					1.000

The first four axes capture 67.2% of cumulative variance, a good proportion given the noise in this large, mixed-value data-set. There are many approaches to determine how many components should be interpreted in PCA (Jackson, 1993) and the most consistent results have been obtained from the broken-stick model. This model is based on eigenvalues from random data and assumes that if the total variance (i.e. sum of eigenvalues) is divided randomly amongst the various components, then the expected distribution will follow a broken-stick distribution in a 'scree plot' of eigenvalue versus ordination axis number. Observed eigenvalues are considered interpretable if they exceed eigenvalues generated by the broken-stick model. The program BSTICK (H.J.B. Birks,

unpublished) uses the number of variances, i.e. 44 variables, and the total variance, i.e. 1.000 and specifies cut-off levels. For example, for axis 1, if % variance is >9.938% and the eigenvalue is >0.099, sufficient variance is captured to explain pattern in the data. Successive axes have smaller cut-off values. All four axes in Table 3.10 are significant and should give meaningful interpretations.

The first axis captures 31.2% of variance and defines a gradient between high values for nutrients (total phosphorus, ammonium, total nitrogen) and productivity indicators (phaeopigments, Chl-*a*), major cations, pH, exposed bedrock, *Branchinecta*, seals, high summer water temperatures, conductivity, bird colonies, the open water period and chloride ions versus high values for distance from the sea, high winter water temperatures, benthic vegetation, depth effects, breadth, clarity, % ice-cover. This division clearly represents a nutrient gradient from coastal, eutrophic lakes affected by nutrient enrichment from marine sources (sea-spray, birds and seals) versus inland, oligotrophic lakes. Lakes with positive PCA axis 1 sample scores include (in descending rank order) Amos, Bothy, Heywood, Knob, Tioga, Light and Spirogyra Lakes; those with negative PCA axis 1 sample scores include Emerald, Moss, Tranquil, Changing, Twisted, Gneiss, Sombre, Pumphouse and Orwell Lakes and Lake 13.

The second axis is less influential (0.147) but a significant gradient exists between lake morphometric variables (area, length, breadth, volume), seal numbers, *Pseudoboeckella*, the period of open water, productivity and catchment vegetation cover versus catchment determinants (high values for altitude, catchment:lake area ratio, distance from the sea), % ice-cover, major cations (Ca^{2+}, K^{+} and Mg^{2+}, all potential subglacial weathering products) and % amphibolite. Lakes with positive PCA axis 2 scores (in descending rank order) include Heywood, Knob, Sombre, Emerald, Pumphouse, Tranquil, Twisted, Moss, Light, Changing, Amos, Tioga, Bothy and Spirogyra Lakes. Only Lake 13, Gneiss and Orwell Lakes have negative PCA axis 2 sample scores.

Clear site differences and groupings are evident on the biplot of PCA axis 1 versus axis 2 scores (Figure 3.5). The biplot is a joint representation of site and environmental data using site or sample scores and environmental loadings (Jongman *et al.*, 1987). Variables with high positive correlations have small angles between their biplot arrows (ter Braak, 1990) and longer arrows are more important in the data-set. Clusters of arrows relate to the main environmental gradients and close associations indicate multicollinear relations

Figure 3.5 **Biplots of PCA axis 1 and 2 scores for the 17 sites by 44 environment variables data-set (a) environment variables (b) sites**

(a) Environment variables (n=44)

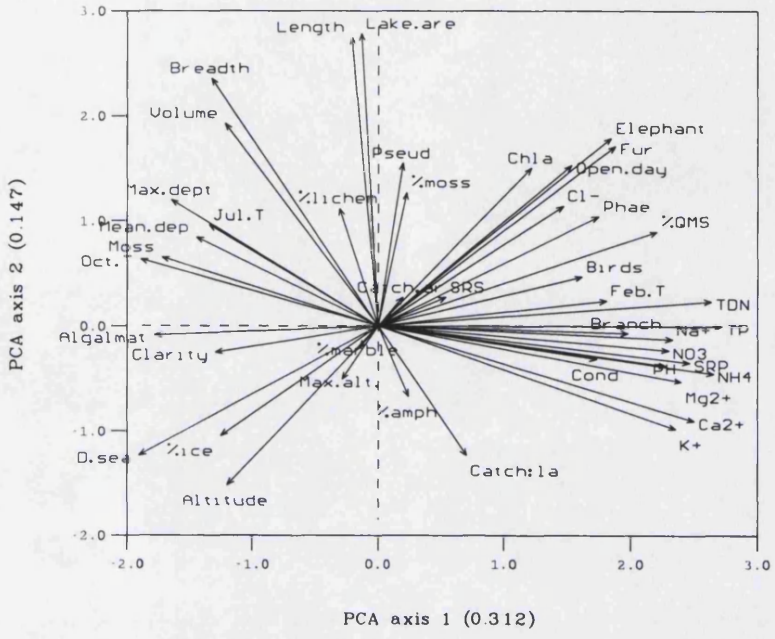

(b) Sites classified by group average cluster groups (n=5)

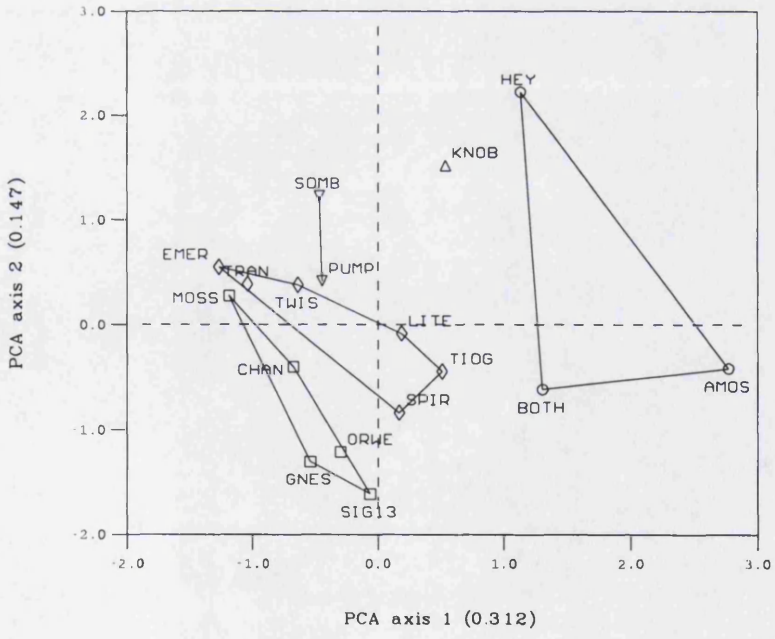

○ Group 1 □ Group 2 ◊ Group 3 △ Group 4 ▽ Group 5

between variables which are also identified in the correlation matrix (Table 3.8). Sites are classified by their memberships in group average cluster analysis (Table 3.9).

The first axis gradient (nutrient-rich versus nutrient-poor) clearly separates Group 1 (Heywood, Amos and Bothy Lakes) from the others, with very high values for nutrients, major cations, conductivity, ammonium, pH, productivity indicators, high summer water temperatures, *Branchinecta*, largely deglaciated catchments and bird colonies and seals. Heywood Lake is determined to a greater degree by the second PCA axis, strongly influenced by lake morphometric parameters (area, length). Group 2 (Changing, Gneiss, Moss, Lake 13 and Orwell Lakes) is associated with the negative end of the axis 1 gradient, with high values for catchment ice-cover, altitude, distance from the sea, clarity, benthic vegetation and high winter water temperatures, all essentially oligotrophic attributes. Group 3 (Light, Spirogyra, Tioga, Tranquil, Twisted, Emerald) includes environmental components across the PCA axis 1 gradient but with a tendency towards more oligotrophic attributes, higher altitudes and greater distances from the sea, marble and amphibolite lithologies and depth effects. Spirogyra, Tioga and Light Lakes occupy intermediate positions along PCA axis 1 with indistinct characteristics. Knob Lake is the sole member of Group 4 and closely relates to Heywood Lake but is more influenced by lake morphometry (length and area), catchment vegetation and *Pseudoboeckella*. Group 5 (Pumphouse and Sombre Lakes) is similar to Group 2 but has a stronger morphometric influence (volume, breadth, area, length) and more catchment vegetation.

Summarily, PCA axis 1 separates lakes on the basis of nutrient-rich, productive, low-lying, shallow basins, with largely deglaciated and vegetated catchments, highly influenced by the marine environment versus oligotrophic, higher altitude sites with a greater proportion of catchment ice-cover, longer periods of lake ice-cover, and clear oligotrophic waters supporting perennial benthic vegetation. Different source lithologies affect certain lakes. These environmental gradients are very similar to those observed by Heywood, Dartnall & Priddle (1980) and Jones, Juggins & Ellis-Evans (1995) reflecting the real nature of the environmental gradients and common origin of the data.

3.7 Discussion

3.7.1 Lake environments

Thirty variables are used to summarise the lake environment including measures of lake

morphometry and site, climate and water chemistry (Figure 3.1). All the lakes are glacial in origin, small (<4.3 hectares) and generally take the form of a central trough surrounded by a sub-lacustrine shelf 1-2 metres deep formed by moraine damming. All the lakes are freshwater, even those close to the coast. With the exception of Pumphouse Lake, which has undergone some anthropogenic modification of its shoreline, all lakes are natural systems. Strong seasonal gradients produce high interannual variability in physical, chemical and biological processes but the synthesis of several years data as mean values to match the resolution of the surface-sediment samples (Chapter 4) smooths interannual variability, so emphasizing spatial effects (site differences) over temporal effects in data analysis. Lake water chemistry, especially nutrient status, strongly determines differences in the lake environments in PCA and this gradient is also reflected in the results of cluster analysis. Site groupings closely match those of Jones, Juggins & Ellis-Evans (1993). The major environmental gradient contrasts indicators of high trophic status (total phosphate, soluble reactive phosphate, total dissolved nitrogen, chlorophyll-*a* and phaeopigments) and associated ions (calcium and magnesium) with nutrient-poor, higher-altitude inland sites with low productivity but high benthic biomass.

The marine influence is ubiquitous and all lakes receive some nutrient and ion inputs from precipitation and snowmelt (Allen, Grimshaw & Holdgate, 1967; Hawes, 1983). Naturally, these effects are greatest near the coast. Eutrophication is most enhanced in lakes which are affected by biotic agents; seals are positively correlated with nutrients (TDN and TP) and productivity indicators, supporting the causal link for enhanced eutrophication identified in Heywood Lake by Ellis-Evans (1990). Shallow lakes of the coastal zone also have higher summer water temperatures and longer periods of open water to sustain a seasonal phytoplankton population. Phytoplankton growth in summer is responsible for the poor clarity of these eutrophic lakes (Heywood, Knob, Amos and Bothy Lakes). Wind exposure additionally increases turbidity of the lake waters. *Branchinecta* positively correlate (r=0.56, p<0.05) with shallow, productive sites as they require algae as food sources and longer summer seasons to complete their life cycle (Björck *et al.*, 1996). The presence of *Branchinecta* in Lake 13 is interesting since it has not been recorded at this site before; shallowing of the lake profile by silting and reduced meltwater inputs with a shift in the ice-front has created a more favourable environment for their existence. *Pseudoboeckella* is less clearly related to lake trophy but favours shallow waters within the photic zone for algal food sources.

Most lakes are ice-free for 3-4 months per year and ice-cover duration has been decreasing over the past 25 years, probably in response to climatic change (Smith, 1990). Unfortunately regression reconstructions with air temperature records have failed to find good agreement (R. Thompson, *pers.comm.*). Maximum summer water temperatures reach 5-6°C. A seasonal temperature component is found in the second ordination gradient; the three temperature variables are the only determinants in the data-set which directly integrate seasonal lake climate. The water temperature gradient reflects lake morphometry, especially basin depth, as well as altitude, exposure, length of the open water period, the influence of influent meltwaters and bottom warming. Lowland eutrophic lakes, such as Heywood, Amos and Bothy, typically have high summer surface water temperatures; longer open water periods allow more warming and the number of open days is positively correlated with high summer water temperatures (r=0.68, p<0.01). Winter temperatures are lower due to heat conduction through the lake ice (Heywood, 1968) with minimal insulation by irregular snow-cover; minimum winter temperatures are close to zero and are observed in Heywood, Knob, Spirogyra, Tioga and Bothy Lakes. The opposite trend is observed in inland oligotrophic lakes. High through-flow of meltwater in summer depresses lake water temperatures, especially in glacier-fed lakes such as Emerald, Tranquil, Sombre, Pumphouse, Moss and Changing; winter temperatures are higher because longer periods of lake ice-cover coupled with a seasonal snow-cover, encouraged at these sites by topographic shelter, insulates the lakes from heat losses by conduction. Data-set bias also enhances these temperature effects since water temperature readings are surface values which show greater variability than bottom waters. Unfortunately, lack of detailed records of snow-cover over the lake ice led to its preclusion as a variable in the analysis.

Morphometric variables have significant collinear relationships (Table 3.8) and morphometry is an important determinant of between-lake variation in PCA, separating lakes on the basis of their overall size and depth. Maximum depth was a highly significant determinant of lake character in a previous lake classification scheme (Heywood, Dartnall & Priddle, 1980). There is a clear gradient in ordination of vegetation type in lakes of contrasting trophies and morphometries. Only the deeper lakes with larger volumes, low concentrations of suspended materials, good light transmission and quiescent conditions favour the support of perennial phytobenthos (Light & Heywood, 1973; Hawes, 1990). A large influx of summer runoff from the surrounding catchment, greatly in excess of the lakes' total volume (Ellis-Evans &

Wynn-Williams, 1985) and short residence times in lakes with a high catchment:lake area ratio (Hawes, 1990) bring sufficient nutrient supplies into even the most oligotrophic lakes to maintain a high benthic biomass in the form of filamentous algae and freshwater mosses which are extremely efficient nutrient sequesters (Hawes, 1988). Therefore, oligotrophic lakes (e.g. Moss Lake) can support complex perennial communities despite their isolation from marine nutrient sources and short periods of open water. Lakes with small basin volumes are prone to winter anoxia (Hawes, 1983), significantly affecting algal mat growth (Gallagher, 1985) and when extreme, causing complete degradation of the phytobenthos (Hawes, 1988). In the deeper lakes, anoxia is restricted to greater depths: for example, below 9 metres in Sombre Lake.

3.7.2 Catchment environments

Fourteen variables in the data-set characterise the catchment environment including measures of site, exposed bedrock, land-cover and fauna (Figure 3.1). Some variables do not possess the same temporal precision owing to lack of recent survey data (e.g. bedrock and vegetation) but their values are still sufficiently representative of the adopted 1993 control year to provide a meaningful addition to the analysis. Catchments vary in complexity from domination by permanent ice-cover to extensive areas of moss vegetation, often frequented by birds and seals. Catchment development is matched by characteristic lake trophies in PCA (cf. Priddle & Heywood, 1980). The principal bedrock - quartz-mica-schist - shows maximal exposure in the deglaciated coastal lowlands. The interplay of % marble and % amphibolite in the second PCA gradient suggests some source-lithology effects on lake characteristics, associated with oligotrophic waters, ice-cover and altitude (Moss, Pumphouse, Light, Gneiss Lakes). Smith (1990) noted the alkaline reactions of morainic materials and cations (Ca^{2+}, Mg^{2+}, K^{+}) in these lakes probably derive from sub-glacial materials independent of marine sources. Mackereth (1966) regarded these cations as glacial indicators in lake sediment sequences.

The overall island altitude is not particularly high (maximum 279 metres) but still provides an environmental gradient affecting lake character. This is strongly associated with distance from the sea and catchment ice-cover. Altitude is a surrogate variable for accessibility by marine organisms to the lakes. Thus lakes at high altitude are too remote for marine organisms and are largely excluded from nutrient-enrichment. Altitude is too close to sea level to significantly affect air temperatures but it indirecly integrates a

climatic component since permanent ice cover is largely restricted to higher ground. Ice cover in PCA has a strong effect on site groupings. Moss and lichen vegetation commonly occur together sharing a significant relationship (r=0.67, p<0.01). In this analysis, the lakes are more sensitive to the presence or absence of vegetation rather than actual vegetation type. The gross categories of 'moss' and 'lichen' lack a significant response to other catchment variables unlike the more detailed study by Jeffers (1977) who identified several significant environmental variables explaining terrestrial vascular plant distributions on Signy Island. The mesotrophic status of Light Lake may be partly explained by percolation through moss stands leading to higher nutrient loadings (Collins, Baker & Tilbrook, 1975).

3.8 Summary

(1) The available environmental data consists of 44 physical, chemical, and biological variables of lake and catchment sources that are thought to be ecologically important. The data are of mixed units (binary, ordinal, percentage, quantitative) calling for special treatment in numerical analysis. Many variables are highly-correlated, introducing redundancy into the data-set. The only explicit climate variables in the data-set are seasonal water temperatures. The open water period and catchment ice cover are climate proxy-variables, known to be responsive to air-temperature variations. Both have shown behavioural changes in the period of recent climate warming, with an increase in the length of the open water period and a significant wastage of the island's ice cover over the last twenty years.

(2) The lakes display large gradients in lake and catchment environment including nutrients, productivity, altitude, depth, duration of lake ice cover, water temperature and catchment ice cover, which are likely to affect lake-sediment characteristics (Chapters 5, 6 and 7). Seals are included as a quantitative variable for the first time. Their effects on water chemistry have been noted by previous authors and strong correlations with nutrient variables confirm the hypothesis that their activities are causing an enhanced eutrophication of lowland lake systems. Results of ordination and classification suggest that catchment complexity is not the only determinant of lake trophic status (cf. Priddle & Heywood, 1980) and a multitude of environmental factors simultaneously determine lake characteristics. The most significant explanatory variables determining lake sediment characteristics are selected in numerical analysis in Chapters 5, 6 and 7.

CHAPTER 4: SAMPLING STRATEGY

4.1 Introduction

Following Birks's (1995) rationale of quantitative reconstructions, modern-species environment relationships - represented by a 'training set' of surface sediment samples and matching contemporary environmental data - can be used to produce a predictive inference model of a past environmental variable by adopting a uniformitarian approach (calibration). Ideally, a modern training set should comprise at least 100 sampling points and should cover long environmental gradients to ensure model robustness (Birks, 1995). Previous diatom-based transfer-functions have used large numbers of lakes to overcome some of the problems associated with calibration and insufficiently long environmental gradients, for example, the SWAP dataset for pH reconstructions (Battarbee & Renberg, 1985; Battarbee *et al.*, 1990; Birks *et al.,* 1990) and the Great Plains Region data-set of Northern North America for salinity reconstructions (Fritz *et al.*, 1991). The diatom-water chemistry training set for the maritime Antarctic (Jones, Juggins & Ellis-Evans, 1993) used single samples from 59 sites to produce a chlorophyll-*a* transfer function for nutrient reconstructions. Signy Island is geographically restricted and the number of lakes is finite (n=17). To capture sediment types representative of the full range of sedimentary environments the training set must be expanded by multiple sampling within each lake basin.

Two austral summer seasons of palaeolimnological sampling were undertaken at Signy Island (1993/94 and 1994/95) and the lakes were sampled for both short and long sediment sequences to provide material for the training set and for calibration. This Chapter presents the sampling strategy adopted, the fieldwork methodology and the resultant number of sampling points in each lake basin. Sediment distribution patterns are described for each lake and an appraisal made of the factors controlling contemporary patterns of sediment deposition.

4.2 Sampling strategy

4.2.1 Spatial resolution

Sedimentation is not necessarily uniform across lake basins and different patterns of sediment accumulation occur over space and time with changing dynamics of the limnic system. In any one year, sediment of uniform composition may be deposited in differing thicknesses at the same location. The greatest accumulations of stratified sediment are

not always found at the deepest point of the lake and may even be absent (Anderson, 1990a). Sediment movement from shallower to deeper water is a recognised phenomenon in lakes (Davis, 1968) and sediment focusing (Lehman, 1975) occurs for a number of reasons in addition to those related to basin morphometry (Hilton, 1985; Hilton, Lishman & Allen, 1986). The non-uniform nature of lacustrine sedimentation can prevent extrapolation to basin-wide characteristics (Dearing, 1986) so that any one core is unrepresentative of a whole lake. An areal spread of short cores at different depths is useful in assessing sediment variability prior to sampling for long sediment sequences, which should be continuous and undisturbed. Multiple-core investigations have become increasingly common (Bloemendal *et al.*, 1979; Anderson, 1990b; Zolitschka, 1996). Variability studies using replicate cores from deep basins have reached different conclusions; in some cases variability may be low (Edwards & Thompson, 1984; Charles *et al.*, 1991; Cumming *et al.*, 1992) and in others it can be high (Downing & Rath, 1988). Anderson (1990a) believed the inherent variability of sediment deposition was responsible in part for the error in diatom-based pH reconstructions.

Littoral-profundal variation can be considerable due to contrasting sedimentological processes (Anderson *et al.*, 1989; 1990a). The distinct morphological transition from shelf to basin in these lakes (Chapter 3) produces strong environmental gradients which are likely to affect sediment composition, increasing the likelihood that one core is unrepresentative of the entire lake. A sampling design formulated for larger lakes using a sample formula based on indices of shoreline development and lake area (Håkanson & Jansson, 1983) can be used to recommend the minimum number of core sampling points but the Signy lakes are too small for this scheme. In keeping with the deterministic system of Håkanson & Jansson (1983) and the prerequisites of the quantitative reconstruction (Chapter 1), the sampling strategy was therefore adopted to sample as much area of each lake basin as possible in the time available. In this way the spatial pattern of sedimentation of each lake could be characterized and the main focus of sediment accumulation located.

4.2.2 Temporal resolution

Samples need to be of comparable time resolution to each other and to the environmental data (Birks, 1995). Dating a large number of cores is an impossible undertaking so chronological control is determined by using a uniform sediment slice - the upper 0-1 cm sediment horizon. According to ^{210}Pb-dated sequences and calculated

rates of sedimentation (Appleby, Jones & Ellis-Evans, 1995) this represents roughly 5-10 years of sediment accumulation. Post-depositional reworking of sediments can introduce older material into surface-sediments and tends to be more pronounced in littoral than profundal sediments (Anderson, 1989, 1990a), requiring some assessment of environments of deposition in each lake basin (Chapter 5).

Long sediment sequences were taken to supplement cores from previous fieldwork seasons so that model calibration and validation could be conducted against the period of historical records. The palaeolimnology of the east coast lakes (Sombre, Heywood, Moss) has been studied in most detail (Jones & Juggins, 1993; Wilson, 1993; Appleby, Jones & Ellis-Evans, 1995; Dyson, 1996; Hodgson & Johnson, 1997). Further material was sought from lakes on the other side of the island to provide insights into the relative synchronicity and magnitude of environmental change in different locations.

4.2.3 Field methodology

4.2.3.1 Surface-sediments

Using available lake bathymetric maps (Heywood, 1967; Light, 1976; Heywood, Dartnall & Priddle, 1979; Sanders, 1984; Rose, 1985; Hawes, 1988; Chalmers, 1992) multiple samples were collected from each lake using a modified Glew gravity corer (Glew, 1991). Recent sediments are often very fluid, requiring careful sampling to minimize disturbance to the sediment-water interface (Battarbee, 1991). The Glew corer extracts relatively undisturbed sediment (Cumming *et al.*, 1993), including the sediment-water interface, with a negligible 'bow-wave' effect. It has been used at Signy in the past and was found to be reliable and well-suited to the range of sediment types and water depths (<15 m) and easy to operate and extrude cores in the field (V. Jones, *pers.comm.*). The core tube length defines the maximum core length (*ca.* 45 cm) and the core diameter is 65 mm, providing plentiful material for analysis. Where surface-sediments were required but no core recovery could be made an Ekman Grab sampler was used. This produced disturbed samples lacking stratigraphic resolution and the Glew was therefore the preferred method. However, its demands for relatively soft sediment introduces an element of bias into the sample-set.

Cores were taken by cutting holes in the lake ice by means of a motorised ice auger or, when ice-free, from the lake surface using an inflatable dinghy. The deepest point of each lake, marked by means of permanent marker buoys or parallel stakes on the

shoreline, was the origin for a series of radial transect lines. In this way disturbance of pristine sediment surfaces associated with the use of anchors was avoided and an accurate record of each core location could be made. Sampling was carried-out at 10 m, 20 m or 30 m intervals along each transect line depending on the size of the lake basin, economies of time and labour availability. Depth readings were taken by a hand-held digital echo-sounder or by a plumbline. The plumbline had the additional use of providing some prediction of the nature of the lake bed by 'feel' so minimising core-tube breakage and allowing adjustments to be made to the rate of drop into the sediment. Some sediments were found to be extremely soft (e.g. Gneiss Lake) requiring a very gentle 'drop' of the corer to prevent overshoot. Sediments on the lake margins (1-2 m depth) were assumed to be too disturbed through ice-scour effects (section 3.5.4) to provide meaningful stratigraphic information.

All seventeen lakes were sampled in the first season of fieldwork in both ice-covered and open water conditions. A total of 112 Glew kajak cores and 7 Ekman grabs were collected from the 17 lakes (Table 4.1). The Glew corer was successful and found to be well-suited to the Signy lake sediments, producing little-disturbed cores with an intact water-surface sediment interface and visible stratification. A further 81 Glew kajak cores were taken from a subset of five lakes (section 4.2.3.2) to supplement the sample net in the second field season.

4.2.3.2 Long-term sediment record

A subset of lakes (Sombre, Moss, Tranquil, Emerald, Gneiss) was chosen for more detailed palaeolimnological study on the basis of the following attributes:

- known bathymetry;
- good supporting site documentation (chemistry, biology, catchment);
- full set of sampling points established in the first field season;
- sediment suitable for Livingstone coring;
- glaciated or part-glaciated catchment, i.e. climate-sensitive; and
- minimal disturbance by fur seals (eutrophication effects) and their possible interference with climate-lake interactions.

A modified piston-corer (Wright, 1980) and Livingstone corer (Wright, 1967) were employed. These were lowered into the water-column by means of 3 metre length steel rods. The piston-corer was used to collect an undisturbed water-sediment interface. Its

clear perspex housing meant that the core could be scrutinised before extrusion. Subsequent, successive drives with the Livingstone corer were given a certain amount of overlap to ensure accurate sequence-matching. A total of 8 long sediment sequences were taken.

Table 4.1 Summary of cores collected from the 17 lakes

Lake	*Glew kajak cores*	*Ekman grabs*	*Long cores*	*Total*
1 Sombre	34	0	2	**36**
2 Heywood	9	3	0	**12**
3 Changing	11	2	0	**13**
4 Moss	16	2	1	**19**
5 Knob	11	0	0	**11**
6 Pumphouse	7	0	0	**7**
7 Light	4	0	0	**4**
8 Spirogyra	4	0	0	**4**
9 Tranquil	25	0	2	**27**
10 Amos	5	0	0	**5**
11 Tioga	4	0	0	**4**
12 Emerald	30	0	2	**32**
13 Lake 13	2	0	0	**2**
14 Twisted	10	0	0	**10**
15 Bothy	1	0	0	**1**
16 Gneiss	19	0	1	**20**
17 Orwell	2	0	0	**2**
Total	**194**	**7**	**8**	**209**

4.2.4 Core extrusion

4.2.4.1 Surface-sediments

All Glew kajak cores were extruded in the field on the day of sampling at 1 cm intervals or 0.5 cm intervals. Samples were placed into labelled Whirlpak® bags. Ekman grab samples were double-bagged. All samples were returned to the laboratory for analysis and stored at +5°C.

4.2.4.2 Long sediment sequences

Piston cores were returned to the laboratory whole, photographed and then extruded into

Whirlpak® bags. Between 0-5 cm the cores were sectioned at 0.25 cm intervals; between 5-20 cm at 0.5 cm intervals; and from 20 cm to the sequence end at 1 cm intervals.

Livingstone cores were extruded in the field into half-sectioned lengths of durapipe and wrapped in cling film. The lengths of sediment were returned to the laboratory whole and all samples were stored at +5°C.

4.2.5 Core description

All cores were described using Munsell colour charts and characterised using the Troels-Smith system (Troels-Smith, 1916; summarised in Birks & Birks, 1990). Analytical laboratory facilities at Signy Island allowed for the estimation of the basic sediment properties (see Chapter 5). Outstanding analyses were completed upon return at University College London (Chapters 5 and 6) and the University of Liverpool (Chapter 7). All cores were allocated an alphanumeric core code and archived at the Environmental Change Research Centre, University College London.

4.3 Sample locations and patterns of sediment deposition

4.3.1 Sombre Lake

Samples were taken along seven transect lines (Figure 4.1) at 10 and 20 metre intervals radiating from the deepest point. Thirty-four Glew cores were taken (SOMB11-41, 44-46 inclusive). The two long sequences - SOMB42 and SOMB43 - were taken in the second season and their surface samples were included in the training set. The long sediment sequence (SOMB42) obtained near the deep spot in the anoxic zone was 231 cm in length, slightly shorter than the core collected in 1991 (V. Jones, *pers.comm.*). SOMB43 was taken outside the zone of winter anoxia to observe potential differences in sediment stratigraphy and composition. Sediment in inflow-proximal cores (SOMB25-27, 45, 46) was notably coarser than those from other locations. Seal hairs were noted in the upper 0-2 cm of SOMB33, SOMB34, SOMB35, SOMB40 along the transect closest to the outflow and have subsequently been found throughout the lake (Hodgson & Johnson, 1997). The outflow is the most direct access route from Stygian Cove for fur seals.

4.3.2 Heywood Lake

Seven Glew kajak cores (HEY5-13) and three Ekman grab samples (HEY14-16) were taken at 10 metre intervals along four transect lines, three crossing the North Basin and

Figure 4.1 Sample locations, Sombre Lake

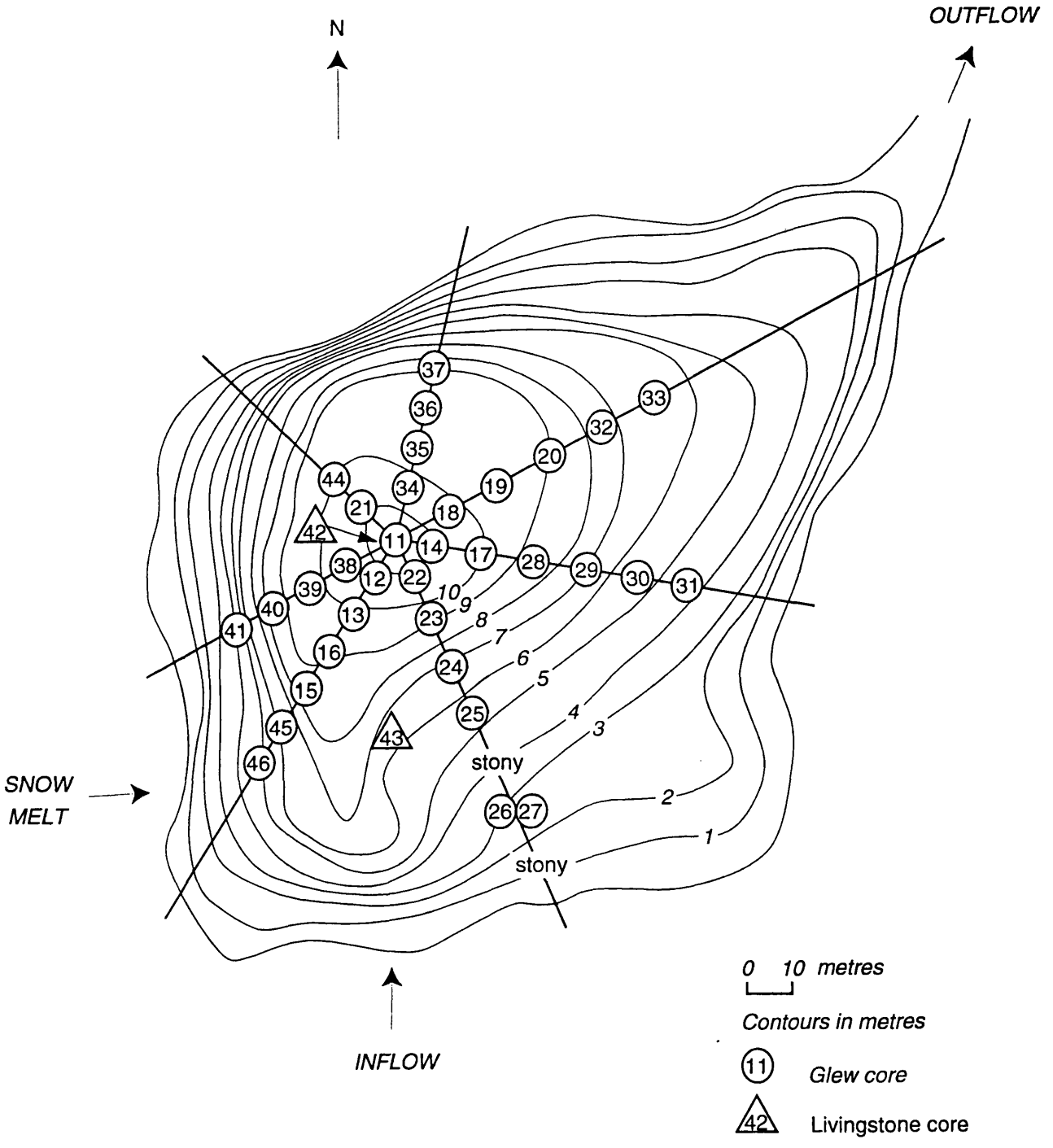

Figure 4.2 Sample locations, Heywood Lake

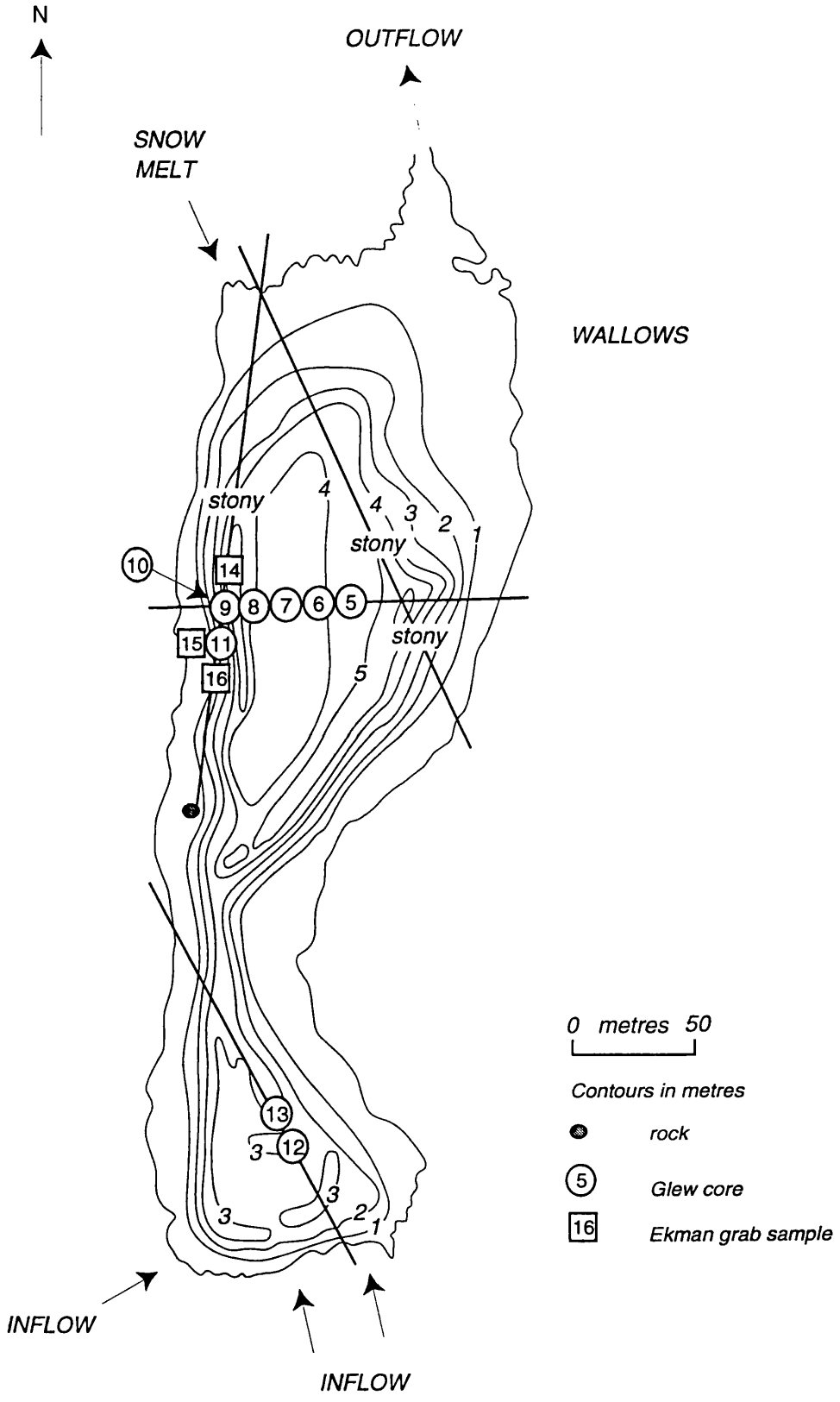

one along a diagonal in the South Basin (Figure 4.2). Organic sediment occurs in localised areas, the remainder of the shelf and trough being too stony for the corer. Just south of the acknowledged deep spot, depth soundings suggested a new recorded maximum depth of 7.2-7.3 metres but no sediment could be collected from this zone, supporting the hypothesis for scouring by water currents (Heywood, 1967). The largest accumulations of organic sediment are concentrated in a narrow trough to the west of the north basin in water depths of 4-5 metres. The shallow south basin is stony and there were difficulties taking samples with the Glew corer. A small mound of sediment occurs in the centre of this basin at depths of around 3 m, the location of Glew cores HEY12 and HEY13.

4.3.3 Changing Lake

This basin was overlain by an advanced ice front as late as 1948 (Light, 1976) and little sediment accumulation was anticipated. Sample locations were sited along five radial transects centred on the deepest point at 10 metre intervals (Figure 4.3). Eleven Glew cores (CHAN2-CHAN12) and two Ekman grab samples (CHAN13 & 14) were collected. Only Ekman grab samples could be taken from the zone of coarse sediments and boulders close to the western inflow and moraine.

4.3.4 Moss Lake

Six transect lines were established radiating from the deepest point (Figure 4.4). A total of 18 Glew kajak cores (MOSS3-8, MOSS11-20) were collected at 20 metre intervals along these transects. Sediments were too coarse and compacted to use the gravity corer on the inflow delta feature. Two Ekman grab samples (MOSS9 and 10) were collected in areas which were too stony for the Glew kajak corer. The long sediment sequence (MOSS21) was located near the deep spot in 8.4 metres of water. The total length retrieved was 95 cm, slightly shorter than the sequence collected in 1991 (V. Jones, *pers.comm.*).

Sampling close to the moraine was difficult because the ice upon the lake had become 'moated' and the ice-thickness and overlying meltwater exceeded the length of the ice auger. Shallow margins were too stony for coring although the shelf area was relatively small. Finer sediments are concentrated in the trough and cores from the deepest part of the basin (MOSS3-8) support a luxuriant growth of aquatic mosses. Inflow-proximal cores (MOSS5, 7 & 8) are notably coarser.

Figure 4.3 Sample locations, Changing Lake

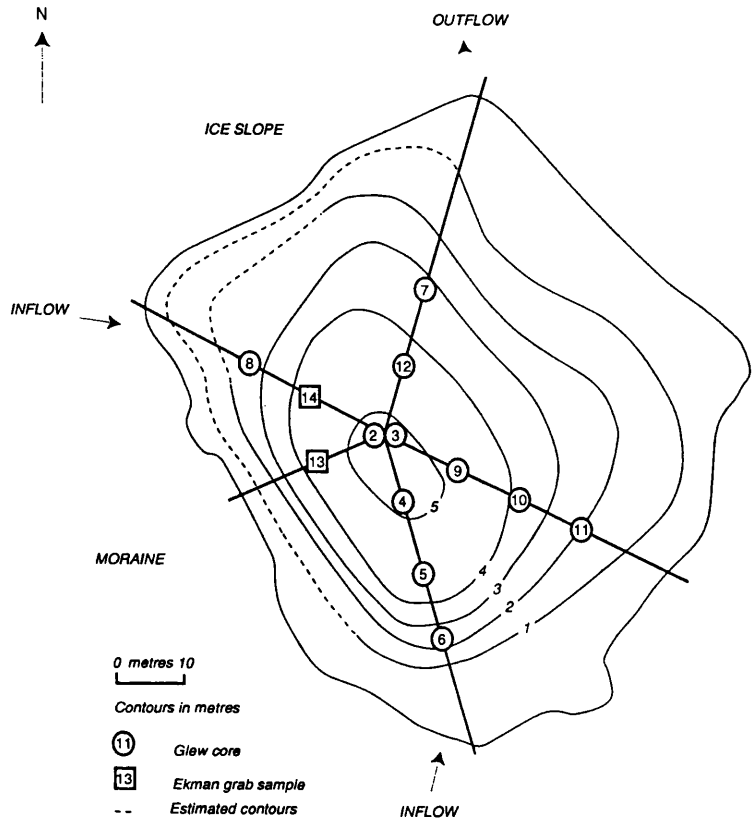

Figure 4.4 Sample locations, Moss Lake

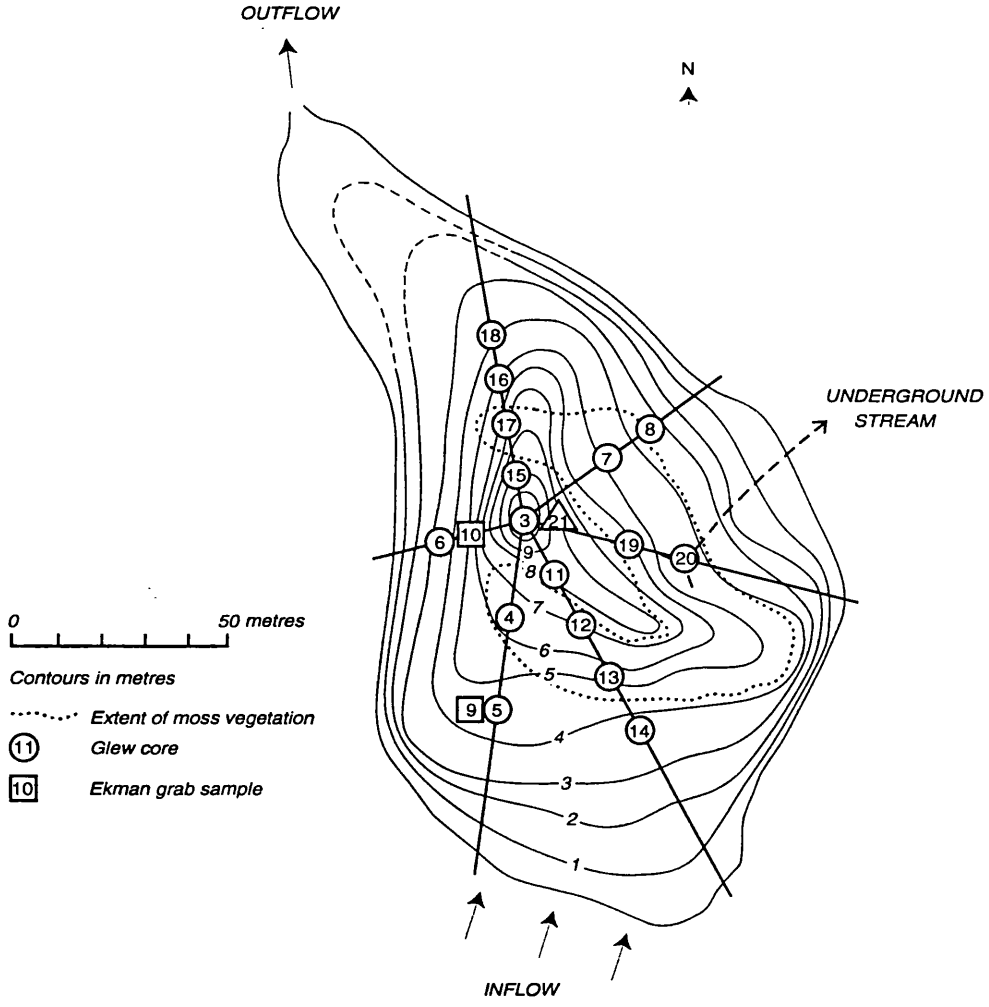

4.3.5 Knob Lake

A large area and complicated bathymetry (Figure 4.5) hindered the sampling exercise and, given time constraints, fewer samples than desirable were collected. Samples were taken along four transect lines, including one established transect line which ran shoreward from the island across the southern deep spot. A total of 11 Glew kajak cores (KNOB1-11) were collected. Sediment is patchy in the southern basin. The central trough is known for its stoniness (Heywood, Dartnall & Priddle, 1980) therefore sampling efforts were directed elsewhere. Soft sediments are found in the northern part of the lake focused in a basin near the outflow. This is in direct alignment with a meltwater inflow draining the col from Changing Lake.

4.3.6 Pumphouse Lake

Complicated bathymetry and irregular sedimentation also restricted sampling efforts (Figure 4.6). Two transect lines, roughly perpendicular to each another, were stretched across the lake in an effort to intersect the deep spot (recorded 4.0 m). Unfortunately the main trough was not encountered and the sampling point with the greatest depth (3.05 m) was devoid of sediment. A total of 7 Glew kajak cores were collected (PUMP1-7) from the central trough along the second transect. No samples were collected from the littoral shelf.

4.3.7 Light Lake

A wall of snow on the northern shore hindered sampling efforts since an excess of 1 metre of snow lay upon the ice, which itself exceeded 1 metre in thickness. Sampling was therefore restricted along two transects running from the deepest point to the north and to the east at 10, 15 and 20 metre intervals (Figure 4.7). Four Glew kajak cores (LITE1-4) were collected with highly loose, flocculent sediments. The extensive shelf zone along the eastern shore was not sampled owing to the rotten state of the lake-ice. The southern shelf is rocky and no sediment was collected from this area.

4.3.8 Spirogyra Lake

Four Glew kajak cores (SPIR2-5) were collected along two transects (Figure 4.8). The principal transect followed the long axis from the inflow to outflow. Sediment is sparsely distributed and the greatest accumulations are close to the deepest point.

Figure 4.5 Sample locations, Knob Lake

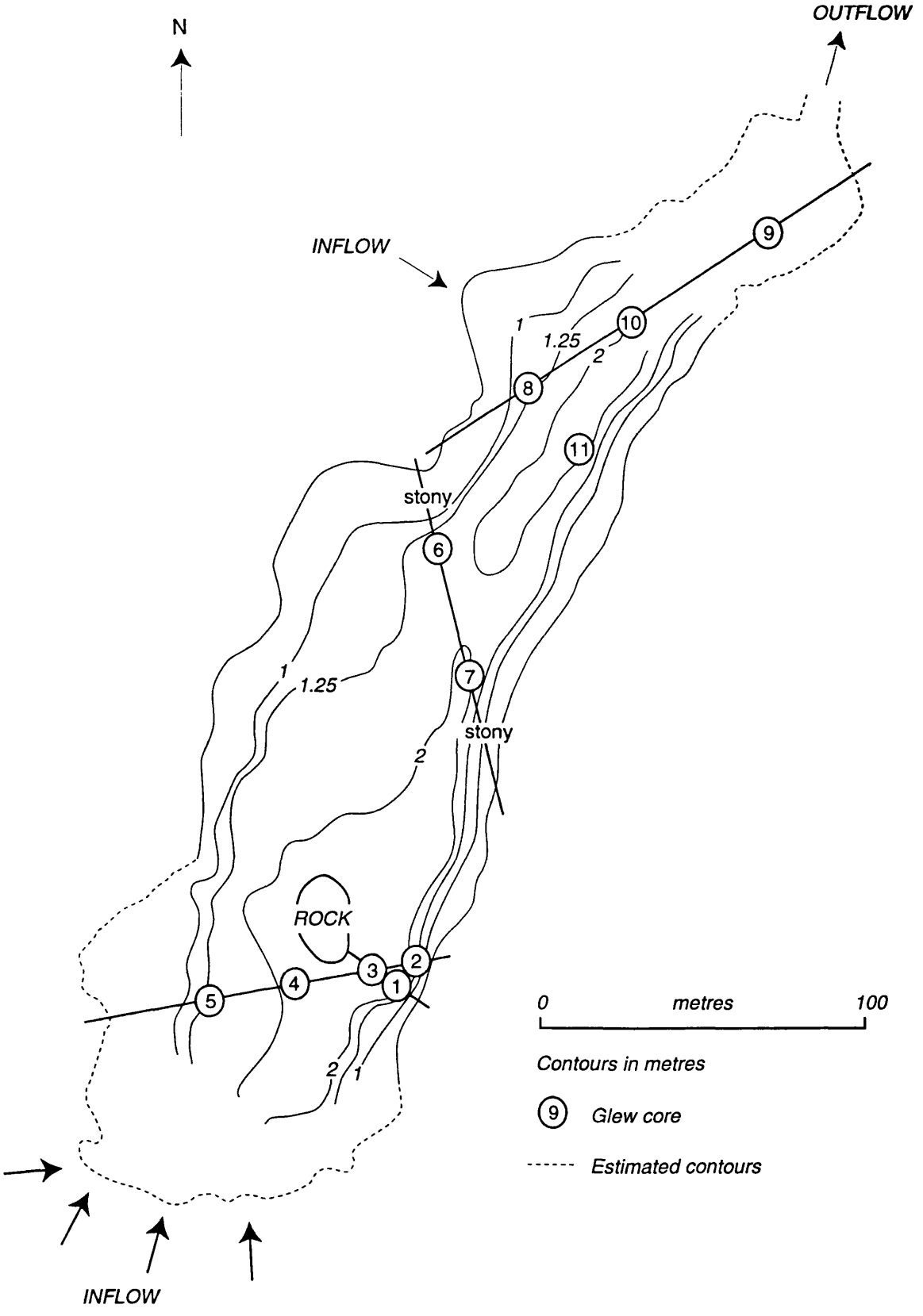

Figure 4.6 Sample locations, Pumphouse Lake

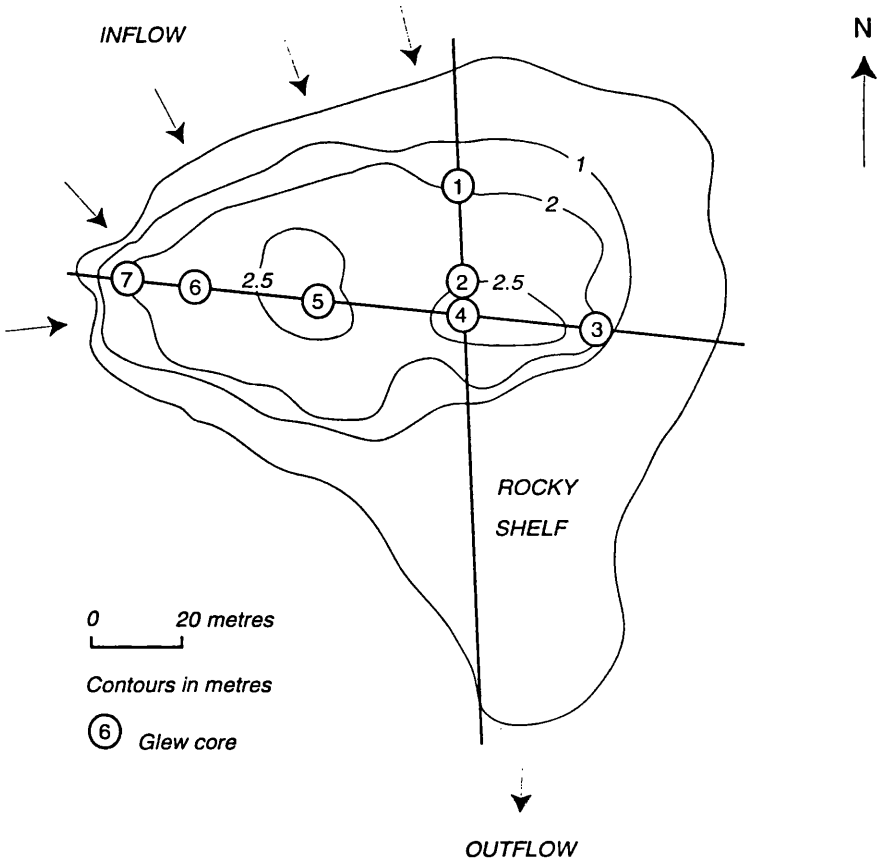

Figure 4.7 Sample locations, Light Lake

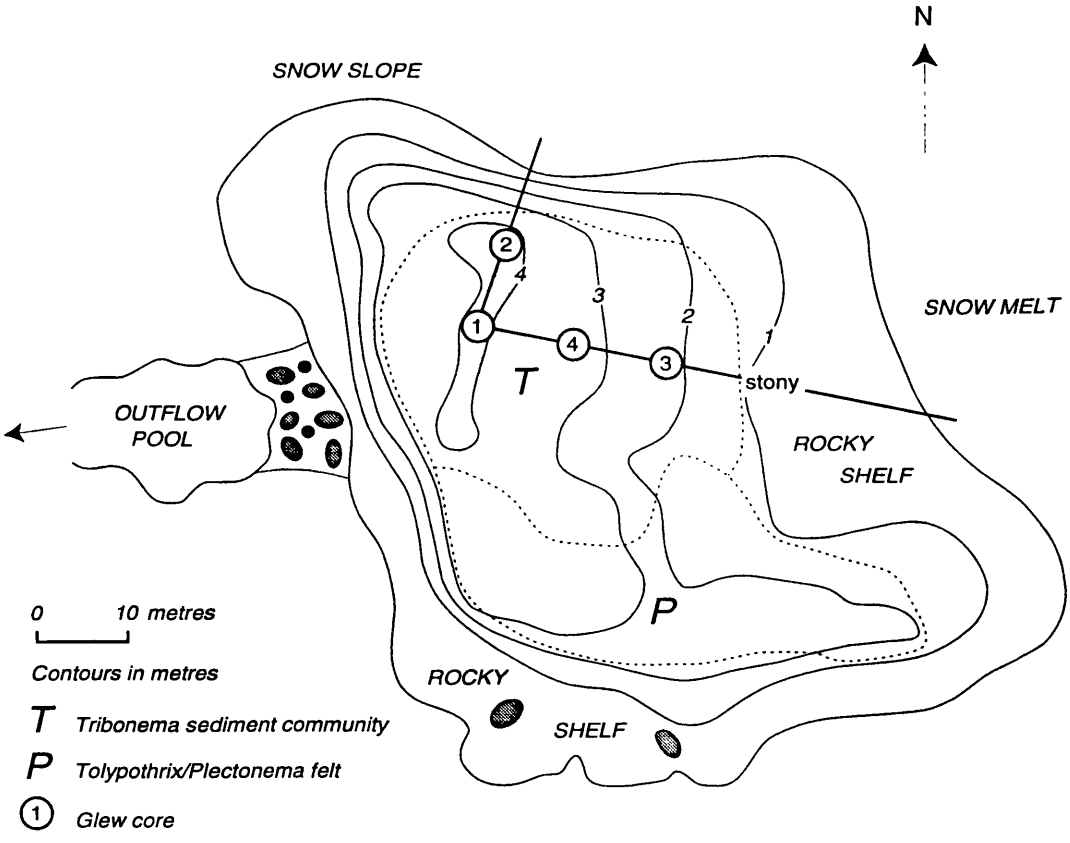

4.3.9 Tranquil Lake

Transects were aligned to intercept the three major basins and to intersect the connecting trough along the southern margin of the lake. A total of 22 Glew kajak cores (TRAN4-28) were sampled from ice along six transect lines at 10 and 20 metre intervals (Figure 4.9). Some cores are laminated, suggesting the presence of varves or rhythmites. Two long sediment-sequences were collected, one from each of the major basins aligned with the inflows. TRAN29 was taken in the southern sub-basin in 6.5 metres of water and a total length of 332 cm was retrieved. TRAN30 was taken from the northern sub-basin near the recorded deep spot in 8.2 metres of water. The total sequence measured 443 cm in length. Both sequences are highly laminated. The material at the base of TRAN30 is highly minerogenic and clayey.

4.3.10 Amos Lake

Two transect lines were set-up, one along the existing rope across the deepest point, the second perpendicular to this along the long axis of the lake (Figure 4.10). A total of 5 Glew kajak cores (AMOS3-7) was collected. Soft sediment is centred along central trough, elsewhere the trough is stony with boulders and little soft sediment. Seal hairs are visible in all cores.

4.3.11 Tioga Lake

Four cores (TIOG1-4) were taken along one transect line trending diagonally along the lake long axis to intersect the deep point (Figure 4.11). A thin layer of sediment was found over the entire basin but the only substantial accumulation was found at the deepest point between 2-3 metres of water depth. Surface-sediments are extremely flocculent and similar to those from Light Lake (section 4.3.7).

4.3.12 Emerald Lake

29 cores (EMER1-32, excluding Livingstone cores EMER16 & 17) were collected along 5 transects (Figure 4.12). These transects were chosen to intersect both the centre and margins of the basin. A long sediment sequence was taken near the deep spot of the basin in 14.65 metres of water (EMER16). The total sequence measured 168 cm. A second piston core (EMER17) and Glew core (EMER18) were taken nearby to provide additional material for analyses. In cores from the profundal zone, the redox boundary was evidenced by a colour change at depths of 10-21 cm in the sediment profile. Cores from the northern shoreline (EMER13-15) are coarse and stony. The first two have a 1

Figure 4.8 Sample locations, Spirogyra Lake

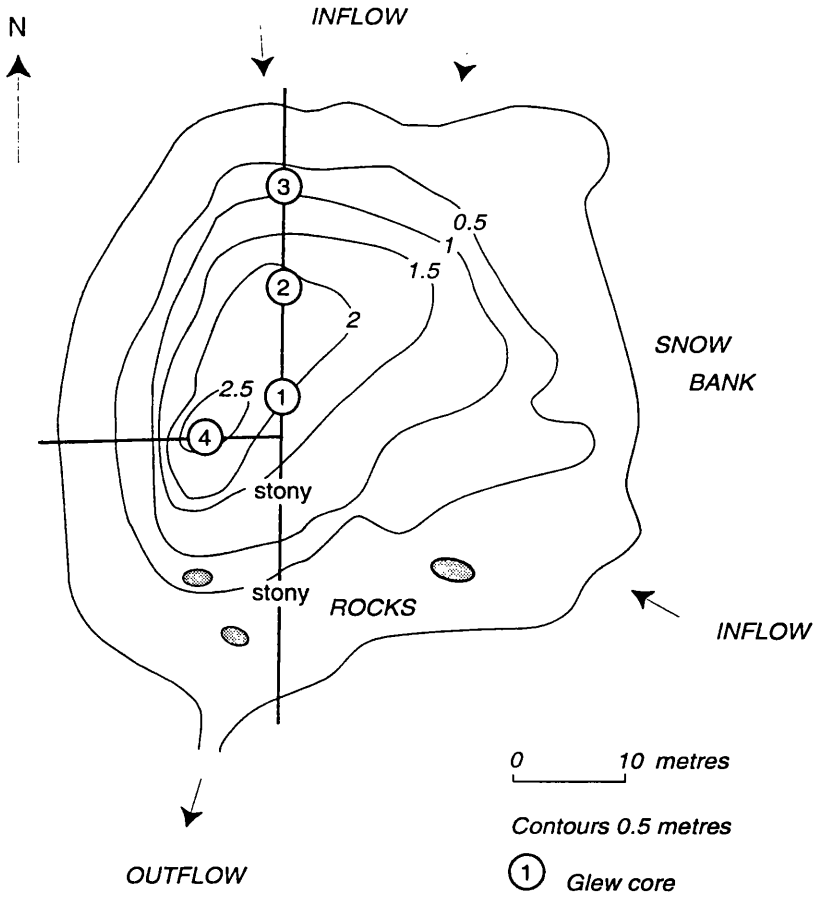

Figure 4.9 Sample locations, Tranquil Lake

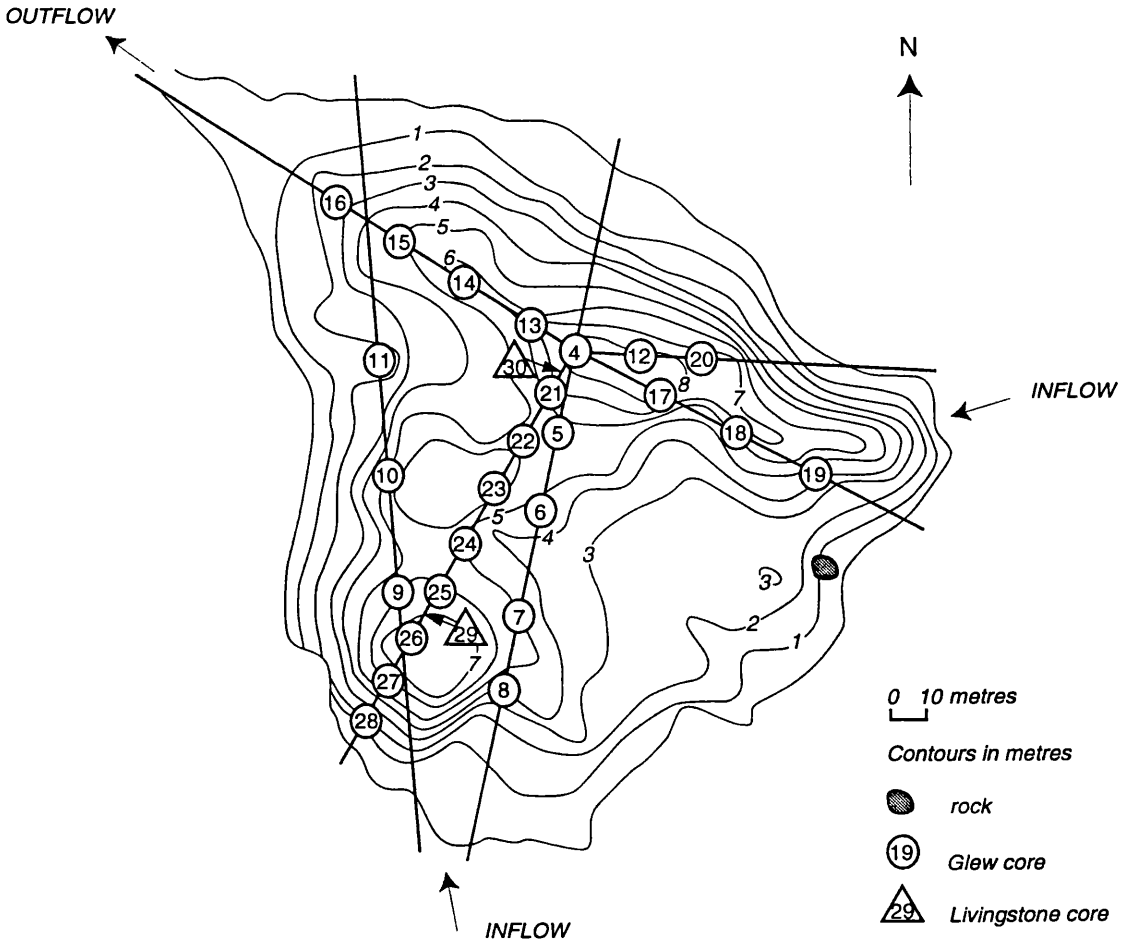

Figure 4.10 Sample locations, Amos Lake

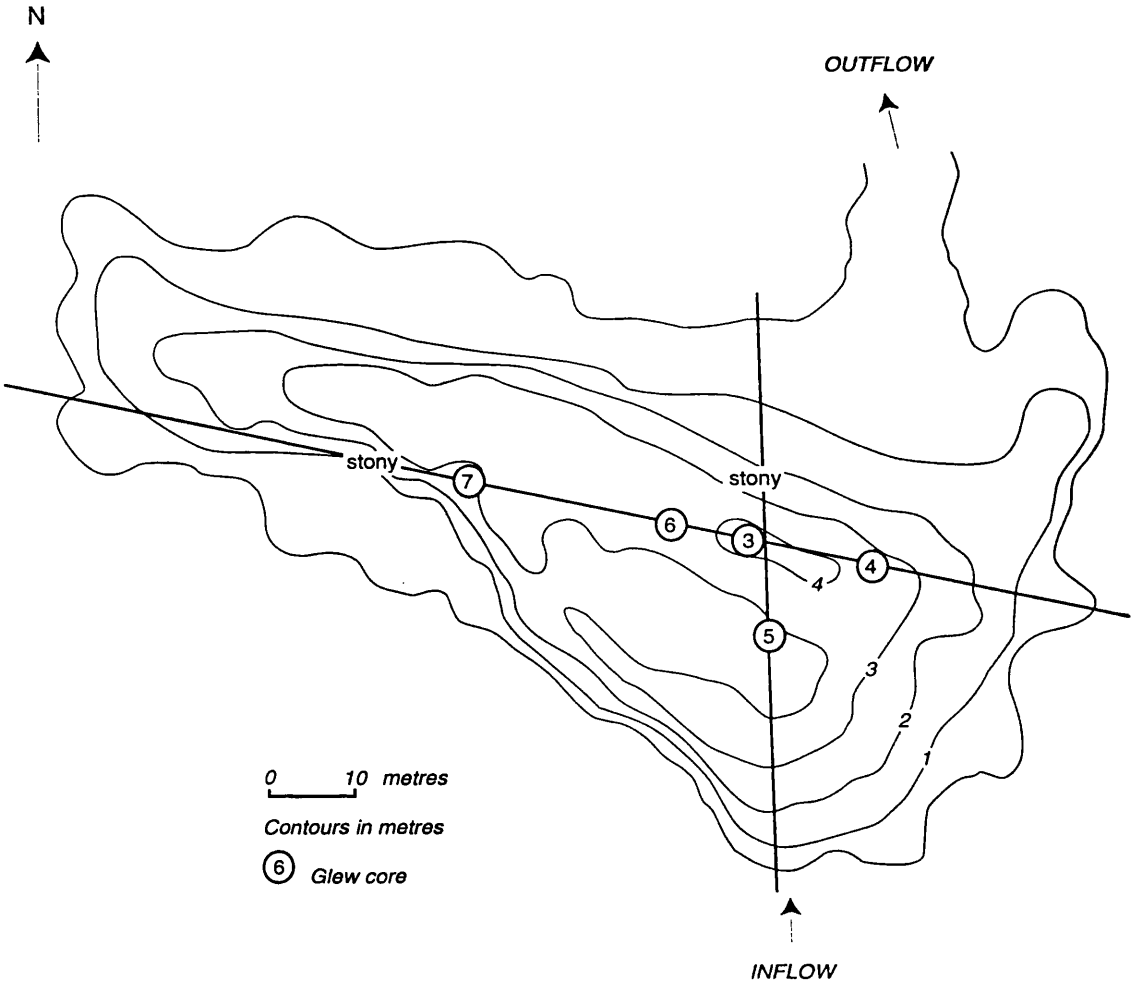

Figure 4.11 Sample locations, Tioga Lake

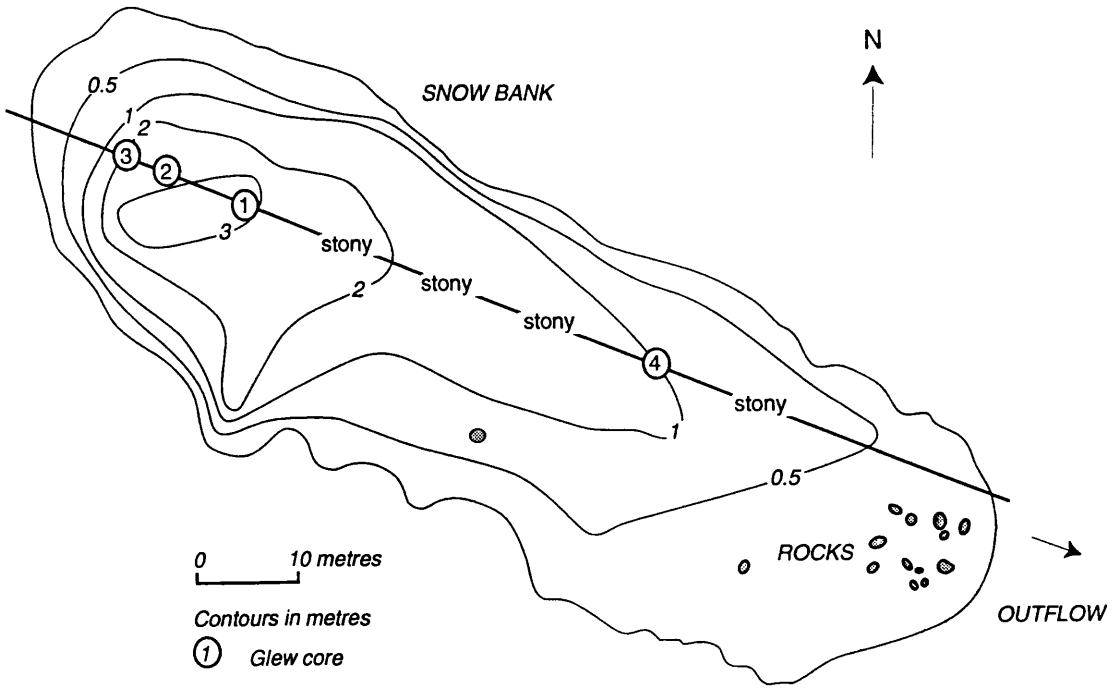

Figure 4.12 Sample locations, Emerald Lake

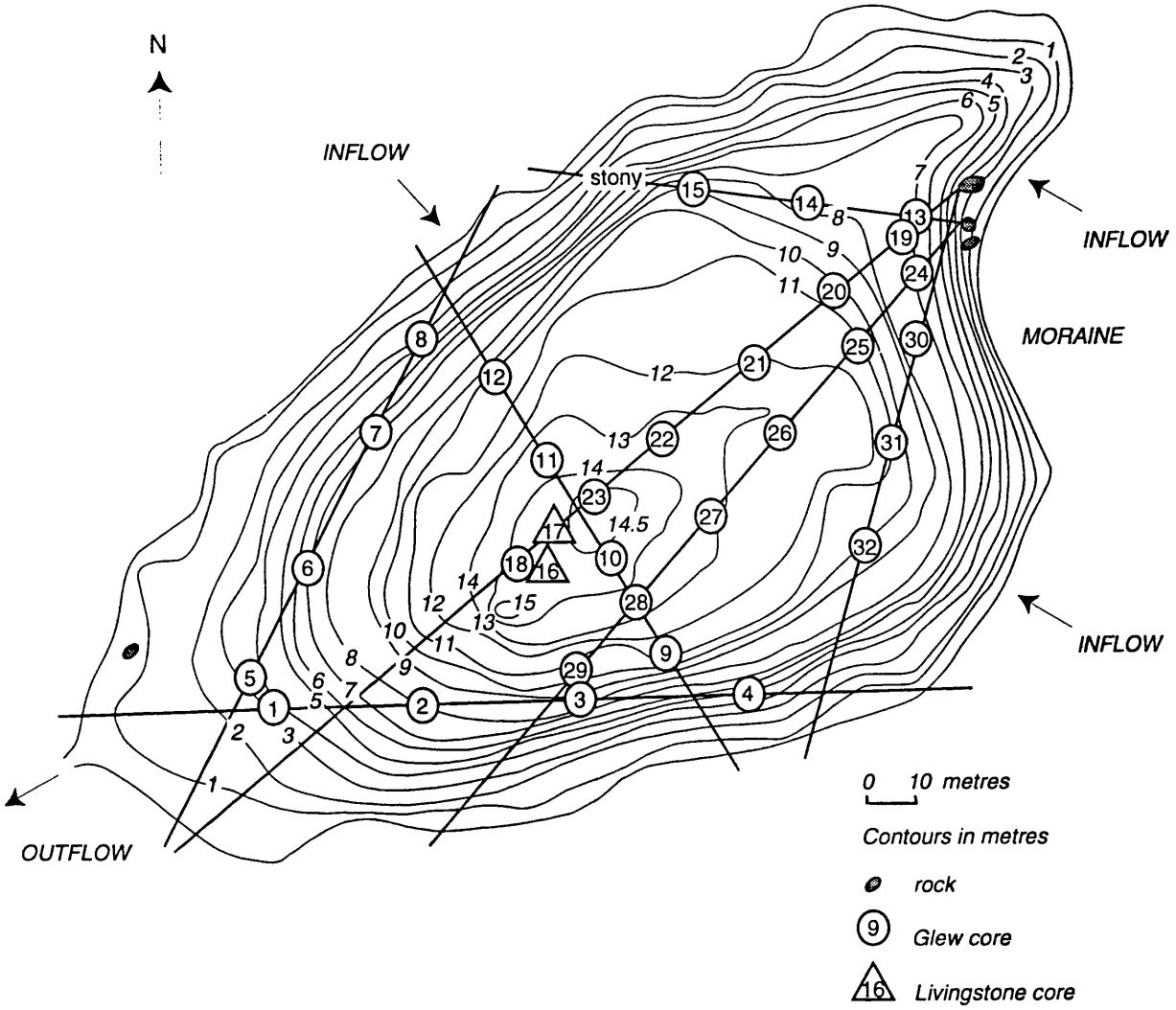

Figure 4.13 Sample locations, Lake13

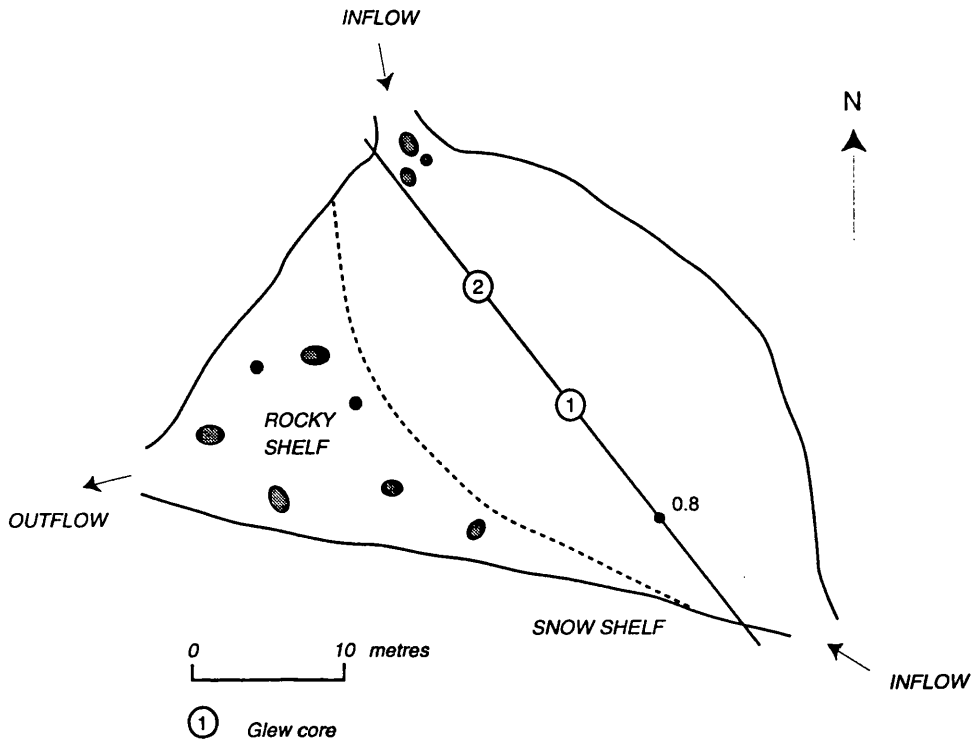

cm surficial algal layer thus despite high suspended sediment concentrations water clarity is adequate enough for the photic zone to extend to at least 8 metres in this part of the basin. The area immediately in front of the main inflow is strewn with many large boulders from the moraine and no cores could be collected from this zone.

4.3.13 Lake 13

Cores were taken along a single transect running parallel to long axis of the lake (Figure 4.13). Depth soundings were taken at 10 metre intervals but soft sediment is only found at water depths of 1.4 and 1.5 metres central to the basin. Elsewhere sediment is very coarse. *Branchinecta* were caught in the core tubes, a new finding in this lake (cf. Heywood, Dartnall & Priddle, 1979). Both Glew cores (SIG131 and SIG132) measured 22 cm in length and discrete laminations are evident in SIG131.

4.3.14 Twisted Lake

Two transects, one across the deepest point and a second from the inflow towards the southern shoreline were established (Figure 4.14). Depth readings were taken at 10 metre intervals and Glew kajak cores at 20 metre intervals. Ten Glew cores (TWIS3-TWIS12) were collected. The basin and shelf are stony in places and soft sediments are found below 4 metres water depth in the largest basin (TWIS9 & 10).

4.3.15 Bothy Lake

Sediment in this small, shallow lake is scant, easily disturbed and focused in a very small area off-centre of the basin (Figure 4.15). Only one core (BOTH1) was collected, composed of coarse sediment including seal hairs.

4.3.16 Gneiss Lake

The deepest point was used as the origin for 4 transect lines (Figure 4.16). Two further transect lines ran from the inflow across the length of the basin. Nineteen Glew kajak cores (GNES2-21) were collected. The steep southern slopes of the basin are very stony and devoid of soft sediment. The eastern end of Gneiss Lake yielded very compact, coarse, orange-brown sediments (GNES11, GNES12), bereft of an organic surface. The sediments closest to the inflow were too dense to be penetrated by the corer beyond 4 cm depth, and the GNES12 sample was obtained by saving a disturbed core-top by pipette. The long sediment-sequence (GNES22) was taken in 6.66 metres of water and measured a total length of 95 cm. Anoxia is most evident at the deepest point where the

Figure 4.14 Sample locations, Twisted Lake

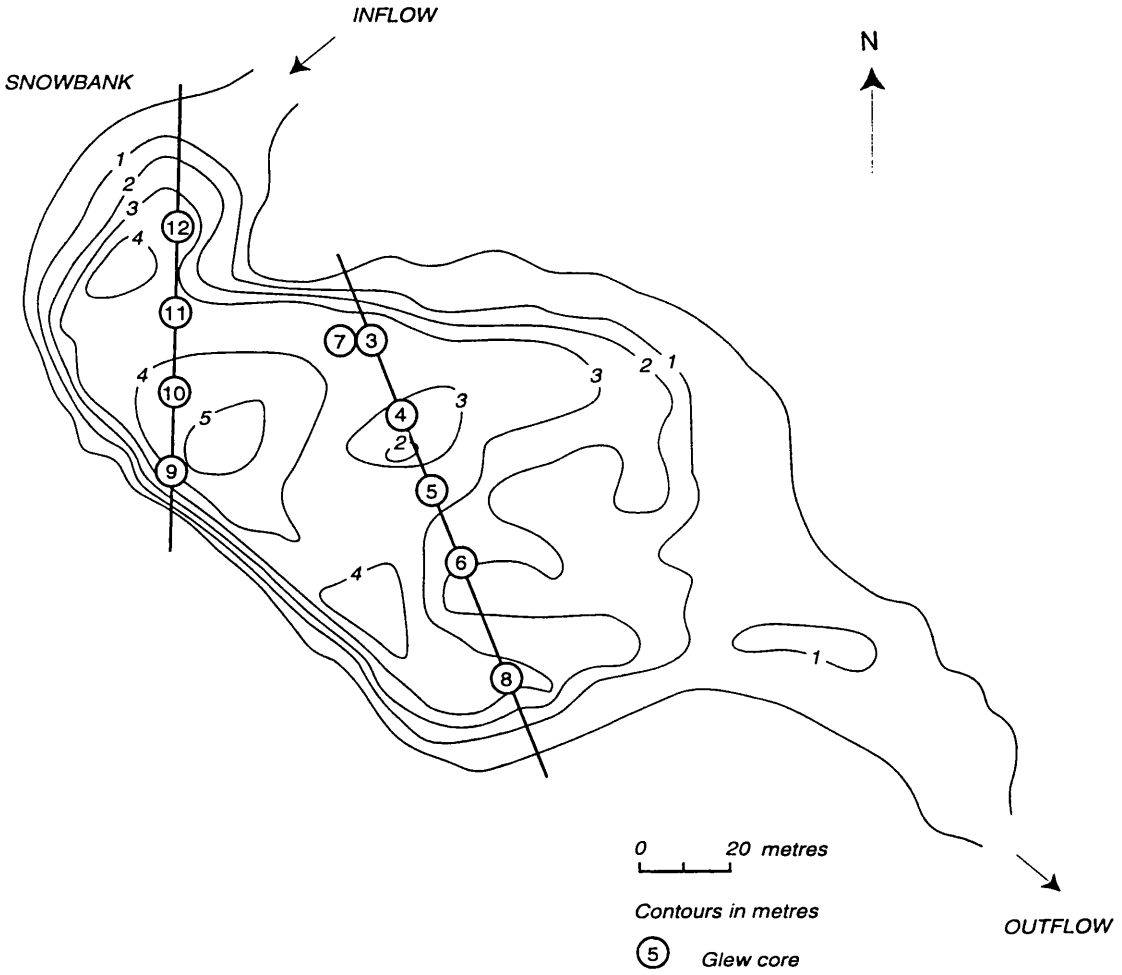

Figure 4.15 Sample location, Bothy Lake

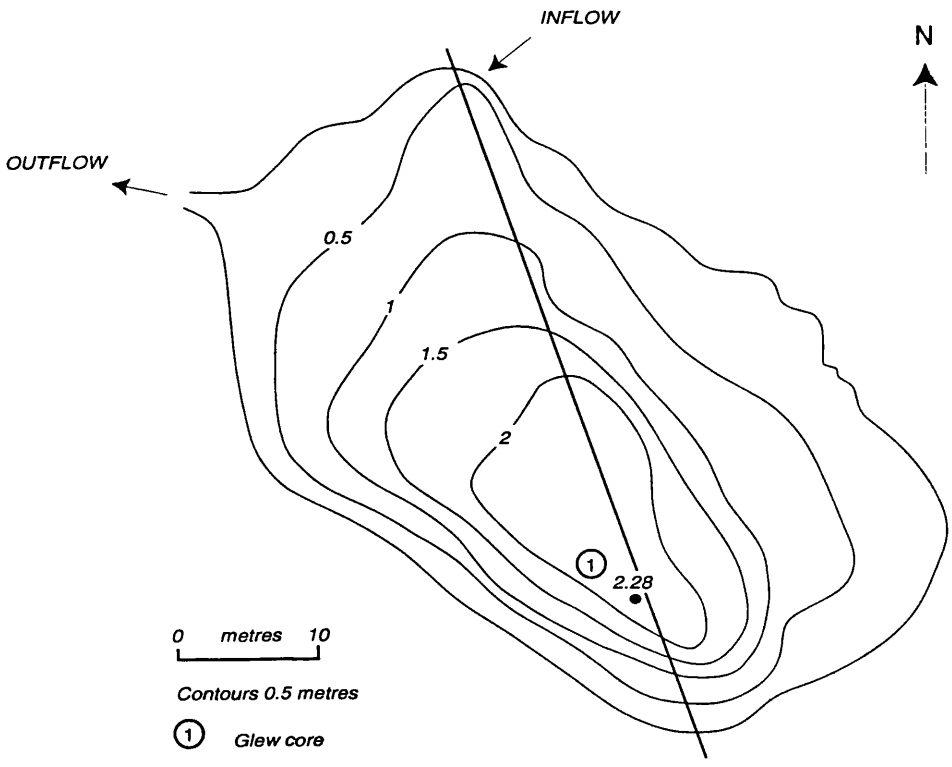

Figure 4.16 Sample locations, Gneiss Lake

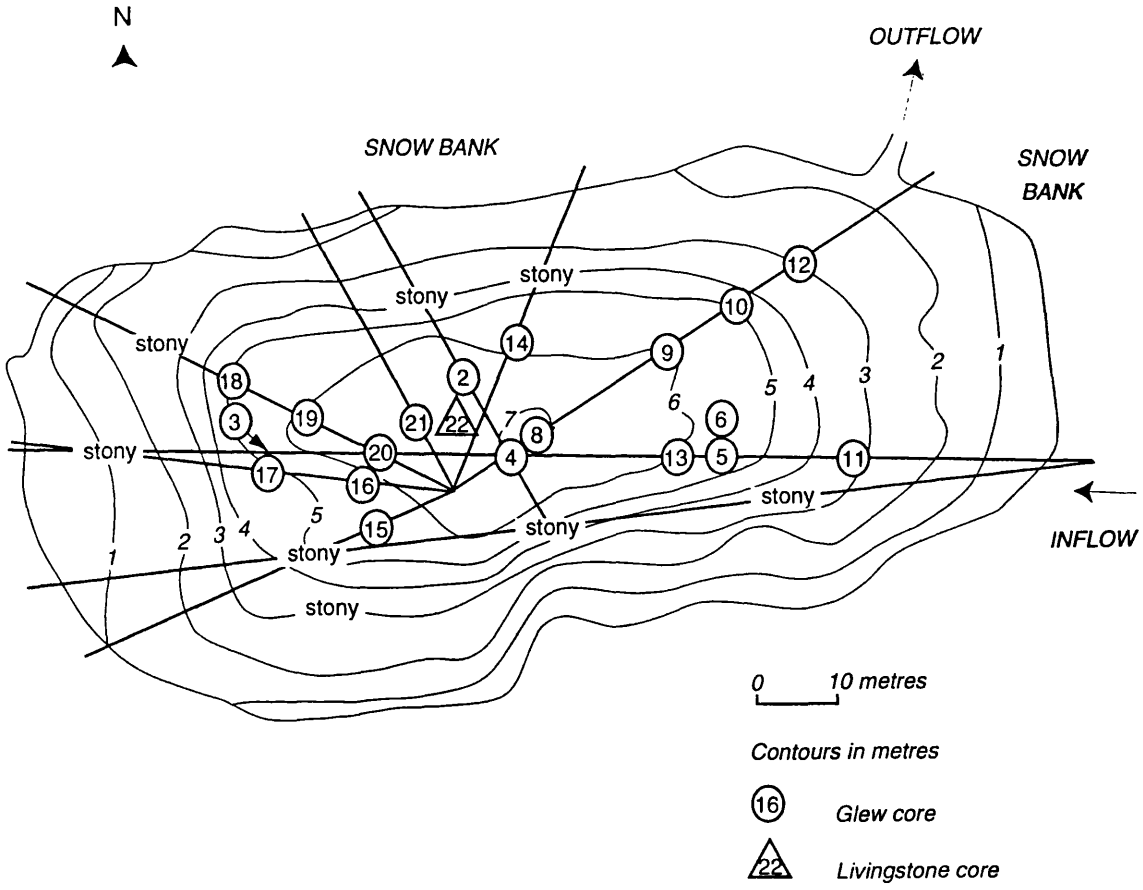

Figure 4.17 Sample locations, Orwell Lake

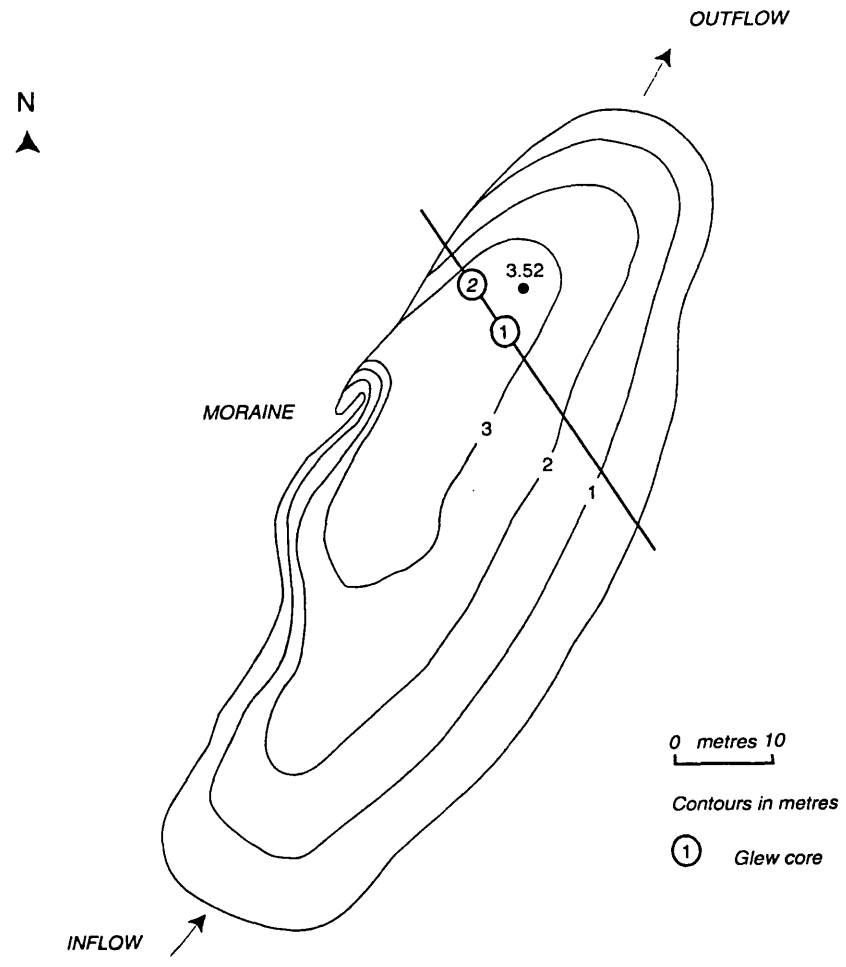

cyanobacterial mats are black, very soft and smell sulphurous upon exposure. At shallower depths (5-6.6 metres) the mats are olive-green in colour and measure up to 30 cm in thickness (GNES19, 20, 21) suggesting stable and continuous accumulation for a considerable length of time. Soft sediment accumulation appears to be maximal in the central and western ends of the lake basin and at its least towards the inflow and outflow where a delta is forming.

4.3.17 Orwell Lake

Two cores (ORWE1, ORWE2) were taken as close to the recorded deep spot as possible (Figure 4.17). Only a maximum of 4.5 cm could be sampled with the Glew corer. The maximum recorded water depth at the time of sampling was 3.4 m. Some days later the lake was seen to be empty.

4.4 Discussion

4.4.1 The sample-set

The Glew, piston and Livingstone corers performed well with the range of sediment types in the different lake basins. A total of 194 Glew cores, 7 Ekman grab samples and 8 piston core tops form the 209 sample training set (Table 4.1). Careful core extrusion provided a surface-sediment resolution of 0-1 cm but only 0-5 cm in the case of the Ekman grab samples. Each sample is best regarded as a running-average of several years' deposition (Davis, 1973), smoothing inter-annual variability. Variable sediment accumulation rates mean that samples taken in areas of relatively low accumulation may include quantities of earlier material. Encouragingly, in a diatom-based transfer function (Anderson, 1990a), fossil diatom assemblages in similar uniform sediment slices gave approximately the same recent history of ecological change in the lake. Different corers have different efficiencies leading to unknown resolution errors but piston core-tops (n=8) were still included in the training-set as more samples are considered to be beneficial to the transfer-function method. The Glew corer can only be used where sediments are suitably soft and this generally means that most samples come from the profundal zone of each basin, at the neglect of the littoral shelf-margins which are characterised by coarser sediments unsuited to gravity coring. The sample-set is therefore inherently biased by the sampling techniques employed so that the full gradient in sedimentary environment has possibly been truncated.

The low-lying eutrophic lakes - Heywood, Knob and Twisted - have the greatest

accumulations of organic sediments. Cores from the photic zone have surficial coverings of annual or perennial phytobenthos. Surprisingly, annual filamentous algae were even captured in core tops from lakes with low clarity for example, Emerald Lake. No surficial algal or moss growth was found in cores taken from the zone of winter anoxia as expected (Heywood, Dartnall & Priddle, 1980). Some Glew cores were dominated in their upper sections by thinly-laminated cyanobacterial mats (Light, Tioga and Gneiss Lakes). These thin laminae probably represent annual growth increments and indicate benthic stability over long time periods. Other laminations - glacial varves, rhythmites or turbidites - are apparent in some cores, notably the long sequences from Tranquil Lake. Varve formation is conditional upon special conditions (Petterson *et al.*, 1993) such as long periods of thermal stratification and anoxia in the profundal zone during summer and winter to minimize water movements and bioturbation. The exact cause and nature of these observed laminations deserve further attention but are beyond the scope of this Thesis.

4.4.2 Factors controlling contemporary sediment distribution

Deposition, resuspension and redeposition of sediment occur non-uniformally within lakes for a variety of reasons and have been reviewed by Håkanson & Jansson (1983). Of the ten redistribution mechanisms for sediment in lakes (Hilton, Lishman & Allen, 1986) at least 6 are likely to be of significance in these lakes: slumping and sliding on slopes, riverine delta formation, river plume sedimentation, intermittent complete mixing, peripheral wave attack and the random redistribution of sediment. The characteristic morphology - a shallow littoral shelf and a trough-shaped basin - imposes an abrupt change in the environment of sedimentation. Lake morphometric form is akin to 'ponds' conforming to the hyperboloid or frustum models of Lehman (1975) which are subject to widespread sediment focusing so that soft sediments are concentrated in the sheltered profundal troughs or sub-basins. The shallow littoral zones lack soft sediments and are stony or boulder-strewn. These are zones of erosion and transportation (Håkanson, 1977) subject to ice-scour, wind and current-induced resuspension. Ice-scour is likely to be even more pronounced in lakes which lose water during the winter months (Moss, Bothy and Gneiss Lakes). In the most shallow basins (Spirogyra, Lake 13, Bothy Lakes) there is little undisturbed sediment. The cone-shaped basins of glacial cirques (Sombre, Moss and Emerald Lakes) probably favour slope-related focusing, slumping and resuspension (Håkanson & Jansson, 1983) and mass-movement from steep slopes is a recognised source of coarse materials in basin margins (Hicks *et al.*, 1990). Delta-front sediments

are typically coarse and it was difficult to extract cores from these locations. Delta formation indicates high allochthonous sediment delivery associated with high erosion rates in the catchment (Appleby, Jones & Ellis-Evans, 1995).

Long winters with permanent ice-cover and a very rapid change from winter to summer (short overturn period) favour even sediment distribution (Petterson *et al.*, 1993) and the absence of thermal stratification and wind-induced mixing in summer (Heywood, 1968) encourages extensive redeposition of sediment. Winds can affect sediments at considerable depths (Johnson, 1980) but is probably maximal in the shallow exposed lakes of the coastal areas (Heywood, Knob, Amos, Twisted), explaining the highly variable nature of sediment accumulation and tendency for concentrations of sediments at the leeward end of the larger lakes (Heywood and Knob Lakes). Water residence times in the larger lakes are of sufficient duration to ensure deposition of most sediments (Hawes, 1983) and rapid sedimentation is assisted by turbidity currents, but some sediment loss probably occurs in smaller lakes with shorter residence times, for example Spirogyra, Lake 13 and Orwell Lake. Bioturbation is at a minimum in these lakes and in quiescent locations sediments should be undisturbed. Many cores are clearly stratified and primary sedimentological events are preserved. The only bioturbation of any significance are seals which stir-up sediments around the margins of visited lakes (Heywood, Knob, Sombre, Pumphouse, Amos, Twisted and Bothy); their presence is recorded in the sediments by their hairs.

4.5 Summary

(1) Analysis of a single core from the deepest point of a lake basin is the most common approach to the study of ontogeny and environmental history (Petterson *et al.*, 1993) but assumes that deposition in such areas is conformable and representative. Palaeoecological studies based on recent sediments however, should not proceed without information about the spacial variability in sedimentation that can be obtained through the correlation of widely sampled cores (Dearing, 1982; Dearing, 1983). This variability should be incorporated into the reconstruction model to cover a broad sedimentological gradient, so enhancing its statistical robustness and applicability.

(2) The sampling strategy was successful and multiple cores were collected from all the lakes to provide material for sedimentological analysis. A total of 194 Glew kajak cores, 7 Ekman grabs and the core tops from 8 Livingstone cores from 17 lakes provide 209

samples for the training-set. Long sediment-sequences provide material for model calibration (Chapter 9). The adopted sampling strategy is slightly biased towards profundal sediments but overall the samples cover the range of different sedimentary environments. A standard method for core extrusion ensured collection of an intact surface sediment-water interface and samples should be broadly contemporaneous within a decadal timescale.

(3) Irregular basin bathymetry reflects the glacial origin of these lakes, complicating patterns of sedimentation. The shallow littoral shelf areas are annually re-worked by seasonal ice-cover and are characterized by shallow, coarse sediments. The largest accumulations of soft sediment are generally central to each basin or in sub-basins. Sediment redistribution is strongly suspected from observed patterns of sediment accumulation which is investigated in subsequent Chapters. Sediment bioturbation is at a minimum and lithostratigraphical variations, including mineral and organic laminations, are well-preserved.

CHAPTER 5: SURFACE-SEDIMENT MINEROGENIC AND ORGANIC CHARACTERISTICS

5.1 Introduction

The shifting proportions of allogenic, endogenic and authigenic materials in sediments over time have been used as diagnostic indicators of changes in the lake-catchment system (Engstrom & Wright, 1984; Engstrom & Hansen, 1985) and by inference, changing climate. Although even crude measures, such as loss on ignition and dry weight have been effectively used to indicate climatic change in the maritime Antarctic (Chapter 1) a need was recognised to undertake a more detailed characterisation of the component sediment fractions to isolate the causal factors responsible for sediment origin and variability. In this chapter, the surface-sediments are analyzed for simple measures of density, water content, and organic matter content using loss on ignition. A sequential extraction procedure (cf. Engstrom & Wright, 1984) is followed to define the relative proportions of allogenic, endogenic and authigenic materials. The fraction corresponding to biogenic silica is used to assess variations in autochthonous production within and between the lakes. The statistical and geographical variations in the selected determinands are analysed and indirect ordination and classification methods are used to explain observed variability in the surface-sediments. The classification is compared to previous lake classification schemes (Chapter 3) and direct ordination is used to examine predictor-response relationships between the minerogenic and organic characteristics and the environment. The principal gradient in the data-set is discussed in the context of lake-catchment development, glacier activity and lake productivity.

5.2 Selected minerogenic and organic determinands

Selected minerogenic and organic sediment determinands are outlined in sections 5.2.1-5.2.4. Laboratory procedures are summarised in Appendix A.

5.2.1 Wet density

Density, water and organic contents co-vary and share similar patterns of distribution in lake basins (Håkanson & Jansson, 1983). Particle-size (Chapter 6) also affects sediment density. As a general rule, organic sediments are generally less dense than minerogenic materials, and density tends to increase with profile depth due to compression. Corrections are possible to account for packing effects using data on water-content and assumed values for the density of solids and water (Björck *et al.*,

1993; Menounos, 1997). Down-core variations in density indicate fluctuations in sediment composition that relate to changes in sediment source, especially in glacier-fed lakes. It can be used to interpret the conditions of deposition and identify features such as varves, rhythmites and turbidites (Zolitschka, 1996). High density layers, implying high minerogenic contents, have been found in Antarctic lake sediment sequences (Bronge, 1992) and, in combination with dry weight and water content, has isolated synchronous event horizons in the Signy lakes (Appleby, Jones & Ellis-Evans, 1995). Values for sediment density are also required for calculations of sediment accumulation rates from radiometric dating (P. Appleby, *pers.comm.*). Wet density was measured for all surface sediments and within key stratigraphic zones of the Glew cores soon after collection to ensure minimal water loss. It was also measured at all depths in the calibration cores (Chapter 9). Values are expressed in volumetric units of g/cm^3.

5.2.2 Percentage dry weight

Dry weight is the antithesis of sediment water-content. In common with wet density, sediment composition determines the percentage weight loss after drying. Sediments with high organic contents generally have more water than those with high mineral contents so that their weight loss upon drying is much greater, yielding low dry weight values. Dense, minerogenic sediments contain very low water contents and have high values for percentage dry weight. Dry weight is a useful determinant of the sedimentary environment; a close relationship between water depth and water content of surficial sediments has been used to predict zones of erosion, transportation and accumulation in lake basins (Håkanson, 1977). Water content tends to increase with depth in association with the focusing of fine materials and organic matter. Dry weight also has an obvious relationship with particle-size, offering another means of defining zones of sedimentation in basins (Chapter 6). Dry weight as a percentage of sediment wet weight was calculated for all core samples at all depths.

5.2.3 Percentage Loss On Ignition

Percentage loss on ignition (%LOI) provides a surrogate measure of the sum of allochthonous and autochthonous organic matter in sediments (Håkanson & Jansson, 1983). As a rapid, simple and accurate method for temporal and spatial comparison in lake basins (Dean, 1974) it is well-suited to the needs of assessing variation in this sample-set. The correlation between the content of organic carbon and %LOI is usually very good (Håkanson & Jansson, 1983) although errors can occur when the minerogenic

fraction contains a high content of crystal water (Dean, 1974; Björck *et al.*, 1993). %LOI also surmounts the problems of organic carbon determination by wet oxidation methods caused by the presence of Fe^{2+}, Mn^{2+} and S^{2-} (Konrad, Chesters & Keeney, 1970) which could be a potential problem in these seasonally anoxic lakes with their redox-related chemical transformations (Ellis-Evans & Lemon, 1989). %LOI is highly correlated with water content and tends to share the same distribution in the sediments (Håkanson & Jansson, 1983). As the inverse of water content, percentage dry weight (section 5.2.2) should show a negative correlation with %LOI. %LOI however, as a composite measure, cannot provide information regarding the origin of organic matter therefore a sequential extraction procedure (section 5.2.4) is used to separate the authigenic sediment fraction, which is non-combustible at the temperatures typically used for %LOI determinations. %LOI was measured for all lake cores at all depths and values are expressed as a percentage of sediment dry weight.

5.2.4 Sequential extraction method

5.2.4.1 Rationale

Analytical separation of the sediment into its constituent fractions has been achieved through selective chemical extraction (Engstrom & Hansen, 1985). Mackereth's (1966) determination of 'mineral matter' in his study of Lake District Lakes was the component remaining after ashing at 550°C which included variable quantities of authigenic oxides and biogenic silica. These components can constitute a large fraction of the total dry weight of freshwater sediments (Engstrom, 1983). For example, Birnie (1990) observed high proportions of diatoms in lake sediment sequences from South Georgia, sometimes dominating the inorganic component. By analogy, sediments from the Signy lakes are probably similar. Deposition rates for authigenic phosphorous or biogenic silica may represent historic levels of lake productivity (Digerfeldt, 1972), and the accumulation rate for allogenic components has been used to indicate erosional intensity in the past (Engstrom, 1983). The sequential extraction procedure (Appendix A) uses a gravimetric method which yields three measures: organic matter as a percentage of dry weight (%OM), biogenic silica as a percentage of dry weight (%BSi) and minerogenic material as a percentage of dry weight (%Min). Extraction was completed for all 209 surface-sediment samples. The environmental relevance of each fraction is discussed below.

5.2.4.2 Organic matter

Organic material is removed by oxidation using 30% hydrogen peroxide at 50-60°C. Organic matter as a percentage of dry weight (%OM) is calculated as the gravimetric weight loss after this digestion. These can be compared with results from the %LOI method (section 5.4.1.2) to assess the reliability of either procedure in gauging sediment organic content. Wet chemical extraction is favoured as ashing at 550°C causes diatom valves to become resistant to alkali-digestion used in the subsequent step of the procedure (Goldberg, 1958, in Flower, 1980).

5.2.4.3 Biogenic silica

Allogenic and biogenic forms of silica are normally abundant in lake sediments so that separation of the two fractions is essential for assessing their relative contributions to the sediment record. The volume of biogenic silica (BSi), including siliceous microfossils (diatom frustules, chrysophytes, sponge spicules), cannot be determined by %LOI. Preferential digestion using alkaline dissolution techniques (Krausse, Schelske & Davis, 1983), has been used to selectively remove biogenic silica from other forms of silica and non-crystalline or amorphous silica (i.e. inorganic ash) in sediments and water samples, causing only minor degradation of clays and silicate minerals. Independent of other authigenic minerals, BSi measurements are a surrogate measure of autochthonous production and diatom concentration (Battarbee, 1986) and a good correspondence has been found for the abundance of diatom valves and BSi concentrations (Flower, 1980: Newberry & Schelske, 1986). Its measurement is less time-consuming than microscopic enumeration and removes the problem of valve fragments which cannot be identified or counted but are still part of the overall diatom production in a lake. Diatoms are more indicative of water chemistry and micro-habitat than temperature (Smol, 1988; Smol, 1991) and increases in the accumulation rate of BSi have been coincident with eutrophication (Digerfeldt, 1972) and can provide a more sensitive index of phosphorus enrichment than actual phosphorus accumulation in the sediments (Schelske *et al.*, 1986). The recent enhanced eutrophication in some of the Signy Lakes should therefore be detectable in the %BSi content of the sediments.

BSi represents the net balance between diatom production and dissolution in the water column and the sediment (Engstrom & Wright, 1984) and Schelske *et al.* (1986) presented a model for predicting the amount of BSi in sediments:

BSi = f (number of diatoms, chrysophytes, dissolution correction)

Even with high annual deposition, shallow water depths, temperature and water chemistry (high pH, high carbonate, high salinity) can lead to poor preservation through diagenetic effects (Flower, 1993) which has been noted in temperate lakes (Parker, Conway & Yaguchi, 1977a, 1977b). Diatom preservation is believed to be good in the Signy lakes (V.Jones, *pers.comm.*) and valve breakage is generally mechanical through turbulence or zooplankton grazing (Oppenheim, 1990). A wet alkaline digestion procedure was used adapted from Rose's (1990) preparation procedure for inorganic ash spheres. The volume of chrysophytes was unknown and no attempt was made to correct for dissolution. Biogenic silica (%BSi) was calculated as the gravimetric loss after digestion in sodium hydroxide. Values are expressed as a percentage of sediment dry weight.

5.2.4.4 Minerogenic material

Minerogenic (clastic) material is the fraction remaining after removal of organic matter by peroxide digestion and removal of biogenic silica by alkaline digestion, i.e. the allogenic fraction. Values are expressed as a percentage of sediment dry weight.

5.2.4.5 Replication

Only the Ekman grab samples provided sufficient material for analytical replication. Three replicate analyses were conducted on 11 samples, representing *ca.*5% of the sample population, allowing a calculation of the standard error of the mean for %OM, %BSi and %Min. The Ekman grab samples however, are more heterogeneous due to mixing of up to 0-5 cm of the surface-sediment layers and are biased towards more coarse, dense minerogenic materials from sampling locations where gravity coring was not possible (Chapter 4). They are not, therefore, fully representative of the %BSi gradient in the sample-set and universal calibration to correct for analytical error is not possible.

5.3 Values and statistical distributions of surface sediment organic and minerogenic determinands

Summary statistics of measures of surface sediment organic and minerogenic determinands are presented in Table 5.1.

Table 5.1 Summary statistics for the surface-sediment organic and minerogenic determinands (209 samples from 17 lakes)

Determinand	*Units*	*Min*	*Max*	*Mean*	*Median*	*S.D.*
Wet density	g/cm^3	0.98	1.72	1.14	1.08	0.15
Dry weight	% of dry weight	1.13	72.03	22.89	19.68	15.63
Loss on ignition	% of dry weight	1.20	66.93	14.73	11.25	12.61
Organic matter	% of dry weight	0.69	81.80	13.63	9.86	12.22
Biogenic silica	% of dry weight	0	46.61	9.12	7.50	7.73
Minerogenic material	% of dry weight	18.20	99.31	86.37	90.14	12.22

5.3.1 Wet density

Wet density attains a maximum of 1.72 g/cm^3 in Orwell (17) Lake and a minimum of 0.98 g/cm^3 in Moss (3) Lake (predominantly moss fragments). The sample population is right-skewed (mean=1.14; median=1.08; S.D.=0.15 g/cm^3). In the box-and-whisker plot (Figure 5.1), 50% of the population lies within the confines of the box and the median is drawn as a solid line; 95% of the population lies within the limits defined by the whiskers. Outliers in the extreme 5% of the distribution are plotted as open circles.

Figure 5.1 Box-and-whisker plot showing variation of wet density by lake number

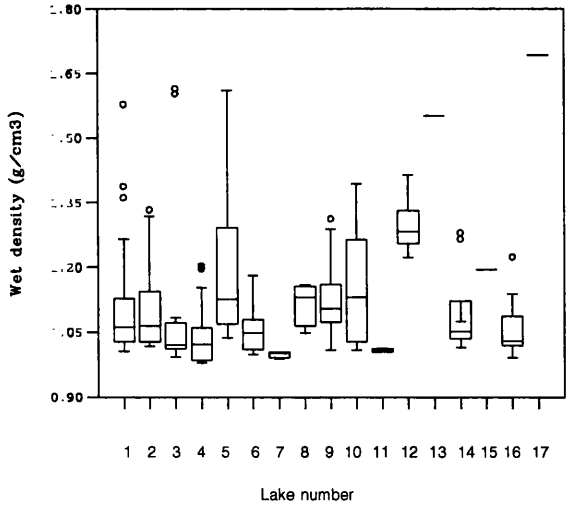

Most lakes have similar median values and relatively limited ranges. Sediments in Knob (5), Tranquil (9) and Amos (10) Lakes are of slightly higher density with larger ranges. Sediments from Emerald (12) Lake are distinctively more dense. Outliers (>2 S.D.)

include SOMB13, SOMB27, SOMB37, HEY14, CHAN13, CHAN14, MOSS9, MOSS21, TRAN20, TWIS8, TWIS5, and GNES12. This list includes Ekman grab samples (HEY14, CHAN13 and CHAN14) reflecting the impenetrability of coarse, dense sediments at these sampling locations.

5.3.1.2 Percentage dry weight

%DW is more variable between lakes than wet density with a maximum value of 72.03% in Lake 13 and a minimum of 1.13% in Moss (4) Lake, predominantly composed of moss fragments (Figure 5.2). The sample population is right-skewed (mean=22.89; median=19.68; S.D.=15.63%). Changing (3), Tioga (11), Twisted (14) and Gneiss (16) share similar median values and distributions, as do Sombre (1), Pumphouse (6) and Bothy (15) Lakes. Knob (5), Spirogyra (8), Tranquil (9) and Amos (10) Lakes have higher median %DW and Emerald (12), Lake 13 and Orwell (17) Lakes have the highest %DW values. Within-lake variability is particularly high in Heywood (2) and Tranquil (9) Lakes. Outliers (>2 S.D.) include SOMB12, SOMB27, SOMB37, CHAN13, CHAN14, KNOB9, GNES12. One sample - EMER5 (19.68%) - has an unusually low value, possibly resulting from laboratory error.

Figure 5.2 Box-and-whisker plot showing variation of % Dry Weight by lake number

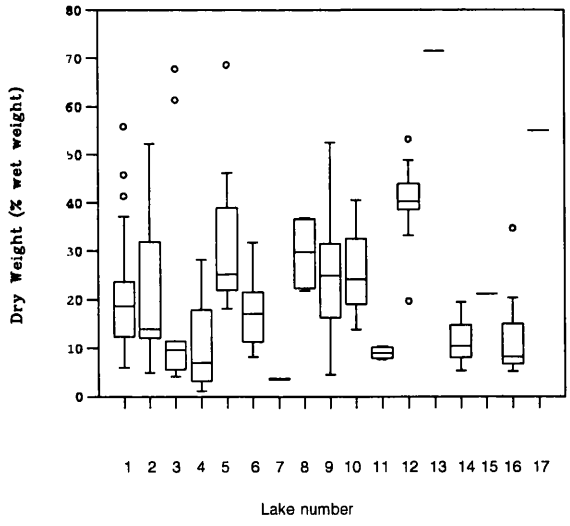

5.3.1.3 Percentage Loss On Ignition

%LOI reaches a maximum of 66.93% in Light (7) Lake and a minimum of 1.2% in Sombre (1) Lake (Figure 5.3). The sample population is right-skewed (mean=14.73; median=11.25; S.D.=12.61%). Heywood (2), Changing (3), Moss (4), Pumphouse (6), Amos (10), Twisted (14) and Gneiss (16) Lakes share similar medians and distributions.

Results from Sombre (1), Knob (5), Spirogyra (8) and Tranquil (9) are slightly lower. %LOI is lowest in Emerald (12), Lake 13 and Orwell (17) Lakes. Light (7) and Tioga (11) Lakes have distinctively higher values for %LOI. Outliers (>2 S.D.) include PUMP4, TRAN28, TRAN11, EMER5 and TWIS4.

Figure 5.3 Box-and-whisker plot showing variation of % Loss On Ignition by lake number

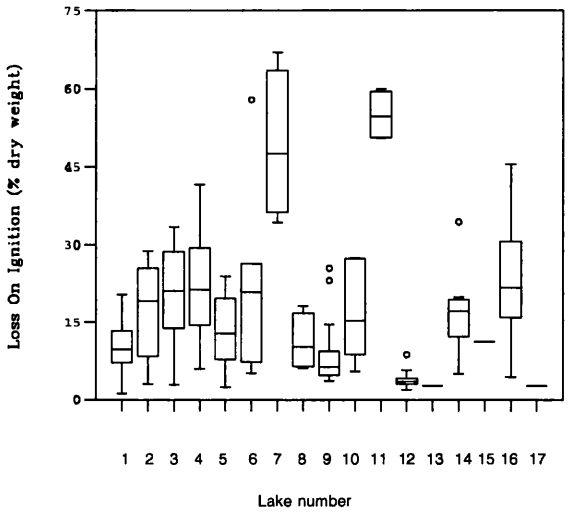

5.3.4 Percentage organic matter

%OM reaches a maximum of 81.80% in Moss Lake (predominantly moss fragments) and a minimum of 0.69% in Changing Lake (Figure 5.4). The overall sample population is right-skewed (mean=13.63; median=9.86; S.D.=12.22%).

Figure 5.4 Box-and-whisker plot showing variation of % Organic Matter by lake number

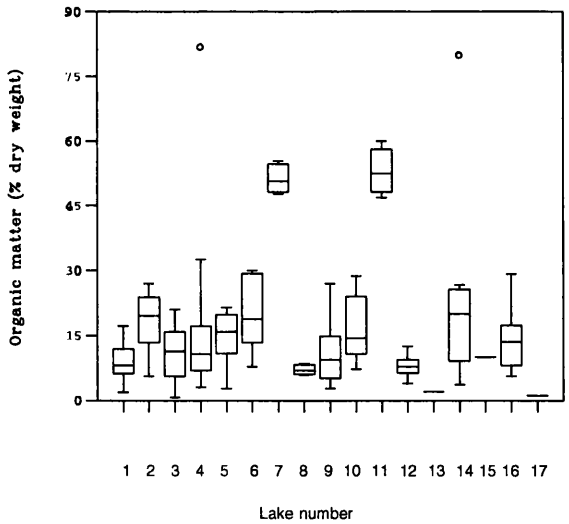

Most lakes have similar values and ranges which closely correspond with values for %LOI. Again, Light and Tioga Lakes have distinctively higher values. Outliers (>2 S.D.)

include MOSS12 and TWIS6, probably a result of laboratory error (section 5.4.1.2). The calculated error from replicate samples (n=11) is ±0.29%.

5.3.5 Percentage biogenic silica

%BSi ranges from a maximum of 46.61% in Light (7) Lake to an absolute minimum of 0% in Emerald (12) Lake (Figure 5.5). The overall sample population is right-skewed (mean=86.34; median=90.14; S.D.=7.73%). There was insufficient material to complete analysis for sample GNES12 and its missing value was replaced by the mean of all the Gneiss Lake %BSi values (mean=13.13%, n=19). Many lakes share similar median values between 5-15 %BSi but high within-lake variability is apparent in Changing (3), Moss (4), Twisted (14) and Gneiss (16) Lakes.

Figure 5.5 Box-and-whisker plot showing variation of % Biogenic Silica by lake number

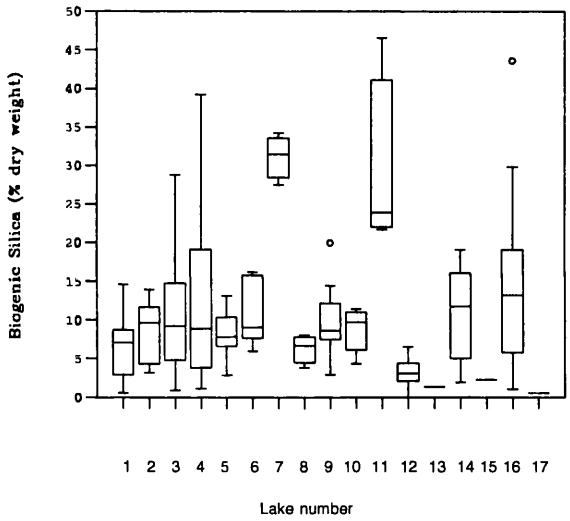

The lowest %BSi values (<5%) are in Emerald, Lake13, Bothy and Orwell Lakes. Light and Tioga Lakes have distinctively higher values. Two outliers (>2 S.D.) include TRAN28 (19.98%) and GNES8 (43.59%). The calculated error from replicate samples (n=11) is ±1.46%.

5.3.6 Percentage minerogenic material

%Min reaches a maximum of 99.31% in Changing (3) Lake and a minimum of 18.2% in Moss (4) Lake (Figure 5.6). Unlike the other determinands, the sample population is left-skewed (mean=86.37; median=90.14; S.D.=12.22%). The missing value for GNES12 (insufficient material) was replaced with the mean for the remaining Gneiss Lake samples (mean=87.04%, n=19). Most lakes display similar ranges of values. Two

exceptions are Light and Tioga Lakes with distinctively low values for %Min. Two outliers (>2 S.D.) are apparent: MOSS12 (18.15%) and TWIS6 (4.02%). The calculated error from replicate samples (n=11) is ±0.29%.

Figure 5.6 Box-and-whisker plot showing variation of % Minerogenic material by lake number

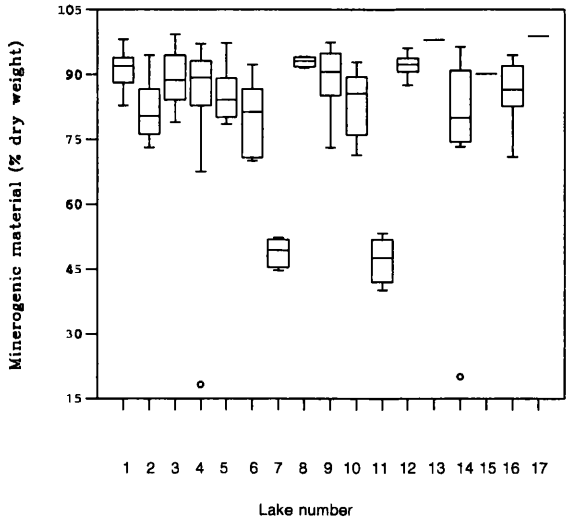

5.4 Spatial distributions of minerogenic and organic determinands

5.4.1 Sombre Lake

The most dense, minerogenic sediments are found proximal to the inflow on the delta feature and along the western margin of the lake basin where the bathymetry slopes steeply from the cirque backslope of the lake (Figure 5.7). The shelf zone, subject to winter ice-scour, is characteristically minerogenic. More organic sediments trend from the deep spot towards the outflow and at mid-depth sites (4-9 metres). %BSi is generally low (<10%) with some suggestion of higher values in the photic zone (4-8 m) near the outflow, matched by higher %LOI. This coupling of higher organic contents and relatively high %BSi suggests an accumulation zone with *in-situ* benthic autochthonous production dominant over allochthonous minerogenic inputs.

5.4.2 Heywood Lake

The sample-net is highly localised (section 4.3.2) restricting interpretation of results. Sediment density is fairly uniform in both the north and south basins (Figure 5.8). Dry weight is more variable, as is %LOI, with large ranges of values over short distances. Peak %LOI does not exceed 30% in either basin, in agreement with %OM values. Organic content is not paralleled by %BSi which is low (<15%) in the samples. Organic matter is probably predominantly allochthonous, matching the observed inwash of

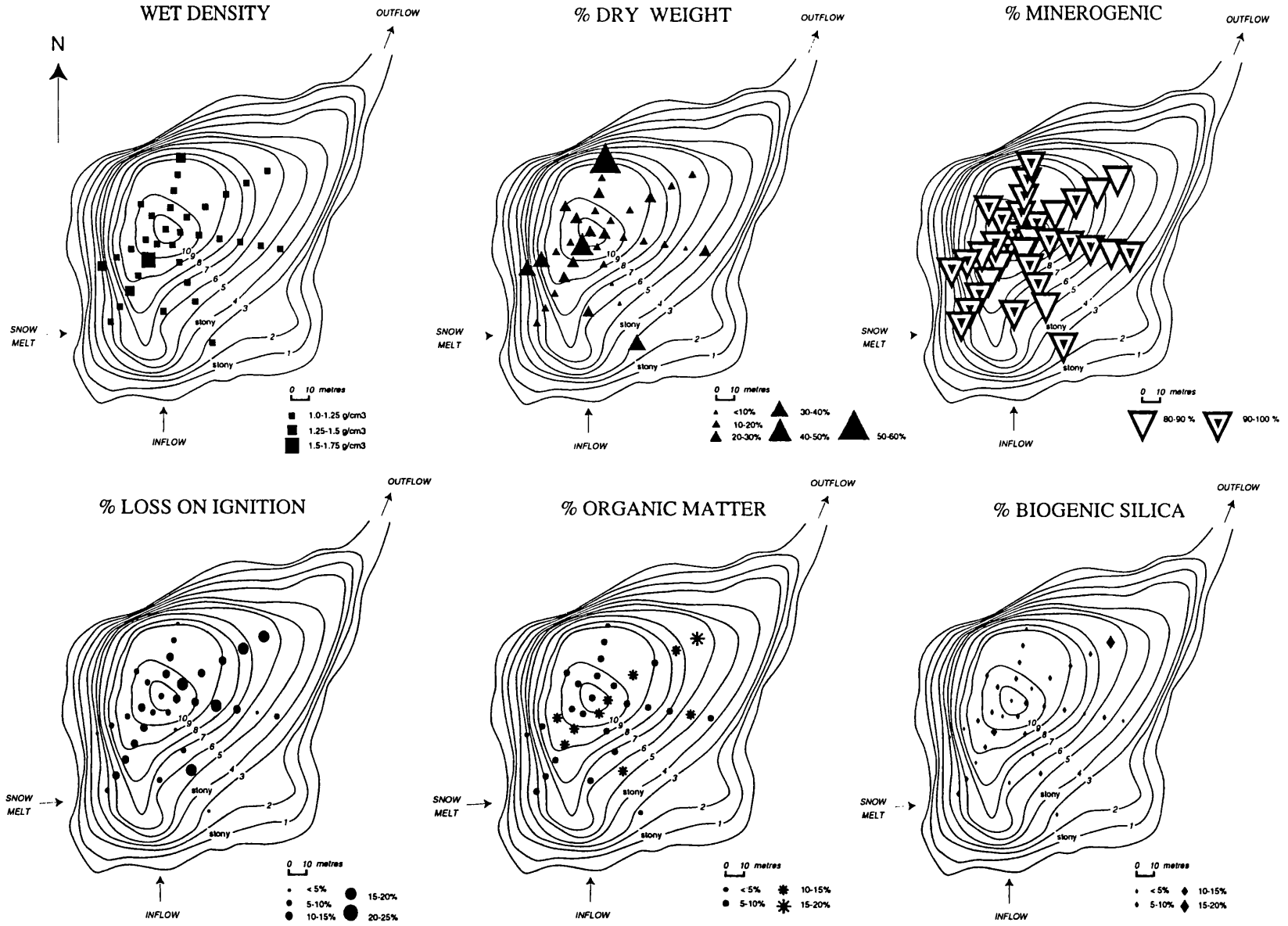

Figure 5.7 Distribution of minerogenic and organic determinands, Sombre Lake

Figure 5.8 Distribution of minerogenic and organic determinands, Heywood Lake

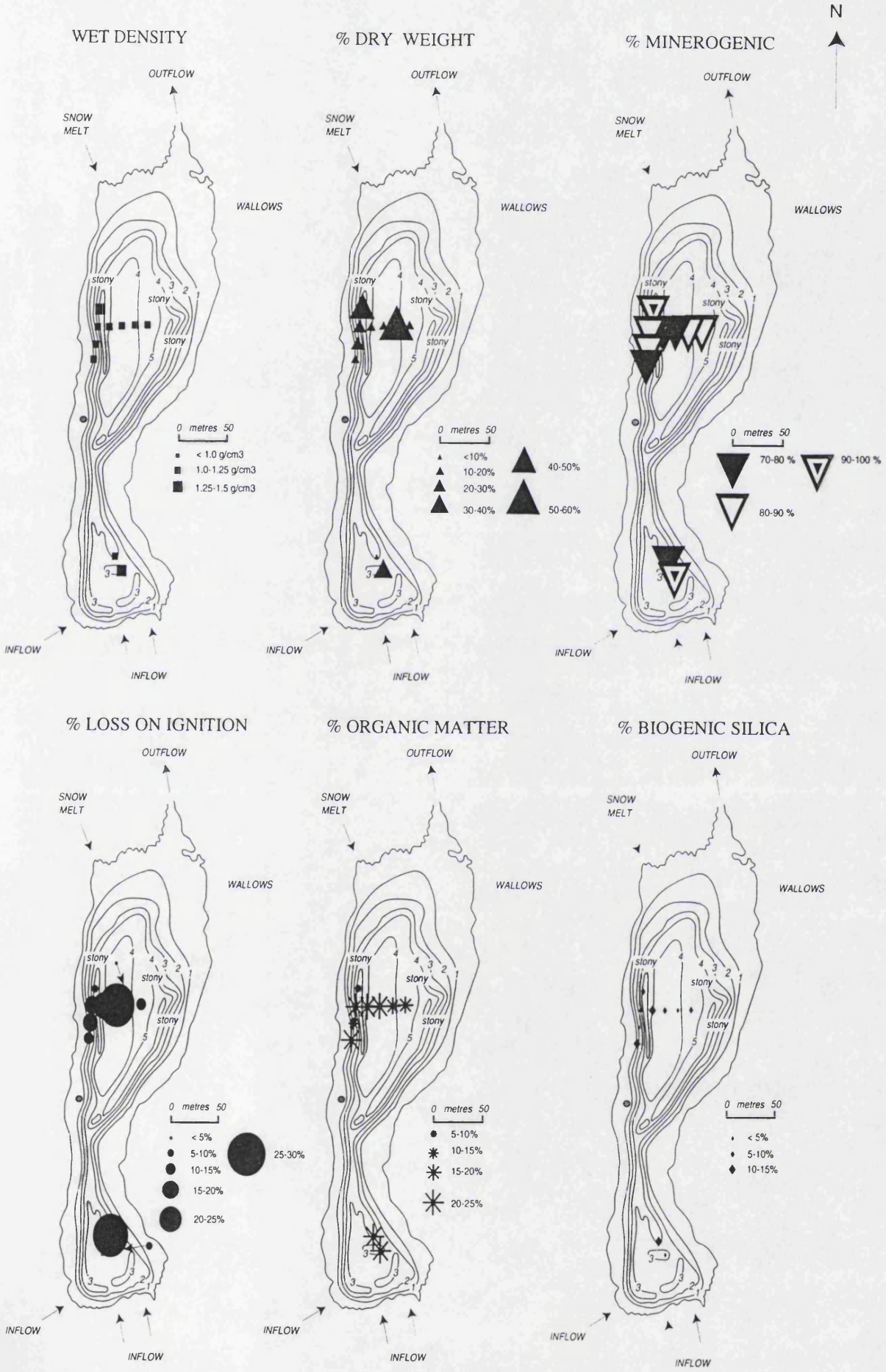

degraded, terrestrial mosses from fur-seal related activities in the catchment (Smith, 1990; Ellis-Evans, 1990). The summer phytoplankton bloom in this lake is known to restrict benthic algal production and high rates of turnover and microbial degradation probably result in little autochthonous input to the sediment. The sediments are therefore relatively minerogenic in character despite the eutrophy of lake waters.

5.4.3 Changing Lake

Surface-sediments are of fairly uniform density (1.0-1.25 g/cm^3) increasing towards the steeper basin slopes of the western shoreline adjacent to the moraine and near the prograding delta feature at the principal inflow draining from Moss Lake (Figure 5.9). The western shore is also the zone where subterranean inflow from Moss Lake enters the lake and currents are probably responsible for resuspension and scouring of more flocculent materials from this zone. High %DW values of the two Ekman grab samples (CHAN13, CHAN14) indicate that this is a zone of erosion (Håkanson, 1977) but these samples also include more minerogenic material from underlying strata (>1 cm). Sediments are highly minerogenic and the surficial water content is also high (%DW <20) suggesting sample sites in the zone of accumulation (Håkanson, 1977). %LOI is surprisingly high (up to 35%) despite the lake's low nutrient status. %LOI is slightly lower in the central basin and higher around the mid-depth zone of 2-4 metres (photic zone). %OM determinations do not fully match patterns in %LOI, possibly owing to local inputs of marble-amphibolite lithologies (Chapter 3) and the effects of carbonate loss during combustion (Dean, 1974). %OM is greatest in the distal part of the basin. This is the oldest zone of the basin as ice retreat only exposed the northern part of the basin in the 1970s (section 2.3.2.3). %BSi is low in the basin (<20%) but higher values are found in the southern basin near the secondary inflow. This meltwater source percolates more slowly through an area of mosses and lichens, perhaps enhancing nutrient inputs at this point in the lake.

5.4.4 Moss Lake

Density values divide the basin along a north-east to south-west transect, with higher densities to the north and west and lower values to the south and east (Figure 5.10). This division is also seen in the distribution of %DW. Steep slopes above the western margins of the basin provide coarse materials by mass-movement, especially on the western margins of the basin. Sediments with higher water contents (%DW <20%) are found in the central basin and towards the east, such that this zone is classified as a

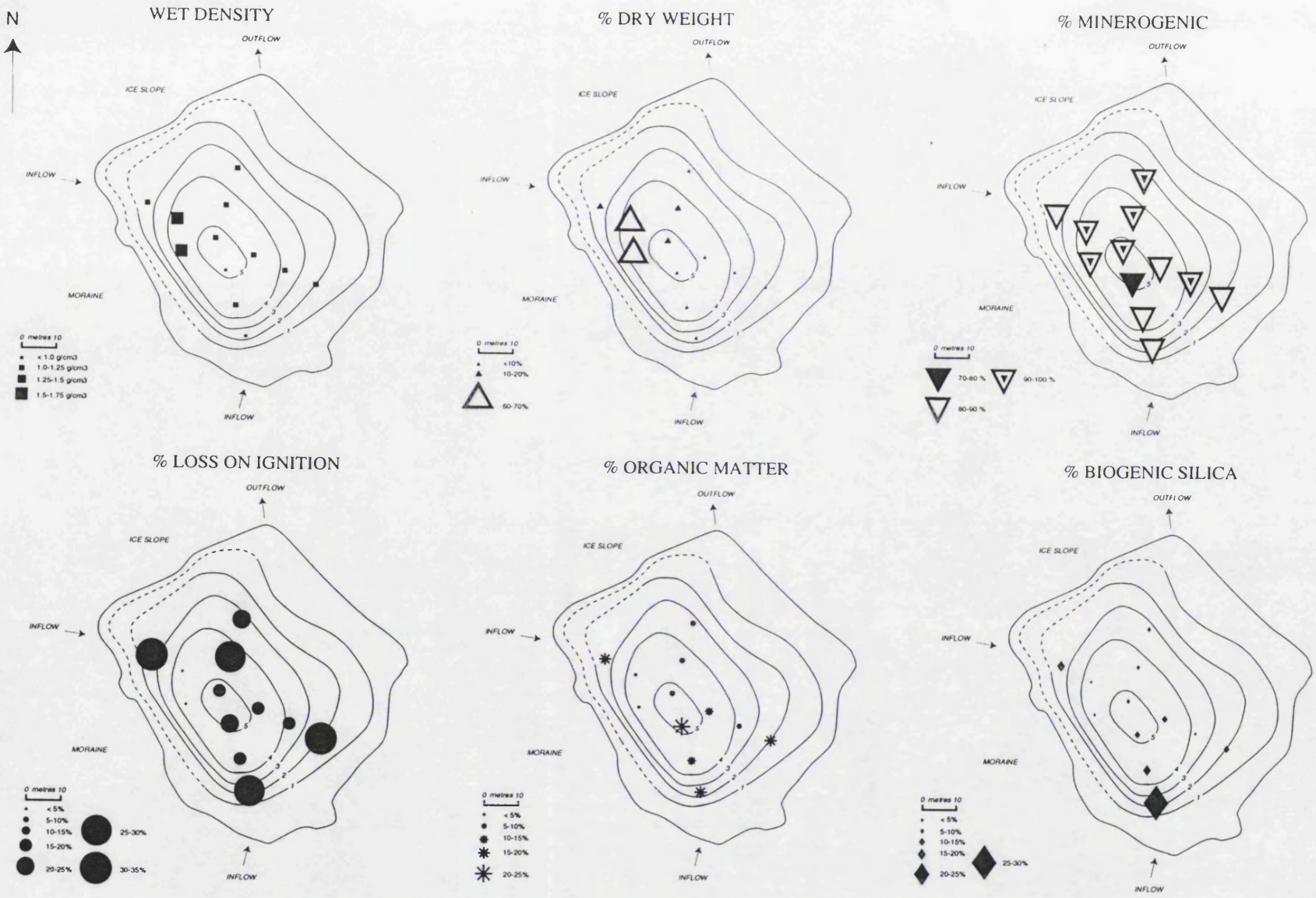

Figure 5.9 **Distributions of minerogenic and organic determinands, Changing Lake**

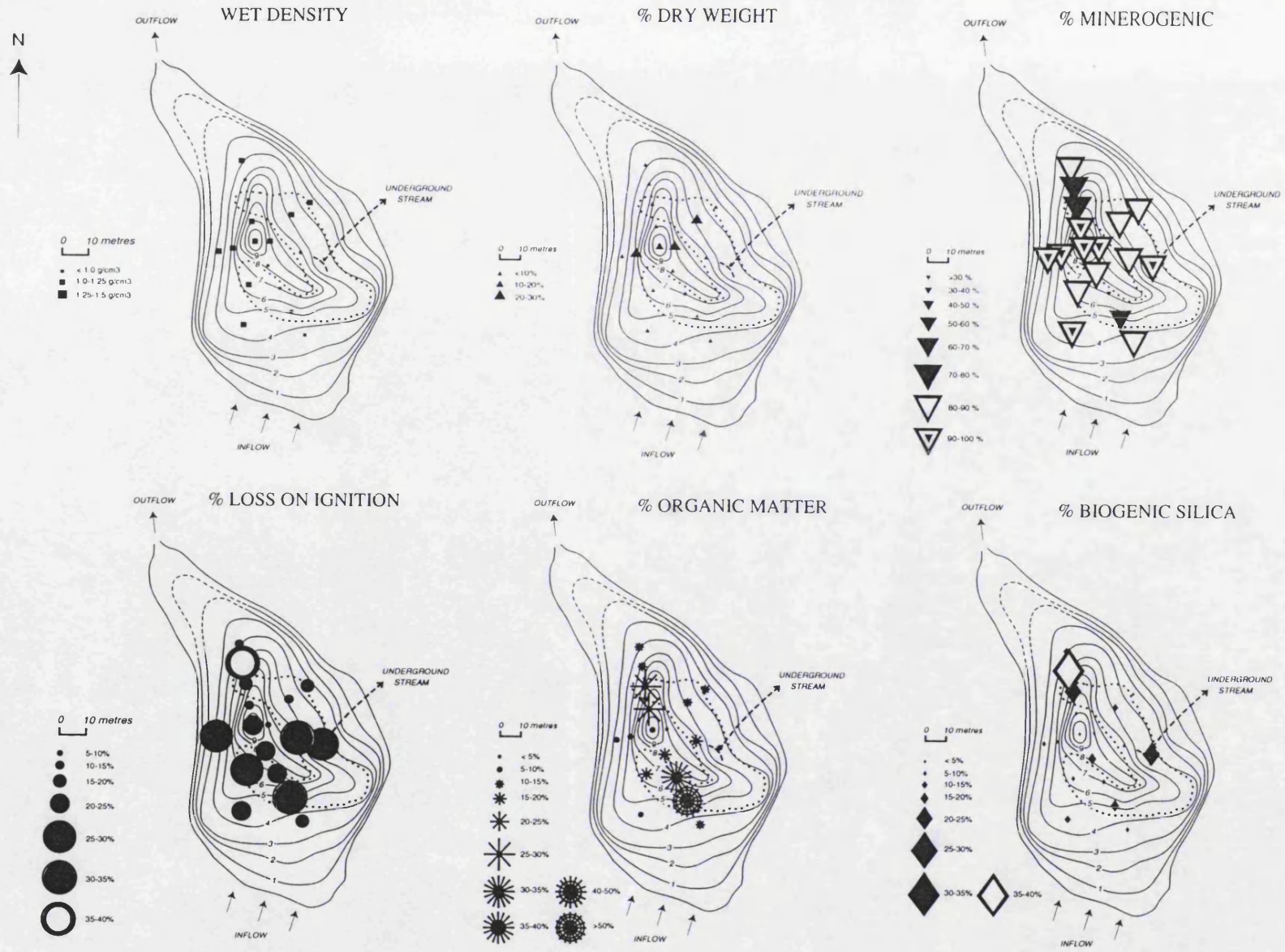

Figure 5.10 Distributions of minerogenic and organic determinands, Moss Lake

zone of accumulation (Håkanson, 1977). Bathymetry and seasonal ice-scour of the margins probably favours the focusing of fine sediments towards the central basin (section 4.4.2). Low density values agree reasonably well with the moss distribution limits mapped by Light (1976) and are matched by high %LOI (25-40%) values. Individual moss stands are localised within the zone and the lowest %LOIs (<20%) are from samples where no mosses were collected with the sediment-water interface. Moss is probably responsible for the entrapment of coarse particulates hence the local variability of sediment type and the high minerogenic contents of samples within the perennial moss zone. %BSi is generally less than 20% but three samples, one close to the subterranean outflow and two near the surface outflow, are higher.

5.4.5 Knob Lake

The values and distributions of determinands (Figure 5.11) are similar to those of adjoining Heywood Lake (Figure 5.8). Sediment density is uniform in the north end of the basin except a single sample near the outflow which is very dense (1.75 g/cm^3) and highly minerogenic (90-100%). Oddly, this sample also has a high organic content but very low %BSi suggesting the dominance of inwashed allochthonous organics rather than autochthonous production. This is an apparent zone of transportation with currents from the secondary inflow and the channelling of water into the funnel-shaped outflow favouring resuspension. Slightly higher densities are found in the southern basin where material is more minerogenic. Water content in these surface-sediments is highly variable (10-70 %DW) and the lowest values (%DW<20), indicating zones of accumulation (Håkanson, 1977), are in the centre of the north basin and at one location in the south basin near the deep spot. Lake eutrophy favours a summer phytoplankton bloom, restricting benthic algal production (Chapter 3). Winter anoxia causes a complete breakdown of organics and biogenic inorganics (Ellis-Evans, 1990) resulting in minimal inputs to the sediment (%BSi <10%) with localised %BSi concentrations (up to 15%) associated with higher sediment organic content in the south basin. Sediments are relatively minerogenic despite lake eutrophy.

5.4.6 Pumphouse Lake

Wet density is uniform in the basin (Figure 5.12) except near the deep spot which has highly organic (LOI >45%), flocculent sediment. Sediments have high water contents (<30% dry weight) except towards the primary inflow where the basin shelves steeply. The inflow-proximal zone has very low %LOI and %BSi values suggesting instability

Figure 5.11 Distributions of minerogenic and organic determinands, Knob Lake

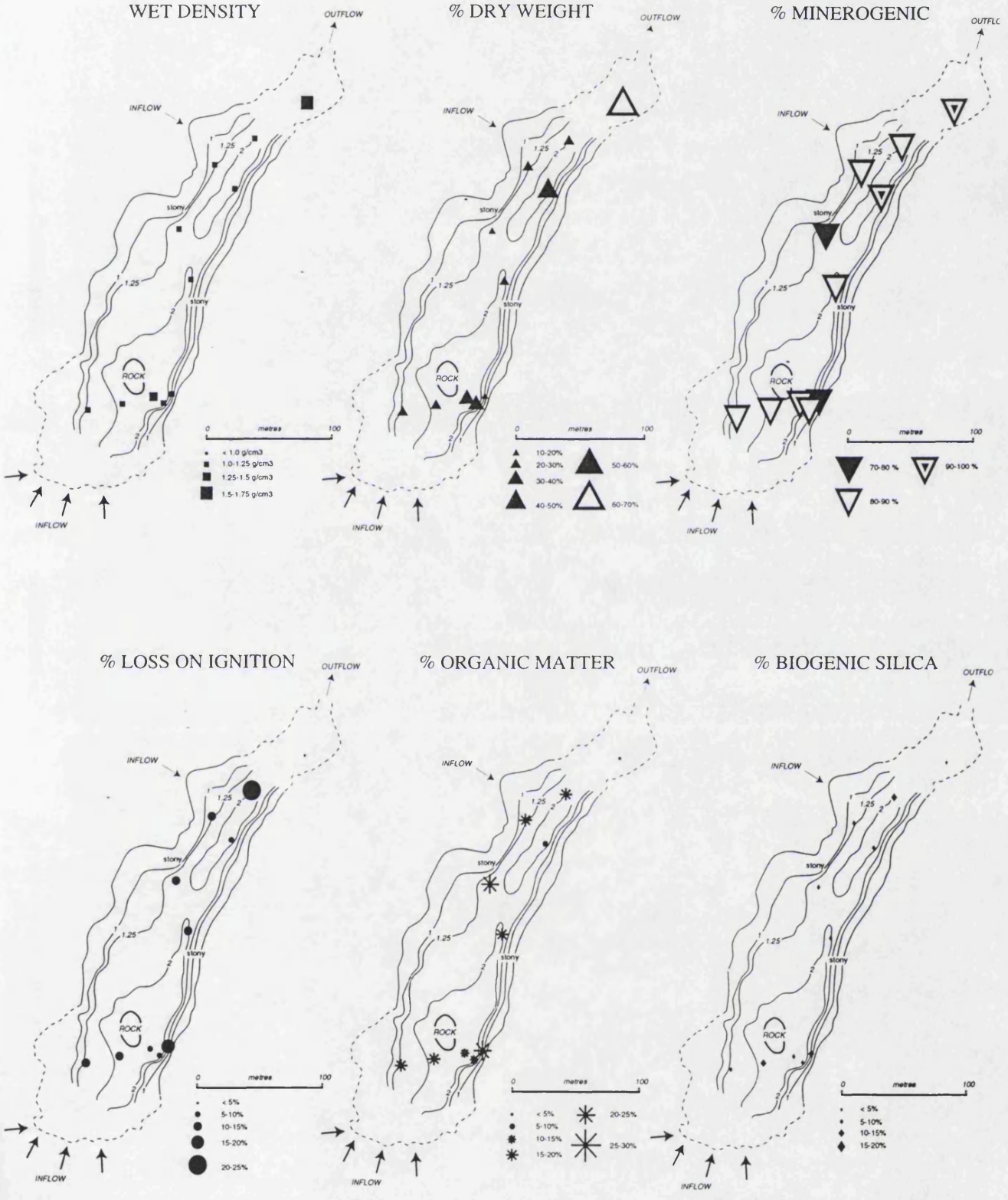

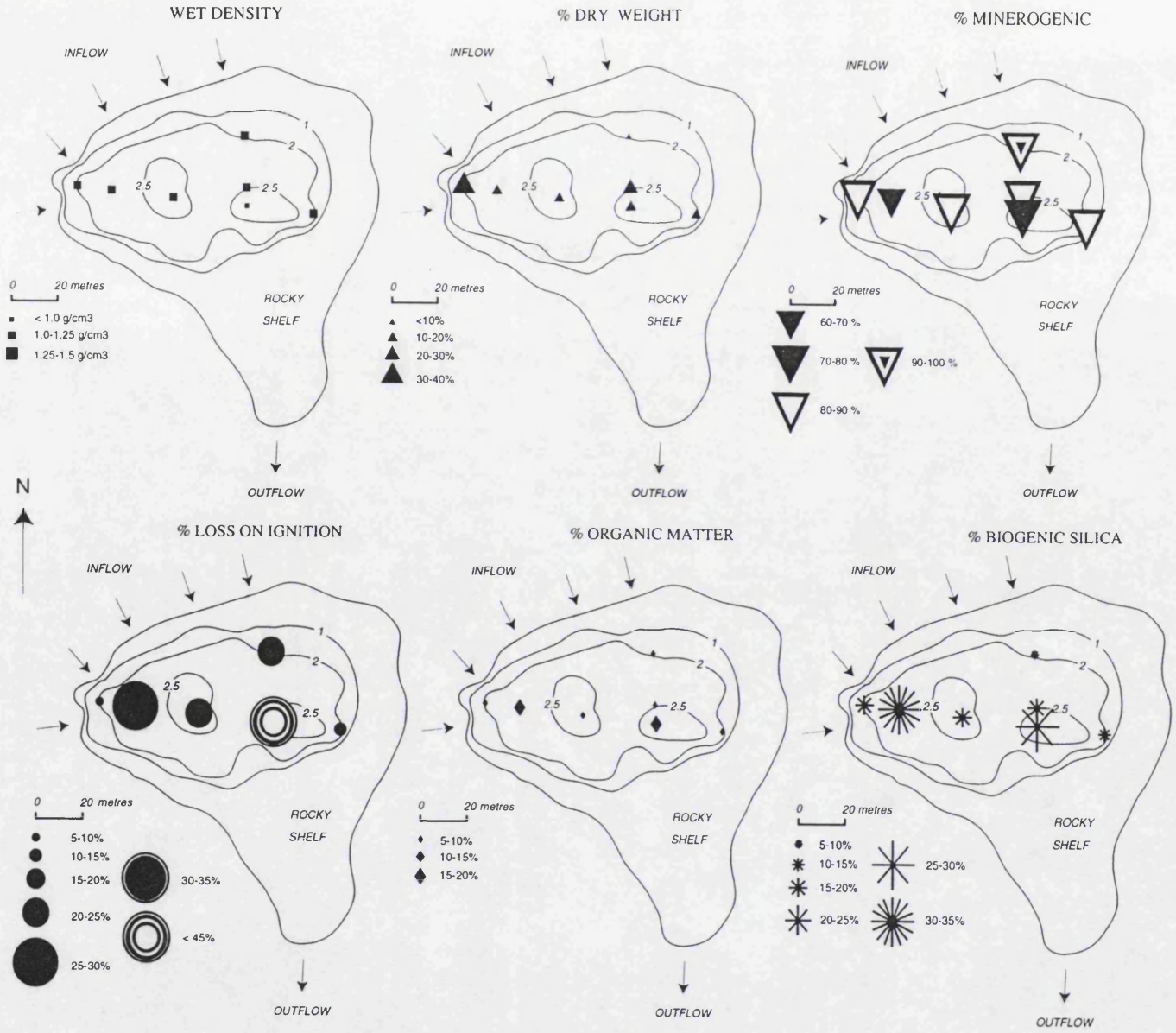

Figure 5.12 Distribution of minerogenic and organic determinands, Pumphouse Lake

and sediment resuspension. Organic materials are restricted to the basin trough and the margins are more minerogenic. The sample-net excludes samples from the extensive littoral shelf, which lack soft sediments (section 4.3.6). %BSi is highly variable and the highest %BSi values are associated with the most organic samples, suggesting *in-situ* autochthonous production in association with algal growth in the trough. Inwashed allochthonous organics probably arise from seal-related erosion of catchment vegetation cover (section 2.2.8.2) but inputs from this smaller catchment are probably less significant than in Heywood and Knob Lakes. %LOI values have a greater range than %OM by peroxide digestion and marble-amphibolite lithologies probably cause some carbonate loss during combustion (Dean, 1974).

5.4.7 Light Lake

The small sample-set (n=4; Figure 5.13) is limited to the central trough (section 4.3.7), an apparently stable accumulation zone. Sediment densities are low (<1.25 g/cm^3) as is %DW (<10%) (Figure 5.13). Sediments are loose, flocculent and water-saturated. They are moderately minerogenic (40-60%) but very high %LOI (30->45%) and high %BSi (25-35%) indicate the predominantly organic nature of the sediments, characterized by finely laminated cyanobacterial mats (section 4.3.7). Sources of organic matter are principally autochthonous. Allochthonous inputs are low.

4.4.8 Spirogyra Lake

The small sample-set (n=4; Figure 5.14) reflects the lack of soft sediments (section 4.3.8). Where found, sediment is of uniform density (1.0-1.25 g/cm^3) and highly minerogenic (90-100%). The two samples proximal to the inflow have higher %DW values indicating a zone of substrate instability and transportation (Håkanson, 1977). Higher water contents near the deep spot (20-30% DW) indicate the sediment accumulation zone. %LOI is slightly enhanced there (15-20%) and the deep spot is probably the focus for low density, organic sediments. %BSi is low in all samples (<10%). The shallow basin morphometry and restricted lake volume are unfavourable to perennial vegetation growth and the samples were taken too early in the summer season to capture the annual growth of filamentous *Spirogyra* characteristic of this lake (Hawes, 1983). Complete mineralisation of refractory organic matter under anoxic conditions occurs over winter (Hawes, 1983) which explains the low organic content and minerogenic nature of the sediments and its classification with proglacial Gneiss and Orwell Lakes (section 3.6.2).

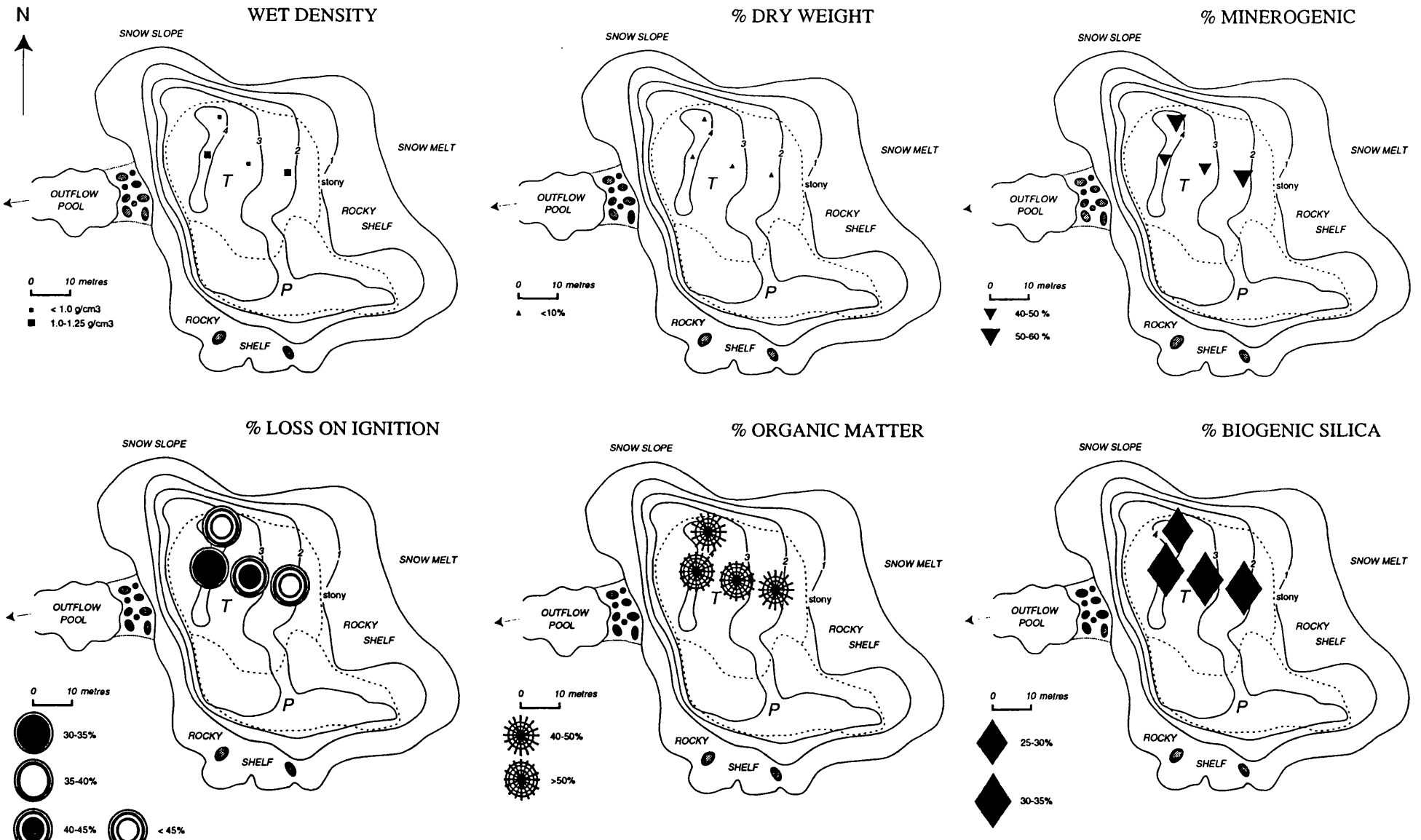

Figure 5.13 Distribution of minerogenic and organic determinands, Light Lake

Figure 5.14 Distributions of minerogenic and organic determinands, Spirogyra Lake

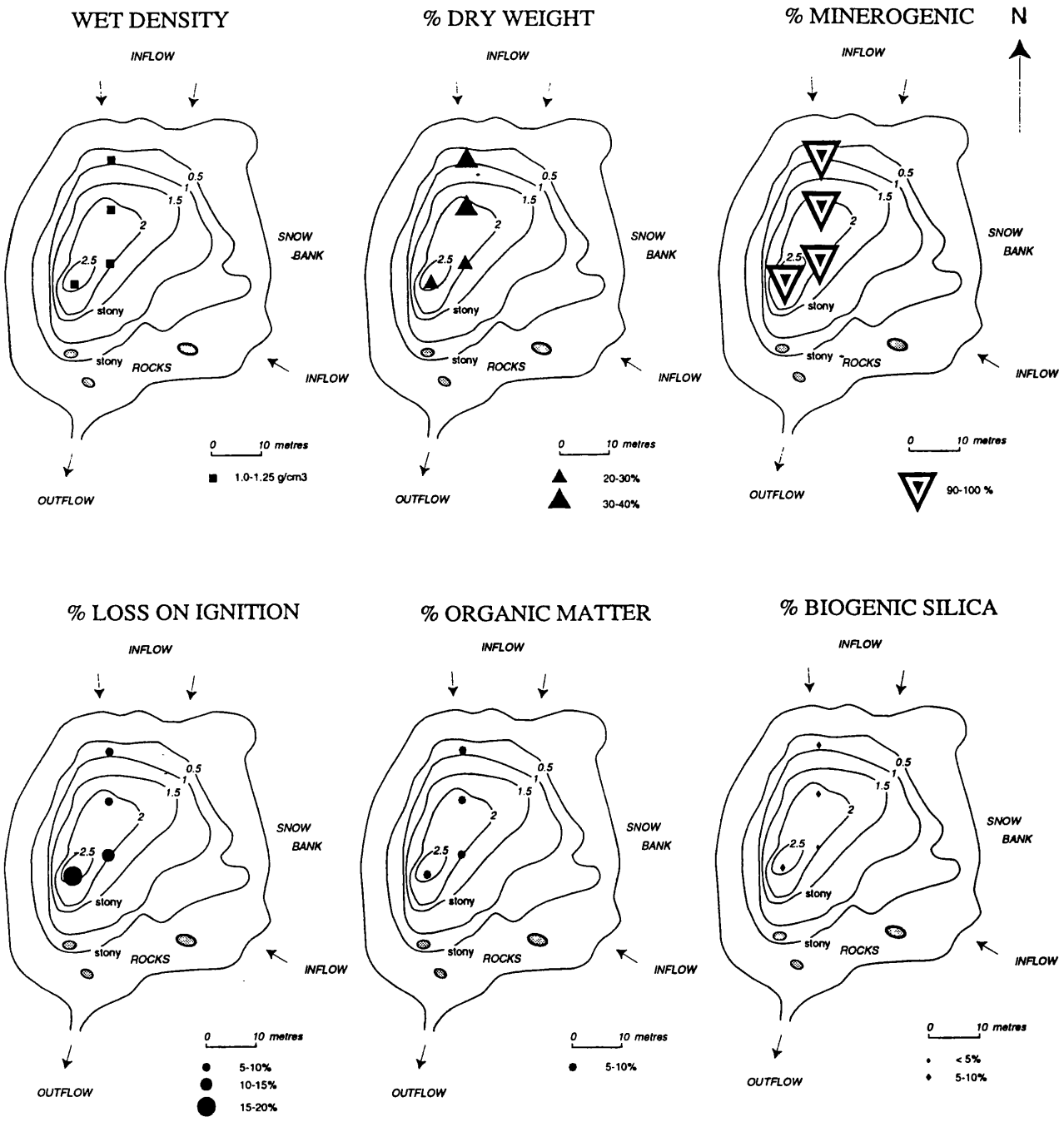

5.4.9 Tranquil Lake

Sediments are uniformly dense (1-1.25 g/cm^3) across the basin (Figure 5.15) with slightly higher densities (up to 1.5 g/cm^3) near the primary inflow which delivers a high volume of minerogenic allochthonous inputs from the glaciated backslope (section 3.3.2.9). Sediment water contents are highly variable across the basin and there is an apparent division between low values in inflow-proximal locations and higher values in distal locations. Highest %DW values (>30%) are found along the trough aligned with the primary inflow with highly minerogenic sediments (90-100%). The inflow-proximal zone and basin slopes are distinguished as zones of sediment transportation on the basis of their water contents (Håkanson, 1977). The secondary inflow basin, the central basin and the outflow trough are zones of accumulation with %DW generally <20%. Organic contents are fairly low (5-10% LOI and %OM) throughout the basin. Only isolated samples along the western margin of the lake at water depths of 3-4 metres in the photic zone have higher organic contents (15-30%) coupled with slightly higher %BSi (10-20%) which probably relates to *in-situ* algal growth. %BSi elsewhere is very low (0-10%). The lake sediments are predominantly minerogenic reflecting the oligotrophic nature of this glacier-fed lake. Only in the more distal parts of the basin does organic matter contribute a greater proportion to the bulk sediment.

5.4.10 Amos Lake

Sediment densities in the central trough are uniform near the deep spot (1.0-1.25 g/cm^3) and slightly more dense towards the stony western part of the basin (1.39 g/cm^3). This pattern is repeated in the %DW and %Min values (Figure 5.16). Water contents of the three samples from the central trough are diagnostic of an accumulation zone (Håkanson, 1977); the fourth is from an unstable zone of sediment transportation. The highest organic contents are found near the deep spot (25-30 %LOI) but these are localised suggesting sediment focusing. Outside this zone organic contents are lower (LOI 5-20%). Sediments are highly minerogenic despite lake eutrophy, a characteristic shared by Heywood and Knob Lakes. The summer phytoplankton bloom precludes the established growth of perennial benthic vegetation due to shading effects and organics are viewed as predominantly allochthonous in origin since %BSi values are very low (0-15%).

5.4.11 Tioga Lake

Wet density is uniform (1-1.25 g/cm^3) and the surface sediments are highly loose and

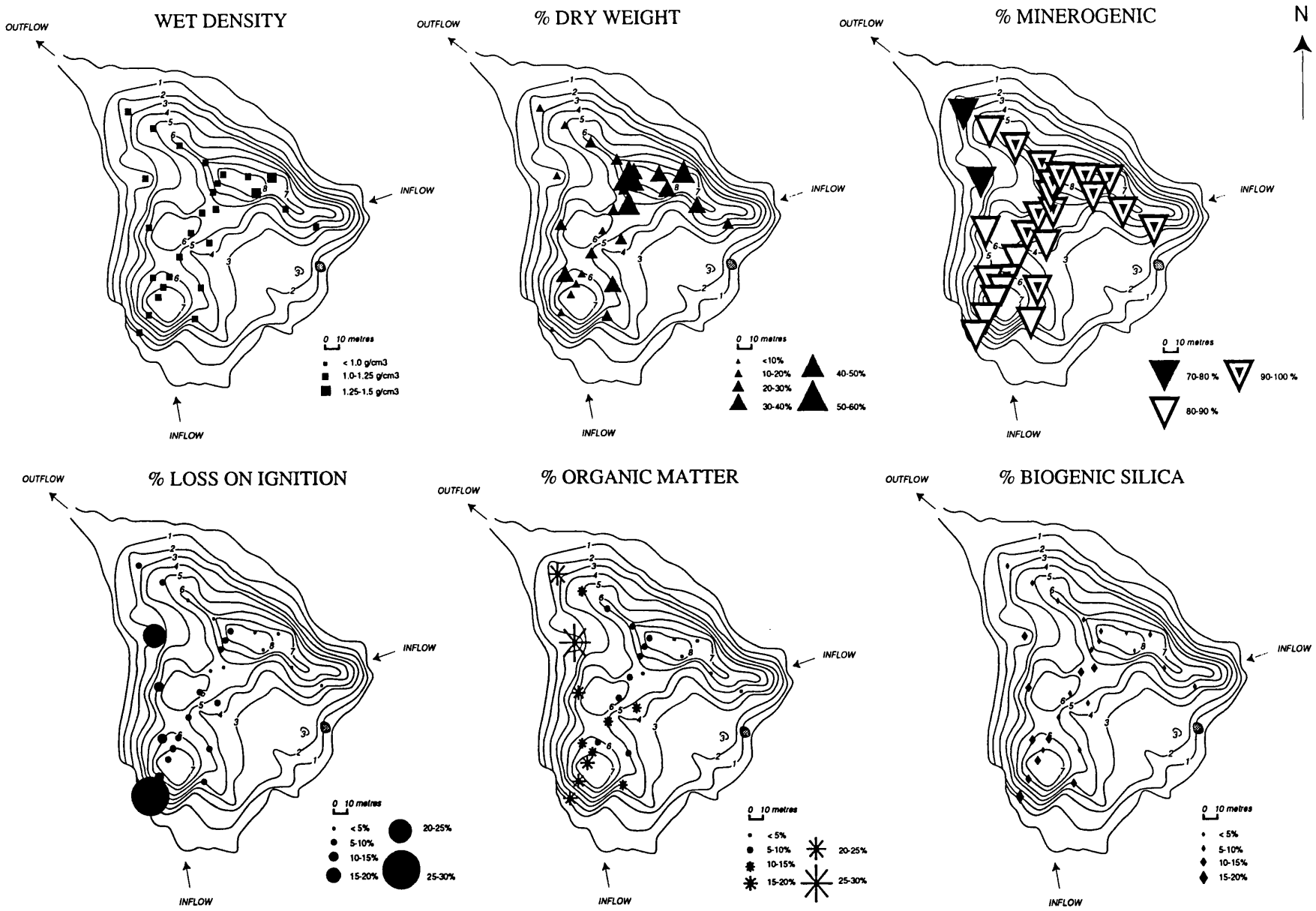

Figure 5.15 Distributions of minerogenic and organic determinands, Tranquil Lake

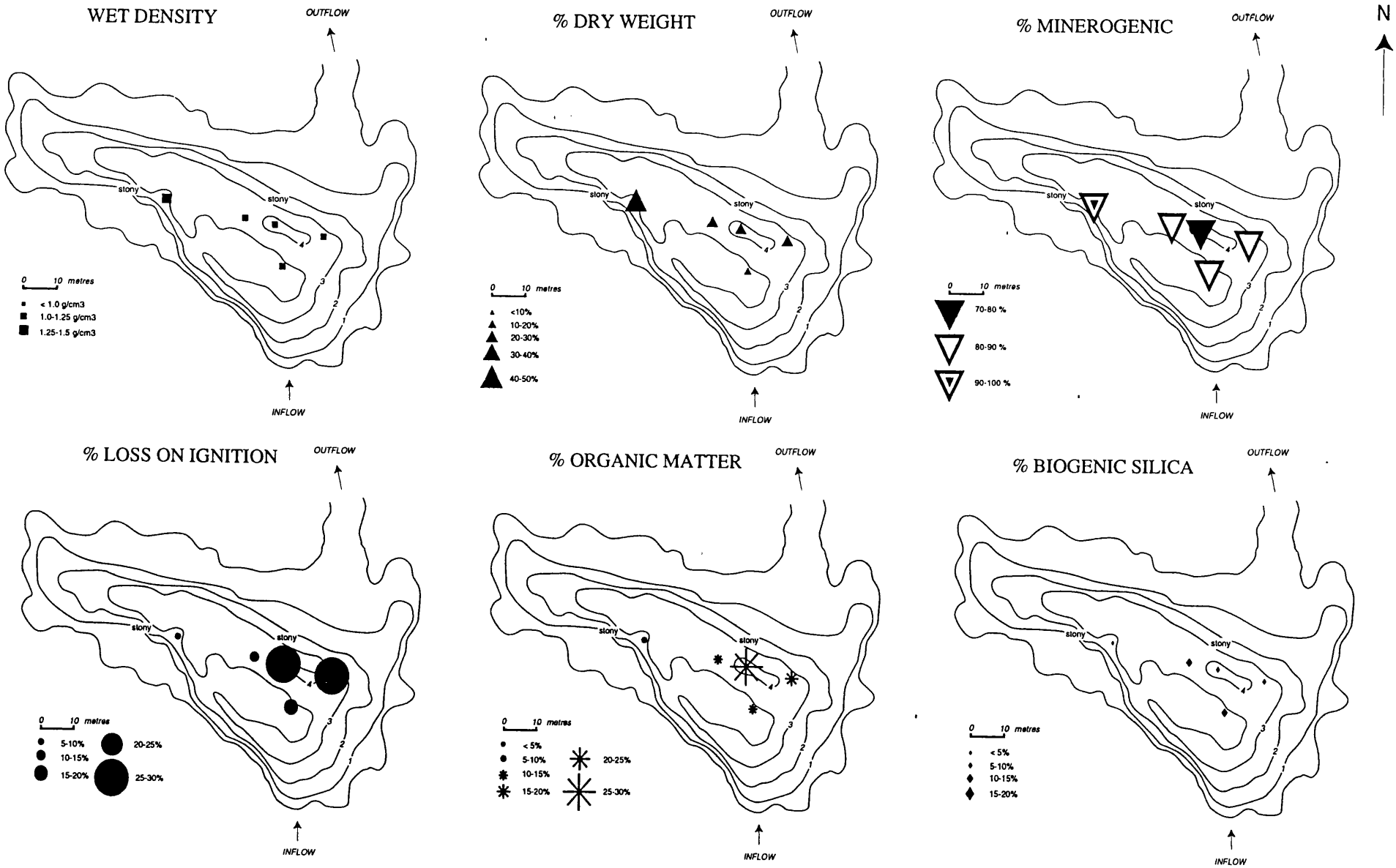

Figure 5.16 Distributions of minerogenic and organic determinands, Amos Lake

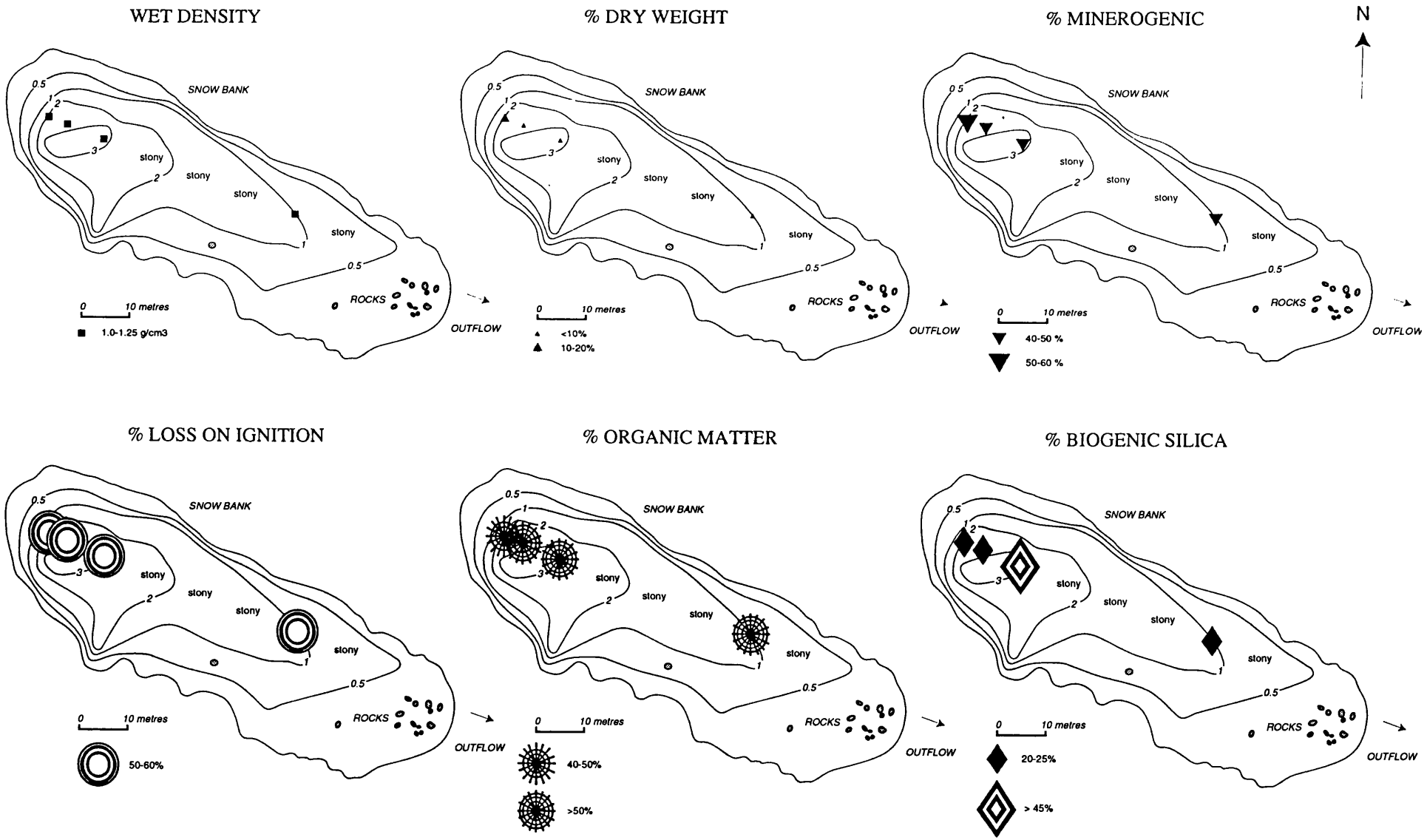

Figure 5.17 **Distributions of minerogenic and organic determinands, Tioga Lake**

water saturated, indicating a zone of accumulation (Håkanson, 1977). Sample locations are restricted to the central basin (Figure 5.17) as little to no soft sediment is found on the littoral shelf (section 4.3.11). The single sample near the outflow shares the same characteristics indicating relative stability of the benthos. %LOI is extremely high (50-60%) and minerogenic content relatively low (40-60%). Surface-sediments are composed of finely-laminated cyanobacterial mats associated with high values for %BSi. The lake environment is stable and sheltered. Inflow is by percolation through moss-stands and marginal snowbank melt offers reduced potential for the inwash of allochthonous minerogenic materials. These sediment characteristics are very similar to Light Lake.

5.4.12 Emerald Lake

Wet density values are moderately high (1.25-1.5 g/cm^3) and fairly uniform across the basin at all water depths (Figure 5.18), paralleled by high values for %DW (30-51%) indicating transportation (Håkanson, 1977), even in the central basin. The highest dry weight (51%) aligns with the secondary inflow to the south-east. %LOI is very low (<10%) confirming the glacial origin of the sediment with marginally higher values only near the outflow where chlorophytes grow in shallow water depths (section 2.3.2.12). %BSi is also slightly higher here indicating *in-situ* autochthonous productivity. Elsewhere %BSi is otherwise low (<10%) and possibly accounted for by clay losses during the laboratory procedure (section 5.5.3). Focusing of fine, organic components is probably promoted by steep basin slopes, evidenced in slightly higher %OM values in the centre of the basin. This however, is not paralleled in the %LOI results.

5.4.13 Lake 13

The two samples are assumed to be representative of the overall basin sediment characteristics. Density is very high (1.5-1.75 g/cm^3) as are %DW (>70%) and %Min (90-100%) indicating a zone of erosion (Håkanson, 1977) (Figure 5.19). %LOI is negligible (<5%) and within the errors associated with loss of crystal water and or carbonate combustion (Dean, 1974), possibly relating to the nearby presence of a marble outcrop (section 2.3.2.13). %BSi is also very low (<5%). Seasonal algal growth is observed which probably supports some epiphytic diatom growth. The lake sediments reflect the nutrient-poor, glaciated nature of the catchment and are dominated by allochthonous minerogenics from the glaciated backslope above.

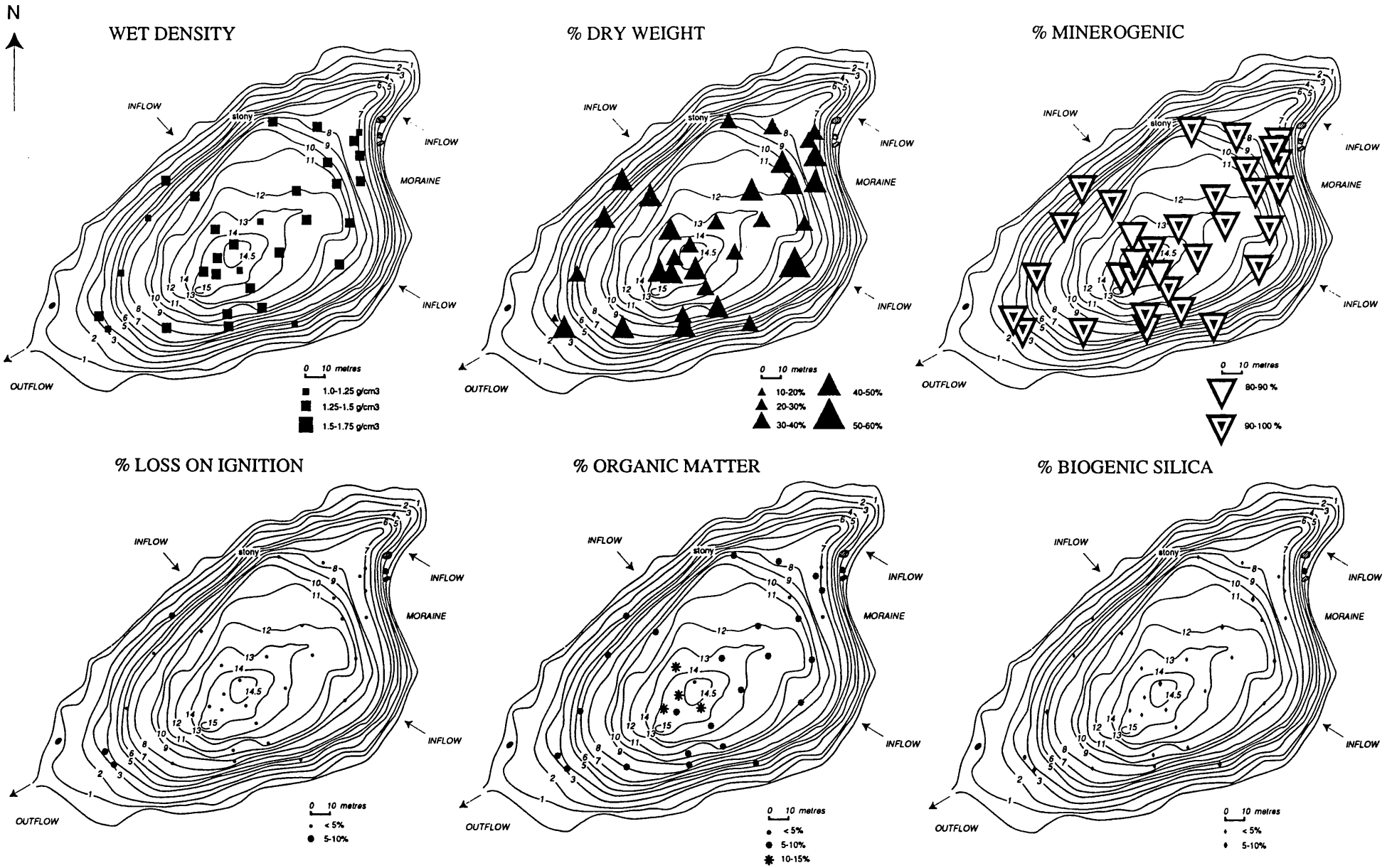

Figure 5.18 **Distributions of minerogenic and organic determinands, Emerald Lake**

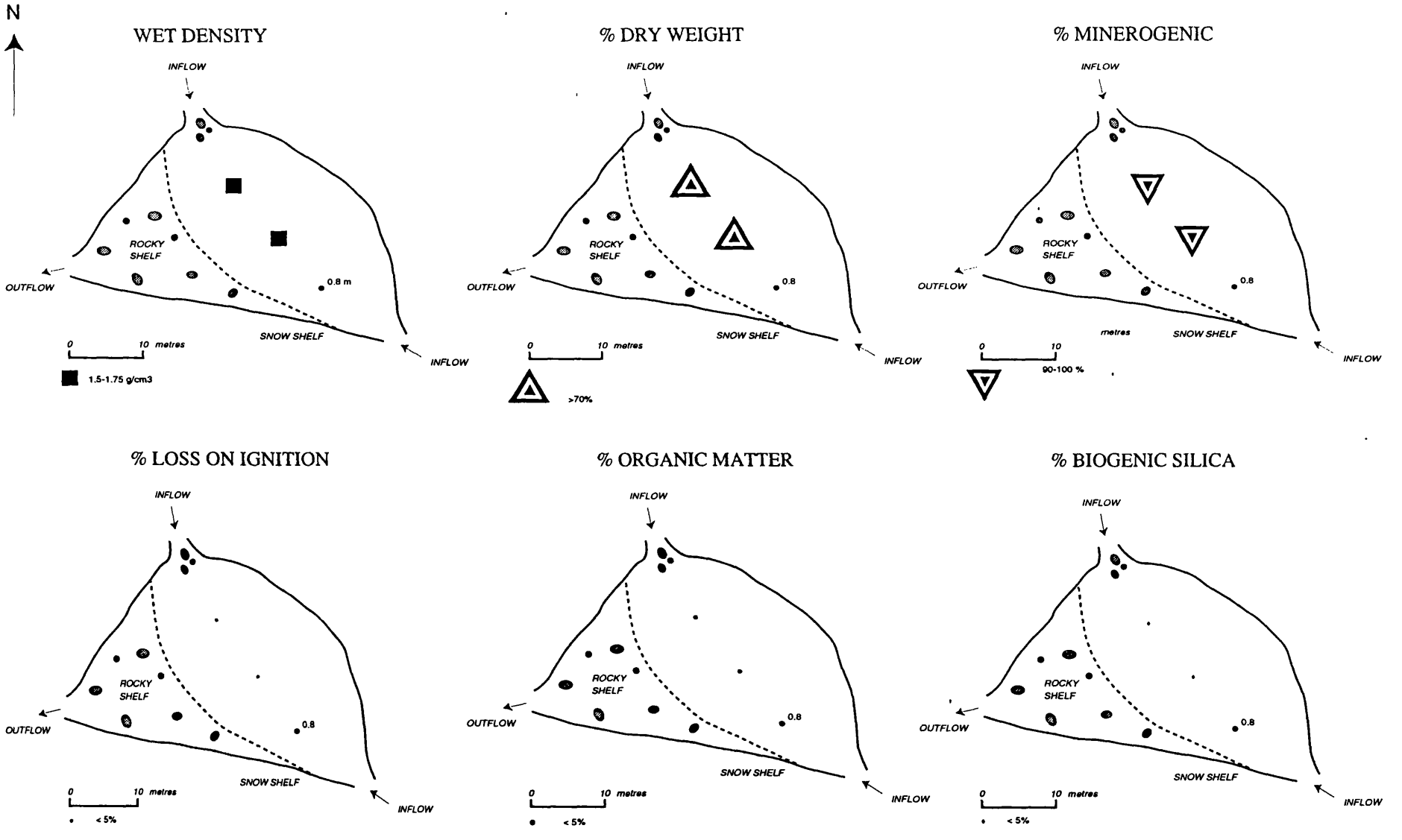

Figure 5.19 Distributions of minerogenic and organic determinands, Lake13

5.4.14 Twisted Lake

The sediment is of relatively low density (1-1.25 g/cm^3) in the north half of the basin and more variable towards the south (Figure 5.20) where the shallow littoral shelf is more extensive. Dry weights are also low (<20%) reflecting the loosely consolidated nature of the surface-sediment in accumulation zones although the minerogenic content is high (70-100%). Shallow basin depths and exposure promote resuspension of more organic sediments and focusing of organic sediment is apparent near the recorded deep spot (30-35% LOI). The deeper basin to the west is probably more influenced by receipt of allochthonous inorganic material from the inflow which drains from Emerald Lake above. %LOI is fairly uniform (10-20%) in this part of the lake. %BSi matches sediment organic content to some degree, with very low values (<5%) along the southern shallow margins of the lake and highest (15-20%) in the central deep spot.

5.4.15 Bothy Lake

Only one sample was collected owing to sediment scarcity (section 4.3.15) and the basin is composed of bare rock and gravel. %LOI is relatively low (10-15%) despite its eutrophy and proximity to the coast and marine nutrient-sources. Sediment is unconsolidated (1-1.25 g/cm^3) and prone to displacement. %BSi is negligible (<5%) and autochthonous productivity low (Figure 5.21). A dry weight of 21% indicates accumulation in this localized zone near the deep spot.

5.4.16 Gneiss Lake

Sediments are of uniform density (1-1.25 g/cm^3), loose, flocculent and water-saturated (Figure 5.22). Very low dry weights (<10 %DW) are recorded except near the inflow and outflow where a delta is actively developing (section 2.3.2.16). %DW in this area indicates a zone of transportation (Håkanson, 1977). The southern margins are highly minerogenic and no sediment was collected due to stoniness (section 4.3.16). Extremely high organic contents (LOI 25-50%) are central to the basin where sediments are composed of finely laminated cyanobacterial mats. High %BSi identifies these mats as habitats for epiphytic diatom growth. %OM is more variable than %LOI in the central basin and values are depressed towards the inflow and outflow where allochthonous minerogenic inputs from the deglaciating catchment are greatest. %BSi values are more site-specific than organic matter and like %OM display depressed values towards the inflow and outflow and in the stony trough towards the western shoreline.

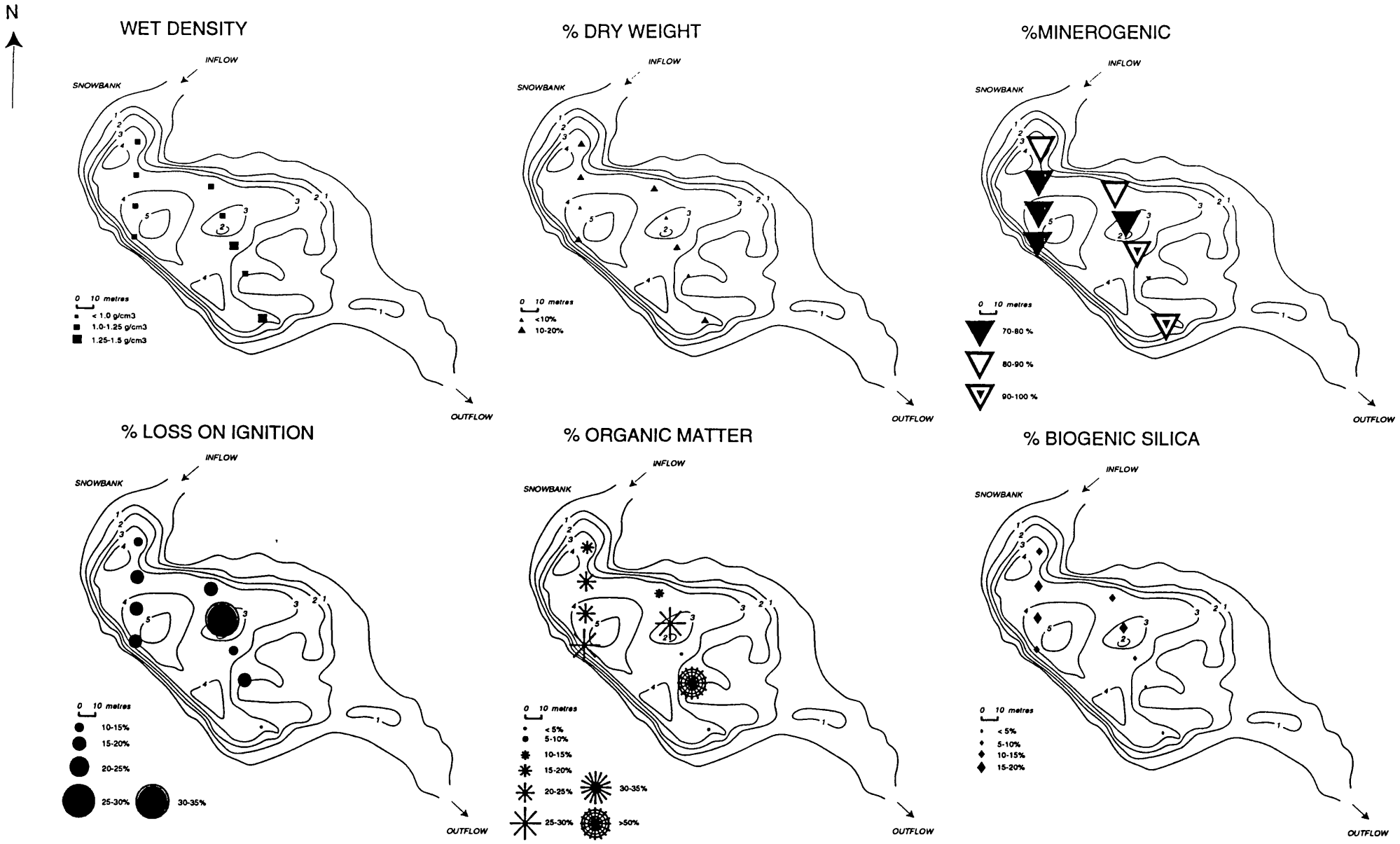

Figure 5.20 **Distributions of minerogenic and organic determinands, Twisted Lake**

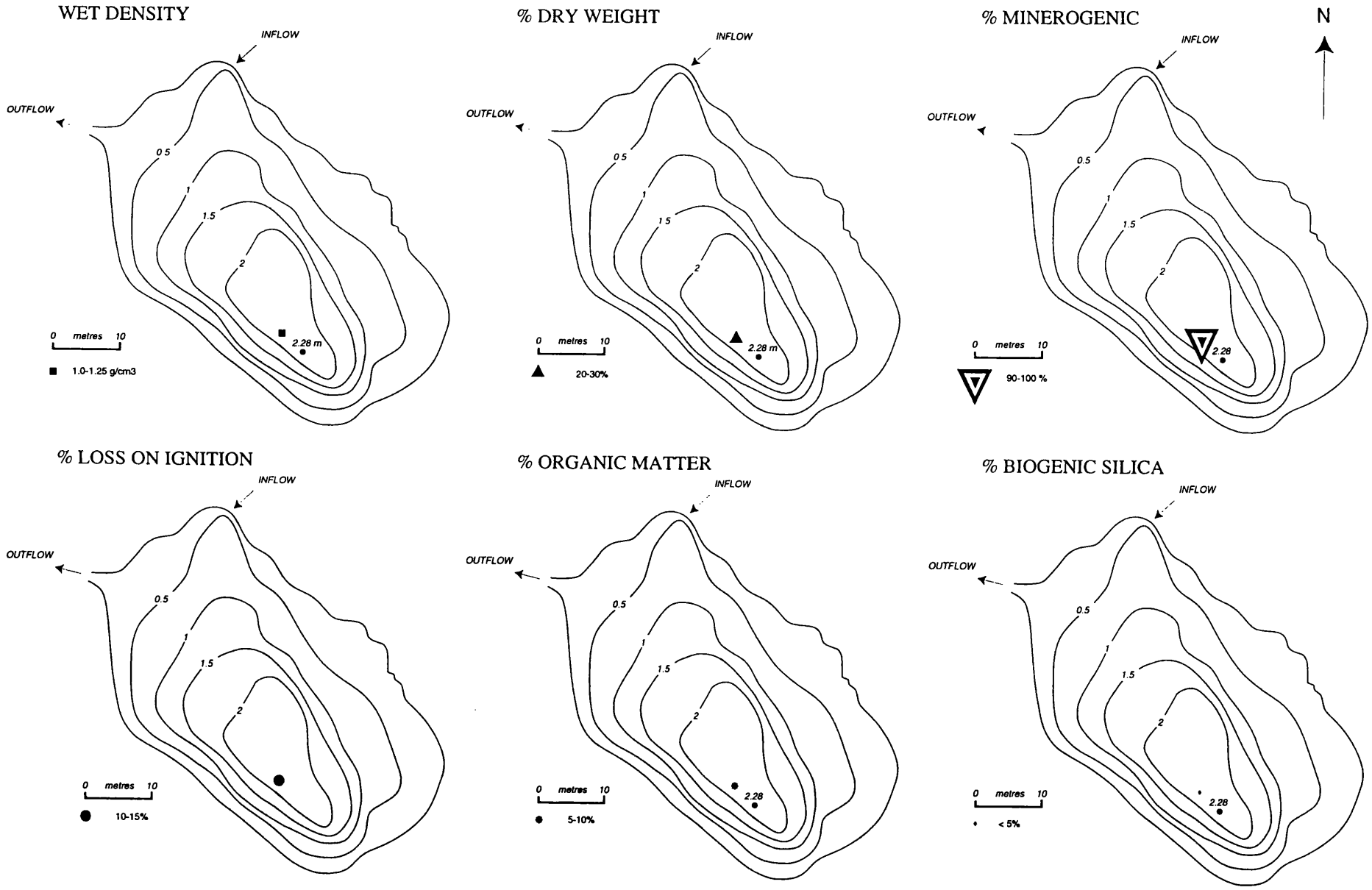

Figure 5.21 Distributions of minerogenic and organic determinands, Bothy Lake

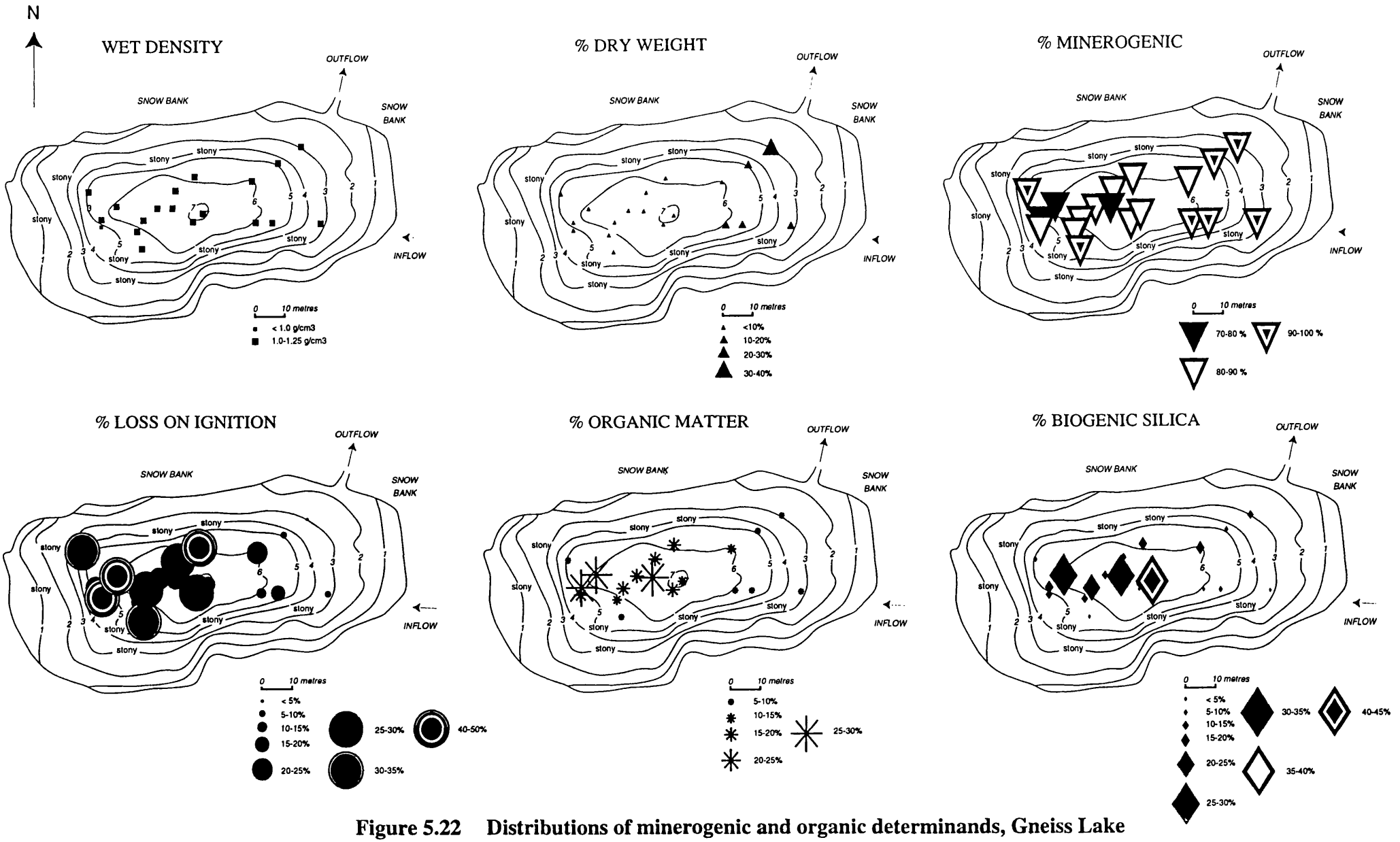

Figure 5.22 Distributions of minerogenic and organic determinands, Gneiss Lake

Figure 5.23 Distributions of minerogenic and organic determinands, Orwell Lake

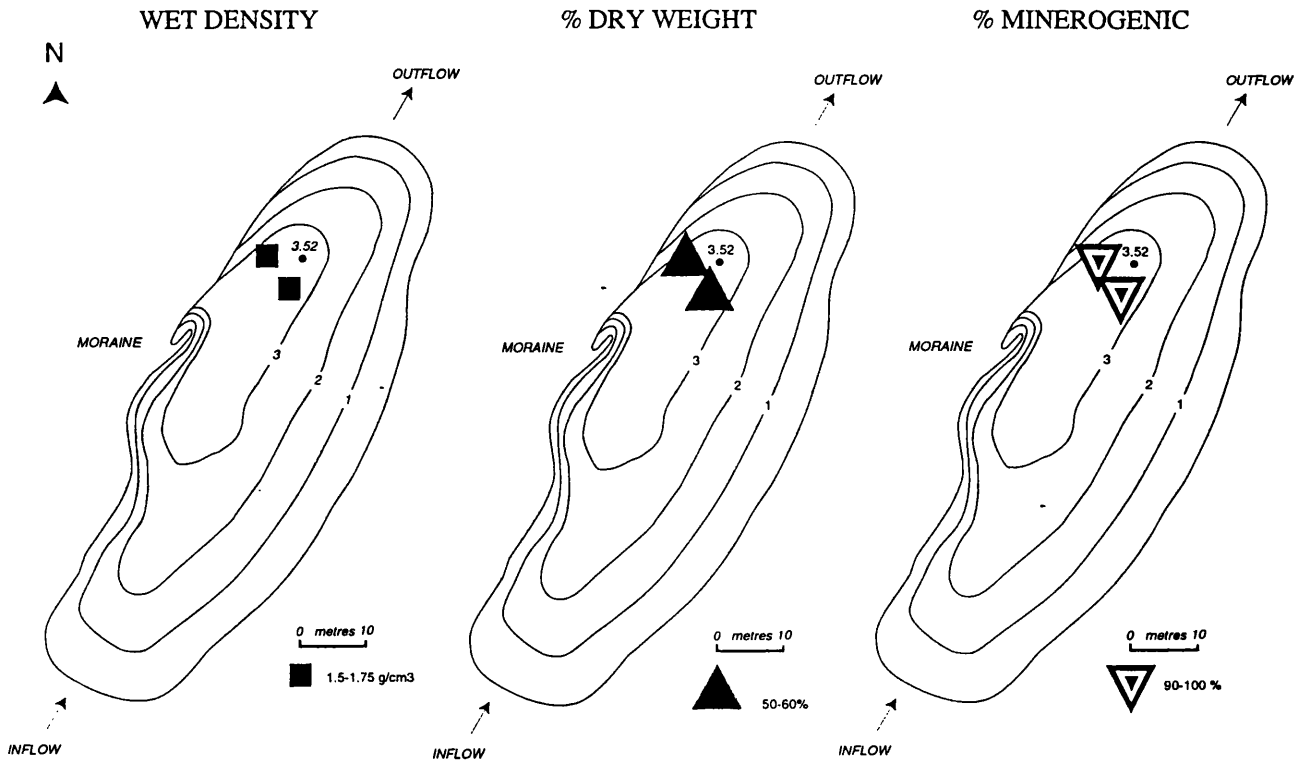

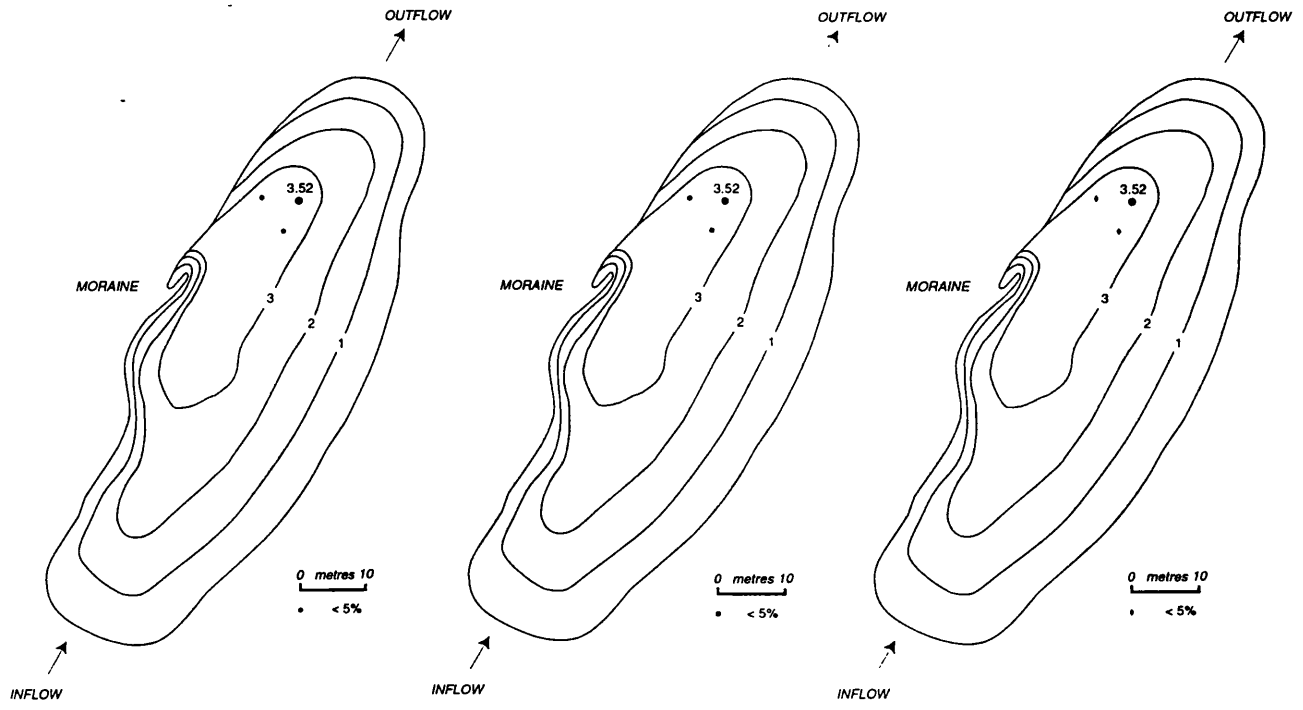

5.4.17 Orwell Lake

Only two samples were taken from this lake (section 4.3.17). Their sediments are dense with a low water content (50-60 %DW) and high minerogenic content (90-100 %Min) (Figure 5.23). They lack organic material (<5 %LOI and %OM) and autochthonous production is low (<5 %BSi). This glacier-fed lake is highly inorganic. High suspended sediment loads and periodic draining restrict seasonal algal growth and preclude perennial vegetation (Chapter 3). Low water contents (>50 %DW) indicate erosion (Håkanson, 1977). Short water-residence times and periodic basin disturbance do not appear to encourage the deposition of fine sediments.

5.5 Relationships between minerogenic and organic sediment determinands

5.5.1 Correlations

Pearson product-moment correlation matrices (Table 5.2) were constructed on both untransformed and $\log_{10}$ transformed data to quantify relationships between the six organic and minerogenic determinands for the 209 sample-set. Shaded cells in the correlation matrices represent relationships which are positive and highly significant ($p<0.001$ for 207 d.f., two-tailed significance test). Six relationships are significant and positively correlated; the remaining 9 relationships are significant and negatively correlated. Log_{10}-transformation does little to improve the strength of the correlations and is therefore of no additional benefit.

Table 5.2 Pearson product-moment correlation matrices for the six organic and minerogenic sediment determinands (a) no transformation (b) $\log_{10}$ transformation

(a) No transformation

WD	1.0000					
% DW	0.8614	1.0000				
% LOI	-0.5912	-0.6611	1.0000			
% OM	-0.4563	-0.4708	0.6815	1.0000		
% BSi	-0.5256	-0.5631	0.7092	0.6159	1.0000	
% Min	0.4563	0.4708	-0.6815	-1.0000	-0.6159	1.0000
	WD	*% DW*	*% LOI*	*% OM*	*% BSi*	*% Min*

Shaded cells have a significance level of $p<0.001$ where $r=0.321$ for 207 degrees of freedom
See text for nomenclature.

(b) Log_{10} transformation

WD	1.0000					
% DW	0.8080	1.0000				
% LOI	-0.6931	-0.7953	1.0000			
% OM	-0.5779	-0.5850	0.7136	1.0000		
% BSi	-0.6177	-0.6586	0.7305	0.7086	1.0000	
% Min	0.4563	0.5122	-0.6464	-0.9504	-0.6108	1.0000
	WD	*% DW*	*% LOI*	*% OM*	*% BSi*	*% Min*

Shaded cells have a significance level of $p<0.001$ where $r=0.321$ for 207 degrees of freedom
See text for nomenclature.

The strongest positive correlation is between %DW and wet density (r=0.86), followed by %LOI versus %OM (r=0.68) and %OM versus %BSi (r=0.62). %OM and %Min have a perfect negative correlation as expected, since the latter is measured weight loss determined from the former (Appendix B). The strongest negative relationship is between %LOI and %Min (r=-0.68).

5.5.2 Comparison of surface-sediment organic content from two independent laboratory procedures

The methods used to determine organic content (sections 5.2.3 & 5.2.4.2) provide the opportunity to assess the results of two independent analyses. Both methods are a combined measure of autochthonous and allochthonous organic fractions. %LOI and %OM are not perfectly correlated (r=0.68) indicating some difference in analytical performance. The scatterplot of %OM versus %LOI (Figure 5.24a) illustrates the mismatch in sample estimates. MOSS12 and TWIS6 are obvious outliers with high %OM values, probably through laboratory error. Removing these two samples yields a near straight-line relationship (Figure 5.24b). Peroxide digestion is assumed to be the more exact procedure and a better surrogate of organic carbon than %LOI (cf. Håkanson & Jansson, 1983). Discrepancies between the two analyses probably result from (i) imperfect burn at 550°C leading to incomplete loss of organic matter for %LOI, (ii) loss of carbonates at 550°C leading to overestimate of %LOI (this may be occurring in Changing and Pumphouse Lakes with higher proportions of marble in the sediments), and (iii) measurement error in weighing of organic matter loss through peroxide digestion.

Figure 5.24 Scatterplots of % Organic Matter versus % Loss On Ignition

(a) All surface-sediments

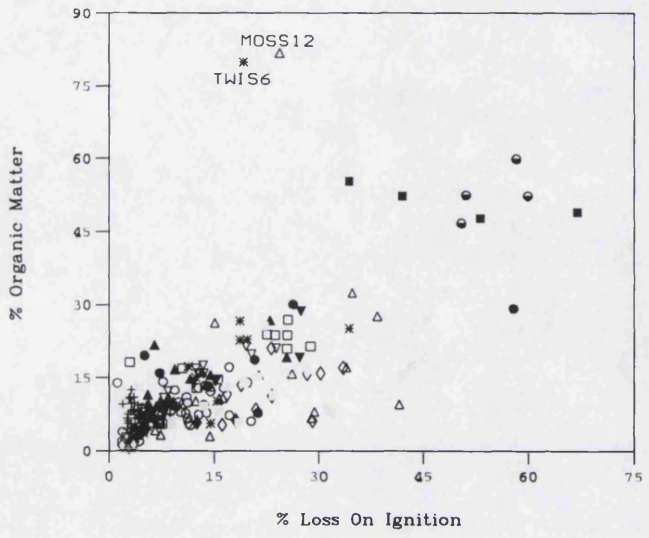

(b) Outliers removed

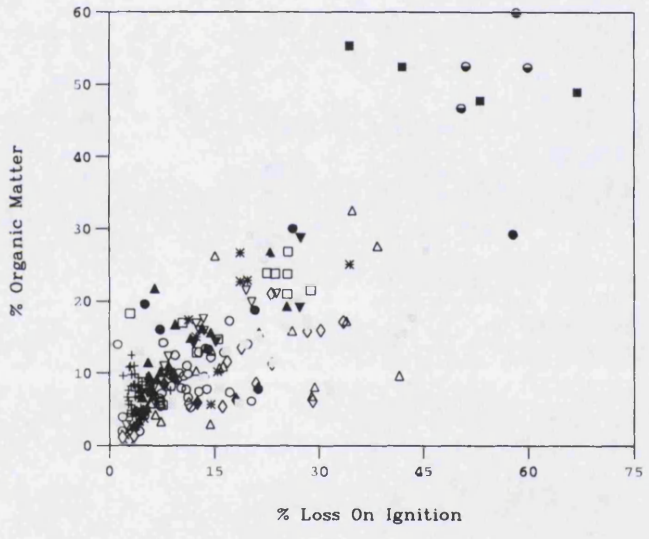

5.5.3 Relationships between sediment organic content and biogenic silica

In early postglacial sediments low levels of %BSi do not always agree with other evidence for relatively high productivity, possibly due to poor preservation and/or silica-limited diatom growth (Renberg, 1976). This could present a problem in some of the Signy Lakes with conditions analogous to those of early post-glacial lakes of temperate latitudes. Silica however, is not limiting (section 3.4.3) and correlations between %BSi and organic matter (section 5.4.2) are positive and high. Spatial distributions of determinands (Figures 5.7-5.22) suggest a covariant relationship between organic matter and %BSi; sites with high organic matter also seem to support or even stimulate the

greatest autochthonous production. The possibility of a cause-effect relationship is explored in this section.

The scatterplot of %OM versus %BSi (Figure 5.25a) isolates the high leverage samples MOSS12 and TWIS6 in the bottom right corner of the graph. Once removed, a linear scatter is achieved (Figure 5.25b).

Figure 5.25 Scatterplots of % Biogenic Silica versus % Organic Matter (a) all samples (b) outliers removed

(a) All surface-sediments

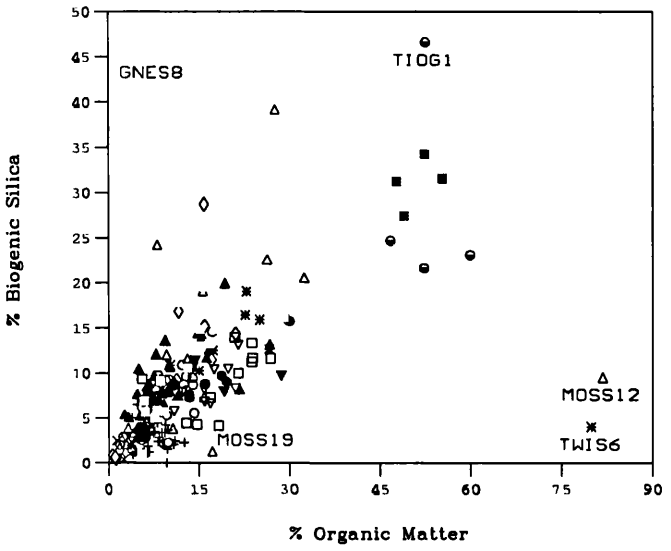

(b) Outliers removed

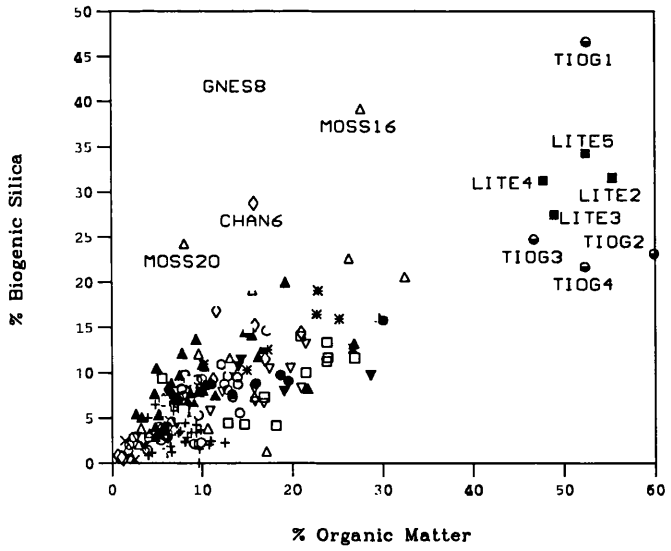

Tioga (half-filled circles) and Light (black squares) Lake samples are outliers with high values for both %BSi and %OM. The lowest values for both measures are in Emerald

Figure 5.27 **Scatterplots of the 6 minerogenic and organic determinands versus water depth (n=209)**

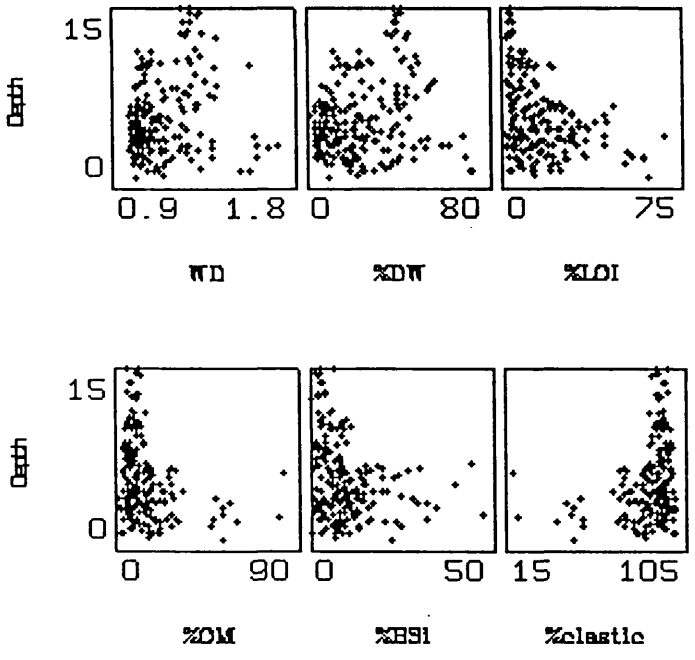

Lake (crosses) and some samples from Sombre (open circles), Changing (open diamonds) and Moss Lakes (open up-triangles). Moss, Pumphouse, Amos and Gneiss lakes have wide ranges suggesting greater within-lake variability and greater site-specific control on autochthonous productivity. Production in these oligotrophic lakes is principally restricted to the benthos. In the lowland coastal lakes (Heywood, open squares, and Knob, open down-triangles) allochthonous organic inputs dominate and overwhelm the signature of autochthonous productivity hence low values for %BSi. The plot of %LOI versus %BSi (Figure 5.26) similarly shows a straight-line relationship. The sample-population is highly influenced by samples from Tioga Lake, LITE3, LITE4 and PUMP4. Neither MOSS12 or TWIS6 exert an extreme influence in this plot for either measure confirming the hypothesis that their extremely high %OM values result from laboratory error (section 5.3.4).

Figure 5.26 Scatterplot of % Biogenic Silica versus % Loss On Ignition

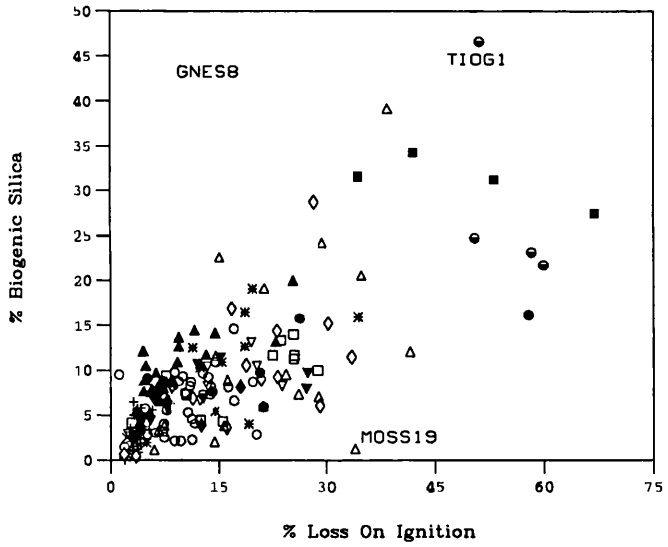

There is a stronger coupling between %OM and %BSi; %LOI appears to be less site-sensitive and the analytical method slightly less accurate. The coupling between organic content and %BSi may be because: (i) benthic and/or epiphytic diatom growth, represented by BSi, is associated with perennial vegetation (mosses or cyanobacterial mats) and senescence and death is succeeded by *in-situ* incorporation into underlying sediments (Oppenheim, 1990), and/or (ii) low-density organic sediments (allochthonous and autochthonous organics) and biogenic siliceous remains are redistributed and focused into deeper parts of the basin or concentrated locally in sub-basins or troughs. The

effects of sediment focusing are considered below.

5.6 The effects of sediment focusing

A close relationship between water depth and the water content of surficial sediments has been observed in previous studies (Håkanson & Jansson, 1983), the latter increasing with depth in association with the focusing of fine materials and organic matter. Water content, the reciprocal of % dry weight, has been used to crudely predict zones of erosion, transportation and accumulation in lake basins (Håkanson, 1977) based on differences in their potential for resuspension. The zone of erosion is marked by coarse-grained, non-cohesive sediments and is found in areas of high water turbulence. Beyond this is the zone of transportation, a zone of discontinuous sedimentation where sediment accumulation is interrupted by infrequent periods of resuspension and associated transport during overturn or storm events. Below this is the zone of accumulation where no further focusing takes place. Håkanson (1977) uses the 50% water content to define the cut-off between areas of erosion and transportation; sediments with >75% water content are representative of zones of accumulation. Håkanson's (1977) scheme has been criticized (Blais & Kalff, 1995) for being over-simplistic as sediment water content tends to overestimate the areal extent of the accumulation zone and does not always accurately define the boundary of the transportation zone. Mean basin slope (Blais & Kalff, 1995) is considered to be a better predictor of the transition zone between the transportation and accumulation but for a crude classification Håkanson's scheme (1977) is seen to be adequate. Here, %DW is used as the inverse of water content (section 5.2.2), a reversal of Håkanson's theorem. The %DW predicts that most samples are taken from accumulation zones (n=134), a third from the zone of discontinuous sedimentation (n=64) and a few from the zone of erosion and transportation (n=11). This sample classification is summarised in Table 5.3 and superimposed on the ordination biplot (Figure 5.29c).

The scatterplots of the six determinands versus water depth for all 209 samples are plotted in Figure 5.27. Scatter is noisy and there are no simple straight-line relationships. Wet density (r=0.1909, p<0.1), %DW (r=0.2249, p<0.05) and %Min (r=0.2671, p<0.01) increase with greater water depth. Values for %LOI (r=-0.3434, p<0.001), %OM (r=-0.2671, p<0.01) and %BSi (r=-0.2567, p<0.01) are negative with increasing water depth, i.e. organic content and the productivity surrogate decrease with increasing water depth. Inter-lake variability is high and there is no conclusive evidence for the depth focusing

of fine, organic materials.

Table 5.3 Surface-sediment sample classification by sediment water content (Håkanson, 1977)

Zone of erosion and transportation	*Zone of discontinuous sedimentation*	*Zone of stable accumulation*
SOMB37; HEY6; CHAN13,14; KNOB9; TRAN30; EMER32; SIG13; ORWE.	SOMB12,14,21,27,31, 40,41; HEY12,14,15; MOSS9,21; KNOB1,3,4,7,11; PUMP7; SPIR3,4; TRAN4,5,7-10,12,13,17,18,20,22; AMOS7; EMER1-4,6-31; GNES12.	SOMB11,13,15-20,22-26,28-30,32-36,38,42-46; HEY5,7-11,13,16; CHAN2-12; MOSS3-8,10-20; KNOB2,4-6,10; PUMP1-6; LITE; SPIR2,5; TRAN6,11,14-16,19,21,23-29; AMOS3-6; TIOG; EMER5; TWIS; BOTH1; GNES2-11,13-22.
n=11	n=64	n=134

Stratigraphic marker horizons offer another means of assessing the effects of sediment focusing (Hilton, Lishman & Allen, 1986) and the differential degradation of organic matter. Three lakes (Sombre, Heywood, Moss) have time-synchronous clay inwash layers (Appleby, Jones & Ellis-Evans, 1995) which are highly apparent in the lithostratigraphic analysis, with high values for wet density and %DW and low %LOI values. It lies between 3.5 and 4 cm in Sombre Lake (Jones, 1993) and two horizons are found at 5.75 and 9.25 cm in Heywood Lake and at 7.5 cm and 25.5 cm in Moss Lake (Appleby, Jones & Ellis-Evans, 1995). Similar inwash horizons are also apparent in cores from Tranquil Lake (V. Jones, *pers.comm.*), suggesting an island-wide event affecting processes of sediment delivery to these lakes.

Plots of sediment accumulation above this layer versus depth for core tops collected in this study for the three lakes (Figure 5.28a-c) illustrate the effects of sediment focusing in Sombre and Moss Lakes but not in Heywood Lake. Sediment focusing should be greatest in cirque lakes (Sombre, Moss) owing to steep basin slopes; the shallow, irregular basin of Heywood Lake is prone to resuspension by peripheral wave attack and random redistribution of sediment (Hilton, 1985; Hilton, Lishman & Allen, 1986) of sufficient magnitude to over-ride the effects of depth focusing.

Hilton, Lishman & Allen (1986) also postulated that if the mean organic content of the

Figure 5.28 Scatterplots illustrating the effects of sediment focusing and organic diagenesis in Sombre, Heywood and Moss Lakes

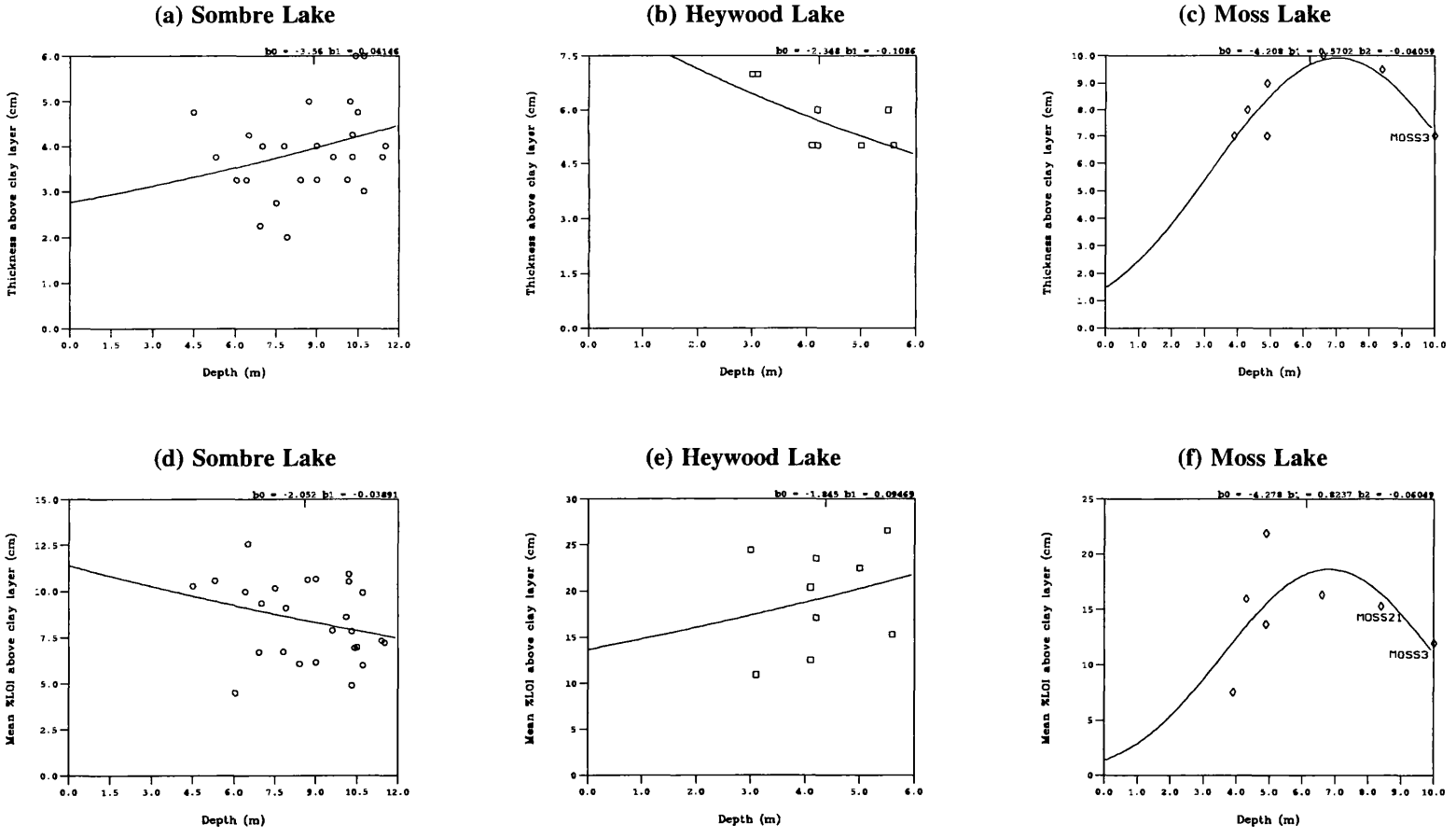

sediment from the marker horizon to the surface showed no significant change then it can be safely assumed that the long-term rates of carbon consumption in the sediments below oxic and anoxic water are the same and focusing is not actually caused by differential organic degradation. The three plots (Figures 5.28d-f) show no apparent trend in mean %LOI above the clay inwash layer with depth. It is therefore likely that focusing is the cause of observed variation rather than spatial differences in organic matter decomposition.

5.7 Classification

5.7.1 Cluster analysis

Agglomerative hierarchical cluster analysis using all 6 determinands was performed using the program CLUSTER (Juggins, 1991) on standardised data in a Euclidean distance matrix. Five types of cluster analysis were undertaken to assess their statistical performance with the data-set (refer to section 3.6.2). Group memberships for the samples in each of the five methods and their relative performances are listed in Table 5.4.

High cophenetic correlations (r>0.7) for three out of five methods suggest that groupings relate to some real structure in the data. Group-average cluster analysis has the highest cophenetic correlation (r=0.85), but this is an artefact of the model as it is designed to maximise the correlation. Minimum variance cluster analysis finds the simplest group structure, producing even divisions across the sample-set but it has a low cophenetic correlation (r=0.57). Minimum variance cluster analysis divides the data-set into 5 groups:

Group 1: n = 10	Group 2: n = 51	Group 3: n = 42
Group 4: n = 61	Group 5: n = 45	

These groups are used to classify the samples in the ordination biplot (Figure 5.30b).

5.7.2 Classification by sediment type and lake trophic status

Lake classification by sediment type has been rarely used (Håkanson & Jansson, 1983) but can provide useful insights into ontogeny and lake dynamics. Hansen (1961) followed Naumann's (1932) original ideas of using sediments for the basis of a classification and postulated that the difference in minerogenic matter (Si) and inorganic

Table 5.4 Comparison of cluster groups of surface-sediment minerogenic and organic data using agglomerative hierarchical cluster methods (209 samples)

Group membership	*Nearest neighbour (single-link)*	*Furthest neighbour (complete link)*	*Weighted group average*	*Group average*	*Minimum variance (Ward's method)*
1	MOSS12; TWIS6.	MOSS12; LITE; TIOG; TWIS6.	SOMB33; HEY7-9,11,13,16; CHAN4-6,8,11,12; MOSS4-6,11-13,16,17,19,20; KNOB2,6,10; PUMP4-6; LITE; TRAN11,28; AMOS3,4; TIOG; TWIS6,9-11; GNES2-4,6,8,9,14,15,17-22.	MOSS12; PUMP4; LITE; TIOG; TWIS6; GNES8,19.	MOSS12; LITE; TIOG; TWIS6.
2	SOMB13; MOSS16; PUMP4; LITE; TIOG; GNES8,19.	SOMB33; HEY7-9,11,13,16; CHAN4-6,8,11,12; MOSS4-6,11,13,16,17,19,20; KNOB2,6,10; PUMP4-6; TRAN11,28; AMOS3,4; TWIS4,9-11; GNES2,3,4,8,9,14,15,17-22.	SOMB13; CHAN13,14; KNOB9; SIG13; ORWE.	SOMB13; CHAN13,14; KNOB9; SIG13; ORWE.	SOMB12,13,27,37,41; HEY12,14; CHAN13,14; KNOB9,11; TRAN12,17,18,20,26,28; AMOS7; EMER1-4,6-32; SIG13; ORWE.
3	CHAN13,14; KNOB9; SIG13; ORWE.	SOMB13; CHAN13,14; KNOB9; SIG13; ORWE.	SOMB12,14,21,27,37,41; HEY6,12,14; MOSS9,21; KNOB1,3,11; SPIR3,4; TRAN4,5,7,8,12,13,17-22,30; AMOS7; EMER1-4,6-32; GNES12.	SOMB33; HEY7-9,11,13,16; CHAN4-6,8,11,12; MOSS4-6,11,13,17,19,20; KNOB2,6,10; PUMP5,6; TRAN11,28; AMOS3-5; TWIS4,9,10,11; GNES2-4,14,15,17,18,20-22;	SOMB33; HEY7-9,11,13,16; CHAN4,5,6,8,11; MOSS5,11,13,16,17,20; KNOB2,6,10; PUMP4,5,6; TRAN11,28; AMOS3,4; TWIS4,9,10,11; GNES2,3,8,9,14,17,19-22.
4	SOMB15,30; HEY6; MOSS5,13,17,19,20; KNOB3; PUMP2,7; TRAN16,30; AMOS3; TWIS4,5; EMER5; BOTH1; GNES12,14,17,22.	SOMB12,27,37,41; HEY6,12,14; KNOB1,3,11; SPIR3,4; TRAN4,5,12,17,18,20,30; AMOS7; EMER1-4,6-32; GNES12.	SOMB11,15-20,22-26,28-32,34-36,38-40,42-46; HEY5,10,15; CHAN2,3,7,9,10; MOSS3,7,8,10,14,15,18; KNOB4,5,7,8; PUMP1-3,7; SPIR2,5; TRAN6,9,10,14-16,23-27,29; AMOS5,6; EMER5; TWIS5,7,8,12; BOTH1; GNES5,6,10,11,13,16.	SOMB12,27,37,41; HEY6,12,14; MOSS9,21; KNOB3,11; TRAN12,17,18,20; AMOS7; EMER1-4,6-32.	SOMB16,17,18-20,22-25,28-30,32,34,36,38,39,42,44-46; HEY5; CHAN2,3,7,9,10,12; MOSS3,4,6-8,14,15,18,19; PUMP1,3; SPIR5; TRAN6,14,15,23-27,29; AMOS5; TWIS3,7,12; GNES4-6,10,13,15,16,18.
5	SOMB11,12,14,16-29,31-46; HEY5,7-16; CHAN2-12; MOSS3,4,6-11,14,15,18,21; KNOB1,2,4-8,10,11; PUMP1,3,5,6; SPIR; TRAN4,5-15,17-29; AMOS4-6; EMER1-4,6-32; TWIS3,7-12; GNES2-6,9-11,13,15,16,18-21.	SOMB11,14-26,28-32,34-36,38-40,42-46; HEY5,10,15; CHAN2,3,7,9,10; MOSS3,7-10,14,15,18,21; KNOB4,5,7,8; PUMP1-3,7; SPIR2,5; TRAN6-10,13-16,19,21-27,29; AMOS5,6; EMER5; TWIS3,5,7,8,12; BOTH1; GNES5,6,10,11,13,16.	nil	SOMB11,14-26,28-32,34-36,38-40,42-46; HEY5,10,15; CHAN2,3,7,9,10; MOSS3,7,8,10,14,15,18; KNOB1,4,5,7,8; PUMP1,2,7; SPIR; TRAN4-10,13-16,19,21-27,29,30; AMOS5,6; TWIS3,7,8; EMER5; TWIS3,5,7,8,12; BOTH1; GNES5,6,10-13,16.	SOMB11,14,15,21,26,31,35,40,43; HEY6,10,15; MOSS9,10,21; KNOB1,3-5,7,8; PUMP2,7; SPIR2-4; TRAN4,5,7-10,13,16,19,21,22,30; AMOS6; EMER5; TWIS5,8; BOTH1; GNES11,12.
Cophenetic correlation	0.806714	0.728660	0.584124	0.856531	0.570287
Delta one-hat	0.677399	1.10972	0.699554	0.250883	31.3674
Gower's delta	232419	-762436	-398147	21195.0	-1.308939E+09

Shaded cells=adopted classification method

biogenic matter (D) can be used to measure lake trophic status. The hypothesis postulates that sediments can be divided into three broad categories: (i) organic matter, expressed crudely by %LOI; (ii) minerogenic matter (Si); and (iii) the inorganic biogenic material (D) containing diatom frustules and biogenic precipitated calcium carbonate. Here, %BSi is substituted for Hansen's 'D' and is regarded solely as a measure of biogenic siliceous matter, since calcium carbonate is negligible in these lakes. The minerogenic material (Hansen's 'Si') is represented as the difference between total silica (quartz) and the alkali-soluble silica, i.e. the difference between %Min and %BSi.

Hansen (1961) found that oligotrophic lakes had a detritus gyttya with a source in the phytobenthos which was strongly mixed with minerogenic materials. The minerogenic component was very large and the content of inorganic biogenic matter low (high Si:D ratio). The more eutrophic a lake the more the biogenic inorganic component would dominate the minerogenic component. Gyttya in eutrophic lakes was more planktonic in character and the Si:D was low. Hansen also used the C/N ratio as a rough measure of humosity to discriminate between polyhumic (dy) sediment and oligotrophic (gyttya) sediment. However, since none of the Signy Lakes are dystrophic and the C/N ratio was not measured, this further classification could not be made. Si:D was calculated for the 209 surface-sediment samples and is summarised in Table 5.5 by lake.

The Si:D ratio is plotted on the box-and-whisker plot (Figure 5.29a) to compare differences between the lakes. High values on the *y* axis specify oligotrophic lakes (high volume of minerogenic to biogenic) and values close to zero are eutrophic. Extremely oligotrophic outlier sites - Lake 13 and Orwell Lake - obscure the pattern in the other samples therefore outlier samples with Si:D values >100 (n=6) were removed (Figure 5.29b) to expand the pattern. This does not improve the interpretability either so more outliers with Si:D >50 (n=18) were removed (Figure 5.29c). This final plot shows the scatter of sites with Si:D <50. Intra-lake variability in Si:D is high in most lakes, reflecting local control on %BSi accumulations (section 5.4.3).

The most oligotrophic lakes in Hansen's Danish data-set had Si:D values of 43.13 and 30.75; values for the Signy Lakes (Table 5.5) largely fall within his range for oligotrophic lakes. Emerald Lake (No.12) is clearly oligotrophic (mean Si:D=36.39). The outlier in Sombre Lake, SOMB27 (Si:D=194.7), is from the strongly minerogenic delta-front. Bothy Lake (15) has a surprisingly high Si:D ratio (39.73) since it is classed as

Figure 5.29 Box-and-whisker plots illustrating Hansen's hypothesis of surface sediment-type and lake trophy for the 17 lakes (a) all surface sediments (b) Si:D <100 (c) Si:D <50

(a) All surface-sediments

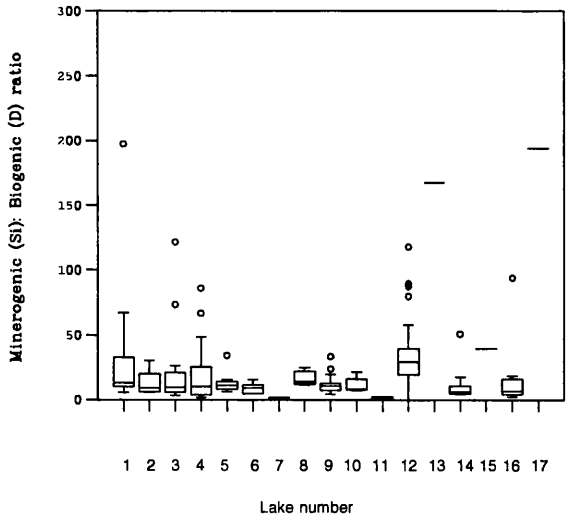

(b) Si:D < 100

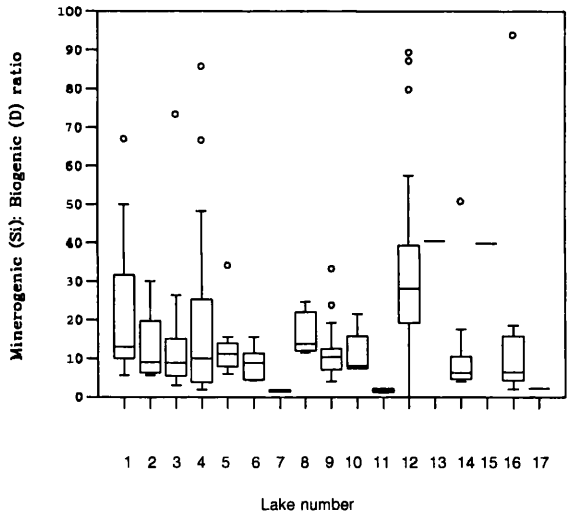

(c) Si:D < 50

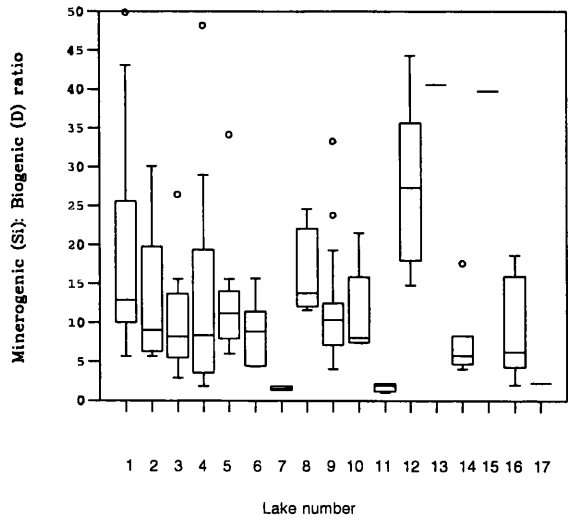

Table 5.5 Summary statistics of Hansen's Si:D ratio for surface sediments from the 17 lakes (n=209)

Lake	*n*	*Min*	*Max*	*Mean*	*Median*	*Std*
1 Sombre	36	5.6747	197.4	25.005	13.194	32.794
2 Heywood	12	5.6619	30.074	12.504	9.0066	7.968
3 Changing	13	2.9317	121.63	23.478	9.6237	34.826
4 Moss	19	1.8469	85.754	19.483	10.04	23.355
5 Knob	11	5.9819	34.134	12.851	11.188	7.6151
6 Pumphouse	7	4.3911	15.61	8.9465	8.8766	3.9193
7 Light	4	1.3892	1.8592	1.5833	1.5425	0.2234
8 Spirogyra	4	11.595	24.58	15.942	13.797	5.8646
9 Tranquil	27	4.041	33.28	11.63	10.39	6.3306
10 Amos	5	7.3717	21.46	10.932	8.0633	5.9949
11 Tioga	4	1.019	2.1994	1.777	1.9449	0.5473
12 Emerald	32	0	117.76	36.389	29.153	25.362
13 Lake 13	2	40.531	294.12	167.32	167.32	179.31
14 Twisted	10	4.0475	50.852	11.581	6.2082	14.348
15 Bothy	1	39.725	39.725	39.725	39.725	0
16 Gneiss	20	1.9739	93.887	12.952	6.4496	19.861
17 Orwell	2	163.55	224.12	193.83	193.83	42.83
All lakes	**209**	**0**	**294.12**	**22.377**	**11.595**	**34.635**

eutrophic but this single sample cannot be considered fully representative of the lake. Spirogyra Lake is similarly oligotrophic (mean=15.94). The most eutrophic lakes using Hansen's scheme are Light Lake (mean=1.58) and Tioga Lake (mean=1.77). This classification is surprising at first because their water chemistries are clearly oligotrophic. It is explained by their high benthic biomass which is not a simple function of lake trophy in maritime Antarctic lakes. In this region, oligotrophic lakes can still support a high benthic biomass despite low nutrient concentrations in lake waters. This produces gyttya sediments with a high biogenic inorganic component. High nutrient status in these lakes does not promote an inorganic gyttya typically observed in Hansen's eutrophic, temperate lakes; the scheme poorly discriminates lakes which are known to be eutrophic on Signy Island (Heywood, Knob, Amos). Clearly, functional relationships in these lakes are very different to the limnic systems which Hansen based his hypotheses on.

5.8 Ordination

5.8.1 Indirect ordination (Principal Components Analysis)

Principal components analysis (PCA) was performed in CANOCO (ter Braak, 1990) for 209 samples and 6 sediment variables. The Euclidean distance matrix used untransformed data, centred and standardised by species. In the ordination biplots of PCA axis 1 versus PCA axis 2 sample scores (Figure 5.30a) variables with high positive correlations have small angles between their biplot arrows; variables with long arrows have high variance and are generally more important within the data-set. Results of the analysis are summarised in Table 5.6.

Table 5.6 Eigenvalues and cumulative variance accounted for in a PCA of the 209 samples by 6 sediment determinands data-set

	Axis 1	*Axis 2*	*Axis 3*	*Axis 4*	*Total variance*
Eigenvalues	0.688	0.167	0.078	0.046	1.000
Cum.%var.sp.dat.	68.8	85.5	93.3	97.8	
Σ *unconstrained eigenvalues*					1.000

Figure 5.30 PCA biplots of surface-sediment organic and minerogenic determinands classified by (a) sites (b) minimum variance cluster groups and (c) Håkanson's energy groups

(a) Sites

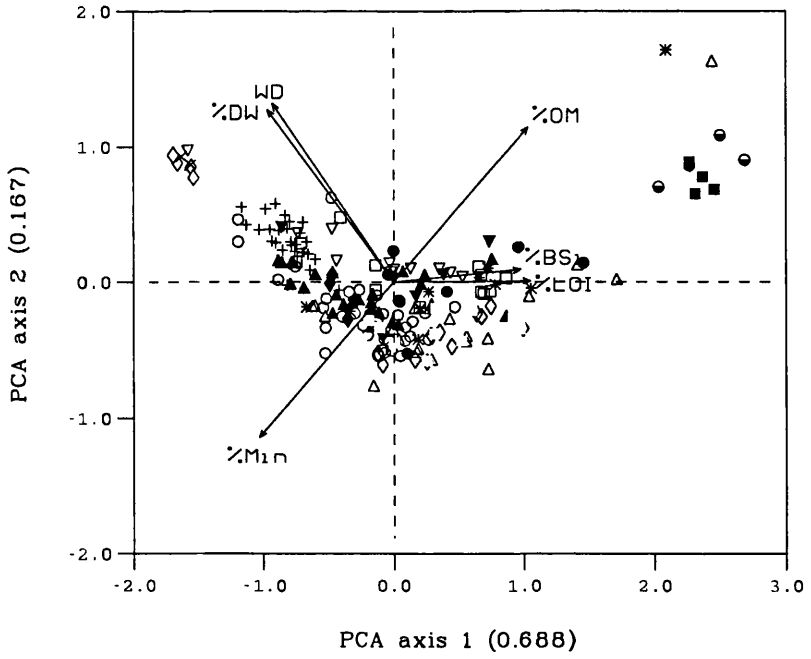

Only the first two PCA axes are significant in the data-set using the program BSTICK (H.J.B. Birks, unpublished). The first PCA axis captures a high proportion (68.8%) of the total variance in the data-set. The major PCA axis 1 gradient contrasts high organic (%LOI and %OM) and %BSi contents versus high minerogenic content, high dry weight and wet density. The second PCA axis (85.5% of cumulative variance in the sediment data) is determined by high values for wet density and %DW versus high values for minerogenic content, %LOI, %BSi and %OM. Both PCA axes therefore capture an organic-minerogenic gradient as expected.

Figure 5.30b Classified by minimum variance cluster groups (n=5)

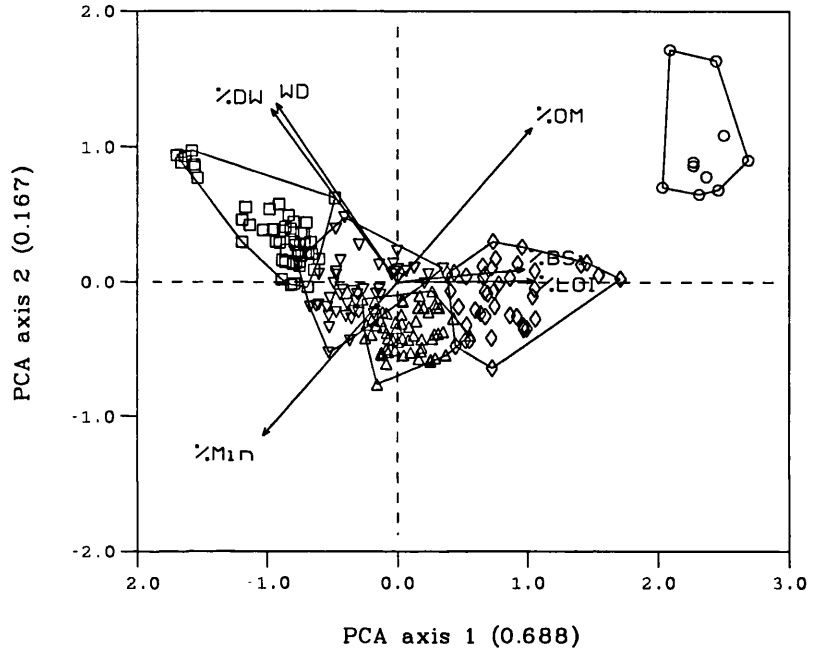

Group 1 ○ Group 2 □ Group 3 ◊ Group 4 △ Group 5 ▽

The first PCA axis (high organic content and high biogenic silica versus low organics and high minerogenics) clearly differentiates the minimum variance cluster groups (Figure 5.30b) with little overlap. Group 1 (circles) to the far right forms an isolated cluster of highly organic sediments, all from Tioga and Light Lakes. Group 2 (squares) is at the opposite end of this gradient, characterised by highly minerogenic, inorganic sediments from Emerald Lake, Lake 13 and Orwell Lake and some samples from Tranquil, Sombre, Heywood, Changing, Knob, Amos Lakes.

Sample groups (n=3) defined by Håkanson's (1977) classification using water content (section 5.6) are added to a further ordination biplot (Figure 5.30c). Samples from the zone of erosion and transportation (Group 3, diamonds), has a very similar distribution

to the second minimum variance cluster analysis group (Figure 5.30b), with high values for wet density and %DW. Group 2 (zone of discontinuous sedimentation, squares) shares the characteristics of minimum variance cluster groups 2 and 5, with slightly lower values for wet density and %DW. Group 1 (zone of accumulation, circles) has an extremely wide range along the first PCA gradient with sediments of highly variable organic and %BSi contents.

Figure 5.30c Håkanson's energy classification

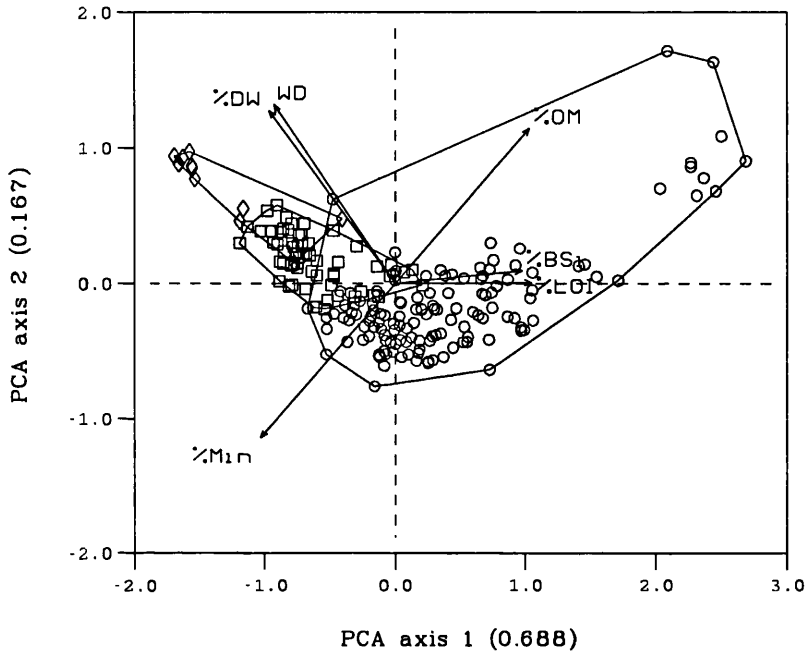

Group 1 ○ Group 2 □ Group 3 ◊

5.8.2 Direct ordination (Canonical Variates Analysis)

In indirect ordination, sediment relationships with the environment are assumed in a latent, intuitive way. Direct ordination techniques, such as Redundancy Analysis or Canonical Correspondence Analysis, combine the two data-types to directly model predictor-response relationships in a quantitative way. Canonical variates analysis (CVA), or Fisher's Linear Discriminant Analysis, is a form of multiple discriminant analysis which combines classification and ordination methods and finds those linear combinations of variables (canonical variates) that discriminate best between *a priori* clusters of samples. Classification methods are based on the assumption that assemblages of variables fall into discontinuous groups; ordination assumes that assemblages vary gradually along gradients (ter Braak, 1994). The CVA method is similar to PCA: it finds the major variation within one group and then extends the analysis using direct

ordination to find the linear combination of environmental variables that maximises the differences *between* groups whilst also maximizing *within-group* variation. It is a dimension-reducing technique which finds the best discrimination possible between groups of samples in fewer dimensions, i.e. on a few synthetic features. CVA has been used to test hypotheses concerning the representativeness of groups of data (Sætersdal & Birks, 1993) and in a similar way here CVA is used to see how groups determined by cluster analysis are explained by statistically significant environmental predictor variables.

In CVA, cluster groups are treated as response variables to environmental predictor variables. The group structure is derived from the five minimum-variance cluster analysis groups (section 5.7.1) and specified as dummy (1/0) variables (e.g. 1, 2, 3, etc..) with equal weights. Scaling of the correlation data matrix uses species scores as weighted mean sample scores. No transformation is necessary and samples and species are given equal weighting. Downweighting of rare-species does not apply with this non-biological data. Forward selection of environmental variables (ter Braak, 1990) is used to reduce the number of explanatory variables to those which were statistically significant in the data-set. Their significance was tested using unrestricted Monte Carlo permutation tests (999 permutations) and adjusted for Bonferroni inequality (ter Braak, 1990; Manly, 1992) to prevent too many variables from being judged significant. A final Monte Carlo permutation test at the end of the analysis is used to test the significance of the ordination results (Hall & Titterington, 1989) for both the first canonical ordination axis and the overall data-set (99 permutations with a more relaxed confidence limit of $p \leq 0.01$). Summary results of this CVA are presented in Tables 5.7 and 5.8 and a biplot of CVA axis 1 and 2 scores (Figure 5.31).

Table 5.7 CVA summary using variables identified in forward selection of sediment minerogenic and organic determinands

Axes	*1*	*2*	*3*	*4*	*Total variance*
Eigenvalues:	0.809	0.589	0.180	0.133	4.000
Gp.env. r:	0.900	0.768	0.424	0.365	
Cum.% variance of gp.dat.:	20.2	35.0	39.5	42.8	
of gp-env relations:	47.3	81.7	92.2	100.0	
Σ *unconstrained eigenvalues*					4.000
Σ *all canonical eigenvalues*					1.711

Thirteen variables were chosen by forward selection and found to be statistically significant ($p \leq 0.001$) (Table 5.8): % ice-cover, % marble, water clarity, elephant seals, maximum altitude, mean depth, % amphibolite, July water temperature, % moss vegetation, Cl^-, phaeopigments, Na^+ and NO_3^{2-}. Tests of canonical axis 1 and the overall trace statistic using 99 unrestricted Monte Carlo permutations found this model to be significant ($p \leq 0.01$).

Table 5.8 Forward selection of environmental variables in CVA of sediment minerogenic and organic determinands (6 sediment variables in 5 cluster groups x 45 environmental variables)

Variable added	*cumulative variance of selected variables*	*number of permutations*	*Bonferroni required significance*	*significance achieved*
% ice-cover	0.42	999	0.05	0.001
% marble	0.60	999	0.025	0.001
Clarity	0.77	999	0.016	0.001
Elephant seals	0.91	999	0.0125	0.001
Maximum altitude	1.05	999	0.01	0.001
Mean depth	1.16	999	0.008	0.001
% amphibolite	1.27	999	0.00714	0.001
July water temp.	1.35	999	0.00625	0.001
% moss	1.43	999	0.0055	0.001
Cl^-	1.50	999	0.005	0.001
Phaeopigments	1.55	999	0.0045	0.001
Na^+	1.65	999	0.00416	0.001
NO_3	1.71	999	0.00385	0.001
Variance explained by all variables	1.74			
No other variables significant				

As in PCA, results of CVA can be conveniently displayed in a biplot of sample scores as CVA group means for the first two CVA axes (Figure 5.31), with vectors of weighted loadings from the origin, scaled by within-group standard deviation. Taking variable scores as the cluster means in the CVA ordination diagram simplifies the pattern in the data.

Figure 5.31 CVA biplot of the 5 cluster groups of surface-sediment minerogenic and organic determinands (n=6) in relation to significant variables on CVA axes 1 and 2

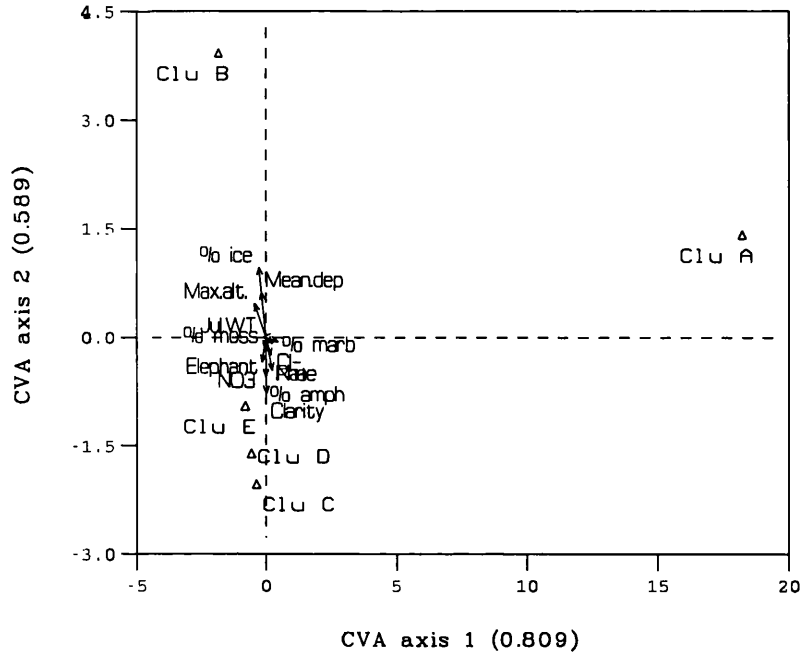

Cluster groups A and B are most distinctive from the others. Group A (circles), including samples from Moss, Light, Tioga and Twisted Lakes, has high CVA axis 1 scores and is associated most strongly with vectors for % marble and Cl^-. Group B (squares), including samples from Sombre, Heywood and Changing Lakes Ekman grab samples, Knob Lake, Tranquil Amos, most of Emerald, Lake 13 and Orwell Lake, has negative CVA axis 1 scores and high CVA axis 2 scores and is most associated with % ice-cover, mean depth and maximum altitude. Clusters C-F are found in the lower left quadrant of the biplot relating to high values for clarity, % amphibolite, nitrate, phaeopigments, elephant seals, chloride ions and % moss vegetation. These groups represent a mixture of samples from different lakes of known contrasting trophies and catchment characteristics.

42.8% (1.711/4.00) of the between-group variation is explained by canonical (constrained) eigenvalues of the thirteen forward-selected environmental variables. Of this, 35.0% of variation in the between-group variance is explained in the first two CVA axes. Both the F-ratio for the significance test of the first canonical axis (49.45) and the overall test statistic (11.22) exceed the critical F value ($F>2.10$, $p<0.05$ for 6 and 207 d.f.). Maximum altitude and % marble have significant inter-set correlations ($r>|0.35|$)

for CVA axis 1; % ice and clarity are significant for CVA axis 2. Canonical coefficients are significant ($r > |1.96|$) for phaeopigments, elephant seals, sodium ions and % moss vegetation; only clarity has a significant canonical coefficients for CVA axis 2.

Group discrimination on the basis of sediment minerogenic and organic characteristics relates to a combination of extrinsic, catchment and intrinsic, limnological variables. The gradient in CVA, especially on the second axis, differentiates groups of oligotrophic lakes with predominantly minerogenic sediments (Emerald, Lake 13, Orwell) with high % catchment ice-cover and high altitudes (central ice-cap influence) in the catchment from those of more mesotrophic or eutrophic status affected by marine influences (sea-spray, seals) with a greater degree of catchment development and unglaciated, vegetated terrain (% moss, % marble, % amphibolite). Outlier group A is most dissimilar from the others, representing an extreme mis-match in lake oligotrophy and largely undeveloped catchment versus a high benthic biomass which result in highly organic sediments at odds with other developmental indicators (refer section 5.6.2). The only intrinsic lake factor which appears to directly affect minerogenic and organic characteristics is mean depth. This reflects the strong littoral-profundal gradient in the lakes data-set (Chapter 3). Larger mean depths are associated with the more oligotrophic lakes, typically occupying cirque basins, in receipt of meltwaters from catchments with greater ice coverage (Sombre, Emerald, Lake 13, Orwell). By contrast, small mean depths associate with the more nutrient-enriched lakes with their characteristic shallow basin morphometries and its effects on lake climate and the extent of the available photic zone (Heywood, Knob, Amos Lakes).

5.9 Discussion

5.9.1 Selected determinands and surface-sediment minerogenic and organic characteristics

The six minerogenic and organic determinands capture the variability in the surface-sediments extremely well, despite the simplicity of their measurement. Coherent lake groupings are apparent in the box-and-whisker plots, cluster analysis and ordination results, despite high inter-lake variability. High correlations show that some relationships are strongly collinear (Håkanson & Jansson, 1983), introducing redundancy into the analysis which will require screening at a later stage in model development (Chapter 8). There is a clear gradient in the surface sediment data-set between organic sediments associated with moderate to high %BSi versus highly minerogenic, inorganic sediments

with variable %BSi. This organic-minerogenic gradient parallels the results of Jones, Juggins & Ellis-Evans (1993) who found a strong nutrient gradient in their diatom-water chemistry training-set and the productivity shift from plankton to benthos suggested in diatom water-chemistry studies of Oppenheim (1990). In planktonic systems for example, eutrophic Heywood, Knob, Amos and Bothy Lakes, autochthonous production takes place in the water column by a limited phytoplankton population dominated by annual chlorophytes, contributing little %BSi to the sediments. Most organic matter is mineralized in the water column or at the sediment surface (Hawes, 1988; Ellis-Evans & Lemon, 1989) so that little is incorporated into the sediments. In benthic systems, typically oligotrophic lakes such as Sombre, Changing, Moss and Pumphouse Lakes, plankton is generally absent and is dominated by sparse periods of cryptophytes during ice-free periods (Hawes, 1983). The productivity signal evident in water chemistry-diatom assemblage data is complicated by the presence of a high benthic biomass (cyanobacterial mats and perennial mosses) sustained by high levels of nutrients in underlying sediments (Ellis-Evans & Lemon, 1989) which support diatom communities and contribute high %BSi inputs to highly organic sediments.

Zones of erosion, transportation and accumulation can be crudely predicted using sediment water content (Håkanson, 1977) and the data-set includes samples from all three energy environments, with a bias towards zones of accumulation, matching the sample-net. A large number of samples, in addition, are from the zone of discontinuous sedimentation, highlighting the importance of resuspension processes in these shallow, wind-stressed lakes. Sediment focusing is detectable and it is highly likely that lower density materials, organic matter and %BSi, are focused into deeper and/or more sheltered parts of each basin.

Analytical methods inevitably contribute some error to measured values. Despite careful removal of most surface water during core extrusion (section 4.2.4.1), variable volumes of water are probably extruded with the first sediment slice, perhaps accounting for some of the variability in the %DW values. Digestion in hydrogen peroxide is considered to be a more reliable measure of organic content than %LOI, especially when organic contents are either very low or very high, and carbonate combustion may occur in some lakes with marble lithologies (e.g. Changing and Moss Lakes). The sequential extraction method is critically dependent on careful sample handling. Even small losses during transfer represent a substantial percentage of the overall sample weight. A small

volume of clay is probably lost in the centrifuge procedure as 2000 r.p.m. is not sufficiently fast to remove all clays from the supernatant, possibly accounting for registered %BSi in Emerald Lake sediments, which other determinands suggest is highly unproductive. Some sorption of silica and/or clays may occur in the polystyrene centrifuge tubes (R.Flower, *pers.comm.*). Incomplete digestion of biogenic silica can occur with structurally more complex diatom valves which take longer to dissolve but examination of the digested residue confirmed that complete digestion had occurred.

5.9.2 Catchment-development and lake-sediment minerogenic and organic characteristics

Direct ordination using CVA (section 3.7.2) clearly shows that the degree of catchment-development is influencing the minerogenic and organic characteristics of these lake-sediments. Karlén (1981) suggests that sediments in lakes fed by glacial meltwater have inorganic contents of sediments 5-10 %LOI; sediments from lakes lower down the valley with larger drainage basins have less inorganic material (15-20 %LOI) and lake sediments from lakes not receiving glacial meltwater are much greater (i.e. 30-40 %LOI). Do the Signy lakes conform to this hypothesis? The organic-minerogenic gradient in PCA is clearly attributable to whether a lake is glacier-fed or not (see section 3.6.2). The most organic sediments (>40% LOI) are found in Light and Tioga Lakes. Neither of these catchments are glaciated and meltwater input is by seepage from melting snowpatches overlying moss-vegetated catchment slopes. Lower sedimentation rates permit the continued survival of a high benthic biomass in the form of perennial vegetation. Gneiss Lake shares similar characteristics, despite high catchment ice-cover, owing to the routing of its meltwaters which largely by-pass the main basin (section 2.3.2.16). Sediment organic content is also enhanced because rates of breakdown and turnover are slow in these oligotrophic lakes (Ellis-Evans, 1982). The range of %LOI in the remaining lakes is generally <30%, suggestive of moderate glacial influence. %LOI of 15-30% is found in the low-lying coastal lakes with larger catchments which are proportionally less glaciated (Heywood, Knob, Pumphouse, Amos, Twisted, Bothy Lakes). These lakes receive higher volumes of allochthonous organic inputs coupled with variable autochthonous production and should, in theory, have the highest %LOI values, but near-complete breakdown of organics during the period of winter anoxia depresses the %LOI of their sediments. Sombre, Tranquil, Emerald, Lake 13 and Orwell Lake all have low %LOI values (<5-10% LOI) and highly dense, minerogenic sediments; all directly receive glacial meltwaters from predominantly glaciated

catchments, conforming to Karlén's predictive model.

5.10 Summary

(1) The six selected determinands represent three basic fractions of the sediment: organic, minerogenic and biogenic inorganic materials. %LOI is a composite measure of both allochthonous and autochthonous organics and a selective extraction method is used to isolate the biogenic inorganic and minerogenic (clastic) fractions. The data-set represents a range of sedimentary environments, is noisy and variables share collinear relationships. The principal gradient is defined by lower density sediments of high organic content and relatively high proportions of biogenic inorganic material versus sediments with low organic contents, high proportions of allochthonous minerogenic contents, low water contents and low biogenic inorganic materials. Changes in %BSi tend to parallel those in organic matter suggesting a link with benthic biomass and associated epiphytic diatom communities and/or the redistribution and focusing of organics and %BSi from shallow to deeper waters.

(2) A division in sediment character can be ascribed to sedimentological differences of lakes with glacier ice and those that are relatively unglaciated, supported by Karlén's (1981) observations from analogous Arctic environments. Sedimentological sensitivity to catchment processes is encouraging for the development of an inferred climate model. The balance of intrinsic (limnological) and extrinsic (catchment) control on lake sediment character is explored using further direct ordination methods in Chapter 8.

(3) A lakes classification is proposed on the basis of sediment organic and minerogenic characteristics, yielding a tripartite division of the 17 lakes: (i) oligotrophic lakes with perennial benthic vegetation (cyanobacterial mat) showing high benthic standing crop, slow turnover and high organic contents in surficial sediments for example, Light, Tioga and Gneiss Lakes; (ii) proglacial, oligotrophic lakes dominated by high density, minerogenic allochthonous inputs with little benthic productivity and basin shapes encouraging focusing for example Tranquil and Emerald Lakes; and (iii) eutrophic lakes with high rates of turnover and decomposition leading to surprisingly minerogenic sediments of lower organic contents and relatively low %BSi contents due to low planktonic and benthic productivity.

CHAPTER 6: SURFACE-SEDIMENT PARTICLE-SIZE CHARACTERISTICS

6.1 Introduction

Sediment particle-size plays a fundamental role in hydraulics, geomorphology and sedimentology. There are natural linkages between the size of inorganic particles in sediments, water content, bulk density and organic content so that measurement of these physical parameters provides a complementary means of interpreting the palaeolimnological record. The particle-size distribution of a material is a sensitive indicator of the environmental conditions under which it is formed (Gale & Hoare, 1991) and is therefore a valuable climate proxy. Sedimentation in glacial lakes can produce characteristic forms of deposition (Church & Gilbert, 1975) and fluctuations in glacier activity in the catchment can be detected in changing particle-size (Nesje *et al.*, 1994) and sedimentation rates (Leonard, 1985). The latest high-resolution quantitative studies have linked sediment particle-size variations in glacial varves to seasonal air temperature variations (Leeman & Niessen, 1994a; Hardy, Bradley & Zolitschka, 1996). A wide range of analytical methods are available for particle-size determination which have different resolutions and degrees of sophistication including microscopy, sieve analysis, sedimentation methods (pipette, hydrometer, settling column), Coulter counter, laser diffraction and X-ray diffraction.

In the maritime- and sub-Antarctic, quantitative particle-size studies of lake sediments have been limited to locations in the South Shetland Islands (Mäusbacher, Müller & Schmidt, 1989; Björck *et al.*, 1993; 1996), James Ross Island (Björck *et al.*, 1996) and South Georgia (Birnie, 1990). At Signy Island, particle-size studies of lake sediments have been observational (Heywood, Dartnall & Priddle, 1980) or semi-quantitative through lithological characterisation (Jones, 1993). Due to the lack of regional examples in the literature, behavioural analogues for these lake systems can be inferred from Arctic and glaciated Alpine regions, which have engendered a proliferation of particle-size studies in contemporary and past lake systems (Church & Gilbert, 1975; Gustavson, 1975; Leonard, 1985; Lemmen *et al.*, 1988; Leeman & Niessen, 1994a, 1994b; Zolitschka, 1997). Late- and Post-Glacial palaeolimnological studies from temperate regions (Holmes, 1968; Snowball & Sandgren, 1996) also provide analogues for the contemporary sedimentological and limnological conditions in the Signy Lakes.

In this Chapter, the particle-size characteristics of the surface-sediment samples are

investigated. Basic methodological considerations are reviewed and a suitable, quantitative method of analysis selected. A statistical approach is taken to characterize the grain-size of the samples and the values and ranges of the particle-size volume-distribution statistics are summarised using 4 determinands for the 17 lakes. Classification and ordination methods are used to explain within-and between-lake variation and the results are compared to other classification schemes. Environments of deposition are derived using basic relationships between the different statistical measures. The endogenic contribution to the overall bulk sediment is considered through a sequential chemical extraction procedure and relationships between particle-size and organic matter are discussed in the context of lake trophic status. The discussion focuses on the processes governing sediment sources and environments of deposition in the lakes, their representivity of catchment processes and how they might, by inference, be linked to climate.

6.2 Methodology

6.2.1 Basic considerations in particle-size studies

Individual grains may be classified into a given size class. However, natural samples of particles generally include individuals of several size classes. There are many different ways of classifying particles according to the mode of measurement and various units exist (Table 6.1). The sand, silt and clay fractions are the most important in lake sedimentological studies (Håkanson & Jansson, 1983). The Troels-Smith (1955) classification provides a semi-quantitative estimate of the relative proportions of sand, silt and clay in a sample as well as the siliceous remains of plants or animals and other endogenic components of the sediment matrix (Birks & Birks, 1980). Two types of distribution frequently arise from particle-size data in natural samples: (i) unimodal, which may have normal or skewed distributions and (ii) bimodal, which are the result of more complex deposition processes. Empirical evidence has shown that deposits composed of lithologies which weather and abrade to sand are likely to possess bimodal distributions; in contrast, deposits which weather and abrade to clay are likely to be unimodal (Gale & Hoare, 1991). A third distribution - polymodal - is less common but can occur in natural sediment samples (Singer *et al.*, 1988).

The grain-size of sediment samples is best described using a statistical approach (Håkanson & Jansson, 1983), commonly the mode, mean, median, standard deviation, sorting, skewness, and kurtosis (section 2.4.4). The specific percentiles of a distribution,

Table 6.1 Classification of sedimentary particles

Wentworth grade	*Wentworth boundary (mm)*	*Millimetres (mm)*	*Micrometres (μm)*	*Phi size (ø)*	*Troels-Smith class*
Boulders		>256	>256,000	>-8.0	
Large cobbles	256	128	128,000	-7.0	
Small cobbles	60	64	64,000	-6.0	
Very large pebbles		44.8	44,800	-5.5	Grana glareosa
		32	32,000	-5.0	majora
Large pebbles	20	22.4	22,400	-4.5	Gg(maj.)
		16	16,000	-4.0	(>6 mm)
Medium pebbles		11.2	11,200	-3.5	
		8	8000	-3.0	
Small pebbles	6.0	5.6	5600	-2.5	Grana glareosa minora
		4	4000	-2.0	Gg(min.)
Granules		2.8	2800	-1.5	(<6mm)
	2.0	2	2000	-1.0	Grana suburralia, Gs
Very coarse sand		1.4	1400	-0.5	(0.6-2 mm)
		1	1000	0.0	
Coarse sand	0.6	0.71	710	0.5	
		0.5	500	1.0	
Medium sand		0.355	355	1.5	Grana arenosa
		0.25	250	2.0	Ga
Fine sand	0.2	0.18	180	2.5	(0.6-0.06 mm)
		0.125	125	3.0	
Very fine sand		0.09	90	3.5	
		0.063	63	4.0	
Coarse silt	0.06	0.045	45	4.5	
		0.0332	32	5.0	
		0.023	23	5.5	Argilla granosa
Medium silt	0.02	0.016	16	6.0	Ag
		0.011	11	6.5	(0.06-0.002 mm)
		0.008	8	7.0	
Fine silt	0.006	0.0055	5.5	7.5	
		0.004	4	8.0	
		0.00275	2.75	8.5	
Clay	0.002	0.002	2.0	9.0	Argilla
		0.00138	1.38	9.5	steatodes, As
		0.001	1.0	10.0	(<0.002mm)

especially the highest and lowest percentiles, are often most sensitive to change and ratios between clay and silt or sand can provide information on energy environments during transport and sedimentation (Sly, 1989; Björck *et al.*, 1993). For this large sample-set (n=209) an automated, quantitative method was sought which was labour-reducing and used small sub-samples. Since the sediments are principally hydraulically derived a complimentary hydraulic-based method of measurement seemed appropriate. Laser diffraction particle-size analysis conforms to these needs and is able to supply quantitative data fulfilling the prerequisites for quantitative environmental reconstructions (Birks, 1995).

6.2.2 Principles of laser diffraction particle-size analysis

Laser diffraction size analysis, or Low Angle Laser Light Scattering (LALLS), relies on an established optical method called 'conventional Fourier optics', the theory that size distributions of fine particles may be inferred from the angular distribution of the intensity of forward-scattered coherent light (Agrawal, McCave & Riley, 1991). The method is fast, accurate and non-destructive for weak particles such as flocs. Small quantities of wet sediment are required for assay (1-2 grammes) and replicate runs minimize instrumentation errors. The size range detected by the machine depends upon the focal length of the focusing lens, the total range for detection using the Malvern Series 2600 Sizer being 0.5-560 μm. This range has been improved considerably using later generation machines (section 6.3.2). However, particles coarser than 900 μm cannot be kept in suspension to perform an accurate assay and require measurement using an alternative technique. Laser diffraction is most accurate with fine sands to silt sized particles but is unreliable in the clay sized fractions due to the base algorithm in the method (based on Fraunhofer diffraction theory). The refractive index of the material must be different from the medium in which it is supported, i.e. each material phase must be optically distinct and the medium must be transparent to the laser wavelength.

The Malvern Series 2600 Sizer used in this study comprises an optical measurement unit which forms the basic particle-size sensor and a computer that manages the measurement and performs results analysis and presentation using integral software. The analyzer beam is from a low power Helium-Neon laser (633 nM wavelength) producing a collimated and monochromatic beam of light, 18 mm in diameter. Particles present within this beam scatter the laser light, and both the scattered light and unscattered remainder are directed incident onto the receiving, range lens. When a particle scatters

light it produces a unique light intensity characteristic with the angle of observation. Light is scattered so that the measured energy on the detector has a peak at a favoured scattering angle which is related to its diameter. Large particles have peak energies in small angles of scatter and vice versa. The receiving lens acts as a Fourier transform lens, forming the far-field diffraction pattern of the scattered light at its focal plane. The detector, in the form of a series of 31 concentric annular sectors, gathering the scattered light to produce an electronic output signal proportional to the light measured over 31 separate solid angles of collection. Unscattered light is brought to focus on the detector and passes through a small aperture out of the optical system. The total laser power passing out of the system is monitored allowing the sample volume-concentration to be calculated. This is corrected against a background measurement of light prior to analysis (section 6.2.3.2).

Many particles are simultaneously present in the analyzer beam and regardless of the optical configuration of their scatter the light measured on the detector is the sum of all individual patterns overlaid on the central axis. The system therefore measures the integral scattering from all particles present in the beam. One instantaneous measurement of the scattering only gives a size distribution based on this small cross-section of the material. This is therefore counteracted by time-averaged observation of the scattering as the material is constantly passed through the analyzer beam, solving two potential problems: (1) inadequate statistical significance and (2) unrepresentative sampling of the bulk material. By making many measurements of the detector readings (sweeps) and averaging over many sweeps of the detector it is possible to build up an integral light scattering characteristic based on millions of individual particles. Time-averaging is performed by successively reading the detector over a predetermined period of time and summing these data. A representative measurement can be built-up quickly, i.e. in 5 seconds, on the basis of sweep measurements of many hundreds or thousands of samples.

The computer uses 'anomalous diffraction theory' and 'Fraunhofer theory' to deduce the volume size-distribution that gives rise to the observed scattering characteristics. It achieves least-squares fitting of the theoretical scattering characteristics to the observed data, and 'Model Independent Analysis' (Malvern Instruments, 1980) assumes no form of size-distribution. The fundamental instrument measurement is one of volume and all other outputs are numerical transformations of this basic output form assuming spherical

particles. The volume-specific basis means that results can only be truly compared to other volumetric measures of particle size (A. Rawle, unpublished).

6.2.3 Analysis

6.2.3.1 Pretreatment

Modification of the particle-size distribution by pretreatment may be beneficial or deleterious according to the materials investigated and the goals of the study (Matthews, 1991). Organic materials interfere with the laser diffraction light-scattering process causing spurious results since the diameters are often much larger than the mineral particles in the matrix. It is standard practice to remove organic matter prior to particle-size analysis and samples were digested in 30% hydrogen peroxide for 3-4 days until reaction had ceased. Cold digestion was adopted to minimize particle breakage. Samples were centrifuged and rinsed twice with distilled water. A certain amount of disaggregation occurs with the removal of the organic component but the benefit is to reduce samples of highly variable organic content to a uniform consistency. Sediment was maintained in a wet state through all stages of the analysis to prevent aggregate formation.

6.2.3.2 Suspension and dispersion

In their natural state, fine particles, especially clays, tend to form polymineralic aggregates or flocculate with organic matter into chains and clusters. Most forms of fine-particle analysis are undertaken on material which has been disaggregated and in which individual particles are maintained in the dispersed state in the suspension (Matthews, 1991) and it is almost impossible to replicate natural conditions in the laboratory. It is possible however, to take steps to ensure that samples are not over-dispersed in the laboratory and to use a standardized procedure for suspension and dispersion and measurement time so that all samples are treated equally allowing direct inter-comparison of results.

The 'Particle In Liquid' method (Malvern, 1980) requires samples in suspension in a clear, optically homogenous liquid which does not interact with the refractive indices of the materials to be analyzed. The relative refractive indices of some common minerals from Signy Island are displayed in Table 6.1. All exceed the index for water and can therefore be measured on the Malvern Sizer. Tap-water can contain a large number of impurities and under pressure may form bubbles which may completely alter the

particle-size distribution, introducing 'particles' in the 150-500 μm range (Loizeau *et al.*, 1994). In a detailed comparative study of the effects of suspension media and dispersion methods on the Malvern Series 2600 Sizer, Chappell (1995) found that analysis using tap-water performed adequately and was more economic and practical than using large volumes of distilled water; he also found little benefit of sample dispersion in sodium hexametaphosphate ($(NaPO_3)_6$). His optimal sample dispersion time in tap-water was three minutes with ultrasonic action.

Table 6.2 Refractive indices of some commonly-occurring mineralogies of Signy Island rocks

Mineral	*Typical formula*	*Refractive Index*
Quartz	SiO_2	1.544
Plagioclase (Muscovite)	$KAl_2Si_3AlO_{10}(OH,F)_2$	1.552
Muscovite	$KAl_2Si_3AlO_{10}(OH,F)_2$	1.552
Garnet	various	1.779 (average)
Iron III oxide	Fe_2O_3	2.94-3.22
Calcite	$CaCO_3$	1.486-1.740
Ferrous oxide	FeO	2.32
Diatomaceous material	SiO_2	1.435
Water	H_2O	1.33

Ultrasonic dispersal causes particle breakage and disaggregation by mechanical action when the particles are agitated by the rapid movement of the liquid due to the transmission of vibrating sound waves (Malvern Instruments, 1980). The breakdown of cohesive aggregates by ultrasonic action increases with time. Conversely, unwanted flocculation of fine particles increases with time of circulation (McCave *et al.*, 1986), thus an optimal time for circulation and disaggregation is required. Chappell (1995) studied time-dependent effects of ultrasonic dispersion on particles by microscopic examination of suspensions retrieved by micro-pipette from the sample cell after 1, 3, and 6 minutes of circulation. Material recovered after 6 minutes showed signs of mechanical degradation with numerous fine, angular shards derived from breakage of mineral. There was also a notable decrease in the red coloration of the sample and the loss of many smaller particles which had previously been attached to larger, mainly rounded quartz particles. Samples selected at 1 and 3 minute intervals had a large number of aggregates in contrast to few found at 6 minutes. A pilot study with Signy

lake-sediments detected the same patterns of time-dependent breakage. Therefore the standard optimum analysis adopted for this study is three minutes of dispersion in tap-water with ultrasonic action.

A measurement of the background light level is taken prior to analysis, which is used to correct the measurement for contamination sources such as ambient light, impurities in the suspension medium, air bubbles and laser speckle (Agrawal, McCave & Riley, 1991). At time zero samples are introduced to the circulation cell by pipette from a sediment-water slurry so that an obscuration of between 10-15% is achieved. Ultrasonic action is discontinued just prior to sample measurement to reduce turbulence in the suspension. Each sample was measured for 5000 sweeps (roughly 20 seconds) and the data averaged to produce a time-averaged reading using the Malvern software (Malvern Instruments, 1980). A typical cycle of measurement lasts approximately 6 minutes per sample, including computing and printout. The rate-determining step is the speed with which the cell can be cleaned and a new dispersion prepared. Up to twenty samples per day can be comfortably run on the Series 2600 Sizer.

6.2.3.3 Lens-size and blended results

The total size-span covered by the Series 2600 Sizer is broken-down into ranges, each selected by fitting the appropriate lens, thus some *a priori* estimation of the size range of the material is required. Three lenses were chosen to cover the estimated size range: (i) 63 mm lens, effective range 1.2-118 μm; (ii) 100 mm lens, effective range 1.9-188 μm; and (iii) 300 mm lens, effective range 5.8-564 μm. It is normally expected that 100% of the particles fall into the effective range of the lens. However, this does not always occur leading to truncated size-distribution histograms in the results output. When the proportion of the distribution in the largest size bin (102-118 μm for the 63 mm lens or 162-188 for the 100 mm lens) exceeded 1% samples were re-analyzed (n=69) using the 300 mm lens (effective range 5.8-564 μm). Results were blended by a normalizing procedure, making the best fit in the centre part of the overlapping region between the two lenses (Malvern Instruments, 1980). A quality factor associated with this fit was quoted with the new blended result, an exact match giving a quality factor of 100%. All blended results on these sediments exceed the 95% quality fit.

6.2.4 Results presentation

The Malvern Sizer generates a volume-distribution curve for the analyzed light-energy

data accompanied by measured and derived diameters. A hard-copy output of the analysis results in the 32 bins with its accompanying distribution histogram and distribution statistics was kept for reference. Four volume-specific summary variables are used to describe the particle-size volume-distribution curve of each sample: median, mean, standard deviation of the mean and the skewness. All units are expressed in micrometres (μm).

6.2.4.1 Median

This is the mid-point of all observations in a population (Figure 6.1). The median is smaller than the mean in positively skewed populations and larger than the mean in negatively skewed populations. For skewed populations the median provides a more adequate description of the most typical characteristic grain size value than the mean, which is heavily influenced by the tail ends of the distribution. The Malvern median, D[v,0.5], is also known as the volume median diameter (Malvern Instruments, 1980).

6.2.4.2 Mean

The mean is an arithmetic average of the data and can be an important tool for interpretations of sediment data in relation to bottom dynamics (Håkanson & Jansson, 1983). The Malvern system can calculate a number of means including the number length mean (D[1,0]), the number mean or number surface mean (D[2,0]), the Sauter mean diameter (D[3,2]) which includes a surface area term (the sphere of equivalent surface area), and the equivalent volume mean diameter (VMD, De Broucker mean or D[4,3]) which relates to spheres of equivalent volume (Malvern Instruments, 1980). The D[4,3] is used in this study, hereafter known simply as the mean particle size, and is calculated as:

$$D[4,3] = \frac{1^4 + 2^4 + 3^4}{1^3 + 2^3 + 3^3} = \frac{\Sigma d4}{\Sigma d3}$$

i.e. the sum of observed diameters to the power of four divided by the sum of cubed diameters in units of micrometres (μm). Converting diameters to spheres allows for some comparison with other sedimentation methods since Stoke's Law is only valid for spheres. Stokes diameter (D_{ST}) is simply a comparison of the particle's settling rate to a sphere settling at the same rate.

Figure 6.1 Statistical definitions of particle-size

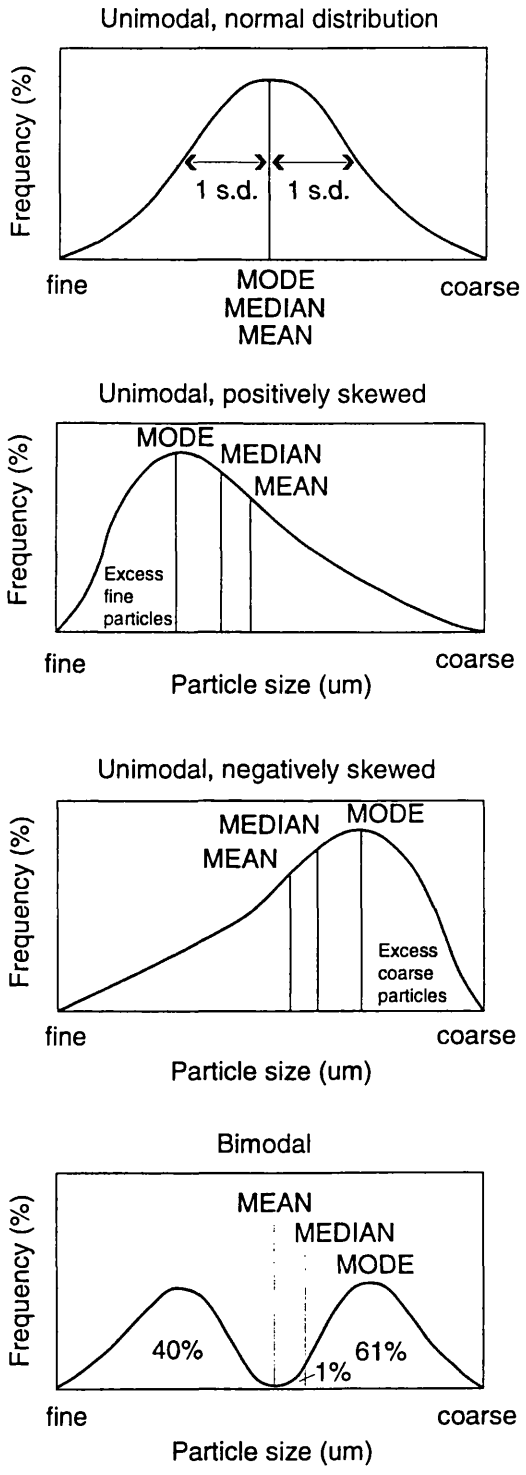

6.2.4.3 Standard deviation of the mean

Standard deviation, or the square root of variance, gives a measure of spread around the mean (Figure 6.1). The gradient of the line is a function of the standard deviation of the distribution. Small standard deviations indicate steep gradients in the distribution curve, with observations clustering tightly around a central value. Larger values of the standard deviation indicate values scattered widely about the mean, with gentle slope gradients and a weak tendency for central clustering. For normal distributions, 1 standard deviation (S.D.) includes two-thirds (66%) of observations; 2 S.D. includes 95% of observations; 3 S.D. includes 99% of observations. The Malvern standard deviation uses μm units.

6.2.4.4 Skewness

Skewness is another measure of spread which can be used to provide measures of energy levels in the profundal zone and the degree of particle mixing (Håkanson & Jansson, 1983). High positive values for skewness indicate samples with particle-size distributions heavily influenced by a preponderance of fine-grained material versus a longer tail of coarser material (Figure 6.1). High negative values for skewness indicate coarser particles in a fine sample. Skewness here relates to the micrometre scale, the opposite to skewness measured on the phi-scale (ø), where negative skew refers to coarse skew and positive skew refers to fine skew (Gale & Hoare, 1991).

6.2.5 Data handling methods

Data from the Malvern Series 2600 Sizer was exported as DOS ASCII text and recovered into Quattro Pro for DOS 5.0 (Borland International, 1991). The data were imported into a Paradox Relational Database, Release 3.0 (Borland International, 1988) and then exported into so-called Cornell Condensed format using the program CHEMOUT (S.Juggins, unpublished). Estimates of the proportions of sand, silt and clay were derived from splitting the results from the 32 sizer bins into 11 Wentworth size classes (>500-<2 μm) and pie charts were created using Adobe Illustrator 5.5 (Adobe Systems Inc., 1993). Numerical analysis was performed using CALIBRATE (Juggins & ter Braak, 1996), CANOCO (ter Braak, 1987; 1990) and Minitab (Minitab Inc., 1989). For cluster analysis using the program CLUSTER (H.J.B.Birks, unpublished), Cornell Condensed data were expanded to Cornell Full Format using EXPAND (H.J.B.Birks, unpublished). There are no missing values in the data-set.

6.3 Values and statistical distributions of surface sediment particle size data

Summary statistics for the 209 surface sediment samples are presented in Table 6.3 and box-and-whisker plots (Figures 6.2-6.5).

Table 6.3 Summary statistics for the surface sediment particle size data (209 samples from 17 lakes)

Determinand	*Min*	*Max*	*Mean*	*Median*	*Standard deviation*
Median	12.08	69.02	25.472	23.21	9.0062
Mean	16.01	104.7	34.451	31.11	12.998
Standard deviation	12.41	131.09	31.843	27.35	15.640
Skewness	0.94	4.46	2.0467	1.93	0.6142

6.3.1 Median particle-size

The median particle-size for all lakes (n=209) has a minimum of 12.08 μm in Emerald Lake and a maximum of 69.02 μm in Heywood Lake. The sample population has a near-normal distribution (mean=25.47; median=23.21; S.D.=9.01). This range coincides with medium silts to fine sands (average coarse silt) (Table 6.1). In the box-and-whisker plot (Figure 6.2) the range of median particle-size varies within each lake, some with fairly discrete distributions (Changing, Light, Tioga) and others highly variable (Heywood, Tranquil, Amos, Gneiss).

Figure 6.2 Box-and-whisker plot showing variation of median particle-size by lake number

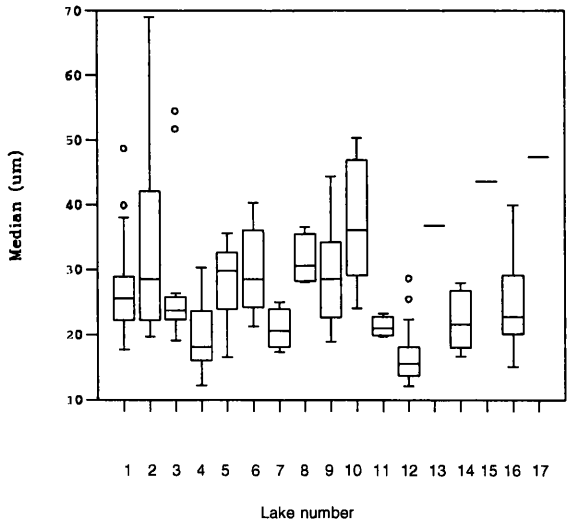

6.3.2 Mean particle-size

Mean particle-size has a minimum value of 16.01 μm in Moss (4) Lake and a maximum of 104.7 μm in Heywood (2) Lake. The sample population-distribution is approximately normal (mean=34.451; median=31.11; S.D.=12.99). This range includes medium silts to fine sands (average coarse silts).

Figure 6.3 Box-and-whisker plot showing variation of mean particle-size by lake number

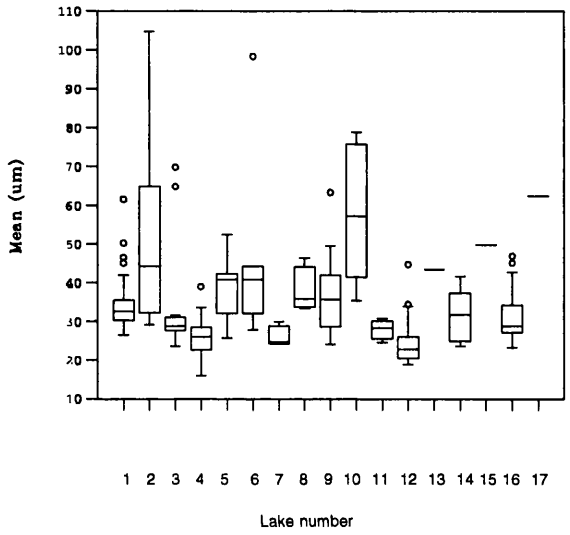

In the box-and-whisker plot (Figure 6.3) most lakes share similar mean particle-sizes. Exceptions with highly variable intra-lake ranges are Heywood (2), Pumphouse (6) and Amos (10) Lakes.

6.3.3 Standard deviation of the mean (S.D.)

The minimum value for standard deviation of the mean (S.D.) is 12.41 μm in Moss (4) Lake and it reaches a maximum of 131.09 μm in Pumphouse (6) Lake. The population distribution is right-skewed (mean=31.84; median=27.35; S.D.=15.64). The box-and-whisker plot (Figure 6.4) shows that intra-lake variation in S.D. is restricted in most lakes. Three exceptions with very large ranges are Heywood (2), Pumphouse (6) and Amos (10) Lakes.

6.3.4 Skewness

Skewness is at a minimum of 0.94 μm in Tranquil (9) Lake and a maximum of 4.46 in Spirogyra (8) Lake. The sample population-distribution is approximately normal

(mean=2.05; median=1.93; S.D.=0.61). The box-and-whisker plot (Figure 6.5) shows reasonable similarity between lakes with larger ranges in skewness (indicating more positive skewness, i.e. predominance of fine material) in Heywood (2), Pumphouse (6), Tranquil (9) and Amos (10) Lakes. All samples are positively skewed, indicating the importance of fine material in these sediments.

Figure 6.4 **Box-and-whisker plot showing variation of S.D. particle-size by lake number**

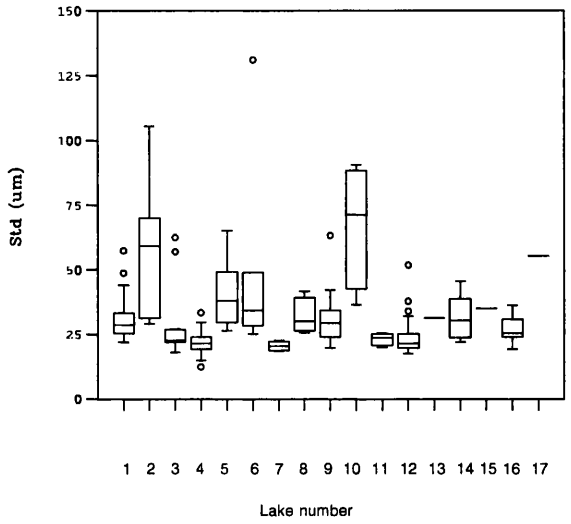

Figure 6.5 **Box-and-whisker plot showing variation of particle-size skewness by lake number**

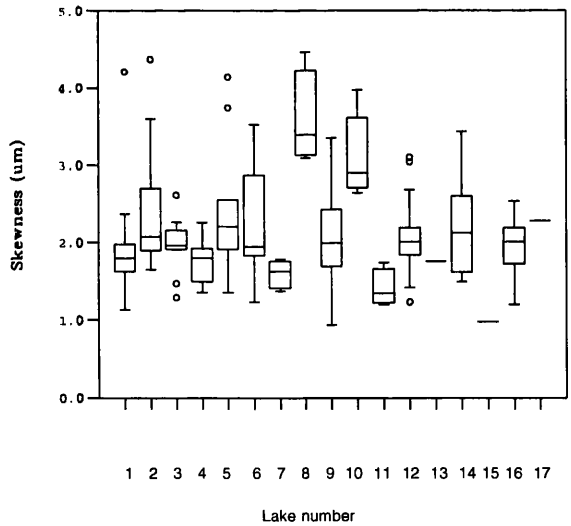

6.4 Comparison of Series 2600 Sizer results and Malvern Mastersizer results

6.4.1 Problems with the Series 2600 Sizer

There has been some highly critical debate in the literature concerning the reliability and precision of laser light-diffraction methods (Singer *et al.*, 1988; Agrawal, McCave & Riley, 1991; Kanerva *et al.*, 1993a, 1993b), in particular the Malvern Series 2600 Sizer (Loizeau *et al.*, 1994) and its detection of fine silt and clay-sized particles. An inherent

problem associated with Fraunhofer diffraction theory, which form the basic algorithm of the Sizer, is that it becomes inappropriate when the particle diameter is close to the wavelength of light because of the interplay of refraction, especially below particle diameters of 10 lambda or 7 μm (Bayvel & Jones, 1981). In consequence, as the relative refractive index between particle and suspension media approach unity the Series 2600 overestimates the mean particle-size for finer samples (Hitchen, 1992). Clay particles have always represented a problem in methods of particle-size analysis. All automated instruments show an increased disparity in results arising from increased particle-particle interference, light dispersion, and influence on fluid viscosity (Singer *et al.*, 1988). The Series 2600 Sizer is further constrained by the effective lens range and poor estimation of the amount of material below the analytical range. The lowest theoretical resolution of the 63 mm lens is 1.2 μm and most clays are consequently below the detection limit. Instrument detection efficiency of clays has been found to be proportional to the actual clay content (Loizeau *et al.*, 1994). For sediments containing less than 10% clay the efficiency is about 40-45% whereas for clay content greater than about 80% it reaches 100%. Small amounts of clay are overlooked in clayey silt by the mixing of particles of different grain-size; clay contents up to 8% do not appear to affect adversely the resolution capabilities of any of the instruments discussed by Singer *et al.* (1988).

Several authors have made comparative studies to gauge the extent of instrumental inaccuracies (Singer *et al.*, 1988; Loizeau *et al.*, 1994). The Malvern Series 2600 Sizer has the lowest correlation against silt and sand standards amongst other methods (Singer *et al.*, 1988) but the r^2 for both standards is still greater than 0.96. Encouragingly, the Malvern Sizer is able to accurately discriminate two size populations of a bimodal distribution but for polymodal samples there is an overall broadening of individual modes. The differentiation of these modes is improved with appropriate disaggregation techniques. Variability between sub-samples can be greater than measurements within one subsample (Loizeau *et al.*, 1994) and the sediment preparation procedure is probably responsible for greater variation in results than the actual optical measurement. Both comparative studies used samples which included the organic matter fraction which cause errors of size estimation (section 6.2.3.1). The pretreatment in this study should have reduced this source of error so that samples are texturally more homogeneous.

In the light of these criticisms an attempt was made to address methodological errors by calibrating the Series 2600 Sizer results against a more accurate method. The results

output was compared with more reliable readings from a compatible, upgraded model of this sizer - the Malvern Mastersizer. Improved algorithms in this instrument use a combination of Fraunhofer and full Mie scattering theory to quantify the presence of fine particles in the volume-distribution.

6.4.2 Analysis on the Mastersizer

A subset of forty samples was selected from the 209 sample-set for calibration using the Malvern Mastersizer at Malvern Instruments, Malvern, Worcestershire, UK. This number was seen as a feasible subset for analysis within one day and represented 19% of the population. Samples were ranked on the basis of mean particle-size and random stratified selection was made within the quartiles of this ranked distribution (ten samples from each quartile). Pretreatment was as above (section 6.2.3.1) using 30% hydrogen peroxide to remove organic material. Samples were analyzed as wet slurries of material using tap-water as the dispersal medium. The Mastersizer covers a size range of 0.05-900 μm using one lens only. Samples were circulated for three minutes with ultrasonic dispersion prior to measurement (3000 sweeps). The volume distribution for the forty calibration samples was calculated using two models: (i) polydisperse OHD which assumes particle behaviour equivalent to sand in water (refractive index 0.52, absorbance 0.1); and (ii) polydisperse OAD which is quoted as the nearest model to the Series 2600 Particle In Liquid (PIL) model, and assumes that particles behave in an manner analogous to the refractive index of sand in water but that all particles are transparent (no absorbance). As above (section 6.2.4), derived statistics from the volume distribution (median, mean, standard deviation of the mean and skewness) were calculated using the integral Malvern software.

6.4.3 Mastersizer results

The Malvern Mastersizer range is essentially unlimited with respect to the size range of the surface-sediments and the volume distributions are more representative than those of the Series 2600 Sizer. Two calibration samples (LITE3, MOSS16) had limited material and produced very low obscuration values in the analysis (5.3% and 2.2% obscuration respectively) and were rejected from calibration-set (section 6.4.4). Satisfactory concentrations were achieved with the remaining samples (average volume concentration=0.03; n=38) producing obscuration values of 10-20%. Only one sample - SOMB37 - had a bimodal distribution with high values for both the median (OHD method=532.19 μm; OAD method=573.64 μm) and mean (OHD method=144.79 μm;

OAD method=158.77 μm). This sample is unusual in that it comes from the delta-front of Sombre Lake and has been subjected to different mixing and sorting processes than the rest of the lake.

6.4.4 Calibration of Series 2600 results using Mastersizer results

Mastersizer results ('truth') are plotted against Series 2600 results (y axis) and a regression trendline fitted to the distribution (Figures 6.6a-e). The correlation coefficient between the two data-sets for the OAD method (nearest analogue to Series 2600 Sizer PIL method) is low (median r^2=0.45; mean r^2=0.22). The OHD model gives a better match when fitting a linear model by least-squares to the sample points with stronger correlations between the OHD and Series 2600 results (median r^2=0.78; mean r^2=0.80). The match between the standard deviation and skewness for the two sample sets is equally poor (S.D. r^2=0.15; skewness r^2=0.06). The reasonably strong correlation of the fitted regression line for the Mastersizer OHD versus Series 2600 results for mean and median particle-sizes means that a calibration of the surface-sediment sample-set can be achieved. Using classical regression, a correction can be applied to the entire sample-set using the following equation:

$$\text{new } y = (\text{initial } y - a)/b$$

where new y = calibrated Series 2600 result
initial y = original Series 2600 result
a = regression line intercept
b = regression line slope

For example, adjusting the median using y = 0.6326x + 11.901 with an original Series 2600 median value of 40.18 μm:

$$\text{new } y = (40.18 - 11.901)/(0.6326) = 45.3479 \text{ μm}$$

All correlations show positive relationships reflecting an improved capture of the real overall volume distribution for each sample. Increasing the lens range to 0.05-900 μm generates new tail ends to the volume distribution, impacting more on the mean which is tail-sensitive. In all forty samples, the mean is greater than the median reflecting positive skew (dominated by materials finer than the mean). The most robust calibration can be achieved with the median value. As the mid-point of all observations this is less

Figure 6.6 Regression plots of Malvern Mastersizer results versus Series 2600 Results

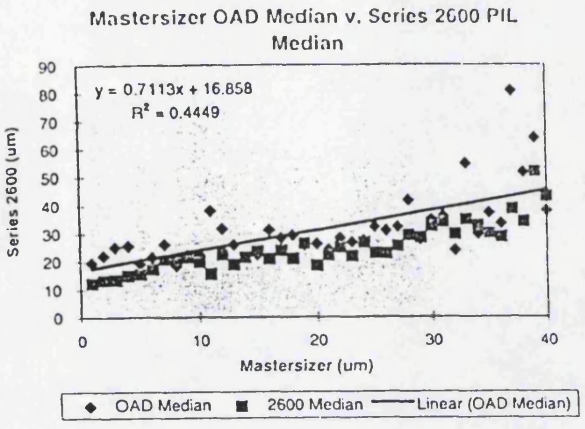

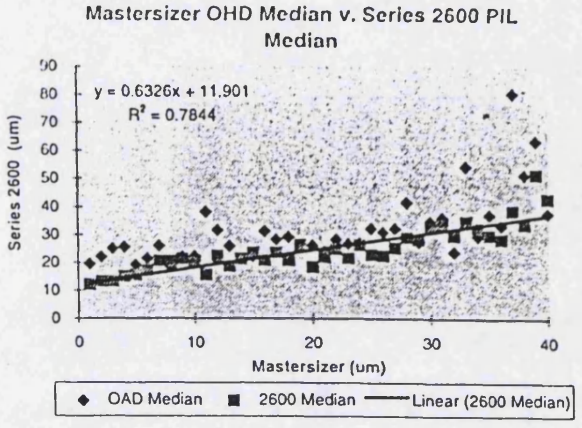

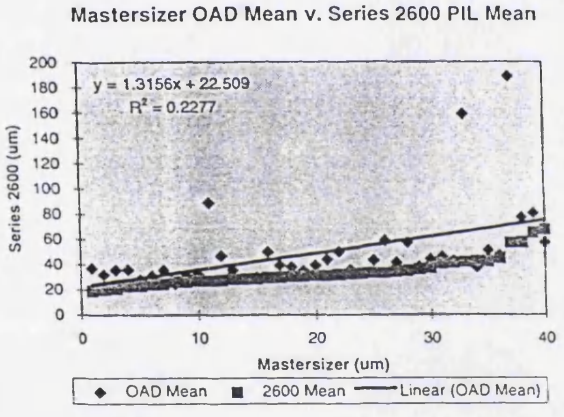

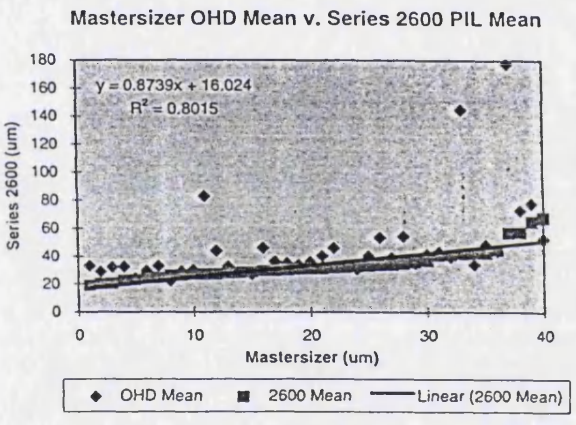

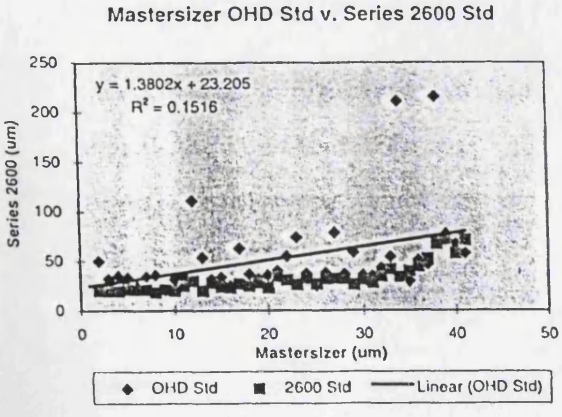

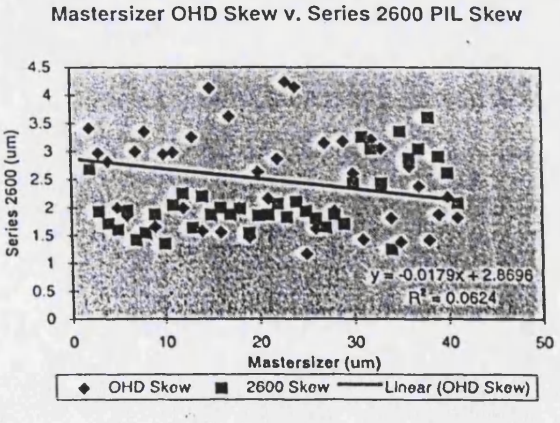

affected by changes to the distribution tails, and from the calibration equation above it is evident that the adjusted median will always be greater than the original median.

The mean and median of fine samples (dominated by fine to medium silts) have a closer match in both instruments. The calibration error is greatest in the coarser samples. Coarse samples also include fine sized fractions, thus they have larger ranges, hence the greater difference in the median but especially the mean, which shifts to the right. The Sizer calculates 100% of the distribution lies within the lens range, 'squashing' the distribution curve. For the Series 2600 100 mm lens, the constraining effect of its focal length limits its effective range of measurement to ≤188 μm. Potential loss of the coarse tail introduces the possibility that the mean and median will be smaller than reality (samples more fine-grained than reality). Where the distribution tail ends before the uppermost size bins (coarse bins) it is assumed that the entire distribution has been captured in measurement. Where the distribution tail is cut-off with a significant proportion of material lost by 'lens vignetting' (Malvern, 1990) it is reasonable to assume a wider volume-distribution actually occurs and the volume statistics, especially the mean, are in error. Each individual sample would be subject to variable error. In blended results (100 and 300 mm lenses) the effective measurement range ≤354 μm captures all particles present in the beam and none of the volume distribution curves are truncated. Blended results are thus considered to be the most reliable.

Since only two of the four variables can be calibrated with reasonable confidence the decision was made to maintain the integrity of the original data-set by leaving values uncorrected. Volume statistics of samples measured on the Mastersizer are all positive, therefore universal application of these calibration coefficients to 'improve' the original data would not actually change the rank sample order and would only lead to relative, and not absolute, improvements in data precision. Calibration would cause the mean and median to the right and skewness and the standard deviation (range) would increase. However, the following limitations of the Series 2600 results should be appreciated in any interpretation of the data:

(1) Distribution ranges are narrower than reality due to effective range of the lens size.

(2) Estimates of the mean and median are smaller than reality.

6.5 Spatial distributions of surface-sediment particle-size

Figures 6.7-6.20 illustrate the particle-size characteristics of the sample-net in each lake

basin. Summary statistics for percentages of sand, silt and clay are presented in Table 6.4. These are not absolute values given the problems associated with the sizing of clays (section 6.3.1).

Table 6.4 Summary statistics for surface sediment percentage sand, silt and clay (209 samples)

Fraction	*Size*	*Min*	*Max*	*Mean*	*Median*	*S.D.*
% sand	>63 μm	0	20.46	9.20	8.61	4.25
% silt	63-2 μm	71.91	95.87	88.79	89.73	3.83
% clay	<2 μm	0	37.28	5.19	2.73	6.23

6.5.1 Sombre Lake

Surface-sediment particle-size is reasonably uniform across the trough (Figure 6.7), with finer materials increasing towards the north and north-western, south and eastern shorelines, probably representing the localised loadings of sub-glacial clays in meltwaters. Percentage silt is generally constant; relative contributions of sand or clay determine the differences between samples. The transect towards the outflow has a higher proportion of fine sand but none of the samples have particles exceeding 188 μm (medium sand).

6.5.2 Heywood Lake

One sample from the south basin has a significantly higher percentage of clay (HEY12). The next nearest sample point, only 10 metres distant, has particle-sizes more characteristic of the north basin (Figure 6.8). Proportions of sand are generally higher in these samples than in Sombre Lake, especially towards the western margin of the north basin. Inter-sample variability is high owing to large particle-size ranges (section 6.3.1.3).

6.5.3 Changing Lake

All samples share similar particle-size characteristics with roughly 90% silt, 10% sand and negligible clays across the range of the basin (Figure 6.9). Two exceptions are the Ekman grab samples (CHAN13 & 14) from the western side of the basin near the inflow and damming moraine, which have significantly higher clay fractions (20-23%). The depth resolution of these samples (Chapter 4) is different to the Glew core samples and they are not strictly contemporaneous.

Figure 6.7 Distribution of surface-sediment particle-size, Sombre Lake

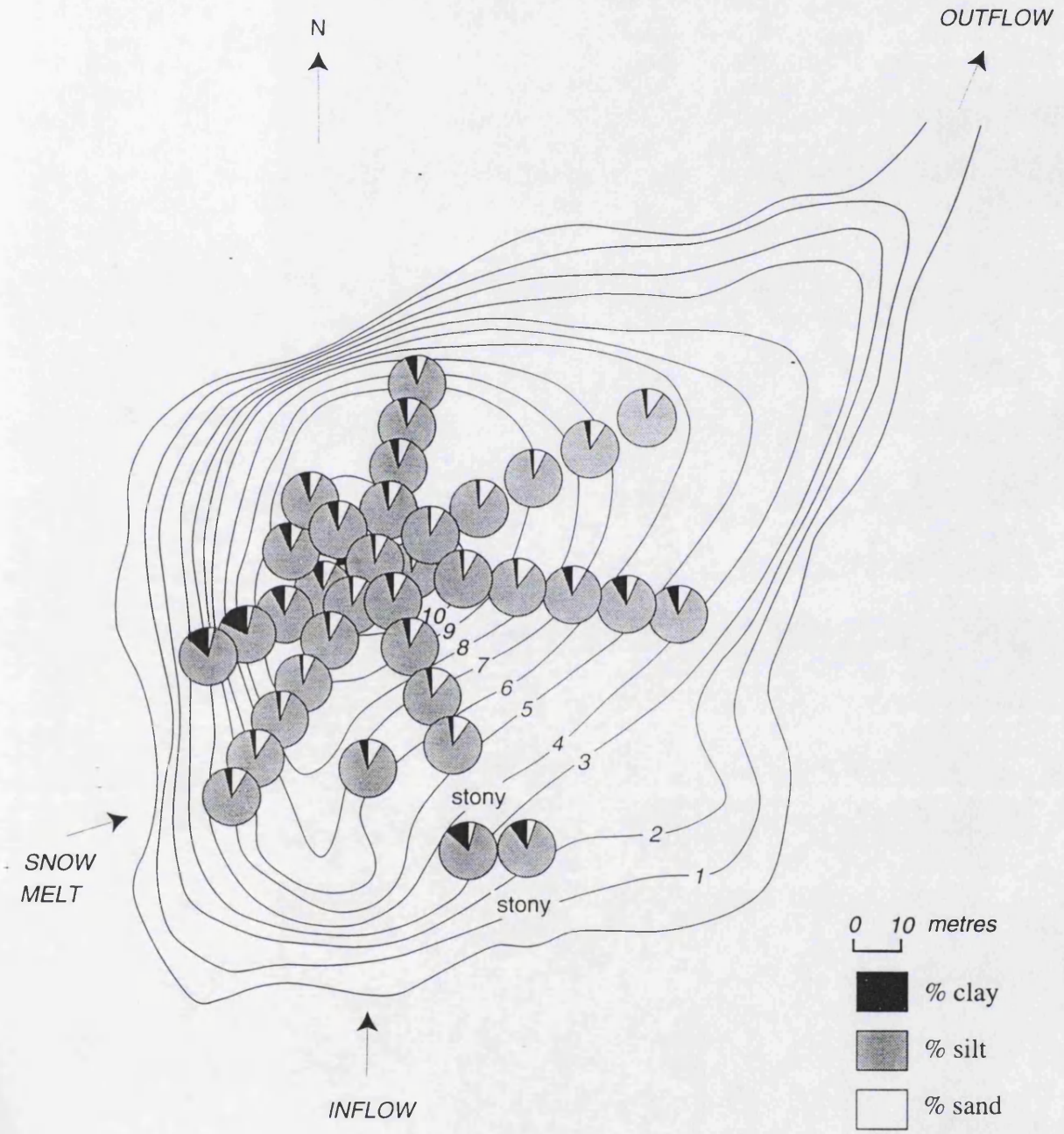

Figure 6.8 Distribution of surface-sediment particle-size, Heywood Lake

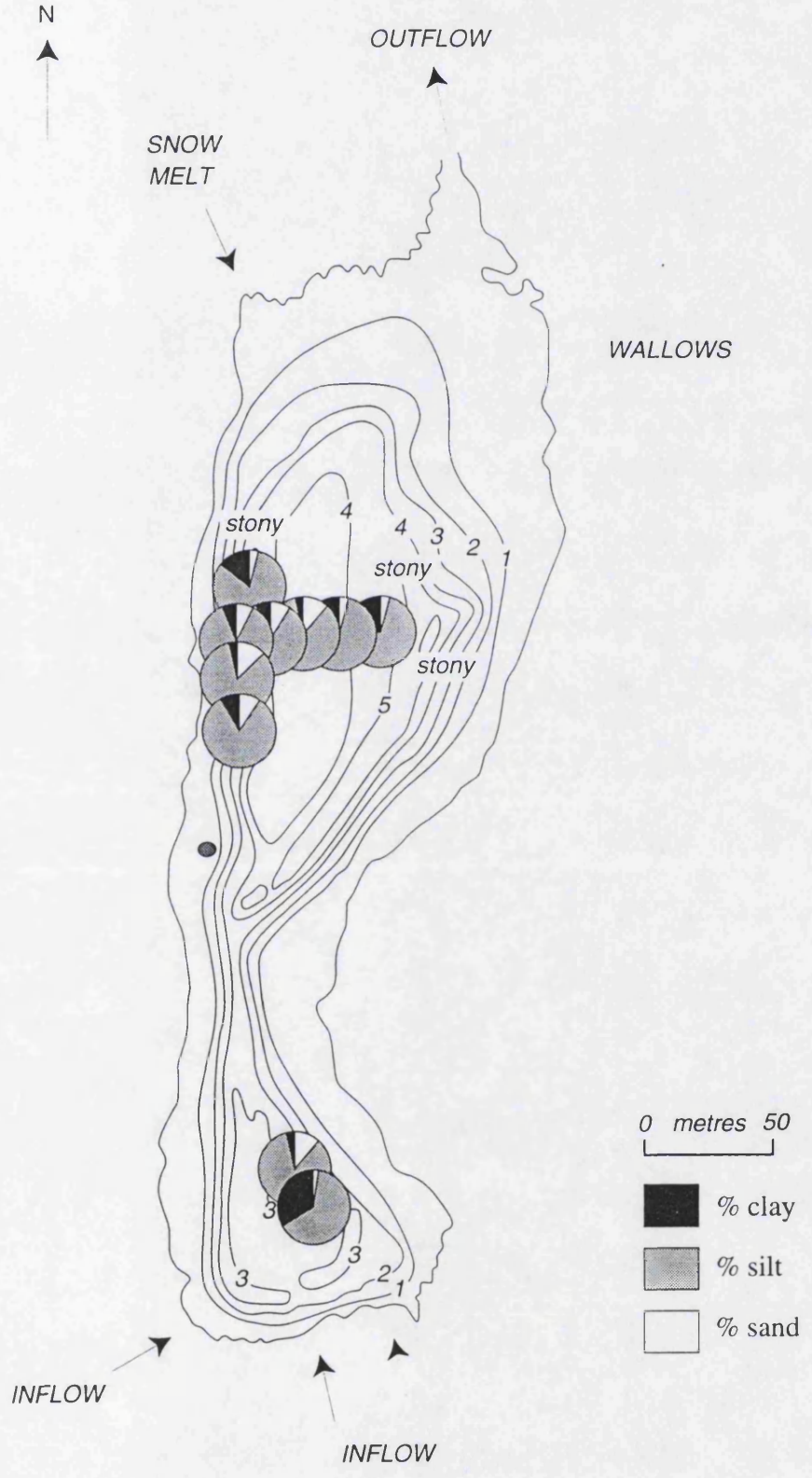

Figure 6.9 Distribution of surface-sediment particle-size, Changing Lake

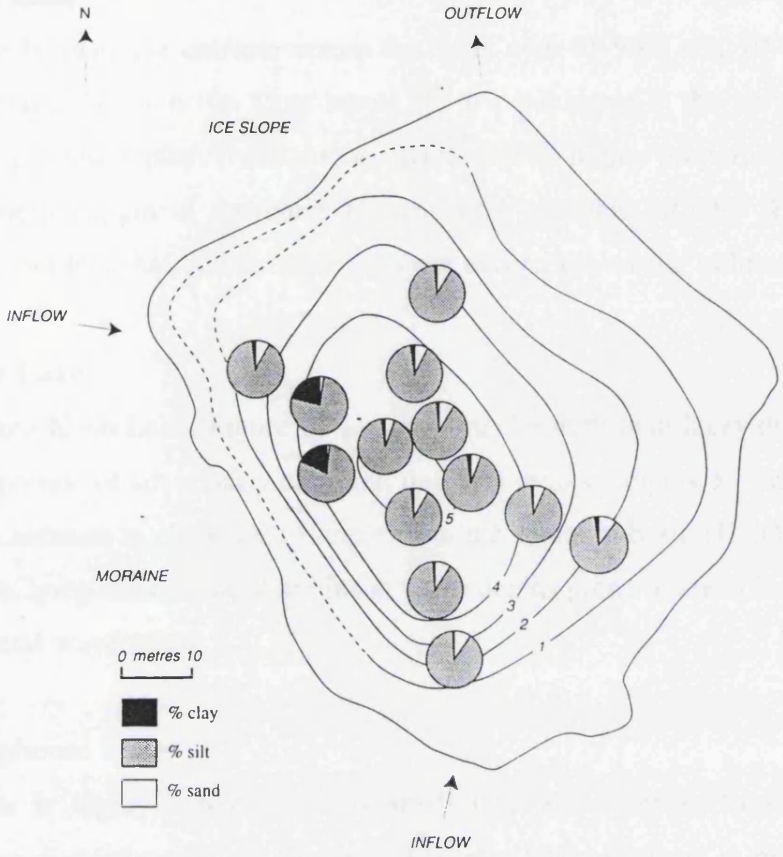

Figure 6.10 Distribution of surface-sediment particle-size, Moss Lake

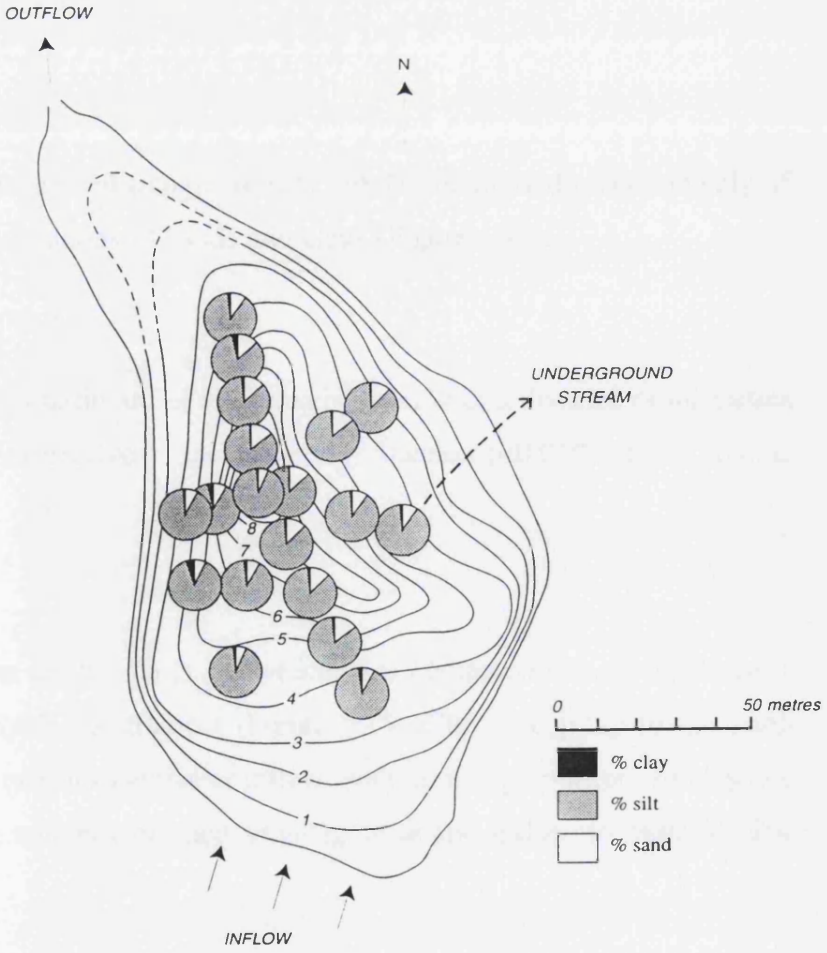

6.5.4 Moss Lake

Particle-size is relatively uniform across the basin with 85-90% silt, 10-15% sand and negligible clays (Figure 6.10). Clay inputs are at a minimum in the very centre of the basin at the greatest depths. Three samples have slightly higher proportions of clay: two on the western margin of the basin (Ekman grab samples MOSS9 & 10) and one towards the outflow (MOSS16). Clay does not exceed 6% of the volume distribution.

6.5.5 Knob Lake

Samples from Knob Lake (Figure 6.11) are more clay-rich than lakes described above but the proportion of silt is fairly constant, thus it is reduced inputs of sand which cause the relative increase in clays. One sample from the southern basin (KNOB2) is notably more coarse, lying close to the shoreline at water depths prone to the effects of ice-scour and peripheral wave attack.

6.5.6 Pumphouse Lake

Particle-size is highly variable in this small lake and samples from neighbouring locations are distinctly different (Figure 6.12), paralleling findings in minerogenic and organic determinands (section 5.3.6). Near the centre of the basin three samples (PUMP1, 2 & 3) have higher proportions of clay. Heterogeneity may reflect disturbance in this shallow basin.

6.5.7 Light Lake

The four samples from the central trough are very similar, composed predominantly of silts with very small contributions of sands and clays (Figure 6.13).

6.5.8 Spirogyra Lake

The four samples from this basin are of uniform character over a distance of 40 metres (Figure 6.14). They are distinctive in lacking a clay fraction (<0.01% of the volume distribution).

6.5.9 Tranquil Lake

Two groups are apparent on the basis of particle-size characteristics, divisible by a north-north-west/south-south-east transect (Figure 6.15). The first group to the north apparently relates to the primary meltwater inflow, with greater proportions of clay and negligible to increasing volumes of sand trending from the inflow to outflow. The

Figure 6.11 Distribution of surface-sediment particle-size, Knob Lake

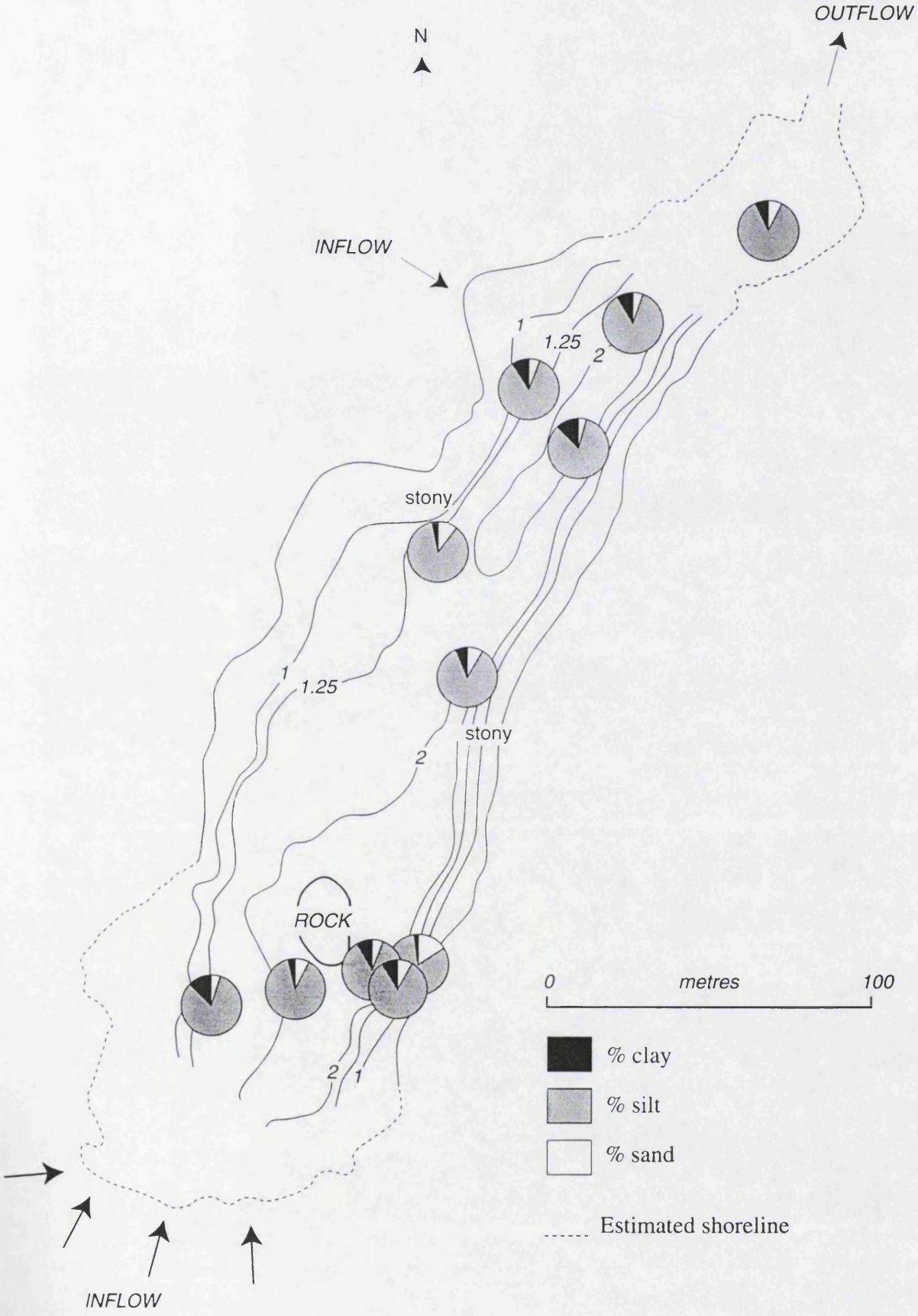

Figure 6.12 Distribution of surface-sediment particle-size, Pumphouse Lake

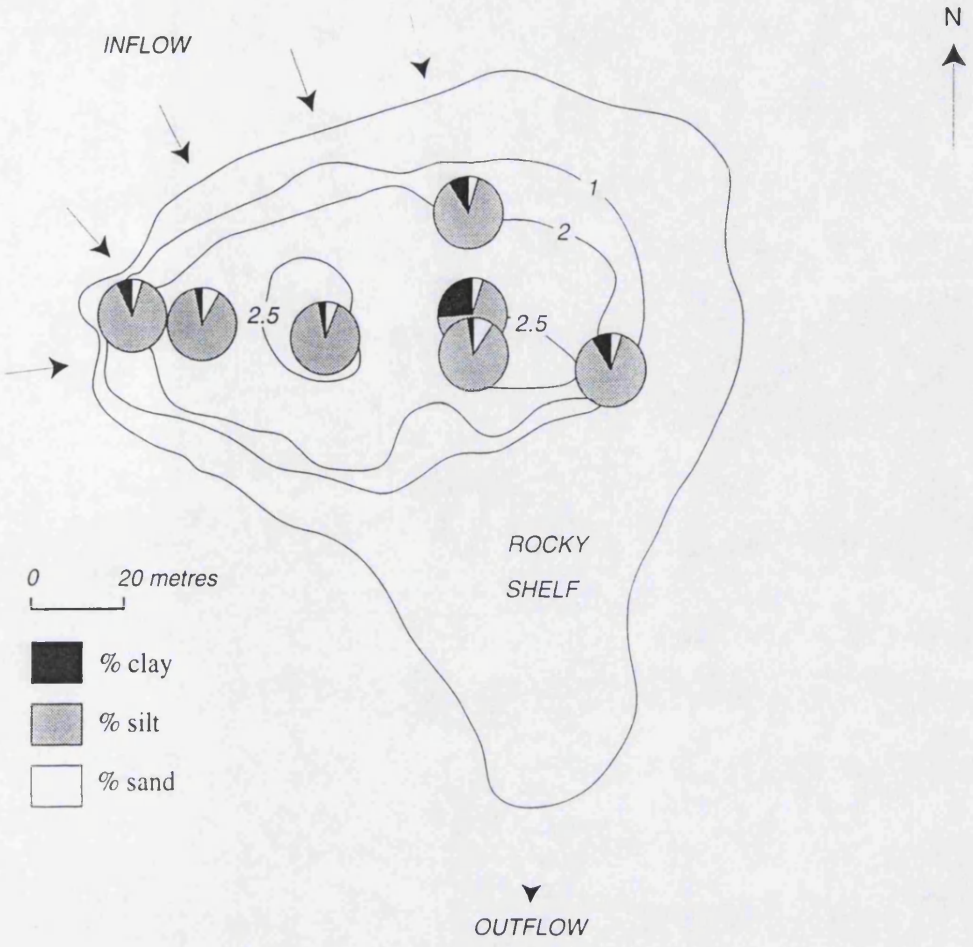

Figure 6.13 Distribution of surface-sediment particle-size, Light Lake

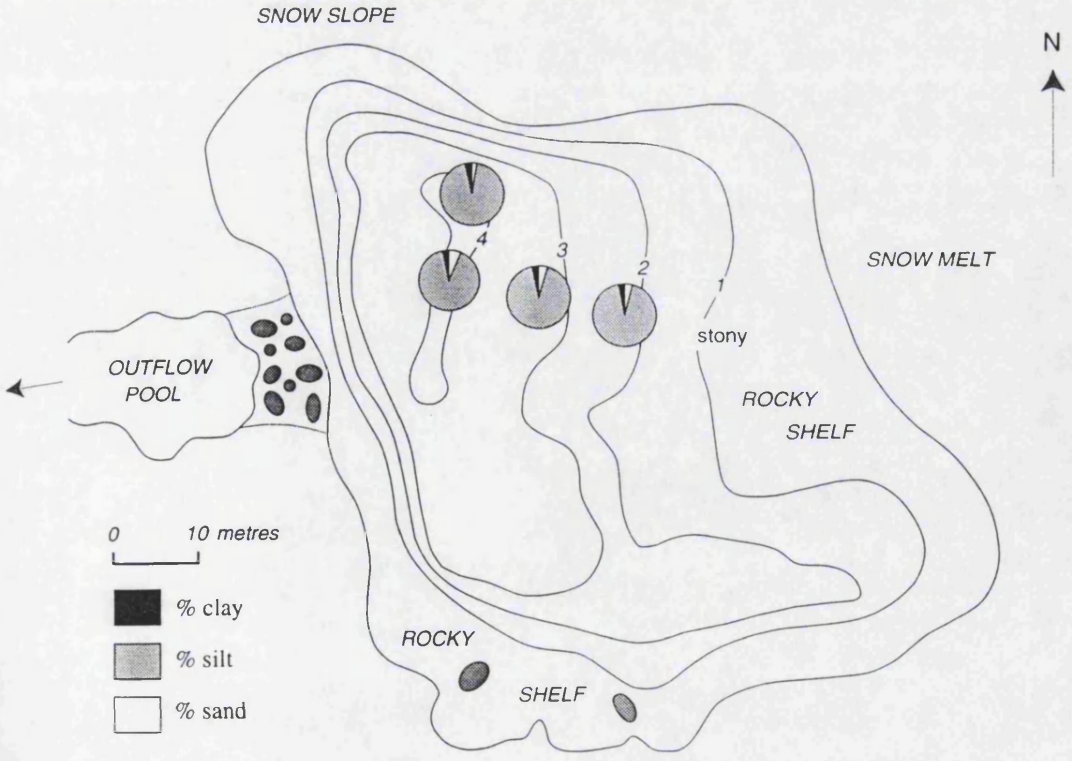

Figure 6.14 Distribution of surface-sediment particle-size, Spirogyra Lake

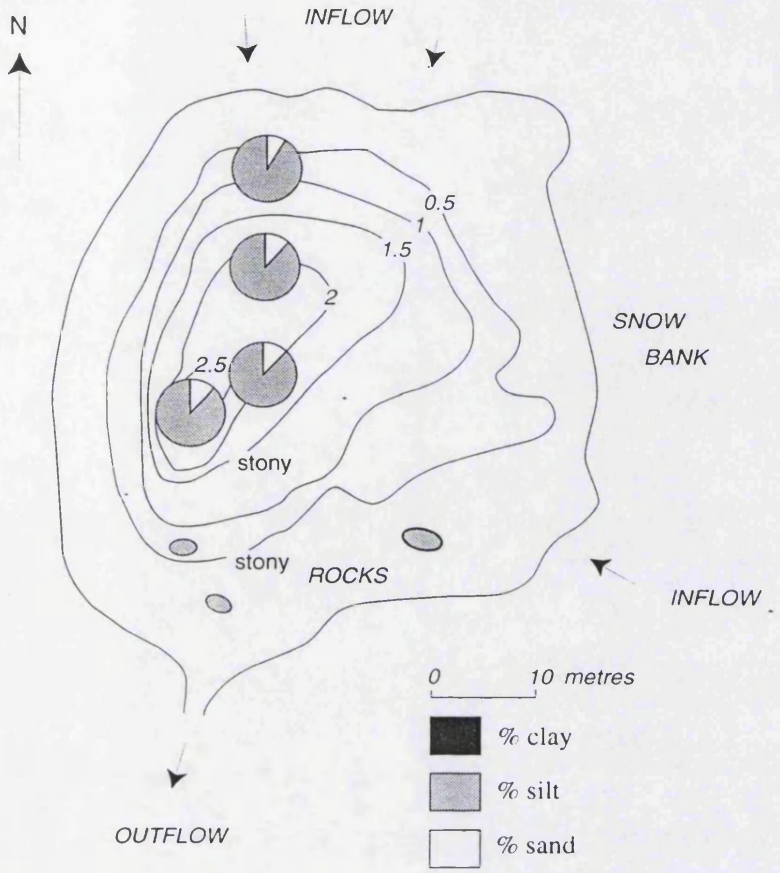

Figure 6.15 Distribution of surface-sediment particle-size, Tranquil Lake

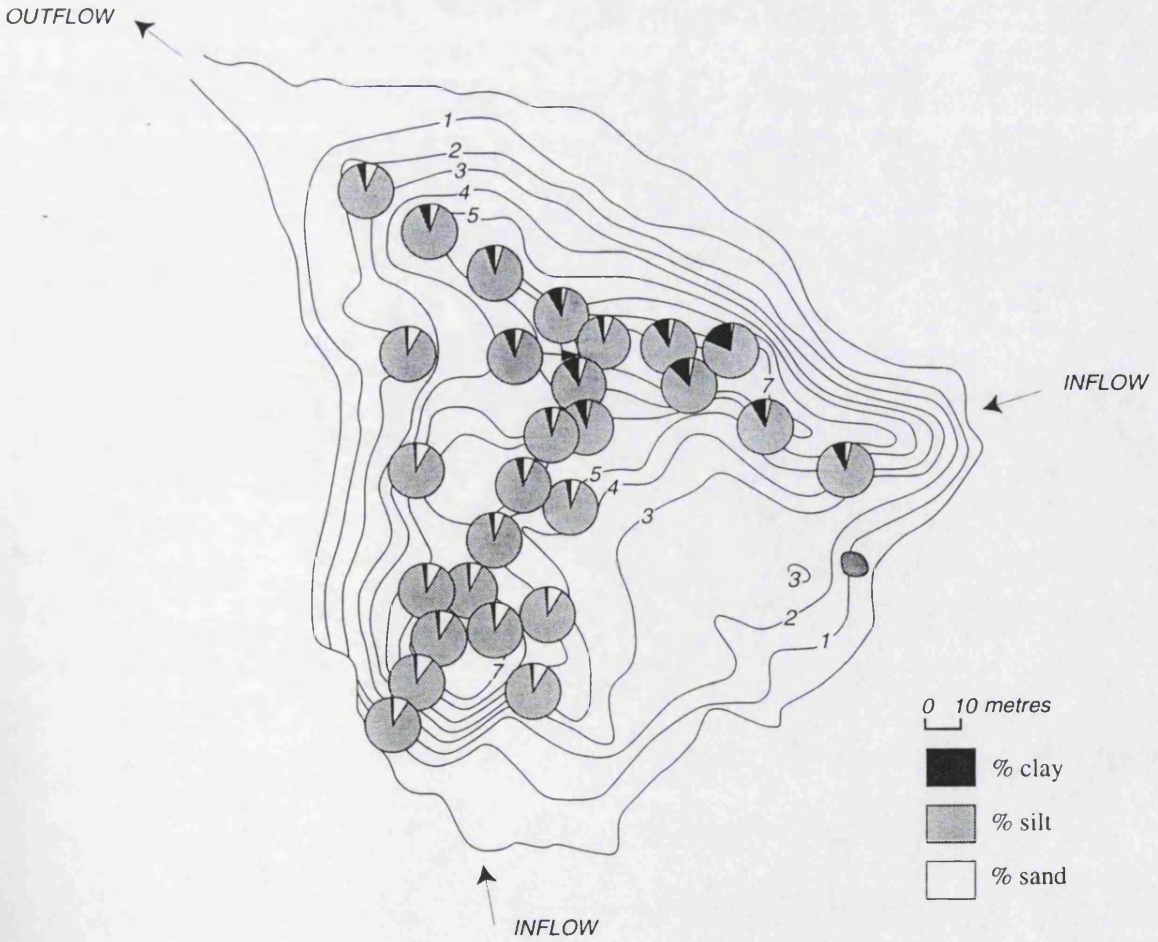

second group, in the southern half of the basin, has very little clay and samples are predominantly silty with a small percentage of sand. This group aligns with the secondary lake inflow. Clay loadings are greater in samples aligned to the principal source of glacial meltwater from the glaciated backslope. The southern group, virtually devoid of clays, is fed by the secondary inflow which drains a more stable area of the catchment. The two groups are reminiscent of patterns seen in Figure 5.11.

6.5.10 Amos Lake

The five samples from the central trough are uniform in character, with roughly 80-95% silt and 10-20% sand (Figure 6.16). Clay is negligible to virtually absent (not exceeding 0.59%).

6.5.11 Tioga Lake

The sediment from the four sample points is very similar (Figure 6.17), composed of 88-95% silt, 20-28% clay and very little sand (<0.1%). These samples are distinctive from the other lakes: they lack sand and have very high proportions of clay. This probably results from analytical bias as there was only sufficient material for measurement on one lens (63 mm lens, effective range 1.2-118μm), leading to an over-representation of fine particles from the shortening of the distribution curve (section 6.4.4).

6.5.12 Emerald Lake

These sediments have uniform particle-size characteristics (*ca.* 85% silt, 15% sand) with very little clay (Figure 6.18). Volumes of clay are higher around the principal inflow which drains the ice-face above the lake. This influence is rapidly dissipated by the volumes of silt received in the remainder of the basin. There are some indications of higher clay receipt from the secondary inflow on the south-east shoreline. The clay component does not exceed 24% (EMER24, proximal to the inflow moraine) and is generally less than 1-2%.

6.5.13 Lake 13

The two samples are slightly different from each other (Figure 6.19). SIG131 near the deep point, proximal to the primary inflow, has a higher percentage of clay and sand (90% silt, 9.6% sand, negligible clay). SIG132 lacks any clays and is predominantly silty with <8% sand).

Figure 6.16 Distribution of surface-sediment particle-size, Amos Lake

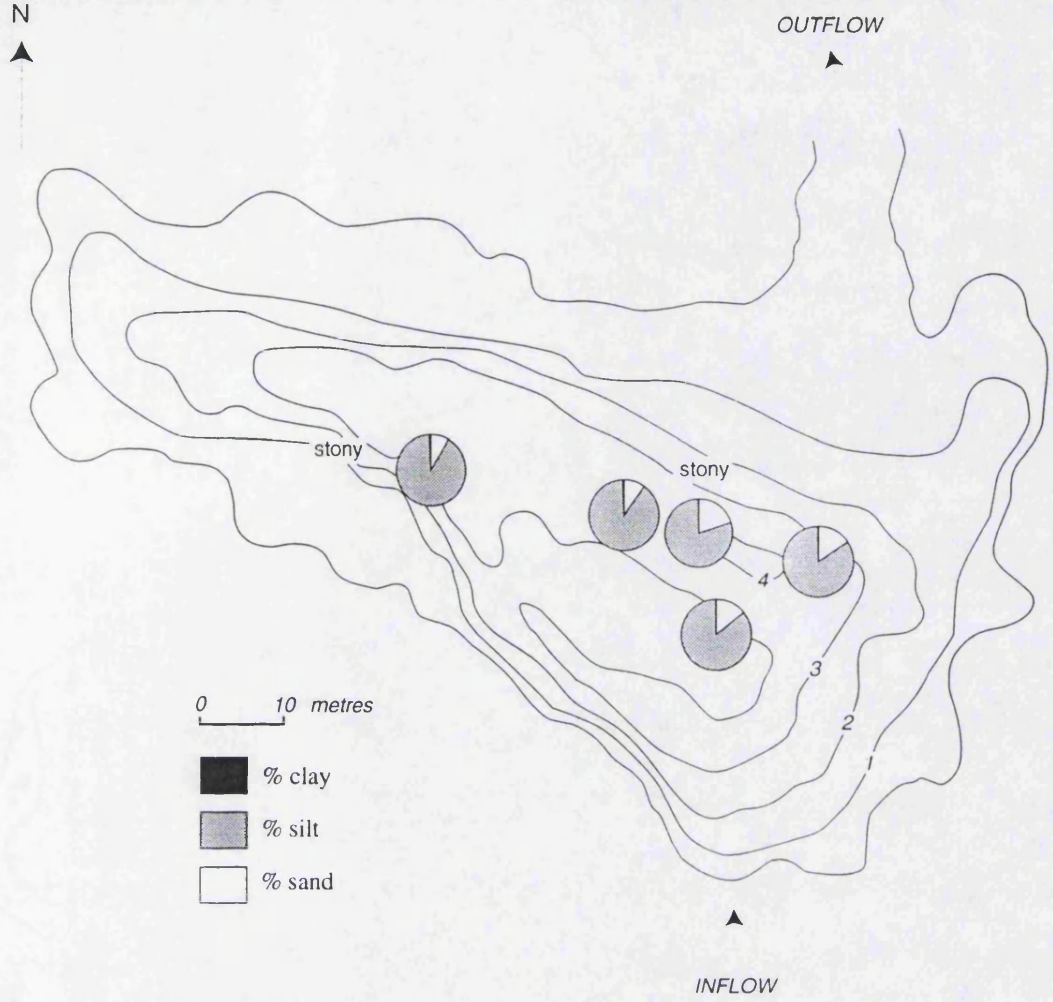

Figure 6.17 Distribution of surface-sediment particle-size, Tioga Lake

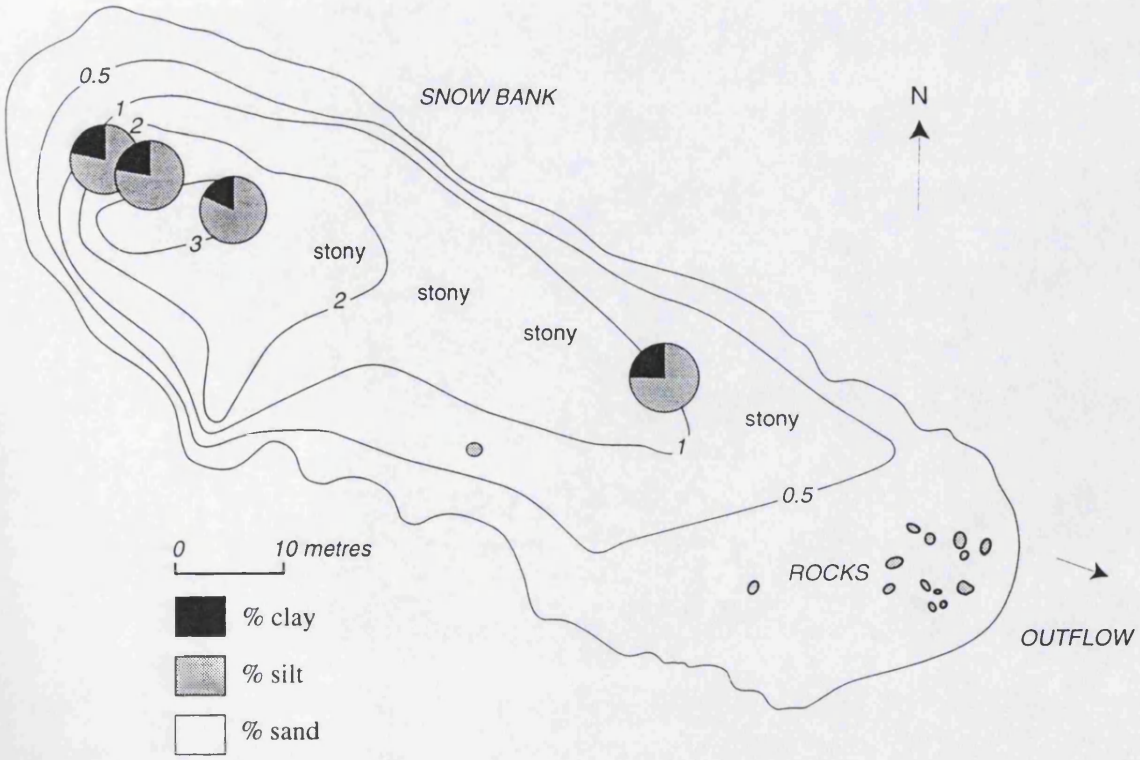

Figure 6.18 Distribution of surface-sediment particle-size, Emerald Lake

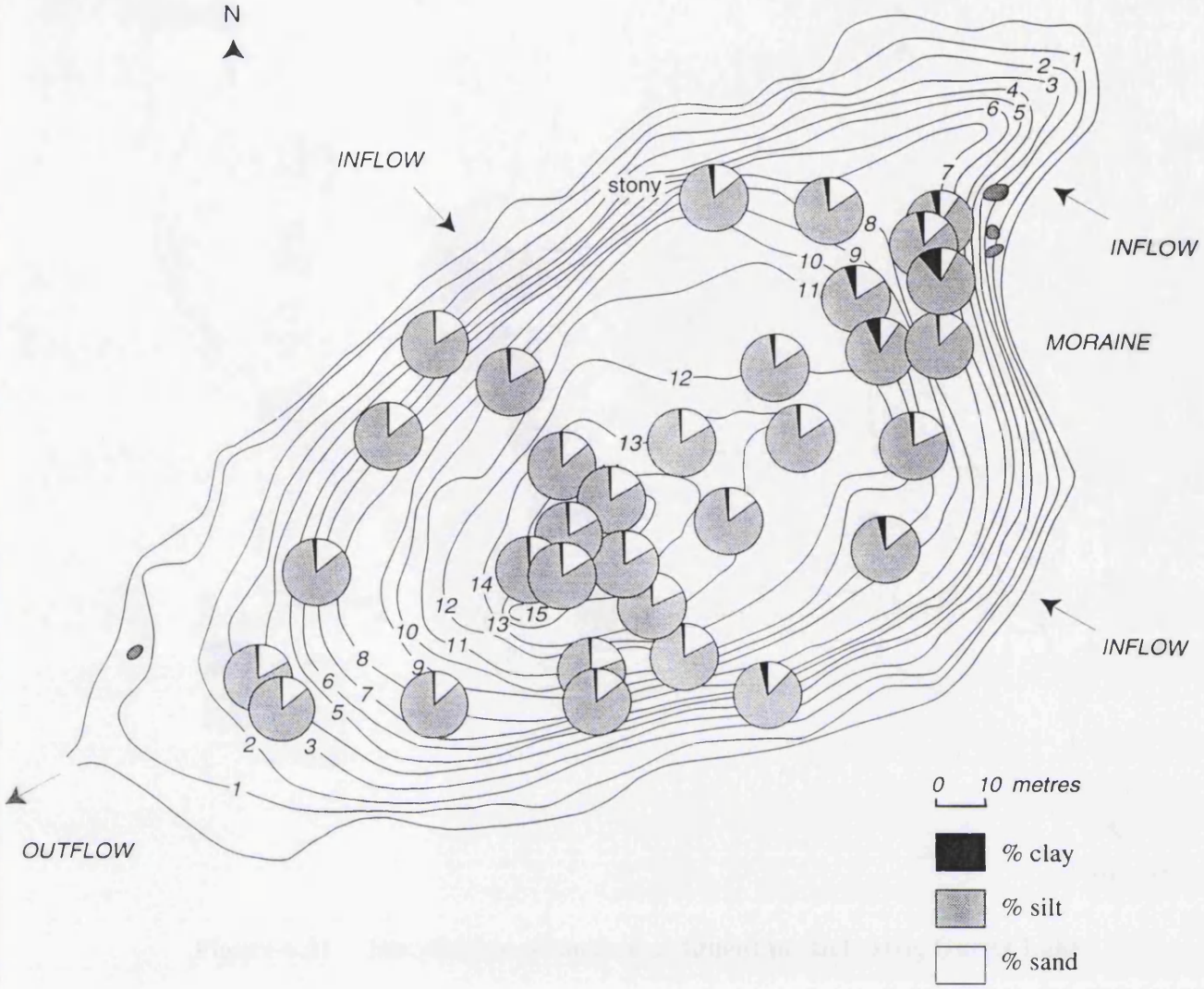

Figure 6.19 Distribution of surface-sediment particle-size, Lake13

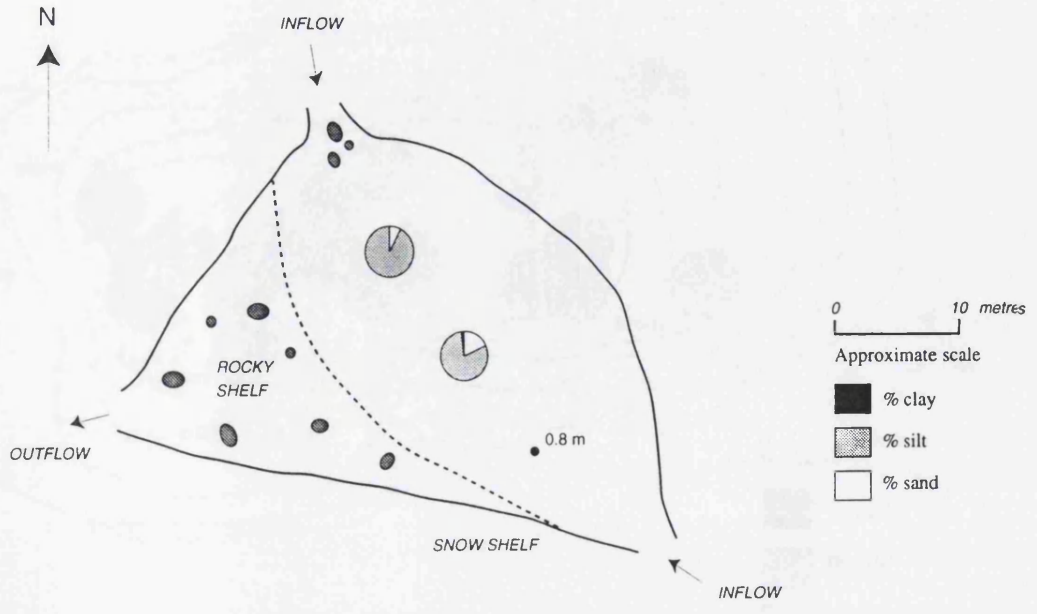

Figure 6.20 Distribution of surface-sediment particle-size, Twisted Lake

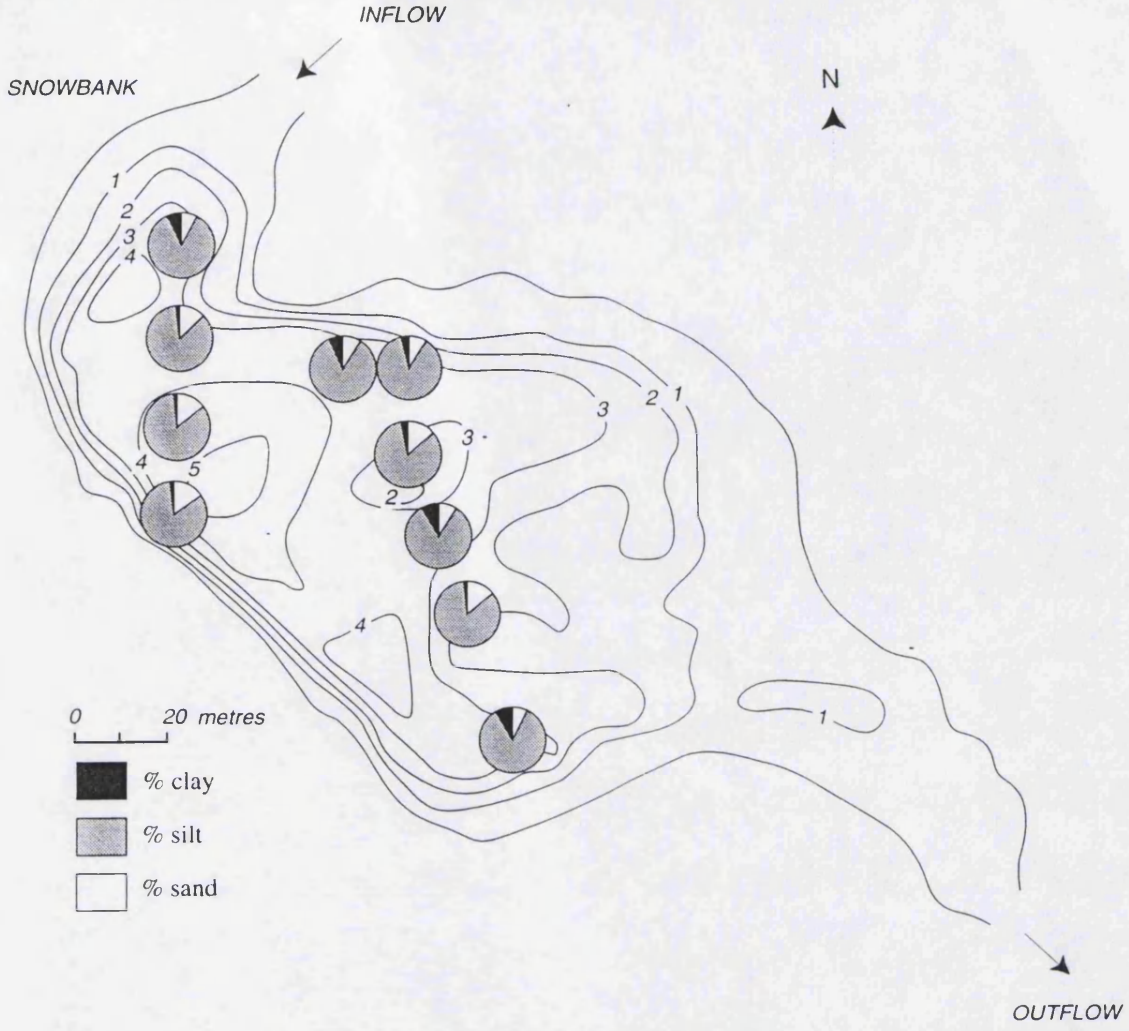

Figure 6.21 Distribution of surface-sediment particle-size, Gneiss Lake

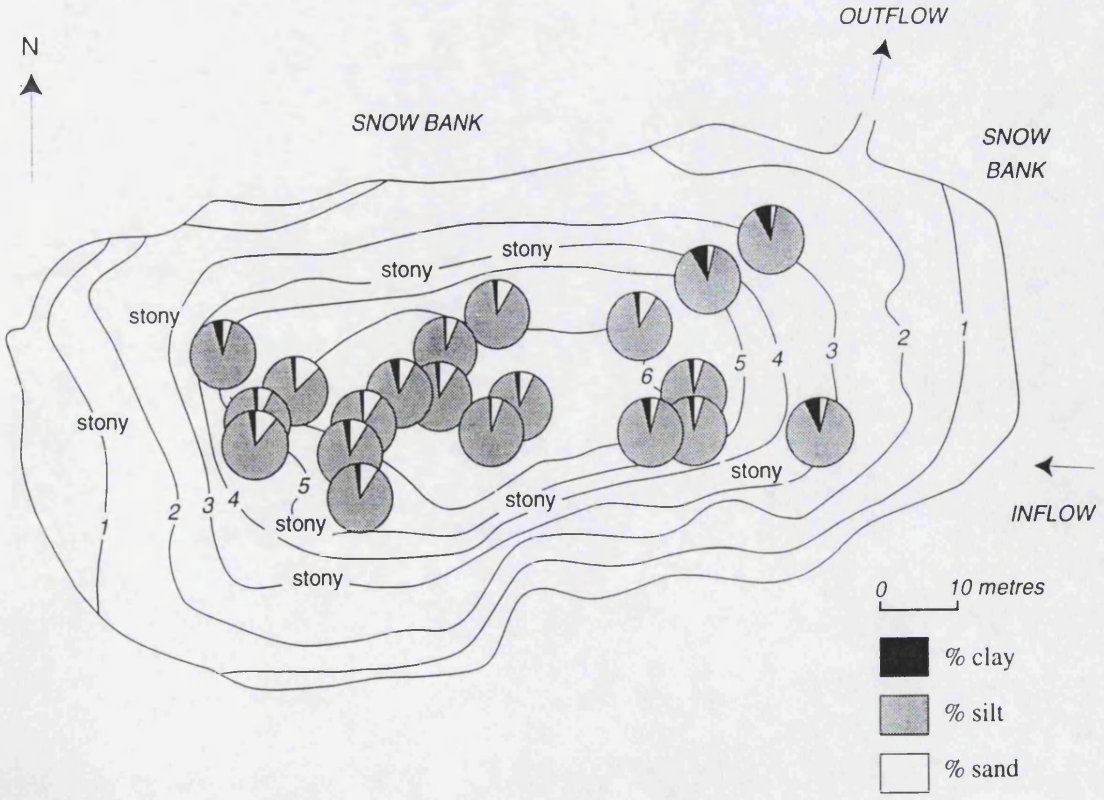

Figure 6.22 Distribution of surface sediment particle size, Orwell Lake

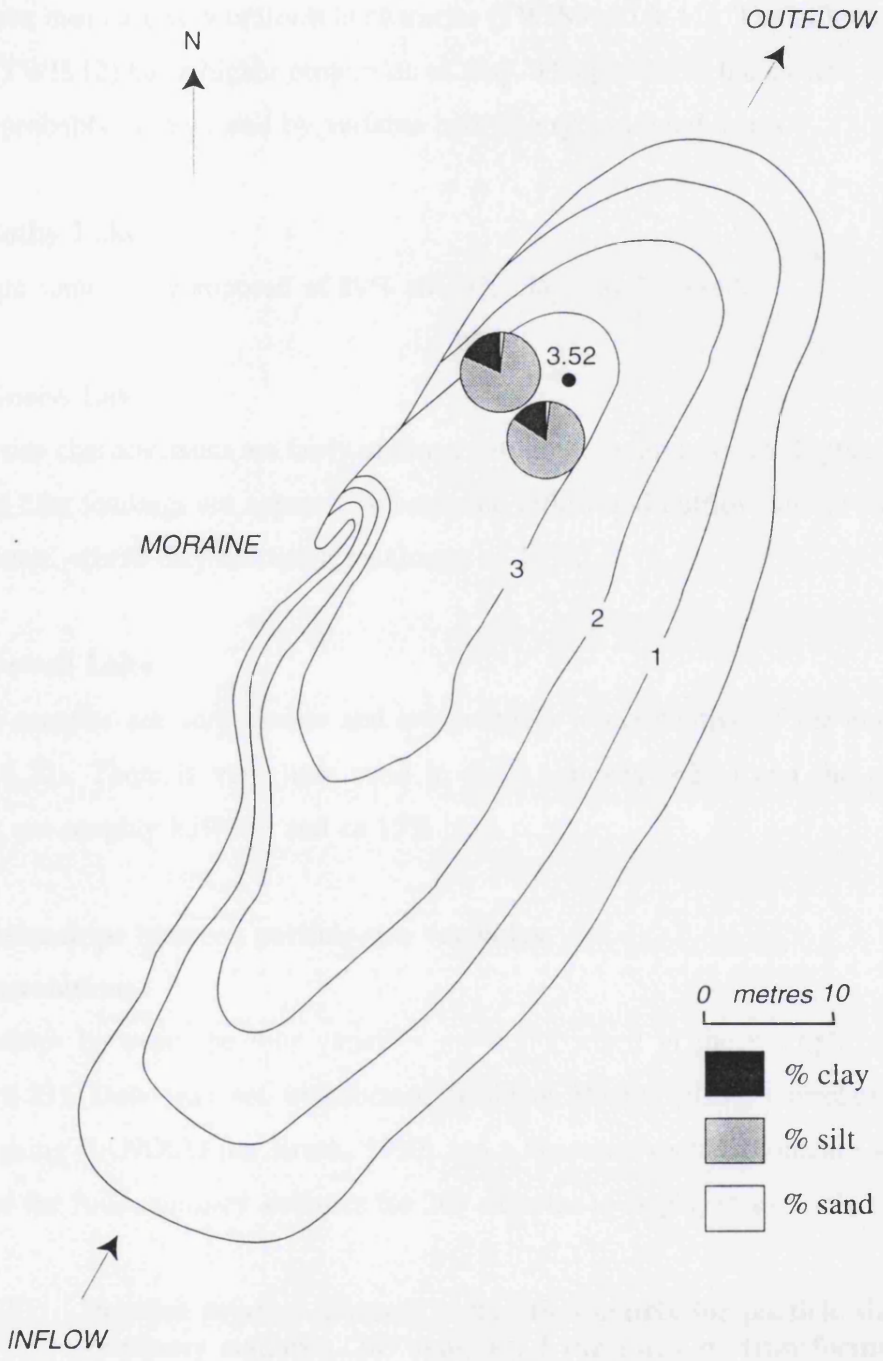

6.5.14 Twisted Lake

Particle-size characteristics are fairly heterogeneous (Figure 6.20). Three samples from the western basin are very uniform in character (TWIS9, 10 & 11). The inflow-proximal sample (TWIS12) has a higher proportion of clay. The pattern in the eastern half of the basin is probably complicated by variable bathymetry and wind-stress.

6.5.15 Bothy Lake

The single sample is composed of 89% silt, 8% clay and 3% sand.

6.5.16 Gneiss Lake

Particle-size characteristics are fairly uniform within the central trough (Figure 6.21) but increased clay loadings are apparent towards the inflow and outflow on the developing delta feature, where clay reaches a maximum of 10%.

6.5.17 Orwell Lake

The two samples are very similar and are probably representative of the entire basin (Figure 6.22). There is very little sand in these samples (<2%) and the other size fractions are roughly 85% silt and *ca.*15% clay.

6.6 Relationships between particle-size variables

6.6.1 Correlations

Relationships between the four variables are summarised in the multiple scatterplot (Figure 6.23). Data was not transformed (Gale & Hoare, 1991). Correlations were derived using CANOCO (ter Braak, 1990) and a Pearson-Product Moment Correlation matrix of the four summary statistics for 209 samples is displayed in Table 6.5.

Table 6.5 Pearson product-moment correlation matrix for particle size summary statistics (209 samples, 4 variables, no transformation)

Median	1.000			
Mean	0.9218	1.000		
S.D.	0.7443	0.9377	1.000	
Skew	0.1656	0.2566	0.4095	1.000
	Median	*Mean*	*S.D.*	*Skew*

Shaded cells have a significance level of $p<0.001$ where $r=0.321$ for 207 degrees of freedom.

All correlations between the four statistical measures of the volume distribution are positive and many are highly significant. The strongest relationship is between mean particle-size and the standard deviation (r=0.9377); the weakest between median particle-size and skewness (r=0.1656). All correlations however, are significant (+ or -) at the p<0.1 level (r=0.164). Mean and median particle-size have a very strong correlation indicating closely matching values and therefore fairly normal particle-size distributions; strong corelations between mean and S.D. particle-size indicate unimodal particle-size distributions with relatively little skew.

Figure 6.23 Multiple scatterplots illustrating the relationships between particle -size summary statistics (untransformed data)

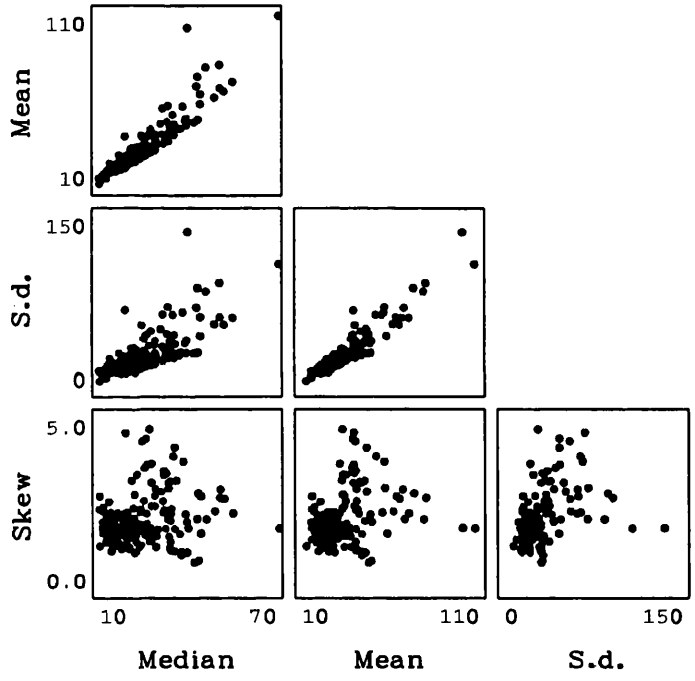

6.7 Classification

6.7.1 Cluster analysis

Five methods of agglomerative hierarchical cluster analysis were tested using the program CLUSTER (H.J.B. Birks) on standardised data in a Euclidean distance matrix and an assessment made of their relative performance with the data-set. Group memberships are displayed in Table 6.6. Nearest-neighbour (single-link) cluster analysis performs poorly with the data, finding little structure beyond the first sixteen samples.

Shaded cells=adopted classification method

Group membership	*Nearest neighbour (single-link)*	*Furthest neighbour (complete-link)*	*Weighted group average*	*Group average*	*Minimum variance (Ward's method)*
1	PUMP2.	HEY12; PUMP2.	HEY5,12; PUMP2; AMOS6,7.	HEY12; PUMP2.	SOMB41; HEY5,6,12,14,15; CHAN13,14; KNOB11; PUMP2; TRAN20; AMOS4,6,7; ORWE2.
2	HEY12.	SOMB27,31,40,41; HEY5,6,10,14-16; CHAN13,14; PUMP3; KNOB1,5,11; SPIR4; TRAN17,18,20; AMOS4-7; EMER24; TWIS8; BOTH1; GNES12; ORWE.	SOMB13,21,26,27,29,31,37,39-41,43,44,46; HEY6,9,10,14-16; CHAN13,14; MOSS9,10; KNOB1,3,5,7-11; PUMP1,3,5,7; SPIR2-4; TRAN4-6,12-15,17-23,30; AMOS3-5; EMER13,24,25; SIG13; TWIS3,5,7,8,12; BOTH1; GNES10-12,18; ORWE.	SOMB41; HEY5,6,14,15,16; CHAN13,14; KNOB11; TRAN20; AMOS4,6,7; ORWE.	SOMB21,26,27,31,37,40; HEY10,16; KNOB1,3,5,8,10; PUMP1,3,7; SPIR4; TRAN4,5,12,13,17-19,21,30; AMOS5; EMER24; SIG13; TWIS5,8; BOTH1; GNES10-12,18; ORWE1.
3	HEY5; AMOS6,7.	SOMB22,24,42; HEY11; CHAN3-7,9; MOSS3,6,7,8,11,12,13,15-21; KNOB2; PUMP4; LITE3-5; TIOG1-3; TRAN7,8,10,11,27,28; EMER1-3,5-12,14-19,21-23,26-31; TWIS4,6,9-11; GNES2,4,8,9,14,15,17,19,20,22.	MOSS3,15,21; EMER5,9,10,16-18,22,23,28,29.	SOMB13,21,26,27,29,31,37,40; HEY10; MOSS9; KNOB1,3,5,7-10; PUMP1,3,5,7; SPIR2-4; TRAN4-6,12-15,17-19,21-23,30; AMOS3,5; EMER24,25; SIG13; TWIS3,5,7,8,12; BOTH1; GNES10-12,18.	SOMB42; CHAN6; MOSS3,6,7,11-13,15,17,19-21; KNOB2; LITE3-5; TRAN28; TIOG1; EMER1-3,5-12,14-18,21-23,26-31; TWIS6,9,10; GNES2,4,19,20.
4	HEY16.	SOMB21,26,37; KNOB3,8,10; PUMP1,7; TRAN4,5,12,13,19,21,30; SIG13; TWIS5; GNES10,11,18.	SOMB22-25,28,30,32-34,36,38,42,45; HEY7,8,11,13; CHAN3-7,9,11; MOSS6,7,11-13,16-20; KNOB2,6; PUMP4,6; LITE3-5; TRAN7,8,10,11,16,27,28; TIOG1-3; EMER1-4,6-8,11,12,14,15,19-21,26,27,30-32; TWIS4,6,9-11; GNES2,4,8,9,14-17,19-22;	SOMB42; CHAN6; MOSS3,6,11-13,15,17,19-21; KNOB2; LITE3-5; TIOG1; EMER1-3,5-12,14-18,21-23,26-31; TWIS6,9,10; GNES19,20	SOMB13,22,24,29,30,32,36,38,39,43,44,45,46; HEY7-9,11,13; MOSS9,10,16; KNOB6,7,9; PUMP5,6; SPIR2,3; TRAN6,14-16,22,23; AMOS3; TWIS3,4,7,12; EMER4,13,19,20,25,32; GNES16,17,21.
5	SOMB41; HEY6,14,15; CHAN13,14; KNOB11; TRAN20; AMOS4; ORWE2.	SOMB11-20,23,25,28-30,32-36,38,39,43-46; HEY7-9,13; CHAN2,8,10-12; MOSS4,5,9,10,14; KNOB4,6,7,9; PUMP5,6; LITE2; SPIR2,3,5; TRAN6,9,14-16,22-26,29; AMOS3; TIOG4; EMER4,13,20,25,32; TWIS3,7,12; GNES3,5,6,13,16,21.	SOMB11,12,14-20,35; CHAN2,8,10,12; MOSS4,5,14; KNOB4; LITE2; SPIR5; TRAN9,24-26,29; TIOG4; GNES3,5,6,13.	SOMB11,12,14-20,22-25,28,30,32-36,38,39,43-46; HEY7-9,11,13; CHAN2-5,7-12; MOSS4,5,7,8,10,14,16,18; KNOB4,6; PUMP4,6; LITE2; SPIR5; TRAN7-11,16,24-27,29; TIOG2-4; EMER4,13,19,20,32; TWIS4,11; GNES2-6,8,9,13-17,21,22.	SOMB11,12,14-20,23,25,28,33-35; CHAN2-5,7-12; MOSS4,5,8,14,18; KNOB4; LITE2; PUMP4; SPIR5; TRAN7-11,24-27,29; TIOG2-4; TWIS11; GNES3,5,6,8,9,13,14,15,22.
6	Remainder, n=193	nil	nil	nil	nil
Cophenetic correlation	0.897633	0.784081	0.735567	0.911940	0.694686
Delta one-hat	0.795466	1.31687	0.600995	0.274303	28.9910
Gower's delta	2.033950E+07	-6.800242E+07	-1.195292E+07	1.789601E+06	-1.230944E+13

Table 6.6 Comparison of cluster groups of surface-sediment particle-size data using agglomerative hierarchical cluster methods

The other methods generally agree, dividing the data-set into five groups respectively, with some clusters sharing similarities. Samples HEY2 and PUMP2 were distinctive at the first level of division in these four cluster methods.

To maintain a direct comparison with the organic and minerogenic data classification (section 5.7.1) minimum variance cluster analysis was selected as it finds the simplest group structure in the large sample-set despite its low cophenetic correlation. Minimum variance cluster analysis divides the data-set into five groups:

Group 1: n = 15	Group 2: n = 38	Group 3: n = 51
Group 4: n = 48	Group 5: n = 57	

These cluster groups are used to classify samples in the ordination biplot (Figure 6.23b) to aid interpretation.

6.7.2 Classification by energy environment

Several approaches have been devised in an attempt to relate particle-size distributions to environments of deposition (Gale & Hoare, 1991). For example, Sly (1983) constructed energies of deposition based on the mean phi size and mean standard deviations of a large number of surface-sediment samples from different sites in the North American Great Lakes. He identified three basic regimes: High Energy, Low Energy (Normal deposition) and Low Energy (Anomalous deposition). Many textural distributions were recognised as anomalous, i.e. they departed significantly from an empirical depositional optimum. Sly defined four additional sectors to characterise these anomalous materials (E_l-H_l) which were generally comparable to sectors A_l-D_l respectively, but contained some coarse particulates in otherwise fine sediments, hence the higher values for standard deviation of the mean. His results are summarised in Table 6.6 with the equivalent mean particle-sizes in μm for comparison.

For exploratory purposes, this classification was tested on the Signy data to predict the depositional environment at each sample point. The mean particle-size in this data-set does not exceed 108 μm (fine sand) therefore none of the samples conform to Sly's 'High Energy' group. The two resultant groups divide the sample-set into a Low Energy (normal deposition) group (n=83) and a Low Energy (anomalous deposition) group (n=126). These groups are used to classify the samples in Figure 6.24. Coarse-grained

Sector	*Niagara*			*Tobermory*			*Kingston*			*Energy*	*Equivalent*
	n	*Mean*	*S.D*	*n*	*Mean*	*S.D.*	*n*	*Mean*	*S.D.*	*regime*	*mean (μm)*
D_h	28	2.23	1.3-1.8	33	1.52	1.3-1.8	82	1.64	1.3-1.8	High Energy	355-180
A_l	47	3.06	1.3-1.8				4	3.65	1.3-1.8	Low	125-63
B_l	48	5.55	2.0-2.5	6	5.25	2.0-2.5	13	5.81	2.0-2.5	Energy	32-16
C_l	128	7.50	1.5-2.0	81	7.83	1.5-2.0	72	7.31	1.5-2.0	(Normal	8-4
D_l				35	8.34	1.5-2.0	2	8.43	1.5-2.0	deposition)	4-2.75
E_l	9	3.28	2.0-2.5	9	3.44	2.0-2.5	15	3.13	2.0-2.5	Low	125-90
F_l	9	4.3	2.5-3.0	48	4.11	2.5-3.0	31	4.27	2.5-3.0	Energy	63-45
G_l	2	5.51	2.5-3.0	42	5.91	2.5-3.0	22	5.55	2.5-3.0	(Anomalous	23-16
H_l				13	6.73	2.5-3.0	1	7.72	2.5-3.0	deposition)	11-4

Three energy regimes were defined by the positive or negative signs of values for skewness/kurtosis. In descending order of hydraulic energy, these were defined as D_h (High Energy) and A_l-D_l (Low Energy). Many textural distributions were recognised as anomalous in that they departed significantly from an empirical depositional optimum. Four additional sectors (E_l-H_l) were used to characterise anomalous materials; they were generally comparable to sectors A_l-D_l, respectively but contained some coarse particulates in otherwise fine sediments.

Table 6.7 Sly's classification using mean phi size and mean standard deviations based on Great Lakes data (1989)

outliers include PUMP2 and HEY12; the finest-grained sample is MOSS3. Some skewness values in the surface-sediment data-set exceed those found by Sly (1989), suggesting that in these small lakes the sediment material is well-mixed with little sorting prior to deposition, a typical characteristic of lacustrine sediments (Gale & Hoare, 1991).

Figure 6.24 Scatterplot of mean versus S.D. particle-size classified by Sly's Low Energy groups

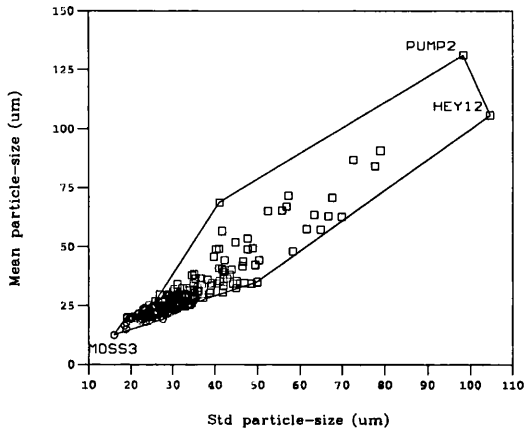

○ Low Energy (Normal Deposition) □ Low Energy (Anomalous Deposition)

A traditional means of plotting particle-size data is using ternary diagrams. Figure 6.25 compares the ternary diagram of Holmes's (1968) Windermere Late- and Post-Glacial sediments and the Signy surface sediment sample-set using derived values for proportions of sand, silt and clay (Table 6.4). In the ternary diagram, low-energy samples plot along the clay-silt edge and high-energy samples along the silt-sand edge. Samples with unimodal distributions group along the clay-silt and silt-sand edges of a triangular diagram, clay being eliminated near the sand apex and vice versa. Points near the centre of the diagram suggest a lack of sorting. The Windermere palaeo-analogue diagram shows that all the Signy sediments are from low energy groups or in an 'overlap' position, confirming the 'Low Energy' Group classification using Sly's (1989) scheme. The sediments are well-sorted, reflecting their glaciofluvial origin, and none plot in the centre of the ternary diagram.

A mean particle-size-depth relationship has been used to define areas of continuous accumulation from zones of active erosion and transportation (Håkanson & Jansson, 1983). Finer, well-sorted materials tend to dominate deep waters with continuous accumulation; coarser, less-sorted materials generally characterize zones of erosion and

Figure 6.25 **Ternary diagrams illustrating energy environments of deposition (a) Holmes's (1968) Windermere samples (b) Signy surface-sediments classified by energy environment (Håkanson)**

(a) Windermere sediment samples

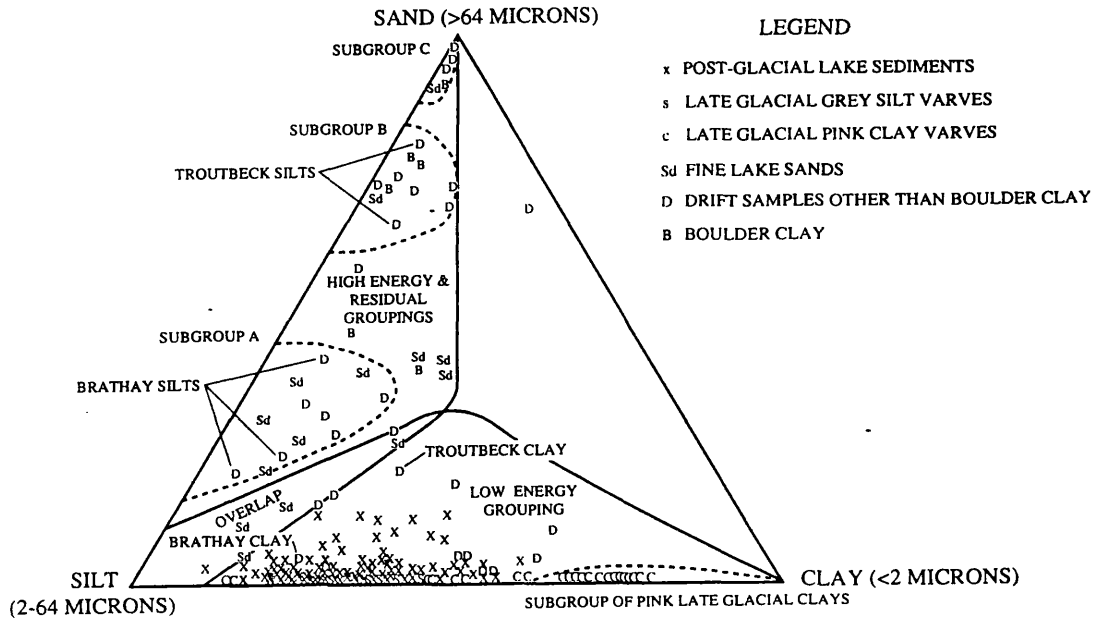

(b) Signy surface-sediments classified by energy environment (Håkanson)

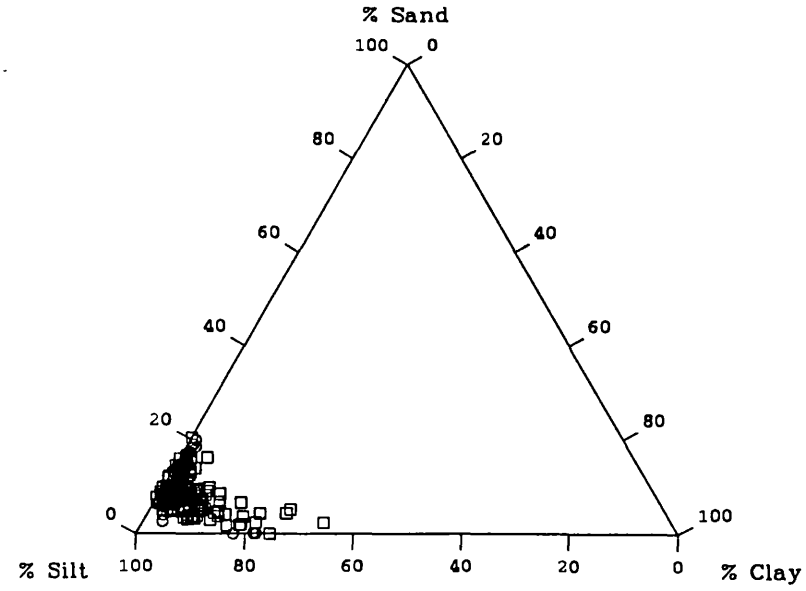

transportation in shallow, littoral margins.

Figure 6.26 Scatterplots of particle-size determinands versus sampling depth (untransformed data)

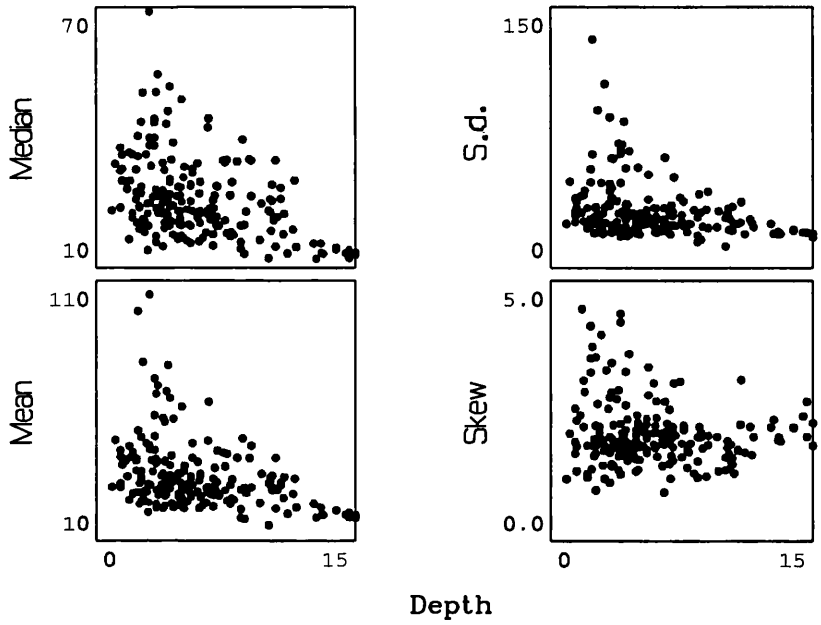

Median v. depth r^2=-0.4005; Mean v. depth r^2=-0.3669; S.D. v. depth r^2=-0.3074; Skew v.depth r^2=-0.1337

The scatterplot (Figure 6.27) illustrates particle size-depth relationships using the four summary determinands. Correlations, derived using CANOCO (ter Braak, 1987; 1990a), are negative in all cases, i.e. materials become finer, less skewed and with narrower distribution ranges, as depth increases, confirming that the bottom zone is characterized by well-mixed, fine-grained sediments. Unfortunately the lakes are too small for the application of the energy-topography formula (Håkanson & Jansson, 1983) to find the critical depth which defines zones of erosion and transportation from zones of accumulation.

Gale & Hoare (1991) believed that particle-size distributions alone are an inadequate means of determining environments of deposition and should be used in conjunction with other evidence. Particle-size shares a natural inter-dependency with sediment minerogenic and organic determinands (Håkanson & Jansson, 1983) and data from Chapter 5 can provide supporting information. Håkanson's (1977) sample classification based on sediment water content (section 5.6) can be used as a crude surrogate for energy environments of deposition. Sample classification on the scatterplot of mean

versus std particle-size however, shows some discrimination between the three energy environment groups, with fine sediments deriving from zones of stable accumulation and coarser more mixed sediments characterising zones of erosion, transportation and discontinuous sedimentation.

Figure 6.27 Scatterplot of mean versus S.D. particle-size classified by water content (Håkanson, 1977)

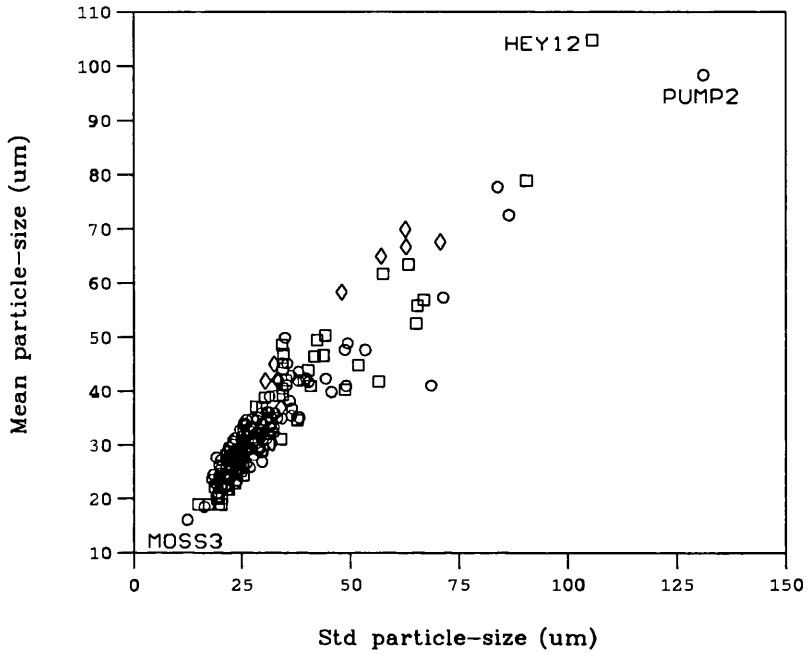

○ zone of stable accumulation □ zone of discontinuous sedimentation ◊ zone of erosion and transportation

Correlations between surface-sediment minerogenic and organic determinands and particle-size summary statistics are summarised in Table 6.8. Particle-size pretreatment (section 6.2.3.1) removes the organic fraction and samples should therefore represent combined minerogenic and biogenic inorganic fractions only. The only highly significant correlations ($p<0.001$) are between median and mean particle-size and wet density. Other correlations are significant at lower levels ($p<0.005$, $r=0.265$) but are still worthy of interpretation given the noise in this large data-set. The wet density distribution is skewed by a sample with a value of 0.98 g/cm^3 (MOSS14) composed almost entirely of aquatic moss remains. The positive correlation between wet density and particle-size is in many ways contradictory, since packing density should decrease with increasing grain-size. Standard deviation, i.e. the range of particle-size in a sample, is more

deterministic. Organic sediments tend to be finer textured and more sorted with lower standard deviations from the mean. Samples with a large variation of particle-sizes (high S.D.) are less sorted and have high values for %DW and wet density. The positive correlation between median particle-size and %Min (r=0.2594) is weak but significant at the p<0.001 level. More minerogenic sediments are associated with larger median grain-sizes, i.e. greater proportions of coarse silts and fine sands indicating more energetic environments of deposition. Skewness has no significance in either direction.

Table 6.8 Pearson product-moment correlation matrix for minerogenic and organic determinands (n=6) and particle-size distribution statistics (n=4) for the 209 sample-set

WD	0.3279	0.3245	0.2818	0.1310
%DW	0.3149	0.3089	0.2716	0.1634
%LOI	-0.2535	-0.2600	-0.2350	-0.1604
%OM	-0.2594	-0.2067	-0.1475	-0.1453
%BSi	-0.2554	-0.2460	-0.2167	-0.1274
%Min	0.2594	0.2067	0.1475	0.1453
	Median	**Mean**	**S.D.**	**Skew**

Shaded cells indicate a significance level of p<0.001 (r=0.321) for 207 degrees of freedom

Other relationships are negatively correlated at lower significance levels (p<0.02), for example median particle-size versus %LOI (r=-0.25) and %OM (r=-0.26) and median, mean and S.D. versus %BSi (r=-0.26, r=-0.25, r=-0.22 respectively). As particle-size increases the organic matter and biogenic silica contents of the sediment declines. Sample classifications in Figures 6.24 and 6.26 show that coarser sediments are from zones of erosion and transportation which are too unstable for the support of perennial phytobenthos or for the deposition of low-density organic sediments. Fine, well-mixed sediments characterize zones of accumulation at greater depths. The profundal zone is the sink for focused sediments (section 5.6) and provides a stable habitat for perennial phytobenthos. The potential effects of autochthonous productivity on particle-size characteristics is considered in the next section.

6.8 The effects of autochthonous production on particle-size

6.8.1 Theory

The endogenic sediment fraction, composed of the siliceous remains of microorganisms,

can have a considerable effect on the size-distribution of material in sediments (Jones & Bowser, 1978) which should be accounted for in particle-size studies (Engstrom & Wright, 1984). In the Signy Lakes an endogenic sediment component is derived from biogenic silica (diatoms and chrysophyte cysts) and varies spatially within and between the lakes, constituting >40% by dry weight in some surface-sediment samples (Chapter 5). Diatoms in these lakes occupy benthic habitats (Oppenheim & Ellis-Evans, 1989) and %BSi values in the sediment seem to indicate either *in-situ* incorporation into the underlying sediment or the focusing of death assemblages in association with low-density organic sediments. The effects of this diatomaceous material is most likely to impact upon the particle-size of sediments where allochthonous minerogenic inputs are low and organic matter is high, principally in zones of accumulation. Two considerations required investigation: (i) the typical size ranges of diatoms in the lakes; and (ii) their contribution to the particle-size volume-distribution. Two experimental hypotheses were established:

Null hypothesis: There is no significant difference in the particle-size characteristics of sediments with and without a biogenic silica (diatom) fraction.

Alternative hypothesis: Particle-size characteristics of sediments with and without a biogenic silica (diatom) fraction are significantly different.

6.7.2 Size-range of diatoms

To quantify the potential contribution of diatom valves to the particle-size distribution an estimate of diatom valve dimensions was required. Prepared diatom slides archived at the Environmental Change Research Centre were used as reference material supported by slides prepared from a sub-set of surface sediment samples. A total of 11 slides from a sub-set of lakes (Sombre, Heywood, Changing, Moss) were examined under a light microscope at x.1000 magnification. These lakes were selected on the basis of plentiful material for replicate analyses. For each slide 100 randomly-selected diatoms were counted and for each valve measurements of its apical- and trans-apical axis lengths were made using an eyepiece graticule. The valve shape (Barber & Haworth, 1981) was recorded. Only whole valves were counted and measured valve dimensions were therefore regarded as a maximum biogenic particle-size. Using the apical valve axis length a particle diameter, equivalent to the Malvern D[4,3] volume mean diameter (section 6.2.4.2), was derived for each valve. The mean diameter of all counts (n=100) was calculated to provide an approximate comparison to the Malvern Sizer results. The

summary of diameters are presented in Table 6.9.

Table 6.9 Summary statistics of valve axis lengths (in μm) and derived volume median (D[3,2]) and mean (D[4,3]) diameters for valve axis 1 (100 counts)

Sample	*Axis*	*Mean*	*Median*	*Std*	*Skew*	*Min*	*Max*	*D[3,2]*	*D[4,3]*
SOMB	1	19.60	11.1	17.40	1.16	3.3	88	45.67	53.56
#5394	2	11.42	8.25	9.03	1.02	2.2	44	w	
SOMB27	1	27.72	22	16.13	1.25	7	90	46.74	55.83
	2	5.39	5	2.59	1.62	2	15		
HEY	1	21.35	16.5	14.74	1.20	4.4	74.8	40.76	47.73
#5391	2	5.45	4.4	2.76	0.87	2.2	13.2		
HEY14	1	25.92	23	13.61	0.55	6	60	38.71	48.78
	2	5.73	5	2.43	0.50	2	12		
HEY15	1	23.22	20	13.15	0.81	4	60	37.04	41.44
	2	5.12	5	2.27	1.78	2	17		
HEY16	1	22.54	20	11.43	2.10	8	83	38.55	42.28
	2	4.63	4	2.42	2.21	1	17		
CHAN	1	23.73	20.35	13.20	1.00	3.3	57.2	38.02	43.17
#5389	2	4.28	4.4	1.73	0.62	2.2	8.8		
CHAN13	1	25.85	22	12.26	1.42	8	70	38.48	45.11
	2	3.88	2	2.22	1.34	1	12		
CHAN14	1	26.22	22	13.80	1.23	8	67	41.21	47.49
	2	4.45	4	2.38	1.34	1	13		
MOSS9	1	26.13	20	16.71	2.22	7	110	51.65	67.64
	2	5.67	5	3.43	1.82	2	20		
MOSS10	1	26.11	20	14.67	1.91	10	90	45.84	57.68
	2	4.85	4	2.74	1.91	1	18		

Where Axis 1 = apical valve axis and Axis 2 = transapical valve axis

Valve shapes are typically pennate, semicircular, rectangular, elliptic, narrow-elliptic, lanceolate or linear. Elliptic valves in Changing Lake are notably smaller than those in Heywood. The recorded fossil valve sizes agree with the length and width dimensions quoted by Oppenheim (1994) for examples of *Achnanthes* species from the Signy lakes and with Birnie's (1990) size estimates for diatomite in lake sediments from South Georgia which ranged between 5.3 (coarse silt, *ca.*32 μm) and 8 phi (fine silt, *ca.*4 μm)

and upper core material ranged from 0.5 phi (coarse sand, *ca.* 710 μm) to *ca.* 8 phi (fine silt, *ca.*4 μm).

6.8.3 Comparison of sediments with and without biogenic silica

To assess for the effects of the endogenic fraction on particle-size distributions, sediment sub-samples were subjected to two treatments: (i) hydrogen peroxide digestion (section 6.2.1), which removes allochthonous and autochthonous organics; and (ii) sequential extraction using hydrogen peroxide and sodium hydroxide (section 5.2.4) which removes organics and the biogenic silica fraction. In theory, samples subjected to the second treatment should show a loss of particles within the size range characterised by diatoms, i.e. coarse silt to fine silt range (section 5.2.4.3). Only the Ekman grab samples from Sombre, Heywood, Changing and Moss Lakes were able to provide sufficient material for replicate analyses. Their lithological characteristics are summarised in Table 6.10. All samples were measured on the Malvern Series 2600 Sizer on both 100 mm and 300 mm range lenses and the results were blended (section 6.2.3.4) yielding an effective particle size range of 1.5-564 μm. Export of results and numerical analysis were performed using the methods in section 6.2.5. Sub-samples retrieved from the circulation cell by micro-pipette were later examined under the light microscope to confirm the loss of diatoms from samples subjected to the second treatment.

Table 6.10 Lithological characteristics of the Ekman grab samples

Sample	*Water depth (m)*	*Wet density (g/cm^3)*	*% Dry weight*	*% Loss on ignition*	*% Biogenic silica*
SOMB27	3.4	1.39	45.79	1.82	0.497
HEY14	4.5	1.33	41.03	7.69	9.316
HEY15	4.0	1.16	28.56	15.58	4.700
HEY16	4.0	1.06	12.47	25.5	11.232
CHAN13	4.3	1.60	67.80	2.84	0.817
CHAN14	3.6	1.60	61.40	3.23	1.337
MOSS9	4.3	1.20	45.98	6.61	3.314
MOSS10	4.2	1.15	42.20	5.96	1.100

6.8.4 Numerical Analysis

Results from the 32 Sizer bins were reduced to nine particle-size classes which matched corresponding Wentworth groups (Table 6.1) from fine sand to very fine silt: 250-125

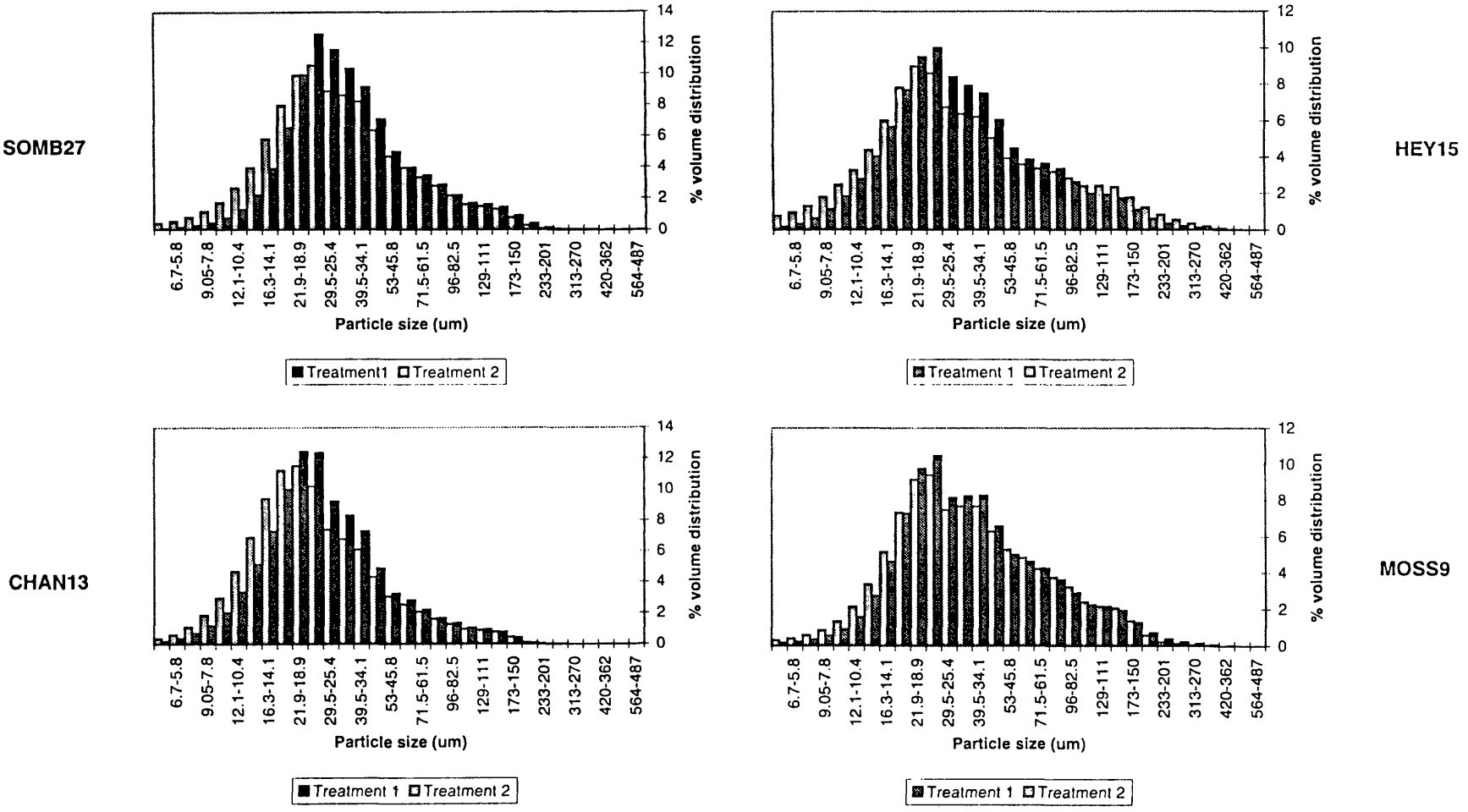

Figure 6.28 Histograms of Ekman grab samples with (Treatment 1) and without (Treatment 2) the biogenic silica fraction

μm, 125-62.5 μm, 62.5-31.2 μm, 31.2-15.6 μm, 15.6-7.8 μm, 7.8-3.9 μm, 3.9-1.95 μm, 1.95-0.98 μm, <0.98 μm. No material >250 μm (medium sand) is found in these samples. Histograms (Figure 6.28) indicate an increase in positive skew (more fine particles) and smoothing of the distribution profile in the second treatment class.

To test for a significant difference between the two populations, two-tailed *t*-tests were performed in Minitab (Minitab, 1989) for the four distribution statistics. Results (Table 6.11) confirm that there is no significant difference between the two populations (p=0.0000). The null hypothesis cannot therefore be rejected and diatoms are not seen to contribute significantly to the particle-size characteristics of these particular surface-sediment samples.

Table 6.11 Results of two-tailed *t*-tests of particle size volume distribution characteristics for a test population (n=61) of samples with and without the biogenic silica fraction

Population	*Mean*	*S.D.*	*S.E.Mean*	*t-value*	*p-value*
Median#1	40.425	12.639	2.270	17.81	0.0000
Median#2	43.605	15.002	2.739	15.92	0.0000
Mean#1	55.670	18.517	3.326	16.74	0.0000
Mean#2	58.607	19.173	3.501	16.74	0.0000
Std#1	55.570	22.870	4.108	13.53	0.0000
Std#2	56.668	20.318	3.710	15.28	0.0000
Skew#1	2.674	0.668	0.120	22.28	0.0000
Skew#2	2.468	0.582	0.106	23.23	0.0000

Where #1 = treatment 1 (organic matter removed) and #2 = treatment 2 (organic matter and biogenic silica removed)

This pattern is confirmed visually in a PCA biplot (Figure 6.29) of axis 1 and 2 scores where the two populations are seen to closely overlap. Results of the ordination are summarised in Table 6.12.

6.8.5 Discussion

Diatoms have a sufficiently different refractive index to be distinguishable from the suspension medium (Table 6.2) and a change in the distribution-curve after treatment to remove biogenic silica (Figure 6.28) should have removed some particles in the

Figure 6.29 Biplot of PCA axis 1 versus axis 2 scores for a test population of samples with and without biogenic silica

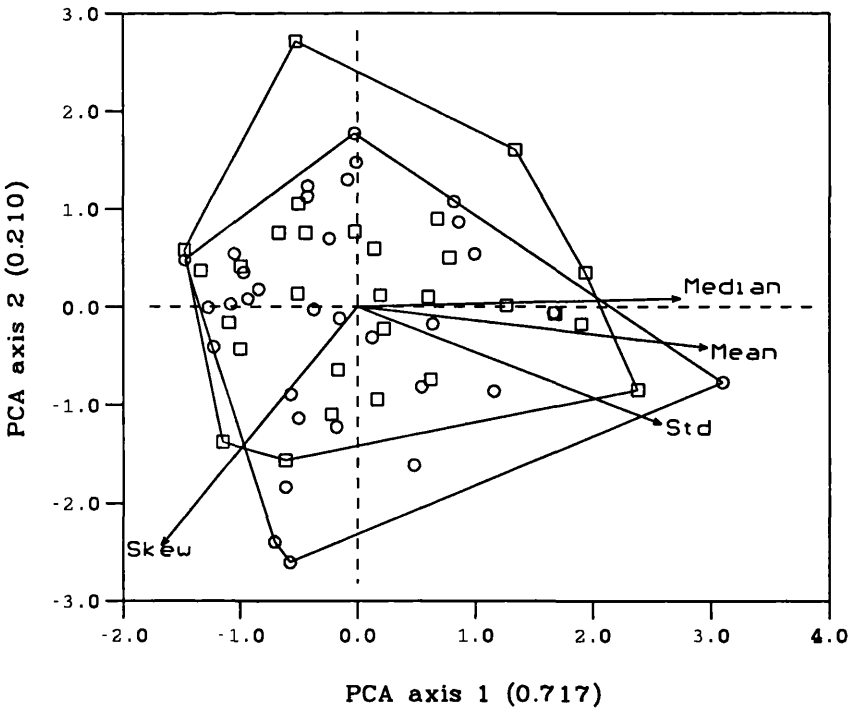

○ Population 1 (includes BSi) □ Population 2 (excludes BSi)

Table 6.13 Eigenvalues and cumulative variance accounted for in a PCA of the 61 samples by 4 particle-size variables data-set

	Axis 1	*Axis 2*	*Axis 3*	*Axis 4*	*Total variance*
Eigenvalues	0.717	0.210	0.073	0.001	1.000
Cum.% variance of sediment data	71.7	92.6	99.9	100.0	
Σ unconstrained eigenvalues					1.000

coarse to fine silt range. Volume-distribution curves are less peaky after the second treatment but there is no significant difference in the distribution statistics of the two populations. A bimodal distribution resulting from the contrasting character of small, high density mineral grains and a larger diameter, lower density biogenic component of diatoms and sponge spicules (Singer *et al.*, 1988) is not observed in this data-set. The Ekman grab samples, with their fairly low %BSi values, are not fully representative of the %BSi gradient in the data-set and diatoms are probably not present in sufficient volume to contribute significantly to the overall particle-size distribution. Many of these

sediments are analogous to the early postglacial sediments from southeastern Labrador (Engstrom & Hansen, 1985) where high erosion rates led to a dominance of allochthonous minerogenics, diminishing the relative autochthonous component to a negligible fraction. An obvious difference might have been seen in sediments with much higher %BSi values for example, Light and Tioga Lakes (section 5.3.5). The Ekman grab samples are more mixed than the 0-1 cm Glew core samples and were taken from locations identified as zones of erosion and transportation (section 5.6). In disturbed conditions many diatom valves break into smaller fragments but these still contribute to the overall biovolume (Flower, 1980) and should be part of the measured %BSi component. The slight fining in the particle-size distribution probably results from particle breakage during the digestion procedure as agitation during digestion causes clay aggregate breakdown (Matthews, 1991) as well as further valve fracture. In the case of these minerogenic samples, attrition and release of clay aggregates is the probable cause of the observed shift in the distribution curves (Figure 6.28).

6.9 Ordination

6.9.1 Principal Components Analysis

PCA provides an overall interpretation of the particle-size data for the 209 samples. PCA performed in CANOCO (ter Braak, 1990) using untransformed data (Gale & Hoare, 1991) in a Euclidean distance matrix, centred and standardised by species. Biplot interpretation is as in previous sections (cf. section 5.8.1) and summary results are presented in Table 6.14.

Table 6.14 Eigenvalues and cumulative variance accounted for in a PCA of the 209 samples by 4 particle-size variables data-set

	Axis 1	*Axis 2*	*Axis 3*	*Axis 4*	*Total variance*
Eigenvalues	0.716	0.230	0.054	0.001	1.000
Cum.%var.sed.dat.	71.6	94.6	99.9	100.0	
Σ *unconstrained eigenvalues*					1.000

Only the first two axes are significant in the data-set using the program BSTICK (H.J.B.Birks, unpublished). The first PCA axis captures a high percentage of the total variance (71.6%) and defines a gradient contrasting high values for median and mean

particle-size and the standard deviation of the mean versus samples with low values for these variables. The rank order of eigenvalues for the first axis is mean > S.D. > median > skewness. The second PCA axis (eigenvalue 0.23) is determined by the degrees of positive skewness, i.e. the greater or lesser influence of fine materials. The rank order of eigenvalues for this axis is skewness > S.D. > mean > median. The sample-set is therefore defined by samples which have larger mean and median particle-sizes associated with larger ranges (higher standard deviations of the mean) versus samples with smaller mean and median particle-sizes and narrower, more normal distributions with few coarse particles.

Figure 6.30 Biplots of PCA axis 1 versus axis 2 scores for surface-sediment particle-size classified by (a) sites (b) minimum variance cluster groups and (c) Sly's energy groups

(a) Sites

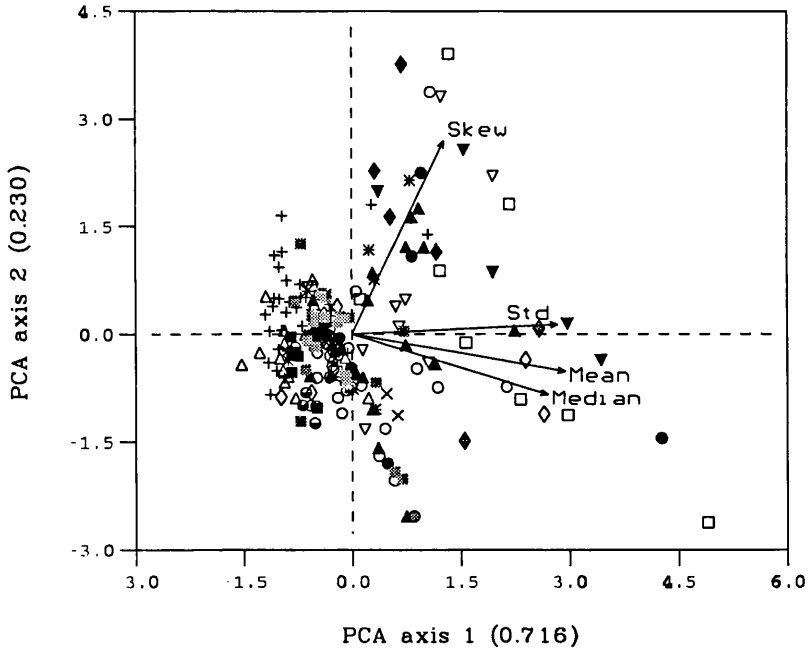

In the biplot of PCA axis 1 and 2 scores (Figure 6.30a), the majority of samples plot just to the left of the origin indicating sediments with finer grain-sizes and narrow ranges, such as Moss (up-triangles), Light (filled squares), Tioga (half-filled circles), Emerald (plus), Twisted (stars) and Gneiss (grey squares) Lakes. Spirogyra Lake (filled diamonds) forms a tight cluster highly correlated with high values for skewness, indicating the predominance of coarse particles in the volume-distribution. Most lakes though display high within-lake variability, most notably Sombre (open circles),

Heywood (open squares), Tranquil (filled up-triangles) and Amos (filled down-triangles) Lakes.

Figure 6.30b Classified by mininum variance cluster groups

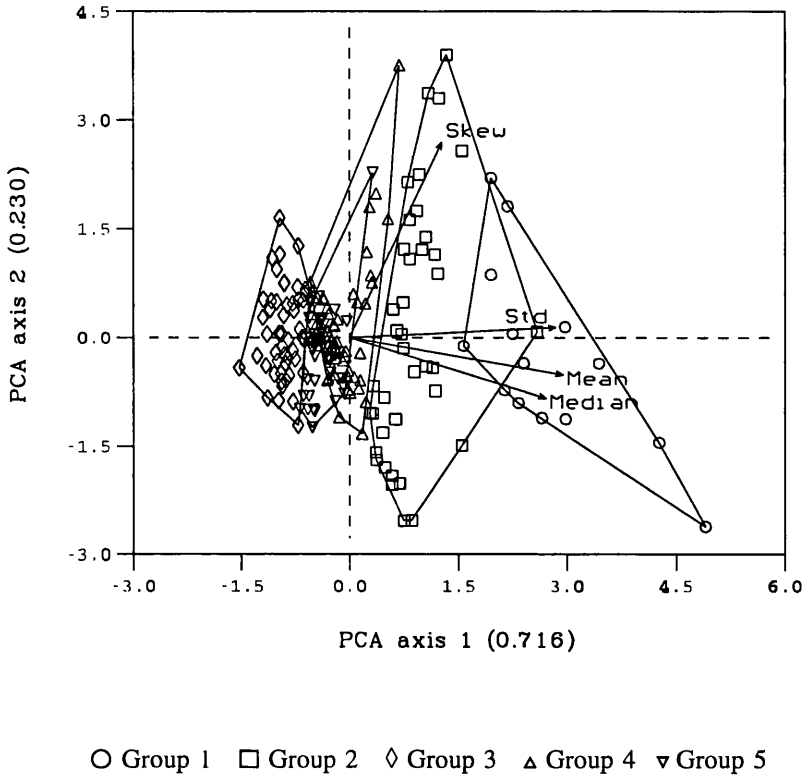

Minimum variance cluster analysis groups (section 6.7.1) are used to classify the samples in Figure 6.30b. All five cluster groups are separated on the basis of PCA axis 1 attributes, and within-group scatter is determined by the PCA axis 2 gradient (high or low skewness). All groups include samples with low or high values for skewness, and are influenced by varying excesses of fine particles. Skewness alone has poor discriminatory power in the data-set. Group 1 (open circles) defines samples with high values for the mean, median and high standard deviations of the mean (large particle ranges) and includes several lakes of contrasting trophies (Sombre, Heywood, Changing, Knob, Pumphouse, Tranquil, Amos, Orwell). Group 2 (open squares) is closer to the origin with more mid-range values, and includes samples from several different lakes, the largest membership contribution from Sombre, Knob, Tranquil and Gneiss Lakes. Group 3 (open diamonds) is at the opposite end of the PCA axis 1 gradient and is defined by low values for the mean, median and standard deviation. These samples cluster more tightly and are dominated by samples from Emerald, Moss and Gneiss Lakes. Group 4 (up-triangles) is aligned along PCA axis 1 near the origin but has a wide

range of values along PCA axis 2. Its distribution overlaps slightly with Group 3 indicating some shared characteristics. Group 4 includes the majority of samples from Sombre, Heywood, Moss, Knob, Tranquil, Twisted, Emerald and Gneiss Lakes. Finally, group 5 (down-triangles) shares its distribution with Group 4 and the cluster definition is weak. It includes remaining samples from Sombre, Changing, Moss, Knob, Tranquil and Gneiss Lakes plus isolated samples from other lakes.

Samples are classified by Sly's (1989) energy environment groups (section 6.7.2) in Figure 6.30c showing the clear definition between the two Low Energy Groups and the 'overlap' group (Holmes, 1968) found in the ternary diagram (Figure 6.21).

Figure 6.29c Classified by Sly's (1989) energy groups

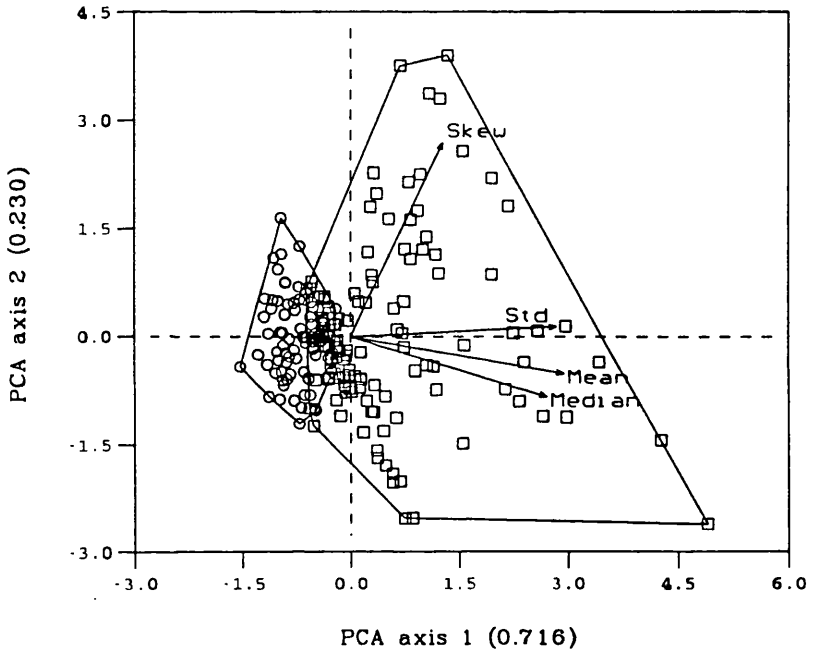

○ Low Energy (Normal Deposition) □ Low Energy (Anomalous Deposition)

6.9.2 Canonical Variates Analysis

As with the minerogenic and organic determinands, CVA can be used to explore direct particle-size-environment relationships as a means of underpinning the environmental controls responsible for the observed particle-size variation within and between sites. CVA was performed in CANOCO using the procedure outlined in section 5.8.2. Cluster groups (n=5) from minimum variance cluster analysis (section 6.7.1) were used in the analysis. Summary results of CVA are presented in Tables 6.14 and 6.15 and a biplot

of CVA axis 1 and 2 scores (Figure 6.31).

Table 6.14 Forward selection of environmental variables in CVA of sediment particle-size determinands (4 sediment variables in 5 cluster groups x 45 environmental variables)

Variable added	*cumulative variance of selected variables*	*number of permutations*	*Bonferroni required significance*	*significance achieved*
Na+	0.24	999	0.05	0.001
Clarity	0.46	999	0.025	0.001
Cl^-	0.54	999	0.016	0.001
Fur seals	0.68	999	0.0125	0.001
Depth	0.76	999	0.01	0.001
Catchment area	0.82	999	0.008	0.006
Variance explained by all variables	0.821			
No other variables significant				

Table 6.15 CVA summary using variables identified in forward selection of sediment particle-size determinands

Axes	*1*	*2*	*3*	*4*	*Total variance*
Eigenvalues:	0.484	0.229	0.087	0.021	4.000
Gp.env. r:	0.696	0.478	0.296	0.145	
Cum.% variance of gp.dat.:	12.1	17.8	20.0	20.5	
of gp-env relations:	59.0	86.8	97.5	100.0	
Σ *unconstrained eigenvalues*					4.000
Σ *all canonical eigenvalues*					0.821

Six statistically significant ($p<0.001$) variables were chosen by forward-selection: sodium ions, clarity, chloride ions, fur seals, sample location depth and catchment area. Tests of the first canonical axis and overall model using 99 unrestricted Monte Carlo permutations were significant ($p<0.01$); both the F-ratio for the significance test of the first canonical axis (27.82) and the overall test statistic (8.70) exceeded the critical F value ($F>5.63$, $p<0.05$ for 4 and 207 d.f.). 20.5% (0.821/4.00) of the between-group variation is explained by canonical (constrained) eigenvalues of these six forward-

selected environmental variables. 22.9% of variance in the between-group variance is explained in the first two CVA axes. Significant inter-set correlations ($r>|0.35|$) for CVA axis 1 include Na^+, fur seals and depth; for CVA axis 2, clarity only. All canonical coefficients are significant ($r>|1.96|$) for CVA axes 1 and 2.

In Figure 6.31, cluster groups A and C are the most dissimilar from the others, at opposite ends of the first CVA axis. Cluster A is strongly associated with large numbers of fur seals, high values for sodium and chloride, and large catchment areas. It has a negative relationship with sample depth, therefore these samples are from shallow water depths from lowland, coastal lakes subject to direct marine influences. Cluster C, conversely, is associated with deep waters and minimal marine influences. Clusters B and D are similar and share characteristics with Group A but are less extreme. Cluster E is very strongly associated with high water clarity and has the lowest chloride inputs, therefore representing inland lakes with a tendency towards samples from greater water depths.

Figure 6.31 CVA biplot of the 5 cluster groups of surface-sediment particle-size variables (n=4) in relation to significant variables on CVA axes 1 and 2

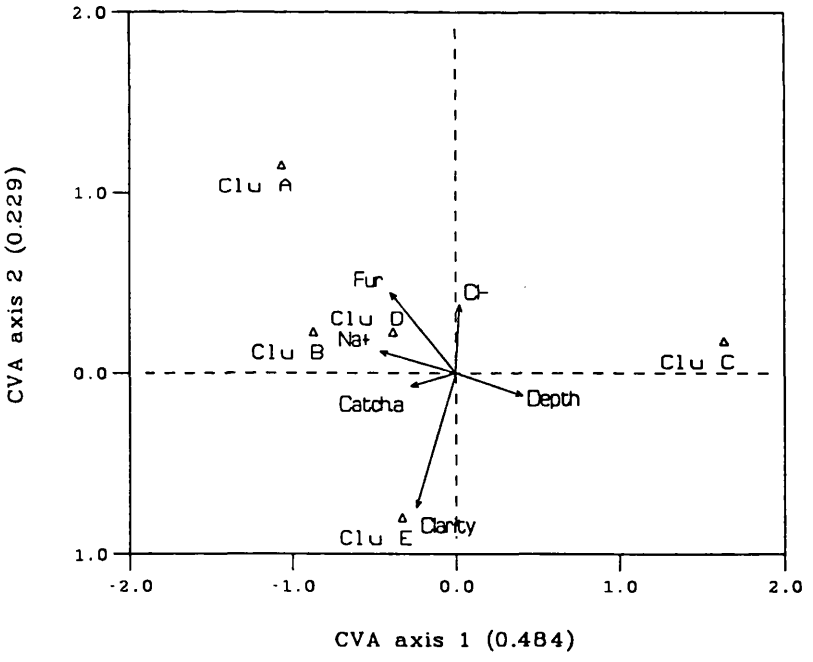

Particle-size cluster groups are discriminated on the basis of a few significant environmental variables of mainly extrinsic origin. Sodium, chloride and fur seals clearly

relate to the effects of the marine environment and in extreme form is represented by the low-lying coastal Heywood, Knob and Amos Lakes. The Group also includes the Ekman grab samples from Changing Lake and Orwell Lakes. Therefore the sediments from this group are characteristically coarse-grained. The group also associates with large catchment areas which include varying proportions of ice-cover; in general, the larger catchments have proportionally less ice-cover and this group therefore represents largely deglaciated terrain. Most lakes feel the effects of the marine factors, and cluster groups A, B and D include samples from 15 out of 17 lakes. This contrasts with cluster group C, predominantly samples from Emerald Lake, associated with fine-grained sediments from deep waters sited inland and away from marine influences. Cluster E is again different and includes fine-grained samples from more moderate water depths in clear-water oligotrophic lakes, largely represented by samples from Sombre, Changing, Moss, Light, Tranquil, Tioga and Gneiss Lakes. The underlying gradient in this ordination is therefore of coastal, lowland, largely deglaciated catchments versus upland, inland lakes with greater ice-cover. The genetic and trophic gradient observed in the minerogenic and organic determinands (section 5.8.1) is not clearly seen in the particle-size data and environmental conditions determining sample variability are more complex and less readily interpretable.

6.10 Discussion

6.10.1 Surface-sediment particle-size characteristics

Sedimentary environments can be characterised by limited sediment textural information (Gale & Hoare, 1991) and the four distribution moments used here (mean, median, standard deviation, skewness) are seen to adequately summarise the surface-sediment particle-size characteristics of these lakes. Samples were pretreated to remove organic materials and were therefore composed of minerogenic and biogenic inorganic particles. *Branchinecta* eggs can constitute a significant proportion of the coarse fraction in maritime Antarctic lakes (Björck *et al.*, 1996) but these low-density grains, potentially present in Sombre, Heywood, Knob, Spirogyra, Tranquil, Amos, Lake 13, Bothy and Orwell Lakes, were lost during pretreatment with the discarded supernatant. Using distribution moments removes problems associated with the accurate resolution of polymodal samples by laser diffraction methods (McCave *et al.*, 1986; Singer *et al.*, 1988) and a standardised method, using blended results from the 100 mm and 300 mm range lenses, is seen to be most reliable. Inaccurate tail-ends of the distribution (section 6.4.1) unfortunately prevent the use of coarse:fine ratios which can provide a prediction

of sediment transport and deposition energies (Sly, 1989; Björck *et al.*, 1996). However, an alternative classification scheme using the distribution moments was still able to provide some determination of samples from zones of erosion and accumulation.

The average median particle-size for the 209 sample-set is 25 μm, within the 0.5-30 μm range of typical lake bottom sediments (Gale & Hoare, 1991) and the 20 μm median grain-size measured in Holocene sediment-sequences from King George Island, South Shetland Islands (Mäusbacher, Müller & Schmidt, 1989). Silts are dominant (mean=88.8%), reaching a maximum (95.9%) in Light Lake, perhaps due to high %BSi contents (section 5.3.5), and a minimum (71.9%) in Heywood Lake. The littoral zone is noted for its coarse-grained and/or stony sediments (Heywood, Dartnall & Priddle, 1979) but these areas were largely neglected by the sample-net (section 4.4.1) and the full gradient of particle-sizes has possibly been truncated. Only five samples record material in the coarse sand range (HEY12, PUMP2, PUMP3, TRAN5, TRAN19) although in negligible volumes (<0.01% of the volume distribution). Coarse grains in otherwise fine samples lead to extremely high values for standard deviation of the mean, most evident in samples HEY12 and PUMP2 (S.D.=105.6 and 131.1 μm respectively). These coarse 'grains' could also be attributable to air bubbles caused by turbulence in the laser diffraction circulation system (Loizeau *et al.*, 1994). The mean sand content in the sample-set is 9% and is maximal in Amos Lake (20.5%, AMOS3). This is greater than comparable surface-sediments from glacial Lake Tasikutaaq, Baffin Island (Lemmen *et al.*, 1988), which had <3% sand in all but the most proximal (prodelta) samples. The lack of sand-sized fractions also indicates that aeolian sediment inputs are low, contrasting with results from Livingston Island where winds have a strong local effect on lake-sediments (Björck *et al.*, 1996). Clays do not exceed 38% in any of the Signy surface samples but these are probably underestimates. McCave *et al.* (1986) found that the amount indicated between 0.5 μm (wavelength of light) and 2 μm by the series 2600 Sizer was only 16% of the amount actually present in the <2 μm size fraction. Different sample types (Glew core or Ekman grab) also affect particle-size for example, the Ekman grab samples in Changing Lake which have higher clay contents.

Volume-distributions are normal or positively skewed, similar to glacial lake-sediments from the Canadian Arctic which all show positive skew (Lemmen *et al.*, 1988). A clear gradient between fine- and coarse-grained sediments is evident in PCA; this trend is also apparent in classification by cluster analysis and by energy environment. Most samples

are from low energy environments, supporting the earlier argument that samples largely come from zones of accumulation (Chapter 5). Below the littoral margins, most surface-sediments are well-sorted, characteristic of non-stratified water columns where suspended sediment is distributed fairly evenly through the water column resulting in continuous accumulation by settling-out of material from suspension (cf. Lemmen *et al.*, 1988). Within-lake variability in particle-size is a function of volume of sediment receipt, bathymetry, size, throughflow and mixing mechanisms. Shallow lakes with more complicated bathymetries, such as Heywood, Pumphouse and Twisted Lakes, have more variable patterns of particle-size distribution, encouraged by resuspension processes. Lakes with well-defined central troughs for example, Emerald Lake, have much more homogenous sediments. Coarse clastic inputs to lakes are normally deposited at or near the lake margins as deltas or fans, seen in the delta formation of Sombre, Changing and Gneiss Lakes. Coarser sediments can occasionally be transported into the profundal zone by subaqueous slumps, slides, debris flows and turbidity currents, especially in basins with steep cirque walls (Hicks *et al.*, 1990) and mass-movement of frost-shattered debris (cf. Björck *et al.*, 1996) may explain the relatively coarse nature of sediments in the trough of Moss Lake. Apart from this example, local source inputs from slope failure are not generally obvious in these surface sediments. Particle-size normally decreases with distance from the inflow (Lemmen *et al.*, 1988) but proximal-distal fining is not apparent in the Signy lakes, perhaps due to their small size, bias of the sample-net and the imposition of resuspension and redistribution mechanisms (winds, currents) on patterns of sedimentation.

6.10.2 Catchment development and lake particle-size characteristics

Catchment development and modes of sediment transport determine the nature of allochthonous material inputs to lake basins and resultant particle-size characteristics of these predominantly minerogenic sediments. Higher inputs of silts and clays to lake sediments are used as diagnostic indicators of glacial activity in the catchment (Nesje, 1994) and the results of CVA indirectly captures a gradient between glaciated and non-glaciated catchment conditions. Glacial meltwaters are responsible for the greatest delivery of allochthonous materials to these lakes, in common with lakes on Livingston Island (Björck *et al.*, 1996). Glacier-fed lakes (Moss, Sombre, Tranquil, Emerald) have finer-grained, more homogenous sediments than those with restricted catchment ice-cover. Transport capacities are determined by channel-form and the median particle-size of the surface sediments matches the 9-37 μm range in median particle-sizes of

sediments transported by rills (Wilkinson & Bunting, 1975). The highly seasonal behaviour of streams on Signy Island (Hawes, 1989) favours rapid sediment mobilisation within a very short time period once streamflow is initiated, often before the major thaw. At this time, principal sediment sources are restricted to unstable channel walls and sub-glacially eroded silts and clays. Clay inwash horizons in sediment sequences from Sombre and Heywood Lakes relate to abrupt changes in the dynamics of sediment transport and deposition in the catchment (Appleby, Jones & Ellis-Evans, 1995) and samples from delta-fronts of Sombre, Changing and Gneiss Lakes are more clayey, indicative of sub-glacially derived materials. Rapid, inflow-proximal deposition of clays is probably encouraged by turbidity currents arising from density effects (Bates, 1953), especially when the lakes are still ice-covered in spring. The distance of the lake from the glacier will determine the volume of sediment receipt and its particle-size characteristics (Desloges, 1994) and normally fluvial sorting leads to decreases in the size of streambed materials with distance downstream. Particle-size characteristics in the Paternoster Valley sequence (Moss, Changing, Sombre) however, do not follow this pattern and the opposite trend in median particle-size is observed: Moss 18.2 μm < Changing 23.7 μm < Sombre 25.5 μm. The exposure of new unstable materials in the lower half of Paternoster Valley, susceptible to reworking and transportation (Leonard, 1986b; Ballantyne & Benn, 1994), has probably overwhelmed any distance-fining effects.

Stabilised, vegetated catchments generally have lower sediment yields and the open texture of lithoskeletal soils in the maritime Antarctic favours mechanical leaching and translocation of fine materials into intermediate soil horizons (Frenot, Van Vliet-Lanoë & Gloaguen, 1995) so becoming unavailable to surface-flow unless perturbed by other weathering processes. Low accumulation rates occur during periods of reduced ice-extent (Leonard, 1985), allowing the autochthonous component to dominate the sediment matrix (Engstrom & Hansen, 1985). An upward-coarsening sequence was observed in lake-sediment profiles from South Georgia (Birnie, 1990) with relative increases in organic content as glacial sediment sources were exhausted post-deglaciation, glacial meltwater inputs assumed less importance and the catchment became increasingly stabilised and vegetated under an ameliorating climate. Coarse grain-size, slow accumulation and high organic carbon content indicate glacial inactivity during the early and mid-Holocene in northern Sweden (Snowball & Sandgren, 1996). Hence the coarser particle-size and higher organic content of sediments in lowland Heywood, Knob and

Pumphouse Lakes indicate relative catchment stabilisation. Karlén (1981) noted that sediments from non-glacial lakes were more homogenous but the opposite trend is observed here: where allochthonous inputs are reduced, local controls on sedimentation such as resuspension through winds and currents create a more heterogeneous sediment matrix, overriding any sediment focusing effects (see section 5.6). Lowland, deglaciated catchments for example, those of Heywood, Knob, Spirogyra and Amos Lakes, have seasonal snow-cover which melts rapidly in spring. High transport velocities of snow-melt streams entrain coarser grains (Wilkinson & Bunting, 1975) and can shift large volumes of coarse sediment over short timescales, in contrast to the less 'flashy' discharges of true glacial meltstreams with a more prolonged season of finer-grained sediment transportation. The effect of different meltwater sources (glacial versus snowpatch) draining contrasting zones of a catchment (glacial versus unglaciated) is most apparent in the striking bipartite particle-size distribution in Tranquil Lake (Figure 6.15).

In lakes with lower allochthonous sediment delivery, there should be a relative increase in the proportion of autochthonous materials in the sediment matrix (section 5.6.2) but it was not possible to detect any difference in particle-size distributions of samples with and without the biogenic inorganic (mainly diatom) component. Derived diatom cell diameters have a number mean of 24.4 μm and median of 19.7 μm (medium to coarse silts) which matches the volume mean and median of the surface-sediment data-set. It is highly likely that silt-sized particles in lakes with high %BSi in their surface-sediments (e.g. Light and Tioga Lakes) are actually diatoms. Some distributions tend towards bimodality, particularly in Heywood Lake, perhaps as a result of contrasting sediment fractions of different origins (cf. Singer *et al.*, 1988). This issue deserves further attention using improved instrumentation and samples of varying %BSi contents.

6.11 Summary

(1) The four statistical moments of the volume distribution adequately explain variance in the data-set. There are some inherent problems with the Malvern Series 2600 Sizer which cause errors in the calculation and results output. Corrections are possible using calibration results from the more accurate Malvern Mastersizer, but a calibration cannot be reliably made for skewness. The decision was taken not to correct results so as to maintain the integrity of the original data-set.

(2) The dominant particle-size fraction is silt, with a mean value of 34.5 μm and median of 25.5 μm for the 209 sample-set. Skewness is positive in all samples, indicating the dominance of fine particles, and is largest in samples with large ranges of particle-sizes (high standard deviations). Coarse fractions are present in very small volumes lending long right-hand tails to the distribution. Most samples have unimodal or weakly polymodal distributions. A coarse-fine grain-size gradient is evident in the data-set which broadly separates samples with small values for mean particle-size (e.g. Emerald Lake) from those with high values, i.e. coarser sediments (e.g. Heywood and Amos Lakes). The sediments from other lakes share similar, overlapping particle-size characteristics. Classification by energy environment of deposition identifies two principal groups associated with 'Low Energy' which also share some overlap. Autochthonous biogenic inorganic remains (diatoms) form a variable component of the overall sediment and contribute to bulk particle-size but the exact effects of this fraction to individual particle-size volume-distributions is uncertain.

(3) The majority of sediment sorting by glaciofluvial action occurs before entry to the lake basins and profundal sediments are well-mixed. Higher clay and fine-silt contents relate to glacial meltwater feed in proglacial lakes (Emerald, Lake 13, Orwell) and delta-front positions (Sombre, Changing Lakes). These samples also have the lowest proportions of coarse materials. Silt content is roughly constant in all samples although the mean and median oscillate between different silt fractions. Normally clay particles are kept in suspension for the longest time and are the last to settle; proximal-distal fining was expected but is not readily recognised. At lake inflows, clay deposition is apparently hastened by density effects leading to turbidity currents and underflows. Forward selection of depth in CVA suggests that depth and, by inference, intrinsic processes, affect particle-size characteristics in these lakes in addition to processes occurring in the catchments. The balance between intrinsic and extrinsic factors is explored further in Chapter 8.

CHAPTER 7: SURFACE-SEDIMENT MINERAL MAGNETIC CHARACTERISTICS

7.1 Introduction

Variations in the type and concentration of magnetic minerals in lake sediments have often been related to, and are indicative of, specific sources and processes within the catchment in response to environmental change (Thompson & Oldfield, 1986). Mineral magnetic measurements of these surface-sediment samples therefore provide another means of differentiating changing proportions of allochthonous and autochthonous (endogenic) sediment components, complementing the measurements of organic and minerogenic and particle-size characteristics discussed in Chapters 5 and 6. Other lake-sediment studies have used mineral magnetic properties to reconstruct erosion histories (Dearing & Flower, 1982; Dearing, 1991), to demonstrate catchment glacial activity (Snowball, 1993a; Nesje *et al.*, 1994; Snowball & Sandgren, 1996), to correlate cores across basins and estimate accumulation rates (Dearing, 1986), to distinguish tephra layers (Björck, Sandgren & Zale, 1991) and for detecting anthropogenic particulate pollutants (Oldfield & Richardson, 1990). Previous mineral magnetic studies of lake sediments in the maritime Antarctic have shown that variations in the concentration of magnetic minerals in lakes over time reflect changes in allochthonous sediment flux and particle-size (Birnie, 1990; Wasell, 1993; Wilson, 1993) which have been related to catchment processes such as glaciation, run-off or post-glacial catchment stabilisation and soil and vegetation development. By inference, these processes have been linked to climatic changes during the Holocene. Additional climate-independent changes in magnetic mineralogy have resulted from tephra deposition (Mäusbacher, Müller & Schmidt, 1989; Björck *et al.*, 1991a; Björck *et al.*, 1993). At Signy Island, tephra has been identified in lake sediment sequences (Dyson, 1996) but the overwhelming proportion of sediment material is considered to be terrigenous.

Two assumptions are made when using the mineral magnetic signature of lake sediments as a proxy record of environmental change in the catchment: (i) magnetic minerals are derived from the catchment and (ii) they are chemically stable. Unfortunately, there is growing evidence for post-depositional alterations in magnetic minerals (Anderson & Rippey, 1988; Hilton, Lishman & Chapman, 1986) which calls into question the long-term stability and interpretability of mineral magnetic parameters in the sediment record. Wilson's (1993) studies of lake-sediment sequences from Sombre and Heywood Lakes,

Signy Island, provided little discussion of the potential for post-depositional modifications in magnetic mineral assemblages although they have been noted in climatically analogous Arctic lakes (Snowball, 1993a). Such transformations complicate mineral source-provenance identification and introduce the 'no analogue' problem (Birks, 1994) into environmental reconstructions. Careful consideration of the sedimentary environment is therefore required before using magnetic assemblages in lake sediments as indicators of catchment processes.

In this chapter the mineral magnetic properties of the surface-sediments from the 17 lakes are characterized in terms of their concentrations and grain-size using a conventional suite of mineral magnetic measurements and derived quotients. Mineral magnetic behaviour is viewed in the context of potential catchment source materials, relationships with sediment particle-size and possible post-depositional modification through diagenesis and/or authigenesis. Classification and ordination methods are used to find patterns in the sample-set which can be related to environmental factors and thus to climate-related processes in the lakes and their catchments.

7.2 Methodology

7.2.1 Screening

To minimize contamination from sources such as dust, sample pots and their packing materials were screened by applying a SIRM (section 7.2.3.3) and measuring the resultant remanence in a Low-Speed Fluxgate Spinner Magnetometer (Molspin Ltd.). Pots with values $\geq 1 \times 10^{-5}$ Am^2 were rejected as a possible source of bias to the overall magnetic signal from the small sediment samples (low mass and volume). New pots and packing material were selected and screened again until a satisfactory value was attained.

7.2.2 Pretreatment

Wet surface-sediment (0-1 cm) was placed on pre-weighed sheets of clear plastic food film and air dried at <50°C. The dried sediment was re-weighed and the mass in grammes calculated. Samples were packed into labelled 10 ml styrene sample pots and clear film was used to firmly pack down the samples in order to prevent particle movement during the course of analysis. Small samples were positioned centrally within the sample pots.

7.2.3 Analysis

Mineral magnetic analyses were conducted at the Institute of Archaeology, University of London, and the Environmental Magnetism Laboratory, Department of Geography, University of Liverpool. The following series of measurements was completed at ambient room temperature: magnetic susceptibility (low and high frequency), ARM (Anhysteretic Remanent Magnetisation), SIRM (Saturation Isothermal Remanent Magnetisation) and IRM (Isothermal Remanent Magnetisation) at backfield strengths of -20, -40, -100 and -300 mT. All measurements were converted to mass-specific values by dividing by the sample mass.

From this basic series, derived parameters were also calculated to provide additional information on the concentration and grain-size of the magnetic minerals. The following series of quotients were calculated:

(1) Mass-specific frequency-dependent susceptibility, κfd (i.e. κlf-κhf)

(2) κfd% (κlf-κhf/κlf*100)

(3) SIRM/ARM

(4) κ_{ARM}

(5) κ_{ARM}/SIRM

(6) SIRM\κ

(7) κ_{ARM}\κ

(8) HARD ('hard' remanence, SIRM+IRM_{-300mT})

(9) HARD% (hard remanence normalised by SIRM)

(10) SOFT ('soft' remanence, SIRM-IRM_{-20mT})

(11) SOFT% (soft remanence normalised by SIRM)

(12) reverse field ratios of demagnetization normalised and expressed as percentages of the SIRM (-20mT%, -40mT%, -100mT%, -300mT%).

Calculations, units and their environmental magnetic interpretation are listed in Appendix B.

7.2.3.1 Magnetic susceptibility (κ)

Magnetic susceptibility was measured on a Bartington Instruments Magnetic Susceptibility Meter (Bartington Instruments Ltd., Oxford, England) using a dual-frequency MS2.B Sensor with a noise level of $1x10^{-6}$ SI units. The equipment was set-up in a quiet environment with stable air conditions and low risk of interference from

external magnetic signals. Once turned-on, the equipment was allowed to settle for 10 minutes to achieve minimum drift. Every time the meter was zeroed, two to three subsequent readings were ignored before introducing the sample into the sensor cell, maintaining constant sample orientation for all replications using the cap stub as a means of alignment. Readings were taken three times for each sample at both high (4.7 kHz) and low (0.47 kHz) frequencies and the mean value calculated for each sample. The mean was divided by the sample mass to yield units of $10^{-8}m^3kg^{-1}$.

7.2.3.2 Anhysteretic Remanent Magnetization (ARM)

ARM was acquired using a DTECH 2000 Demagnetizer (DTECH Ltd., Tim Wasco). The sample was exposed to a gradually decreasing alternating field (peak value 100mT) whilst in the presence in a biasing weak steady field of 0.04mT (31.84 A/m). The value for the ARM was normalised by the biasing field in A/m. Intensity of the ARM was directly proportional to the strength of the steady field, so the normalization procedure was necessary. This produces a parameter called the anhysteretic susceptibility ($\varkappa_{ARM}$). ARM, and all subsequent remanences, was measured on fluxgate spinner magnetometer (Molspin Ltd.) directly linked to a PC-based data-collection system. Measured values in units of $10^{-8}Am^2$ were divided by sample mass (g) to give units of $10^{-5}Am^2kg^{-1}$.

7.2.3.3 Saturation Isothermal Remanent Magnetization (SIRM)

An Omitec Trilec Pulse Magnetizer was used to rapidly generate a digitally accurate magnetic field of 1 T (1000mT). The remanence was measured immediately on the magnetometer. To reduce the viscous loss of the applied field, SIRM (and IRM below) was applied to small batches, i.e. 10 samples, then measured immediately afterwards. The lapse-time between magnetization and measurement was made as short and as constant as possible. Additionally, the instrument was calibrated every 10 samples. Measured values in units of $10^{-8}Am^2$ were divided by sample mass (g) to give units of $10^{-5}Am^2kg^{-1}$.

7.2.3.4 Isothermal Remanent Magnetization (IRM)

SIRM grown in samples using the Omitec Trilec Pulse Magnetizer were DC-demagnetized in reverse fields of increasing strength (coercivity) using the Molspin Pulse Demagnetizer (Molspin Ltd.). Partial stepwise demagnetization was applied at strengths of -20mT, -40mT, -100mT, and -300mT. The remanence was measured immediately. The instrument was calibrated every 10 samples. Measured values in units

of $10^{-8}Am^2$ were divided by sample mass (g) to give units of $10^{-5}Am^2kg^{-1}$.

7.2.4 Data handling

Results of analyses conducted at Liverpool University (ARM, SIRM, IRM) were entered into a Quattro Pro for Windows version 5.0 spreadsheet (Borland International, 1993) with an automated template for results calculation (B.Jude, unpublished). Hand-logged susceptibility readings were appended to this spreadsheet. The values were transposed into a Paradox Relational Database, Release 3.0 (Borland International, 1988) and then converted to Cornell Condensed Format using CHEMOUT (S.Juggins, unpublished). All statistical summaries and analyses were conducted using CALIBRATE (Juggins & ter Braak, 1996) and CANOCO (ter Braak 1987; 1990). Cluster analysis was performed using the methods outlined in section 3.6.2. *T*-tests were performed using Minitab (Minitab, 1989). There were no missing values in the data-set.

7.3 Values and statistical distributions of surface-sediment mineral magnetic data

209 samples from 17 lakes were measured for their mineral magnetic properties yielding 16 relevant mineral magnetic parameters. Summary statistics are listed in Table 7.1. The samples are of small mass (*ca.*1 g dry weight) so that many of the measurements are close to the noise levels of the instruments and/or the contamination levels of the sample pots responsible for some intractable problems in the data-set (section 7.3.2).

7.3.1 Magnetic susceptibility (κlf, κhf)

Mass-specific susceptibility integrates and expresses the contributions from all the magnetic components in a sample. It is widely used to detect the presence of secondary ferrimagnetic minerals (Thompson & Oldfield, 1986). Results for κlf and κhf are summarised in the box-and-whisker plots (Figures 7.1 & 7.2). κlf ranges from a minimum of -6.3 $x10^{-8}m^3kg^{-1}$ (Moss Lake) to an extreme 1098.4 $x10^{-8}m^3kg^{-1}$ (Pumphouse Lake). The negative susceptibility values result from a lack of calibration between the high- and low-frequency electronic circuits in the susceptibility sensor (section 7.3.1.2). The extremely high value in Pumphouse Lake may be due to contamination or the presence of authigenic minerals (section 7.7.2). The sample-set population is heavily right-skewed owing to the overwhelming influence of sample PUMP2 (mean=27.2, median=22.3, S.D.=75.1 $x10^{-8}m^3kg^{-1}$).

Table 7.1 Summary statistics of surface-sediment mineral magnetic parameters from the 209 sample-set

Measure	*Minimum*	*Maximum*	*Mean*	*Median*	*S.D.*
κlf $10^{-8}m^3kg^{-1}$	-6.3	1098.4	27.2	22.3	75.1
κhf $10^{-8}m^3kg^{-1}$	-12.6	1058.4	26.8	22.3	72.4
κfd $10^{-8}m^3kg^{-1}$	-2.7	40.0	0.4	0.1	2.9
κfd%	-100.0	25.0	-0.2	0.5	9.2
SIRM $10^{-5}Am^2kg^{-1}$	30.7	16266.0	274.2	184.1	1119.5
κ_{ARM} $10^{-8}m^3kg^{-1}$	19.9	7006.6	230.1	150.9	499.5
κ_{ARM}**/SIRM** $10^{-3}mA^{-1}$	0.3	4.3	1.0	0.9	0.6
SIRM/κ 10^3Am^{-1}	-93.1	95.5	8.1	7.5	13.7
κ_{ARM}/κ	-75.9	140.9	9.2	6.9	14.6
HARD $10^{-5}Am^2kg^{-1}$	-28.3	52.6	8.3	6.5	7.1
HARD%	-1.7	29.5	5.0	3.8	4.2
SOFT $10^{-5}Am^2kg^{-1}$	6.0	11912.0	107.7	47.4	821.1
SOFT%	12.8	49.8	40.8	43.3	6.5
-40mT%	-16.6	49.7	34.0	38.010.9	
-100mT%	-63.9	49.7	23.8	30.0	17.7
-300mT%	-106.4	49.7	15.8	24.9	24.6

Figure 7.1 Box-and-whisker plot showing variation of κlf by lake number

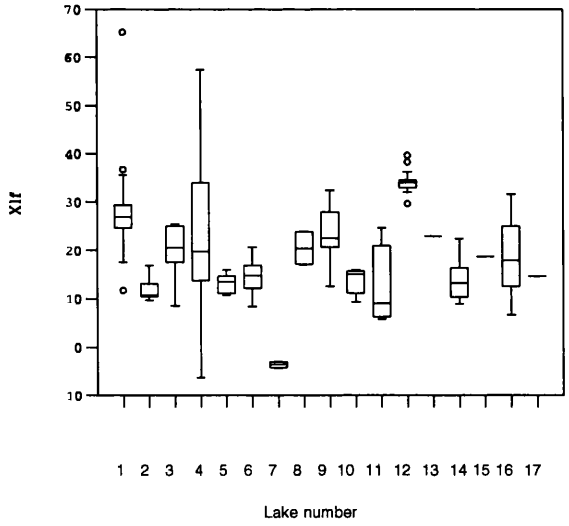

κhf values range from a minimum of -12.6 $x10^{-8}m^3kg^{-1}$ in Moss (4) Lake to a similarly extreme value of 1058.4 x $10^{-8}m^3kg^{-1}$ in Pumphouse (6) Lake (sample PUMP2). The overall sample distribution parallels the κlf distribution as expected and is right-skewed (mean=26.8, median=22.3, S.D.=72.4 $x10^{-8}m^3kg^{-1}$).

Figure 7.2 Box-and-whisker plot showing variation of κhf by lake number

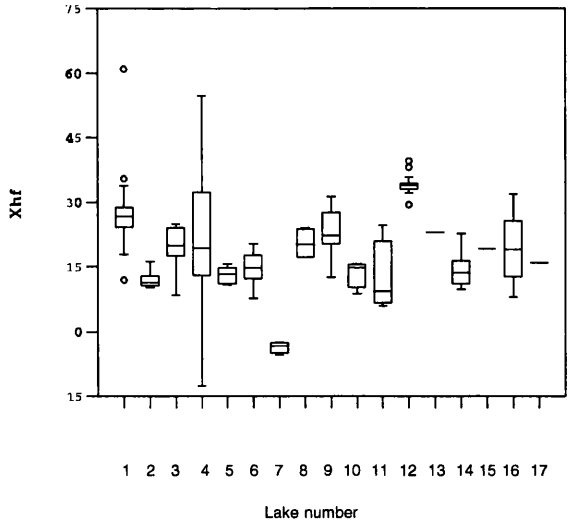

7.3.2 Frequency-dependent susceptibility (κfd, κfd%)

κlf alone does not discriminate well between ferrimagnetic grain-sizes or mineral type. The loss of κ between two frequencies - κfd - provides the main evidence for the presence of secondary ferrimagnetic minerals within a narrow size band of 0.0018-0.020 μm, close to the SP/SSD grain size boundary (Maher, 1988). Grains within this size range are unlikely to include primary minerals or industrially-derived spherules. Quantitative interpretation of this parameter is difficult since it is affected by both grain-size and grain concentrations within the SP grain-size range. Values for κfd and κfd% are summarised in the box-and-whisker plots (Figures 7.3 and 7.4).

Figure 7.3 Box-and-whisker plot showing variation of κfd by lake number

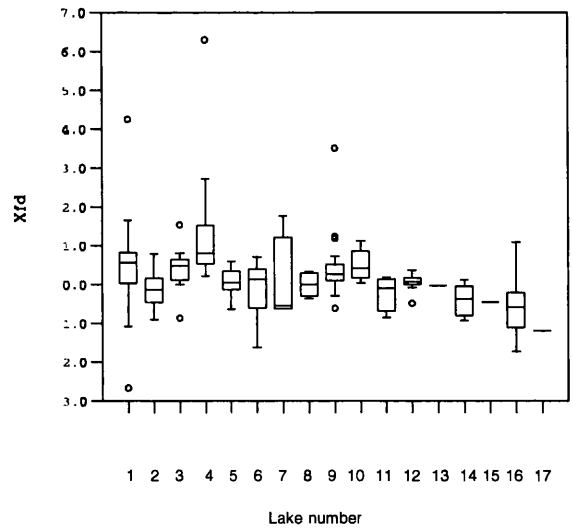

κfd values ranges from -2.7 x $10^{-8}m^3kg^{-1}$ in Sombre (1) Lake to 40.0 x $10^{-8}m^3kg^{-1}$ in

in Pumphouse (6) Lake (sample PUMP2). Values for Sombre and Heywood (2) Lakes fall within the range found by Wilson (1993; Table 7.2). The population distribution, like κlf and κhf, is right-skewed (mean=0.4, median=0.1, S.D.=2.9 $x10^{-8}m^3kg^{-1}$).

Values of κfd% in natural samples range from 0-15% dependent on mineralogy (magnetite or maghemite) and grain-size distribution and a maximum value of 14-17% occurs in assemblages of spherical ferrimagnetic grains lying between 0 μm and the SP/SSD boundary (Dearing *et al.*, 1996a). The full range of κfd% values are found in Moss (4) lake, from a minimum of -100% to a maximum of 25%. The population distribution is left-skewed (mean=-0.2%, median=0.5%, S.D.=9.2%). κfd% is very low, reflecting the lack of FV grain sizes in these samples. Negative κfd% values and values >14% indicate measurement errors, contamination from metal fragments or sample anisotropy (Dearing *et al.*, 1996a). MOSS16 and TRAN30 are Wilson's (1993) positive κfd% values for surface sediments from Sombre and Heywood Lakes (Table 7.2) fall within the limits of this sample-set distribution.

Figure 7.4 Box-and-whisker plot showing variation of κfd% by lake number

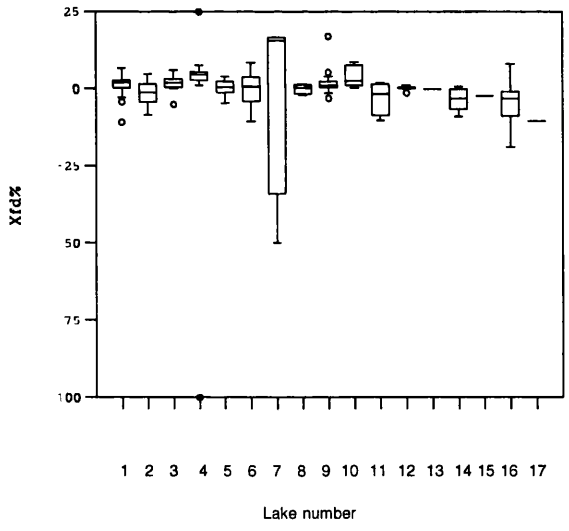

Problems with the precise measurement of κfd were anticipated in these relatively dilute natural materials of small mass (Oldfield, 1994). 77 samples have negative κfd and κfd% readings. Diamagnetic inclusions in the samples (quartz, organic matter) cause low κ values and sample pots and their packing materials add a diamagnetic component to small sediment samples. A diamagnetic correction was applied to the κ readings. Background readings of pots and their packing materials were taken at both high and low frequencies. The mean of 10 background readings yielded a value of $-0.5\ x10^{-10}m^3$.

This was added to the meter output reading and mass-specific values were recalculated. Despite this diamagnetic correction negative values remain negative. The suspected cause of this is improper calibration between the high- and low-frequency settings on the susceptibility meter (J. Bloemendal, *pers.comm.*). Attempts to calibrate the values met with little success. Conclusions which could be drawn from κfd and κfd% values are therefore limited.

Table 7.2 Summary of mineral magnetic parameters of surface-sediments (0-1 cm) from Sombre and Heywood Lakes (Wilson, 1993)

Measure	*Sombre*	*Heywood*
κlf $10^{-8}m^3kg^{-1}$	27.7	10.2
κhf $10^{-8}m^3kg^{-1}$	26.8	10.2
κfd $10^{-8}m^3kg^{-1}$	0.9	0.1
κfd%	3.2	0.1
SIRM $10^{-5}Am^2kg^{-1}$	339.1	66.7
κ_{ARM} $10^{-8}m^3kg^{-1}$	117.0	34.0
κ_{ARM}**/SIRM** $10^{-5}mA^{-1}$	34.5	51.1
SIRM/κ 10^3Am^{-1}	12.2	65.1
ARM/κ 10^2Am^{-1}	1.3	1.1
HARD $10^{-5}Am^2kg^{-1}$	2055.7	75.1
HARD%	3.0	0.6
SOFT $10^{-5}Am^2kg^{-1}$	13648.0	4965.2
SOFT%	20.1	37.2
-40mT%	42.9	58.8
-100mT%	72.2	80.4
-300mT%	97.0	99.4

7.3.3 Anhysteretic Remanent Magnetisation (κ_{ARM})

ARM is more sensitive to the concentration and grain-size of ferrimagnetic minerals in a sample than κ or SIRM and is highly selective of true SSD ferrimagnetic grains around 0.02-0.1 μm (Maher, 1988). Values for κ_{ARM} are consistently low for the data-set except one sample, PUMP2, which has an extremely high reading of 7006.6 $x10^{-8}m^3kg^{-1}$, forcing the sample-set distribution to be highly right-skewed (mean=230.1, median=150.9, minimum=19.9, S.D.=499.5 $x10^{-8}m^3kg^{-1}$).

Results for κ_{ARM} are summarised in the box-and-whisker plot (Figure 7.5). Lakes with

greatest internal variability based on their standard deviations from the mean include Sombre (1), Heywood (2), Changing (3) and Moss (4) Lakes, closely followed by Gneiss (16) and Tioga (11) Lakes. The most homogenous group of data is from Emerald (12) Lake which has a large number of samples (mean=73.7, median=73.4, minimum=55.7, maximum=88.5, S.D.=7.4 x $10^{-8}m^3kg^{-1}$). High intra-lake variability is seen to be a function of mixed mineral magnetic assemblages and not a result of the number of samples within each basin.

Figure 7.5 Box-and-whisker plot showing variation of $\varkappa_{ARM}$ by lake number

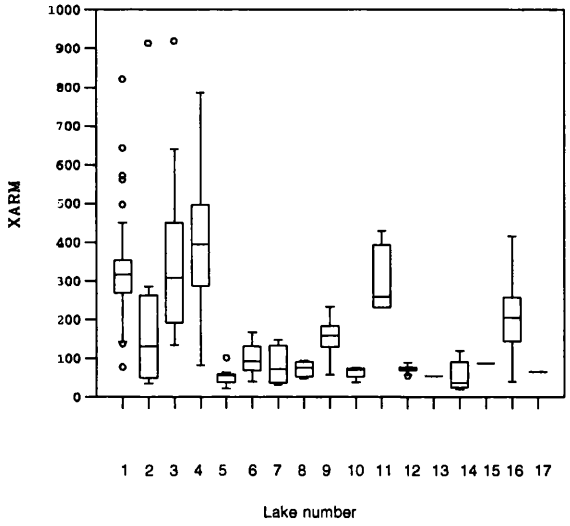

7.3.4 Saturation Isothermal Remanent Magnetization (SIRM)

SIRM expresses the combined effect of all the remanence carrying minerals and shows some response to grain-size variations, particularly fine grains. The range of values for SIRM are summarised in the box-and-whisker plot (Figure 7.6). The median SIRM is close to the expected value for the dominant schist geology (section 7.7.1). Again, PUMP2 is an outlier with an extreme SIRM of 16266 $x10^{-5}Am^2kg^{-1}$ inconsistent with the remainder of the dataset (minimum=30.7, mean=274.2, median=184.1, S.D.=1119.5 $x10^{-5}Am^2kg^{-1}$). The lowest SIRM value is for sample HEY12 (30.7 $x10^{-5}Am^2kg^{-1}$).

Removing PUMP2, the remaining samples from Pumphouse Lake have a mean of 182.9 $x10^{-5}Am^2kg^{-1}$, more in line with SIRM values from the other lakes and reducing intra-lake variability (minimum=97.2, median=181.1, maximum=297.2). Moss (4) and Tioga (11) Lakes show the greatest intra-lake variability (largest standard deviations from the mean), and Amos (10) Lake the least, suggesting more uniform magnetic behaviour. Tioga Lake has unusually high SIRM values (mean=600.7, median=430.0, S.D.=366.5

$x10^{-5}Am^2kg^{-1}$).

Figure 7.6 Box-and-whisker plot showing variation of SIRM by lake number

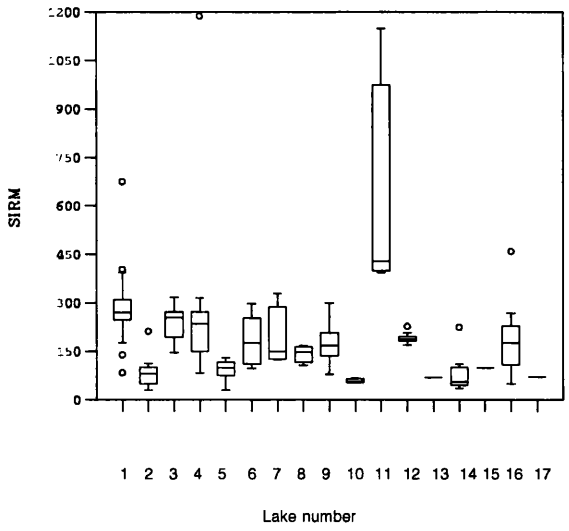

The median SIRM value for each lake can be used define a broad lakes classification (descending rank order):

(1) Sombre, Changing and Moss Lakes (269-234 $x10^{-5}Am^2kg^{-1}$).
(2) Pumphouse, Emerald and Gneiss Lakes (187-181 $x10^{-5}Am^2kg^{-1}$).
(3) Light, Spirogyra and Tranquil Lakes (168-149 $x10^{-5}Am^2kg^{-1}$)
(4) Heywood, Knob and Bothy Lakes (98-81 $x10^{-5}Am^2kg^{-1}$).
(5) Lake 13 and Orwell Lake (70-69 $x10^{-5}Am^2kg^{-1}$).
(6) Amos and Twisted Lakes (57.0-55.2 $x10^{-5}Am^2kg^{-1}$).

7.3.5 κ_{ARM}/SIRM

The κ_{ARM}/SIRM quotient can be used to assess ferrimagnetic grain-size (section 7.6.2). Values for this quotient have a maximum of 4.3 $x10^{-3}mA^{-1}$ in sample HEY13, forcing the distribution to be right-skewed (mean=1.0, median=0.9, S.D.=0.6 $x10^{-3}mA^{-1}$). Sample LITE4 has the minimum value of 0.3. κ_{ARM}/SIRM values for the 17 lakes are summarised in the box-and-whisker plot (Figure 7.7).

Normalized to SIRM, the lowest intra-lake variability is in Emerald (12) Lake (n=32, mean=0.4, median=0.4, min=0.3, max=0.5, S.D.=0.03 $x10^{-3}mA^{-1}$). Knob (5) and Pumphouse (6) Lakes also cluster tightly (mean and median values ≈5, standard deviations ≈0.9), even including outlier sample PUMP2. Spirogyra (8) Lake is very similar (mean and median ≈5, S.D.=0.1). Heywood (2) Lake has the greatest heterogeneity in κ_{ARM}/SIRM values (minimum=0.7, maximum=4.3, mean=1.9,

median=1.8, S.D.=1.1). Changing (3) and Gneiss (16) Lakes also display fairly high intra-lake variability for this quotient. Wilson's (1993) κ_{ARM}/SIRM value for Sombre Lake surface-sediment (0.4 $x10^{-3}mA^{-1}$) matches the median in this data-set, however, her value for Heywood Lake (0.5 $x10^{-3}mA^{-1}$) exceeds the maximum value here.

Figure 7.7 Box-and-whisker plot showing variation of κ_{ARM}/SIRM by lake number

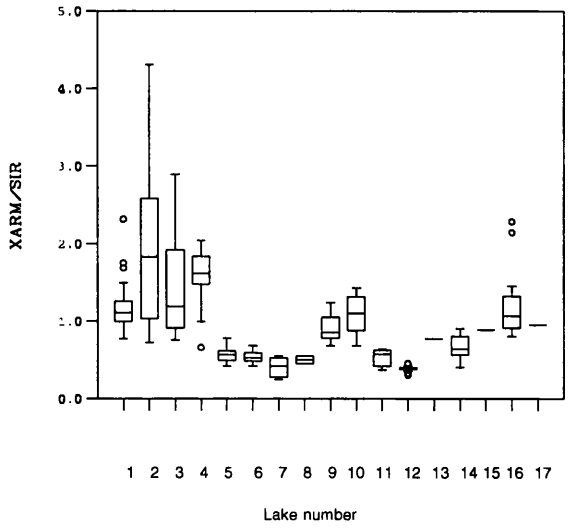

7.3.6 SIRM/κ

Variations in SIRM/κ can arise from changing contributions from non-remanence components, whether paramagnetic or superparamagnetic, from changes in the proportion of different grain-size populations among the ferrimagnetic and imperfect antiferromagnetic components, or from changes in the mineralogy of the sample giving rise to differences in the ferrimagnetic:imperfect antiferromagnetic quotient (Oldfield, 1991). SIRM/κ values are summarised in the box-and-whisker plot (Figure 7.8) and range from -93.1 $x10^3Am^{-1}$ in Light (7) Lake to 95.5 $x10^3Am^{-1}$ in Moss (4) Lake. The population distribution is close to normal about the mean (mean=8.1, median=7.5, S.D.=13.7 $x10^3Am^{-1}$). Outliers with low values of this quotient include LITE2, MOSS12 and all Light Lake samples; high value outliers, suggesting the presence of greigite, include MOSS16 and all Tioga Lake samples. The remaining samples have values between 0 and 20 $x10^3Am^{-1}$ indicating the *absence* of greigite (J. Dearing, *pers.comm.*), faithfully reflecting typical values for schist lithologies (Thompson & Oldfield, 1986).

Wilson's (1993) values for SIRM/κ in surface-sediments of Sombre (12.2 $x10^3Am^{-1}$) and Heywood (65.1 $x10^3Am^{-1}$) Lakes are within the range of values found in this sample-set.

Figure 7.8 Box-and-whisker plot showing variation of SIRM/κ by lake number

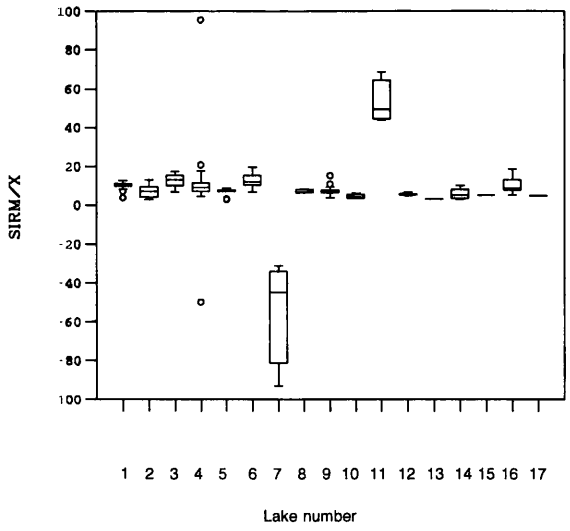

7.3.7 κ_{ARM}/κ

This dimensionless quotient is also used to diagnose grain-size variations (section 7.6.2) and results are summarised in Figure 7.9. The sample population is normally distributed (mean=9.2, median=6.9, S.D.=14.6). Outliers with low values include MOSS12 and all four samples from Light Lake. Outliers with high values include MOSS16, HEY13, CHAN4, TIOG2, and GNES8. The largest intra-lake variation is in Moss Lake with values ranging from -75.9 to 140.9.

Figure 7.9 Box-and-whisker plot showing variation of κ_{ARM}/κ by lake number

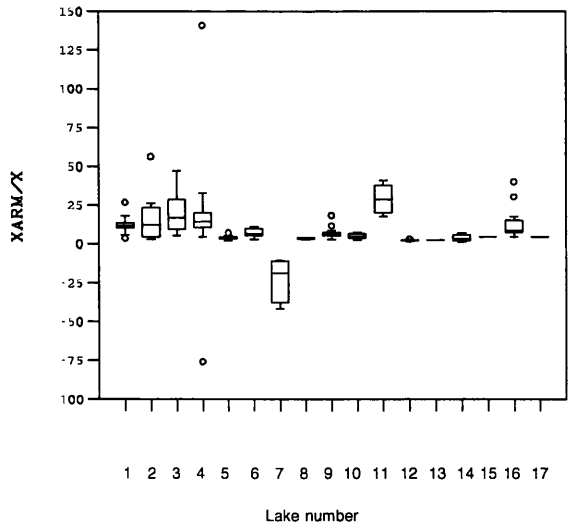

7.3.8 HARD

HARD or HIRM (High Induced Remanent Magnetization or 'Hard' IRM) is exclusively related to the imperfect antiferromagnetic component and is a rough guide to the concentration of haematite in a sample. HARD ranges from -28.3 (PUMP2) to 52.6

(TIOG4) $x10^{-5}Am^2kg^{-1}$. The sample distribution is slightly right-skewed (mean=8.3, median=6.5, S.D.=7.1 $x10^{-5}Am^2kg^{-1}$. Sample HEY14 has an unusual negative value of -1.5 $x10^{-5}Am^2kg^{-1}$; the remaining values in the data-set are positive as expected. Values for the 17 lakes are summarised in the box-and-whisker plot (Figure 7.10).

Figure 7.10 Box-and-whisker plot showing variation of HARD by lake number

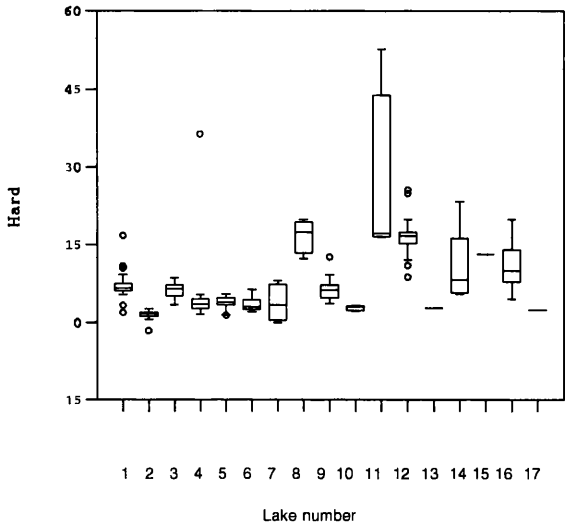

Sample MOSS9 has the second highest value in the sample-set (36.3). Spirogyra, Tioga and Emerald Lakes have high mean and median values for HARD although once the weighting of sample TIOG4 is removed the intra-lake mean value decreases to 16.9 $x10^{-5}Am^2kg^{-1}$, which is still high relative to the other lakes. High intra-lake variability is apparent in Moss, Twisted and Gneiss Lakes and to a lesser degree in Sombre, Light and Spirogyra Lakes. HARD values are much lower than those found in the surface-sediments of Sombre Lake (205.6 $x10^{-5}Am^2kg^{-1}$) by Wilson (1993) however, her results from Heywood Lake (7.5 x $10^{-5}Am^2kg^{-1}$) are in agreement.

7.3.9 HARD%

HARD% is the percentage of the SIRM requiring fields strengths greater than 300mT to be demagnetized. In common with HARD it corresponds to the imperfect anti-ferromagnetic component and acts as a rough guide to the haematite/goethite concentration in samples. HARD% ranges from -1.7 (Heywood Lake) to 29.5 (Twisted Lake). Normalising HARD by the SIRM makes the sample distribution more right-skewed (mean=5.0, median=3.8, S.D.=4.2). The values for HARD% are summarised in the box-and-whisker plot (Figure 7.11). The antiferromagnetic concentration in these samples is low but mineral magnetic assemblages are mixed and none are exclusively

ferrimagnetic. Outliers with low values, i.e. the smallest antiferromagnetic component, include HEY14 and PUMP2; outliers with high values, indicating strong antiferromagnetic mineral presence, include TWIS8, TWIS5, TWIS4, TWIS7, TWIS3, EMER30 and SPIR4. Wilson (1993) found similarly low values for HARD% in surface-sediments from Sombre (3.0%) and Heywood (0.6%) Lakes (Table 7.2).

Figure 7.11 Box-and-whisker plot showing variation of HARD% by lake number

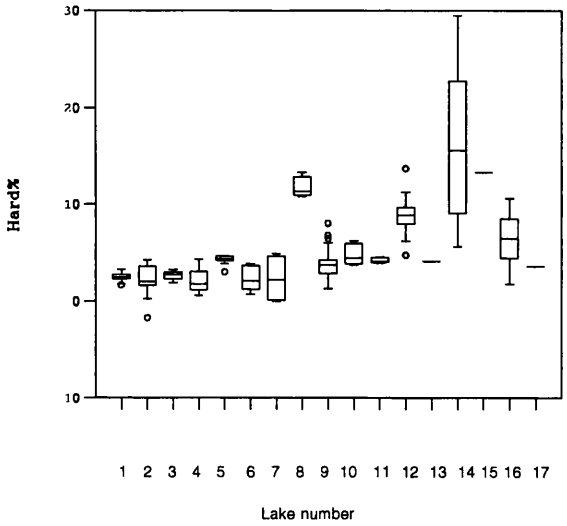

7.3.10 SOFT

SOFT is the part of the SIRM that can be demagnetized in the lowest reverse field (-20mT). It relates to the ferrimagnetic contribution, especially the influence of coarser grains, and can be used as a crude index of multi-domain magnetite concentration.

Figure 7.12 Box-and-whisker plot showing variation of SOFT by lake number

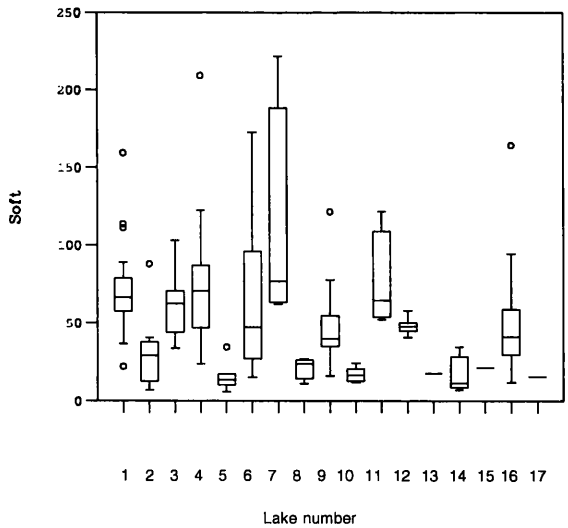

Values for SOFT for the 17 lakes are summarised in the box-and-whisker plot (Figure

7.12).

SOFT ranges from 6.0 $x10^{-5}Am^2kg^{-1}$ (Knob Lake) to an extremely high 11912 $x10^{-5}Am^2kg^{-1}$ (Pumphouse Lake; PUMP2), forcing the sample distribution to be highly right-skewed (mean=107.7, median=47.4, S.D.=821.1 $x10^{-5}Am^2kg^{-1}$). Removing PUMP2 reduces the intra-lake variability in Pumphouse Lake considerably (minimum=62.1, maximum=221.7, mean=109.2, median=76.5, S.D.=75.8 $x10^{-5}Am^2kg^{-1}$) although values are still generally higher than the other lakes (PUMP1 also has a high value for SOFT: 172.6 $x10^{-5}Am^2kg^{-1}$). SOFT values indicate that all samples include a MD magnetite component. Interestingly, the SOFT values found by Wilson (1993) from surface sediments in Sombre and Heywood Lakes (Table 7.2) are also very high and exceed those found in this data-set.

7.3.11 SOFT% and S-ratios normalized to SIRM

SOFT% are all positive and range from 12.8% (Heywood Lake) to a maximum of 49.8% (Pumphouse Lake). The sample population distribution is highly left-skewed (mean=40.8%, median=43.3%, S.D.=6.5%) and results are summarised in Figure 7.13. The lowest median values for SOFT% are in Heywood (28.9%), Amos (27.4%), Light (33.5%) and Twisted (32.3%) Lakes indicating the most antiferromagnetic behaviour. The median values for the remaining lakes are all between 40-50%. The highest median is in Tioga Lake (48.3%). Outliers with low values for SOFT% and more antiferromagnetic behaviour include HEY12, KNOB9 and AMOS4; outliers with high values, i.e. ferrimagnetic, include PUMP2, TIOG4 and MOSS9.

Figure 7.13 Box-and-whisker plot showing variation of SOFT% by lake number

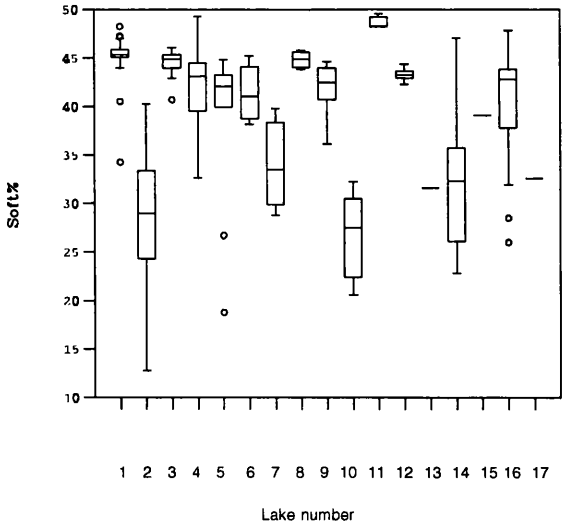

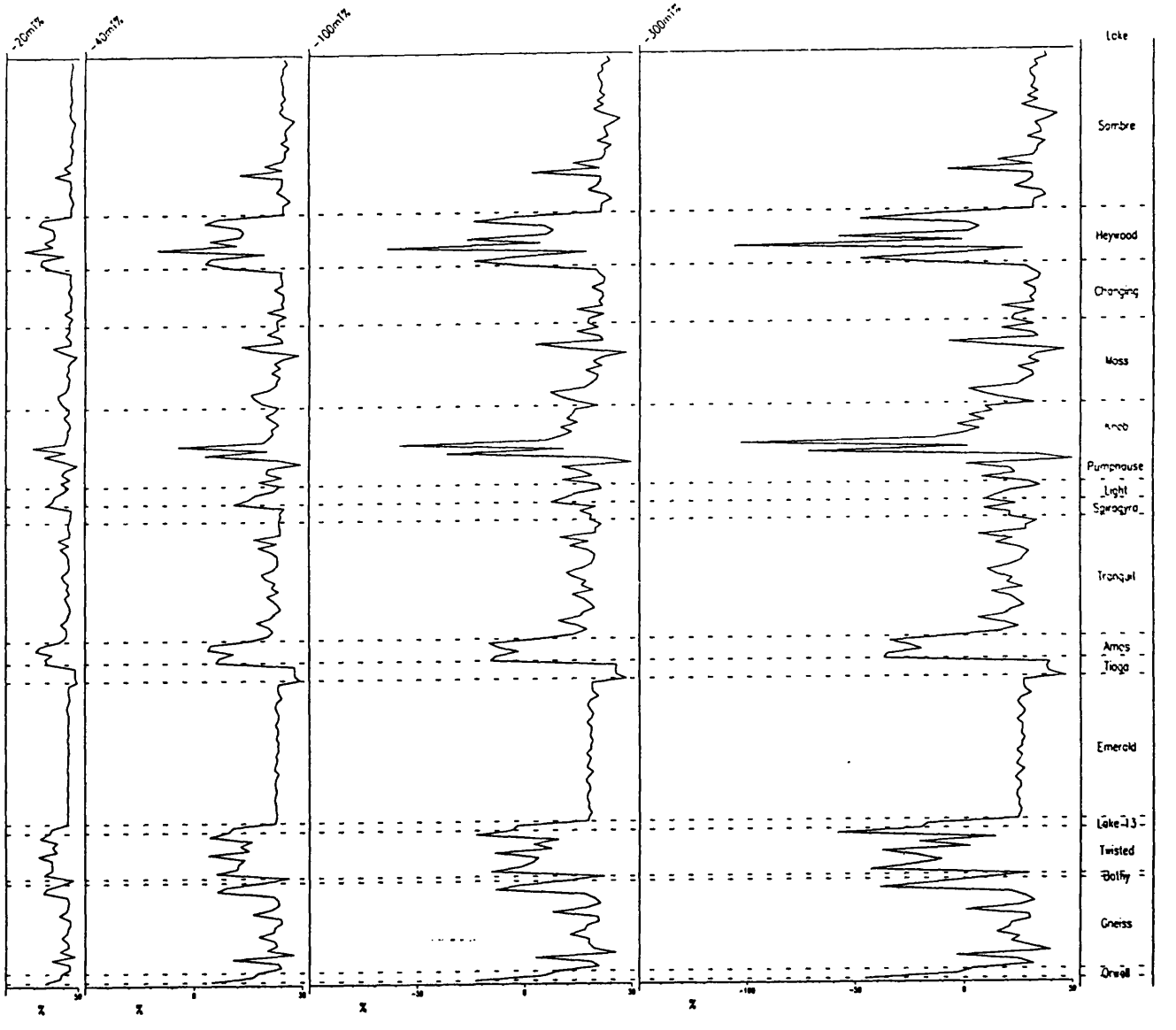

Figure 7.14 **Normalized reverse-field magnetic response at -20mT%, -40mT%, -100mT% and -300mT% for 209 surface-samples from 17 lakes**

Some samples at -40mT% are negative (Heywood, Knob Lakes) indicating demagnetization has already occured and samples are very soft. At -100mT% and -300mT% the number of samples with negative values increases and includes samples from other lakes - Amos (10), Lake 13, Twisted (14), Gneiss (16) and Orwell (17) - in addition to Heywood (2) and Knob (5) Lakes. Demagnetization exceeds 100% in Heywood (2) and Pumphouse (6) Lakes indicating extremely 'soft' ferrimagnetic samples.

The demagnetization response of samples using reverse field ratios normalized by SIRM is illustrated in Figure 7.14. The response is similar across the data-set although samples from Pumphouse and Light Lakes are noticeably more 'soft' and ferrimagnetic in behaviour as are outlier samples from Sombre, Moss and Gneiss Lakes. Sombre and Emerald Lakes show internally-consistent behaviour implying uniform magnetic mineralogy within these lake basins.

7.4 Testing for the effects of storage diagenesis

7.4.1 Storage diagenesis and hypothesis testing

Oldfield *et al.* (1992) discussed the important implications of storing samples in the moist state over a period of months prior to drying and magnetic analysis. Both the rate of drying-out and the chemical changes that accompany drying exercise an important influence on a sample's remanence. This loss following prolonged storage was previously ascribed solely to the oxidation of authigenic iron sulphides such as greigite (Hilton, 1985; Hilton, Lishman & Chapman, 1986). However, fine-grained ferrimagnetic oxides such as magnetite and/or maghaemite can also be transformed to paramagnetic or imperfect antiferromagnetic minerals, including goethite. In these surface sediment samples, some of which were derived from anoxic zones, a loss of remanence could be potentially attributed to a number of oxidative changes which occur post-extrusion. Williams (1991) studied oxic storage diagenesis of samples from dystrophic Loch Ba, Rannoch Moor, Scotland, and found high losses of magnetic response (28-37% of the initial volume magnetic susceptibility) upon oxidation.

Fortunately, the collection of material over two field seasons presents the opportunity to test hypotheses concerning the potential effects of storage diagenesis. Of the seventeen lakes sampled in the 1993/94 field season, five lakes were re-sampled in the

1994/95 (Sombre, Moss, Tranquil, Emerald and Gneiss). Sediment drying and magnetic analyses were not undertaken until June 1996, thus 17 months had elapsed between collection and drying of first season sediments and 5 months for the second season samples. These samples are prime candidates for the type of diagenetic changes described by Oldfield *et al.* (1992) as they have been cold-stored in moist conditions. As this decay is time-dependent it should be greater in the first season samples. Thus two hypotheses can be tested:

$$H_0: \mu_1 = \mu_2$$

Null hypothesis: there is no significant difference in the susceptibility or remanence characteristics of samples collected in 1993/94 (population 1) and those collected in 1994/5 (population 2).

$$H_1: \mu_1 < \mu_2$$

Alternative hypothesis: the susceptibility and remanence measures of population 2 are higher than those of population 1 as the latter has been subject to a longer period of 'storage diagenesis'.

The key magnetic parameters to test these losses are $\varkappa$lf, $\varkappa$fd, ARM, SIRM, SOFT and HARD (Oldfield *et al.*, 1992). *T*-tests, based on the *t* probability distribution, are useful for testing the equivalency of two samples (Davis, 1986). The likelihood of magnetic enhancement with storage time is very unlikely, therefore a decay (population 1 < population 2) is assumed and a one-tailed *t*-test is appropriate to test the alternative hypothesis. Since HARD is the most conservative parameter (Oldfield *et al.*, 1992) it is used as a control; in theory *t*-tests for HARD should support the null hypothesis (i.e. no difference between the two populations) with a *p*-value of 0.000.

Samples were selected from the five lakes (Sombre, Moss, Tranquil, Emerald, Gneiss) and divided according to year of collection. Owing to the problems with the susceptibility readings samples were screened and those with values of $\varkappa$fd and $\varkappa$fd% ≤ 0 were removed. This unfortunately precludes all but one sample from Gneiss Lake so this lake was dropped from the analysis. The remaining four lakes supplied 27 samples from the first season (population 1) and sixty from the second season (population 2).

7.4.2 Results

Results of both two- and one-tailed *t*-tests for the six magnetic indicators from the four lakes are summarised in Table 7.3. None of the *t*-tests detect any significant differences

between the two sample populations (p=0.0), probably because the test population is too small and the within sample-set variability is high, hiding any storage diagenesis effects in the general noise of the data-set.

Table 7.3 Results of one-tailed *t*-tests of storage diagenesis indicator variables for a test population of samples collected in 1993/94 (n=27) and 1994/95 (n=60) from four lakes

Population	*Mean*	*S.D.*	*S.E.Mean*	*t-value*	*p-value*
κlf#1	29.456	7.955	1.531	19.89	0.0000
κlf#2	27.717	8.954	1.156	24.84	0.0000
κfd#1	0.701	0.634	0.122	13.95	0.0000
κfd#2	0.627	0.743	0.096	16.96	0.0000
ARM#1	9.522	6.917	1.331	7.90	0.0000
ARM#2	6.925	4.563	0.589	13.45	0.0000
SIRM#1	270.708	195.787	37.679	7.21	0.0000
SIRM#2	216.208	92.591	11.953	18.17	0.0000
HARD#1	9.441	7.812	1.503	6.94	0.0000
HARD#2	8.551	5.267	0.680	14.05	0.0000
SOFT#1	69.983	36.689	7.061	10.05	0.0000
SOFT#2	55.124	22.835	2.948	19.04	0.0000

Where #1 denotes samples collected in 1993/94 and #2 refers to samples collected in 1994/95. For population #1 17 months had elapsed between collection and drying; 5 months had elapsed between collection and drying for population#2.

The *t*-tests were repeated on an individual lake basis to remove the effects of between-lake variability. Significant differences between the two sample populations are immediately apparent using the one-tailed *t*-test (Table 7.4a-d). The only significant difference in the Sombre Lake samples is registered by ARM. Both Moss and Tranquil Lakes display significant differences for all determinands. The greatest difference is found in HARD (p<0.059 and 0.028 respectively). In Moss Lake some of these losses may additionally represent diagenesis of greigite. In Emerald Lake, HARD is the only determinand registering a significant difference between the two populations (p<0.0001). The fact that the differences are greatest for the most conservative, 'control' parameter implies that storage diagenesis is not the only reason for differences between the two populations. In all cases n(population 1) < n(population 2) and it might be a statistical bias of the mean for two different-sized populations. Also, the second season samples

Table 7.4 Results of one-tailed *t*-tests of storage diagenesis indicator variables for a test population of samples collected in 1993/94 and 1994/95 from four individual lakes (type in bold indicates significant difference)

(a) Sombre Lake (population 1, n=8; population 2, n=19)

Population	*Mean*	*S.D.*	*S.E. Mean*	*t-value*	*p-value*
xlf#1	28.125	4.258	1.505	19.35	0.0000
xlf#2	30.234	9.119	2.092	14.93	0.0000
xfd#1	0.915	0.387	0.137	13.98	0.0000
xfd#2	0.827	0.900	0.206	8.85	0.0000
ARM#1	**13.597**	**6.088**	**2.153**	**6.78**	**0.0002**
ARM#2	10.305	4.128	0.947	11.94	0.0000
SIRM#1	295.124	54.797	19.374	15.28	0.0000
SIRM#2	300.459	115.663	26.535	11.36	0.0000
HARD#1	6.635	0.614	0.217	35.20	0.0000
HARD#2	7.460	2.977	0.683	12.39	0.0000
SOFT#1	78.109	22.363	7.907	10.01	0.0000
SOFT#2	72.381	27.276	6.258	11.73	0.0000

Population 1: n= 8 (SOMB11,12,13,14,16,17,20,21)
Population 2: n=19 (SOMB22,24,25,26,27,28,31,32,33,34,36,37,38,39,40,41,42,43,44)

(b) Moss Lake (population 1, n=8; population 2, n=10)

Population	*Mean*	*S.D.*	*S.E.Mean*	*t-value*	*p-value*
xlf#1	**29.600**	**13.057**	**4.616**	**6.63**	**0.0003**
xhf#2	**19.315**	**11.159**	**3.529**	**5.76**	**0.0003**
xfd#1	**1.003**	**0.892**	**0.315**	**6.35**	**0.0004**
xfd#2	1.018	0.442	0.140	14.45	0.0000
ARM#1	**13.195**	**7.143**	**2.526**	**5.62**	**0.0009**
ARM#2	10.810	3.907	1.235	9.56	0.0000
SIRM#1	336.275	353.239	124.889	2.70	0.0300
SIRM#2	3.338	1.083	0.343	12.66	0.0000
HARD#1	**8.098**	**11.446**	**4.047**	**2.25**	**0.0590**
HARD#2	3.338	1.083	0.343	12.66	0.0000
SOFT#1	**80.791**	**57.288**	**20.254**	**4.04**	**0.0051**
SOFT#2	62.671	20.684	6.541	9.73	0.0000

Population 1 (n=8: MOSS3,4,5,6,7,8,9,10)
Population 2 (n=10: MOSS11,13,14,15,16,17,18,19,20,21)

(c) Tranquil Lake (population 1, n=5; population 2, n=17)

Population	*Mean*	*S.D.*	*S.E. Mean*	*t-value*	*p-value*
xlf#1	**26.335**	**5.426**	**2.427**	**11.26**	**0.0004**
xlf#2	23.989	4.384	1.063	23.50	0.0000
xfd#1	**0.524**	**0.450**	**0.201**	**7.57**	**0.0016**
xfd#2	0.574	0.807	0.196	8.05	0.0000
ARM#1	**5.545**	**1.716**	**0.767**	**8.53**	**0.0010**
ARM#2	4.731	1.235	0.300	19.13	0.0000
SIRM#1	**210.486**	**60.781**	**27.182**	**7.78**	**0.0015**
SIRM#2	160.223	37.998	9.216	17.49	0.0000
HARD#1	**5.910**	**2.355**	**1.053**	**6.56**	**0.0028**
HARD#2	6.144	1.253	0.304	23.52	0.0000
SOFT#1	**63.001**	**33.455**	**14.962**	**4.28**	**0.0130**
SOFT#2	39.256	9.909	2.403	16.75	0.0000

Population 1: n= 5 (TRAN4,5,6,8,9)
Population 2: n=17 (TRAN12,13,14,15,16,17,18,19,20,21,22,23,24,25,26,27,30)

(d) Emerald Lake (population 1, n=6; population 2, n=14)

Population	*Mean*	*S.D.*	*S.E. Mean*	*t-value*	*p-value*
xlf#1	33.643	2.787	1.138	30.45	0.0000
xlf#2	34.830	1.635	0.437	81.99	0.0000
xfd#1	0.1624	0.0733	0.0299	38.83	0.0000
xfd#2	0.1377	0.0954	0.0255	44.62	0.0000
ARM#1	2.5034	0.1383	0.0565	62.05	0.0000
ARM#2	2.2264	0.2384	0.0637	50.63	0.0000
SIRM#1	200.914	13.289	5.425	37.22	0.0000
SIRM#2	181.675	9.408	2.515	72.65	0.0000
HARD#1	**17.914**	**3.856**	**1.574**	**12.01**	**0.0001**
HARD#2	16.679	3.082	0.824	21.46	0.0000
SOFT#1	50.554	3.905	1.594	32.34	0.0000
SOFT#2	45.580	3.598	0.962	48.44	0.0000

Population 1 (n=6: EMER1,2,4,7,11,12)
Population 2 (n=14: EMER13,14,17,19,22,23,24,25,26,27,28,30,31,32)

are more variable in character owing to a wider range of sampling locations outside the profundal zone.

Major diagenetic changes probably take place within the first few months of storage, thereafter losses of concentration and remanence are less significant. The changes are still sufficiently significant though to be detected in this sample-set. Even the second season samples had been stored in a moist state for 5 months prior to drying. Oldfield *et al.* (1992) compared samples stored at room temperature. These sediments have been stored at +5°C and low temperatures have probably inhibited some of the diagenetic changes. Also, the mineral magnetic signature of predominantly primary-weathered, minerogenic material with relatively low organic contents, is much more stable and less subject to the oxidative changes witnessed in Yates's highly organic carbon sediments (30-50% organic carbon) from Peckforton Mere (Yates, 1988; discussed by Oldfield *et al.*, 1992). The organic carbon contents in some of the Signy sediments are relatively high (e.g. Light, Tioga and Gneiss Lakes) and changes of a similar magnitude should be anticipated.

7.5 Relationships between mineral magnetic determinands

7.5.1 Correlations

To assess relationships between determinands quantitatively, a Pearson product-moment correlation matrix was prepared in CANOCO (ter Braak, 1987; 1990) with untransformed data (negative values could not be log-transformed) for 208 samples (PUMP2 removed). The output matrix is displayed in Table 7.5. Shaded cells indicate positive correlations at the $p<0.001$ significance level ($r=0.321$ for 206 degrees of freedom, two-tailed significance test). Excluding measures of autocorrelation, 50 positive correlations are significant at $p<0.001$ and 52 are significant at $p<0.005$ ($r=0.276$ for 206 d.f.). The highest positive correlations are between the normalized reverse field ratios which share an obvious relationship with each other. There are also strong positive correlations between $\varkappa$ and other concentration measures such as SIRM and HARD. The highest r is between $\varkappa$lf and $\varkappa$hf, as expected. $\varkappa$fd and $\varkappa$fd% are strongly correlated to other fine-grain size indicators such as SIRM/$\varkappa$, $\varkappa_{ARM}/\varkappa$ and SOFT as well as overall concentrations ($\varkappa_{ARM}$, SIRM).

Five correlations are negatively significant at $p<0.001$ level; nil at the $p<0.005$ level. These mostly relate to measures of hard induced remanence (HARD, HARD%) versus

×lf	1.000															
×hf	0.9962	1.000														
×fd	0.2670	0.1826	1.000													
×fd%	0.2648	0.2762	-0.0671	1.000												
SIRM	0.4637	0.4424	0.3421	0.0001	1.000											
$\times_{ARM}$	0.2373	0.2093	0.3655	-0.0014	0.6368	1.000										
$\times_{ARM}$/SIRM	-0.1988	-0.2122	0.1048	-0.0313	0.0324	0.7086	1.000									
SIRM/×	0.1355	0.1533	-0.1676	0.3808	0.2667	0.2329	0.1534	1.000								
$\times_{ARM}$/×	-0.0362	-0.0211	-0.1758	0.4507	0.1607	0.4491	0.5136	0.7980	1.000							
HARD	0.4967	0.5110	-0.0474	0.0305	0.5319	-0.0388	-0.4466	0.2017	-0.0727	1.000						
HARD%	0.0663	0.0897	-0.2454	-0.0352	-0.2703	-0.4730	-0.4368	-0.0620	-0.2208	0.5206	1.000					
SOFT	0.3216	0.2950	0.3690	-0.1624	0.7757	0.6746	0.1788	-0.0694	0.0673	0.1770	-0.4015	1.000				
SOFT%	0.5388	0.5293	0.2276	0.0481	0.6032	0.4436	-0.0512	0.2594	0.1552	0.4102	-0.1838	0.4858	1.000			
-40mT%	0.5229	0.5133	0.2244	0.0416	0.6177	0.4390	-0.0729	0.2237	0.1326	0.4231	-0.1664	0.5375	0.9915	1.000		
-100mT%	0.4942	0.4839	0.2254	0.0380	0.6286	0.4843	-0.0023	0.1838	0.1480	0.3962	-0.1975	0.6104	0.9522	0.9788	1.000	
-300mT%	0.4835	0.4730	0.2260	0.0398	0.6179	0.4999	0.0468	0.1600	0.1580	0.3644	-0.2494	0.6358	0.9146	0.9467	0.9903	1.000
	×lf	**×hf**	**×fd**	**×fd%**	**SIRM**	**$\times_{ARM}$**	**$\times_{ARM}$/ SIRM**	**SIRM/×**	**$\times_{ARM}$/×**	**HARD**	**HARD%**	**SOFT**	**SOFT%**	**-40mT%**	**-100mT%**	**-300mT%**

Shaded cells have a significance level of $p<0.001$ where $r=0.321$ for 206 degrees of freedom

Table 7.5 Pearson product-moment correlation matrix for the 16 surface-sediment mineral magnetic parameters

ferrimagnetic concentration (κ_{ARM}) and fine-grained indicators (κ_{ARM}/SIRM, κ_{ARM}/κ), indicating that the overall concentration is determined by a ferrimagnetic component which is highly dissimilar to the hard component. Characteristic magnetic grain-sizes of the mineral assemblage are investigated further in the next section.

7.6 Magnetic grain-size variations

7.6.1 Grain-size dependence of mineral magnetic behaviour

Magnetic methods offer the potential for rapid and non-destructive granulometry. The grain-size dependence of various mineral magnetic parameters has been defined using measures of κ, κfd, SIRM, κ_{ARM} and the coercivity of remanence ((BO)CR) (Maher, 1988). All except the latter have been measured in this study, providing the opportunity to explore grain-size variations in the surface sediment samples. At Signy Island, there are only minor excursions from the dominant geology (section 3.5.2), thus fulfilling criteria for determining grain-size variations from various quotients which would otherwise be affected by mineralogical-related differences of mixed assemblages.

Two important magnetic grain-size boundaries vary with grain shape. These are (i) the division between ultrafine superparamagnetic grains (SP) and small stable single-domain grains (SSD), theoretical boundary 0.012-0.069 μm for magnetite (Maher, 1988) and (ii) the division between multidomain (MD) and SSD grains, roughly 0.1 μm (Thompson & Oldfield, 1986) (see Appendix B). Where samples have escaped the influence of diagenesis and authigenic greigite formation, ferrimagnetic grains in natural samples, with diameters from *ca.*0.2 μm diameter upwards, are of detrital and overwhelmingly terrigenous origin. The origin of fine (<0.1 μm) diameter SSD and SP grains in sediments is controversial. Magnetite grains in the size region SP<0.02μm>SP,SD can form a significant component of some natural magnetic assemblages occurring in soils and sediments.

7.6.2 Magnetic granulometry

Dearing *et al.* (1996a) proposed a granulometric method using κlf and κfd% which can be used to detect the presence of SP grains lying within a narrow band of grain sizes between ≈ 0.018 μm and 0.020 μm diameter. These essentially represent secondary ferrimagnetic minerals and the size-range is unlikely to include coarser-grained primary minerals or industrially-derived spherules. A model predicts a maximum κfd% of 14-17% in assemblages of spherical ferrimagnetic grains lying between 0 μm and the

SP/SSD boundary. Values of κfd% >10 indicate the increasing dominance of SP grains exceeding 20% of the total grain content which can be used to make a quantitative estimate of their total concentration; actual values depend on mineralogy (magnetite or maghemite) and grain-size distribution. Values of 10-12% are typical for an equal distribution of SP grains and κfd% values exceeding 14% indicate measurement errors (section 7.3.2). κfd% is depressed by the presence of frequency-dependent grains and is affected when the paramagnetic component >50% of the total susceptibility.

Figure 7.15 Plots of κfd% versus (a) κlf and (b) κfd for samples of soil and synthetic magnetite and maghemite minerals (cf. Dearing *et al.*, 1996a).

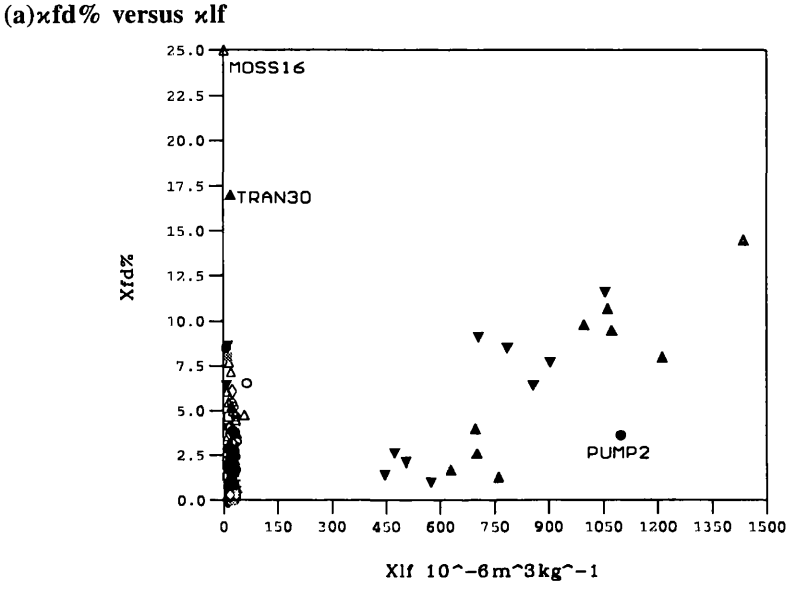

In this sample-set, κlf and κfd and κfd% share weak, but positive correlations (*ca.* r=0.26, p<0.01; Table 7.5). Following Maher's (1988) recommendations, the sample-set was screened and samples with κlf-κhf>'noise' were rejected (section 7.3.2), leaving a compliment of 125 surface-sediments. Figure 7.15 plots κfd% versus κlf and κfd% versus κfd for the Signy surface-sediments (n=125) and Maher's synthetic magnetite and maghemite grains (see Dearing *et al.*, 1996a) are also plotted for comparison (black up- and down-triangles respectively). The pattern of distribution shares similarities with Lees's (1994; in Dearing *et al.*, 1996a) environmental samples. Dearing *et al.* (1996a) use these plots to identify three types of magnetic assemblage: samples with κfd% <2% dominated by frequency-independent grains; samples with κfd% >6% dominated by frequency-dependent grains; and an intermediate group where κfd% is 2-6% in which there is a mixture of grain types. In Figure 7.15a, the Signy surface-sediments plot close to the origin with a linear spread along the vertical axis. Outlier samples include

PUMP2, TRAN30 and MOSS16. κfd% values for the latter two exceed 15% and are improbable, therefore indicating measurement errors (section 7.3.2). Sample PUMP2 has a very high SIRM and associates with the synthetics. The remaining samples have values for κfd% <10%. In figure 7.15b, the effect of frequency independent grains is excluded by using κfd instead of κfd%. Samples shift closer towards the vertical axis, the greatest movement occurring where κfd% <2.5%, i.e. in frequency-independent grains. Samples above κfd% >5% show little change in position; these samples are dominantly frequency-dependent grains.

Fig.7.15b κfd% versus κfd

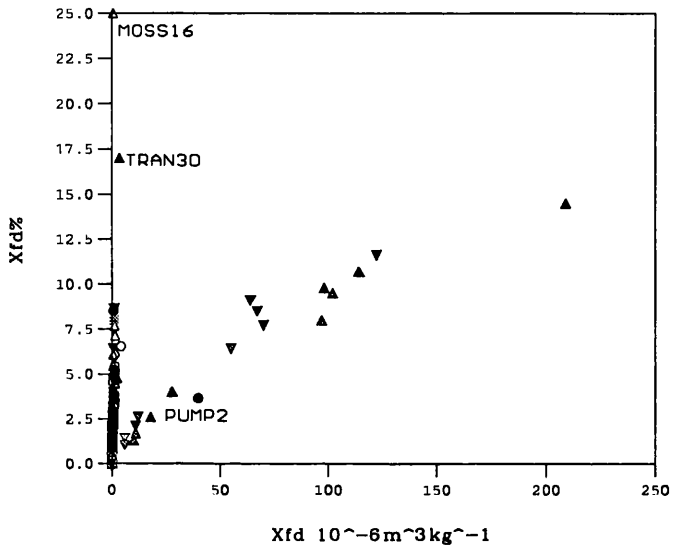

According to the Dearing *et al.* (1996a) model, samples showing relatively high κlf but virtually zero κfd are dominated by coarse-grained MD ferrimagnets, represented in this sample-set by samples from Emerald, Lake 13, Amos, Orwell, Tranquil, Knob, Spirogyra with κlf values of *ca.*0.3 $x10^{-6}m^3kg^{-1}$ and κfd% <1%. Samples with κfd% <5% are typical for samples where SSD grains dominate the assemblage or where extremely fine-grains dominate the SP fraction and the majority of samples (n=114) have κfd% values <5%. Samples with κfd% >6% have a significant proportion of SP grains and occupy an envelope bounded by limits defining grains <0.015 μm and > 0.015 μm. Only samples CHAN12, MOSS13, AMOS3, SOMB25, MOSS11, MOSS19, GNES22, PUMP6 and AMOS4. Samples with κfd% >10% are dominated by SP grains and only two samples - TRAN30 and MOSS16 - conform to this category. However, their κfd% values exceed the theoretical maximum and are likely to be in error.

It is inadvisable however, to depend wholly on granulometric models based on κ when

source lithologies are suspected to be predominatly paramagnetic (section 7.7.1). An alternative granulometric method proposed by Maher (1988) uses models based on κ_{ARM}/SIRM and κfd%. κ_{ARM}/SIRM is sensitive within the MD range and as a remanence parameter, is unaffected by paramagnetic contributions which can strongly influence κ measures and quotients.

Figure 7.16 plots κ_{ARM} versus SIRM for the 208 sample-set. The two measures are significantly correlated (p<0.001) (Table 7.5) and the samples follow a linear trend along a size gradient. Coarser-grained MD samples close to the origin include Emerald (plusses), Moss (open up-triangles), Knob (open down-triangles) and Gneiss (grey squares). MOSS9 is an outlier with a very high SIRM but relatively low κARM. SOMB25 also has a relatively high SIRM. Finer-grained samples include MOSS16, which was identified as an outlier in Figure 7.16 on the basis of its extremely high κfd% value. Other plausible, fine-grained samples come from Moss, Changing and Sombre Lakes including MOSS17, CHAN4, CHAN5, MOSS13, SOMB11, MOSS11, some of which were identified in Figure 7.15 as having a significant SP sized component.

Figure 7.16 Maher's first stage granulometry - κ_{ARM} versus SIRM

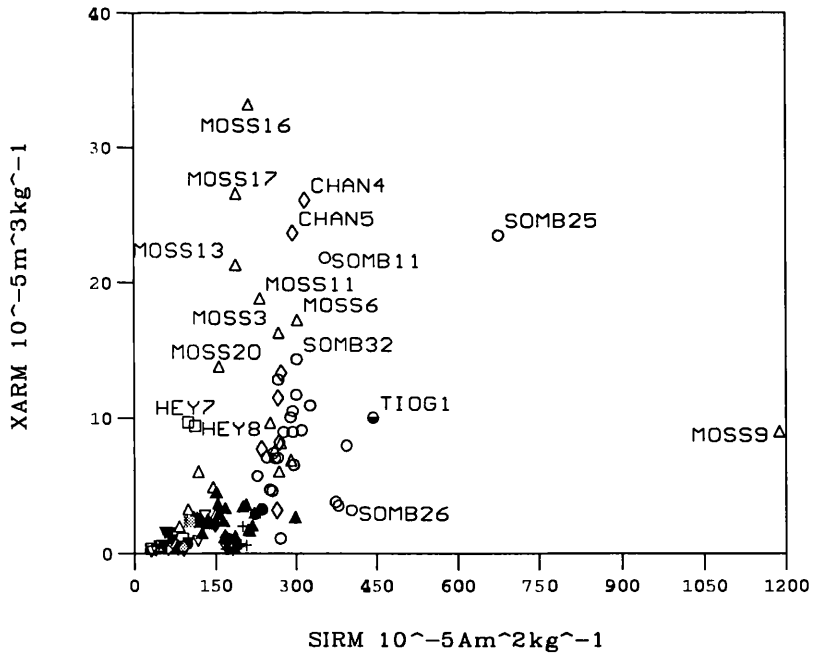

The first stage of granulometry does not discriminate grains of 0.012 μm and the 150

-250 μm magnetites therefore Maher (1988) proposed a second granulometric model which discriminates the coarse tail from the fine tail. The κ_{ARM}/SIRM quotient can be used to define the boundary between MD and PSD/SSD magnetite grains (0.069 μm). In Figure 7.17 Maher's New MT29 sample (0.069 μm) is labelled, defining this grain-size boundary. Values of κ_{ARM}/SIRM <20 $10^{-5}mA^{-1}$ are associated with grain-sizes exceeding 1.0 μm, i.e. MD while those around 40 indicate finer grains ~0.1 μm, i.e. SSD. Samples MOSS16 and TRAN30 are clearly outliers associated with unnaturally high κfd% values. The other samples follow a linear trend along the κ_{ARM}/SIRM axis with some spread along the κfd% axis also. All samples exceed the κ_{ARM}/SIRM cut-off at 20 $x10^{-5}mA^{-1}$ and therefore have grain-sizes smaller than 1.0 μm. There is a gradient within the SSD grain sizes: coarse SSD grains in Emerald (plusses), Pumphouse (black circles), Knob (down-triangles) and Twisted (stars) Lakes and finer-grained SSD with a greater SP component, all lying above the 0.069 μm boundary. The finest samples with the highest κ_{ARM} values include samples from Changing, Heywood, Sombre and Moss Lakes and some of these values are in excess of 200 $x10^{-5}mA^{-1}$, indicating the presence of bacterial magnetosomes (Oldfield, 1994).

Figure 7.17 Maher's second stage granulometry - κ_{ARM}/SIRM versus κfd%

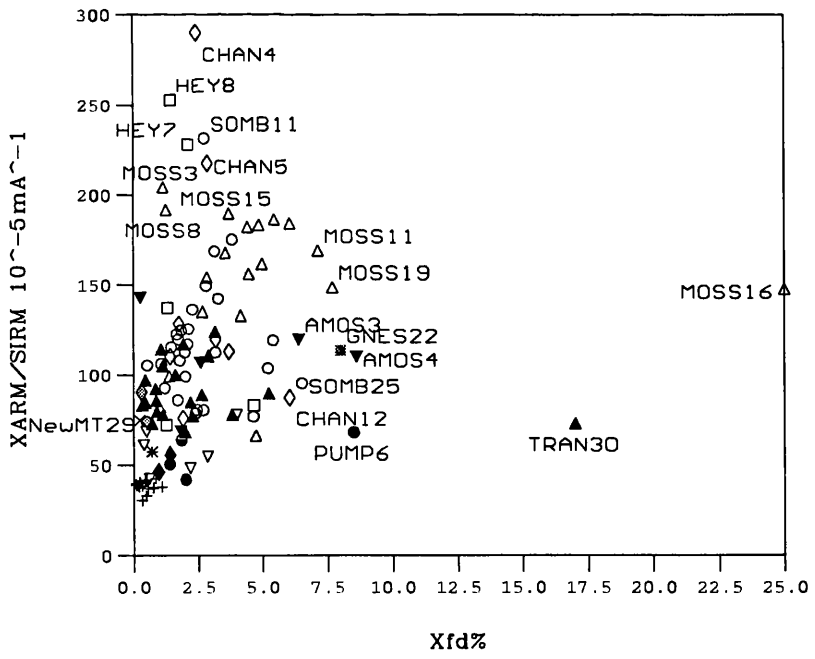

Oldfield (1994) proposed further methods to discriminate fine-grained ferrimagnets using κ_{ARM}/κ and κfd%. The two quotients have a near-negative correlation and as values for

κfd% decline and κ_{ARM}/κ increase, grain-size generally increases. Normalizing κ_{ARM} by κ removes the effects of concentration variations in the data-set. In Figure 7.18, MOSS16 is a clear outlier with a high κ_{ARM}/κ value, affecting the distribution of the remaining surface-sediment samples. Maher's New MT Series synthetic magnetites (grey circles) are plotted for comparison. PSD and MD grains should lie in an envelope close to the origin, with values of κ_{ARM}/κ <10 and with negligible values for κfd% (Oldfield, 1994). A few samples from Emerald (plusses), Spirogyra (filled up-diamonds) lie close to this theoretical envelope but the majority plot outside in the realm of finer SSD (<0.1 μm) grain-sizes. Some samples from Heywood (squares), Changing (diamonds) and Tioga (half-filled circles) are very similar to the Maher's New MT series magnetites, confirming the SSD nature of these grains.

Figure 7.18 Scatterplot of κ_{ARM}/κ versus κfd%

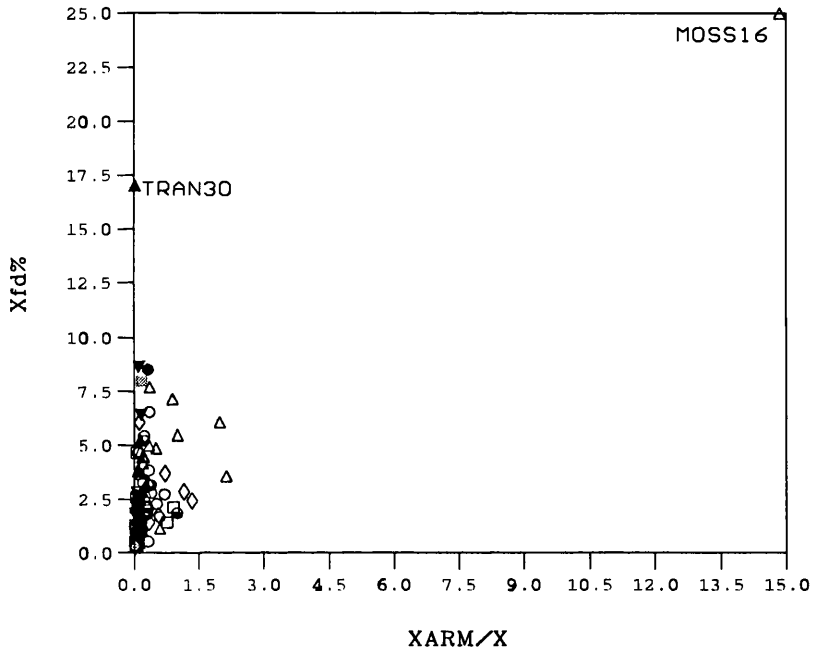

7.6.3 Mineral magnetic behaviour and relationships with sediment particle-size

The actual magnetic crystal-size varies little with sediment particle-size however, mineralogy to some extent determines particle-size (Dearing & Flower, 1982) and fluctuations in mineral concentrations can occur in response to changing depositional environments and grain-size. Gravity sorting has been known to concentrate magnetite and haematite in different depositional environments (Stober & Thompson, 1979). The concentration of magnetic minerals into specific particle-size fractions of the bulk

sediment, combined with a changing particle-size distribution of the bulk sediment due to detrital source variations, is often used to interpret down-core variations in magnetic properties (Oldfield *et al.*, 1985). Some coarse materials have fine-grained (1-10 μm) inclusions. Separation of magnetic behaviour into specific particle-size fractions was not an objective in this Thesis but the availability of particle-size data for these surface-sediments (Chapter 6) presents the opportunity to further characterise magnetic granulometry and explore its relationships with the bulk sediment matrix.

SSD, SP and MD magnetic grain-sizes are all below the measurable limits of conventional particle-sizing techniques (<2 μm) however, clear trends in κ are apparent through the entire size-range (0.01-500 μm) (Maher, 1988). Data from Dankers (1978; in Maher, 1988) show a significant increase in κ with particle-size, reaching a secondary, lower peak (relative to the lower, sub-micron fraction) at 50 μm. Above 50 μm, κ gradually decreases. Other authors have noted a κ peak at slightly smaller grain sizes (Thomspon & Morton, 1979; Dearing & Flower, 1982). In the scatterplot (Figure 7.19) there is a generally linear trend with a low, negative correlation (r=-0.11), indicating some decrease in κ with particle-size. The lack of sand-sized material means that the distribution minimum observed by Maher (1988) has not been reached. The highest κ values lie within a similar range of grain-size (10-40 μm) with peak values

Figure 7.19 Scatterplot of κlf versus median particle-size

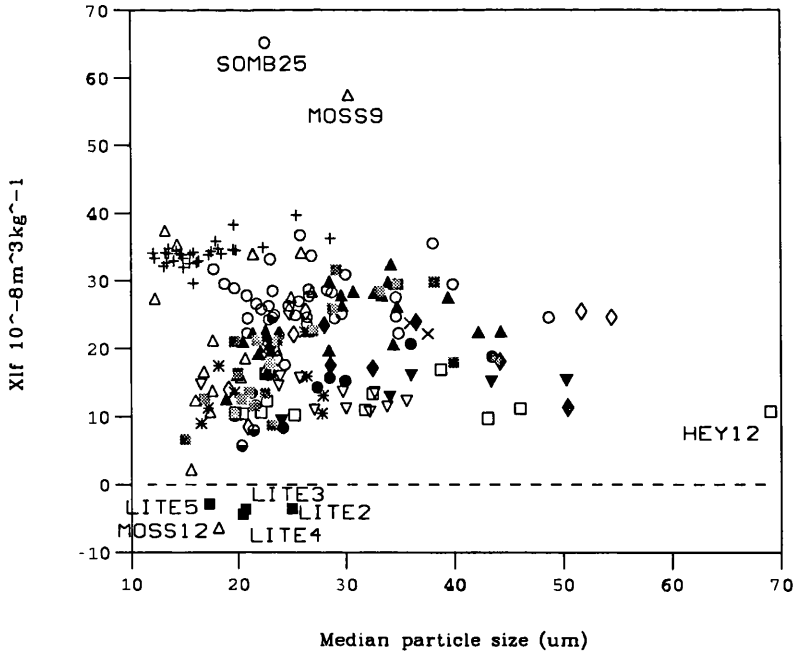

at median grain-sizes of 25-29 μm. Dankers's (1978) 50 μm peak is not evident. These results are more analogous to those from Loch Lomond (Thompson & Morton, 1979) where the highest specific χ was in the <32 μm fraction. Samples from Emerald (plusses) and Sombre (open circles) Lakes have relatively high χ values, probably relating to concentration effects in relatively dense, minerogenic sediments from glacial sources. Negative χ values in the surface-sediments are found in samples that are highly organic (Light Lake, MOSS12). Heywood Lake (open squares) has consistently low χ values and highly organic and notably coarse-grained sediments. One possible explanation is the loss of χ with resuspension at shallower water depths (Dearing & Flower, 1982) which characterizes sedimentation processes in this wind-stressed lake (section 5.6).

Figure 7.20 Scatterplot of SIRM versus median particle-size

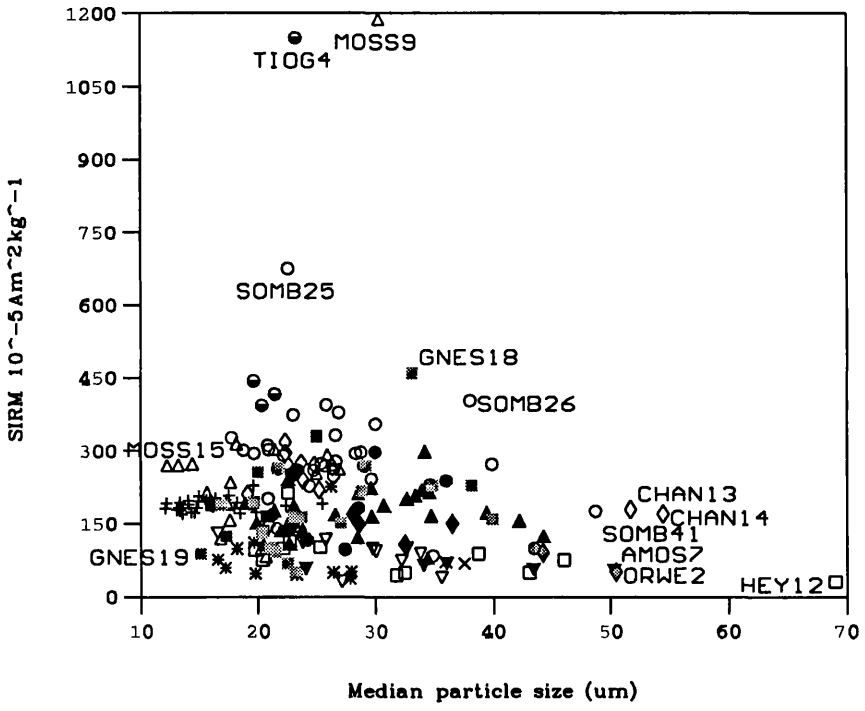

Maher (1988) also noted a SIRM-grain-size relationship with two distinct spikes in SIRM at grain-sizes of 0.03-0.036 μm (SD) and the <5-10 μm range of Dankers (1978). In the scatterplot (Figure 7.20) samples follow a slightly left-skewed distribution and a negative correlation (r=-0.1294) confirms Dankers's (1978) observation for decreasing magnetic concentrations with increasing particle-size. The highest SIRM intensities are

found at median particle-sizes of 20-35 μm and are especially strong in Tioga (half-filled circles) and Sombre (open circles) Lakes. The coarsest samples - HEY12, CHAN13, CHAN14, ORWE2, AMOS7 - with median particle-sizes between 20-35 μm, have the lowest SIRM intensities (≤150 $10^{-5}Am^2kg^{-1}$).

Figure 7.21 Scatterplot of κ_{ARM} versus median particle-size

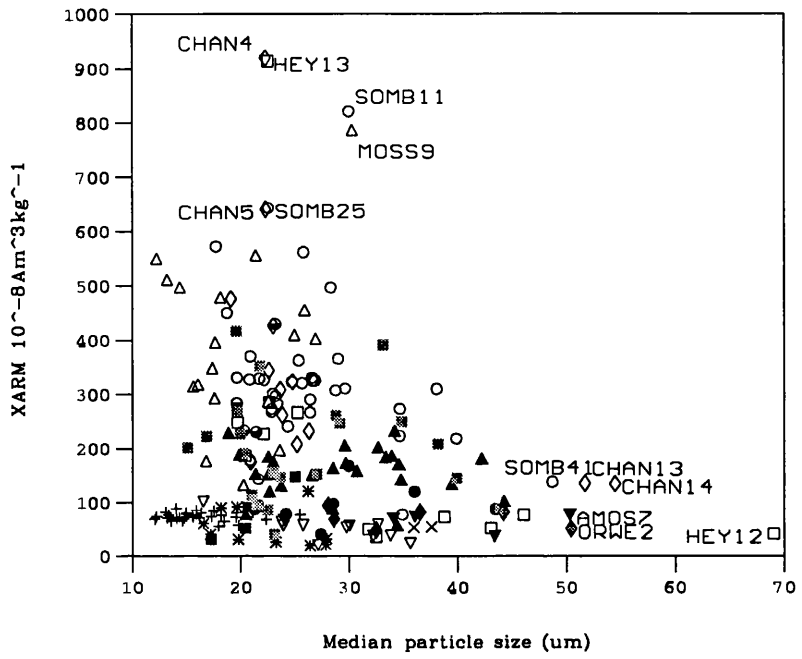

κ_{ARM} versus grain-size should show a slow continuous decrease extending across the coarser end (5-100 μm) of the grain-size spectrum (Maher, 1988) and this decline is evident in Figure 7.21 where the two measures share a negative correlation (r=-0.13). Peak κ_{ARM} occurs in samples with median grain-sizes between 20-30 μm and κ_{ARM} is especially high in samples CHAN14, HEY13, SOMB11 and MOSS9. High κ_{ARM} values are also sustained at finer median grain-sizes (<15 μm). Low values are found at both ends of the particle-size spectrum, particularly in the cluster of fine-grained samples from Emerald Lake (plusses) and in the coarse distribution tail (CHAN13, AMOS7, ORWE2, CHAN14, HEY12).

The κ_{ARM}/SIRM quotient is sensitive to magnetic grain-size variations (section 7.6.2) and the scatterplot of surface-sediments (Figure 7.22) has a weak, left-skewed distribution with peak values at median particle-size values of around 20 μm. Low κ_{ARM}/SIRM values are also found in coarse samples (HEY12, CHAN14, CHAN13). The lowest

Figure 7.22 Scatterplot of κ_{ARM}/SIRM versus median particle-size

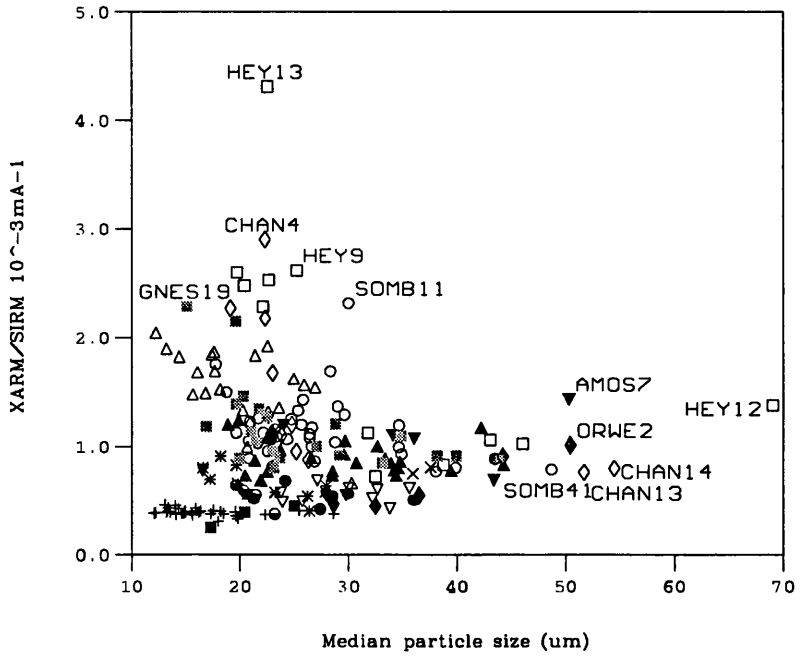

values are found in the finest samples from Emerald Lake (plusses) which cluster close to the origin.

The figures above illustrate that the relationships between mineral magnetic behaviour does share some relationship with particle-size in the surface-sediments. Magnetic concentrations are relatively independent of particle-size but follow the expected model and decline as particle-size becomes coarser. Magnetic grain-size on the other hand, is more responsive to particle-size and the finest grain-sizes are associated with particles in the mid-silt range, the dominant size-fraction. Arguments concerning detrital versus non-detrital control on magnetic mineralogy and grain-size characteristics are explored in the following section.

7.7 Sources of mineral magnetic behaviour

7.7.1 Catchment source mineralogies

Characterising the mineral magnetic behaviour of catchment source materials helps to define a baseline against which post-depositional changes in the lake sediments (section 7.7.2-7.7.4) can be assessed. Mineralogical alterations resulting from diagenesis and authigenesis can affect magnetic behaviour so that it is no longer fully representative of the catchment geology, reducing the potential for accurate sediment source ascription

and consequently, for inferred climate predictions using sediment proxies. Source-provenance identification was not a goal in this study thus assumptions concerning magnetic behaviour have been inferred from the island's geology (Matthews & Maling, 1967; Thomson, 1968; Storey & Meneilly, 1985), lake-sediment geochemistry (Dyson, 1996) and lake-sediment mineral magnetism (Wilson, 1993) and by analogy with known values for magnetic determinands from other sources in the Antarctic and elsewhere (Thompson & Oldfield, 1986; Oldfield, 1991; Karlén & Matthews, 1992; Cromack, 1993; Snowball, 1993a, 1993b; Wasell, 1993; Nesje *et al.*, 1994; Battarbee *et al.*, 1996).

Common minerals at Signy Island include quartz, plagioclase, orthoclase and oligoclase feldspars, biotite (mica), chlorite, ilmenite, calcite, ferrous oxide, maghaemite, iron pyrites, haematite, amphibole, magnetite, garnet, epidote, graphite and goethite (Thompson, 1968). Many of these are paramagnetic (calcite, garnet, feldspar), diamagnetic (quartz) or canted antiferromagnetic (haematite) (Thompson & Oldfield, 1986). Metamorphic assemblages typically have coarse grain-sizes with MD minerals displaying unstable remanences (Thompson & Oldfield, 1986). Quartz is virtually ubiquitous and is probably the dominant mineral constituent of the lake-sediments (Dyson, 1996). Using Electron Microprobe Analysis, Dyson (1996) identified high iron contents in some of these lake sediments. On Signy Island, garnet has an unusually high iron content; it is noted for its paramagnetic behaviour (Thompson & Oldfield, 1986). Soil development is generally limited in these catchments and weathering products should form a small component of the transported sediment budget, especially in glaciated catchments. Therefore, allochthonous sediments should be representative of their catchment geologies.

By analogy, Late-Glacial lake-sediments from temperate regions generally reflect the primary magnetic mineralogy of freshly exposed catchment material at the close of the last glaciation. Rank $\varkappa$ values for Late Glacial sites of varying geologies are listed with $\varkappa$ values for the Signy surface-sediments in Table 7.6. Maximum $\varkappa$ values from poorly-sorted, unweathered Late Glacial sediments typically range from 0.4-200 $x10^{-8}m^3kg^{-1}$ (Thompson & Oldfield, 1986). Median values in the Signy surface-sediments relate more to parent materials; extreme values, which affect the mean, may relate to post-depositional enhancements in concentration (section 7.7.3-7.7.4). Surprisingly, Gneiss Lake has a mid-rank position despite its catchment geology, which should yield materials with higher magnetic concentrations (Thompson & Oldfield, 1986). The $\varkappa$

Table 7.6 Rank maximum χ values from Late-Glacial lake sediments and results from Signy Island surface and basal lake sediments

Site	*Locality*	*Bedrock*	*Maximum* χ $10^{-8}m^3kg^{-1}$
Loch Garten	Speyside, Scotland	schist/granite	0.4
Paajarvi	Southern Finland	schist/granite	1.2
Loch Morlich	Speyside, Scotland	schist/granite	1.2
Lochan Uaine	Cairngorms, Scotland[5]	granite	2.0 (basal)
Kiteenjarvi	Eastern Finland	schist	4.0
Vuokonjarvi	Eastern Finland	granite/gneiss	9.0
Tioga Lake	**Signy Island**	**schist**	**24.6 (9.1)**
Ormajarvi	Southern Finland	gneiss	10.0
Heywood Lake	**Signy Island**	**schist**	**16.9 (10.8)**
Twisted Lake	**Signy Island**	**schist**	**22.4 (13.3)**
Knob Lake	**Signy Island**	**schist**	**16.0 (13.5)**
Orwell Lake	**Signy Island**	**schist**	**18.0 (14.7)**
Heywood Lake	**Signy Island**	**schist**	**15.0 (@118 cm)**
Amos Lake	**Signy Island**	**schist/amphibolite**	**16.0 (15.1)**
Pumphouse Lake	**Signy Island**	**schist/marble**	**1098.4 (15.2)**
Gneiss Lake	**Signy Island**	**gneiss/amphibolite**	**31.6 (17.9)**
Bothy Lake	**Signy Island**	**schist/gneiss**	**18.8**
Moss Lake	**Signy Island**	**schist/amphibolite**	**57.5 (19.8)**
Hjortsjon	Southern Sweden	granite/gneiss	20.0
Spirogyra Lake	**Signy Island**	**schist**	**23.9 (20.5)**
Changing Lake	**Signy Island**	**schist/amphibolite**	**25.5 (20.6)**
Windermere	Northern England	slate/andesite	22.0
Tranquil Lake	**Signy Island**	**schist**	**32.4 (22.5)**
Lake 13	**Signy Island**	**schist/marble**	**23.7 (23.0)**
Sombre Lake	**Signy Island**	**schist**	**65.2 (26.8)**
Block Lake	Husvik, S.Georgia[2]	volcaniclastic sandstones/shales	>30 (@10 cm)
Emerald Lake	**Signy Island**	**schist**	**39.7 (34.0)**
Kløsa, Erlingvatnet	N.W. Spitsbergen[3]	schist/marble	40.0 (basal)
Loch Davan	Deeside, Scotland	schist/granite	50.0
Hajeren	N.W. Spitsbergen[3]	schist/marble	>60 (basal)
Sombre Lake	**Signy Island**	**schist**	**61.9 (@248 cm)**
Parochlus Lake	Husvik, S.Georgia[2]	volcaniclastic sandstones/shales	>90 (basal)
Bjorkerods Mosse	Southern Sweden	gneiss/dolerite	100
Isdalsvatn	Hardangerjøkulen, Norway[4]	Precambrian (granite?)	100 (basal)
Midtivatnet, Storevatnet	Jostedalsbreen, S.Norway[1]	granite	>100 (basal)
Loch Lomond	Southern Scotland	schist/basalt	130
Geitabergsvatn	Iceland	basalt	160
Lake Måns	Husvik, South Georgia[2]	volcaniclastic sandstones/shales	>250 (basal)

Median value for Signy surface sediments in brackets. Data from Thompson & Oldfield (1986), [1] Karlén & Matthews (1992), [2] Wasell (1993), [3] Cromack (1993), [4] Nesje *et al.* (1994) and [5] Battarbee *et al.* (1996).

peak of basal sediments in Sombre Lake (Wilson, 1993) probably results from particle-size interactions and packing density but it still lies within the range found in the surface-sediment data-set (Table 7.1).

Tephra is a potential allogenic source of ferrimagnetic minerals to the lake sediments. Tephra has been identified in very dilute quantities in cores from Sombre and Heywood Lakes in sufficient concentrations to enhance κ (Dyson, 1996). The last significant eruption from the nearest source, Deception Island, was in 1967-70 and the uppermost tephra horizon in Sombre Lake corresponding to this event is at 3.4 cm. According to calculated rates of sediment accumulation (Appleby, Jones & Ellis-Evans, 1995), this event horizon should lie below the 0-1 cm surface layer. Tephra could however, affect the contemporary mineral magnetic behaviour in lakes where resuspension is active. Shard presence can only be confirmed by microscopic analysis, which is beyond the scope of this Thesis.

7.7.2 Reductive diagenesis

The most common magnetic minerals found in lake-sediments include impure magnetite, haematite, magnetite and greigite (Jones & Bowser, 1978). Reductive diagenesis (dissolution) can significantly modify magnetic mineralogy in productive lakes under anaerobic conditions (Hilton, Lishman & Chapman, 1986), leading to a continuous percentage loss of magnetic properties in the fine-grained magnetite range (Anderson & Rippey, 1988), a coarsening of the magnetic grain-size and a reduction in the overall magnetic concentration. It most commonly affects κ_{ARM}, SIRM and SOFT. In Arctic Sweden, Snowball (1993b) demonstrated that down-core variations in magnetic properties were attributable to post-depositional magnetite dissolution, rather than climate-related sediment source changes. In the Signy lakes, iron can occur in extremely high concentrations in the water column and sediments (Gallagher, 1985; Ellis-Evans & Sanders, 1988; Ellis-Evans & Lemon, 1989) and is active in microbially mediated reactions in the surface-sediments, with activities peaking in the 0-0.5 cm layer and detectable to depths of 5 cm. However, permanently low temperatures restrict dissolution, which is principally located at sites where the supply of ferric iron is greatest (Ellis-Evans & Lemon, 1989). Despite their predisposition to chemical transformations, Wilson (1993) was unable to identify reductive diagenesis effects in these lake sediments and confirmation of this conclusion is sought.

Dissolution processes in these lakes are likely to be highly variable according to lake trophy, morphology, development of the anoxic zone, sediment type and availability of iron. In theory, indications should be greatest in the most organic sediments (Hilton, Lishman & Chapman, 1986) at the greatest basin depths. In Figure 7.24, the reductive diagenesis indicators - $\varkappa_{ARM}$, SIRM and SOFT - are plotted against %LOI and water depth (proxy for anoxia). Correlations are positive but weak in this noisy data-set. On a sample-set basis, no decrease in magnetic concentration, symptomatic of dissolution, can be identified. In fact, values are seen to increase with increasing water depth and with increasing organic contents. Higher concentrations of ferrimagnetic minerals at depth suggests either sediment focusing, already indicated in previous chapters, or *in-situ* authigenesis.

Figure 7.23 Scatterplots of reductive diagenesis determinands (SIRM, $\varkappa_{ARM}$ and SOFT) versus % Loss On Ignition and water depth

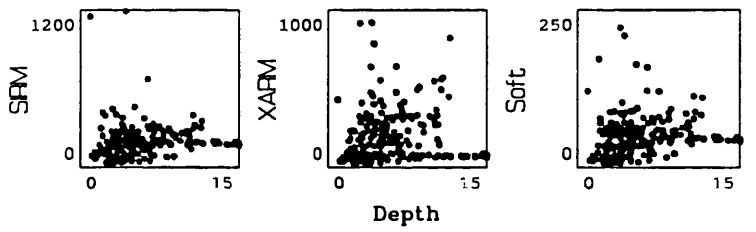

r=0.886, not significant *r*=0.0979, not significant *r*=0.1459 not significant

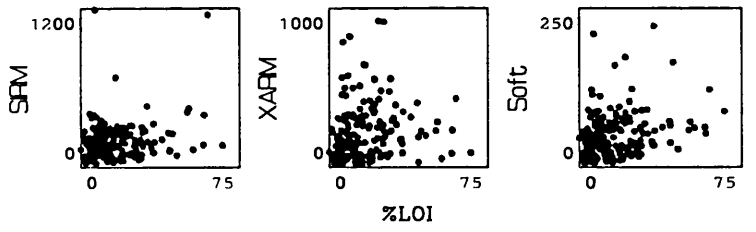

r=0.1772, *p*<0.10 *r*=0.2073, *p*<0.05 *r*=0.2211, *p*<0.05

7.7.3 Effects of authigenesis

Sulphurization reactions in sediments can result in authigenic iron sulphide formation (Jones & Bowser, 1978). This has more commonly been noted in saline environments but there is increasing evidence for their importance in both eutrophic and oligotrophic

freshwater environments (Bloemendal, 1982; Hilton, Lishman & Chapman, 1986; Snowball, 1991; Williams, 1991; Ariztegui & Dobson, 1996). Williams (1991) concluded that the sedimentary environments most prone to magnetic alterations are organic-rich, surficial strata hosting active Fe^{3+} and SO_4 reduction with periodic oxidation for the elemental sulfur. These are typical conditions in the Signy lakes (Ellis-Evans, 1989) thus sulphide authigenesis, leading to the production of greigite (Fe_3S_4), is anticipated but is not supported by the data.

Table 7.7 Correlation coefficients of grain-size diagnostic determinands and % Loss on Ignition and Depth for a screened data-set of surface -sediments (n-125)

	κlf	κfd%	κ_{ARM}/SIRM	κ_{ARM}/κ	κ_{ARM}/κfd
Depth (m)	0.4927 *p*<0.001	-0.1072 *n/s*	-0.0348 *n/s*	-0.0339 *n/s*	0.4572 *p*<0.001
% LOI	-0.4545 p<0.001	0.4541 *p*<0.001	0.4667 *p*<0.001	0.5141 *p*<0.001	-0.1872 *p*<0.10

Shaded cells highly significant ($p<0.001$ for 124 d.f)
n/s not significant

Correlation coefficients between concentration and grain-size indicators and % loss on are highly significant (Table 7.7) suggesting a link between fine-grained magnetite and organic-rich sediments, i.e. authigenic magnetic mineral formation. Organic matter is diamagnetic and makes no contribution to magnetic concentration. Greigite is identified by high values for SIRM/κ and a large loss of remanence between -40mT and -100mT (F. Oldfield, *pers.comm.*). Only one sample - PUMP2 - displays extreme behaviour possibly indicative of greigite but its value for SIRM/κ (19.505 x10^3Am^{-1}) is not especially high. Samples display a uniform response to demagnetization (Figure 7.14). The highest SIRM/κ (section 7.3.8) is in sample MOSS16 (95.5 x10^3Am^{-1}) which may include greigite, since it repeatedly occurs as an outlier in granulometry (section 7.6.2). Samples from Tioga Lake (Figure 7.8) also have very high SIRM/κ values but these values are artefacts of negative κlf values due to small sample mass, paramagnetic effects and measurement problems (section 7.3.2) and should be disregarded. Otherwise, SIRM/κ values match their typical paramagnetic schist geologies (Thompson & Oldfield, 1986; Snowball, 1993a). It is possible that greigite has been lost from these samples through storage diagenesis effects (section 7.4).

The lack of evidence for sulphide authigenesis suggests that another process may be responsible for the non-detrital magnetic characteristics of this sample-set. An alternative mode of magnetic mineral formation is through the action of magnetotactic bacteria.

7.7.4 Bacterial magnetite formation

Bacterial magnetosomes can contribute a significant authigenic component to the magnetic properties of soils (Dearing *et al.*, 1996b), freshwater and marine sediments (Oldfield, 1991). In lake sediments, magnetite formed by stricly anaerobic bacteria as magnetosomes has extremely high κ_{ARM}/SIRM values, far higher than the range produced by abiotically-produced synthetic materials (Maher, 1988). Bacterial magnetite are characterised by coarse SSD-sized grains relating to their cell size (diameters <50 nm) rather than SP size grains. In Arctic Sweden, Snowball (1994) demonstrated high concentrations of bacterial intra-cellular magnetite in the upper 70 cm of gyttya from the profundal zone (19 m) of an oligotrophic Lake Pajep Njaukjaure, which contrasted strongly with the mixed grain-size assemblages of the remainder of the core and the coarse MD minerals in the basal sediments. At Signy Island, fine-grained magnetites are lacking in catchment sources (7.7.1) and greigite formation is apparently rare (section 7.7.2) thus, magnetosomes are predicted as the most likely source of the SSD ferrimagnetic component indicated in magnetic granulometry (section 7.6.2).

Oldfield (1991) used the κ_{ARM}/κfd quotient to detect the presence of bacterial magnetite in sediments. Values in the screened sample-set (n=125) used in granulometry range from 16.61 to an incredible 8.92e+16; the latter indicates problems with κ discussed in section 7.3.2. This quotient displays a significant positive correlation with depth (r=0.46, p<0.001; Table 7.7) and indicates that the greatest concentrations of non-detrital ferrimagnets occur at greater depths, as controlled by the extent of the anoxic zone. κ_{ARM}/SIRM values in the 208 sample-set range from 25-431 $x10^{-5}mA^{-1}$, exceeding the maximum in Maher's (1988) New MT series magnetites. Values for κlf vary over three orders of magnitude (Table 7.1), matching the range of variability found in a large data-set of English topsoils. However, the modes of this ferrimagnetic mineral formation differ. The English topsoils were demonstrated to have a significant proportion of secondary SP/SSD ferrimagnetic minerals that has formed through bacterially-mediated reactions (Dearing *et al.*, 1996b). This is entirely different to magnetotactic bacteria which produce intracellular magnetite crystals wholly within the SSD domain range as controlled by cell-size. In soils, the magnitude of this ferrimagnetic concentration is

strongly associated with elevated values for iron. If the ferrimagnets in these lake sediments are of pedogenic origin then it would be logical to find the greatest concentrations of SSD minerals in catchments with significant outcrops of iron-rich (marble and amphibolite) bedrock, e.g. Changing, Moss, Pumphouse Lakes.

The association of enhanced ferrimagnetic concentrations and fine grain-sizes with sediments of higher organic content suggests a link to the benthic environments of the lake independent of catchment effects thus supporting the hypothesis for magnetotactic bacteria. Ellis-Evans & Lemon (1989) isolated iron-reducing bacteria from Sombre Lake which utilize the abundant Fe(III) oxyhydroxides and constitute an important component of the anaerobic mineralisation of organic carbon in the anoxic zone. It is possible that these anaerobic bacteria are intimately associated with benthic vegetation such as cyanobacterial mats which coexist in anaerobic conditions. Also, fine, organic sediments are prone to focusing (section 5.6) to deeper parts of the basins which may, in part, be responsible for the significant correlation between $\varkappa_{ARM}/\varkappa$fd and depth.

In the next stage of the data-analysis, classification (section 7.8) and ordination methods (section 7.9) are used to consolidate and simplify relationships between variables and between variables and the environment.

7.8 Classification

7.8.1 Cluster analysis

Agglomerative hierarchical cluster analysis was performed using the program CLUSTER (H.J.B.Birks, unpublished) on standardised data in a Euclidean distance matrix. Five methods of cluster analysis were chosen and their performance with the 208 sample by 16 variables data-set was assessed. Group memberships for each of the five methods are listed in Table 7.8.

Common groupings are evident in all methods. In four out of five methods, MOSS12 and LITE2 are sole members of the first and/or second groups. SOMB25, MOSS9 and TIOG4 also often group together. MOSS16 tends to occur singly. The remaining samples from Light Lake tend to occur together. Twisted Lake samples define a discrete group. SOMB11, HEY13, CHAN4 and CHAN5 form members of the lowest groups, often as single members of individual groups. Samples from Emerald and Amos Lakes tend to remain together with the majority of samples from Sombre and Tranquil Lakes.

Group membership	*Nearest neighbour (single-link)*	*Furthest neighbour (complete-link)*	*Weighted group average*	*Group average*	*Minimum variance (Ward's method)*
1	MOSS12; LITE2.	MOSS12; LITE2.	MOSS12; LITE2.	MOSS12; LITE2.	SOMB37; HEY5,6,10,12,14,15; MOSS7; KNOB1,3-11; PUMP3,5; SPIR; TRAN16,20,30; AMOS; EMER; SIG13; TWIS3-5,7-12; BOTH; GNES2-4,9,12,13,16; ORWE2.
2	MOSS16.	SOMB25; MOSS9; TIOG4.	SOMB25; MOSS9; TIOG4.	MOSS16.	MOSS12; PUMP1; LITE; GNES17.
3	TIOG4.	HEY13; CHAN4; MOSS16.	MOSS16.	SOMB25; MOSS9; TIOG4.	SOMB13,15-21,23,24,26-36,38-41,43-46; HEY7-9,11,16; CHAN2,3,6-14; MOSS4,8,11,13,16-20; KNOB2; PUMP4,6,7; TRAN4-15,17-19,21-29; TIOG; TWIS6; GNES5,6,8,10,11,14,18-22; ORWE1.
4	SOMB25; MOSS9.	SOMB35,37,41; HEY5-12,14-16; CHAN6,11,13,14; MOSS4,7,8,13,17-20; KNOB; PUMP3-7; LITE3-5; TRAN7-11,14-18,20-22,24-30; AMOS; SIG13; TWIS; GNES2-4,8,9,14,16,19,20,22; ORWE.	SOMB12-24,26-46; HEY5-12,14-16; CHAN2,3,6-14; MOSS4-8,10,11,13-15,17-21; KNOB; PUMP; LITE; SPIR; TRAN; AMOS; TIOG1-3; EMER; SIG13; TWIS; BOTH; GNES; ORWE.	HEY12; KNOB9.	SOMB25; MOSS9.
5	LITE3,4,5.	SOMB15,18,19,23,30,45,46; CHAN3,11; PUMP1; SPIR; TIOG1-3; EMER; TWIS12; BOTH; GNES5,6,10-13,15,17,18,21;	HEY13.	HEY13; CHAN4.	SOMB12,14,22,42; CHAN5; MOSS3,5,6,10,14,15,21.
6	TIOG1,2,3.	SOMB13,14,16,17,20-22,24,26-29,31-34,36,38-40,43,44; CHAN2,7-10,12; MOSS5,11,14; TRAN4-6,12,13,19,23.	CHAN4.	LITE.	SOMB11; HEY13; CHAN4.
7	HEY13; TRAN30.	SOMB12,42; MOSS6,10,15,21.	SOMB11; CHAN5; MOSS3.	SOMB37; HEY5,6,10,14,15; MOSS7; KNOB11; TRAN7; AMOS; SIG13; TWIS; GNES2,3,9; ORWE.	nil
8	PUMP1; TWIS5,8; GNES17.	SOMB11; CHAN5; MOSS3.	nil	TRAN30; TIOG.	nil
9	TWIS4.	nil	nil	PUMP1; GNES17.	nil
10	HEY12; CHAN4; KNOB9.	nil	nil	HEY7-9,11,16;CHAN6; MOSS8,13,17,20; GNES19.	nil
	remainder (n=186)	nil	nil	remainder n = 146	nil
Cophenetic correlation	0.800858	0.676019	0.826086	0.881683	0.263651
Delta one-hat	0.554258	1.21554	0.357272	0.187765	23.0877
Gower's delta	731486	-2.256057E+06	-380716	47527.3	-8.575247E+09

Table 7.8 Comparison of cluster groups of surface-sediment mineral magnetic data using agglomerative hierarchical cluster methods (208 samples, 16 variables)

Differences in calculation cause some structural differences in the groupings. The first four methods have relatively high cophenetic correlations (r>0.75) and groups relate to some underlying structure in the data. Each method has variable usefulness in interpreting group structure. Nearest neighbour cluster analysis yields a high number of groups (n=11) and is dominated by single samples. The majority of samples (n=186) occur in the final group. Furthest-neighbour cluster analysis forms 8 groups. Group-average and weighted-group average methods appear similar but order the samples differently. Minimum-variance cluster analysis provides the most even distribution of samples within 6 groups, although the cophenetic correlation is low (r=0.26) in line with the classification results from the other sediment determinands (Chapters 5 and 6). Minimum variance cluster analysis divides the data-set in the most regular manner into 6 groups:

Group 1: n = 94	Group 2 = 7	Group 3 = 100
Group 4: n = 2	Group 5 = 12	Group 6 = 3

This sample classification is imposed on the results of ordination (Figure 7.24b).

7.9 Ordination

7.9.1 Analysis

Indirect ordination by PCA was performed in CANOCO (ter Braak, 1990) using the 208 samples by 16 variables data-set (sample PUMP2 removed) in a Euclidean distance matrix, centred and standardised by species. Results are summarised in Table 7.9. In the biplots of PCA axis 1 versus axis 2 sample scores (Figures 7.24a&b) variables with high positive correlations have small angles between their biplot arrows; variables with long arrows have high variance, and are generally more important within the data-set.

Table 7.9 **Eigenvalues and cumulative variance accounted for in a PCA of the 208 samples by 16 mineral magnetic variables data-set**

	Axis 1	*Axis 2*	*Axis 3*	*Axis 4*	*Total variance*
Eigenvalues	0.399	0.182	0.136	0.079	1.000
Cum.%var.sed.dat.	39.9	58.1	71.7	79.7	
Σ *unconstrained eigenvalues*					1.000

Capture of variance is very good and 79.9% of sample variance is accounted for in the

first four axes. Only the first three axes are significant in the ordination using the program BSTICK (H.J.B.Birks, unpublished). PCA axis 1 (0.399) defines a gradient between concentration measures, dominated by high values for all reverse field ratios, SIRM, magnetic susceptibility and $\varkappa_{ARM}$, versus HARD% and antiferromagnetic behaviour on the negative side of the biplot (Figure 7.24a). This gradient separates samples from Sombre, Changing, Moss, Emerald and Tranquil Lakes from Heywood, Knob, Amos, Twisted, Lake 13 and Bothy Lakes, and essentially follows a site classification based on lake trophy (Chapters 3, 5 and 6). A second gradient in the data-set on PCA axis 2 (0.182) defines samples with high values for $\varkappa_{ARM}$/SIRM, $\varkappa_{ARM}$, $\varkappa_{ARM}/\varkappa$, essentially measures of fine ferrimagnetic minerals and concentration, versus HARD% and HARD, displaying antiferromagnetic, coarser-grained properties. The outlier samples identified by their grain size characteristics (section 7.6.2) are strongly associated with diagnostic vectors for example, HEY13 and MOSS16 with $\varkappa_{ARM}$/SIRM, CHAN4 with $\varkappa_{ARM}/\varkappa$, SOMB11 with SIRM/$\varkappa$ and MOSS9, TIOG4 and SOMB25. Samples from Twisted, Emerald, Spirogyra, Bothy and Orwell Lakes are typically antiferromagnetic.

Figure 7.24 Biplots of PCA axis 1 and 2 scores for 208 samples and 16 mineral magnetic variables (a) classified by site (b) classified by minimum variance cluster groups

(a) Sites

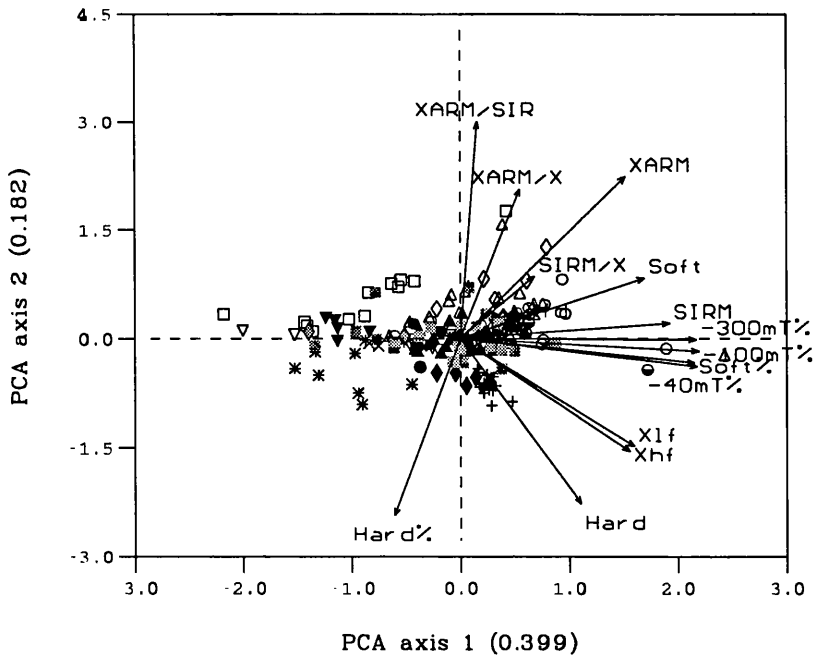

Figure 7.24b Classified by minimum variance cluster groups

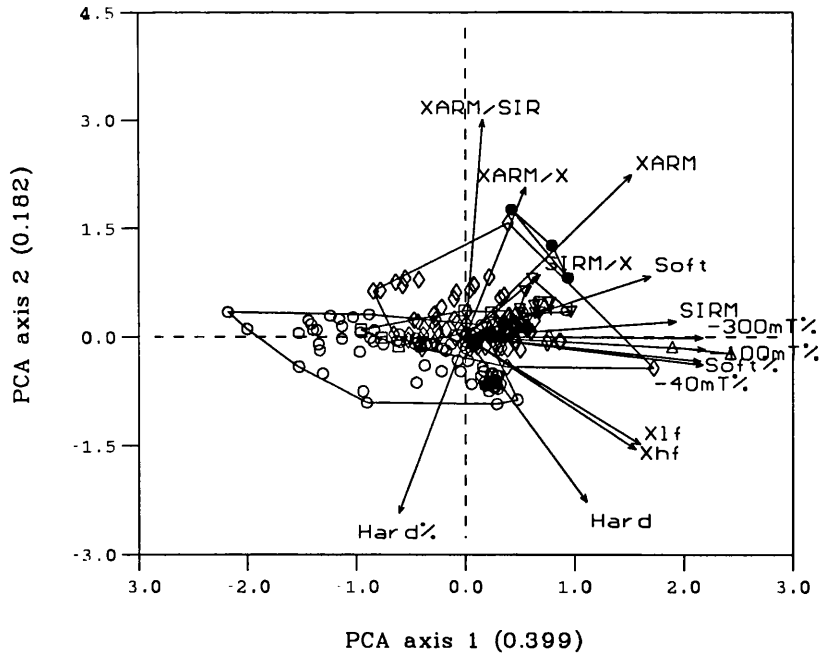

Group 1 ○ Group 2 □ Group 3 ◊ Group 4 ▵ Group 5 ▿ Group 6 ●

Sample classification by minimum-variance cluster analysis (Table 7.8) is imposed on the biplot (Figure 7.24b) to aid interpretation. Group 1 (open circles) is associated with the negative end of the first axis gradient with low values for concentration measures and fine-grain indicators, influenced by higher values for HARD and HARD% on axis 2. Group 2 (open squares) lies central to the ordination origin, with a linear spread towards the negative end of the axis 1 gradient, sharing characteristics with group 1. Group 3 (open diamonds) has a large distribution associated with both positive values for axes 1 and 2 but with tendencies towards higher concentrations and finer grain-sizes (high values for κ_{ARM}/SIRM, κ_{ARM}/κ, κ_{ARM}, SIRM/κ). Group 4 (up-triangles) has only two members - SOMB25 and MOSS9 - associated with extreme values of SIRM and normalized S-ratios. Group 5 (down-triangles) is a fairly discrete cluster associated with SOFT, SIRM/κ and SIRM. Group 6 (filled circles) has only three members - SOMB11, HEY13, and CHAN4 - and is associated with extreme values for ferrimagnetic indicators (κ_{ARM}, κ_{ARM}/κ, κ_{ARM}/SIRM, SOFT) as an outlier group, unusual with respect to the remainder of the data-set.

The PCA therefore differentiates samples on the basis of both their magnetic concentrations and grain-size variations. In summary, the first PCA axis defines a gradient of high concentrations to the right of the origin, versus low concentrations to

the left. The samples generally have a linear spread along this axis. The second PCA axis relates to grain-size variations. To the top, a non-detrital, bacterial signal indicated by high values for SSD determinands $\varkappa_{ARM}$/SIRM and $\varkappa_{ARM}/\varkappa$. Towards the bottom, a coarse-grained, detrital (haematite) signal indicated by HARD%. Within-lake variability is high and greatest for Moss, Heywood, Sombre, Gneiss and Changing Lakes. The smallest within-lake variability is found in Emerald, Spirogyra and Amos Lakes.

7.9.2 Canonical Variates Analysis

In previous chapters, CVA proved to be a useful method to simplify and model sediment-environment relationships (sections 6.8.2) to provide an interpretation of the causal factors responsible for variability in the contemporary sediment characteristics. CVA was performed in CANOCO (ter Braak, 1987; 1990) following the method outlined in section 5.8.2 using the 6 cluster groups from minimum variance cluster analysis (Table 7.9). Results of CVA are summarised in Tables 7.10 and 7.11.

Table 7.10 Forward selection of environmental variables in CVA of sediment mineral magnetic determinands (16 sediment variables in 6 cluster groups x 45 environmental variables)

Variable added	*cumulative variance of selected variables*	*number of permutations*	*Bonferroni required significance*	*significance achieved*
Clarity	0.52	999	0.05	0.001
% marble	1.02	999	0.025	0.001
July water temp.	1.14	999	0.016	0.001
% amphibolite	1.24	999	0.0125	0.002
Variance explained by all variables	1.54			
No other variables significant				

Five variables were chosen by forward-selection (Table 7.11) and found to be statistically significant ($p \leq 0.001$) and an unrestricted Monte Carlo permutation test (99 permutations) found both the first canonical axis 1 and the overall trace statistic to be significant at $p \leq 0.01$. In the biplot of CVA axis 1 versus CVA axis 2 scores (Figure 7.25), cluster groups D, E, C and F are similar and plot in the lower left quadrant of the biplot, associated with clarity, July water temperature and % amphibolite. Clusters A and

Table 7.11 CVA summary using variables identified in forward selection of sediment mineral magnetic determinands

Axes	*1*	*2*	*3*	*4*	*Total variance*
Eigenvalues:	0.633	0.522	0.128	0.019	5.000
Gp.env. r:	0.795	0.722	0.358	0.137	
Cum.% variance of gp.dat.:	12.7	23.1	25.7	26.0	
of gp-env relations:	48.6	88.7	98.6	100.0	
Σ *unconstrained eigenvalues*					5.000
Σ *all canonical eigenvalues*					1.302

B oppose each other and are highly dissimilar from Clusters D, E, C and F. Cluster B is found in the upper left quadrant, associated with high values for % marble. Cluster A is found along the positive end of the first CVA axis gradient with low clarity, low July water temperatures and the influence of Chl-*a*, the surrogate for lake trophy.

Figure 7.25 CVA biplot of the 6 cluster groups of surface-sediment mineral magnetic variables (n=4) in relation to significant variables on CVA axes 1 and 2

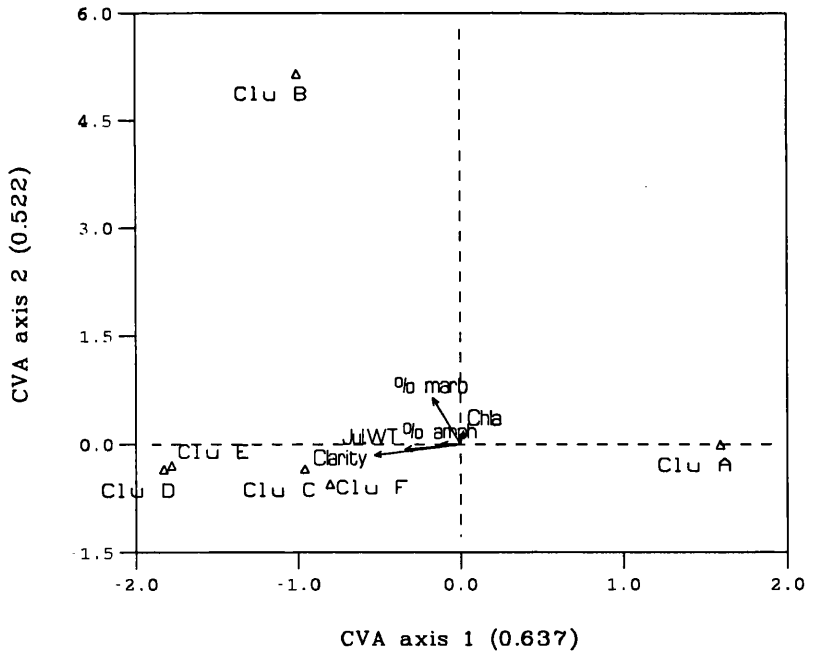

26.04% (1.302/5.0) of the between-group variation is explained by the canonical (constrained) eigenvalues of the five forward-selected environmental variables. 23.1% of variance in the sediment data was explained by the first two CVA axes. Both the F-ratio for the significance test of the first canonical axis (16.59) and the overall test

statistic (9.83) exceed the critical F value ($F>1.57$, $p<0.05$ for 16 and 206 degrees of freedom). Significant inter-set correlations ($r>|0.195|$) for CVA axis 1 are found for clarity, July water temperature and % marble; for CVA axis 2, % marble and Chl-*a*. Canonical coefficients for clarity, July water temperature, Chl-*a* and % marble are significant ($r>|1.96|$) for CVA axis 1; for CVA axis 2 the canonical coefficients for % marble, % amphibolite, clarity and Chl-*a*.

Source lithology clearly affects mineral magnetic behaviour in the sediments and resultant group discrimination. Both amphibolite and marble geologies are noted for their high iron contents (section 7.7.1). There is also a lake climate component in the ordination (light climate and July water temperature). High winter water temperatures affect rates of chemical transformations, especially those that are microbially-mediated (Ellis-Evans & Lemon, 1989) and possibly responsible for authigenic magnetite formation which has produced a non-detrital magnetic mineral signature (section 7.6.3). Clarity relates to the volume of suspended materials in the water column, either minerogenic from allochthonous sources or organic through the phytoplankton. The selection of Chl-*a* reflects an underlying trophic gradient which affects organic contents in the sediments and therefore the predisposition to authigenic magnetic mineral formation through abiotic (section 7.7.3) or biotically-mediated reactions (section 7.7.4).

7.10 Discussion

7.10.1 Surface-sediment mineral magnetic characteristics

The mineral magnetic data in this Chapter provides another source of information on the contemporary sediments and environmental processes responsible for their characteristics. In keeping with Arctic lakes (Snowball, 1994), the results show that high mineral magnetic concentrations can exist in surface sediments in steady state environments which are relatively unaffected by human activity. Numerical analysis suggests that many processes of interest to the environmental magnetist are occurring within sub-sets of lakes but the noise in the full sample-set obscures these details (for example, the *t*-tests of all lakes versus individual lakes). Many questions remain unanswered but more detailed analysis was beyond the objective of this Thesis. The principal concern at this stage is whether (i) the mineral magnetic parameters are sensitive to the environmental variable of interest (i.e. catchment ice-cover as a proxy for climate) and (ii) they are conservative enough to be preserved in the sediment record without any major diagenetic changes ('no analogue' problem).

Fine ferrimagnetic grains are usually scarce in unweathered parent materials (Oldfield, 1991) and the bedrock of Signy Island is a source of predominantly coarse-grained (MD), paramagnetic minerals to the lake sediments. Paramagnetism complicates the measurement of $\varkappa$ in these samples. Despite these analytical problems and increased random noise in the data-set through oxidative diagenetic changes during storage, it is apparent that a large number of samples are mixtures of fine-grained, SSD and/or coarser MD magnetites (cf.Thompson & Morton, 1979) given the relatively low values for haematite indicators HARD and HARD%. Thus, the mineral magnetic behaviour of the surface-sediments has a two-component signature which varies both within and between lakes: (i) a terrigenous, detrital signal and (ii) a fine ferrimagnetic, non-detrital signal. The second component is most unlikely to have been derived from the dominant catchment source mineralogies, although availability of iron from certain lithologies probably plays a role in determining concentrations. Authigenic mineral formation is apparently active in these lakes, probably in association with bacteria. This fine-grained, high-concentration versus coarse-grained, lower concentration gradient is clearly captured in the ordinations and classifications. Variability in the sample-set is largely dependent on concentration effects and the grain-size of this second component (i.e. varying proportions of ferrimagnetic minerals relative to the baseline terrigenous magnetic minerals) such that some lakes have considerably enhanced concentrations (Light, Moss, Tioga) and others are only marginally affected (Emerald). This ferrimagnetic enhancement is associated with mid-silt range particles, the dominant size-fraction (section 6.9.1). These materials might also provide the best substrates for bacterial magnetosome activity and authigenic magnetic mineral formation is commonly associated with sediments of higher organic contents.

An imperative assumption of the reconstruction method is that the underlying catchment signature can be identified in the sediments, since the allochthonous 'detrital' materials are responsive to processes in the catchment and, by inference, climate effects. The constancy of this detrital material is most evident in Emerald Lake, which displays highly homogenous mineral magnetic characteristics. Wilson (1993) qualitatively linked parallel variations in magnetic parameters in Sombre and Heywood Lakes as responses to processes occurring in the catchments (and by inference, climate) and believed that authigenesis and/or diagenesis was minimal in core profiles. This is encouraging since reuslts here suggest that surface-sediment samples from these lakes appear to include variable proportions of SSD sized materials of non-detrital origin. It is possible that they

are not preserved at lower levels in the stratigraphy.

Redox conditions at the surface-sediment-water interface are complex in these lakes, and iron is active in many reactions (Ellis-Evans & Lemon, 1989). Seasonal anoxia promotes ideal conditions for the production of authigenic iron sulphides but there is no convincing evidence for authigenic greigite formation, except in one sample (PUMP2), although it is highly likely that any greigite may have been lost during storage. Tephra offers another potential source for magnetic minerals but its influence is probably minimal owing to dilute concentrations and its presence below the resolution of the surface samples, except in zones of active erosion and resuspension. Storage diagenesis have taken some effects, with a likely loss of fine-grained ferrimagnetic minerals but the magnitude of this loss is impossible to gauge. Despite evident post-depositional modifications of the suface sediments in this sample-set, Wilson (1993) was unable to find evidence for post-depositional changes in Holocene sediment sequences from Sombre or Heywood Lakes.

7.10.2 Catchment development and mineral magnetic characteristics

Results from previous chapters show that clear trends can be observed between glacier-fed and non-glacier fed lakes relating to changing volumes of allochthonous inputs relative to the autochthonous component. With maturation and stabilisation of the catchment the volume of allochthonous mineral inputs should decrease. Stober & Thompson (1979) noted the gradual depletion of sources of fine-grained ferrimagnetic minerals with maturation of the drainage basin coupled with declining allochthonous contribution to the lake sediments. The authors postulated that as the catchment developed, allogenic inputs were diluted by varying volumes of allochthonous and autochthonous organics, reducing the strength of mineral magnetic behaviour. They used the ARM gradient in ferrimagnetic mineral concentration as a proxy for lake evolutionary status. Adopting the hypothesis that the Signy lakes follow an evolutionary series (Heywood, Dartnall & Priddle, 1980), the same rationale was applied, but no clear ARM gradient could discern 'mature', coastal lowland from 'young' upland lakes. Rank minimum ARM (using the minimum removes the effects of the authigenic ferrimagnetic component, thus showing the underlying trend in allochthonous source materials) produces the following order: Tioga > Changing > Bothy > Moss > Sombre > Tranquil > Emerald > Lake 13 > Orwell > Spirogyra > Pumphouse > Gneiss > Amos > Heywood > Light > Knob > Twisted. Lower ARM values show a slight tendency to be found in

the lowland lakes but the pattern is not exclusively a function of age. The clear division between glacier-fed and non-glacier fed lakes seen in the other data-sets is less easily discriminated using mineral magnetic measurements. Unlike Stober & Thompson's (1979) study area in Northern Ireland, ferrimagnetic minerals are scarce in these catchments because of the nature of the parent materials and the lack of soil development and secondary mineral formation.

Instead, declining allochthonous sediment inputs seem to favour greater production of authigenic magnetic minerals with longer exposure time of the surface-sediment with the water column. The highest concentrations of ferrimagnetic minerals are found in lakes with cyanobacterial mats and/or freshwater mosses which require relatively low rates of sedimentation to allow their sustained growth. On the basis of research in Arctic Sweden, Snowball (1993b) argued that under ameliorating climates, low sediment accumulation rates, enhanced lake productivity and higher organic carbon contents produce intense reducing conditions with almost complete magnetite loss; climatic deterioration, glacier reformation and increased sedimentation rates reduce organic carbon input to the sediments, permitting good magnetite preservation. The Signy surface sediments are also representative of geochemical environments of deposition but the causal mechanisms for variation are less clearly defined. Certainly, the more eutrophic lakes (Heywood, Knob, Amos) appear to have lower magnetic concentrations, perhaps resulting from diagenetic loss of magnetite but more likely a function of lower sediment receipt and higher proportions of inwashed allochthonous organics diluting overall mineral concentrations. Other oligotrophic lakes with low sediment accumulation rates and high organic contents have the highest magnetic concentrations indicating authigenic magnetite production. Oligotrophic lakes with higher rates of sediment delivery (Sombre, Emerald) have moderate magnetic mineral concentrations but minerals are coarse-grained and representative of low-concentration, catchment source materials. These questions may only be answered by more detailed laboratory and statistical analyses.

7.11 Summary

(1) The values of many of the measures and quotients match the results of a previous study of Holocene sediment sequences at Sombre and Heywood Lakes (Wilson, 1993) and are of comparable magnitude to those from Late-Glacial lake-sediments from temperate latitudes. The Signy lake-sediments are characterized by large, multi-domain

grain-sizes of terrigenous, detrital origin, i.e. catchment-derived. Magnetic behaviour matches expected values from predominantly coarse-grained, paramagnetic minerals from unweathered source materials and coarse MD magnetite material typical of lake sediments. The lack of pedogenesis in the catchments limits the potential allochthonous input of secondary ferrimagnetic minerals which would otherwise be useful diagnostic indicators of erosion. Deviations in magnetic behaviour with changing lithology (amphibolites and marbles) are not obviously apparent against the clear grain-size and concentration gradient in the sample-set.

(2) A second magnetic component is superimposed on the baseline, catchment-derived, detrital signal dominating the overall behaviour of most samples. This is of fine-grained (SSD) ferrimagnetic minerals which, given the nature of catchment materials, can only be of authigenic origin. Redox-mediated reactions and bacterial activity have been noted in the iron chemistry of these lakes and post-depositional modification of magnetic mineral assemblages has led to magnetite formation, rather than diagenetic magnetite loss. One sample (PUMP2) is highly unusual and possibly contains greigite, arising from the local weighting of marble lithology and reducing conditions. Owing to previous anthropogenic impacts at this site the decision was taken to exclude the sample from further analysis until its mineralogical make-up could be explained.

(3) Storage diagenesis has probably affected the samples, decreasing overall values for magnetic phases sensitive to oxidative changes and in doing so, increasing the overall sample-set variability in an uneven manner. It is impossible to assess the overall magnitude of these changes. Most results match those of Wilson (1993) for Sombre and Heywood Lakes. This benchmark however, is also unreliable as Wilson worked on material that had been stored in cold, moist conditions for two years prior to measurement.

(4) There is no clear evidence for tephra in the surface sediment sample-set. The uppermost tephra horizon, corresponding to 1957-1968 AD, lies below the 0-1 cm surface-sediment layer in accumulation zones. Areas subject to resuspension and mixing could feasibly include a tephra component and with variable sedimentation rates in different parts of each lake basin and between each lake the introduction of tephra noise to the mineral magnetic behaviour cannot be entirely discounted. It is however, seen to be a minor potential addition to the overall behaviour in the sample-set.

CHAPTER 8: A SYNTHESIS OF CONTEMPORARY SEDIMENT CHARACTERISTICS AND SEDIMENT-ENVIRONMENT INTERACTIONS

8.1 Introduction

In previous chapters, data characterising the contemporary environment of the Signy lake catchments were presented and analyzed to find the major environmental gradients and an updated classification of the lakes (Chapter 3). Sediment samples were collected from multiple point locations in all the lake basins (Chapter 4) and surface-samples were analyzed for their organic and minerogenic, particle-size and mineral magnetic characteristics (Chapters 5, 6 and 7). Analysis of these separate data-sets has shown that these quantitative sedimentological data behave in a similar way to quantitative biological data (Birks, 1995), in that they are highly complex and variable with skewed distributions, show collinear relations and therefore possess some redundancy. In the first part of this Chapter, the surface-sediment data from the individual data-sets are merged into one data-matrix of 208 samples and 26 variables and relationships are summarised using classification and indirect ordination methods. The full data-set is termed the 'training-set' (refer Figure 1.2) and this analysis forms an intermediate step before deriving the quantitative reconstruction in Chapter 9.

In the second part of this Chapter, a combination of direct ordination and classification methods are used to study sediment-environment interactions and to reduce the data into manageable, environmentally-relevant components. Applied ecological studies require direct methods of ordination (ter Braak, 1994), typically with a limited number of qualitative or quantitative environmental variables. Data screening in direct ordination allows for data-reduction, leaving a sub-set of relevant, statistically significant explanatory environmental variables known as the *minimum adequate model*, thus removing redundant variables with little influence on the lake sediments. Variance partitioning of the different sediment fractions is used to assess the relative balance of intrinsic, limnological factors and extrinsic, catchment factors in determining sediment characteristics. A climatically-relevant environmental variable is selected from this sub-set of variables to form the basis of the reconstruction (Chapter 9).

The aims of this Chapter are thus (i) to combine the different sediment data-sets and to provide an overall summary of the surface-sediment characteristics (section 8.2) and (ii) to model relationships between the sediments and the environment data-set (sections 8.4-

8.6) as a precursor to the environmental reconstruction in Chapter 9.

8.2 Analysis of combined surface-sediment data

8.2.1 Classification

This data-set, with its large numbers of samples and variables, is typically noisy. Classification can be used to improve the distinction between sample and site (di)similarities. Five methods of agglomerative hierarchical cluster analysis were performed using the program CLUSTER (H.J.B.Birks, unpublished) using the procedure outlined in section 3.6.2. Group memberships are listed in Table 8.1.

MOSS12 and LITE2 are clearly outliers, occurring singly or together in the classifications from four methods. Other outlier samples include LITE2, MOSS16, SOMB25, MOSS9, TWIS6, ORWE2 and other samples from Light and Tioga Lakes. Single-link cluster analysis performs poorly and is only able to resolve variation into 18 groups, the first ten of which are mostly of single samples. Group-average cluster analysis has the highest cophenetic correlation (r=0.89) but also finds a large number of groups (n=14). Furthest-neighbour cluster analysis has a better spread of samples in 13 groups, similar group memberships and a relatively high cophenetic correlation (r=0.84). Weighted-group average cluster analysis finds 10 groups which are similar in structure to furthest-neighbour groups but has a lower cophenetic correlation (r=0.68). Minimum variance finds the simplest structure with regular groupings (n=6) and is less affected by outlier samples. It divides the data-set into the following groups:

Group 1: n = 77	Group 2: n = 62	Group 3: n = 54
Group 4: n = 2	Group 5: n = 2	Group 6: n = 11

In common with the minimum variance cluster analyses of the individual sediment data-sets, the cophenetic correlation is low (r=0.31). Group 1 includes all samples from Light, Amos and Tioga Lakes and the majority of samples from Heywood, Moss, Knob, Tranquil, Twisted and Gneiss Lakes. Other samples in the group are from Sombre, Changing, Pumphouse, and Orwell Lakes. Group 2 includes all samples from Spirogyra, Emerald, Lake 13 and Bothy Lakes, the majority of samples from Knob Lake and other samples from Sombre, Pumphouse, Tranquil, the delta-front sample from Gneiss Lakes, the Ekman grab samples from Changing Lake and one sample from Orwell Lake. Group 3 includes outlier samples SOMB25 and MOSS9 only. Group 4 includes a third of the

Group membership	*Nearest neighbour (single-link)*	*Furthest neighbour (complete-link)*	*Weighted group average*	*Group average*	*Minimum variance (Ward's method)*
1	MOSS12.	MOSS12: LITE2.	MOSS12: LITE2.	MOSS12: LITE2.	SOMB23.30.35: HEY5-12.14-16: CHAN6.11: MOSS4.7.8.11-13.16-20: KNOB2.4.6.9.11: PUMP4.5.6: LITE: TRAN7-10.16.25-29: AMOS: TIOG: TWIS3-8.10-12: GNES2.3.4.8.9.13-16.19.20.22: ORWE2.
2	LITE2.	HEY12: KNOB9: ORWE2.	SOMB37.41: HEY5.6.10.12.14-16: CHAN13.14: KNOB1.9.11: PUMP3: TRAN20.30: AMOS: SIG13: TWIS3-5.7-11: GNES2.3.9: ORWE.	MOSS16.	SOMB26.27.31.37.40.41: CHAN13.14: KNOB1.3.5.7.8.10: PUMP3.7: SPIR: TRAN4.5.12-15.17-21.30: EMER: SIG13: BOTH: GNES12: ORWE1.
3	MOSS16.	SOMB25: MOSS9: TIOG.	MOSS16.	SOMB25: MOSS9.	SOMB25 MOSS9.
4	TIOG4.	HEY13: CHAN4.5: MOSS16.	SOMB25: MOSS9.	TIOG.	SOMB13.15-21.24.28.29.32-34.36.38.39.43-46: CHAN2.3.7-10.12: MOSS5.6.14: PUMP1: TRAN6.11.22-24: GNES5.6.10,11,17.18.21.
5	SOMB25: MOSS9: TWIS6.	LITE3-5: TWIS6.	TIOG.	LITE3.4.5: TWIS6.	HEY13; CHAN4.5.
6	HEY12: TRAN9.	SOMB37.41: HEY5.6.10.14.15: CHAN13.14: KNOB11: TRAN20.30: AMOS: SIG13: TWIS3-5.7-11: GNES2.3.9: ORWE1.	LITE3.4.5: TWIS6.	HEY13.	SOMB11.12.14.22.42: MOSS3.10.15.21.
7	LITE3.4.5: TIOG.	HEY7-9.11: CHAN6.11: MOSS4.8.11.13.17.19.20: KNOB2: PUMP4.6: TRAN27.28: GNES8.14.19.20.22.	TRAN9.	HEY5.6.10.14.15.16: KNOB9.11: AMOS3.4.6.7: ORWE2.	nil
8	KNOB9.	SOMB13.20.21.23.26.27.30.31.35.40.43: CHAN2: MOSS7.18: KNOB1.3-8.10: PUMP3.5.7: SPIR: TRAN4-8.10.12-19.21-26.29: EMER: TWIS12: BOTH: GNES4.10.11-13.16:	SOMB12-24.26-36.38-40.42-46: HEY7-9.11: CHAN2.3.6-12: MOSS4.5.7.8.10.11.13.14.17-20: KNOB2-8.10: PUMP1.4-7: SPIR: TRAN4-8.10-19.21-29: EMER: TWIS12: BOTH: GNES4-6.8.10-22.	TRAN9.	nil
9	ORWE2.	SOMB15-19.24.28.29.32-34.36.38.39.44.45.46: CHAN3.7-10.12: MOSS14: PUMP1: TRAN11: GNES5.6.15.17.18.21.	HEY13.	TWIS3-5.7-11: GNES2.3.9.	nil
10	TRAN30. Remainder (n=189) in 8 groups.	MOSS5.6. Remainder (n=9) in 3 groups.	SOMB11: CHAN4.5: MOSS3.6.15.21.	SOMB37.41: CHAN13.14: TRAN20.30: SIG13: ORWE1. Remainder (n=57) in 4 groups.	nil
Cophenetic correlation	0.854846	0.834945	0.677718	0.884740	0.313895
Delta one-hat	0.479646	0.666868	0.562074	0.166720	19.1624
Gower's delta	805997	-1.805636E+06	-1.684757E+06	46465.0	-7.655353E+09

Table 8.1 Comparison of cluster groups of all surface-sediment variables using agglomerative hierarchical cluster methods (26 variables, 208 samples)

samples from Sombre Lake, the majority of samples from Changing and Gneiss Lakes, other samples from Moss and Tranquil Lakes and one sample from Pumphouse Lake (PUMP1). Group 5 has only three samples: HEY13, CHAN4 & 5. Group 6 has only 9 members from Sombre and Moss Lakes only, indicating some sedimentological similarity in the two lakes. These groups are used to classify samples on the ordination biplot (Figure 8.1c) to simplify the interpretation.

8.2.2 Indirect ordination

Principal Components Analysis was performed using CANOCO (ter Braak, 1987; 1990) on untransformed data in a Euclidean distance matrix. As in previous chapters, samples were centred and standardized by variables, removing the need to transform mixed-unit data. Results are summarised in Table 8.2.

Table 8.2 Eigenvalues and cumulative variance accounted-for by PCA of the 208 samples by 26 sediment variables data-set

	Axis 1	*Axis 2*	*Axis 3*	*Axis 4*	*Total variance*
Eigenvalues	0.279	0.221	0.110	0.089	1.000
Cum.%var.sp.dat.	27.9	50.0	61.1	69.9	
Σ *unconstrained eigenvalues*					1.000

The capture of variance in the sediment data-set by the first two PCA axes (50.0%) is low relative to the individual data-sets but reasonable. The PCA axis 1 gradient is determined by all particle-size determinands, %DW, wet density, HARD% and %Min versus normalized reverse field ratios, SIRM, SOFT, κ_{ARM}, magnetic susceptibility, HARD and remaining determinands. Samples most associated with the positive end of this gradient are from Heywood, Knob, Orwell and Amos Lakes; those least associated are samples from Moss, Tioga, Gneiss, Changing and Sombre Lakes. The second PCA axis defines a gradient on the basis of high organic content and %BSi, κ_{ARM}/SIRM, κ_{ARM}/κ and SOFT versus minerogenic content, magnetic susceptibility, %DW, wet density, HARD, median particle-size and remaining magnetic and particle-size determinands. Samples most associated with the positive end of this gradient include those from Moss, Light, Tioga, Gneiss and Twisted Lakes; samples from Changing, Moss, Emerald and Sombre Lakes are most associated with the negative end of this gradient.

Figure 8.1 **Biplot of PCA axis 1 and 2 scores for all surface-sediment determinands (n=26) (a) sediment determinands (b) samples classified by sites (c) samples classified by minimum variance cluster groups**

(a) Sediment determinands only

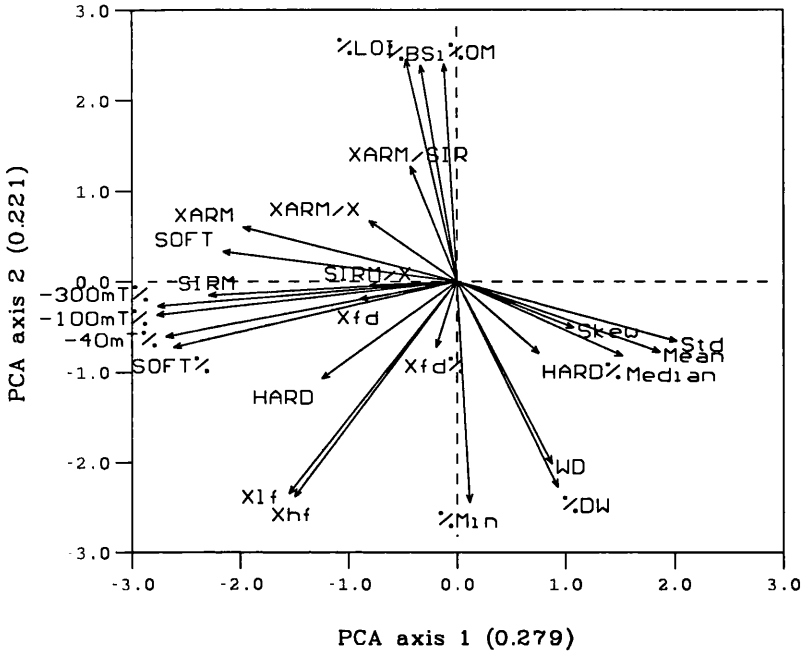

(b) Samples classified by sites

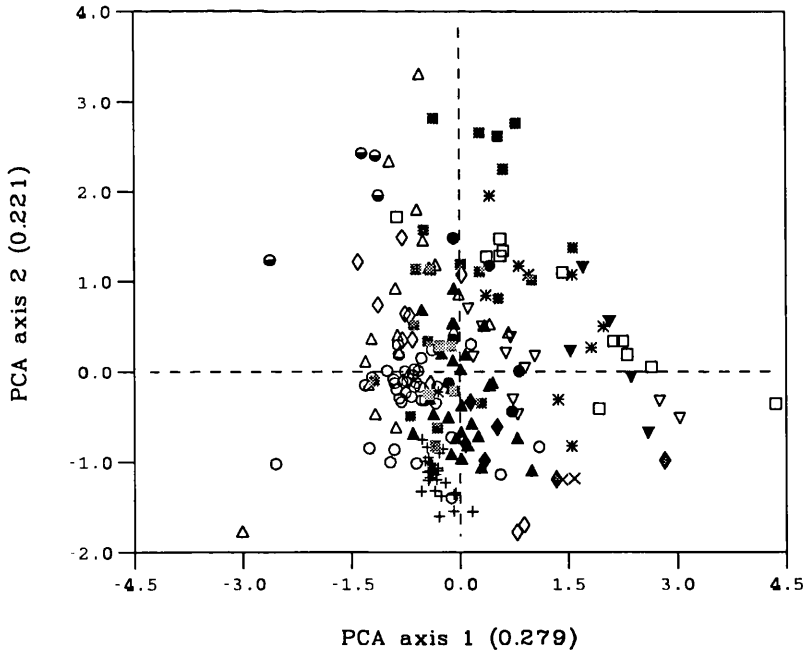

In the PCA biplot of axis 1 versus axis 2 scores (Figure 8.1a) sediment determinands are represented by arrows. In Figure 8.1b, samples are classified by sites. Sombre (open circles), Moss (open up-triangles), Changing (open diamonds), Knob (open down-

down-triangles), Pumphouse (filled circles), Heywood (open squares), Tranquil (filled up-triangles), Gneiss (grey squares) and Twisted (stars) Lakes have wide distributions. Of these, only Heywood Lake plots far from the origin, associated more with organic matter, %BSi, high κ_{ARM}/SIRM (SD magnetic grain-sizes) and coarse particle-size. Samples from Emerald (plusses), Lake 13 (crosses), Spirogyra (filled diamonds), Tioga (half-filled circles), Tranquil (filled up-triangles), Amos (filled down-triangles) and Light (filled squares) have tighter distributions.

Figure 8.1c **Samples classified by minimum variance cluster groups**

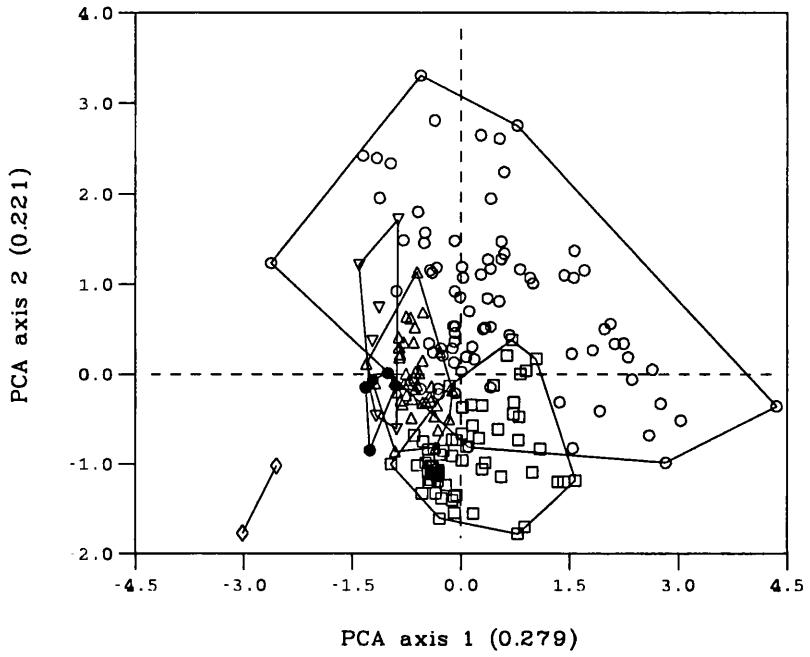

In Figure 8.1c samples are classified by their group memberships from minimum variance cluster analysis (Table 8.1). Five of the six groups share overlapping distributions. Group 1 (open circles) has a wide-ranging distribution along the PCA axis 1 gradient, but is predominantly associated with higher values for particle-size determinands, i.e. coarser samples, and high values for organic contents and %BSi. Group 2 (open squares) shares some overlap with group 1 but its distribution is predominantly determined by the PCA axis 2 gradient, samples having high minerogenic contents and high values for %DW, wet density and HARD% (antiferromagnetic concentration). Group 3 (open diamonds) has only two members (SOMB25, MOSS9) and plots as an outlier group at the extreme negative end of the PCA axis 1 gradient,

with the highest values for normalized reverse field-ratios (very soft ferrimagnetic behaviour) but also high values for HARD and magnetic susceptibility, indicating higher magnetic concentrations arising from two sources. Group 4 (up-triangles), close to the origin but along the negative side of the PCA axis 1 gradient, is most associated with high values for magnetic concentration parameters and with finer particle-size and higher organic contents. Group 5 (down-triangles) has a restricted distribution along the negative end of the PCA axis 1 gradient but has characteristics across the range of the PCA axis 2 gradient, displaying both highly minerogenic and organic behaviour. Group 6 (filled circles) plots to the right of the origin in a fairly tight cluster and is most associated with measures of ferrimagnetic concentration and behaviour ($\varkappa_{ARM}$, ARM, SOFT) and the finest particle-sizes.

The variance explained in a PCA of the combined data-set is considerably less than the individual data-sets (Table 8.3) and greater noise with more variables weakens the strength of the first axis gradient, which is principally determined by minerogenic versus organic sediment characteristics. In common with diatom species assemblage data-sets, some determinands have a negligible influence (short gradient) and others profound (long gradient). Grain-size is highly influencial in the data-set and the standard deviation of the mean particle-size had the largest eigenvector or loading in the PCA.

Table 8.3 Percentage variance explained in the sediment data in PCA of individual and combined surface sediment data-sets

Data-set	*n determinands*	*n samples*	*Axis 1*	*Axis 2*	*Axis 3*	*Axis 4*	*Total variance*
organic & minerogenic	6	209	68.8	85.5	93.3	97.8	1.000
particle-size	4	209	71.7	92.6	99.9	100	1.000
mineral magnetic	16	208	39.9	58.1	71.7	79.7	1.000
combined	**26**	**208**	**27.9**	**50.0**	**61.1**	**69.9**	**1.000**

8.2.3 Canonical Variates Analysis

In chapters 5, 6 and 7 direct ordination of sediment cluster groups and environmental variables in CVA was used to clarify the possible origin of the respective fractions of the sediment. Here, CVA provides a summary of the major environmental influences controlling overall sediment character. Cluster groups from minimum variance cluster

analysis (Table 8.1) were used in CVA using the procedure outlined in section 5.8.2.

Figure 8.2 CVA biplot of the 6 cluster groups of surface-sediment data (26 variables) in relation to significant environmental variables on CVA axes 1 and 2

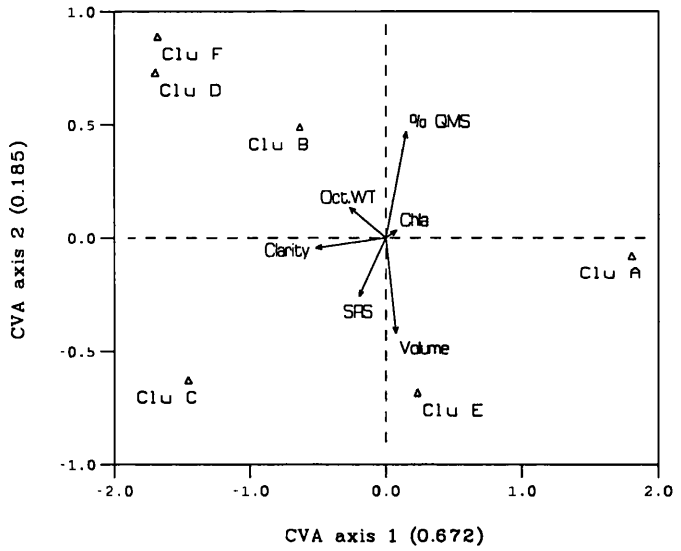

Six variables were chosen by forward-selection and found to be statistically significant ($p \leq 0.001$) (Table 8.4) and both the first canonical and the overall trace statistic using 99 unrestricted Monte Carlo permutations confirmed the significance ($p \leq 0.001$) of the model. Lake water temperature (winter maxima) and light climate (clarity) clearly affect sediment type, also relating to lake morphology (volume) and indirectly relating to catchment development (%QMS as a surrogate for deglaciated terrain). The lake productivity gradient is represented by Chl-*a* and soluble reactive silicate which to some degree also reflects catchment development.

In Figure 8.2, environment variables are plotted as vectors relative to the sample cluster groups in a biplot of CVA axis 1 versus axis 2 scores. The pattern of clusters is well-dispersed. The CVA axis 1 gradient, determined by clarity and October water temperature versus their negative scores, separates Cluster A from the remaining groups. The second CVA axis gradient (volume, SRS and clarity versus %QMS, Chl-*a* and high October water temperature) separates Clusters A, C and E from Clusters B, D and F. Clusters B, D and F are most associated with positive scores for October water temperature and % quartz-mica-schist. Cluster A has a strong positive association with the CVA axis 1 gradient, with low clarity and high Chl-*a*. Cluster E is determined more

by the second CVA axis, strongly associating with lake volume and soluble reactive silicate. Cluster C plots in the bottom left quadrant and is associated with high clarity, soluble reactive silicate but opposite to the vectors for Chl-*a* and % quartz-mica-schist.

Table 8.4 Summary results for CVA of the surface-sediment data-sets (208 samples)

Data type	*All variables*	*Organic & minerogenic*	*Particle-size*	*Mineral magnetic*
No. of variables	26	6	4	16
No.of clusters	6	6	4	7
Axis 1 λ	0.672	0.776	0.422	0.637
Axis 2 λ	0.185	0.601	0.202	0.522
Axis 1 r	0.820	0.881	0.650	0.795
Axis 2 r	0.431	0.775	0.449	0.722
Axis 1 % gp var.	13.4	15.5	14.1	12.7
Axis 2 % gp var.	17.2	27.6	20.8	23.1
Axis 1 % gp-env	65.2	41.6	63.8	48.6
Axis 2 % gp-env	83.2	73.9	94.3	88.7
Σ *unconstrained eigenvalues*	5.000	5.000	3.000	5.000
Σ *all canonical eigenvalues*	1.031	1.865	0.662	1.302
% explained	20.6	37.3	22.1	26.04
Forward selected environmental variables (rank order of influence)	Clarity October WT Volume SRS Chlorophyll-*a* % quartz-mica-schist	% ice Catchment area % amphibolite Elephant seals Cl^- Phaeopigments Maximum altitude SRS Maximum depth Catchment:lake area % quartz-mica-schist	Maximum depth Clarity Volume Maximum altitude % quartz-mica-schist	Clarity % marble July WT % amphibolite Chlorophyll-*a*

λ = eigenvalue; *r* = species-environment correlation; % gp var. = explained percentage variance of the groups data; % gp-env = explained percentage variance of group-environment relationships.
Underlined variables also selected in CVA using 209 sample-set (incl. PUMP2).

All forward-selected environmental variables significant ($p \leq 0.001$) in unrestricted Monte Carlo permutation tests (999 permutations) with Bonferroni Adjustment.

20.6% (1.031/5.00) of the between-group variation is explained by the canonical (constrained) eigenvalues of the six forward-selected environmental variables (Table 8.4). Only 17.2% of variance in the sediment data is explained in the first two CVA axes. Both the F-ratio for the significance test of the first canonical axis (31.22) and the overall test statistic (8.70) exceed the critical F-ratio value ($F>1.46$, $p<0.05$ for 30 and 206 d.f.). Significant inter-set correlations ($r>|0.195|$ at $p\leq0.05$) for CVA axis 1 are met by clarity, October water temperature, soluble reactive silicate and % quartz-mica-schist; for CVA axis 2, % quartz-mica-schist and volume. Only the canonical coefficient for clarity is significant ($r>|1.96|$) for CVA axis 1; none are significant for CVA axis 2.

Results of this CVA are compared with results of individual CVAs of the respective data-types in Table 8.4. Since outlier sample PUMP2 was removed in Chapter 7 on the basis of its extreme magnetic behaviour, all the CVAs were repeated using minimum variance cluster groups for 208 samples (Table 8.5). There are therefore subtle differences in the environmental variables chosen by forward selection illustrating the sensitivity of the method to differing numbers of cluster groups and their constituent memberships. For example, in the updated CVA of the minerogenic and organic determinands (n=208), there are 6 cluster groups, not 5. Fewer variables (n=11) are selected and of these, only 6 (% ice-cover, % amphibolite, elephant seals, maximum altitude, Cl^- and phaeopigments) match the earlier results (section 5.8.2). None of the variables selected in the new CVA with the particle-size summary-statistics match those before (section 6.8.2). Sample PUMP2 also displayed unusual particle-size characteristics and exerted considerable leverage in cluster analysis (section 6.6.1).

Relationships between the forward-selected variables from these 208-sample CVAs are summarised in the venn diagram (Figure 8.3). Clearly, different sediment fractions relate to different combinations of explanatory variables. October water temperature was selected in the full model of all sediment determinands but was not represented in the individual CVAs. Explanatory variables which recur in the data-sets include lake climate (clarity, water temperature) and productivity determinands (Chl-*a*, soluble reactive silicate) and % quartz-mica-schist as a surrogate for catchment development. CVA is therefore a useful means of illustrating the subtle response of sediments to different explanatory variables in a broad sense. This is repeated in a more detailed and deterministic way using variance partitioning (section 8.5).

Group membership	*Minerogenic and organic (n=6)*	*Particle-size (n=4)*	*Mineral magnetic (n=20)*	*All sediment variables*
1	MOSS12; LITE; TIOG; TWIS6.	SOMB21.26.27.31.37.40.41; HEY5.6.10.12.14-16; CHAN13.14; KNOB1.3.5.8.10.11; PUMP1.3.7; SPIR4; TRAN4.5.12.13.17-20.21.30; AMOS4-7; EMER24; SIG13; TWIS5.8; BOTH1; GNES10.11.12.18. ORWE.	SOMB37; HEY5.6.10.12.14.15; MOSS7; KNOB1.3-11; PUMP3.5; SPIR; TRAN16.20.30; AMOS; EMER; SIG13; TWIS3-5.7-12; BOTH; GNES2-4.9.12.13.16; ORWE2.	SOMB23.30.35; HEY5-12.14-16; CHAN6.11; MOSS4.7.8.11-13.16-20; KNOB2.4.6.9.11; PUMP4.5.6; LITE; TRAN7-10.16.25-29; AMOS; TIOG; TWIS3-8.10-12; GNES2.3.4.8.9.13-16.19.20.22; ORWE2.
2	SOMB12.13.37.41; HEY12.14; CHAN13.14; KNOB9.11; TRAN12.17.18.20; AMOS7; EMER1-4.6-32; SIG13. ORWE.	SOMB42; CHAN6; MOSS3.6.7.11-13.15.17.19-21; KNOB2; LITE3-5; TRAN28; TIOG1; EMER1-3.6-12.14-18.21-23.26-29.30.31; TWIS6.9.10; GNES2.4.19.20.	MOSS12; PUMP1; LITE; GNES17.	SOMB26.27.31.37.40.41; CHAN13.14; KNOB1.3.5.7.8.10; PUMP3.7; SPIR; TRAN4.5.12-15.17-21.30; EMER; SIG13; BOTH; GNES12; ORWE1.
3	SOMB33; CHAN5.6.8.11; MOSS5.11.13.16.17.20; PUMP5; TRAN28; AMOS4; TWIS4.10; GNES2.5.8.14.17.19-22.	SOMB13.22.24.29.30.32.36.38.39.43-46; HEY7.8.9.11.13; MOSS9.10.16; KNOB6.7.9; PUMP5.6; SPIR2.3; TRAN6.14-16.22.23; AMOS3; EMER4.13.19.20.25.32; TWIS3.4.7.12; GNES16.17.21.	SOMB13.15-21.23.24.26-36.38-41.43-46; HEY7-9.11.16; CHAN2.3.6-14; MOSS4.8.11.13.16-20; KNOB2; PUMP4.6.7; TRAN4-15.17-19.21-29; TIOG; TWIS6; GNES5.6.8.10.11.14.18-22; ORWE1.	SOMB25 MOSS9.
4	SOMB16-20.22-25.28-30.32.34.36.38.39.42.44-46; HEY5; CHAN2.3.7.9.10.12; MOSS3.4.6.8.14.15.17-19; PUMP1.3; SPIR5; TRAN6.14-16.23-27.29; AMOS5; TWIS3.7.12; GNES4.5.6.10.13.15.16.18.	SOMB11.12.14-20.23.25.28.33; CHAN2-5.7-12; MOSS4.5.14.18; KNOB4; PUMP4; LITE2; SPIR5; TRAN7-11.24-27.29; TIOG2.3.4; TWIS11; GNES3.5.6.8.9.13-15.22;	SOMB25; MOSS9.	SOMB13.15-21.24.28.29.32-34.36.38.39.43-46; CHAN2.3.7-10.12; MOSS5.6.14; PUMP1; TRAN6.11.22-24; GNES5.6.10.11.17.18.21.
5	SOMB14.21; HEY6.10.15; KNOB1.3-5.7.8; PUMP7; SPIR3.4; TRAN4.5.7-10.13.19.21.22.30; AMOS6; GNES12.	nil	SOMB12.14.22.42; CHAN5; MOSS3.5.6.10.14.15.21.	HEY13; CHAN4.5.
6	SOMB11.15.26.31.35.40.43; MOSS9.10.21; SPIR2; TWIS5.8; EMER5; BOTH1; GNES11.	nil	SOMB11; HEY13; CHAN4.	SOMB11.12.14.22.42; MOSS3.10.15.21.
Cophenetic correlation	0.570388	0.460823	0.263651	0.313895
Delta one-hat	31.3536	48.4577	23.0877	19.1624
Gower's delta	-1.293234E+09	-2.100202E+13	-8.575247E+09	-7.655353E+09

Table 8.5 Comparison of cluster groups of surface-sediment component fractions using minimum variance cluster analysis (208 samples)

Figure 8.3 **Results of forward-selection of significant explanatory environmental variables in CVA of collective sediment variables data-set and organic and minerogenic, particle size and mineral magnetic data-sets**

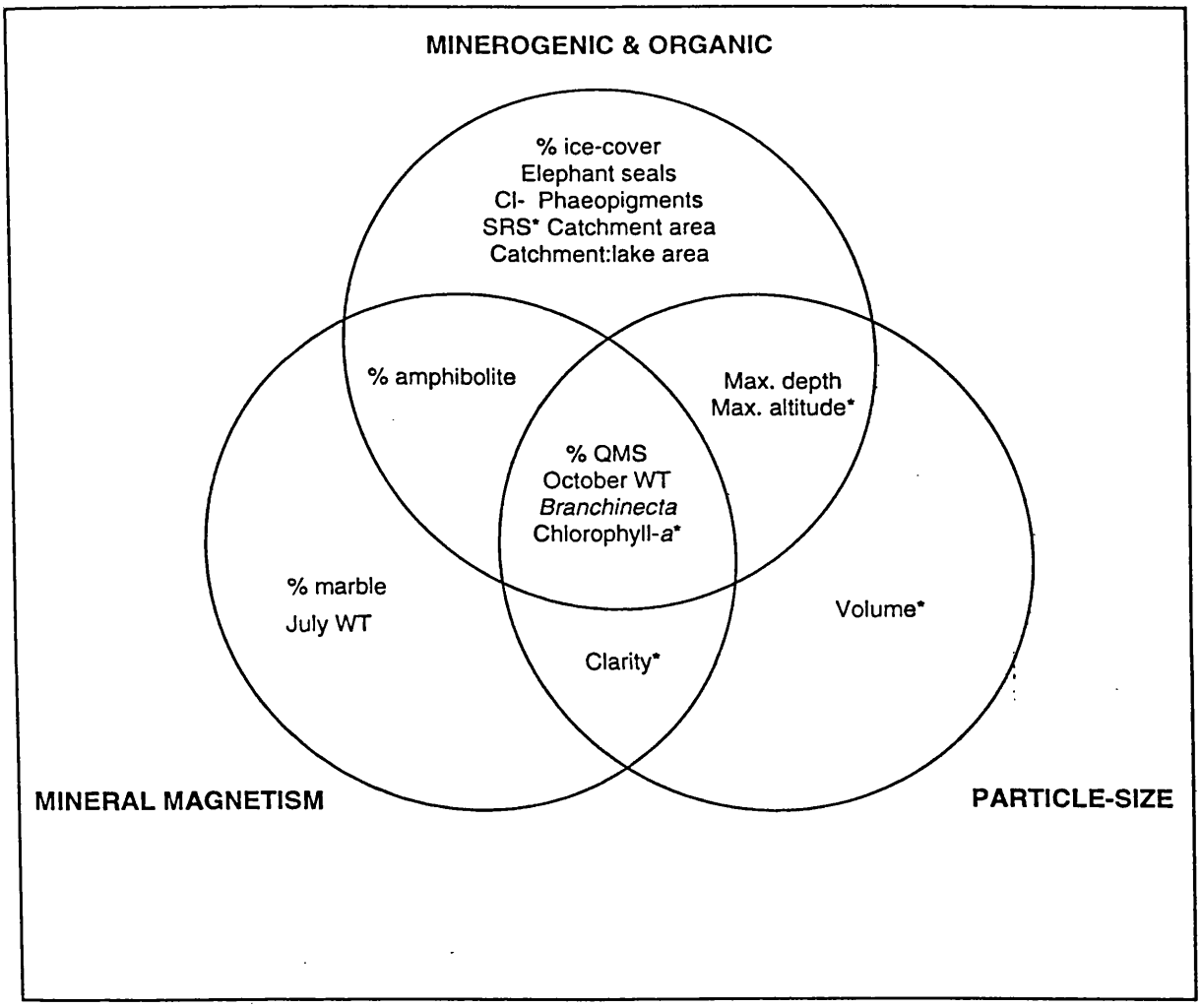

This venn diagram is a pictorial summary of the results presented in Table 8.4. Each circle represents a specific sediment data-set; the central area of overlap defines the group of all sediment variables (n=26). Environmental variables chosen in forward selection in Canonical Variates Analysis are alloted to their respective sediment data-sets. Environmental variables marked * are also forward-selected in CVA of all sediment variables. Environmental variables selected independently by different data-sets in CVA but with more than one data-set in common are alloted to a position of overlap between the two circles (e.g. % amphibolite is selected independently in CVA of both minerogenic and organic and mineral magnetic variables). Environmental variables in the centre of the diagram have been chosen in a CVA of all variables but are not necessarily selected in CVA of single data-sets.

8.3 Summary of surface-sediment characteristics

In diatom-based transfer-function models, the species data-set is composed of counts of diatoms, often expressed as relative abundances, per site. Here, each sample is analogous to a diatom slide and the numerous sediment determinands (n=26) are akin to diatom taxa which form the species data-set. This is only a third of the number of variables typically used for diatom-based transfer functions (e.g. Bennion, 1994; Pienitz & Smol, 1993; Jones & Juggins, 1995; Pienitz, Smol & Birks, 1995; Korsman & Birks, 1996). Capture of variance in CVA shows that only between 20-38% of variance in the sediment data is explained by the selected variables, leaving a considerable proportion of variance unexplained. It is not feasible however, to measure or collate everything and the choice of variables was made in the early stages of the study using *a priori* knowledge. The choice of variables obviously limits the scope of the quantitative reconstruction. Inevitably, not all variables will prove useful in modelling and reconstruction, and screening of redundant variables is undertaken in section 8.4.

Ideally, the sediment determinands should be responsive to climate-related processes in either the lakes or their catchments. Variables selected in CVA of all sediment determinands capture lake-climate and catchment development gradients through the sediment characteristics, which is highly encouraging for the modelling of climate effects. Lake morphometry is also clearly influential, as are unusual source lithologies (% marble and % amphibolite) and the marine influence (nutrients and ions). There is a division between samples taken in the shallow littoral zone and those from the profundal, as well as between sample types; the Ekman grab samples tend to occur as outliers. The other clear division is between glacier-fed and non-glacier-fed lakes, showing the importance of the allochthonous sediment flux in defining sediment variability. Higher rates of sedimentat accumulation in glacier-fed lakes appear to produce more homogeneous sediments. More productive, non-glacier-fed lakes have much more heterogeneous sediment characteristics resulting from resuspension, diagenesis and authigenesis, contrasting with Karlén's (1981) findings for more homogenous sediments in non-glacier-fed lakes.

8.4 The selection of statistically significant predictor variables

8.4.1 Background

When the number of environmental variables exceeds the number of response variables (n=26) there is no constraint in the ordination (ter Braak & Prentice, 1988) and linear

gradient analysis (redundancy analysis, RDA) effectively becomes a PCA. Many of the environmental variables are multicollinear (Chapter 3) and therefore of limited explanatory power, necessitating data-screening and elimination of redundant variables. It is possible to partial-out "nuisance" variation using partial ordination methods (ter Braak & Verdenschodt, 1995). Alternatively, direct ordination can be used as a data-reduction tool, reducing a large set of variables to a small sub-set, finding the minimum adequate model that can explain variation in the sediment data almost as well as the full model. Criteria for the justified deletion of variables are outlined by Birks (1995). In the context of this study, the principal concern is to retain as many quantitative climate-proxy variables in the sub-set model without a significant loss of overall explanatory power. Where prediction and estimation of responses are the primary objective regression can be fairly tolerant towards the elimination of variables (Rawlings, 1988).

Two procedures for reducing the number of environmental predictor variables are explored in the following sections (8.4.2 & 8.4.3). *Forward-selection* (section 8.4.2) has already been introduced in CVA (section 5.8.2) and uses an agglomerative method to select statistically significant environmental variables in turn, so building-up a model in stages which finally approximates the full model of sediment and environment data with a minimal loss of explained variance. The second method - *backward elimination* (section 8.4.3) reverses this strategy. Both methods isolate the most significant variables and identify those variables which do not exert an independent influence on the surface-sediment distributions because of multicollinear relations.

8.4.2 Predictor variables reduction by forward selection

8.4.2.1 Theory

The iterative process of forward selection in CANOCO (ter Braak, 1990) allows the identification of a minimum set of environmental variables that explains variation in the sediment data almost as well as the full set. The process used in RDA or CCA is analogous to the forward-selection process used in step-wise multiple regression (ter Braak, 1990b). This is the most common method for eliminating unwanted variables in ecological studies. In the maritime Antarctic, Björck *et al.* (1993) used forward-selection in RDA in their palaeoclimatic reconstruction from lake sediments on Livingston Island to find a sub-set of 6 significant variables from a full set of 21, providing a climatic explanation for Holocene lake-sediment variability independent of the dominating local effects of tephra.

8.4.2.2 Analysis

Forward selection of environmental variables was performed using RDA in CANOCO (ter Braak, 1987). The method uses a step-wise analysis as follows:

(1) RDA is performed on each environmental variable separately and their marginal effects (predictive power) are listed in rank order according to the size of their eigenvalues.

(2) The variable with the largest marginal effect (eigenvalue) is selected and its statistical significance tested using an unrestricted Monte Carlo permutation test (999 permutations); the variable is accepted as making a significant contribution to variance in the sediment data if $p \leq 0.001$.

(3) The selected variable is used as a covariable and the succeeding variables are listed in order of their conditional effects (i.e. variance explained when allowing-for the effects of the first selected variable); the next ranked environmental variable is selected and a Monte Carlo permutation test is run, applying a Bonferroni-type correction (ter Braak, 1990; Manly, 1992) for simultaneous multiple tests.

(4) Selection is continued until the nth variable is judged non-significant; the forward-selection is halted and a final RDA is run with only the selected variables. The reduced sub-set model is tested for significance ($p<0.05$) with a Monte Carlo permutation test (99 iterations).

(5) The sum of canonical eigenvalues is compared with that of the full RDA model to observe the loss of explanatory power.

8.4.2.3 Results

Forward selection found that 11 of the 45 environmental variables make significant contributions to explaining the variance in the surface-sediment data. Table 8.6 summarises the results of forward selection in RDA, including the cumulative variance explained by the addition of each variable identified by the forward selection procedure, the Bonferroni adjusted significance level and the number of permutations required to determine it. The final model summary is presented in Table 8.7 and the canonical coefficients, t-values and inter-set correlations of the selected environmental variables are summarised for the first two RDA axes in Table 8.8.

The sum of constrained eigenvalues (linear combinations of environmental variables) of the full RDA model is 0.523. The sum of canonical eigenvalues (0.480) for the 11 forward-selected variables indicates an inevitable loss of explanatory power in selection

of a minimally-adequate sub-set (i.e. 52.3-48.0 = 4.3% loss of explained variance). This loss is fairly small and the eleven variable model is considered to be almost as robust as the full set.

Table 8.6 Forward selection of environmental variables in RDA of all sediment variables (208 samples, 26 sediment variables, 45 environmental variables)

Variable added	*cumulative variance of selected variables*	*number of permutations*	*Bonferroni required significance*	*significance achieved*
Mean depth	0.11	99	0.05	0.010
Clarity	0.19	999	0.025	0.001
% marble	0.25	999	0.016	0.001
Cyanobacterial mat	0.31	999	0.0125	0.001
Maximum altitude	0.35	999	0.01	0.001
Conductivity	0.38	999	0.008	0.001
SRS	0.40	999	0.00714	0.001
October WT	0.43	999	0.00625	0.001
% ice	0.45	999	0.0055	0.001
Branchinecta	0.47	999	0.005	0.001
Phaeopigments	0.48	999	0.0045	0.002
Variance explained by all variables	0.52			
No other variables significant				

Canonical coefficients (judged significant by approximate *t*-tests) and inter-set correlations (Table 8.8) were examined to estimate the relative contributions of the individual environmental variables to the ordination axes (ter Braak, 1987). The first axis (0.150) is significantly different ($p \leq 0.01$) from random expectation, indicating that the sediments are significantly related to the selected environmental variables.

Mean depth is the most significant environmental variable for RDA axis 1 with the largest canonical coefficient, largest inter-set correlation and *t*-value (Table 8.8). The most significant environmental variables associated with RDA axis 2 are October water

Table 8.7 Summary statistics for RDA of statistically significant explanatory variables (n=11) chosen by forward selection

RDA axes	*1*	*2*	*3*	*4*	*Total variance*
Eigenvalues	0.150	0.138	0.078	0.057	1.000
Sediment-environment correlations	0.783	0.809	0.796	0.817	
Cumulative % variance					
(i) of sediment data	15.0	28.8	36.6	42.3	
(ii) of sediment-environment relationship	31.2	60.0	76.3	88.1	
Σ *of all unconstrained eigenvalues*					1.000
Σ *of all canonical eigenvalues*					0.480

Table 8.8 Canonical coefficients of the 11 forward-selected environmental variables, their *t*-values and their inter-set correlations

environmental variable	*canonical coefficients*		*t-values of canonical coefficients*		*inter-set correlation*	
	axis 1	*axis 2*	*axis 1*	*axis 2*	*axis 1*	*axis 2*
Maximum altitude	0.4163	-0.1018	4.7501*	-1.2713	-0.0112	-0.5047
% ice	-0.0898	-0.1387	-0.6245	-1.0571	-0.1313	-0.5939
% marble	-0.0989	0.4205	-1.5508	7.2183*	0.0691	0.4402
Mean depth	-0.7775	-0.1449	-7.0586*	-1.4405	-0.5589	-0.3167
Conductivity	0.0058	0.4503	0.0547	4.6269*	0.2892	0.2568
Phaeopigments	0.1662	0.6886	0.9219	4.1820*	0.4809	0.2589
SRS	-0.1158	-0.0173	-1.3266	-0.2166	-0.0660	0.3774
Clarity	-0.3257	0.3734	-3.3165*	4.1640*	-0.4846	0.3001
October WT	0.0315	0.7706	0.2121	5.6865*	-0.5115	0.0586
Branchinecta	0.0310	-0.4194	0.3397	-5.0340*	0.1785	0.0597
Cyanobacterial mat	-0.2186	-0.1141	-2.3766*	-1.3586	-0.5086	-0.2166

* *t*-test significant at $p \leq 0.05$; n=30, 207 d.o.f., $t \geq 1.96$)

temperature (on the basis of its canonical coefficient and *t*-value) and % ice-cover (significant inter-set correlation only). Other significant variables associated with axis 1 include maximum altitude, clarity and cyanobacterial mat. Axis 2 is more noisy and significant variables include % marble, conductivity, phaeopigments, clarity, October water temperature and *Branchinecta*. A large number of degrees of freedom mean that

most variables have significant inter-set correlations for both axes. A common additional constraint imposed on CCA (and RDA) is the removal of samples with >8X influence on any of the forward-selected environmental variables (Pienitz, Smol & Birks, 1995). Leverage diagnostics in CANOCO (ter Braak, 1990) were examined for such outliers and five samples outliers with >8X influence were identified: all Light Lake samples, on the basis of their association with % marble, and the single sample from Bothy Lake, associated with conductivity.

The two RDA correlation biplots (Figure 8.4a&b) emphasize the patterns of variation in the sediment data and the main relationships between sediments and each environmental variable. The site scores are linear combinations of environmental variables and these canonical coefficients represent the best weights or parameters of the final regression. Quantitative environmental variables are represented by arrows and the angles between them represent environment x environment correlations. It is therefore possible to see the relative influence of the selected environmental variables in terms of the length of the arrows (long arrows indicate variables that are important in the analysis).

Vectors for phaeopigments, conductivity and *Branchinecta* are associated with high values for particle-size determinands, i.e. coarse, unsorted sediments, in Heywood (open squares), Amos (filled down-triangles), Twisted (stars), and Gneiss (grey squares) Lakes. These oppose the vectors for cyanobacterial mat, maximum depth and October water temperature, which link with high values for magnetic normalized reverse field ratios and concentration parameters, suggesting ferrimagnetic behaviour associated with intrinsic (authigenic) lake processes. Sombre (open circles) and Moss (open up-triangles) Lakes conform to these characteristics. Clarity is highly linked to high values for κ_{ARM}, SOFT and SIRM, supporting the hypothesis for authigenic production of ferrimagnetic minerals independent of source lithologies (low suspended sediment volume, short open water season, anaerobic conditions). Samples from Tioga (half-filled circles) and others from Sombre (open circles), Changing (open diamonds) and Moss (open up-triangles) Lakes link with these vectors. Vectors for SRS and %marble are found with high values for %LOI, %OM, %BSi, high κ_{ARM}/SIRM and reverse field-ratios. Sediments from Light (filled squares), Pumphouse (filled circles) and to a lesser degree Heywood and Changing Lakes match these characteristics. This gradient indicates productivity and lithology effects on magnetic grain-size variations and concentrations (iron-bearing

Figure 8.4 **Correlation biplots of 11 forward-selected environmental variables (a) samples and environment (b) sediment determinands and environment**

(a) Samples and environment

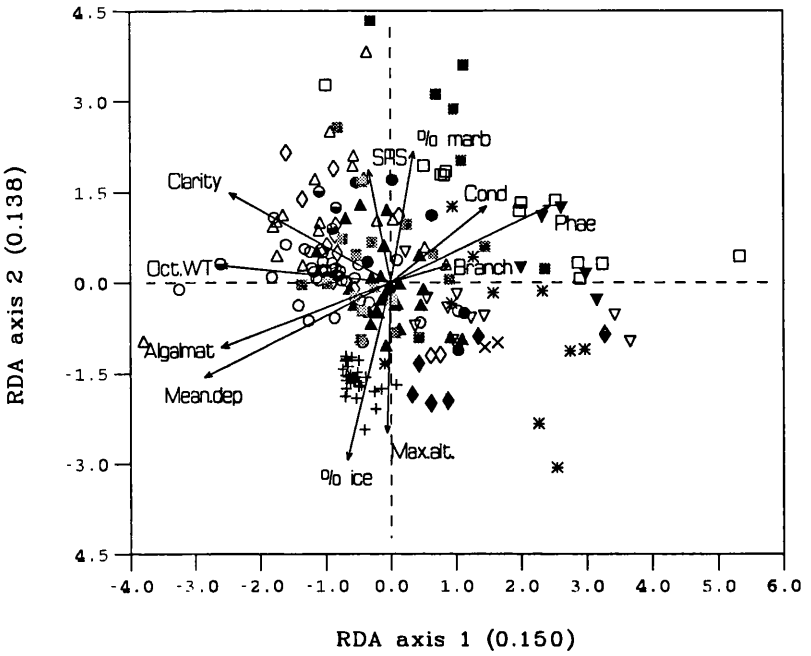

(b) Sediment determinands and environment

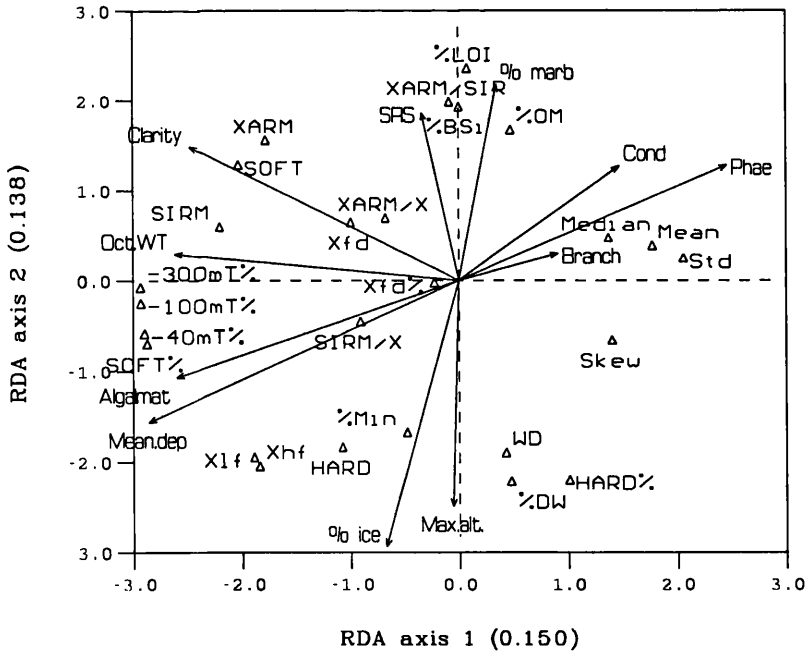

amphibolite and marble lithologies). Sediments also tend to be coarser in these lakes (see above). Vectors for % ice-cover and maximum altitude associate with minerogenic

sediments (high wet density, %DW, %Min) and antiferromagnetic behaviour (high HARD and HARD%), characterising sediments from Emerald Lake (plusses). $\varkappa$lf and $\varkappa$hf plot near these determinands, supporting the hypothesis for mixed magnetic assemblages which are predominantly detrital reflecting their catchment source lithologies.

8.4.3 Predictor variables reduction by backward elimination

8.4.3.1 Theory

Environmental variables can be eliminated from regression analyses on the basis of their variance inflation factors or VIFs (Montgomery & Peck, 1982). These are a measure of the correlation between environmental factors. Variables with high VIFs have the least significance in the regression model. The variance of estimated regression (canonical) coefficients (c_j) are proportional to their VIF (ter Braak, 1987):

$$\text{Var } (c_j) = \text{VIF x (residual variance) / } (n\text{-}q\text{-}1)$$

where n is the number of samples and q is the number of predictor variables. The VIF is related to the (partial) multiple correlation coefficient R_j between variable j and the other environmental variables:

$$\text{VIF} = \quad 1 / (1\text{-}R_j^2)$$

If the VIF for a variable is greater than 20 this indicates that the variable is almost perfectly correlated with other variables and does not contribute any extra fit to the regression model. Variables with high VIFs have unstable canonical coefficients and ter Braak (1986) warns against interpreting them. Deletion is made on the basis of the correlation structure. Elimination using VIFs is a useful means of finding a minimal set of variables which allow some *a priori* knowledge in the selection of the final sub-set. It is therefore less rigid in its approach than forward-selection and also more intuitive in that selection is made using a combination of statistical rigour and personal objectivity.

8.4.3.2 Analysis

RDA was performed in CANOCO as above. As with forward-selection (section 8.4.2), the aim is to simplify the full model by deleting redundant variables with minimal

reduction of model performance (sum of canonical eigenvalues). The following procedure is followed:

(1) All explanatory variables are initially included in the analysis (full model); the sum of canonical eigenvalues (variance explained), eigenvalues and species-environment correlations are noted.

(2) The model output is examined for its VIFs and those with values >20 noted.

(3) A second RDA is performed, this time eliminating several variables with high VIFs (4-5 variables at a time); at the end of the analysis an unrestricted Monte Carlo permutation test (99 permutations) is run to test the significance of the first constrained axis and the overall test statistic ($p<0.01$); the sum of canonical eigenvalues of the sub-set model of explanatory variables is noted.

(4) A third RDA is performed, eliminating more variables with high VIFs, and so on; the model output after each run is examined; the RDA is repeated, eliminating further variables, and the significance of the reduced model is tested each time using significance tests of the first canonical axis and overall test statistic.

(5) For the first few runs no change in the sum of canonical eigenvalues is noted; eventually a change is observed, thereafter variables are eliminated more judiciously (one to two at a time); elimination is continued until the model is tested to be non-significant; the penultimate selection of variables (tested to be significant) forms the final sub-set of environmental variables.

(6) Substitutions of more satisfactory explanatory variables are made on an individual basis to replace those which are considered to be less relevant.

(7) A final model is run with the selected variables and its significance tested at $p<0.01$ with a Monte Carlo permutation test. The sum of canonical eigenvalues is compared with that of the full model to observe any loss of explanatory power.

8.4.3.3 Results

Eliminating variables with VIFs >20 in RDA left a complement of 14 environmental variables with optimal explanatory power. All variables have VIFs <10 except for open days (13.67), thus the residual variation is reasonably low. The final model summary is presented in Table 8.9 and the canonical coefficients, their VIFs, *t*-values and inter-set correlations for the first two RDA axes for the 14 variables model are summarised in Table 8.10.

Table 8.9 Summary statistics for RDA of statistically significant explanatory variables (n=14) selected by VIFs

RDA axes	*1*	*2*	*3*	*4*	*Total variance*
Eigenvalues	0.149	0.133	0.080	0.058	1.000
Sediment-environment correlations	0.807	0.771	0.804	0.825	
Cumulative % variance					
(i) of sediment data	14.9	28.3	36.2	42.1	
(ii) of sediment-environment relationship	30.9	58.5	75.0	87.0	
Σ *of all unconstrained eigenvalues*					1.000
Σ *of all canonical eigenvalues*					0.483

Table 8.10 Canonical coefficients of the 14 environmental variables selected by VIFs, their *t*-values and their inter-set correlations

environmental variable	*VIF*	*canonical coefficients*		*t-values of canonical coefficients*		*inter-set r*	
		axis 1	*axis 2*	*axis 1*	*axis 2*	*axis 1*	*axis 2*
Sample depth	2.56	0.0367	0.1009	0.4332*	1.0536	-0.4355	-0.0960
Max.altitude	6.10	0.0335	-0.5677	0.2576*	-3.8618*	-0.1823	-0.4468
Catchment area	5.93	0.4627	0.3620	3.6051*	2.4968*	-0.1225	-0.1339
% ice	5.26	-0.4838	-0.2948	-4.0030*	-2.1588*	-0.3222	-0.4938
% amphibolite	6.06	-0.1166	0.4301	-0.8988	2.9341*	0.0404	0.2952
% marble	1.84	0.0985	0.5525	1.3800	6.8501*	0.2156	0.3749
% moss	2.06	0.0424	-0.1439	0.5613	-1.6850	0.1959	-0.1384
Volume	5.38	-0.5559	0.3491	-4.5490*	2.5284*	-0.4421	-0.2344
Open days	13.67	-0.1268	0.0578	-0.6506	0.2626	0.0812	-0.1256
SRS	4.07	-0.3040	-0.0788	-2.8584*	0.6557	0.0464	0.3735
Clarity	2.75	-0.5134	0.2395	-5.8761*	2.4266*	-0.3763	0.4483
Branchinecta	7.22	-0.2112	-0.3499	-1.4917	-2.1877*	0.1837	-0.0073
Moss	7.06	-0.1199	-0.0975	-0.8567	-0.6162	-0.2351	-0.2330
Cyanobacterial mat	4.59	-0.5451	-0.1069	-4.8274*	-0.8379	-0.5521	-0.0236

* *t*-test significant at $p \leq 0.05$; n=30, 207 d.o.f., $t \geq 1.96$.

This sub-set explains nearly 30% of the variation in the sediment data in the first two RDA axes (Table 8.9). All variables are significant at $p<0.01$ in unrestricted Monte Carlo permutation tests (99 permutations). The full model sum of eigenvalues is 0.523;

the loss in explained variance using only 14 variables is only 4.0% (i.e. 0.523-Σ canonical eigenvalues 0.483). Removing 25 variables has resulted in a loss of explanatory power of roughly similar magnitude to that observed when eliminating data by forward selection (section 8.4.2.3). This model includes more variables than the forward-selection sub-set model but selection here was made in a more discerning manner using a combination of statistics and objectivity. The model was forced to include catchment ice-cover. It was possible to remove the marine influence (cations, conductivity, Cl^-) completely, as well as the seal influence, a modern environmental perturbation likely to obscure other climatically-relevant trends recorded in the sediments.

Using their canonical coefficients, *t*-values and inter-set correlations (Table 8.10), the most significant variables associated with RDA axis 1 are volume, clarity and cyanobacterial mat; for RDA axis 2, maximum altitude, % marble, % ice-cover. The associations with each axis are more noisy than the patterns seen in the forward-selected sub-set. Once again, a high number of variables display significant inter-set correlations owing to the large number of degrees of freedom. The coefficients suggest that climatic influences affect RDA axis 1 and lithology affects RDA axis 2. The Monte Carlo permutation test of the first axis ($\lambda 1$=0.149) is significantly different from random expectation (p<0.01) indicating that the sediments are significantly related to the environmental variables. Nine samples with >8X influence on the environmental variables are identified in leverage diagnostics (ter Braak, 1990): samples from Knob Lake, associating with % moss vegetation, samples from Light Lake which associate again with % marble (as in forward-selection) and the single sample from Bothy Lake, associated with catchment area.

The two biplots of RDA axis 1 and 2 results (Figure 8.5) show the fourteen variables plotted as vectors on a correlation biplot with (a) sites as weighted sums and (b) sediment variables. RDA axis 1 variables - *Branchinecta*, % moss vegetation and open days - are most associated with high values for particle-size determinands, corroborating the hypothesis that lake populations of *Branchinecta* bear some relation to the length of the open season to allow completion of their life-cycle (Björck *et al.*, 1996) as well as substrate preference (Heywood, Dartnall & Priddle, 1980). Lowland, eutrophic lakes are most associated with these characteristics, i.e. Heywood (open squares), Knob (open down triangles), Amos (filled down triangles) and Twisted (stars) Lakes. The opposite

Figure 8.5 **Correlation biplots of 14 environmental variables selected by low VIFs (a) samples and environment (b) sediment determinands and environment**

(a) Samples and environment

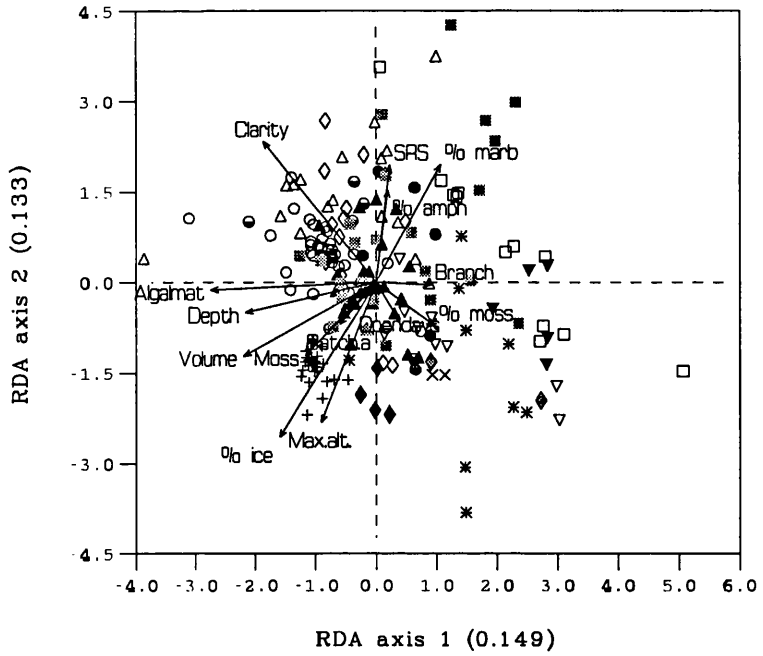

(b) Sediment determinands and environment

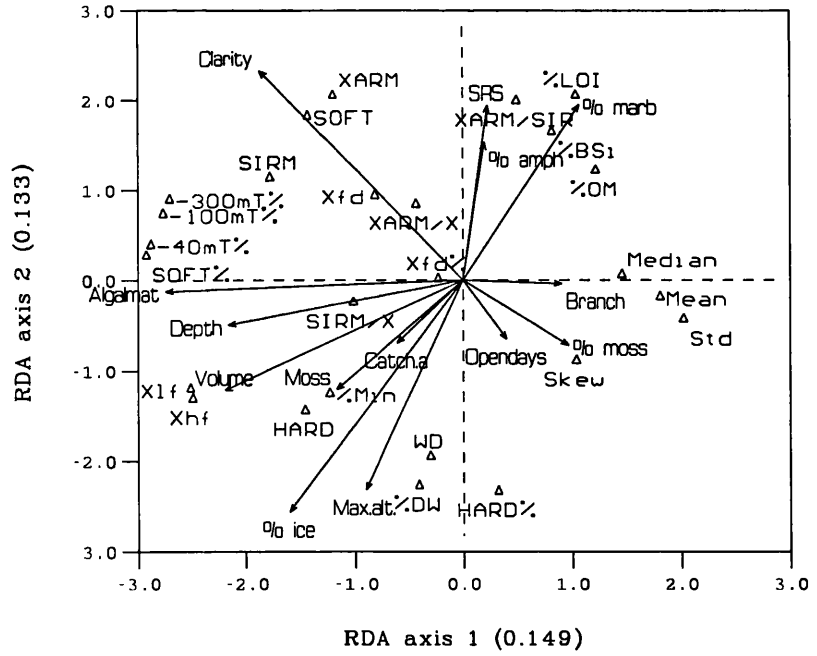

end of the RDA axis 1 gradient, cyanobacterial mat and depth, are associated with high values for particle-size determinands, corroborating the hypothesis that lake populations of *Branchinecta* bear some relation to the length of the open season to allow completion

of their life cycle (Björck *et al.*, 1996) as well as substrate preference (Heywood, Dartnall & Priddle, 1980). Lowland, eutrophic lakes are most associated with these characteristics: Heywood (open squares), Knob (open down-triangles), Amos (filled down-triangles) and Twisted (stars) Lakes. The opposite end of the RDA axis 1 gradient, cyanobacterial mat and depth, are associated with high values for SOFT% and normalized reverse field-ratios indicating fine-grained ferrimagnetic behaviour, possibly representing bacterial production of fine-grained magnetites, also suggested latently in indirect ordination (section 7.10). Sombre (open circles), Changing (open diamonds) and Moss (open up-triangles) Lakes are most associated with this end of the RDA axis 1 gradient. The vector for clarity opposes the vector for open days. Lakes with longer periods of ice-cover are less turbulent with less suspended sediment and less phytoplankton productivity. These sediments have the highest magnetic concentrations (high SIRM) and highest proportions of fine-grained magnetite minerals (κ_{ARM}, SOFT). Environmental vectors for SRS, % amphibolite and % marble are associated with high scores for %BSi, %LOI, %OM, κ_{ARM}/SIRM and normalized reverse-field magnetic ratios (soft magnetic behaviour). Lithology therefore determines magnetic grain-size and possibly also authigenic magnetic mineral formation. High SRS in the water column associates with high %BSi in the sediments. Light Lake (filled squares), and to a lesser degree Heywood (open squares) and Gneiss (grey circles) Lakes match these characteristics. Finally, the lower left quadrant of the biplot includes vectors for water depth at the sampling point, lake volume, freshwater moss, % ice-cover, maximum altitude and catchment area. The most significant determinant (longest vector) is % ice-cover, associating with HARD (antiferromagnetic behaviour) and minerogenic sediments (high values for wet density, %DW, % Min). Emerald (plusses) and Spirogyra (filled diamonds) Lakes correlate most strongly with these variables. Magnetic susceptibilities are high but are divorced from SIRM and κ_{ARM} in the upper left quadrant of the biplot, suggesting that overall magnetic concentrations are from mixed magnetic mineral assemblages, paralleling the results seen in the forward-selected variables (section 8.4.2).

8.4.4 Discussion

Commonly, more than one minimum adequate model can be derived from one data-set and a unique solution is not always possible. It is usually impossible to remove variables without some loss of information. Using these methods it was possible to remove a large number (two-thirds) without any marked effect (<5% loss of explained variance). Deletion by two different methods in this instance yielded two different models: eleven

variables and fourteen variables, both explaining nearly the same amount of variance in the sediment data (*ca.* 30% in RDA axes 1 & 2) and sharing several variables in common, suggesting authenticity of the selected predictors. Although forward selection is the most common method of deletion it should be used judiciously because: (i) several sets can be almost equally as good and automatic selection might find one which is not optimal to the study aims; (ii) the selection order might change the result and important variables might not be selected; (iii) small changes in the data can change the selected variables; and (iv) it can be difficult to draw reliable conclusions about the relative importance of variables.

The VIF selection model was therefore chosen as the 'best set' of explanatory variables. Although it had a larger number of variables (n=14), their selection was semi-intuitive. Undesirable effects (marine and seal influences) were removed and more relevant climate parameters maintained in the model in keeping with the aims of the study. Statistical testing with Monte Carlo permutation tests confirmed the model's statistical robustness. Eliminating data in this way by-passed the need for the additional complication of imposing covariable effects on ordinations, thereby maintaining the simplicity of the analysis. It was not felt necessary to remove any samples at this stage.

In the next section this best set of explanatory variables is used in variance decomposition to see how patterns in sediment characteristics can be related to extrinsic, catchment and intrinsic, limnological predictors, so helping to explain sediment origin and formation.

8.5 Variance partitioning of sediment-environment interactions

8.5.1 Theory

The method of variance partitioning is linked to the concept that ecological phenomena are explained by non-mutually-exclusive abiotic or biotic processes that overlap in space and time. In order to formulate causal hypotheses from predictor-response relationships, it is useful to know the relative weights of explained and unexplained fractions of the variance. Direct ordination methods above show that explanatory variables share colinear relationships. Collinearity can have beneficial properties in numerical analysis, for example, in dimension reduction and predictive model construction in which a few factors integrate a great amount of information (e.g. Kernan, 1996). However, intercorrelations are problematic when trying to identify cause and effect relations, for

example, indicator response to certain pollutants. It is not possible to decompose the variance in data-sets in the same way that can be achieved in an analysis of variance (ANOVA). Instead, a method of variance decomposition has been developed in ecological studies involving a series of (partial) constrained ordinations (Borcard, Legendre & Drapeau, 1992). Partial constrained ordinations (ter Braak, 1988) in RDA or CCA provide a major improvement towards the detailed causal interpretation of natural phenomena. The effects of known or undesirable variables - covariables - can be removed from the ordination, such as geography, time, climate or anthropogenic influences. The technique used in CANOCO (ter Braak, 1988) for estimating the desired variation is known as residuals regression. The partitioning is based on a few general measurements of the variation of analyzed data-sets involving the eigenvalues of different constrained and partial analyses.

Variance partitioning has been used to remove spatial effects (Borcard, Legendre & Drapeau, 1992; Quinghong & Bråkenhielm, 1995) and/or temporal effects (Lotter & Birks, 1993). It can be used as a predictive tool in bioindication studies (Qinghong & Bråkenhielm, 1995) linked to pollution deposition and has also been used to explain present-day distributions of Norwegian mountain plants (Birks, 1993). In aquatic ecology, variance partitioning has been used to explain relationships between diatom species distributions and hydrochemistry (Gasse, Juggins, & Ben Khelifa, 1995). In the maritime Antarctic, Jones & Juggins (1995) used partial CCAs to partition variance in diatom surface-sediment assemblages using forward-selected explanatory variables. The fraction of variance explained by lake-water chlorophyll-*a* and ammonium alone were significantly independent of other chemical or biogeographic effects to merit their reconstruction in WA regression techniques. In the same way here an assessment can be made of the effects of extrinsic (catchment) and intrinsic (limnological) environmental factors and their interaction on the variation in sediment characteristics in the suite of lakes, so helping to justify the selection of relevant environmental variables for reconstruction (section 9.2).

8.5.2 Analysis

The best-set of 14 environmental variables chosen by their low VIFs in section 8.4.3 were used to partition the variance in the sediment data for 208 samples. The explanatory variables can be divided into two broad groups: catchment factors and limnological factors.

Catchment (n=6)	**Limnology** (n=8)
Maximum altitude	Depth
Catchment area	Volume
% ice cover	Open days
% amphibolite	SRS
% marble	Clarity
% moss	*Branchinecta*
	Freshwater moss
	Cyanobacterial mat

A sequence of direct ordinations using RDA and partial RDA were used to decompose the variance explained in the species data-set using combinations of these explanatory variables and covariables in CANOCO (ter Braak, 1990) against the full data-set and the three different sediment data-series (organic and minerogenic, particle-size and mineral magnetism). The method shares parallels with that used by Lotter & Birks (1993), who decomposed variation in three different palaeoecological species data-sets (pollen, aquatic pollen and spores and diatoms) into depth, age and tephra-affected components, so allowing for a prediction of climatic change effects.

In (partial) RDA the explanatory variables are used as covariables so that their effects on variation in the sediment-site matrices can be allowed for and eliminated in the analysis. In this way it is possible to determine the variation in the sediment data that is uniquely attributable to a selected set of explanatory variables, taking into account the effects of other covariables (ter Braak & Prentice, 1988). The effect of the covariables is removed before performing the canonical analysis so that the sum of canonical eigenvalues has a value less than that of the full model.

The following decomposition was used to partition each data-set:

(1) RDA with 14 environmental variables; the residual variance (total - $\sum$canonical eigenvalues) gives a measure of unexplained variance in the model.

(2) RDA with only the catchment (n=6) environmental variables, limnology as covariables, to assess the unique catchment contribution to variation in the sediment data.

(3) RDA with only the limnology (n=8) environmental variables, catchment as covariables, to assess the unique limnology contribution to variation in the sediment data.

(4) The covariance between limnology and catchment is calculated as the ∑canonical eigenvalues [1] - ∑canonical eigenvalues for catchment [2] - ∑canonical eigenvalues for limnology [3].

For each analysis the correlation matrix of variable-environment data was centred and standardized by variables. At each stage the fraction of variation accounted for by the canonical (constrained) axes is given by their sum of eigenvalues. When performing partial RDAs the sum of eigenvalues drops below that obtained in the full model RDA and gives a measure of the remaining variation in the sediment data. The statistical significance of each separate analysis was tested using unrestricted Monte Carlo permutation tests (99 permutations) of the first canonical eigenvalue for (partial) RDA axis 1 and the overall test.

8.5.3 Results

Table 8.11 and Figure 8.6 summarise the results of (partial) redundancy analysis of the sediment-environment data-sets under different models of explanatory variables and covariables. The minerogenic and organic determinands and mineral magnetic determinands explain roughly similar proportions of variance in the sediment data-set. Particle-size determinands perform less well with a greater proportion of unexplained variance (61.8%).

Table 8.11 Results of partitioning the variance in the sediment data-sets under models of catchment and limnology explanatory variables

Source	*Organic + minerogenic*	*Particle size*	*Mineral magnetism*
Catchment + limnology	0.506, $p<0.01$	0.382, $p<0.01$	0.503, $p<0.01$
Catchment only	0.298, $p<0.01$	0.084, $p<0.02$	0.163, $p<0.01$
Limnology only	0.163, $p<0.01$	0.254, $p<0.01$	0.258, $p<0.01$
Catchment-limnology interactions	0.045, $p<0.01$	0.044, $p<0.01$	0.082, $p<0.01$
Total variance	1.000	1.000	1.000
Unexplained variance	0.494	0.618	0.497

Values are the sum of squares (=variance) expressed as proportions of total variance in each data-set. Significance values for each model were tested for the first canonical axis and overall trace statistic using Monte Carlo permutation tests (99 iterations).

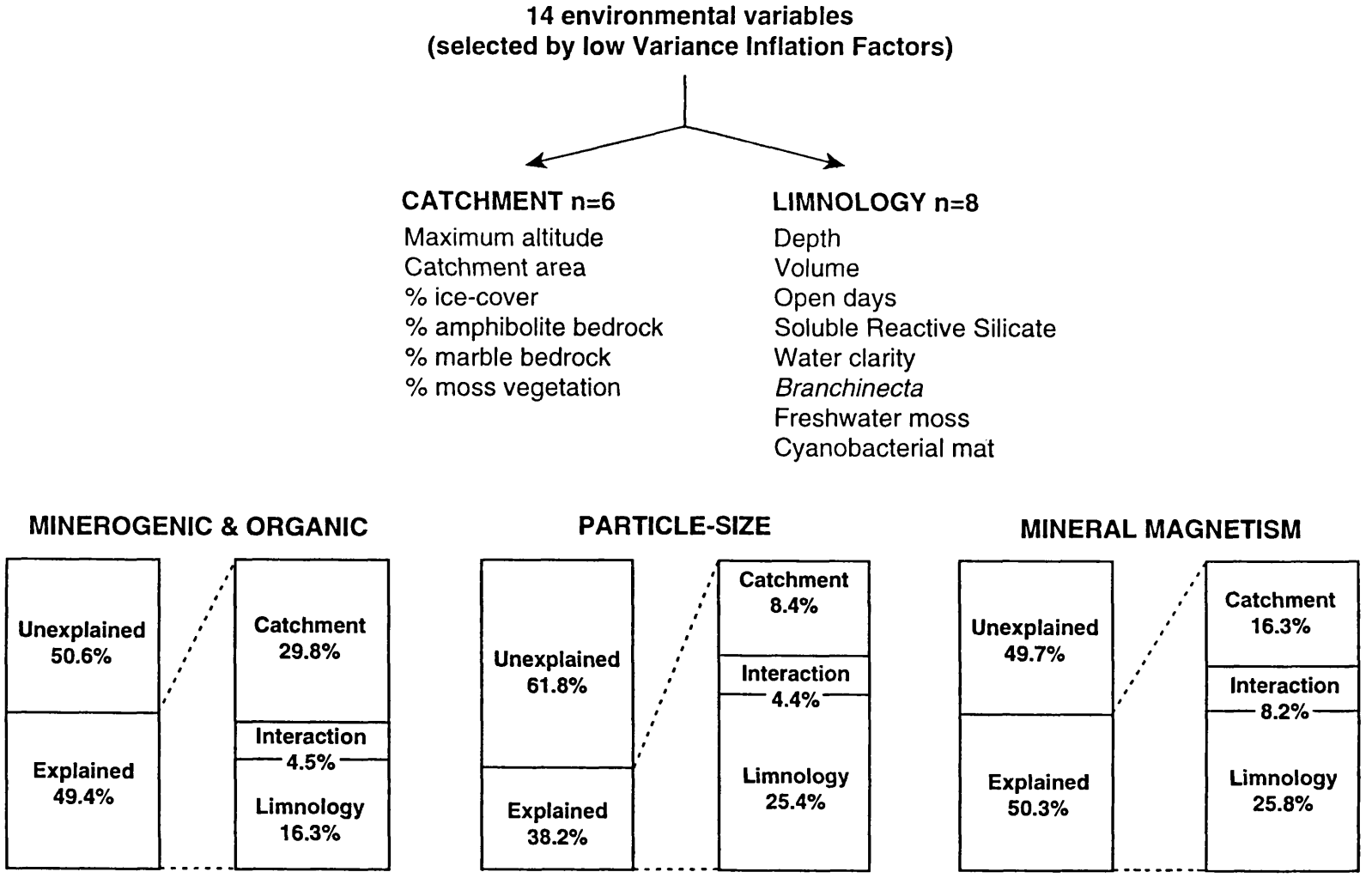

Figure 8.6 **Results of partitioning the variance in the sediment data-sets under models of catchment and limnology explanatory variables**

The capture of explained variance in all three series is generally very good (close to 50%) in comparison with similar variance partitioning exercises using diatom-water chemistry data-sets and (partial) CCA (Gasse, Juggins & Ben Khelifa, 1995; Jones & Juggins, 1995). Linear methods are less complicated than their unimodal equivalents and the sediment variables used here lack the taxonomic and taphonomic complications of diatom-assemblage data. The processes linking the sediments to the environment are probably more simplistic and therefore more easily modelled. The fraction of unexplained variance (*ca.*50-60%) results from quantitative variables (either environmental or sedimentological) not measured in this study.

Unique catchment effects explain significantly different proportions of variance using the different suites of determinands. Minerogenic and organic determinands (n=6) explain 29.8% of variation, compared with 16.3% using mineral magnetic determinands and 8.4% using particle-size volume-distribution statistics. This suggests that the organic and minerogenic measures are most responsive to catchment-derived influences including land-cover (ice-cover, vegetation) and lithology. These determinands are most likely to provide the key to linking causal processes in the catchment with response in the lake sediments (see Chapter 9). Significance levels of first canonical axes assessed using Monte Carlo permutation tests (99 permutations) for the various models are all significant at $p<0.01$ except for the relationship between unique catchment effects and particle-size data. Particle-size is surprisingly unresponsive to catchment variables in variance partitioning. This could be the result of incomplete capture of the full particle-size gradient through sampling bias (Chapter 4) and/or the result of methodological problems discussed in section 6.4.1. Unique limnology however, explains 25.4% of variation in the particle-size data and it is possible that intrinsic controls relating to morphology and lake climate are strongly affecting the receipt of sediment and processes of deposition. Certain selected variables - depth, volume and the duration of open water - in the CVA certainly suggest that this is possible and Heywood, Dartnall & Priddle (1980) emphasised the strong seasonality of the lakes. Benthic vegetation is also a strong determinant of sediment character and both cyanobacterial mat and freshwater moss are included in this partial model (Table 8.10).

The mineral magnetic determinands share a similar pattern of behaviour to particle-size. Unique limnology explains the greatest proportion of variance in the sediment data (25.8%), supporting the hypothesis for authigenic, fine-grained magnetic mineral

formation. The catchment contribution to mineral magnetic characteristics is slightly greater (16.3%) than particle-size (13.6%). The coupling between the lakes and catchments is greatest in the mineral magnetic data: catchment-limnology interactions account for 8.2% of variation versus roughly 4% for the minerogenic and organic and particle-size determinands. The decoupling of catchment and limnology in the latter is of interest in modelling as the ability to discriminate single causal environmental controls (i.e. climate through glaciation) may be enhanced. Results of CVA (section 8.3) also suggest a relative independence of cathment and limnological controls on sediment characteristics. Variance partitioning is therefore a useful exercise as it gives some indication of the respective performances of the data-sets (sediment and environment) and highlights where future research efforts can be directed to improve the modelling base.

8.6 Summary

(1) The combined data-set includes 208 samples and 26 determinands of minerogenic and organic, particle-size and mineral magnetic origin. Classification and ordination using the sediment data alone indicate a division of sites on the basis of whether or not a lake is glacier-fed which affects the balance of allochthonous minerogenic materials relative to organics and biogenic inorganics. Between-lake variability is reduced in the combined data-set, and local site factors are more influential in determining variability. A crude division of sediment types can be defined:

high minerogenic content		high organic content
low %BSi		higher %BSi
high sediment density		lower sediment density
low water content	versus	higher water content
finer particle-size, sorted		coarse particle-size, unsorted
detrital magnetic behaviour		non-detrital magnetic behaviour
coarse (MD) magnetic grain size		fine (SSD) magnetic grain size

Recurrent outlier samples are identified in classification, PCA and from leverage diagnostics in RDA. They include SOMB25, MOSS9, MOSS12, MOSS16, all samples from Light Lake, TWIS6 and BOTH. It was considered inappropriate at this stage to eliminate outlier samples as there were no justifiable criteria for their deletion.

(2) Direct ordination with the environment data provides an environmental explanation for observed differences in the sediment sample-set. Canonical variates analysis (CVA) was used to explore broad groupings of data with significant explanatory variables.

Climate effects on lake sediments are controlled directly through water temperature and indirectly through clarity, a surrogate for inwash and productivity, and chlorophyll-a, a productivity and lake developmental indicator. Extrinsic climate effects are conditioned through the degree of catchment development; % quartz-mica-schist represents the proportion of deglaciated catchment and maximum altitude acts as a surrogate for the influence of the central ice-cap on the lake catchments.

(3) Many environmental variables display multicollinearity and are therefore redundant. Data elimination in redundancy analysis (RDA) was used to find a minimum adequate model which explains variation in the sediment data almost as well as the full model. Reduction on the basis of Variance Inflation Factors (VIFs) was favoured as a more intuitive method versus the more traditional means of forward selection. A sub-set of 14 statistically significant explanatory variables was able to explain 30% of variation in the sediment data in the first two RDA axes. Elimination inevitably means some loss of explanatory power in the model but this data loss is minimal (roughly 5%). The 14 variables model includes climatically-relevant variables: the duration of open water, October water temperature, % catchment ice-cover and *Branchinecta*. The inclusion of the water depth at the sampling location makes the model inherently more sensitive to local site factors. It was possible to remove nuisance variation (marine effects). The gradient in water chemistry determinands was relatively weak and the sediments were fairly unresponsive to them, in contrast to diatom studies in the same lakes where water-chemistry determinands such as TP, TN, ammonium and Chl-*a* are dominant in determining between-lake variability in diatom species-assemblages (Jones & Juggins, 1995). The lack of sedimentological response to water chemistry corroborates the poor performance of Hansen's trophic classification (section 5.7.2).

(4) Variance partitioning of the sediment data on the basis of these 14 explanatory variables provides a novel insight into the balance of intrinsic and extrinsic factors controlling sediment variability. The minerogenic and organic determinands are seen to be more responsive to extrinsic, catchment-related factors; particle-size and mineral magnetic behaviour are more strongly affected by intrinsic limnological factors. Limnological dominance on mineral magnetic behaviour supports the hypothesis for non-detrital, authigenic magnetic mineral formation superimposed on a weaker, detrital signal from the catchment. A proportion of unexplained variance (roughly 50%) relates to determinands not quantified in this study. The origin of the different sediment fractions

has a crucial bearing on the construction of a transfer-function model to reconstruct climate as the selected sediment predictor variables in inverse multiple regression must be responsive to the environmental variable being reconstructed. This environmental variable and the sediment predictor variables are selected in the following Chapter.

CHAPTER 9 - A QUANTITATIVE RECONSTRUCTION OF RECENT ENVIRONMENTAL CHANGE

9.1 Introduction

In Chapter 8 direct interactions between the surface-sediment training-set and contemporary environmental data were explored in numerical analysis. Variance partitioning (section 8.6) found that a significant fraction of the variation in the sediments was attributable to catchment-only or limnology-only factors but it was not certain at this stage where the balance of climate control in the sediment was; it could be conditioned through limnology or the catchment. Direct ordination (section 8.4.2) hinted at three possible, climatically-relevant candidates for a quantitative environmental reconstruction: October water temperature, % catchment ice-cover and the period of open water. Birks (1995) provides a proforma for making a quantitative palaeoenvironmental reconstruction using an example of planktonic foraminiferal species data and environmental data. The same rationale is adopted with these data-sets in this Chapter.

The variable to be reconstructed is selected using constrained inverse multiple regression. A transfer-function model uses a training-set of significant sediment response variables in a parsimonious regression model to reconstruct catchment ice-cover in quantitative units. Its performance is assessed and compared with results from an alternative reconstruction technique, the Modern Analog Technique. The best models are used to perform a quantitative palaeoenvironmental reconstruction using matching lithostratigraphical data from dated sediment sequences from four different lake-catchment systems on Signy Island. Accurate supporting chronological control through radiometric dating allows a correlation between sites and offers a means of assessing the rates of environmental change. The ice-cover predictions are validated using historical records of catchment ice-cover and compared with local air temperature records spanning the Twentieth Century to make inferences of the causal effects of ice retreat and the effects of climatic change on the island, its lakes and their sedimentology. The overall aim is to simplify relationships and to produce a robust and repeatable methodology which can be applied to lake-catchment systems on Signy Island with potential for application elsewhere under analogous climatic regimes in either the present or the past.

9.2 Selection of an appropriate environmental variable for reconstruction

9.2.1 Theory

Robust reconstructions of environmental variables from quantitative stratigraphical sedimentological data require a strong statistical relationship between the sediments and the variable to be reconstructed (ter Braak, 1987; 1988). Direct gradient analysis (RDA, CCA) has frequently been used in palaeolimnology as a preliminary analysis for determining whether particular variables influence present-day variation in species assemblage data to sufficiently warrant palaeo-reconstruction from fossil assemblage data (e.g. Pienitz, Smol & Birks, 1995). To test for the effect of an environmental variable on sediment variations, direct gradient analysis (RDA) is performed with one environmental variable as the sole explanatory variable (i.e. sedimentary data constrained by one variable only) to study the marginal effects of each environmental variable. This is a form of linear regression analysis. When response data are constrained to one environmental variable, a high ratio of the first constrained eigenvalue ($\lambda 1$) to the second unconstrained eigenvalue ($\lambda 2$) indicates the relative importance of that variable in explaining the response data (ter Braak, 1987; 1988) and consequently which environmental variables can be used to develop inference models. The objective of this section is to confirm which climatically relevant, quantitative environmental variables sufficiently influence present-day sediment characteristics to warrant reconstruction using fossil sediment data.

9.2.2 Analysis

RDA was performed in CANOCO using one active environmental variable (remainder were deleted). The data were centred and standardized by variables by using a correlation matrix of the response variables to make the regression coefficients of the different sedimentary variables comparable. Each model was tested for significance with unrestricted Monte Carlo permutation tests (99 permutations). This analysis was repeated for each environmental variable to achieve a ranking of potential explanatory power (Table 9.1).

9.2.3 Results

Table 9.1 summarises the results of each RDA with a single explanatory variable versus all sediment variables. The largest axis 1 gradients (largest eigenvalue) are for mean depth (0.106), maximum depth (0.100), % ice-cover (0.089) and clarity (0.089). Their correlations with the sediment data are r=0.717, r=0.706, r=0.699 and r=0.640

respectively.

Table 9.1 Results of RDA (=multiple linear regression) to find suitable environmental variables for reconstruction

Variable tested	λ_1	λ_2	*r*	*p*	*Variable tested*	λ_1	λ_2	*r*	*p*
Depth	.059	.250	.571	0.01	Ammonium	.052	.241	.504	0.01
Altitude	.020	.253	.411	0.01	Nitrate	.051	.248	.549	0.01
Maximum altitude	.073	.251	.644	0.01	TDN	.060	.245	.559	0.01
Distance from sea	.017	.249	.335	0.01	TP	.077	.243	.607	0.01
Catchment area	.024	.255	.401	0.01	SRP	.045	.241	.468	0.01
% ice	**.089**	**.254**	**.699**	**0.01**	SRS	.054	.251	.614	0.01
% QMS	.074	.252	.618	0.01	Cl^-	.047	.255	.507	0.01
% amphibolite	.026	.249	.366	0.01	Na^+	.066	.253	.613	0.01
% marble	.065	.254	.622	0.01	K^+	.073	.242	.591	0.01
% moss	.026	.243	.400	0.01	Mg^{2+}	.048	.245	.496	0.01
% lichen	.013	.255	.420	0.04	Ca^{2+}	.066	.242	.572	0.01
Catchment:lake area	.012	.250	.285	0.02	**Clarity**	**.089**	**.215**	**.640**	**0.01**
Maximum depth	**.100**	**.249**	**.717**	**0.01**	Feb.WT	.023	.245	.374	0.01
Mean depth	**.106**	**.246**	**.706**	**0.01**	Jul.WT	.078	.227	.629	0.01
Length	.024	.248	.381	0.01	Oct.WT	.082	.229	.619	0.01
Breadth	.025	.255	.411	0.01	*Pseudoboeckella*	.026	.241	.373	0.01
Lake area	.028	.242	.396	0.01	*Branchinecta*	.033	.250	.504	0.01
Volume	.070	.254	.616	0.01	Moss	.040	.256	.539	0.01
Open days	.028	.248	.420	0.01	Algal mat	.090	.241	.665	0.01
pH	.053	.240	.524	0.01	Birds	.050	.245	.500	0.01
Conductivity	.047	.253	.518	0.01	Fur seals	.052	.252	.574	0.01
Chlorophyll-*a*	.077	.251	.617	0.01	Elephant seals	.084	.239	.625	0.01
Phaeopigments	.079	.245	.619	0.01					

λ_1 = eigenvalue of RDA axis 1
λ_2 = eigenvalue of unconstrained axis 2
r = species-environment correlation
p = significance level (Monte Carlo unrestricted permutation test, 99 permutations)
Variables in bold with largest axis 1 eigenvalue

The only suitable quantitative predictor variable selected by its large eigenvalue is % ice-cover in the catchment (0.089). The eigenvalue for open days - the period of open water - is too low (0.028) to make a meaningful or reliable reconstruction. A poor match between historical records of lake ice-cover and air temperature variations (R. Thompson, *pers.comm.*) indicates that it would be unwise to attempt a reconstruction until the mechanisms for break-out and freeze-over are fully established. Clarity, as a

nominal variable, has poor predictive potential. Maximum depth, similarly, is of little use. In the selection of a minimum adequate model of 14 explanatory variables (section 8.4.2) the *t*-values of canonical coefficients for clarity and % ice-cover are statistically significant ($p \leq 0.05$). Thus the only climatically-relevant variable suitable for reconstruction is % ice-cover in the catchment, a most fortuitous outcome given the observed loss of permanent snow and ice cover over the last 40 years in probable response to increases in mean annual air temperature (Smith, 1990). These preliminary results suggest that there is a link between the sediments and catchment ice-cover which could form the basis of a reconstruction model. The correlation between air temperature variations and glacier response is well-established and these, in turn, have been linked to features in lake sediment records using sophisticated multivariate techniques (Leeman & Niessen, 1994a; Hardy, 1996).

9.3 Selection of statistically significant response variables

9.3.1 Theory

A sub-set of significant response variables can be extracted from the sediment data-set in a similar way to the selection of the minimum adequate model of explanatory variables (section 8.4.1). Using the selected environmental predictor for reconstruction - % ice-cover - an inverse regression with the sediment data, combined with forward selection, is used to find which combinations of sediment determinands are most strongly linked to variations in catchment ice-cover.

9.3.2 Analysis

Inverse multiple linear regression was performed in CANOCO using % ice-cover as the sole response variable. Sediment determinands are used as predictor variables. This directly tests the hypothesis that there is a causal effect of catchment ice-cover on the sediment characteristics. Data were scaled on a correlation matrix and centred and standardised by species. Forward selection of the sediment variables was applied and each forward-selected variable was tested for its significance ($p \leq 0.001$) using unrestricted Monte Carlo permutation test (999 permutations), adjusted for Bonferroni inequality with each successive selection. The forward selection was stopped when this *p*-value was exceeded and a full model run with the selected variables. The significance of the first canonical axis and the overall trace statistic were tested with an unrestricted Monte Carlo permutation test (99 permutations).

9.3.3 Results

Only four significant sediment determinands were chosen by forward selection: % dry weight, mean particle-size, % loss on ignition and HARD% (Table 9.2), explaining 74% of variation in catchment ice-cover (Table 9.3). This is a highly satisfactory percentage of the explained variance. The first canonical axis and overall model was significant to $p \leq 0.01$ (Table 9.4). All VIFs attained values <2 indicating very low multicollinear relations (section 8.4.3).

Table 9.2 Forward selection of sediment determinands in constrained inverse multiple regression using % ice as the sole response variable

Variable added	*cumulative variance of selected variables*	*number of permutations*	*Bonferroni required significance*	*significance achieved*
% DW	0.27	999	0.05	0.001
Mean particle size	0.44	999	0.025	0.001
% LOI	0.50	999	0.016	0.001
HARD%	0.55	999	0.0125	0.002
Variance explained by all variables	0.74	99	0.05	0.01
No other variables significant at $p<0.01$				

Table 9.3 Summary statistics for constrained multiple regression of sediment determinands using % ice as the sole response variable

RDA axes	*1*	*2*	*3*	*4*	*Total variance*
Eigenvalues	0.547	0.453	0.000	0.000	1.000
Variable-environment correlations	0.740	0.000	0.000	0.000	
Cumulative % variance					
(i) of response variable data	54.7	100.0	0.0	0.0	
(ii) of response variable-environment relationship	100.0	0.0	0.0	0.0	
Σ of all unconstrained eigenvalues					1.000
Σ of all canonical eigenvalues					0.547

Table 9.4 **Canonical coefficients of the four forward-selected determinands, their *t*-values and their inter-set correlations for axis 1**

sediment determinand	*canonical coefficients*	*t-values of canonical coefficients*	*inter-set correlations*
% DW	-0.587	-0.677*	-0.524
Mean particle-size	0.564	0.824*	0.212
% LOI	0.393	0.465*	0.506
HARD%	-0.302	-0.459*	-0.379

* *t*-test significant at $p \leq 0.05$; n=30, 207 d.f., $t \geq 1.96$.

Scatterplots of the selected determinands' response to ice-cover are plotted in Figure 9.1, each fitted with a LOWESS smoother (span=0.35) (Juggins & ter Braak, 1997). %DW increases with increasing ice-cover. Mean particle-size shows fairly constant behaviour as ice-cover increases although at low observed ice-coverage samples are slightly coarser. %LOI decreases with increasing ice-cover. HARD% shows a staggered increase with increasing ice-cover, and is strongly influenced by some high values mid-range.

Figure 9.1 **Scatterplots of % dry weight, mean particle-size, % loss on ignition and HARD% versus observed catchment ice-cover with fitted LOWESS smoother (span=0.35)**

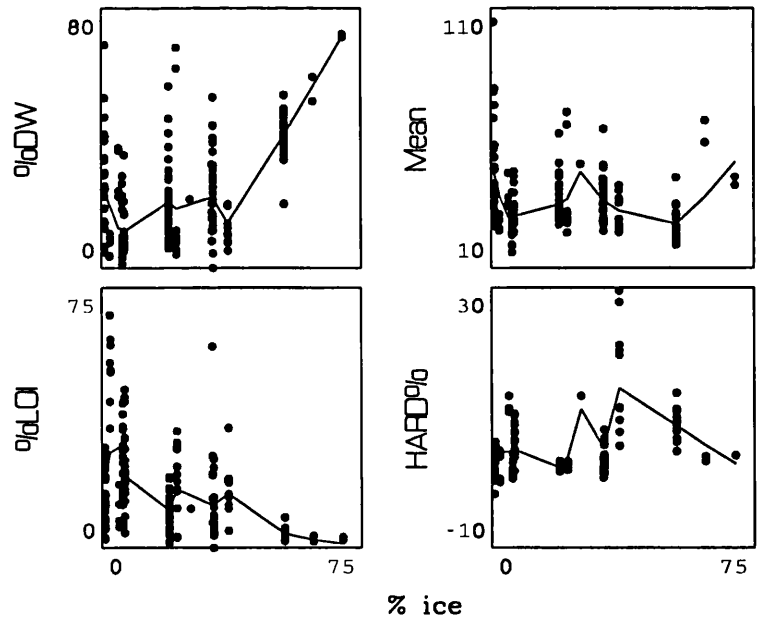

Leverage diagnostics in CANOCO (ter Braak, 1990) were used to check the influence of unusual samples. Only five samples associated with the four forward-selected sediment determinands had >8X leverage: HEY12 (mean particle-size), LITE3 (%LOI), TWIS4 and TWIS5 (both HARD%). There is clearly something unusual about the magnetic characteristics of samples from Twisted Lake. At this stage the decision was taken to retain all outliers in the model since there were no justifiable criteria for their deletion.

An ice prediction equation which forms the basis of the reconstruction model can be proposed on the basis of this regression analysis, with sediment determinands in rank order of predictive ability:

$$\% \text{ ice} \propto \%DW - \%LOI - \text{mean particle-size} - HARD\%$$

Physical and chemical conservatism are important considerations in the selection of appropriate predictor variables and unfortunately diagenesis tends to be greatest in surface-sediments from which training-sets are formed. Despite the occurrence of seasonal anoxia (Ellis-Evans & Lemon, 1989) post-depositional diagenesis of the measured determinands, once incorporated into the sediments, seems to be minimal (section 5.4.2). However, a lack of SSD-sized magnetic material in Wilson's (1993) cores from Sombre and Heywood Lakes suggests some magnetic diagenesis. In light of these unknown post-depositional modifications and given the interpretational problems of the magnetic mineralogy, an even more parsimonious model can be constructed stopping forward selection after the first three determinands (%DW, mean particle-size, %LOI). This model is still capable of explaining 50% of variation in catchment ice-cover (Table 9.2).

All these determinands can be linked to processes occurring in the catchment. %LOI and %DW are well-supported by other studies (Mackereth, 1966; Karlén, 1981; Karlén & Matthews, 1992) as indicators of catchment development and glacial activity. Mean particle-size is related to the weathering processes occurring in the catchments, processes of sediment entrainment and transportation, and environments of deposition in the lake basins. Differences in mean particle-size are apparent between the lakes on the basis of catchment character, i.e. glaciated or non-glaciated (Chapter 6). Removal of the magnetic determinand from the model is advisable given likely variations in source lithology over

time (Stober & Thompson, 1979) and especially in light of the sensitivity of the surface-sediments to the influence of marble and amphibolite geologies (Chapters 6, 7 and 8). Exposures of these geologies have varied over time with fluctuations in ice-cover and subject to weathering will have yielded variable volumes of marble- and amphibolite-rich sediments to the lakes, thus affecting long sediment-sequences. HARD% however, is the most conservative magnetic parameter (Oldfield *et al.*, 1992) and the least susceptible to dissolution or diagenetic changes in the sediments. Its conservatism reduces the potential occurrence of a no-fossil analogue in an environmental reconstruction but model predictions including HARD% should be treated with caution.

9.4 A quantitative reconstruction of catchment ice-cover

Comparative studies, where the same environmental variable is reconstructed using different reconstruction techniques to develop a concensus reconstruction (Bartlein & Whitlock, 1993) are remarkably few (Birks, 1995). Limited comparisons of different reconstruction techniques include ter Braak & van Dam (1989), Birks *et al.* (1990a), Le (1992), ter Braak & Juggins (1993), ter Braak *et al.* (1993), ter Braak (1995), Bartlein & Whitlock (1993), Juggins, Battarbee & Fritz (1994) and Korsman & Birks (1996). Since this was a developmental exercise in an untested environment, the comparison of two different methods was an advantageous means of assessing model performance (section 9.4.5). Two contrasting reconstruction methods were tested - a transfer function based on Partial Least Squares (PLS) regression and analogue matching (Modern Analogue Technique, MAT).

9.4.1 The transfer function approach

Quantitative palaeoenvironmental reconstructions follow two sequential steps (Birks, 1995): regression (this section) and calibration (section 9.5). It is not possible to build an explanatory model of modern sediment responses because of imperfect knowledge. Instead, direct empirical models based on observed patterns of response in modern sediment samples in relation to their environment are used to derive empirical calibration functions. Modern ecological response functions, U_m, (also known as calibration functions, transfer functions or regression coefficients) can be estimated from the modern training set of X and Y using either classical or inverse regression methods:

Classical: $Y_m = \hat{U}_m X_m$

Inverse: $X_m = U_m Y_m$

where Y_m is the matrix of modern surface sediment data and X_m is the matrix of associated environmental data. The environmental variables are assumed to be causally related to Y_m and the results of variance partitioning (section 8.5) confirm that the catchment has a significant, detectable effect on sediment character. Y_m, the modern response data, are formed from the sub-set of statistically significant sediment variables (section 9.3.3).

In this study, an inverse approach is used to achieve the reconstruction. The multiple inverse regression approach has its origins in the work of Imbrie & Kipp (1971) and their reconstructions of sea-surface temperatures and salinity from planktonic foraminifera using calibration functions. This approach is most efficient statistically if the relation between each response variable and the environment is linear with a normal error distribution and the environmental variable has a normal distribution (Brown, 1982). Exploratory data analysis of these data found that many of the response and predictor variables had skewed distributions but this problem is solved by standardisation in CANOCO. The data therefore fulfil the requirement to display a linear response between the sediments and their environment, an assumption which is normally more difficult to satisfy with biological data (pollen, diatoms, foraminifera) as they generally follow unimodal response models.

The regression method best suited to this data-set is Partial Least Squares regression (PLS). PLS has been little used in palaeoenvironmental reconstructions to date. The PLS method was pioneered by Herman Wold in Sweden from the 1930s to mid 1960s for modelling information-scarce situations in the social sciences. The first definitive version of PLS was published in 1977 (Geladi, 1988) using a NIPALS algorithm. Ideas of PLS modelling are closely connected with the evolution of chemometrics (de Jong, 1991; Burnham, Viveros & McGregor, 1996) and the method was introduced mainly as a path-modelling device (studying relations between blocks of manifest variables). PLS performs a similar role to principal components regression (PCR), ridge regression (RR) and stepwise multiple linear regression (SMLR), differing from PCR in that fewer components are selected to maximize covariance with the response variables and it gives a lower prediction error than PC regression. It produces latent variables (pseudoinverse) that contain the essentials of the original data and can be used in a simplified path model. Both PLS and PCR are 'biased' methods of inverse regression because some data

are discarded when only a limited number of uncorrelated orthogonal components are selected from the original data. In this way it avoids collinearity and is more robust, i.e. the model parameters do not change very much when new calibration samples are taken from the total population (Geladi & Kowalski, 1986).

The basic equation for PLS (Geladi, 1988) is:

$$Y = XB + F$$

where Y = a matrix of responses (N x J) (in PLS1 J=1)
X = a matrix of measured features (N x K)
B = a matrix of PLS regression coefficients (K x J)
F = a matrix of residuals (N x J)
N = number of objects, samples
J = number of responses (=1 in PLS1)
K = number of predictor variables

PLS can be used in an exploratory way when no physical models are known that link the dependent (response) and independent (predictor variables). Manifest variables, in this case the sediment determinands, are directly measurable but might have no meaning for the phenomenon being investigated. That is, none may directly give any information about catchment ice-cover. The latent variables in PLS are intuitive, hidden, summarizing variables that are not directly measurable and therefore provide a tool for developing a predictive model. The distinction between latent and manifest variables only appears in multivariate situations. With the help of PLS, it is possible to construct a latent variable that is a very good predictor of % ice-cover. PLS was implemented in CALIBRATE (Juggins & ter Braak, 1997). It has been used by ter Braak & Juggins (1993) and ter Braak *et al.* (1993). Korsman *et al.* (1992) used PLS to calibrate near infra-red spectra of lake sediments to pH. Korsman (1994) and Korsman & Birks (1996) used PLS for calibrating diatom assemblages to pH, colour and alkalinity for lakes in northern Sweden.

Quantitative model validation is an implicit feature of PLS, thereby providing an estimate of the accuracy of prediction. The optimal pseudo-rank (which gives the optimal calibration model) is selected using a validation statistic (the root mean square error of prediction, RMSEP). The correct selection is important because the model is required to describe the significant sources of variance but should not over-fit the data

using irrelevant information in the model from the calibration set. These include non-random components in the noise or fluctuations due to experimental or sampling conditions. Overfitted models have poorer prediction errors. Validation can be achieved through either bootstrapping or jack-knifing methods (Miller, 1974); both are computer resampling procedures. They define a root mean square error of prediction ($RMSEP_{boot}$, $RMSEP_{jack}$) for the PLS model. The most realistic RMSEP estimation involves independent test sets but in palaeoecology usually all the available modern data are used in developing the calibration model.

When only the calibration data are available, as is the case here, an approximation to the real prediction error can be calculated using cross-validation. Jack-knifing is one such cross-validation procedure. It can be used to estimate bias and the standard error using a sub-set of data, assuming that the statistic has a normal error distribution. If the analysis starts with a training-set of 100 samples, one sample is dropped-out and a transfer function model built from the 99 samples. This 99 sample transfer function is then applied to the left-out sample and the predicted value is compared with the observed value and the error or residual calculated for the predicted value. The sample is then re-inserted into the training set, the next sample taken out, and the procedure repeated for all 99 samples in the training set until all samples have been left out once. Errors are accumulated and a prediction error calculated on the basis of these leave-one-out samples. Jackknifing is computationally expensive but it gives a more efficient estimate of the prediction error and the optimal number of PLS model components than simple model fit and 'apparent' errors (ter Braak & Juggins, 1993). The only source of variability in jackknife estimates come from the original data, and larger training-sets improve the accuracy of the technique.

9.4.2 The Modern Analog Technique (MAT)

A second, more simple environmental reconstruction was undertaken to compare with the results from PLS regression. The Modern Analog Technique (MAT) is a numerical comparison technique which uses an appropriate similarity or dissimilarity measure to compare the sediment assemblage in a fossil sample with sediment assemblages in all available modern samples that have associated environmental data. When the model finds the modern sample or group of modern samples that most closely match the fossil sample, the past environment for that sample is inferred to be the modern environmental value(s) for analogous modern sample(s) which have the closest match. Analogues are

identified using the standardised Euclidean distance, a numerical measure of the dissimilarity. The procedure can be repeated for all fossil samples and a simultaneous reconstruction for several environmental variables is made for the stratigraphical sequence on the basis of modern analogues.

Ter Braak (1995) considers MAT to be a *k*-nearest neighbours method of regression via smoothing (Stone, 1977; Hastie & Tibshirani, 1990). Like PLS regression, it is an inverse procedure because it estimates the environmental variable x_0 given the fossil assemblage y_0 (ter Braak, 1995). It could be based on, for example, the mean of the 5 or 10 most similar modern samples (Anderson *et al.*, 1989; Hutson, 1980; Thunell *et al.*, 1994), or the weighted mean of the 5 or 10 most similar modern samples, with the weights being the inverse of the dissimilarity values so that modern samples that have the lowest dissimilarity (i.e. are the most similar) have the greatest weight in the reconstruction (e.g. Prell, 1985; Morley, 1989b; Bartlein & Whitlock, 1993). The requirements for MAT are very similar to other reconstruction techniques (Birks, 1995).

MAT was used by Bartlein & Whitlock (1993) in their study of environmental change at Elk Lake, Minnesota, using fossil pollen assemblages to reconstruct January temperature, July temperature and annual precipitation. They compared their MAT reconstructions with reconstructions based on regression and response surface techniques. Peng *et al.* (1993) used analogue-matching to reconstruct vegetational "ecosystems" in Europe at 6000 BP. Guiot (1990) and Guiot *et al.* (1993a, 1993b) developed a more mathematically complex variant of MAT to reconstruct a range of past climatic variables from fossil pollen assemblages including January, April, July & October temperature and precipitation anomalies for the last interglacial-glacial cycle. Its relative performance with other reconstruction techniques has been assessed with training-sets of modern diatom samples from saline lakes in the Northern Great Plains of North America (Juggins *et al.*, 1994) and with the Imbrie & Kipp (1971) marine planktonic foraminifera training-set (Birks, 1995) and it has been found to produce reasonable reconstructions. Other examples of the use of this simple MAT include Hutson (1980), Prell (1985), Morley (1989b), Anderson *et al.* (1989), Le (1992) and Thunell *et al.* (1994). MAT was therefore seen to be well suited to this type of quantitative reconstruction where these linear response data lack the complexity of non-linear biological species-environment responses.

9.4.3 Analysis

9.4.3.1 PLS regression

The transfer function was created in CALIBRATE using inverse regression of both the four- and three-determinands models (section 9.3.3). Catchment ice-cover was selected as the variable to be reconstructed. The X matrix (dependent variables, i.e. sediments) was standardized. Model validation was achieved using 'jackknifing' (leave-one-out) cross-validation for the default number of components (n=6) suggested by CALIBRATE. The model performance was assessed on the basis of its apparent errors (RMSE) and errors of prediction ($RMSEP_{jack}$) supported by values for r^2 (coefficient of determination) and bias (systematic prediction error), and sample leverage and residuals (predicted - inferred) given in the CALIBRATE output.

9.4.3.2 MAT

The program MAT (Juggins, 1994) was used to derive measures of dissimilarity between modern samples for present-day ice coverage (1993) using standardised data. The squared-Euclidean distance dissimilarity coefficient for the second percentile, i.e. the extreme 10% of the dissimilarities calculated between all modern samples, was taken as an approximate threshold value to indicate a good analogue (cf. P.Anderson *et al.*, 1989; Bartlein & Whitlock, 1993). The optimum number of analogues, namely the number of matches that give the lowest RMSE, was selected for reconstruction using the fossil data (section 9.5.2).

9.4.4 Results

Error estimates of PLS regression and MAT with the four and three determinands models and different training-sets are summarised in Tables 9.5 and 9.6 respectively.

9.4.4.1 Four-determinands model (208 samples)

The four determinands model uses %DW, mean particle size, %LOI and HARD% to predict % ice for the 208 sample training-set. A three component PLS model gives the best model prediction with the lowest RMSEP (ter Braak & Juggins, 1993). The apparent root-mean-square error (RMSE) for the % ice calculations is 12.33 with a r^2 of 0.55 and maximum bias of 36.02 (Table 9.5). The jack-knifed root mean square error of prediction ($RMSEP_{jack}$) is 12.69 with a r^2 of 0.52 and maximum bias of 38.13.

Table 9.5 Error estimates for various reconstruction models using different training-sets for four sediment determinands (%DW, mean particle-size, %LOI, HARD%) (NA = not applicable)

Model	*n*	*RMSE*	r^2	$RMSE_{(jack)}$	r^2
PLS 3 components	**208**	**12.3289**	**0.5491**	**12.6860**	**0.5231**
MAT (squared Euclidean distance, mean of optimal number of closest matches = 10)	"	15.8049	0.2624	NA	NA
MAT (squared Euclidean distance, weighted mean of optimal number of matches = 10)	"	NA	NA	15.6496	0.2922
PLS 3 components	205	12.3488	0.5486	12.7251	0.5211
MAT (squared Euclidean distance, mean of optimal number of closest matches = 10)	"	15.8203	0.2617	NA	NA
MAT (squared Euclidean distance, weighted mean of optimal number of matches = 10)	"	**NA**	**NA**	**15.5546**	**0.2991**
PLS 3 components	103	12.4118	0.5318	13.1117	0.4796
MAT (squared Euclidean distance, mean of optimal number of closest matches = 9)	"	16.0994	0.2345	NA	NA
MAT (squared Euclidean distance, weighted mean of optimal number of closest matches = 10)	"	NA	NA	15.9940	0.2401

Best reconstruction methods in bold.
Best regression method = 3 components PLS for 208 samples.
Best analogue method = MAT weighted mean of optimal number of closest number of matches (n=10) for 208 samples.

Scatterplots of samples in relation to observed ice versus PLS-predicted values, leverage and residuals leverage are displayed in Figure 9.3. The plot of PLS-predicted versus observed ice cover with a fitted LOWESS smoother (Figure 9.2) gives a reasonable straight-line fit, with a slight 'shoulder' at mid-range values. The values for high % ice cover are highly dependent on the samples from Lake 13 and Orwell Lake; ideally more samples with high observed ice-covers are required to improve the accuracy of prediction. A downward trend in the residuals (Figure 9.3) is apparent: the model over-estimates at low % ice-cover and under-estimates at high % ice-cover. HEY12, TWIS8 and TWIS5 are apparent outliers with high leverage. HEY12 has a very low SIRM (section 7.3.5) which affects the calculation of HARD%, making the sample more 'hard' than others in Heywood Lake. HARD% relates to glacial activity and Heywood catchment has limited ice-coverage, hence the mismatch. The core was sampled from the South basin (section 4.3.2) which is notably more minerogenic and probably more susceptible to inwash and sediment translocation than the North basin with its organic gyttyas. TWIS5 and TWIS8 have unusually high values for HARD% (section 7.3.11). KNOB9 has an unusually high residual (Figure 9.3) with predictions exceeding observed; it was noted for its very low SOFT% value (section 7.3.13) and

Figure 9.2 Predicted versus observed % ice-cover using the 4 determinands 3 component PLS model with fitted LOWESS smoother (span=0.35)

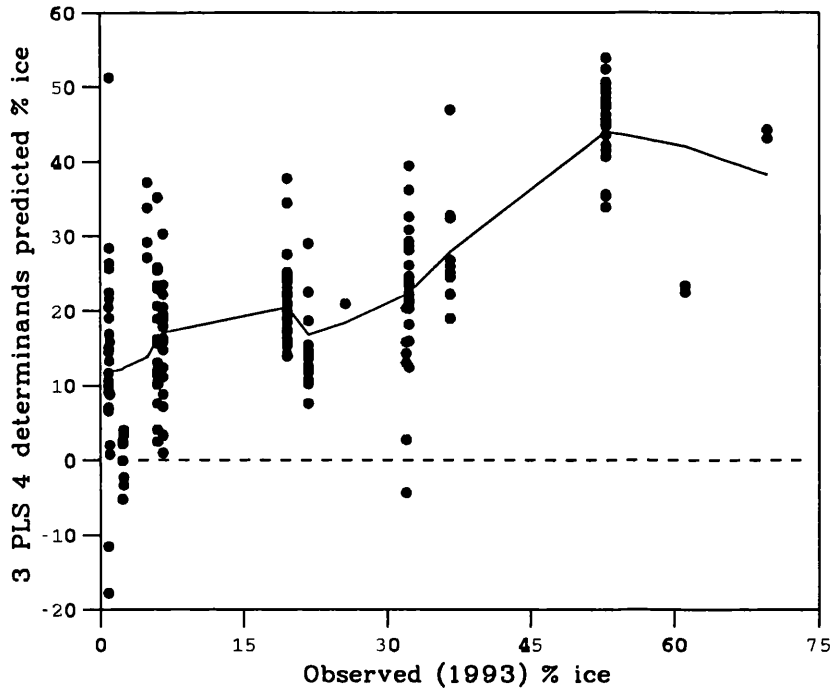

antiferromagnetic behaviour. Its leverage however, is low. PUMP1 and PUMP4 have unusually low residuals, with predicted far lower than observed. These samples were disproportionately 'soft' (7.3.12) for their recorded ice-coverage, possibly due to source mineralogy differences (presence of iron-bearing rocks), and had relatively coarse particle-size (mean 52.54 and 40.93 μm respectively).

The MAT model second percentile (DC=28.31) was used to indicate a good analogue. The majority of samples have DC values below this cut-off, indicating good matching. 'Poor' analogue samples with values exceeding the second percentile cut-off include SOMB21, PUMP3 & 7, TRAN12 & 21, EMER28 and GNES5, 10, 17 & 22. The overall MAT model has DC values below this cut-off. The RMSE and RMSEP are slightly higher than the equivalent PLS model (*ca.*15.7%) and the r^2 between observed and predicted is much lower (*ca.*0.27) indicating a weaker performance (Table 9.5).

9.4.4.2 Three determinands model (208 samples)

The three-determinands model used %DW, mean-particle size and %LOI to predict % ice using the 208 sample training-set. A two component PLS model gives the lowest prediction error: RMSE=12.99, r^2=0.5, maximum bias=35.38; RMSEP=13.27, r^2=0.48

Figure 9.3 **Scatterplots of (a) sample leverages and (b) residuals (predicted-observed) versus observed % ice-cover for the 4 determinands 3 PLS model**

(a) Sample leverages

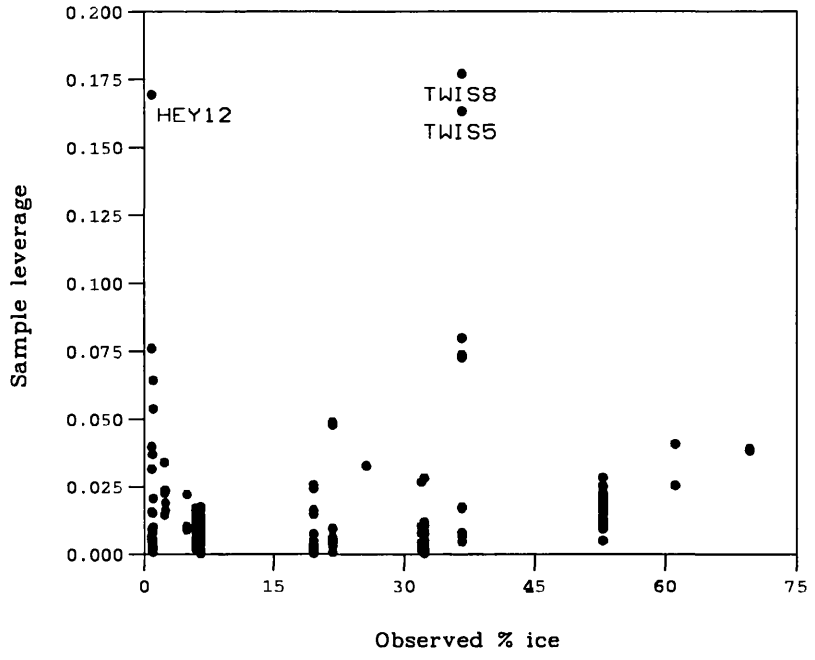

(b) Prediction residuals

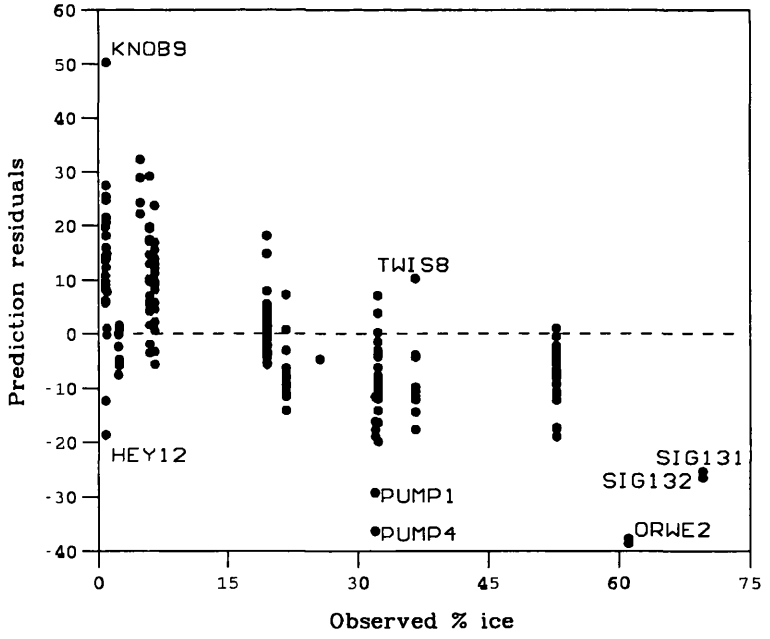

and maximum bias=36.74 (Table 9.6). The predictive capability is marginally worse than the four determinands PLS model (Table 9.5). This time, only HEY12 occurs as an

outlier with high leverage. HARD% is not the only property responsible for its unusual characteristics in the training-set as this sample also has an unusually coarse particle-size (mean=104.7 μm) and low organic content (7.16% LOI) in comparison with the other samples from Heywood Lake.

Table 9.6 Error estimates for various reconstruction models using different training-sets for three sediment determinands (%DW, mean particle-size, %LOI) (NA=not applicable)

Model	*n*	*RMSE*	r^2	$RMSE_{(jack)}$	r^2
PLS 2 components	**208**	**12.9868**	**0.4997**	**13.2712**	**0.4780**
MAT (squared Euclidean distance, mean of optimal number of closest matches = 6)	"	16.0141	0.2718	NA	NA
MAT (squared Euclidean distance, weighted mean of optimal number of matches = 10)	"	NA	NA	16.2274	0.2672
PLS 2 components	207	12.9930	0.4982	13.2713	0.4768
MAT (squared Euclidean distance, mean of optimal number of closest matches = 10)	"	16.0053	0.2543	NA	NA
MAT (squared Euclidean distance, weighted mean of optimal number of matches = 10)	"	NA	NA	16.0787	0.2678
PLS 2 components	103	13.1286	0.4761	13.8039	0.4238
MAT (squared Euclidean distance, mean of optimal number of closest matches = 10)	"	**14.8529**	**0.3388**	**NA**	**NA**
MAT (squared Euclidean distance, weighted mean of optimal number of closest matches = 10)	"	NA	NA	15.0444	0.3456

Best reconstruction methods in bold.
Best regression method = 2 components PLS for 208 samples.
Best analogue method = MAT weighted mean of optimal number of closest number of matches (n=10) for 103 samples.

The MAT model second percentile (DC=1.27) was taken as the threshold value to indicate a good analogue. The majority of samples have DC values well below this threshold indicating good analogues but the following samples are 'poor' analogues with DC values exceeding the threshold: SOMB12 & 26, HEY8, CHAN8 & 11, MOSS9 & 16, PUMP5, LITE2 & 5, TRAN10, 13, 19 & 21, EMER3, 7, 11, 19 & 30, TWIS4 & 5, and GNES11, 14, 15 & 19. The best MAT model with the lowest RMSEP uses the mean of 6 closest matches (RMSEP=16.01, r^2=0.27); the weighted mean of the 10 closest matches gives a marginally worse performance (RMSEP=16.23, r^2=0.27). Both MAT models are considerably weaker than the corresponding PLS regression results.

9.4.4.3 Four-determinands model screened for outliers (205 samples)

The samples HEY12, TWIS5 and TWIS8 identified in the scatterplot (Figure 9.3) on the

basis of their unusually 'hard' mineral magnetic behaviour were removed from the training-set leaving a total of 205 samples. PLS model calibration was performed in CALIBRATE using jackknifing as above. A three component PLS model gives the lowest error of prediction: RMSE=12.35, r^2=0.55, maximum bias=37.77, RMSEP=12.73, r^2=0.52, maximum bias=39.58 (Table 9.5). This performance is marginally worse than PLS with the 208 sample training-set. Results for MAT give a second percentile cut-off of DC=8.19. A few samples exceed this critical threshold indicating 'poor' analogues: SOMB21, PUMP3, PUMP7, TRAN12 & 21, EMER14, 15, 26 & 28, TWIS10 and GNES5, 10, 17 & 22. The mean and weighted mean of the 10 closest matches give the optimal predictions (mean RMSEP=15.82, r^2=0.26; weighted mean RMSEP=15.56, r^2=0.3). These results are an improvement on the 208 sample training-set but are weaker than PLS regression.

9.4.4.4 Three-determinands model screened for outliers (207 samples)

HEY12 is the only sample with high leverage in the 3 determinands, 208 sample PLS model (section 9.4.4.2) and was therefore removed to leave a total of 207 samples in the training-set. A two component PLS model gives the best model prediction with the 207 sample training-set: RMSE=12.99, r^2=0.5, maximum bias=36.71; RMSEP=13.27, r^2=0.48, maximum bias=38.32 (Table 9.6). Again, MAT performs less well than PLS; the optimal model performance with this training-set uses the mean of the 10 closest matches (RMSEP=16.01, r^2=0.25). Several samples exceed the second percentile cut-off (DC=0.78) indicating 'poor' analogues: SOMB12 & 26, HEY8 & 9, MOSS9 & 15, PUMP4, LITE2 & 5, SPIR2, TRAN10, 13, 19 & 21, EMER3, 8, 12, 13, 19 & 30, TWIS4 & 5, and GNES10, 11, 14, 15 & 19. Removal of outlier HEY12 makes little improvement to the performance of the three determinands models and the sample was therefore re-inserted into the training-set.

9.4.4.5 Subset of profundal sediments (103 samples)

In lakes of regular morphometry, cores from the profundal zone are commonly assumed to be representative of basin-wide processes and cores for palaeoenvironmental reconstruction are frequently taken from the deepest point to ensure continous sedimentation (see Chapter 4). The 208 sample training-set encompasses a wide sampling range within each lake to ensure a full gradient covering the range of contemporary sediment types for reconstruction purposes. At this stage the question of

sample-set size was addressed. Was this large training-set (n=208) really necessary and could the transfer-function have been derived from a smaller number of samples selected from the profundal zone?

To test the representativeness of the profundal zone, a smaller training-set was extracted from the 208 sample training-set. This comprises 103 samples from sampling sites at greater than the mean depth of each lake basin. This still includes a large number of samples, fulfilling the need for a minimum of 100 samples in a training-set (Birks, 1995). Both the four- and three-determinands models were tested using this training-set.

A two component PLS model gives the best error of prediction for both the four and three determinands models (RMSE=12.41, r^2=0.53, maximum bias=34.82; RMSEP=13.11; r^2=-.48; maximum bias=38.37). The second percentile (DC=0.09) was chosen for the critical cut-off in MAT and many samples (n=59) exceeded this threshold. Model results are still worse than PLS regresssion but better than the 208- or 207-sample MAT models. The optimal four-determinands MAT model uses the weighted average of the 10 closest matches (RMSEP=15.99, r^2=0.24).

The three determinands PLS model yields a RMSE=13.13, r^2=0.48 and maximum bias=34.71; RMSEP=13.80, r^2=0.42, maximum bias=38.14 (Table 9.6). The second percentile cut-off (DC=0.05) isolated fewer 'poor' analogues (n=27) than the four determinands MAT model. The optimal MAT model uses the mean of the 10 closest matches (RMSEP=14.85, r^2=0.34), the best of all the MAT model results.

9.4.5 Discussion

Variance in the sediment data is sufficient to reconstruct catchment ice-cover (section 9.2) and the prediction models for inferring catchment ice-cover are good given the noise in the lake-catchment systems. There is negligible difference between the prediction errors for four or three determinands using either the 208, 207 or 103 sample training-sets but in most cases the four-determinands model is more accurate. The RMSEP for the various models is fairly low, and certainly no worse proportionally than the errors associated with other climate-related transfer functions based on diatom data (e.g. Pienitz, Smol & Birks, 1995; Vyverman & Sabbe, 1995). For any reconstruction of catchment ice-cover using four sediment determinands, the errors of estimation and prediction are approximately 12-16% and the correlation between observed and predicted

ice cover is between r^2=0.25-0.55. These correlations are low but are not reliable indicators of model performance as they are more dependent on the size of the training-set (H.J.B.Birks, *pers.comm.*). The RMSEP provides a better, unbiased measure of performance but in MAT the RMSEP is strongly over-estimated by cross-validation (ter Braak, 1995) and performance is probably worse than indicated. Screening for outlier samples makes only marginal improvements to the PLS models. The best PLS model performance is with the 208 sample training-set using four sediment determinands ($RMSEP_{jack}$=12.69%, r^2=0.52). Either a two or three component PLS model yields the best regression model predictions. The inability of further components in PLS to improve the ice-cover predictions suggests that the residual structure in the sediment data after extracting the first component contained much random noise.

The mean or weighted mean of the 10 closest matches generally gives the best MAT model predictions and the best MAT model using four determinands is for the mean of the 10 closest matches using the screened 207 sample training-set (RMSEP=15.56, r^2=0.3). MAT is therefore more sensitive to unusual samples. The best MAT model overall uses three determinands and the mean of 10 closest matches using the 103 sample training-set (RMSEP=14.85, r^2=0.34). The loss of samples from the shallow, littoral zones produces a more homogeneous data-set but it is the loss of the magnetic determinand, HARD%, which reduces heterogeneity in the training-set, enabling better analogue-matching. PLS regression with jack-knife cross-validation is relatively insensitive to this loss of data, even with the exclusion of over half the samples. This is because some samples at the extreme ends of the gradient, particularly those from Lake 13 and Orwell Lake, are still part of the 103 sample training-set, and their coarse, bottom-sediments are analogous to sediments from the shallow littoral zones of other lakes. In general, the full gradient from littoral to profundal is not captured in the sample-net (Chapter 4) the model is already biased to some degree towards profundal samples resulting in a relatively homogenous sediment data-set. Loss of the within-lake variability gives more emphasis to between-lake variability and associated differences in catchment ice-cover.

A clear bias can be seen in the PLS errors. All PLS models under-estimate ice-cover at low observed % ice-cover and slightly over-estimate at high observed % ice-cover. This is an inherent problem with inverse regression methods which is difficult to adjust for. Ter Braak (1995) stated that the inverse approach performs slightly better when the

fossil samples are from the central part of the distribution of the modern training-set (see also Birks, 1995). Classical regression methods, on the other hand, ensure that the model works at the extreme ends of the gradients with reduced errors. The best model predictions for ice cover using the PLS model are therefore mid-range values, i.e. 30-50% ice cover.

9.5 Model calibration

9.5.1 Theory

Calibration is the second step in a quantitative palaeoenvironmental reconstruction (Birks, 1995). In calibration, X_f, the past environment, in this case catchment ice-cover, is reconstructed from fossil core data:

$$X_f = \hat{U}_m \, Y_f$$

where Y_f is fossil core data (fossil set) and $\hat{U}_m$ is the transfer function derived from modern response data in the regression step (section 9.4). The fossil core data are a set of variables from the core that match the sediment determinands used in the transfer function model (i.e. %DW, mean particle-size, %LOI, HARD%). Calibration by analogue-matching can be achieved in a similar way with MAT to provide down-core reconstructed values for catchment ice-cover. PLS and MAT give statistical estimations of standard errors of prediction for each reconstructed value but only PLS gives sample-specific standard errors of prediction. The cut-off value (Bartlein & Whitlock, 1985) in analogue-matching is an alternative means of assessing, through dissimilarity, which samples are 'poor' analogues thus representing conditions which are not found in the modern training-set.

Model calibration is possible at four sites on Signy Island. Several long sediment-sequences have radiometric chronologies (Appleby, Jones & Ellis-Evans, 1995; V.J. Jones, *pers.comm.*) and an absolute timescale is necessary to achieve model validation of observed ice-cover in the past from model-predicted estimates. Lakes with dated sediment sequences include Sombre, Heywood, Moss, Tranquil and Emerald Lakes. The Moss Lake chronology is considered unreliable owing to an apparent hiatus in the sequence in the late 1960s, truncating the radiometric signal (Appleby *et al.*, 1995) and a second dated sequence also gives unreliable dates (P.G. Appleby, *pers.comm*). It was therefore excluded from the calibration. The four selected lakes all have different

present-day catchment ice-coverages, are at different altitudes and are found on either side of the island's central ice-cap (Sombre and Heywood to the east, Tranquil and Emerald to the west). Model performance can therefore be tested with respect to sensitivities of glacier response with local geographic variation. If the model is unstable under local influences such as topography or lithology then its application at other sites and extrapolation of results to regional climate reconstructions is severely questionable. Core ^{210}Pb chronologies are summarised in Appendix D.

9.5.2 Analysis

Cores SOMB2, HEY2, TRAN1 were collected by V.J. Jones in 1991 and analytical data are archived at the Environmental Change Research Centre, University College London. Core EMER16 was collected as part of this study in 1994. Surface-sediments of SOMB2, HEY2 and TRAN1 are not included in the training-set. Radiometric dating of the sediment sequences was undertaken by P.G. Appleby, University of Liverpool.

Core lithology (%DW, %LOI) was measured according to the methods outlined in Appendix A. Mean values from adjacent levels were used to replace missing values in archive data for SOMB2, HEY2 and TRAN1. Particle-size analysis of all four cores was undertaken on the Malvern Series 2600 using the methodology outlined in Chapter 6 and results were derived using the blending algorithm from the 100 mm and 300 mm range lenses. Mineral magnetic measurements were referenced from Wilson (1993) to obtain down-core values for HARD% for cores SOMB2 and HEY2 only. No magnetic measurements were available for cores from Tranquil and Emerald Lakes.

PLS calibration was implemented by CALIBRATE (Juggins, 1997). The regression model (four and three determinands) was applied to core data to obtain a prediction of % ice-cover over the timescale of the ^{210}Pb chronology (i.e. from the late-Nineteenth Century to present). Unlike bootstrapping, jackknifing is unable to give sample-specific error estimates for fossil samples.

The modern data-fossil match in MAT calibration was carried out using the program MAT (Juggins, 1994) using the output data file from the earlier analysis (section 9.4.3.2) and the squared Euclidean distance dissimilarity coefficient using a default of the mean and weighted mean of 10 closest matches. The 208 sample-training set was used (weighted mean of 10 closest matches), despite its slightly poorer performance, to

maintain comparability with reconstructions based on PLS calibration. Fossil data were standardised using means and standard deviations of the 208-sample training-set (4 and 3 determinands respectively) owing to the small number of samples in the fossil sets (cf. Overpeck, Webb & Prentice, 1985). Reconstructions were made with the optimal four and three determinands MAT models with the lowest RMSEPs: four determinands = weighted mean of 10 closest matches; three determinands = mean of 10 closest matches (Tables 9.6 & 9.7).

Stratigraphic plots were prepared using Tilia Version 2.0 (Grimm, 1993) and Tiliagraph Version 1.10 (Grimm, 1991).

9.5.3 Sombre Lake

9.5.3.1 Ice-cover reconstructions using four sediment determinands

^{210}Pb activities span the core from 0-10.25 cm and the CRS chronology dated 7.25 cm to 1856±25 yrs AD (Appleby, Jones & Ellis-Evans, 1995). Results of optimal model calibration using 4 sediment determinands (3 components PLS, MAT weighted mean of 10 closest matches) are presented in Table 9.7 and as a stratigraphic plot in Figure 9.4.

The PLS predicted ice-cover in the 0.5 cm sample (17.05%) is very close to the observed ice-cover in the Sombre Lake catchment (19.55%). Most MAT fossil samples have good analogues in the modern data-set (minimum DC<28.31); poorer matches occur at 4.75 cm (1947±2 AD), 6.5 cm (*ca.*1871 AD) and 6.75 cm (1867±17 AD) where DC values exceed the second percentile cut-off indicating sediment characteristics not represented in the modern set.

PLS predicted % ice-cover is fairly constant (*ca.*25%) at the end of the 19th Century and then decreases slightly at the turn of the 20th Century to a minimum of 21.48% in 1905 AD. MAT predictions are roughly 10% lower for the same time period, suggesting under-prediction, but closely match PLS predictions at 1905 AD (19.63%). PLS predicted ice-cover then shows a steady increase from 1913 (24.51%) to 1947 AD (32.68%) in line with increasing %DW and mean particle-size and decreasing %LOI and HARD%; MAT results parallel this trend, also reaching a maximum at 1947 AD (24.59%). A slight dip in PLS predicted ice-cover occurs in 1955 AD (30.76%), matched by a dip in MAT predictions (12.20%), prompted by stasis in %DW and HARD%, a slight increase in mean particle-size and a decrease in %LOI. A sharp shift in the curve

Table 9.7 Comparison of reconstruction results using PLS regression and analogue matching using the 208 sample training-set and fossil data for Sombre Lake (SOMB2)

Mean depth (cm)	*^{210}Pb year AD (0cm=1991)**	*Predicted % ice*					
		PLS Model 4[3]	*MAT 4 mean*	*MAT 4 weighted mean*	*PLS Model 3*[2]	*MAT 3 mean*	*MAT 3 weighted mean*
0.50	1987	17.0539	22.0940	21.7915	19.2453	26.7780	27.9452
0.75	1986	15.2449	24.6380	23.9130	17.3129	25.7210	27.0330
1.25	1984±2	20.4656	23.3660	22.2760	22.8281	24.6380	23.5159
1.50	1980	21.5704	27.5310	14.1818	23.9029	14.3170	12.5547
1.75	1978	18.0208	21.5780	21.0158	20.3985	17.5550	18.6233
2.25	1974±2	19.3681	16.8990	19.3641	21.7011	18.6220	2.9375
2.50	1971	26.3736	16.8830	16.4527	29.1076	25.4530	18.6277
2.75	1968±2	28.2322	24.0010	30.7791	31.3088	27.3130	53.1112
3.25	1963±2	34.5084	22.6400	20.3271	37.6700	26.2330	31.7954
3.50	1961	34.5150	25.6460	20.7346	37.8871	26.2330	32.8816
3.75	1960±2	35.9875	22.6400	20.2321	39.0430	25.9860	26.5511
4.25	1957±2	36.6656	22.6400	20.5040	39.7492	25.9860	23.6642
4.50	1955	30.76Mw	14.1300	12.2006	33.3708	17.8410	7.0352
4.75	1947±2	32.6816	31.2090	24.5853	34.9521	20.1660	22.9286
5.25	1923±4	26.1719	19.3800	20.7963	28.3392	33.8480	26.7477
5.50	1913	24.5085	16.4070	17.8402	26.0913	13.4930	10.1564
5.75	1905±6	21.4792	16.8990	19.6327	22.6305	17.3500	18.1863
6.25	1886±10	26.2494	10.3220	8.2558	27.6829	16.8210	11.3674
6.50	1871	26.1270	15.1050	13.7359	27.3038	12.2500	8.4613
6.75	1867±17	25.4301	11.7770	10.3824	26.7677	15.8610	13.9199
7.25	1851±25	25.0695	17.1360	14.0994	26.3752	16.2220	8.0473

* CRS method. Ages without error estimates derived by interpolation between adjacent stratigraphic levels based on calculated rates of sedimentation (cm yr^{-1})

[3] 3 component PLS; [2] 2 component PLS. See Tables 9.5 & 9.6 for model RMSEP, r^2 and maximum bias.

MAT 4 mean = squared Euclidean distance, mean of optimal number of closest matches = 10

MAT 4 weighted mean = squared Euclidean distance, weighted mean of optimal number of closest matches = 10

MAT 3 mean = squared Euclidean distance, mean of optimal number of closest matches = 10

MAT 3 weighted mean = squared Euclidean distance, weighted mean of optimal number of closest matches = 10

occurs between 1955 AD and 1957 AD in both models coupled with an abrupt increase in %DW and relative decrease in %LOI.

Post-1957 AD both PLS and MAT predicted ice remained at a higher level (*ca.*35% for PLS, *ca.*20% for MAT), principally in response to elevated %DW. This time period

Figure 9.4 Catchment ice-cover reconstruction for Sombre Lake (n=4)

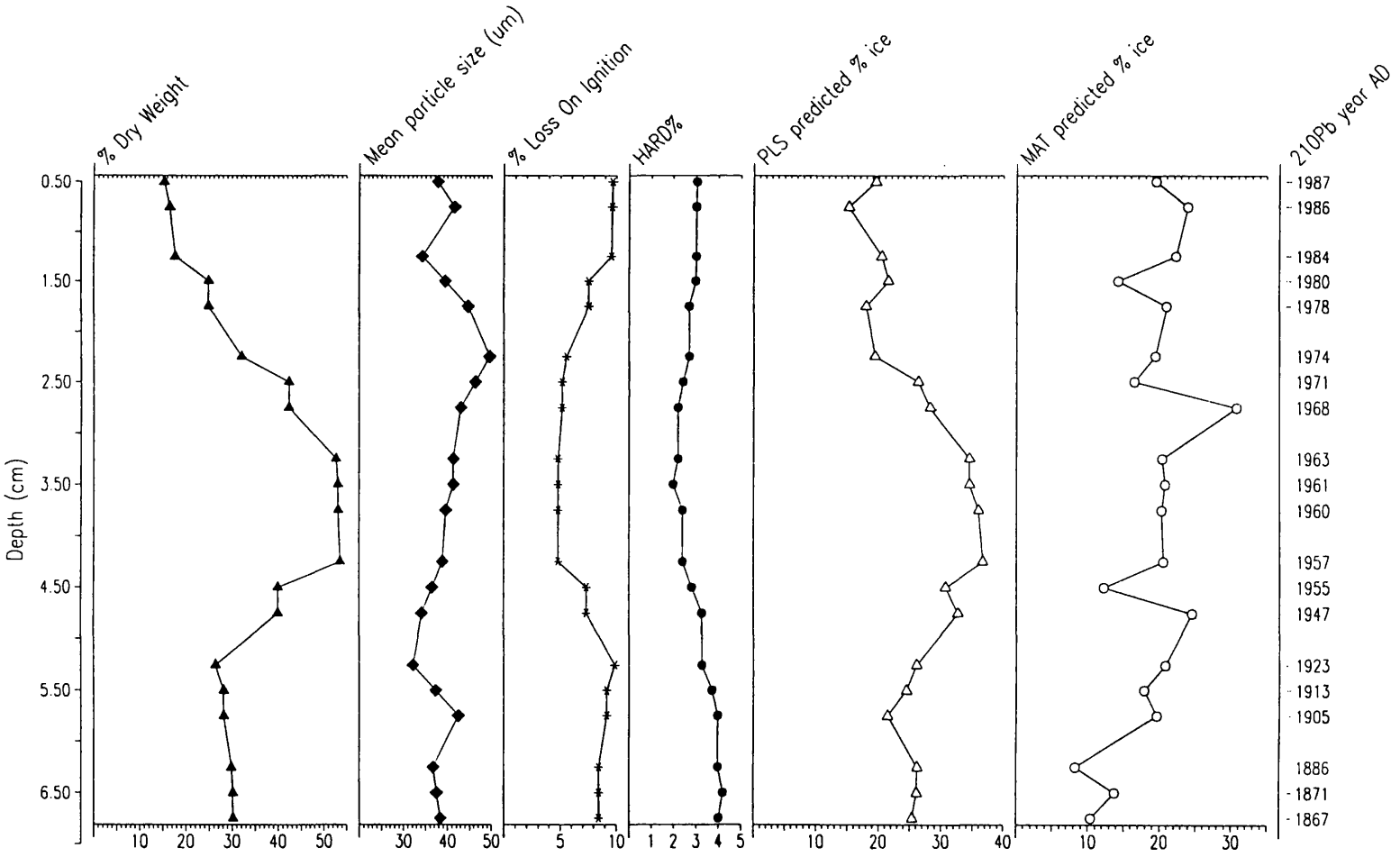

corresponds to the inwash horizon noted by Appleby, Jones & Ellis-Evans (1995) between 4.5 cm (*ca.*1955) and 2.5 cm (*ca.*1971) (section 4.3.1). MAT shows a peak ice-cover of 30.78% in 1968 AD. A steady decline is evident from the mid-1960s as %DW decreases. From 1971-1974 AD results from the two models start to diverge; PLS shows continued ice-cover decline in close parallel with trends in %DW but MAT shows a slight increase in response to a slight coarsening of particle-size. Thereafter the two models continue to show a decrease in tandem. Around 1980-1984 AD ice-cover shows a slight recovery to *ca.*20% in both models and a short steady-state period. Both %DW and %LOI are constant at this time. Post-1984 AD the decline continues, steadily in PLS results and in parallel with decreasing %DW. The dip in PLS predicted ice-cover at 1986 AD (15.25%) corresponds to a particle-size peak (mean *ca.*40 μm). MAT predictions are unaffected by this change in particle-size. %LOI and HARD% are constant. At the top of the core sequence, an increase in ice-cover is seen in PLS and slight decrease in MAT. This is an artefact of the stratigraphic plot. The first sample is the observed catchment ice-cover in 1993 AD (19.55%) and shows that PLS is slightly under-predicting recent ice-cover (17.05%); MAT predictions are slight over-predictions (21.79%) at this time. These errors are small and well-within the PLS (RMSE-12.33% and RMSEP=12.69%) and MAT (RMSEP=16.01%) prediction errors.

9.5.3.2 Ice-cover reconstructions using three sediment determinands

The reconstruction was repeated using fossil data from Sombre Lake and 2 components PLS model and MAT model of the mean of 10 closest matches. Results are summarised in Table 9.7 and Figure 9.5. Two fossil horizons have poor analogue matches exceeding the second percentile threshold value (min.DC=1.27), at 0.75 cm (*ca.*1986 AD) and 1.5 cm (*ca.*1980 AD). Patterns in down-core predictions are very similar to the four determinands model results above (section 9.5.3.1) and generally parallel changes in %DW. The 0.5 cm PLS predicted ice-cover (19.25%) is much closer to the observed 1993 ice cover (19.55%). MAT over-estimates modern ice-cover by 5% (predicted value=26.78%).

In the stratigraphic plot (Figure 9.5). MAT predictions show some slight deviations from the four determinands MAT results, showing a strong peak in ice cover in 1923±4 AD (33.85%) which is not evidenced in PLS or in Figure 9.4. The behavioural shift from relatively constant ice-cover (*ca.*15%) at the turn of the Century occurs after 1905 AD in PLS and after 1913 AD in MAT. Ice-cover continues to increase in PLS through the

Figure 9.5 Catchment ice-cover reconstruction for Sombre Lake (n=3)

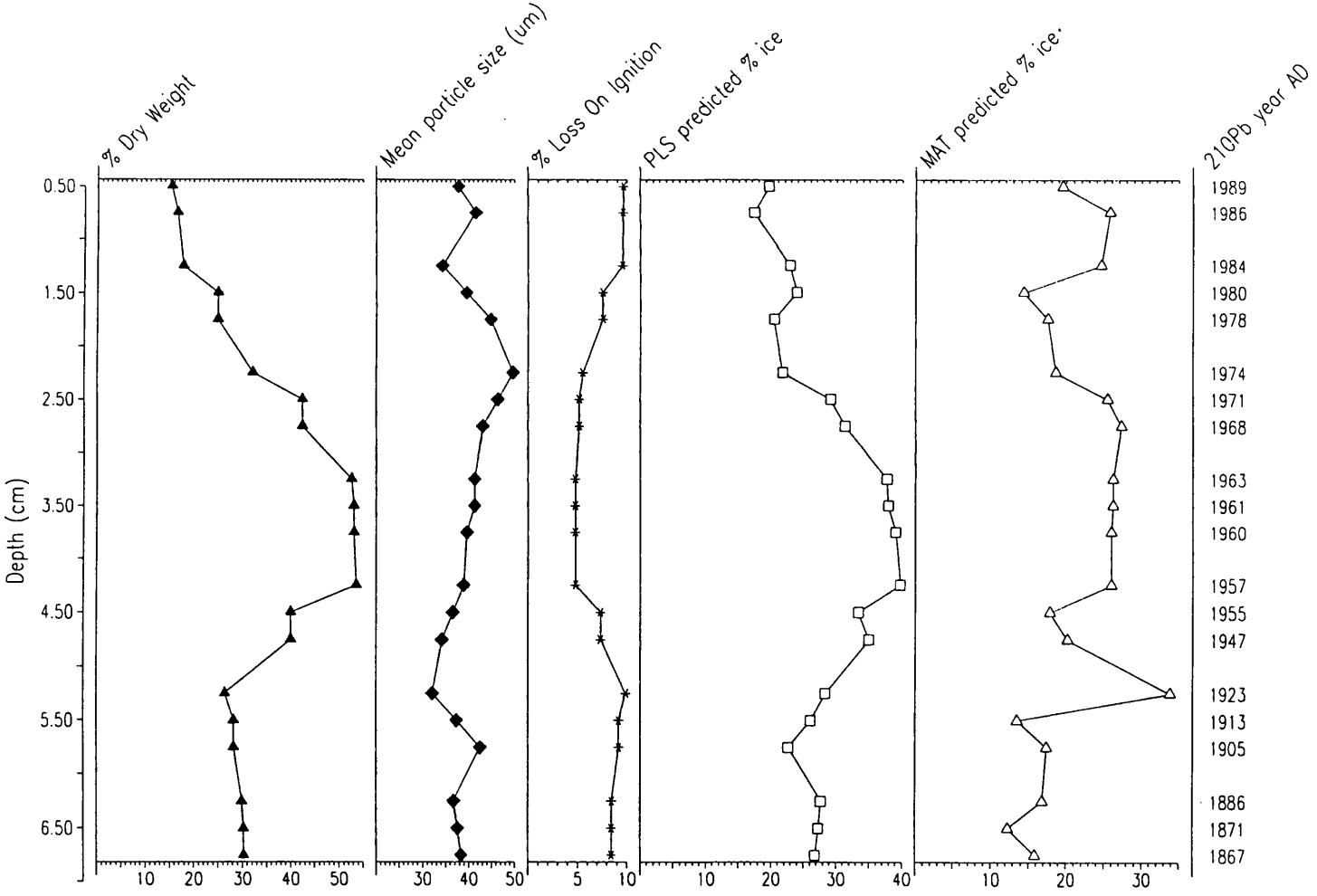

1920s to late-1940s, reaching a minimum in 1955 AD (12.20%); MAT predictions decline from the 1923 AD peak, to a synchronous minimum (17.84%). Ice-cover increases again in both models to a sustained coverage of *ca.*20-25% until 1963 AD. Then, PLS predictions show a steady decline whereas MAT predictions remain at this level until *ca.*1970 AD. The curve suggests a period of relative stasis in ice-cover. Decline in the early 1970s is then rapid and synchronous in both models, following trends in decreased %DW and increased mean particle-size (*ca.*50 μm). The two reconstruction methods deviate *ca.*1980: PLS shows a slight increase in ice-cover, relating to constancy in %DW and %LOI and MAT shows a slight decrease relating to a decrease in mean particle-size. Reconstructed values for both methods at this time deviate strongly; PLS predicts 23.90% and MAT predicts 14.31% ice-cover. Post-1980, PLS ice-cover declines steadily. MAT predictions rise sharply to 22% and then decrease post-1986 towards present values, showing the tendency for the model to over-predict by *ca.*6% at this time. PLS model predictions are very similar to 1993 AD observed ice-cover with a marginal error (<0.3%). These errors are well-within the prediction errors of either model (PLS RMSE=12.99%, RMSEP=13.27%; MAT RMSEP=13.37%). The three determinands models are therefore able to accurately reproduce the main trends seen in the four determinands models despite the loss of HARD%.

9.5.4 Heywood Lake

9.5.4.1 Ice-cover reconstructions using four sediment determinands

^{210}Pb activities span the core from 0-15.25 cm and 15.0 cm was dated by the CRS model to 1874 AD (P.G. Appleby, *pers.comm.*). Results are presented from 1892±14 yr AD to the present in Table 9.8 and Figure 9.6. The predicted ice-cover fluctuates between 0 and 22% in PLS and 0-46% in MAT over the Century timescale. Analogue matching performs well and only two samples have dissimilarity coefficients above the critical threshold (min.DC=28.308491) at 3.75 cm (*ca.*1981 AD) and 10.25 cm (*ca.*1909 AD).

At the end of the 19th Century catchment ice-cover is relatively constant and stable in both models (*ca.*15% in PLS and *ca.*34% in MAT) reflecting constant sedimentological characteristics. Ice-cover started to decline in the first decade of the Twentieth Century in PLS with decreasing HARD% and increasing mean particle-size; contrarily, MAT predictions show an increase to a peak in 1909 AD (40.33%), then a sharp decline to 2-3% by the early 1920s. Ice-cover increased from the mid-to late-1920s, the respective models slightly out-of-phase, with MAT lagging behind PLS predicted response by some

Table 9.8 Comparison of reconstruction results using PLS regression and analogue matching using the 208 sample training-set and fossil data for Heywood Lake

Mean depth (cm)	^{210}Pb *year AD* (0cm=1991)*	*Predicted % ice*					
		PLS Model 4^3	*MAT 4* mean	*MAT 4 weighted* mean	*PLS Model* 3^2	*MAT 3* mean	*MAT 3 weighted* mean
1.25	1989±2	7.3363	48.6860	46.9009	10.7567	7.6870	5.2635
1.75	1988	5.5621	6.0820	4.5807	8.7348	1.4140	1.2250
2.25	1987	4.0392	34.1780	36.8484	5.4315	17.5640	18.1846
2.50	1986	15.1672	0.8900	0.8870	17.2730	1.9130	1.5191
2.75	1985	11.4988	11.2740	10.9525	11.6486	1.4140	1.2445
3.25	1983±2	5.5963	35.1880	37.9692	7.3167	5.0580	3.2577
3.50	1982	7.4620	34.4800	34.1906	9.2605	1.4140	1.1519
3.75	1981	10.2221	39.5740	39.9591	14.1920	1.4140	1.1585
4.25	1979±2	11.7173	11.5080	7.6198	14.9023	4.5330	1.3805
4.50	1977	5.1955	2.7540	3.8022	8.0207	12.6430	6.2700
4.75	1975	9.2103	5.8900	4.1557	11.3580	12.6430	6.2879
5.25	1973	9.8246	5.8900	3.1729	11.3915	6.6160	3.7196
5.50	1972	$-5.7932e^{-2}$	12.1270	6.1383	0.8318	13.1500	5.6575
5.75	1969	2.0708	6.6160	4.2003	2.4144	13.1500	5.6446
6.25	1967±3	2.1524	12.6430	6.8111	2.1363	13.1500	5.4334
6.50	1966	0.3426	4.5410	1.6202	0.1509	5.0480	2.5083
6.75	1964	-0.8554	6.6160	2.5396	-1.4420	7.1400	3.5965
7.25	1962	6.0076	12.6430	1.1869	5.6103	5.0660	3.3441
7.50	1960	12.7565	4.5410	32.4237	12.8320	21.7810	24.6008
7.75	1957	15.8027	6.6160	7.1321	15.8126	12.6190	11.2134
8.25	1950±4	19.4221	1.3970	23.1956	19.7760	16.5560	23.4368
8.50	1942	15.7376	26.0840	22.3857	15.8450	22.3620	21.2527
8.75	1937	22.1831	8.3160	16.1657	22.8042	11.3380	9.1438
9.25	1928	19.1425	23.4450	2.7463	20.4757	13.1500	5.1599
9.50	1923	3.6931	21.8370	3.1054	4.0400	7.1400	3.8548
9.75	1918	8.4574	15.2370	2.3775	9.9973	7.1400	3.7366
10.25	1909	7.1517	6.6160	40.3251	9.2837	5.0660	2.9358
10.5	1904	13.4378	5.8900	34.0445	15.9547	5.0600	2.8125
10.75	1899	13.6728	2.7450	36.8001	16.9027	8.1940	3.6092
11.25	1892±14	15.2507	37.2440	32.2686	17.8408	8.1490	4.0717

* CRS method. Ages without error estimates derived by interpolation between adjacent stratigraphic levels based on calculated rates of sedimentation (cm yr^{-1})

[3] 3 component PLS; [2] 2 component PLS. See Tables 9.5 & 9.6 for model RMSEP, r^2 and maximum bias.

MAT 4 mean = squared Euclidean distance, mean of optimal no. of closest matches = 10

MAT 4 weighted mean = squared Euclidean distance, weighted mean of optimal no. of closest matches = 10

MAT 3 mean = squared Euclidean distance, mean of optimal no. of closest matches = 10

MAT 3 weighted mean = squared Euclidean distance, weighted mean of optimal no. of closest matches = 10

Figure 9.6 Catchment ice-cover reconstruction for Heywood Lake (n=4)

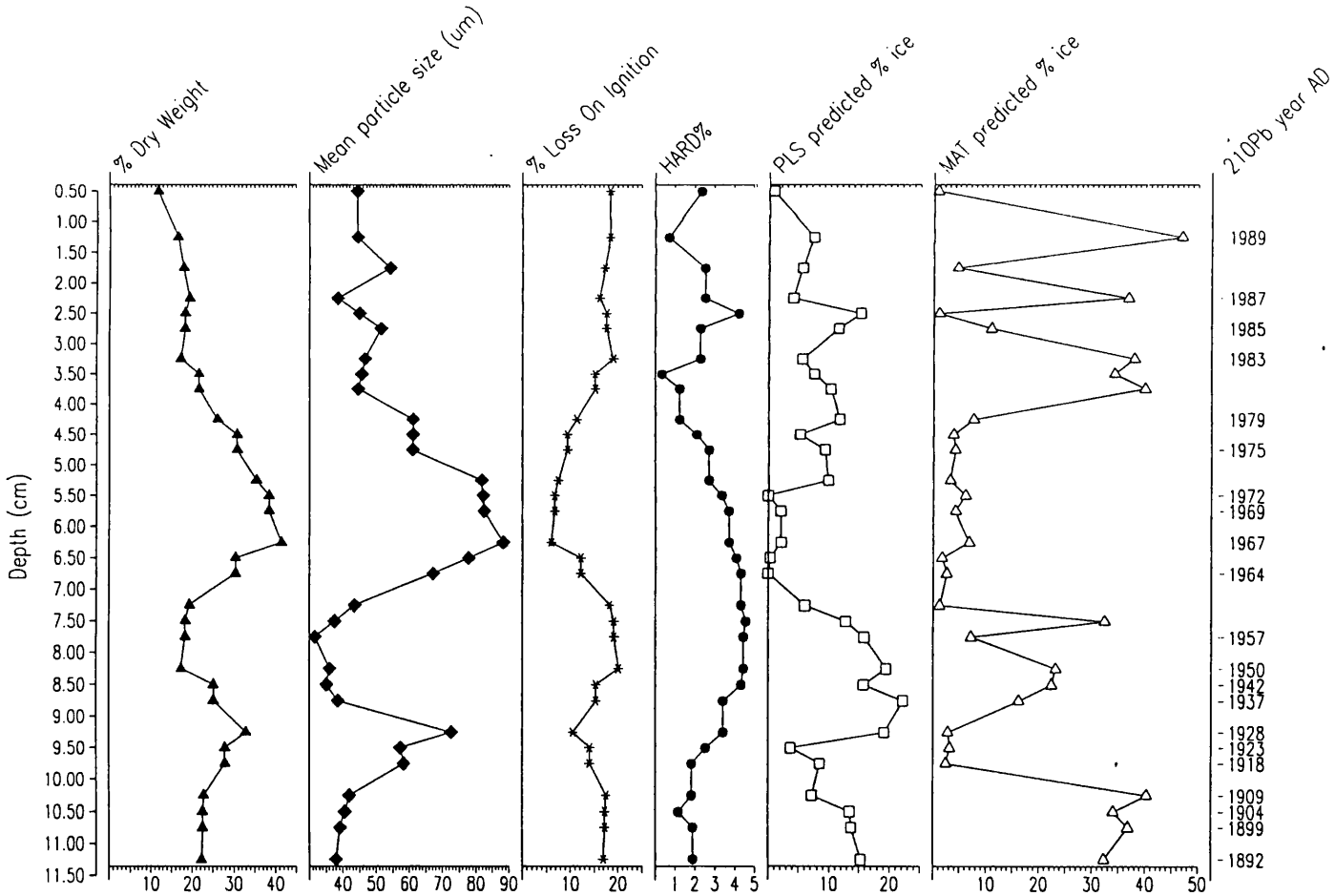

5 years. The inwash horizon at 9.25 cm (*ca.*1928) observed by Appleby, Jones & Ellis-Evans (1995) is detected in the model response as increased ice-cover in PLS and the MAT mean of 10 closest matches models, but not in the MAT weighted mean of 10 closest matches. PLS predictions show a slight decrease *ca.*1942 AD, followed by a recovery by 1950 AD, thereafter followed by a pronounced decline towards zero ice-cover by 1964 AD, paralleled by decreasing %LOI and increasing %DW and mean particle-size. The PLS model actually predicts negative values in two instances (6.75 cm and 5.50 cm) which have been plotted as zero; this is a result of the inherant bias in the PLS inverse regression model (section 9.4.5). MAT predictions are more 'noisy', with a peak ice-cover in 1950 AD (23.2%) followed by a sharp dip *ca.*1957 AD (7.13%) and a sharp peak again *ca.*1960 (32.42%), rapidly falling to near-zero ice-cover by 1962 AD. Ice-cover is maintained at this new steady-state through the 1960s. The inwash horizon noted by Appleby, Jones & Ellis-Evans (1995) at 5.75 cm (*ca.*1969 AD) is not detected in the models response, with the exception of the MAT three determinands mean of 10 closest matches model. PLS predictions show a slight increase to *ca.*10% in the early 1970s which is not registered in the MAT model.

MAT is very noisy towards the core-top, showing abrupt fluctuations in ice-cover, largely in response to shifts in particle-size and HARD%. PLS predictions are more steady, showing a slight increase *ca.*1986 to 15% followed by a steady decline towards present values. MAT lags behind the PLS predictions here by a year and this increase occurs in 1987 AD, reaching 36.85%, clearly due to a peak in HARD% and decrease in mean particle-size. Another sharp peak occurs *ca.*1989 AD (46.90%). The sharp decline towards the core-top is an artefact of the discrepancy between model predictions and observed 1993 AD ice-cover. MAT grossly overpredicts contemporary ice-cover (>40% error), well outside the limits of the model errors of prediction (RMSEP=15.6496). PLS on the other hand, performs better with a smaller discrepancy between 1993 AD observed (0.82%) and 1989 AD predicted (7.34%), well within its error of prediction (RMSEP=12.6860). Both models therefore over-predict contemporary ice-cover.

9.5.4.2 Ice-cover reconstructions using three sediment determinands

Reconstructed values using the three deteminands PLS and MAT models are very similar to those of the four-determinands models (Table 9.8, Figure 9.7). The exclusion of HARD% has reduced some of the noise in the MAT predictions which show a closer

Figure 9.7 Catchment ice-cover reconstruction for Heywood Lake (n=3)

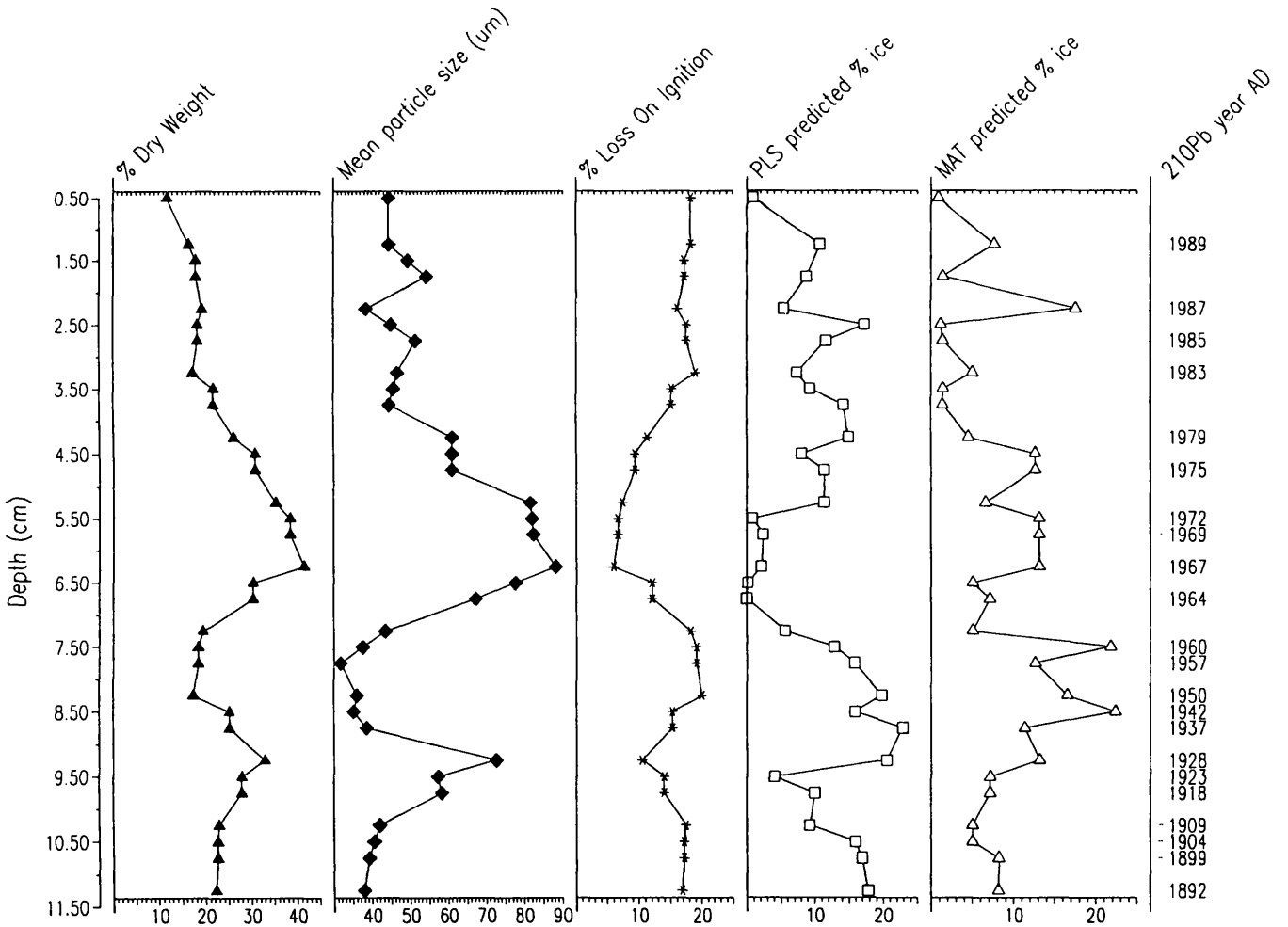

correspondence to trends in PLS results, but also show some lag in response as observed above. Predicted ice-cover ranges from 0-22% in PLS and 1-22% in MAT over the Century timescale. Increases in PLS predicted ice-cover are seen to respond principally to a fining of particle size, decreasing %DW and increased %LOI; decreasing ice-cover, conversely, is in response to increasing %DW, a coarsening of particle-size and lower %LOI. These results are unexpected and contradict findings from other glacier-sediment response studies (Karlén, 1981; Karlén & Matthews, 1992) suggesting that glacier activity is not the dominant determinant of sedimentological responses in this lake and biotic impacts may play a role in this signal (see section 9.7.2).

The match between observed 1993 ice-cover (0.82%) and model predictions in the nearest stratigraphic level (*ca.*1989) is poorer for PLS than the four determinands model (PLS=10.76%). MAT predictions however, are improved with a 1989 AD prediction of 7.69%. Both models therefore over-predict but are still within their errors of prediction (PLS RMSEP=13.37; MAT RMSEP=16.01).

9.5.5 Tranquil Lake

The rate of sedimentation rate in this lake is very slow and the entire ^{210}Pb chronology is found above 2.5 cm, dated by the CRS model to 1897 AD (P.G. Appleby, *pers.comm.*). No magnetic measurements were made on this core so the three-determinands models only could be applied (Table 9.9).

Table 9.9 Comparison of reconstruction results using PLS regression and analogue-matching using the 208 sample training-set and fossil data for Tranquil Lake

Mean depth (cm)	*^{210}Pb year AD (0cm=1991)**	*% DW*	*Mean particle size (μm)*	*% LOI*	*Predicted % ice*		
					PLS 3²	*MAT 3 mean*	*MAT 3 weighted mean*
0.5	1976±2	28.69	43.52	7.5	23.0228	17.5690	19.4279
1.5	1940±8	38.96	45.93	4.35	28.1008	21.9500	19.3020
2.5	1897±15	41.45	40.37	4.51	32.9571	17.8680	14.8868

* CRS method
² 2 component PLS. See Table 9.6 for model RMSEP, r^2 and maximum bias
MAT mean 3 = squared Euclidean distance, mean of optimal no. of closest matches = 10
MAT weighted mean = squared Euclidean distance, weighted mean of optimal number of closest matches = 10

The match between the fossil and modern samples is good and no predictions exceed

the second percentile threshold for dissimilarity coefficients (min DC=1.27). In 1897 AD, PLS predicts ice-cover of 32.96%, less than the present extent (1993 AD = 42.64%) and outside the limits of the model error of prediction (RMSEP=13.37%). MAT gives an even lower estimate at this time (17.87%), also well outside its error of prediction (RMSEP=16.0141%). PLS predicted ice-cover declines over the Century (1897 to 1976 AD) by over 10%, matched by decreasing %DW (41.45% to 28.69%), increasing mean particle-size (40.37 μm to 43.52 μm) and increasing %LOI (4.51% to 7.5%). MAT predictions show an increase towards the mid-Twentieth Century followed by a decline to conditions similar to those at the end of the Nineteeth Century. The pattern of decreasing ice-cover with decreasing %DW and increasing %LOI follows the expected pattern in this glacial lake however, it is highly likely that the low rate of sedimentation in this lake is affecting the models' ability to discriminate changes in sedimentological characteristics.

9.5.6 Emerald Lake

The sedimentation rate in this lake is also rather slow and the entire ^{210}Pb chronology is restricted to the upper 4.25 cm (from 1896 AD onwards). No magnetic measurements were made on this core so only the three-determinands models could be applied. Results are summarised in Table 9.10 and Figure 9.8.

Six fossil samples are poor analogues with dissimilarity coefficients exceeding the critical threshold (min.DC=1.27) at 1.375 cm, 1.625 cm, 3.125 cm, 4.125 cm, 5.25 cm, 9.25 cm and 9.75 cm, indicating sedimentological characteristics without close matches in the modern set. Catchment ice-cover predictions (Table 9.10, Figure 9.8) are much more constant (*ca.*45%) in the 2 components PLS model than the MAT model, which shows more marked fluctuations over the Twentieth Century, largely in response to particle-size changes. Other fossil sediment determinands are fairly constant, with only minor fluctuations in the %DW curve which are mirrored in the MAT predictions, i.e. decreasing %DW indicates increased MAT predicted ice-cover.

Catchment ice-cover declined in the first decade of the Twentieth Century and MAT predictions reach a minimum in 1904 (31.01%). There is then an apparent increase in ice-cover towards the 1930s as %LOI increases and then falls again and mean particle-size decreases. Another trough in the MAT predictions is encountered in 1937 AD (32.18%) which is not seen in the PLS predictions and coincides with a peak in %DW.

Table 9.10 Comparison of reconstruction results using PLS regression and analogue-matching using the 208 sample training-set and fossil data for Emerald Lake

Mean depth (cm)	*^{210}Pb year AD (0cm=1991)**	*Predicted % ice*		
		PLS 3[2]	*MAT 3 mean*	*MAT 3 weighted mean*
0.38	1989	46.2965	48.6860	42.9068
0.63	1986	49.3445	23.9470	24.1291
0.83	1982	45.6071	21.6490	52.8060
1.13	1978	46.1790	23.9470	21.3704
1.38	1973	43.1928	25.8120	34.0949
1.63	1966	43.5687	45.5410	46.8568
1.88	1958	44.9933	20.6680	21.5934
2.13	1952	49.4499	22.9490	42.0226
2.38	1948	45.3294	23.5130	22.8967
2.63	1944	50.6305	23.9470	24.3344
2.88	1941	46.7870	45.5410	50.9671
3.13	1937	48.6574	32.1840	39.9085
3.38	1932	40.4670	52.8300	52.8300
3.63	1924	38.2832	43.5170	36.3771
3.88	1912	37.1991	38.8890	19.1212
4.13	1904	43.3499	31.0130	39.9279
4.38	1878	43.3510	45.5410	46.6837

* CRS method. Dates interpolated from adjacent stratigraphic levels.
[2] 2 component PLS. See Table 9.6 for model RMSEP, r^2 and maximum bias.
MAT 3 mean = squared Euclidean distance, mean of optimal number of closest matches = 10
MAT 3 weighted mean = squared Euclidean distance, weighted mean of optimal number of closest matches = 10

The next peak in MAT at 1941 AD (45.54%) opposes the slight decline seen in the PLS predictions and is determined by a trough in %DW. MAT predictions then decline significantly to a plateau of *ca.*23% from 1944 to 1958 AD; PLS behaviour is also relatively constant over this period, but with higher predicted values (*ca.*45%). Post-1958 AD, MAT ice-cover increases sharply to a peak in 1966 AD (45.54%) which is also not seen in the PLS predictions which remain roughly constant. MAT ice-cover declines sharply again from the 1966 AD peak and assumes relatively constant behaviour from 1973-1986 AD. Both models show an increase in ice-cover towards the core top which is an artefact of the error between predicted (PLS=46.3%, MAT=48.69%) and observed (52.84%) values, showing that both models under-predict recent ice-cover and probably also in the past.

Figure 9.8 Catchment ice-cover reconstruction for Emerald Lake (n=3)

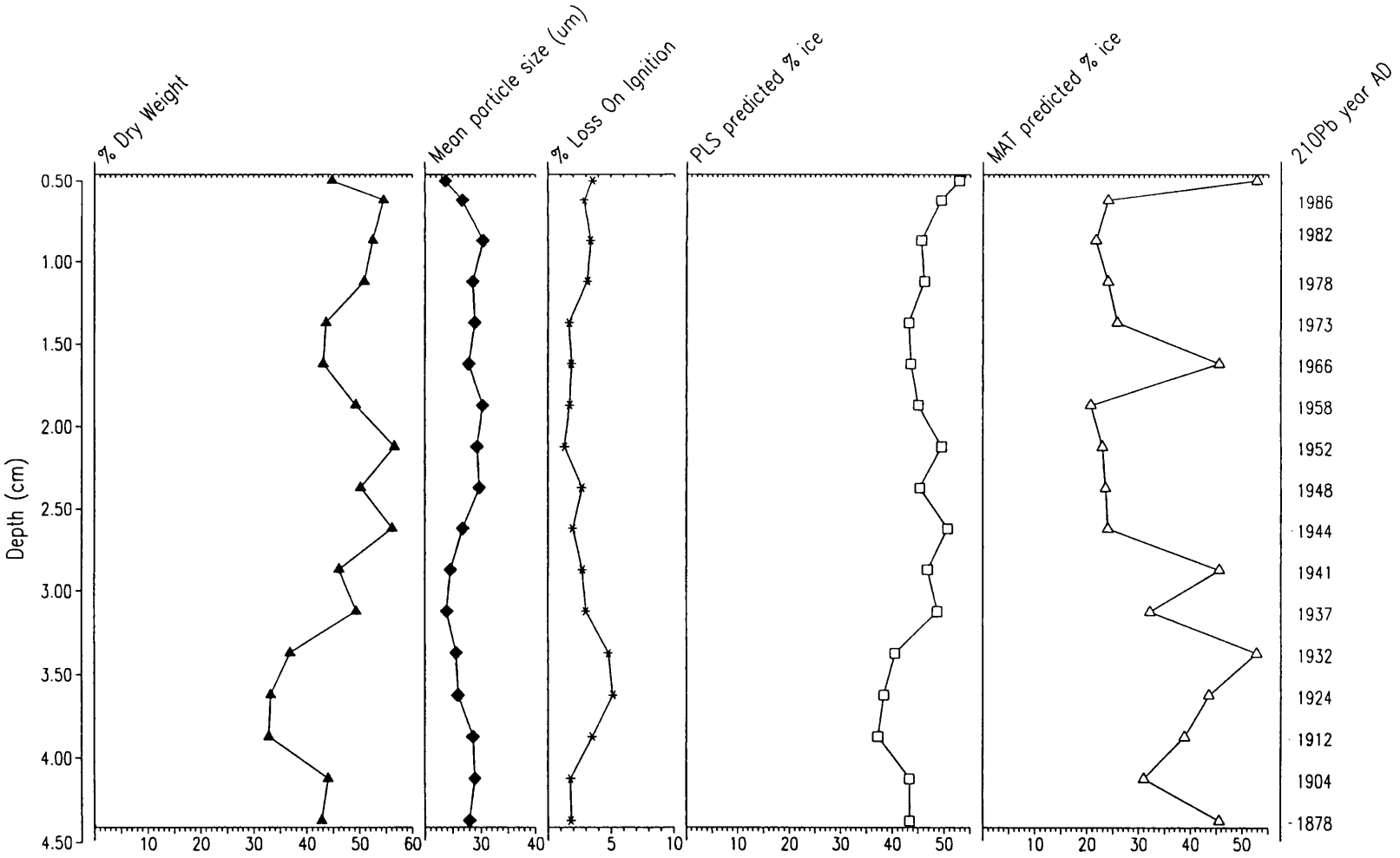

9.5.7 Comparison of the models

The four and three-determinands PLS and MAT ice-cover reconstruction models integrate the effects of fluctuations in the sediment determinands over time. The PLS and MAT models appear to react to sedimentological changes in different ways, causing discrepancies in the directional prediction of ice-cover so that results are not always in agreement. PLS ice-cover prediction curves (Figures 9.4-9.8) strongly reflect shifts in %DW, the first regression predictor. MAT appears to be slightly more responsive to changes in particle-size. PLS integrates the sediment determinands in a smoother manner and HARD% modulates the effects of minor fluctuations in the other predictors. In MAT however, HARD% tends to introduce more noise through lack of good analogues in the modern set, possibly a result of post-depositional changes in magnetic mineralogy. For the most recent sediments, Sombre and Emerald Lakes are obviously subject to under-prediction and Heywood Lake to over-prediction. In PLS, this is in part a result of the inherent bias in the regression model (section 9.4.4).

Similar trends in predicted ice-cover over time suggest an island-wide glacial response and the potential causal factors are investigated in section 9.7. The model response to environmental perturbation is at times somewhat surprising and at odds with conventional hypotheses regarding climate, ice-cover and glacial activity and resultant lake-sediment characteristics. Increasing %DW and decreasing %LOI usually cause the model to predict increased ice-cover as expected but in several instances an inverse relationship occurs between the predictors and the response. This is most notable in the Heywood Lake reconstruction between 1928 and 1962 AD (Figure 9.6) where decreasing %DW, a fining of particle-size and increasing %LOI and HARD% suggest increased ice-cover in both models. In Sombre and Emerald Lakes, sediment predictors behave as expected in PLS regression: increased dry weight, a fining of particle-size and decreased %LOI indicate increased ice-cover, and vice versa. HARD% in this environmental context is an indicator of glacial activity and higher values for HARD% therefore represent greater ice-cover. The model is therefore sensitive to the combinations and magnitudes of sediment variables.

9.6 Model validation using historical data

9.6.1 Historical records of ice coverage

The PLS model has inherent validation (section 9.3) using the $RMSEP_{jack}$ based on the original data, which assumes that the whole gradient of possibilities has been captured

in the training-set population to produce a linear model. Fortunately it is also possible to validate the model with real, historical data on ice-extent. The original 1:10,000 scale map of Signy Island was drawn-up on the basis of aerial photographs taken in 1968 fixed by trigonometric survey. The Island and its ice-coverage were digitized in ARC/INFO and are held in a Geographical Information System (GIS) at the British Antarctic Survey. Catchment boundaries defined for this study (Chapter 3) were superimposed on the GIS and catchment-based estimates of historical ice-cover were calculated (P. Cooper, *pers.comm.*). The 1968 ice-cover estimates present a unique opportunity to validate the model predictions at the matching time horizon in the calibration cores, fixed by radiometric dating. Dates from this period have a standard error of roughly ±3 years (Appendix D) ensuring a fairly close time-horizon match.

9.6.2 Comparison of historical ice-cover and model predictions

Table 9.11 compares the results of PLS regression and MAT (optimal models) at time horizons which equate with 1968 AD, the year of observed ice-cover.

Table 9.11 Comparison of historical observations of ice-cover (1968 AD) and predicted ice-cover for the four calibration sites

	Sombre	Heywood	Tranquil	Emerald
Horizon depth	2.75	6.25	0.75	1.50
^{210}Pb year AD	1968	1967	1967	1968
Observed % ice	47.09	9.39	55.95	67.98
PLS predicted % ice	28.2322[4] 31.3088[3]	2.1524[4] 2.1363[3]	- 23.0228[3*]	- 43.3808[3**]
Observed-predicted	18.8578 15.7812	7.2376 7.2537	- 32.9272	- 24.5992
MAT predicted % ice	30.7791[4] 27.3130[3]	12.6430[4] 2.1363[3]	- 17.5690[3*]	- 35.6765[3**]
Observed-predicted	16.3109 19.2946	-3.2530 7.2537	- 38.3810	- 32.3035

[4] 4 determinands model; [3] 3 determinands model
[*] model result at 0.5 cm; [**] mean of predicted results at 1.38 and 1.63 cm
RMSEP Four determinands, 3 components PLS model = 12.6860
RMSEP Three determinands, 2 components PLS model = 13.2712
RMSEP Four determinands MAT model, weighted mean of 10 closest matches = 15.6496
RMSEP Three determinands MAT model, mean of 10 closest matches = 16.0141

All PLS models under-predict historical ice-cover by varying orders. The discrepancy between observed and predicted is greatest for Tranquil and Emerald Lakes, which

under-predict ice cover by 32.9% and 24.6% respectively, far outside the range of their RMSEPs. Sombre Lake PLS predictions are slightly better but still under-predict with a range in excess of its RMSEP. Heywood Lake has the best match between observed and predicted within therange of the RMSEP but actually over-predicts, with an error of 7.2% for both the three and four determinand models.

MAT performs slightly differently. Historical ice-cover in Tranquil and Emerald Lakes is still greatly under-predicted by 38.38% and 32.30% respectively, probably a result of inadequate horizon resolution given the slow rate of sedimentation. The difference between observed and predicted at these sites is in excess of the range of their model RMSEPs. The discrepancy is smaller at Sombre Lake where under-predictions are 16% and 19% for the four and three determinands models respectively. The four and three determinands MAT models produce different results at Heywood Lake; the four determinands model over-predicts by 3% whereas the three determinands model under-predicts by 7%. The lowest error between observed and predicted for all calibration sites is at Heywood Lake using the four determinands MAT model however, the error of reconstruction is weaker for MAT (RMSEP=15.6496, r^2=0.2624) and the probability that this match has occurred through chance is greater. All PLS results, with their lower errors of prediction, are therefore considered to be more robust than MAT.

The principal reasons for poor validation are therefore considered to be: (i) training-set error due to the mis-match between estimated and actual contemporary (1993 AD) ice-cover due to lack of accurate survey information; (ii) error in the estimation of historical ice-cover (this should be minimal since the 1:10,000 version of the Island map was drawn-up on the basis of aerial survey); (iii) inability to discriminate between permanent snow and ice, which are responsible for contrasting styles of sediment delivery to the lakes; and (iv) inability to resolve the time-period accurately in the sediment record.

9.7 Comparison with air-temperature records

9.7.1 Temperature and ice relationships

Twentieth Century temperature records for the Antarctic Peninsula region have registered many fluctuations (Jones, Raper & Wigley, 1986; Jones *et al.*, 1993). At Signy Island, moraine deposition events, dated by lichenometry, are coincident with cold spells in the early 1910s, early 1920s to mid-1930s and late 1940s (Smith, 1990) and the observed warming trend since the mid-Twentieth Century is considered to have been responsible

for the significant loss of permanent snow and ice on the Island (Chapter 2). Smith (1990) proposed that the status of the ice-cap is dependent largely on the air-temperature attained during the austral summer (particularly December to February) although the amount of cloud cover and precipitation as rain could also be critical. Summer air temperatures have been linked to glacier ablation and lake-sediment response elsewhere (Leeman & Niessen, 1994) and at Signy Island the summer months have been getting warmer since the mid-1950s. The availability of mean monthly air temperature records (British Antarctic Survey) from Orcadas (1903 onwards) and Signy (1947 onwards) provide the opportunity to test the sensitivity of catchment ice-cover to temperature fluctuations and to underpin cause-process relationships using these quantitative ice prediction models derived from the palaeolimnological record. Unfortunately, precipitation records are unreliable and lack the consistent trends observed in the temperature series data.

9.7.2 Temperature and model relationships

The optimal PLS and MAT model results and 3 year running-means of summer maximum monthly air temperatures for the 20th Century at the four calibration sites are plotted in Figure 9.9. The diagram is divided into three main time periods.

In the first period, from the turn of the Century to the early 1920s, ice-cover appears to be in a state of decay or is relatively static in most lake catchments. Regional instrumental and climate-proxy records show that the period around 1900 AD was extremely cold (Jones *et al.*, 1986; Boninsegna, 1992) and 1898 and 1900 were among the coldest 15 of the last 500 years. Ice-extent on Signy Island was probably maximal at the turn of the Century. Warmer summers in the early 1900s seemed to promote some ice-recession, especially in Heywood and Emerald Lake catchments, but this was halted by the cold spell around 1910 (Smith, 1990) where in two summers temperatures did not exceed 0°C and ablation would have been negligable. Warmer years around 1915 AD do not appear to have had any significant effect on catchment ice-cover.

The second period commenced around 1920 AD when both Heywood and Emerald Lakes show an abrupt increase in ice-cover. In Heywood Lake this is more evident in the PLS results; in Emerald Lake in MAT results. At Sombre Lake, catchment ice-cover remains relatively constant. Cold spells observed in the 1920s and 1930s led to moraine deposition (Smith, 1990) which indicate increased ice extent in certain parts of the

Figure 9.9 Catchment ice-cover predictions and summer air temperatures

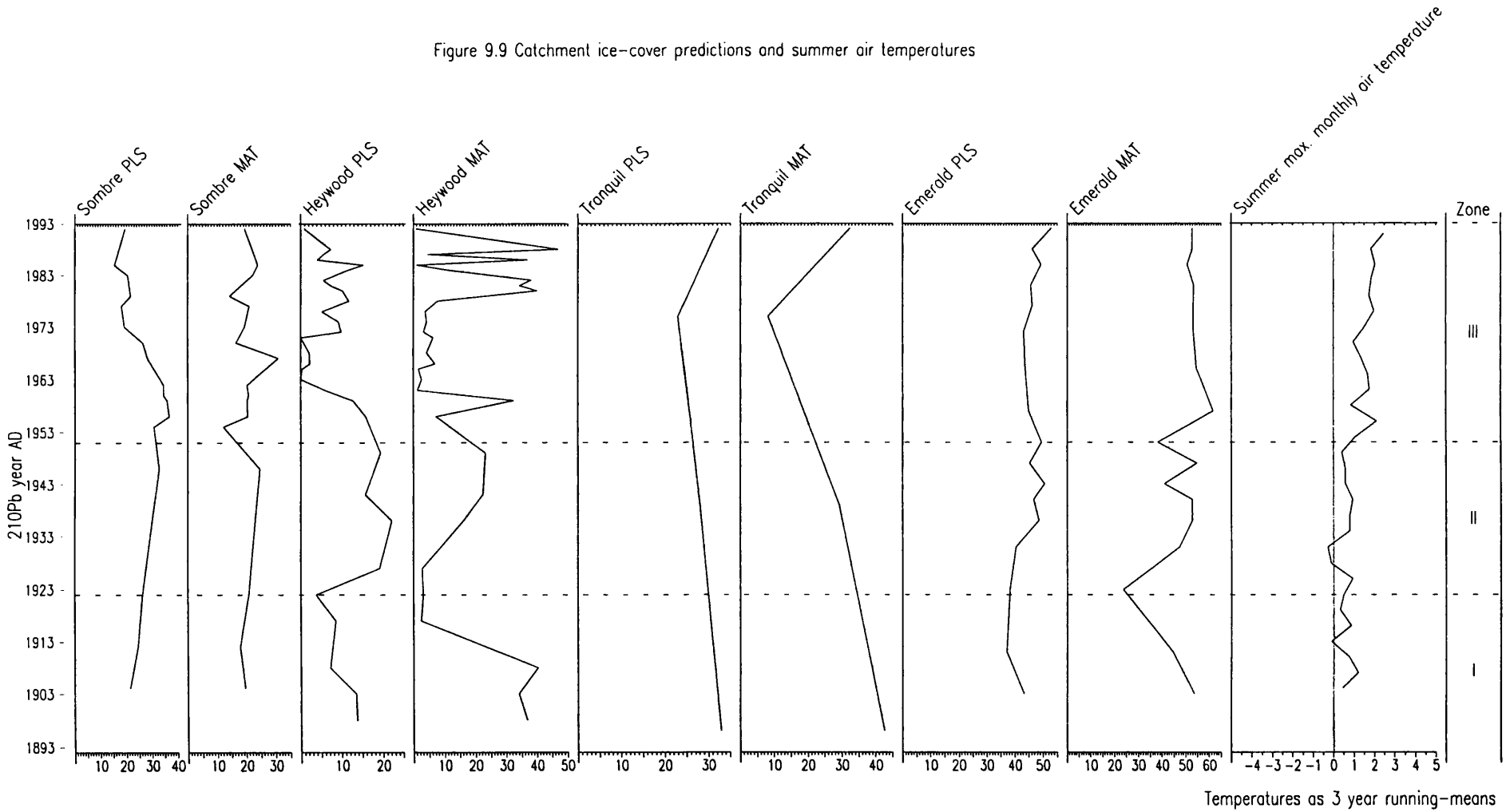

Island. Summer maximum air-temperatures continued to oscillate around zero and seasonality was sufficient to maintain relative stasis in ice cover but after 1934 AD the trend in summer air temperatures became increasingly positive. This period of increased ice extent continued throughout the 1930s and 1940s and aerial photographs in 1948 evidence greater Island ice cover, particularly in Paternoster Valley (the location of Moss, Changing and Sombre Lakes).

The third period commenced in the early 1950s and continues to the present-day. In 1951 AD the mean annual air temperature shifted from negative to positive (Smith, 1990). Predicted catchment ice-response differed between the lakes. Predictions in Sombre Lake (PLS and MAT) and Emerald Lake (MAT) closely followed this temperature change within a couple of years, indicating increased ice-extent. This probably represents the release of sub-glacially eroded material from melting ice fronts and the model response is actually symptomatic of active ice retreat. This trend continued through the mid-1950s in Sombre and Emerald Lakes. PLS and MAT predictions in Heywood Lake responded rapidly to increased temperatures with a sharp decrease in ice-cover. By 1960, ice-cover in Sombre and Heywood catchments was in chronic decline, matching the increasing temperature trend. Emerald Lake, however, remained relatively inert; the bulk of the ice-sheet on this part of the Island seems to have a greater inherant lag-time response to climate forcing. Ice-cover achieved an apparent minimum in Heywood Lake in the mid-1960s and then recovered slightly in the early 1970s. Predictions in the most recent period are complicated by the effects of the increasing fur-seal population and their erosive effects in the lowland catchments, causing an inwash of allochthonous materials. Increased noise in the predictions for this period is also a function of a greater number of data-points. A succession of cold summers in the early 1980s was seen as a slight stand-still event around 1980, most strongly in the Sombre Lake PLS predictions. The apparent increase in ice-cover towards present-day values is an artefact of model under-prediction in Sombre, Tranquil and Emerald Lakes and over-prediction in Heywood Lake (section 9.4.5).

These results can be summarised using a correlation log which integrates the multivariate stratigraphical data in a low-dimensional, geometric way, so helping to find the latent structure in the data and illustrate the direction and magnitude of systems changes. Principal Components Analysis was undertaken on the fossil sediment determinands (%DW, mean particle-size and %LOI) and the summer maximum monthly

Figure 9.10 PCA axis 1 scores and summer maximum air temperatures

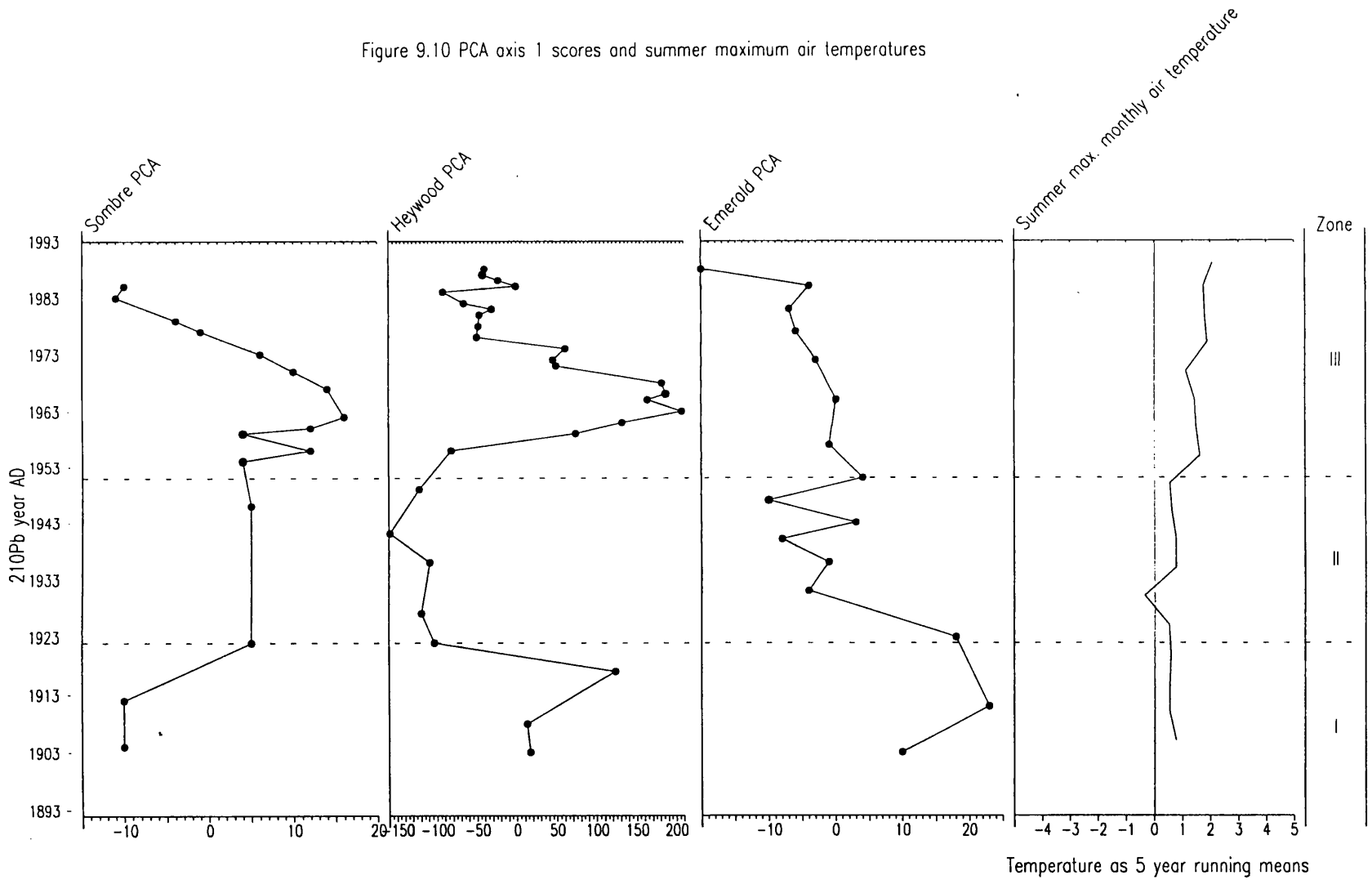

temperature at each stratigraphic horizon using CANOCO (ter Braak, 1987; 1990). PCA axis 1 sample scores are plotted for Sombre, Heywood and Emerald Lakes in Figure 9.10. Tranquil Lake was excluded from the analysis owing to a limited number of data-points over the last century. The summer maximum monthly temperature is also plotted as a reference. In the PCA logs, strong shifts in PCA scores implies stronger correlations between the variables, indicating a significant change in behaviour registered in all proxies. Shifts to the left indicate relative decreases in ice-cover; those to the right indicate an increase in ice-cover.

The three broad periods identified in Figure 9.9 are also captured by the PCA axis 1 scores (Figure 9.10). In the early Twentieth Century, the lake catchment systems were in apparent equilibrium. Some time around 1910 AD perturbation occurred and PCA axis 1 scores for the three lakes shift to the right. This coincides with a cold period in the instrumental records (Smith, 1990). The period was of comparable duration in Sombre and Heywood Lakes but lags slightly in Emerald Lake, reflecting a differential in ice-sheet response on the east and west coasts of the Island.

The second phase was from the 1920s to the early 1950s; lake-catchments were in relative equilibrium, especially at Sombre Lake. Emerald Lake oscillated around some systematic mean. Ice-cover was at a minimum in Heywood Lake.

The third phase occurred in the early 1950s, with another behavioural shift in all three lakes. PCA axis 1 scores swing significantly to the right, indicating increased ice-cover. The change occurs first in Emerald Lake, then Sombre and then in Heywood. This is coincident with the shift in mean annual air temperatures from being negative to positive in 1951 AD (Smith, 1990). The sharp increase in ice-cover is therefore actually indicating a change in glacier dynamics and sediment release from retreating ice-fronts, the type of paraglacial effects discussed by Church & Ryder (1972) and Leonard (1985, 1986b). From the early 1960s onwards, PCA scores drift slowly back to the left again, showing a relatively constant decay in ice-cover in the Sombre and Heywood Lake catchments but a more gradual change at Emerald Lake.

9.8 Discussion

Measured temperature fluctuations over the Twentieth Century produce a sedimentological response in all the calibration cores. The trends in predicted ice-cover

are better regarded as predictors of catchment stability or instability, in response to either climatic (glacial) or biotic (fur seal) perturbations. PCA provides a useful summary of temperature-ice-sediment correlations and forcing is broadly contemporaneous at different sites on the Island. Radiometric chronologies provide a means of making an accurate comparison between different sediment-sequences from different lakes with an error of only a few years, so that decadal-and sub-decadal timescale changes can be accurately modelled and interpreted from the sediment record.

Temperature oscillations in the first half of the Twentieth Century led to a rapid response in terms of both glacial advance and retreat. In the second half of the Twentieth Century the warming trend led to a significant depletion of ice-cover, authenticated by historical records (Smith, 1990). Glacial retreat was an Island-wide phenomenon registered in all four calibration lakes on either side of the central ice-cap. Lakes on the west coast seem to be less responsive to this climatic forcing; Emerald Lake is a more inert system with considerable temperature-buffering capacity and response lag-time. A limited number of data points in the Tranquil Lake core make it difficult to discern changes on less than a century timescale. Slow sedimentation rates in themselves indicate relative glacial geomorphic stability. Temperature is not the sole control on advance and retreat although clearly it is significant. Exclusion of precipitation data from the analysis leaves questions concerning changes in the hydrological balance on glacial activity unanswered.

The relationship between glacial activity and downvalley sedimentation rate is not as simple as Karlén (1981) envisaged (Leonard, 1986a) and is timescale-dependent. Over the centuries to millennial timescales, high overall sedimentation rates directly relate to periods of increased ice-extent (Leonard, 1986a, 1997), supporting Karlén's argument (Karlén, 1981; Karlén & Matthews, 1992) that increased glacier extent in a basin, possibly with concomitant increases in ice thickness and velocity, results in increased erosion of fine-grained material. Variations in factors which control short-term sedimentation rate variability, including rate of release of sediment by the ice, and competence and capacity of meltwater streams, are smoothed-out over longer timescales and variation in erosion rates relating to changing ice-extent and activity becomes a more important controlling factor. The ice-cover reconstructions in Tranquil Lake, limited to century-scale resolution due to low sedimentation rates, are probably fairly representative of upvalley ice-extent, and the observed loss from the end of the 19th

Century to the present is a real phenomenon which can be linked to known climatic warming. The 0-1 cm sample resolution in the training-set itself limits the temporal resolution of any reconstructions. These samples integrate strong seasonal influences into a period of several years, which varies between sites according to the sedimentation rate. This is advantageous to medium-scale (10^2-10^3 yr) environmental reconstructions in that short-term environmental fluctuations ('noise') are smoothed-out.

Over shorter timescales (10^2) the simple relationship between upvalley ice-extent and downvalley lacustrine sedimentation rate breaks down and interpretation of the sedimentary record is not simple (Leonard, 1997). This in particular affects the interpretation of ice-cover reconstructions for Sombre and Heywood Lakes. At these sites higher rates of sedimentation allow an accurate ^{210}Pb chronology enabling model predictions of decadal or sub-decadal resolution. Factors affecting medium-timescale variability (Leonard, 1986a) in sedimentation rate (changing erosion rates, exposure of unstable material during ice recession, shifting stream courses) which remain essentially constant, are integrated and smoothed in the resolution of the sedimentary record. The highest rates of sedimentation are not always coincident with maximum ice extent and in fact tend to be associated with transitional periods such as the period of most rapid glacier advance or recession, rather than the maximum stand. Periods of stasis, coincident with cold periods in the 1910s and around 1980 are evidenced by a plateau or reduction in ice-cover as the lakes were 'starved' of inwashed glacigenic sediment. Secondary peaks in sedimentation rate are easily explicable by paraglacial effects (Church & Ryder, 1972) which occur one to two decades later in the early phases of ice recession (Ballantyne & Benn, 1994), often with rates at least as high as those associated with the maximum ice stand. The notably more dense, minerogenic sediments on the delta features currently evident in Sombre, Changing and Gneiss Lakes are symptomatic of these processes following catchment glacial retreat. Relative fining of particle-size up-core can be used as indirect evidence of changing proximity to a glacier terminus at the coring site but this upward fining was not evident, probably owing to the effects of local ice-cover and unstable glacigenic materials between the glacier terminus and lakes.
High paraglacial sedimentation rates can persist for up to a century after maximum ice-stands, a complication which Leonard (1985) believed limited the resolution in glacial chronologies reconstructed from lacustrine sequences to about a century. Model results here suggest sensitivity within the decadal timescale but in the future, paraglacial reworking of sediments could lead to enhanced erosion rates and therefore abnormally

high model predictions where ice recession has already occurred.

Diagenesis largely affects the surface-sediments and some of the variability witnessed in the upper profile may result from compression effects which would strongly affect % dry weight determinations. The reliance of the transfer function on % dry weight is problematic in that variable volumes of water are extruded with each sediment slice leading to bias in the training-set and with increasing core depth, compression leads to decreasing water content and increasing dry weight such that model predictions would show apparent increases in ice-cover, as evidenced by increases in reconstructed ice-cover at the end of the 19th Century at all the calibration sites. However, time-synchroneity between lakes where events are recorded at different depths suggests that the sediment is responding to a real climate effect. The interdependency between dry weight, particle-size and organic matter has long been recognised (Håkanson & Jansson, 1983) and introduces appreciable difficulties in the interpretation of down-core variations in % dry weight. This interplay has been discussed recently by Menounos (1997). Cores could be adjusted for compression effects. Ultimately it may be possible to integrate the three predictor determinands (% dry weight, particle-size and %LOI) into one composite regression equation term (cf. Kernan, 1996). The model performance might also be improved by universal calibration of particle-size results (section 6.3.4.). The effects of a relative increase in mean values, i.e. samples to become coarser, would lead to relative decreases in model predictions of ice-cover. Discrepancies in the particle-size values might explain some of the over-estimation of validated reconstructions in Heywood Lake (+7%) but does not explain the under-prediction of historical ice-cover in Sombre, Tranquil and Emerald Lakes (section 9.6.2) .

One further consideration is the representativeness of the fossil core. All cores were taken from the deepest point of each basin which is theoretically, the most stable part of the basin. Sediment focusing is evident in some basins and changes in basin shape occur with lake development over time. In the early stages, lake basins have steeper slopes and more conical basins favouring sediment focusing, especially of light, fine materials. Over recent timescales (last 100 years) morphological changes in deep lakes with broad central troughs (e.g. Sombre, Emerald) should be minimal and cores from these locations should be representative of basin-wide processes. Over longer, Holocene timescales ontological changes might affect reconstructions, favouring the use of models based on profundal sediments (section 9.4.4.5) which, for MAT, would provide a better

chance of analogue-matching. If the lakes were perenially ice-covered in the past, depositional regimes might have been very different, including sediment characteristics (e.g. dropstone influence, cf. Björck *et al.*, 1996) not included in the gradient of the modern training-set, so increasing the likelihood of a no analogue situation.

9.9 Summary

(1) Catchment ice-cover was chosen for reconstruction on the basis of its explanatory power in the data-set. An ice-prediction equation was developed using either four or three conservative sediment determinands, representative of sediment lithology (%DW), particle-size (mean), organic content (%LOI) and magnetic behaviour (HARD%). Using inverse methods, where catchment ice-cover is the response to sediment predictors, two methods of reconstruction (PLS regression and analogue-matching) were tested using the 208 sample training-set. Prediction errors for all models are between 12-16% and although correlations between observed and predicted are low they are reasonable given the noise in environmental systems. The optimal PLS model has 4 determinands and 2 components using the full training-set (RMSE=12.33%, r^2=0.55; $RMSEP_{jack}$=12.69%, r^2=0.52). The optimal analogue-matching model uses 3 determinands and the weighted-mean of 10 closest matches using a screened training-set of 103 profundal sediment samples ($RMSEP_{jack}$=15.04%, r^2=0.35). The PLS model does not perform equally across the range of observed catchment ice-covers: it under-predicts high observed ice-cover and over-predicts low observed ice-cover. This fault is typical of inverse regression and cannot presently be corrected for. PLS regression gains from a large number of samples but performs nearly as well as the full model using a reduced training-set (n=103) providing the overall gradient length is maintained. MAT model performance is disrupted by high sample heterogeneity and is more robust using a training-set of more homogenous sediments from the profundal zone in which it can readily find matches.

(2) Prediction errors are sufficiently modest to allow useful, unbiased quantitative reconstructions of past ice-cover. Reconstruction (calibration) was performed at 4 contrasting sites on Signy Island using PLS regression and MAT techniques. Core sequences had radiometric chronologies which spanned a timescale from the end of the 19th Century to the present. Model predictions were validated against historical observations of catchment ice-cover (1968 AD) with reasonable agreement between observed and predicted and generally within the model errors of prediction. The resolution of the model predictions was highly dependent on the sedimentation rate.

MAT depends entirely on the range and composition of the modern training-set and as a result of this, MAT reconstructions show greater short-term variation than reconstructions based on other, more statistically based techniques (Bartlein & Whitlock, 1993). This short-term variation is highly evident at Heywood Lake in response to minor variations in lithology and particle-size. Errors with historical ice-cover (1968 AD) are generally larger, especially for the highly glaciated catchments (Tranquil and Emerald Lakes). Sources of prediction error include the inherant bias in the models, noise in the natural system such as differential sediment delivery from ice- and snow-melt, errors in the present-day estimates of ice-cover, measurement errors of the sediment determinands, post-depositional changes and systems inertia to change.

(3) Catchment ice-cover is seen as a climate-proxy and model results can be linked to observed ice-loss and temperature trends over the 20th Century. Temperature-ice cover relationships can be gauged from the sediment-proxies over a timescale of years rather than decades supporting the hypothesis that small catchments with partial ice-cover are highly sensitive to climate forcing (Karlén, 1981). Stable permanent ice-fields are relatively insensitive compared to smaller glacier features such as valley glaciers, yielding less sediment to be detected as a glacial response, hence the low sedimentation rates in Tranquil Lake (0.012 cm^2y^{-1}) reveals little information about activity of ice in the catchment. The models require sediment variability to register changes and where sediment inputs are very uniform, eg. Emerald Lake, the highly homogenous minerogenic character of the sediments obscures any short-term changes. Although the climate at Signy Island is strongly affected by local factors such as pack-ice extent (section 3.2.4), some of the climatic events registered in air-temperature records are global phenomena, for example, the Little Ice Age maximum which reached its peak in high-latitude regions at the end of the 19th Century, the mid-1940s warm period and 'Greenhouse Warming' which has been particularly marked since the 1970s. Reconstructions from this region therefore form an important link in the global correlation of climate proxy-records. However, model predictions support other authors' obeservations that it is not easy to discriminate from the palaeolimnological record whether an ice-field is in advance or retreat as the sub-glacial or paraglacial product in the sediment record is very similar (cf. Leonard, 1985; Karlén & Matthews, 1992). Post-1950 the mechanisms linking catchment ice and sediments are less simple and other factors, including biotic processes, may be responsible for apparent increases in predicted ice-cover. Evidence from Heywood Lake suggests a biotic impact on the

predictions through the erosive effects of fur seals in the catchment. The model is therefore better regarded as a proxy for catchment instability and erosion. The exact effects of fur seals on erosion rates are unknown and their quantification could be a future research objective.

CHAPTER 10: RECOMMENDATIONS AND SUMMARY

10.1 Introduction

Quantitative lake-sediment studies (Chapters 5, 6, 7) and analysis of the contemporary environment data (Chapter 3) provides a firm foundation and justification for making causal inferences between observed sediment characteristics and environmental predictor variables, and therefore, by inference, climate. This knowledge-base provides a framework for the critical evaluation of model results. Without this preliminary analysis many of the complex and subtle contemporary sediment-environment interactions would have been overlooked, making interpretation of the model results far more difficult. This Chapter proposes ways in which the current model could be applied, potential improvements in the methodologies used and recommendations for future research including links to other climate-proxy records. The final part presents a summary of findings.

10.2 Model application

Application of the optimal model (PLS, 208 sample training-set) in its present form is envisaged at Signy Island beyond the historical period and over Holocene timescales to the point of lake inception (*ca.*6000 BP). Long sediment-sequences with supporting radiocarbon chronologies are available from Sombre, Heywood, Moss, Tranquil, Emerald and Gneiss Lakes. Obviously, over longer timescales and with less precise dating control, the objective of reconstruction is altered slightly. The ^{14}C chronology provides less strict temporal resolution than that of ^{210}Pb, especially in light of problems associated with radiocarbon dating in the Antarctic (Björck *et al.*, 1991b; Zale, 1994), and coarser sampling resolution typically used in analyses of long sediment sequences means that the decadal and sub-decadal reconstructions seen in this study cannot be achieved. Model interpretation over longer timescales must be adjusted accordingly; instead of responding to short-medium term ice-cover fluctuations and paraglacial effects discussed by Leonard (1986a), the model should be more indicative of actual up-valley ice-extent and activity, analogous to Karlén's (1981) hypotheses.

The model could also be used outside its current geographical and temporal range in locations with similar environmental regimes, such as Arctic or Alpine regions, or to analogous Late and Post-Glacial sediments of temperate latitudes where calibration lakes are, or have been, affected by glacier activity. Local calibration would be required to

account for differences in geology, which affect weathering and resultant particle-size characteristics and the mineral magnetic properties. As a first stopping point, the model could be applied to lake-sediment sequences from Elephant Island, maritime Antarctic, which has a similar geology (Thomson, 1968). Tephra however, from local sources, could be a problem there and more sophisticated numerical analysis may be required to screen its effects from the background, terrigenous signal. In general though, the model based on three simple determinands (% dry weight, mean particle-size, % loss on ignition) has universal application independent of source lithology variations and rate of sediment accumulation.

10.3 Model improvements

Year-to-year variations in sediment accumulation rate cannot be resolved in this study owing to the lack of annual varves, although some of the long-sediment sequences are visibly laminated and deserve further attention. Annual variability is affected principally by ablation rate, which controls meltwater stream discharge, in itself largely determined by summer air temperature (Gilbert, 1975; Perkins & Sims, 1983; Leeman & Niessen, 1994; Bradley *et al.*, 1996). This study shows that relatively high-resolution reconstructions are still possible in these non-laminated systems using appropriate coring technology and fine-interval sampling. Accuracy could be improved further using finer sectioning (<0.5 cm resolution) of both training-set and fossil samples and perhaps freezer coring techniques. Freeze-drying of samples would circumvent some of the problems associated with diagenetic changes in the sediments post-extrusion but would be detrimental to particle-size analysis.

Variance partitioning confirms the need for sequential extraction techniques (Engstrom & Hansen, 1993; Engstrom & Wright, 1994) to underpin the processes of sediment formation. The sequential extraction techniques used here are very simplistic. Organic matter is clearly a highly important variable but % LOI is a crude, composite measure which gives no indication of the source of the organic carbon. Geochemical analysis, such as C/N ratios, could help understand the mechanisms by which % LOI reflects the balance of erosion versus within-like productivity, as affected by climate. A more specific analysis of major cations and nutrients in the sediments would also be useful but not necessarily helpful to model development as the overall objective was to produce a simple model which could be easily replicated elsewhere. Mineral magnetism received a somewhat cursory treatment in this Thesis as a component part of a much wider

scheme to produce a climate reconstruction model; many queries remain unanswered in these lake-systems, especially concerning the provenance of magnetic minerals in the sediments.

In this study, lake macro-vegetation is recorded on a lake-wide, presence-absence basis but this obscures the local effects that vegetation can play on bottom dynamics and sedimentation. Modelled relationships between the sediments and the lake environment would be improved by a presence-absence notation of vegetation on a sample basis. Given the significance of *Branchinecta* as a climatic and sedimentary predictor (section 8.5) it might be useful to include more indicator fauna. Heywood, Dartnall & Priddle (1980) noted the presence of nematodes and oligochaetes in the lakes which as benthic dwellers are also representative of the sedimentary environment.

10.4 Recommendations for future research

A rigorous and reliable comparison of the predictive abilities of different methods requires an independent test or evaluation set (Juggins, 1992). Very few independent evaluation sets are currently available (Birks, 1995) so an alternative approach is to use simulated data of known properties for both training and test-sets (e.g. ter Braak & Juggins, 1993; ter Braak *et al.*, 1993; Le & Shackleton, 1994) to discover the strengths and weaknesses of current reconstruction procedures with data of different properties. The use of simulated data with this model is a valid consideration after adjustments have been made for inherent errors associated with data in the training-set, such as the problems with particle-size and magnetic susceptibility. Further screening of the training-set could be undertaken, for example, removing samples from lakes recently affected by fur-seals (Heywood, Amos, Bothy), leaving a sub-set of lakes that should be purely responsive to glacier variations.

In common with lakes on Livingston Island (Björck *et al.*, 1996), sediments are clearly influenced by streamflow and the type of transported materials. More detailed studies are required into annual sedimentation regimes and sediment flux, including the deposition of diatom valves, to aid interpretation of climate reconstructions from the sedimentary record. Sediment-trap studies have met with limited success (A.Caulkett, *pers.comm.*) but ideally, the employment of sediment-traps in ice-proximal to ice-distal transects in key lakes would provide critical information on the magnitude, timing and composition of delivered sediments. It may be possible to develop a 'Lotic Index' (cf.

Ludlum, Feeney & Douglas, 1996) to study past changes in runoff.

Meteorological measurements continue at Signy Island and future studies could include the high-resolution measurement of meteorology and glacier movement, coupled with detailed monitoring of sediment transport and deposition, paralleling the exciting developments in the Arctic where integrated lake-climate studies have been carried-out using a 'systems approach' to palaeoclimatic reconstruction (Bradley *et al.*, 1996). Antarctic lake-sediment studies are currently lagging behind those of their Arctic counterparts, partly a result of the difficulty of accessibility and expense.

The results of ice-cover modelling in this Thesis could be compared with the nutrient-reconstructions of Jones & Juggins (1995), particularly in light of the ice-cover reconstruction results for Heywood Lake, to see if nutrient enrichment is purely in response to biotic forcing from migratory fur seals or whether it is more climatic in origin. The exact nature of seal-related erosion of the lowland catchments remains unquantified and again, sediment trapping would be useful. Although true glacial varves are apparently lacking from the most recent sediments in these lakes, annual algal growth layers could form the basis of an alternative chronology in lakes such as Light, Tioga and Gneiss Lakes, with careful sampling by freezer-coring techniques.

Lichens form an expansive land cover-type, and lichenometry (Beschel, 1973), supported by more detailed geomorphological mapping and comparison with the moraine record (cf. Cromack, 1993), could provide additional information on past ice-cover. Most attention on past ice extent has focused in Paternoster Valley on the east coast of Signy Island (J.C. Ellis-Evans, *pers.comm.*), at the neglect of the west coast. The clear advantage of using lakes rather than moraines however, is their greater sensitivity and their continued survival during periods of increased glacier extent.

It was not possible to make a valid reconstruction of lake ice-cover using the measured sediment determinands which is unfortunate since lake ice-cover is also sensitive to recent warming trends (cf. Anderson, Robertson & Magnusson, 1996). Observations at Signy Island have been recorded irregularly and records of freeze-in and break-out dates are rather poor for remote lakes. It might be more useful to develop a quantitative index of lake ice-cover on the basis of air temperature records and lake morphometric parameters. A large volume of literature relates to the modelling of lake ice-cover from

studies in the Arctic and Scandinavia and models have been developed on lake thermal regimes, for example, PROBE (Svensson, 1978) and LIMNOS (Vavrus, Wynne & Foley, 1996). Simulations of lake ice-cover response to climatic warming in Finnish lakes (Huttula, Peltonen & Kaipainen, 1996) indicate that warming will lead to earlier melt-out and overall increase the duration of the open water season. This has enormous implications for lake productivity and its registration in the sediment record.

There is great potential for linking lacustrine and marine sediment records in the environs of Signy Island, tying-in with the objectives of the International Geological Correlation Project (IGCP) approved project 374 ('Palaeoclimatology and palaeoceanography from late Quaternary and Holocene laminated sediments: a global joint approach using marine and lacustrine sediments'). In the 1993 austral summer, sediment cores were taken from nearshore marine locations adjacent to the outlet from the Orwell Glacier (S. Vanhove, *pers.comm.*). Sediments deposited here should be of largely terrestrial origin, representing outwash from the Orwell Glacier. A similar climate response should be detectable in appropriate marine sediment proxies. The stretch of water between Signy and Coronation Islands - Normanna Strait - is extremely deep (section 3.2.1) and is likely to contain an extremely long and continuous marine sediment record.

10.5 Summary

(1) This Thesis has presented an integrated study of the contemporary surface-sediment characteristics of Signy Island's 17 freshwater lakes and the corresponding catchment and limnological factors that influence them. Signy Island is recognised for its sensitivity to environmental perturbations and a 20th Century climatic warming trend is believed to have caused significant loss of permanent snow and ice. In this region, palaeolimnology can contribute much to environmental monitoring (Smol & Douglas, 1996) and the simplicity of these ecosystems and absence from direct human disturbance increases the possibilities for discriminating cause-effect relationships in the sediment record. Following the rationale of Birks (1995), numerical methods have been adapted from palaeoecological studies to produce a quantitative ice-cover reconstruction model using physical sediment determinands. This novel and exploratory development has made a contribution to basic research endeavours in palaeolimnology, providing an exact means of predicting glacier activity and extent using lake-sediments and inferring past climate and climatic fluctuations.

(2) Signy Island is affected by strong seasonal climatic gradients and its landscape has been, and continues to be, shaped by glacial activity. Topographic depressions support a series of 17 freshwater lakes, including glacial and non-glacial types which are suitable for the modelling of glacier variations following the rationale of Karlén (1981). The scientific programme of the British Antarctic Survey has resulted in a vast collection of environmental data, providing a base for the modelling and validation of environmental change. An environmental data-set of 44 variables was assembled on a catchment basis and numerical methods were used to characterize the lakes, providing an updated lake classification (cf. Heywood, Dartnall & Priddle, 1980). Marine influences have always been responsible for the eutrophic state of lowland lakes which contrasts with the oligotrophy of inland, isolated waters. The effects of the rising migratory seal population, driving an enhanced eutrophication, are increasing the disparity between the eutrophic and oligotrophic lakes.

(3) There is a strong contrast between the littoral and profundal zones in these lakes and a sampling strategy was devised to collect surface-sediments across a wide range of sedimentary environments, providing a long gradient for modelling. 209 cores were taken from multiple points at a range of different depths, including long-sediment sequences from 5 lakes to provide historical material for model calibration. The 0-1 cm resolution of the samples represents *ca.*5-10 years of sediment accumulation. Distribution of sediment in each lake basin suggests that redistribution by wind and water currents is probably significant and samples from different zones are not strictly contemporaneous thus contributing to training-set 'noise' (cf. Anderson 1990a).

(4) Measures of sediment lithology included 6 determinands: wet density, percentage dry weight, % loss on ignition, % organic matter by peroxide digestion, % biogenic silica and % minerogenic (clastic) content. These represent 3 fractions of the overall sediment: organic, minerogenic (both either allochthonous and/or autochthonous) and biogenic inorganic (autochthonous only, mainly diatoms and chrysophytes). The contrasting sediment characteristics between glacier-fed and non-glacier fed lakes can be clearly recognised in numerical analysis. Glacier-fed lakes are heavily influenced by allochthonous minerogenic inputs by meltstreams, although where sediment receipt is reduced, some of these sediments can have high organic contents owing to high standing biomass (moss and/or cyanobacterial mat) which decomposes very slowly. Non-glacier-fed lakes generally follow the convention for more organic sediments, lower

minerogenic contents and higher biogenic inorganic contents. This is complicated however, by seasonal anoxia in some lakes which promotes complete breakdown of annual organic matter, producing highly minerogenic sediments, even in the most eutrophic lakes. A model of sediment focusing (Håkanson, 1977) supports the suggestion for a significant movement of sediment in these lakes. The sheltered profundal zone is therefore the preferred sampling location for long, continuous sediment sequences.

(5) Particle-size was measured by laser diffraction analysis and the volume distribution of each sample was summarised by 4 statistical moments: median, mean, standard deviation and skewness. Problems are associated with the sizing technique which can potentially be corrected for. Medium silt is the dominant size fraction, exhibiting some positive skew, indicating the importance of fine particles. The absence of sand-sized particles means that sediments mainly derive from low-energy environments of deposition and are well-mixed by fluvial sorting before entry to the lake basins. The distinction between glacier- and non-glacier-fed lakes is also reflected in particle-size. Turbidity currents appear to hasten the deposition of clays at lake inflows, probably in early spring under lake ice-cover, and neither proximal-distal nor down-valley fining of particle-size is apparent owing to local effects.

(6) Mineral magnetic measurements of the surface-sediments strongly suggest a largely non-detrital origin to magnetic behaviour. Catchment source lithologies contribute low-concentration, coarse-grained (MD or coarse SSD) paramagnetic minerals and rudimentary soils in the catchments provide a limited source of secondary ferrimagnetic minerals. The catchment signal is most apparent in glacier-fed lakes with heavy allochthonous minerogenic inputs (e.g. Emerald Lake). Unusual lithologies with high iron contents (e.g. marble and amphibolite) have a strong local effect on magnetic mineralogy. Superimposed on this background, terrigenous signal is an apparently non-detrital, fine-grained (SSD) component which affects sediments from all the lakes to some degree. There is no strong evidence for abiotic authigenesis although clearly, early diagenetic changes in these samples during storage may have led to the loss of greigite and other fine-grained ferrimagnets. The origin of this fine-grained fraction is most likely to be bacterial, matching findings in analogous Arctic lakes. There is no strong evidence for tephra from the 1967-70 Deception Island eruptions affecting contemporary sediments. One unusual sample was removed from the data-set, suspected for contamination.

(7) All surface-sediments were assembled to form a training-set. Discriminant analysis identifies the major environmental variables affecting overall sediment character and the constituent fractions. The glacier versus non-glacial fed division is still apparent but is weakened by greater noise in this larger data-set. Climate effects on the sediment are largely indirect, conditioned through the limnology (clarity, water temperature, productivity) and catchment (proportion of deglaciated terrain, altitude as a surrogate for the effects of the central ice-cap). Redundant environmental variables can be screened and a sub-set of 14 statistically significant environmental variables explains variation in the sediment data almost as well as the full model. Variance partitioning of the sediment data using these variables is able to show how the balance of response of the respective sediment fractions to catchment and limnological predictors. Variance unexplained relates to variables not quantified in this study, highlighting areas for future research.

(8) Catchment ice-cover was chosen for reconstruction and an ice-prediction equation was established using 4 sediment determinands: % dry weight, mean particle-size, % loss on ignition and HARD%. Two ice-prediction models were developed using a transfer function approach (Partial Least Squares regression) and analogue matching (Modern Analog Technique). Prediction errors for all models and various training-sets vary between ±12-16%. PLS regression is the more robust method and the optimal 2 components PLS model uses 4 sediment determinands and the 208 sample training-set (RMSE=12.3229%, r^2=0.5499; RMSEP=12.6860, r^2=0.5231). This model however, under-predicts at high observed ice-cover and over-predicts at low observed ice-cover. Models were validated using historical records (1968 AD) of ice-cover and most estimates are within the model errors of prediction.

(9) The model is a proxy for erosion and instability, caused by either climate (deglaciation response to rising air temperatures) or biological agents (disturbance of catchment soils and vegetation by fur-seals). Comparison of model results to changes in summer air temperatures over the 20th Century shows that the lake-sediments are responsive on a sub-decadal time resolution, dependent on (i) sediment accumulation rates (≥0.01 g/cm^2yr^{-1}) and (ii) inertia in glacial response to climate forcing. Small valley glaciers are more responsive than large, stable ice-fields. Even so, the ice-cover response to regional and global climate phenomena can be recognised using model predictions from physical determinands in lake-sediment records, adding a further dimension to the use of quantitative palaeoenvironmental reconstructions and the study of global climatic

changes over time.

BIBLIOGRAPHY

Adobe Systems Incorporated (1993) *Adobe Illustrator User Guide, Version 5.0.* Adobe Systems Incorporated, 1585 Charleston Road, P.O. Box 7900, Mountain View, California 94039-7900, USA. US Patent No.4,837,613.

Agrawal, Y.C., McCave, I.N. & Riley (1991) Laser diffraction size analysis. In J.P.M. Syvitski (Ed.) *Principles, methods and application of particle size analysis*, Cambridge University Press, 1991, pp. 117-128.

Allen, S.E., Grimshaw, H.M. & Holdgate, M.W. (1967) Factors affecting the availability of plant nutrients on an Antarctic island. *Journal of Ecology* **55**, 381-396.

Anderson, D.M., Prell, W.L. & Barratt, N.J. (1989) Estimates of sea surface temperature in the Coral Sea at the Last Glacial Maximum. *Palaeoceanography* **4**, 615-627.

Anderson, N.J. (1986) Diatom biostratigraphy and core correlation within a small lake basin. *Hydrobiologia* **143**, 105-112.

Anderson, N.J. (1990a) Variability of sediment diatom assemblages in an upland, wind-stressed lake (Loch Fleet, Galloway, S.W. Scotland). *Journal of Palaeolimnology* **4**, 43-59.

Anderson, N.J. (1990b) Variability of diatom concentrations and accumulation rates in sediments of a small lake basin. *Limnology and Oceanography* **35**, 497-508.

Anderson, N.J. & Rippey, B. (1988) Diagenesis of magnetic minerals in the recent sediments of a eutrophic lake. *Limnology and Oceanography* **33**, 1476-1492.

Anderson, P.M., Bartlein, P.J., Brubacker, L.B., Gajewski, K. & Ritchie, J.C. (1989) Modern analogues of late-Quaternary pollen spectra from the western interior of North America. *Journal of Biogeography* **16**, 573-596.

Anderson, W.L., Robertson, D.M. & Magnuson, J.J. (1996) Evidence of recent warming and El Niño-related variations in ice breakup of Wisconsin lakes. *Limnology and Oceanography* **41**, 815-821.

Appleby, P.G. & Oldfield, F. (1978) The calculation of lead-210 dates assuming a constant rate of supply of unsupported 210Pb to the sediment. *Catena* **5**, 1-8.

Appleby, P.G., Nolan, P.J., Gifford, D.W., Godfrey, M.J., Oldfield, F., Anderson, N.J. & Battarbee, R.W. (1986) ^{210}Pb dating by low background gamma counting. *Hydrobiologia* **143**, 21-27.

Appleby, P.G., Jones, V.J., & Ellis-Evans, C.J. (1995) Radiometric dating of lake sediments from Signy Island (maritime Antarctic): evidence of recent climatic change. *Journal of Palaeolimnology* **13**, 179-191.

Ariztegui, D. & Dobson, J. (1996) Magnetic investigations of framboidal greigite

formation: a record of anthropogenic environmental changes in eutrophic Lake St Moritz, Switzerland. *The Holocene* **6**, 235-241.

Ballantyne, C.K. & Benn, D.I. (1994) Paraglacial slope adjustment and resedimentation following recent glacier retreat, Fåbergstølsdalen, Norway. *Arctic and Alpine Research* **20**, 255-269.

Barber, H.G. & Haworth, E.Y. (1981) *A guide to the morphology of the diatom frustule*. Freshwater Biological Association Scientific Publication No.44, 112 pp.

Bartlein, P.J. & Whitlock, C. (1993) Palaeoclimatic interpretation of the Elk Lake pollen record. *Geological Society of America Special Paper* **276**, 275-293.

Bates, C.C. (1953) Rational theory of delta formation. *American Association of Petroleum Geologists* **37**, 2119-2162.

Battarbee, R.W. (1978) Observations on the recent history of Lough Neagh and its drainage basin. *Philosophical Transactions of the Royal Society of London* **281**, 303-345.

Battarbee, R.W. (1984a) Diatom analysis and the acidification of lakes. *Philosophical Transactions of the Royal Society of London B* **305**, 451-477.

Battarbee, R.W. (1984b) Spatial variations in the water-quality of Lough Erne, Northern Ireland, on the basis of surface sediment diatom analysis. *Freshwater Biology* **14**, 539-545.

Battarbee, R.W. (1991) Recent palaeolimnology and diatom-based environmental reconstruction. In L.C.K. Shane & E.J. Cushing (Eds.) *Quaternary Landscapes.* Minneapolis, University of Minnesota Press, pp. 129-174.

Battarbee, R.W. & Renberg, I. (1990) The surface-water acidification project (SWAP) palaeolimnology program. *Philosophical Transactions of the Royal Society of London B - Biological Sciences* **327**, 227-232.

Battarbee, R.W., Mason, J., Renberg, I. & Talling, J.F. (Eds.) (1990) *Palaeolimnology and lake acidification*, The Royal Society, London, 219 pp.

Battarbee, R.W., Barber, K.E., Oldfield, F., Thompson, R., Stevenson, A.C., Eglington, G., Haworth, E.Y., Brooks, S.J., Holmes, J., Cameron, N.G., Rose, N.L. & Maddy, D. (1996) *Proxy records of climatic change in the UK over the last two millennia. Final Report for the NERC Special Topic Grant GST /02/701.* Environmental Change Research Centre, University College London, London, April 1996.

Bayly, I.A.E. (1992) Fusion of the Genera *Boeckella* and *Pseudoboeckella* (Copepoda) and revision of their species from South America and sub-Antarctic Islands. *Revista Chilena de Historia Natural* **65**, 17-63.

Bayvel, L.P. & Jones, A.R. (1981) *Electromagnetic scattering and its applications.* Applied Science, London, 289 pp.

Bennion, H. (1994) A diatom-phosphorous transfer function for shallow, eutrophic

ponds in southeast England. *Hydrobiologia* **275/276**, 391-410.

Berglund, B.E. (1986) Palaeoecological reference areas and reference sites. In B.E. Berglund (Ed.) *Handbook of Holocene Palaeoecology and Palaeohydrology*, John Wiley & Sons Ltd., pp. 111-126.

Beschel, R.E. (1973) Flechten als Altersmasstab rezenter Moranen. *Zeitschrift für Gletshcerkunde und Glazialgeologie* **1**, 152-161. Translated by W.Barr (1973) Lichens as a measure of recent moraines. *Arctic and Alpine Research* **5**, 303-309.

Birks, H.J.B. *Program CLUSTER. Agglomerative hierarchical cluster analysis (seven methods).* Unpublished.

Birks, H.J.B. *Program EXPAND.* Unpublished.

Birks, H.J.B. (1993) Quaternary palaeoecology and vegetation science - current contributions and possible future developments. *Review of Palaeobotany and Palynology* **79**, 153-177.

Birks, H.J.B. (1994) The importance of pollen and diatom taxonomic precision in quantitative palaeoenvironmental reconstruction. *Review of Palaeobotany and Palynology* **79**, 153-177.

Birks, H.J.B. (1995) Quantitative palaeoenvironmental reconstructions. In Maddy, D. & Brew, J.S. (1995) *Statistical modelling of Quaternary science data*, Technical Guide 5, Quaternary Research Association, Cambridge, pp. 161-254.

Birks, H.J.B. & Birks, H.H. (1980) Sampling and description of organic sediments, In H.J.B. Birks & H.H. Birks, H.H. (Eds.) *Quaternary Palaeoecology*, Edward Arnold, pp. 37-45.

Birks, H.J.B. & Gordon, A.D. (1985) *Numerical Methods in Quaternary Pollen Analysis.* Academic Press, London, 317 pp.

Birks, H.J.B., Juggins, S. & Line, J.M. (1990) Lake surface-water chemistry reconstructions from palaeolimnological data. In B.J. Mason (Ed.) *The Surface Waters Acidification Programme*, Cambridge University Press, Cambridge, pp. 301-313.

Birks, H.J.B., Line, J.M., Juggins, S., Stevenson, A.C. & ter Braak, C.J.F. (1990) Diatoms and pH reconstruction. *Philosophical Transactions of the Royal Society of London B* **327**, 263-278.

Birnie, J. (1990) Holocene environmental change in South Georgia: evidence from lake sediments. *Journal of Quaternary Science* **5**, 171-187.

Björck, S., Håkansson, H., Zale, R., Karlén, W. & Jonsson, B.L. (1991a) A late Holocene lake sediment sequence from Livingston Island, South Shetland Islands, with palaeoclimatic implications. *Antarctic Science* **3**, 61-72.

Björck, S., Hjort, C., Ingolfsson, O. & Skog, G. (1991b) Radiocarbon dates from the Antarctic Peninsula Region - problems and potential. *Quaternary Proceedings* **1**, 55-65.

Björck, S., Sandgren, P. & Zale, R. (1991) Late Holocene tephrochronology of the Northern Antarctic Peninsula. *Quaternary Research*, 36, 322-328.

Björck, S., Håkansson, H., Olsson, S., Barnekow, L. & Janssens, J. (1993) Palaeoclimatic studies in South Shetland Islands, Antarctica, based on numerous stratigraphic variables in lake sediments. *Journal of Palaeolimnology* **8**, 233-272.

Björck, S., Olsson, S., Ellis-Evans, C., Håkansson, H., Humlum, O., & de Lirio, J.M. (1996) Late Holocene palaeoclimatic records from lake sediments on James Ross Island, Antarctica. *Palaeogeography, Palaeoclimatology, Palaeoecology* **121**, 195-220.

Blais, J.M. & Kalff, J. (1995) The influence of lake morphometry on sediment foucusing. *Limnology and Oceanography* **40**, 582-588.

Bloemendal, J. (1982) *The quantification of rates of total sediment influx to Llyn Goddionduon, Gwynedd.* Unpublished PhD Thesis, University of Liverpool.

Bloemendal, J., Oldfield, F. & Thompson, R. (1979) Magnetic measurments used to assess sediment influx at LLyn Goddionduon. *Nature* **280**, 5717, 50-53.

Boninsegna, J.A. (1992) South American dendroclimatological records. In R.S. Bradley & P.D. Jones (Eds.) *Climate Since A.D. 1500*, Routledge, pp. 446-462.

Borland International (1988) *Paradox user's guide, release 3.0*, Borland International, Scotts Valley, California, 310 pp.

Borland International (1991) *Quattro Pro, version 3.0 user's guide*, Borland International, Scotts Valley, California.

Borcard, D., Legendre, P. & Drapeau, P. (1992) Partialling out the spatial component of ecological variation. *Ecology* **73**, 1045-1055.

Bradbury, J.P. (1975) Diatom stratigraphy and human settlement in Minnesota. *Geological Society of America Special Paper* **171**, 74 pp.

Bradbury, J.P. (1986) Continental diatom biostratigraphy and palaeolimnology: a review and evaluation of research directions and applications. *Proceedings of the 8th International Diatom Symposium*, Otto Koeltz, Königstein, pp. 667-686.

Bradbury, J.P. (1988) A climatic-limnologic model of diatom succession for palaeolimnological interpr+wation of varved sediments at Elk Lake, Minnesota. *Journal of Palaeolimnology* **1**, 115-131.

Bradbury, J.P., Leyden, B., Salgado-Labouriau, M., Lewis, W.M. Jnr., Schubert, C., Binford, M.W., Frey, D.G., Whitehead, D.R. & Weibezahn, F.H. (1981) Late Quaternary environmental history of Lake Valencia, Venezuela. *Science* **214**, 1299-1305.

Bradley, R.S., Retelle, M.J., Ludlam, S.D., Hardy, D.R., Zolitschka, B., Lamoureux, S.F. & Douglas, M.S.V. (1996) The Taconite Inlet Lakes Project: a systems approach to palaeoclimatic reconstruction. *Journal of Palaeolimnology* **16**, 97-110.

British Antarctic Survey (1989) Sea mammals report 1988-89. J.R. Ashford. BAS Reference H/1988/N2.

British Antarctic Survey (1990) Sea mammals report 1989-90. N. Forsyth. BAS Reference H/1989/N2.

British Antarctic Survey (1991) Sea mammals report 1990-91. N. Forsyth. BAS Reference H/1990/N13.

British Antarctic Survey (1992) Sea mammal report 1990-91. L. Bullough. BAS Reference H/1991/NM3.

British Antarctic Survey (1992) Signy sea mammal report 1992. L. Bullough. BAS Reference H/1992/NM3.

British Antarctic Survey (1993) Sea mammal report 1993-94. S. Brockington. BAS Reference H/1993/NM3.

Bronge, C. (1992) Holocene climatic record from lacustrine sediments in a freshwater lake in the Vestfold Hills, Antarctica. *Geografiska Annaler* **74A**, 47-58.

Brown, P.J. (1982) Multivariate calibration. *Journal of the Royal Statistical Society B* **44**, 287-321.

Burnham, A.J., Viveros, R., MacGregor, J.F. (1996) Frameworks for latent variable multivariate regression. *Journal of Chemometrics* **10**, 31-+w.

Chalmers, M.O. (1992) Terrestrial Assistants Report, Signy Island, 1991-1992. *British Antarctic Survey*, Unpublished report H/1992/N1.

Chambers, M.J.G. (1966) Investigation of patterned ground at Signy Island, South Orkney Islands, II - temperature regimes in the active layers. *British Antarctic Survey Bulletin*, No.10, 71-83.

Chappell, A. (1995) *Geostatistical mapping and ordination analyses of ^{137}Cs-derived net soil flux in south-west Niger.* Unpublished PhD Thesis. University College London. 297 pp.

Charles, D.F. & Norton, S.A. (1986) Palaeolimnological evidence for trends in atmospheric deposition of acids and heavy metals. In *Acid Deposition: Long-term trends*, National Academy Press, Washington D.C., pp. 335-431.

Charles, D.F. & Whitehead, D.R. (1986) The PIRLA project: Palaeoecological investigations of recent lake acidification. *Hydrobiologia* **143**, 13-20.

Charles, D.F., Dixit, S.S., Cumming, F. & Smol, J.P. (1991) Variability in diatom and chrysophyte assemblages and inferred pH: palaeolimnological studies of Big Moose Lake, New York, USA. *Journal of Palaeolimnology* **5**, 267-284.

Church, M. & Gilbert, R. (1975) Proglacial fluvial and lacustrine environments. In A.V. Jopling & B.C. McDonald (Eds.) *Glaciofluvial and glaciolacustrine sedimentation.* Society of Economic Palaeontologists and Mineralogists, Tulsa, Oklahoma, Special

Publication, 23, pp. 22-100.

Church, M. & Ryder, J.M. (1972) Paraglacial sedimentation: A consideration of fluvial processes conditioned by glaciation. *Geological Society of America Bulletin* **83**, 3059-3072.

Collins, N.J., Baker, J.H. & Tilbrook, P.J. (1975) Signy Island: maritime Antarctic. In Rosswall, T. & Heal, O.W. (Eds.) *Structure and function of tundra ecosystems*, Ecological Bulletin (Stockholm), 20, pp. 345-374.

Croxall, J.P., Rootes, D.M. & Price, R.A. (1981) Increases in penguin populations at Signy Island, South Orkney Islands. *Bulletin of the British Antarctic Survey* **54**, 47-56.

Cromack, M. (1991) *A glacial sedimentary system in Northwest Spitsbergen.* Unpublished PhD Thesis, University of Cambridge.

Cumming, B.F., Smol, J.P., Kingston, J.C., Charles, D.F., Birks, H.J.B., Camburn, K.E., Dixit, S.S., Uutala, A.J. & Selle, A.R. (1992) How much acidification has occurred in Adirondack Region Lakes (New York, USA) since pre-industrial times? *Canadian Journal of Fisheries and Aquatic Science* **49**, 128-141.

Cumming, B.F., Glew, J.R., Smol, J.P., Davis, R.B. & Norton, S.A. (1993) Comment on "Core compression and surficial sediment loss of lake sediments of high porosity caused by gravity coring" (Crusius and Anderson), *Limnology and Oceanography* **38**, 695-699.

Dankers, P.H. (1978) *Magnetic properties of dispersed natural iron oxides of known grain size.* Unpublished PhD Thesis, University of Utrecht.

Davey, M.C. (1988) Ecology of terrestrial algae of the fellfield ecosystems of Signy Island, South Orkney Islands. *British Antarctic Survey Bulletin* **81**, 69-74.

Davey, M.C. (1993) Carbon and nitrogen dynamics in a maritime Antarctic stream. *Freshwater Biology* **30**, 319-330.

Davey, M.C., Pickup, J. & Block, W. (1992) Temperature variation and its biological significance in fellfield habitats on a maritime Antarctic island. *Antarctic Science* **4**, 383-388.

Davis, J.C. (1986) *Statistics and data analysis in geology.* Second edition. John Wiley & Sons Ltd., New York.

Davis, M.B. (1968) Pollen grains in lake sediments: redeposition caused by seasonal water circulation. *Science* **162**, 796-799.

Davis, M.B. (1973) Redeposition of pollen grains in lake sediment. *Limnology and Oceanography* **18**, 44-52.

Davis, M.B. & Ford, M.S.J. (1982) Sediment focusing in Mirror Lake, New Hampshire. *Limnology and Oceanography* **27**, 137-150.

Davis, M.B., Moeller, R.E. & Ford, J. (1984) Sediment focusing and pollen influx. In E.Y. Haworth & J.W.G. Lund (Eds.) *Lake sediments and environmental history*, University of Leicester Press, Leicester, pp. 261-293.

Dean, W.E., Bradbury, J.P., Anderson, R.Y. & Barnosky, C.W. (1984) The variability of Holocene climatic change: evidence from varved lake sediments. *Science* **226**, 1191-1194.

Dearing, J.A. (1983) Changing patterns of sediment accumulation in a small lake in Scania, southern Sweden. *Hydrobiologia* **103**, 59-64.

Dearing, J.A. (1986) Core correlation and total sediment influx. In B.E. Berglund (Ed.) *Handbook of Holocene Palaeoecology and Palaeohydrology*, John Wiley & Sons Ltd., pp. 247-270.

Dearing, J.A. (1991) Lake sediment records of erosional processes. *Hydrobiologia* **214**, 99-106.

Dearing, J.A. & Flower, R.J. (1982) The magnetic susceptibility of sedimenting material trapped in Lough Neagh, Northern Ireland, and its erosional significance. *Limnology and Oceanography* **27**, 969-975.

Dearing, J.A., Hay, K.L., Baban, S.M.J., Huddleston, A.S., Wellington, E.M.H. & Loveland, P.J. (1996a) Magnetic susceptibility of soil: an evaluation of conflicting theories using a national data-set. *Geophysical Journal International* **127**, 728-734.

Dearing, J.A., Dann, R.J.L., Hay, K., Lees, J.A., Loveland, P.J., Maher, B.A. & O'Grady, K.O. (1996b) Frequency-dependent susceptibility measurements of environmental materials. *Geophysical Journal International* **124**, 228-240.

Dean, W.E. (1974) Determination of carbonate and organic matter in calcareous sediments and sedimentary rocks by loss on ignition: comparison with other methods. *Journal of Sedimentary Petrology* **44**, 242-248.

Deevey, E.S. (1955) The obliteration of the hypolimnion. *Memorie Dell'Istituto Italiano Di Idrobiologia Supp.* **8**, 9-38.

de Jong, S. (1991) Chenometrical applications in industrial food research laboratory. *Mikrochimica Acta* **2**, 93-101.

Desloges, J.R. (1994) Varve deposition and the sediment yield record at three small lakes of the Southern Canadian Cordillera. *Arctic and Alpine Research* **26**, 130-140.

Digerfeldt, G. (1972) The post-glacial development of Lake Trummen. *Folia Limnologica Scandinavica* **16**, 1-104.

Domack, E.W., Jull, A.J.T., Anderson, J.B., & Linick, T.W. (1991) Mid-Holocene ice sheet recession from the Wilkes Land Continental Shelf, East Antarctica. In M.R.A. Thompson, J.A. Crame & J.W. Thomson (Eds.) *Geological Evolution of Antarctica*, Proceedings of the 5th International Symposium on Antarctic Earth Sciences, Cambridge: Cambridge University Press, pp. 693-698.

Doran, P.T., Wharton Jnr., R.A., & Berry-Lyons, W. (1994) Paleolimnology of the McMurdo Dry Valleys, Antarctica. *Journal of Paleolimnology* **10**, 85-114.

Downing, J.A. & Rath, L.C. (1988) Spatial patchiness in the lacustrine sedim+wtary environment. *Limnology and Oceanography* **33**, 447-458.

Dyson, C. (1996) *Antarctic tephrological studies at Midge Lake, Livingston Island, South Shetland Islands and at Sombre Lake, Signy Island, South Orkney Islands.* MSc Dissertation, University College London, 68 pp.

Ebdon, D. (1985) *Statistics in geography.* Second edition. Blackwell, Oxford. 232 pp.

Edwards, K.J. & Thompson, R. (1984) Magnetic, palynological and radiocarbon correlation and dating comparisons in long cores from a northern Irish lake. *Catena* **11**, 83-89.

Ellis-Evans, J.C. (1982) Seasonal microbial activity in Antarctic freshwater lake sediments. *Polar Biology*, 1, 129-140.

Ellis-Evans, J.C. (1983) A full list of officially recognized names for the lakes of Signy Island, South Orkney Islands. *British Antarctic Survey Bulletin*, No. 59, 79-80.

Ellis-Evans, J.C. (1990) Evidence for change in the chemistry of maritime Antarctic Heywood Lake. In K.R. Kerry & G. Hempel (Eds.) *Antarctic Ecosystems. Ecological Change and Conservation*, Springer-Verlag Berlin Heidelberg, pp. 77-82.

Ellis-Evans, J.C. & Lemon, E.C.G. (1989) Some aspects of iron cycling in maritime Antarctic lakes. *Hydrobiologia* **172**, 149-164.

Ellis-Evans, J.C. & Sanders, M.W. (1988) Observations on microbial activity in a seasonally anoxic, nutrient enriched maritime Antarctic lake. *Polar Biology* **8**, 311-318.

Ellis-Evans, J.C. & Wynn-Williams, D.D. (1985) The interaction of soil and lake microflora at Signy Island. In W.R. Siegfried, P.R. Condy & R.M. Laws (Eds.) *Antarctic Nutrient Cycles and Food Webs*, Springer-Verlag Berlin Heidelberg, pp. 662-668.

Engstrom, D.R. (1983) *Chemical stratigraphy of lake sediments as a record of environmental change.* Unpublished PhD Thesis, University of Minnesota.

Engstrom, D.R. & Hansen, B.C.S. (1985) Postglacial vegetational change and soil development in southeastern Labrador as inferred from pollen and chemical stratigraphy. *Canadian Journal of Botany* **63**, 543-561.

Engstrom, D.R. & Wright Jnr., H.E. (1984) Chemical stratigraphy of lake sediments as a record of environmental change. In E.Y. Haworth & J.W.G. Lund (Eds.) *Lake sediments and environmental history. Studies in palaeolimnology and palaeoecology in honour of Winifred Tutin*, Leicester University Press, pp. 11-67.

Environmental Systems Research Institute Inc. (1989-92) *ARC/INFO Geographical Information System (GIS). ARC Version 6.1*, June 30 1992, Copyright ©1989, 1990, 1991, 1992 Environmental Systems Research Institute Inc., USA.

Everitt, B.S. (1978) The graphical display of clusters and similarity matrices. In Everitt, B.S. (1978) *Graphical techniques for multivariate data.* Heinemann Educational Books Ltd, London, pp. 42-64.

Everitt, B.S. & Dunn, G. (1991) Cluster analysis. In Everitt, B.S. & Dunn, G. (Eds.) *Applied multivariate data analysis.* Edward Arnold, London, pp. 99-126.

Fenton, J.H.C. (1980) The rate of peat accumulation in Antarctic moss banks. *Journal of Ecology* **68**, 211-228.

Flower, R.J. (1980) *A study of sediment formation, transport and deposition in Lough Neagh, Northern Ireland, with special reference to diatoms.* Unpublished PhD Thesis, New University of Ulster.

Flower, R.J. (1993) Diatom preservation: experiments and observations on dissolution and breakage in modern and fossil material. *Hydrobiologia* **269/270**, 473-484.

Frenot, Y., Van Vliet-Lanoë, B., Gloaguen, J.-C. (1995) Particle translocation and initial soil development on a glacier foreland, Kerguelen Islands, Subantarctic. *Arctic and Alpine Research* **27**, 107-115.

Frey, D.G. (1969) The rationale of palaeolimnology. *Mitt.Int.Vereinigung Limnologie 17*, 7-18.

Fritz, S. (1989) Lake ontogeny and limnological response to prehistoric and historic land use in Diss, Norfolk, England. *Journal of Ecology* **77**, 182-202.

Fritz, S. (1990) Twentieth-century salinity and water level fluctuations in Devil's Lake, North Dakota: Test of a diatom-based transfer function. *Limnology and Oceanography* **35**, 1771-1781.

Fritz, S., Juggins, S., Battarbee, R.W. & Engstrom, D.R. (1991) Reconstruction of past changes in salinity and climate using a diatom-based transfer function. *Nature* **352**, 706-708.

Gaillard, M.-J, Birks, H.J.B., Karlsson, K. & Lageråas, P. (1995) Quantitative reconstruction of past land-use and soil conditions using the modern analog approach - a case study in south Sweden. *PACT Volume for Urve Miller* (Submitted).

Gale, S.J. & Hoare, P.J. (1991) *Quaternary sediments. Petrographic methods for the study of unlithified rocks.* Belhaven Press, London, 323 pp.

Gallagher, J.B. (1985) The influence of iron and manganese on nutrient cycling in shallow freshwater lakes. In W.R. Siegfried, R.M. Laws & P.R. Condy (Eds.) *Antarctic nutrient cycles and food webs*, Springer Verlag Berlin Heidelberg, pp. 234-237.

Gasse, F., Juggins, S. & Ben Khelifa, L. (1995) Diatom-based transfer functions for inferring past hydrochemical characteristics of African lakes. *Palaeoclimatology, Palaeolimnology, Palaeoceanography* **117**, 31-54.

Gauch, H.G. (1982) *Multivariate analysis in community ecology.* Cambridge University

Press, Cambridge, 298 pp.

Geladi, P. (1988) Notes on the history and nature of partial least squares (PLS) modelling. *Journal of Chemometrics* **2**, 231-246.

Geladi, P. & Kowalski, B.R. (1986) Partial least-squares regression: a tutorial. *Analytica Chimica Acta* **185**, 1-17.

Gilbert, R. (1975) Sedimentation in Lillooet Lake, British Columbia. *Canadian Journal of Earth Sciences* **12**, 1697-1711.

Glew, J.R. (1991) Miniature gravity corer for recovering short sediment cores. *Journal of Palaeolimnology* **5**, 285-287.

Gordon, J.E. & Timmis, R.J. (1992) Glacier fluctuations on South Georgia during the 1970s and early 1980s. *Antarctic Science* **4**, 215-226.

Grimm, E.C. (1991) *Tilia-graph Version 1.19.* Illinois State Museum, Research and Collections Center, 1920 South 10½ Street, Springfield, IL 62703, USA.

Grimm, E.C. (1993) *Tilia Version 2.0.* Illinois State Museum, Research and Collections Center, 1920 South 10½ Street, Springfield, IL 62703, USA.

Grobbelaar, J.U. (1975) The lentic and lotic freshwater types of Marion Island (sub-Antarctic): a limnological study. *Verhandlungen der internationalen Vereinigung für theoretische und angewandte Limnologie* **19**, 1442-1449.

Guinet, C., Jouventin, P. & Georges, J-Y. (1994) Long term population changes of fur seals *Arctocephalus gazella* and *Arctocephalus tropicalis* on subantarctic (Crozet) and subtropical (St.Paul and Amsterdam) islands and their possible relationship to El Nino Southern Oscillation. *Antarctic Science* **6**, 473-47S.

Guiot, J. (1990) Methodology of the last climatic cycle reconstruction in palynology based on multivariate time series analysis. *Géographie physique et Quaternaire* **39**, 115-125.

Guiot, J., de Beaulieau, J.L., Cheddadi, R., David, F., Ponel, P. & Reille, M. (1993) The climate in western Europe during the last glacial/interglacial cycle derived from pollen and insect remains. *Palaeogeography, Palaeoclimatology, Palaeoecology* **103**, 73-93.

Gustavson, T.C. (1975) Sedimentation and physical limnology in proglacial Malaspina Lake, southeastern Alaska. In A.V. Jopling & B.C. McDonald (Eds.) *Glaciofluvial and glaciolacustrine sedimentation.* Society of Economic Palaeontologists and Mineralogists, Tulsa, Oklahoma, Special Publication, 23, 249-263.

Håkanson, L. (1977) The influence of wind, fetch and water depth on the distribution of sediments in Lake Vanern, Sweden. *Canadian Journal of Earth Sciences* **14**, 397-412.

Håkanson, L. & Jansson, M. (1983) *Principles of lake sedimentology.* Springer-Verlag Berlin Heidelberg New York Tokyo. 316 pp.

Hall, D. & Titterington, D.M. (1989) The effect of simulation on level accuracy and power of Monte Carlo tests. *Journal of the Royal Statistical Society B* **51**, 459-467.

Hansen, K. (1961) Lake types and lake sediments. *Verhandlungen der internationalen Vereinigung für theoretische und angewandte Limnologie* **14**, 285-290.

Hardy, D.R. (1996) Climatic influences on streamflow and sediment flux into Lake C2, northern Ellesmere Island, Canada. *Journal of Palaeolimnology* **16**, 133-149.

Hardy, D.R. & Bradley, R.S. (1996) Climatic change in Nunavut. *Geoscience Canada* **23**, 217-224.

Hardy, D.R., Bradley, R.S. & Zolitschka, B. (1996) The climatic signal in varved sediments from Lake C2, northern Ellesmere Island, Canada. *Journal of Palaeolimnology* **16**, 227-238.

Harper, P.P. (1981) Ecology of streams at high latitudes. In M.A. Lock & D.D. Williams (Eds.) *Perspectives in running water ecology.* Plenum Press, New York, pp.313-337.

Harrison, R.B. (1960) Geology, geomorphology and glaciology report. Signy Island, South Orkney Islands. *British Antarctic Survey unpublished report.* G/1960/H, 8 pp.

Hastie, T.J. & Tibishirani, R.J. (1990) *Generalized additive models.* Chapman & Hall, London, 335 pp.

Hawes, I. (1983) Turbulence and its consequences for phytoplankton development in two ice-covered Antarctic lakes. *British Antarctic Survey Bulletin* **60**, 69-81.

Hawes, I. (1988) The seasonal dynamics of Spirogyra in a shallow, maritime Antarctic lake. *Polar Biology* **8**, 429-437.

Hawes, I. (1989) Filamentous green algae in freshwater streams on Signy Island, Antarctica. *Hydrobiologia* **172**, 1-18.

Hawes, I. (1990) Eutrophication and vegetation development in maritime Antarctic Lakes. In K.R. Kerry & G. Hempel (Eds.) *Antarctic Ecosystems. Ecological Change and Conservation*, Springer-Verlag Berlin Heidelberg, pp. 83-90.

Haworth, E.Y. & Lund, J.W.G. (Eds.) (1984) *Lake sediments and environmental history*, Leicester University Press, Leicester. 411 pp.

Heywood, R.B. (1967) Ecology of the freshwater lakes of Signy Island, South Orkney Islands: I. Catchment areas, drainage systems and lake morphology. *British Antarctic Survey Bulletin* **14**, 25-43.

Heywood, R.B. (1968) Ecology of the freshwater lakes of Signy Island, South Orkney Islands: II. Physical and chemical properties of the lakes. *British Antarctic Survey Bulletin* **18**, 11-44.

Heywood, R.B. (1977) Antarctic freshwater ecosystems - a review and synthesis. In

G.A. Lano (Ed.) *Adaptations within Antarctic Ecosystems.* Third SCAR Symposium on Antarctic Biology, 1974. Gulf Publishing, Texas, pp.801-828.

Heywood, R.B., Dartnall, H.J.G., & Priddle, J. (1979) The freshwater lakes of Signy Island, South Orkney Islands, Antarctica: data sheets. *British Antarctic Survey Data*, No.3, 1979. British Antarctic Survey & Natural Environment Research Council.

Heywood, R.B., Dartnall, H.J.G., & Priddle, J. (1980) Characteristics and classification of the lakes of Signy Island, South Orkney Islands, Antarctica. *Freshwater Biology* **10**, 47-59.

Hicks, D.M., McSaveney, M.J., & Chinn, T.J.H. (1990) Sedimentation in proglacial Ivory Lake, Southern Alps, New Zealand. *Arctic and Alpine Research* **22**, 26-42.

Hilton, J. (1985) A conceptual framework for predicting the occurrence of sediment focusing and sediment redistribution in small lakes. *Limnology and Oceanography* **30**, 1131-1143.

Hilton, J. & Lishman, J.P. (1985) The effect of redox change on the magnetic susceptibility of sediments from a seasonally anoxic lake. *Limnology and Oceanography* **35**, 497-508.

Hilton, J., Lishman, J.P. & Allen, P.V. (1986) The dominant processes of sediment distribution and focusing in a small, eutrophic, monomictic lake. *Limnology and Oceanography* **31**, 125-133.

Hilton, J., Lishman, J.P. & Chapman, J.S. (1986) Magnetic and chemical characterization of a diagenetic magnetic mineral formed in the sediments of productive lakes. *Chemical Geology* **56**, 325-335.

Hitchen, C.J. (1992) The effect of suspension medium refractive index on the particle size analysis of quartz by laser diffraction. *Particle and Particle Systems Characterization* **9**, 171-175.

Hodgson, D.A. & Johnston, N.M. (1997) Inferring seal populations from lake sediments. *Nature* **387**, 30-31.

Holdgate, M.W. (1964) Terrestrial ecology in the Maritime Antarctic. In R. Carrick, M.W. Holdgate & J. Provost (Eds.) *Biologie Antarctique*, Hermann, Paris, pp. 181-194.

Holdgate, M.W., Allen, S.E. & Chambers, M.J.G. (1967) A preliminary investigation of the soils of Signy Island, South Orkney Islands. *British Antarctic Survey Bulletin*, No. 12, 53-71.

Holmes, P.W. (1968) Sedimentary studies of Late Quaternary material in Windermere Lake (Great Britain). *Sedimentary Geology* **2**, 201-224.

Houghton, J.T., Jenkins, G.J. & Ephraums, J.J. (1990) *Climate change: the IPCC assessment.* Cambridge University Press, Cambridge.

Hutchinson, G.E. (1957) *A treatise on Limnology. Volume 1: Geography, physics and*

chemistry. New York, London, Wiley & Sons, 1015 pp.

Hutson, W.H. (1980) The Agulhas Current during the last Pleistocene: analysis of modern faunal analogs. *Science* **207**, 64-66.

Huttula, T., Peltonen, A. & Kaipainen, H. (1996) Effects of climatic change on ice conditions and temperature regime in Finnish lakes (sensitivity analysis of wind forcing and other climatic variables). *The Finnish Research Programme on Climate Change (SILMU), Final Report*, Publications of the Academy of Finland 4/96, Edita, Finland, pp. 167-189.

Huttunen, P., Meriläinen, J. & Tolonen, K. (1978) The history of a small dystrophied forest lake, southern Finland. *Polskie Archiv Hydrobiologie* **25**, 189-202.

Imbrie, J. & Kipp, N.G. (1971) A new micropalaeontological method for quantitative palaeoclimatology application to a late Pleistocene Caribbean core. In K.K. Turekian (Ed.) *The Late Cenozoic Glacial Ages*, Yale University Press, New Haven and London, pp. 71-181.

Ingólfsson, O., Hjort, C., Björck, S. & Lewis-Smith, R.I. (1992) Late Pleistocene and Holocene glacial history of James Ross Island, Antarctic Peninsula. *Boreas* **21**, 209-222.

IPCC (1990) *Scientific assessment of climate change*. Policy makers' summary of the report of Working Group 1, WMO-UNEP. 26 pp.

Jackson, D.A. (1993) Stopping rules in principal components analysis: a comparison of heuristical and statistical approaches. *Ecology* **74**, 2204-2214.

Jeffers, J.N.R. (1977) Discriminant functions: a case study. *Bias* **4**, 24-38.

Jones, B.F. & Bowser, C.J. (1978) The mineralogy and related chemistry of lake sediments. In A. Lerman (Ed.) *Lakes: chemistry, geology, physics*. Springer-Verlag New York Heidelberg Berlin, pp. 179-227.

Jones, P.D., Marsh, R., Wigley, T.M.L. & Peel, D.A. (1993) Decadal timescale links between Antarctic Peninsula ice-core oxygen-18, deuterium and temperature. *The Holocene* **3**, 14-26.

Jones, P.D., Raper, S.C.B. & Wigley, T.M.L. (1986) Southern hemisphere surface air temperature variations: 1851-1984. *Journal of Climate and Applied Meteorology* **25**, 1213-1230.

Jones, J.G. (1980) Some differences in the microbiology of profundal and littoral lake sediments. *Journal of General Microbiology* **47**, 57-83.

Jones, J.G. & Simon, B.M. (1981) Differences in microbial decomposition processes in profundal and littoral lake sediments with particular reference to the nitrogen cycle. *Journal of General Microbiology* **123**, 297-312.

Jones, V.J. (1993) The use of diatoms in lake sediments to investigate environmental history in the Maritime Antarctic: an example from Sombre Lake, Signy Island.

Antarctic Special Topic, 91-95.

Jones, V.J. (1996) The diversity, distribution and ecology of diatoms from Antarctic inland waters. *Biodiversity and Conservation* **5**, 1433-1449.

Jones, V.J. & Juggins, S. (1995) The construction of a diatom-based chlorophyll-*a* transfer function and its application at three lakes on Signy Island (maritime Antarctic) subject to differing degrees of nutrient enrichment. *Freshwater Biology* **34**, 433-445.

Jones, V.J., Juggins, S. & Battarbee, R.W. (1993) The palaeolimnology of Antarctic lakes using diatom:water quality transfer functions. *Final Report for the NERC Antarctic Special Topic Award*, GST/02/448, September 1993.

Jones, V.J., Juggins, S. & Ellis-Evans, C.J. (1993). The relationship between water chemistry and surface sediment diatom assemblages in maritime Antarctic lakes. *Antarctic Science* **5**, 339-348.

Jongman, R.H.G., ter Braak, C.J.F. & van Tongeren, O.F.R. (Eds.) (1987) *Data analysis in community and landscape ecology*. Pudoc, Wageningen.

Juggins, S. (1992) Diatoms in the Thames Estuary, England: Ecology, palaeoecology, and salinity transfer function. *Bibliotheca Diatomologica* **25**, 216 pp.

Juggins, S. (1994) *Program MAT - Modern Analog Technique, Version 1.0*, Department of Geography, University of Newcastle, Newcastle-upon-Tyne NE1 7RH, UK.

Juggins, S., Battarbee, R.W. & Fritz, S.C. (1994) Diatom/salinity transfer functions and climate change: an assessment of methods and application to two Holocene sequences from the Northern Great Plains, North America. In B.M. Funnell & R.L.F. Kay (Eds.) *Palaeoclimate of the last Glacial/Interglacial Cycle*, Special publication 94/2 of the NERC Earth Sciences Directorate, pp. 37-41.

Juggins, S. & ter Braak, C.J.F. (1996) *CALIBRATE Version 0.61 (Beta Test) - A Computer Program for Species-Environmental Calibration by [Weighted-Averaging] Partial Least Squares Regression.* ECRC, University College London.

Kanerva, H., Kiesvaara, J., Muttonen, E. & Yliruusi, J. (1993b) Evaluation of the capability of laser-light diffraction to determine the size distributions of spherical particles. *Pharmazeutische Industrie* **55**, 775-779.

Karlén, W. (1981) Lacustrine sediment studies. A technique to obtain a continuous record of Holocene glacier variations. *Geografiska Annaler* **63A**, 273-279.

Karlén, W. & Matthews, J.A. (1992) Reconstructing Holocene glacier variations from glacial lake sediments: studies from Nordvestlandet and Jostedalsbreen-Jötunheimen, southern Norway. *Geografiska Annaler* **74A**, 327-347.

Kernan, M. (1996) *Predicting surface water critical loads at the catchment scale.* Unpublished PhD Thesis, University of London. 349 pp.

Korsman, T. (1994) *Acidification trends in Sweden. An assessment of past water*

chemistry conditions using lake sediments. Doctoral Thesis, University of Umeå, 72 pp.

Korsman, T. & Birks, H.J.B. (1996) Diatom-based water chemistry reconstructions from northern Sweden: a comparison of reconstruction techniques. *Journal of Palaeolimnology* **15**, 65-77.

Korsman, T., Nilsson, M., Ohman, J. & Renberg, H.J.B. (1992) Near-infrared reflectance spectroscopy of sediments - a potential method to infer the past pH of lakes. *Environmental Science and Technology* **26**, 2122-2126.

Krausse, G.L., Schelske, C.L. & Davis, C.O. (1983) Comparison of three wet-alkaline methods of digestion of biogenic silica in water. *Freshwater Biology* **13**, 73-81.

Le, J. (1992) Palaeotemperature estimation methods: sensitivity test on two western equatorial Pacific cores. *Quaternary Science Reviews* **11**, 801-820.

Le, J. & Shackleton, N.J. (1994) Estimation of palaeoenvironment by transfer functions: simulation with hypothetical data. *Marine Micropalaeontology.* In press.

Leeman, A. & Niessen, F. (1994a) Varve formation and the climatic record in an Alpine proglacial lake: calibrating annually laminated sediments against hydrological and meteorological data. *The Holocene* **4**, 1-8.

Leeman, A. & Niessen, F. (1994b) Holocene glacial activity and climatic variations in the Swiss Alps: reconstructing a continuous record from proglacial lake sediments. *The Holocene* **4**, 259-268.

Lehman, J.T. (1975) Reconstructing the rate of accumulation of lake sediment: the effect of sediment focusing. *Quaternary Research* **5**, 541-550.

Lemmen, D.S., Gilbert, R., Smol, J.P. & Hall, R.I. (1988) Holocene sedimentation in glacial Tasikutaaq Lake, Baffin Island. *Canadian Journal of Earth Sciences* **25**, 810-823.

Leonard, E.M. (1985) Glaciological and climatic controls on lake sedimentation, Canadian Rocky Mountains. *Zeitschrift für Gletcherkunde und Glazialgeologie* **21**, 35-42.

Leonard, E.M. (1986a) Varve studies at Hector Lake, Alberta, Canada, and the relationship between glacial activity and sedimentation. *Quaternary Research* **25**, 199-214.

Leonard, E.M. (1986b) Use of lacustrine sedimentary sequences as indicators of Holocene Glacial History, Banff National Park, Alberta, Canada. *Quaternary Research* **26**, 218-231.

Leonard, E.M. (1997) The relationship between glacial activity and sediment production: evidence from a 4450-year varve record of neoglacial sedimentation in Hector Lake, Alberta, Canada. *Journal of Palaeolimnology* **17**, 319-330.

Lewis-Smith, R.I. (1988) Destruction of Antarctic terrestrial ecosystems by a rapidly increasing fur seal population. *Biological Conservation* **45**, 55-72.

Light, J.J. (1976) An unusual drainage system in an Antarctic valley. *British Antarctic Survey Bulletin*, No.43, 77-84.

Light, J.J. & R.B. Heywood (1973) Deep-water mosses in Antarctic lakes. *Nature* **242**, 5399, 535-536.

Likens, G.E. & Moeller, R.E. (1985) Chemistry. In G.E. Likens (Ed.) *An ecosystem approach to aquatic ecology, Mirror Lake and its watershed.* Springer-Verlag New York.

Loizeau, J.-L., Arbouille, D., Santiago, S., & Vernet, J.-P. (1994) Evaluation of a wide range laser diffraction size analyser for use with sediments. *Sedimentology* **41**, 353-361.

Lotter, A.F. & Birks, H.J.B. (1993) The impact of the Laacher See Tephra on terrestrial and aquatic ecosystems in the Black Forest, southern Germany. *Journal of Quaternary Science* **8**, 263-276.

Ludlum, S.D., Feeney, S. & Douglas, M.S.V. (1996) Changes in the importance of lotic and littoral diatoms in a high arctic lake over the last 191 years. *Journal of Palaeolimnology* **16**, 184-204.

McCave, I.N., Bryant, R.J., Cook, H.F. & Coughanowr, C.A. (1986) Evaluation of a laser-diffraction-size analyzer for use with natural sediments. *Journal of Sedimentary Petrology* **56**, 561-564.

McKay, C.P., Clow, G.D., Wharton Jnr., R.A., & Squyres, S.W. (1985) Thickness of ice on perennially frozen lakes. *Nature* **313**, 561-562.

Mackereth, F.J.H. (1966) Some chemical observations on post-glacial lake sediments. *Philosophical Transactions of the Royal Society of London B* **250**, 165-213.

Maher, B.A. (1988) Magnetic properties of some synthetic sub-micron magnetites. *Geophysical Journal* **94**, 83-96.

Malvern Instruments Ltd (1980) *System 2600 Instruction Manual, IM026, Issue 2.* Malvern Instruments Ltd., Spring Lane South, Malvern, Worcestershire, UK.

Malvern Instruments Limited (1996) *Sample dispersion and refractive index guide. MAN0079. Version 3.0. May 1996.* Malvern Instruments Limited, Spring Lane South, Malvern, Worcestershire, UK.

Manly, B.F.J. (1992) *The design and analysis of research studies.* Cambridge University Press, 353 pp.

Matsumoto, G.I. (1993) Geochemical features of the McMurdo Dry Valley Lakes, Antarctica. Physical and Biogeochemical Processes in Antarctic Lakes, *Antarctic Research Series* **59**, 95-118.

Matthews, D.H. & Maling, D.H. (1967) The geology of the South Orkney Islands I. Signy Island. *Falkland Islands Dependencies Survey Scientific Reports*, No.25, 27 pp.

Matthews, M.D. (1991) The effect of pretreatment on size analysis. In J.P.M. Svyitski (Ed.) *Principles, Methods and Application of Particle Size Analysis*, pp. 34-42.

Mäusbacher, R., Müller, J. & Schmidt, R. (1989) Evolution of postglacial sedimentation in Antarctic lakes (King George Island). *Zeitschrift für Geomorphologie N.F.* **33**, 219-234.

Menounous, B. (1997) The water content of lake sediments and its relationship to other physical parameters: an alpine case study. *The Holocene* **7**, 207-212.

Miller R.G. (1974) The jack-knife - a review. *Biometrika* **61**, 1-15.

Minitab, Inc. (1989) *Minitab. Data analysis software. Release 7.2 -- Standard version.* Copyright Minitab Inc.

Morley, J.J. (1989) Variations in high-latitude oceanographic fronts in the Southern Indian Ocean. An estimation based on faunal changes. *Palaeoceanography* **4**, 547-554.

Naumann, E. (1932) Grundzuge der regionalen Limnologie. *Der Binnengewasser* **11**, 176.

Nesje, A., Dahl, S.O., Løvlie, R. & Sulebak, J.R. (1994) Holocene glacier activity at the southwestern part of Hardangerjøkulen, central-southern Norway: evidence from lacustrine sediments. *The Holocene* **4**, 377-382.

Newberry, T.L. & Schelske, C.L. (1986) Biogenic silica record in the sediments of Little Round Lake, Ontario. *Hydrobiologia* **143**, 293-300.

Oldfield, F. (1977) Lakes and their drainage basins as units of sediment-based ecological study. *Progress in Physical Geography* **1**, 460-504.

Oldfield, F. (1991) Environmental magnetism - a personal perspective. *Quaternary Science Reviews* **10**, 73-85.

Oldfield, F. (1994) Toward the discrimination of fine-grained ferrimagnets by magnetic measurements in lake and near-shore marine environments. *Journal of Geophysical Research* **99**, 9045-9050.

Oldfield, F., Darnley, I., Yates, G., France, D.E., & Hilton, J. (1992) Storage diagenesis versus sulphide authigenesis: possible implications in environmental magnetism. *Journal of Palaeolimnology* **7**, 179-189.

Oldfield, F., Maher, B.A., Donaghue, J., Pierce, J. (1985) Particle-size related mineral magnetic source sediment linkages in the Rhode River catchment, Maryland, USA. *Journal of the Geological Society of London* **142**, 1035-1046.

Oldfield, F. & Richardson, N. (1990) Lake sediment magnetism and atmospheric deposition. *Philosophical Transactions of the Royal Society of London Series B* **327**, 325-330.

Oppenheim, D.R. (1990) A preliminary study of benthic diatoms in contrasting lake

environments. In K.R. Kerry. & G. Hempel (Eds.) *Antarctic Ecosystems. Ecological Change and Conservation*, Springer-Verlag Berlin Heidelberg, pp. 91-99.

Oppenheim, D.R. (1994) Taxonomic studies of Achnanthes (Bacillariophyta) in freshwater maritime Antarctic lakes. *Canadian Journal of Botany* **72**, 1735-1748.

Oppenheim, D.R. & Ellis-Evans, J.C. (1989) Depth-related changes in benthic diatom assemblages of a maritime antarctic lake. *Polar Biology* **9**, 525-532.

Oppenheim, D.R. & Greenwood, R. (1990) Epiphytic diatoms in two freshwater maritime Antarctic lakes. *Freshwater Biology* **24**, 303-314.

Oppenheim, D.R. & Paterson, D.M. (1990) The fine structure of an algal mat from a freshwater maritime antarctic lake. *Canadian Journal of Botany* **68**, 174-183.

Overpeck, J.T., Webb, T. & Prentice, I.C. (1985) Quantitative interpretation of fossil pollen spectra: dissimilarity coefficients and the method of modern analogs. *Quaternary Research* **23**, 87-103.

Parker, J.I., Conway, H.L. & Yaguchi, E.M. (1977) Dissolution and diatom frustules and recycling of amorphous silicon in Lake Michigan. *Journal of the Fisheries Research Board of Canada* **34**, 545-551.

Parker, J.I. & Edgington, D.N. (1976) Concentration of diatom frustules in Lake Michigan sediment cores. *Limnology and Oceanography* **21**, 887-93.

Peel, D.A. (1992) Ice core evidence from the Antarctic Peninsula region. In R.S. Bradley & P.D. Jones (Eds.) *Climate Since AD 1500*, Routledge, pp. 549-571.

Pennington, W. (1978) Responses of some British lakes to past changes in land use on their catchments. *Verhandlungen der internationalen Vereinigung für theoretische und angewandte Limnologie* **20**, 636-641.

Pennington, W., Haworth, E.Y., Bonny, A.P. & Lishman, J.P. (1972) Lake sediments in northern Scotland. *Philosophical Transactions of the Royal Society of London B* **264**, 191-294.

Perkins, J.A. & Sims, J.D. (1983) Correlation of Alaskan varve thickness with climatic parameters, and use in palaeoclimatic reconstruction. *Quaternary Research* **20**, 308-321.

Petterson, G., Renberg, I., Geladi, P., Lindberg, A. & Lindgren, F. (1993) Spatial uniformity of sediment accumulation in varved lake sediments in northern Sweden. *Journal of Palaeolimnology* **9**, 195-208.

Pienitz, R. & Smol, J.P. (1993) Diatom assemblages and their relationship to environmental variables in lakes from the boreal forest-tundra ecotone near Yellowknife, Northwest Territories, Canada. *Hydrobiologia* **269/270**, 391-404.

Pienitz, R., Smol, J.P. & Birks, H.J.B. (1995) Assessment of freshwater diatoms as quantitative indicators of past climatic changes in the Yukon and Northwest Territories, Canada. *Journal of Palaeolimnology* **13**, 21-49.

Prell, W.L. (1985) The stability of low-latitude sea-surface temperatures: an evaluation of the CLIMAP reconstruction with emphasis on the positive SST anomalies. *Technical Report TR025*, Department of Energy, Washington, 60 pp.

Priddle, J. (1985) Terrestrial habitats - inland waters. In W.N. Bonner & D.W.H. Walton (Eds.) *Key Environments - Antarctica*, Pergamon Press, pp. 118-132.

Priddle, J. & H.J. Belcher (1982) An annotated list of benthic algae (excluding diatoms) from freshwater lakes on Signy Island. *British Antarctic Survey Bulletin* **57**, 41-53.

Priddle, J. & Heywood, R.B. (1980) Evolution of Antarctic lake ecosystems. *Biological Journal of the Linnaean Society* **14**, 51-66.

Qinghong, L. & Bråkenhielm, S. (1995) A statistical approach to decompose ecological variation. *Water, Air and Soil Pollution* **85**, 1587-1592.

Ragotzkie, R.A. (1978) Heat budgets of lakes. In A. Lerman (Ed.) *Lakes: chemistry, geology, physics*, Springer-Verlag New York Heidelberg Berlin, pp. 1-18

Rawle, A. *Basic principles of particle size analysis.* MRK034/02. Unpublished Report. Malvern Instruments Limited, Malvern, Worcestershire, UK.

Rawlings, R.O. (1988) *Applied Regression Analysis: A Research Tool.* Wadsworth and Brooks/Cole Advanced Books and Software, Pacific Grove, California.

Renberg, I. (1976) Palaeolimnological investigations in Lake Prätsjön. *Early Norrland* **9**, 113-159.

Rose, N. (1985) Limnological Assistants Report, 1985-1986, Signy Island. *British Antarctic Survey*, unpublished report H/1985/N1.

Rose, N.L. (1990) A method for the selective removal of inorganic ash particles from lake sediments. *Journal of Palaeolimnology* **4**, 61-67.

Sætersdal, M. & Birks, H.J.B. (1993) Assessing the representativeness of nature reserves using multivariate analysis: vascular plants and breeding bird in deciduous forests, western Norway. *Biological Conservation* **65**, 121-132.

Sanders, M.W. (1984) Limnological Assistants Report, 1984, Signy Island. *British Antarctic Survey*, unpublished report H/1984/N1.

Schelske, C.L., Conley, D.J., Stoermer, E.F., Newberry, T.L. & Campbell, C.D. (1986) Biogenic silica and phosphorous accumulation in sediments as indices of eutrophication in the Laurentian Great Lakes. *Hydrobiologia* **143**, 79-86.

Schmidt, R., Mäusbacher, R. & Müller, J. (1990) Holocene diatom flora and stratigraphy from sediment cores of two Antarctic lakes (King George Island). *Journal of Palaeolimnology* **3**, 55-74.

Simola, H. & Tolonen, K. (1981) Diurnal laminations in the varved sediment of Lake

Lovojärvi, south Finland. *Boreas* **10**, 19-26.

Singer, J.K., Anderson, J.B., Ledbetter, M.T., McCave, I.N., Jones, K.P.N. & Wright, R. (1988) An assessment of analytical techniques for the size analysis of fine-grained sediments. *Journal of Sedimentary Petrology* **58**, 534-543.

Sly, P.G. (1983) Sedimentology and geochemistry of recent sediments off the mouth of the Niagara River, Lake Ontario. *Journal of Great Lakes Research* **9**, 134-159.

Sly, P.G. (1989) Sediment dispersion: part 1, fine sediments and significance of silt/clay ratio. *Hydrobiologia* **176/177**, 99-110.

Smith, R.I. Lewis (1972) Vegetation of the South Orkney Islands with particular reference to Signy Island. *Scientific Papers of the British Antarctic Survey No. 68*, 1-124.

Smith, R.I. Lewis (1988) Destruction of Antarctic terrestrial ecosystems by a rapidly increasing fur seal population. *Biological Conservation* **45**, 55-72.

Smith, R.I. Lewis (1990) Signy Island as a paradigm of biological and environmental change in Antarctic terrestrial ecosystems. In K.R. Kerry & G. Hempel (Eds.) *Antarctic Ecosystems - Ecological Change and Conservation*, Proceedings 5th SCAR Symposium on Antarctic Biology, Springer-Verlag, Berlin, pp. 30-48.

Smol, J.P. (1988) Palaeoclimate proxy data from freshwater arctic diatoms. IV. Palaeolimnology. *Verhandlungen der Internationalen Vereiningung von Limnologen* **23**, 837-844.

Smol, J.P. (1990) Palaeolimnology - recent advances and future challenges. In R. de Bernardi (Ed.) *Scientific Perspectives in Theoretical and Applied Limnology*, CNDR, Pallantz.

Smol, J.P., Walker, I.R. & Leavitt, P.R. (1991) Palaeolimnology and hindcasting climatic trends. *Verhandlungen der internationalen Vereiningung für theoretische und angewandte Limnologie* **24**, 1240-1246.

Smol, J.P. & Douglas, M.S.V. (1996) Long-term environmental monitoring in Arctic lakes and ponds using diatoms and other biological indicators. *Geoscience Canada* **23**, 225-230.

Smol, J.P. (1988) Palaeoclimate proxy data from freshwater arctic diatoms. IV. Palaeolimnology. *Verhandlungen der internationalen Vereinigung für theoretische und angewandte Limnologie* **23**, 837-844.

Snowball, I.F. (1993a) Mineral magnetic properties of Holocene lake sediments and soils from the Karsa Valley, Lappland, Sweden, and their relevance to palaeoenvironmental reconstruction. *Terra Nova* **5**, 258-270.

Snowball, I.F. (1993b) Geochemical control of magnetite dissolution in sub-arctic lake sediments and the implications for environmental magnetism. *Journal of Quaternary Science* **8**, 339-346.

Snowball, I.F. (1994) Bacterial magnetite and the magnetic properties of sediments in a Swedish lake. *Earth and Planetary Science Letters* **126**, 129-142.

Snowball, I.F. & Sandgren, P. (1996) Lake sediment studies of Holocene glacial activity in the Kårsa valley, northern Sweden: contrasts in interpretation. *The Holocene* **6**, 367-372.

Stober, J.C. & Thompson, R. (1979) An investigation into the source of magnetic minerals in some Finnish lake sediments. *Earth and Planetary Science Letters* **45**, 464-474.

Stone, C.J. (1977) Consistent non-parametric regression. *Annals of Statistics* **5**, 595-645.

Storey, B.C. & Meneilly, A.W. (1985) Petrogenesis of metamorphic rocks within a subduction-accretion terrane, Signy Island, South Orkney Islands. *Journal of Metamorphic Geology* **3**, 21-42.

Svensson, U. (1978) *A mathematical model of the seasonal thermocline.* Department of Resources Engineering, University of Lund, Sweden, Report No.1002.

ter Braak, C.J.F. (1987a) Ordination. In R.H.G. Jongman, C.J.F. ter Braak & O.F.R. Tongeren (Eds.) *Data analysis in community and landscape ecology.* Pudoc: Wageningen, pp.91-173.

ter Braak, C.J.F. (1987b) Calibration. In R.H.G. Jongman, C.J.F. ter Braak & O.F.R. Tongeren (Eds.) *Data analysis in community and landscape ecology.* Pudoc: Wageningen, pp.78-90.

ter Braak, C.J.F. (1987c) *CANOCO - a FORTRAN program for canonical community ordination by [partial] [detrended] [canonical] correspondence analysis, principal components analysis and redundancy analysis (version 2.1)*, Technical Report LWA-88-02. Wageningen: TNO Institute of Applied Computer Science, 95 pp.

ter Braak, C.J.F. (1990) *Update notes: CANOCO version 3.10.* Wageningen: Agricultural Mathematics Group, 35 pp.

ter Braak, C.J.F. (1994) Canonical community ordination. Part I: Basic theory and linear methods. *Ecoscience* **1**, 127-140.

ter Braak, C.J.F. (1995) Non-linear methods for multivariate calibration and their use in palaeoecology: a comparison of inverse (K-Nearest Neighbours, PLS and WA-PLS) and classical approaches. *Chenometrics and Intelligent Laboratory Systems* (in press).

ter Braak, C.J.F. & Juggins, S. (1993) Weighted-averaging partial least squares regression (WA-PLS): an improved method for reconstructing environmental variables from species assemblages. *Hydrobiologia*, **269/270**, 485-502.

ter Braak, C.J.F., Juggins, S., Birks, H.J.B., & van der Voet, H. (1993) Weighted-averaging partial least squares regression (WA-PLS): definition and comparison with other methods for species-environment calibration. In G.P. Patil & C.R. Rao (Eds.) *Multivariate Environmental Statistics*, Elsevier Science Publishers, Amsterdam, pp. 525-

560.

ter Braak, C.J.F. & Looman, C.W.N. (1986) Weighted averaging, logistic regression and the Gaussian response model. *Vegetatio* **65**, 3-11.

ter Braak, C.J.F. & Prentice, I.C. (1988) A theory of gradient analysis. *Advances in Ecological Research* **18**, 271-317.

ter Braak, C.J.F. & van Dam, H. (1989) Inferring pH from diatoms: a comparison of old and new calibration methods. *Hydrobiologia* **178**, 209-223.

ter Braak, C.J.F. & Verdenschodt (1995) Direct gradient analysis, Chapter 8. Compendium I.

Thomson, J.W. (1968) The geology of the South Orkney Islands. II. The petrology of Signy Island. *British Antarctic Survey Scientific Reports*, No. 62, British Antarctic Survey, Natural Environment Research Council, 30 pp.

Thompson, R. & Morton, D.J. (1979) Magnetic susceptibility and particle-size distribution in recent sediments of the Loch Lomond drainage basin, Scotland. *Journal of Sedimentary Petrology* **49**, 802-811.

Thompson, R. & Oldfield, F. (1986) *Environmental magnetism.* Allen & Unwin, London, 227 pp.

Thunell, R., Anderson, D., Gellar, D. & Miao, Q. (1994) Sea-surface temperature estimates for the Tropical Western Pacific during the Last Glaciation and their implications for the Pacific Warm Pool. *Quaternary Research* **42**, 255-264.

Timmis, R.J. (1986) *Glacier changes in South Georgia and their relationship to climatic trends.* Unpublished PhD Thesis, University of East Anglia, Norwich.

Trenberth, K.E. (1984) The atmospheric circulation affecting West Antarctic region in summer. In *Environment of West Antarctica: Potential CO_2-Induced Changes,* Natural Environment Research Council, National Academy Press, pp. 73-87.

Troels-Smith, J. (1955) Karakterisering af løse jordater. Characterisation of unconsolidated sediments. *Danmarks geologiske Undersogelse IV* **3**, 73 pp.

van Tongeren, O.F.R. (1987) Cluster analysis. In Jongman, R.H.G., ter Braak, C.J.F. & van Tongeren, O.F.R. (Eds.) *Data analysis in community and landscape ecology.* Pudoc: Wageningen, pp. 174-212.

Vavrus, S.J., Wynne, R.H. & Foley, J.A. (1996) Measuring the sensitivity of southern Wisconsin lake ice to climate variations and lake depth using a numerical model. *Limnology and Oceanography* **41**, 822-831.

Vyverman, W. & Sabbe, K. (1995) Diatom-temperature transfer functions based on the altitudinal zonation of diatom assemblages in Papua New Guinea: a possible tool in the reconstruction of regional palaeoclimatic changes. *Journal of Palaeolimnology* **13**, 65-77.

Wasell, A. (1993) Records of Holocene environmental changes in selected sedimentary basins on South Georgia. *Stockholm University Department of Quaternary Research*, Report 23, Paper III, 19 pp.

Wasell, A. & Håkanson, H. (1992) Diatom stratigraphy in a lake on Horseshoe Island, Antarctica: a marine-brackish freshwater transition with comments on the systematics and ecology of the most common diatoms. *Diatom Research* **7**, 157-194.

Watson, A., Davison, R.W. & French, D.D. (1994) Summer snow patches and climate in Northeast Scotland, U.K. *Arctic and Alpine Research* **26**, 141-151.

Wentworth, C.K. (1922) A scale of grade and class terms for clastic sediments. *The Journal of Geology* **30**, 377-392.

Whitehead, D.R., Charles, D.F. Jackson, S.J., Reed, S.E. & Sheehan, M.C. (1986) Late glacial and Holocene acidity changes of Adirondack (N.Y.) lakes. In J.P. Smol, R.W. Battarbee, R.B. Davis & J. Meriläinen (Eds.) *Diatoms and lake acidity*, W. Junk, Dordrecht, pp. 251-274.

Wilkinson, T.J. & Bunting, B.T. (1975) Overland transport of sediment by rill water in a periglacial environment in the Canadian high Arctic. *Geografiska Annaler* **57A**, 105-116.

Williams, T.M. (1991) Ferrimagnetic sulphide formation in recent sediments of Loch Ba, Scotland and implications for magnetostratigraphic interpretation. *Quaternary Research* **35**, 208-221.

Williams, T.M. (1992) Evidence for the dissolution of magnetite in recent Scottish peats. *Quaternary Research* **37**, 171-182.

Wilson, B.J. (1993) *A study of environmental change on Signy Island, Antarctica, using magnetic measurements on lake sediments.* Unpublished MSc. Thesis, Department of Geography, University of Liverpool.

Wold, S., Ruhe, A., Wold, H. & Dunn, W.J. (1984) The collinearity problem in linear regression. The partial least squares (PLS) approach to generalized inverses. *SIAM Journal Of Science and Statistical Computing* **5**, 735-743.

Wright, H.E. (1967) A square-rod piston sampler for lake sediments. *Journal of Sedimentary Petrology* **37**, 975-976.

Wright, H.E. (1980) Cores of soft lake sediments. *Boreas* **9**, 107-114.

Zale, R. & Karlén, W. (1989) Lake sediment cores from the Antarctic Peninsula and surrounding islands. *Geografiska Annaler* **71A**, 211-220.

Zale, R. (1994) C-14 age corrections in Antarctic lake sediments inferred from geochemistry. *Radiocarbon* **36**, 173-185.

Zolitschka, B. (1996) Recent sedimentation in a high arctic lake, northern Ellesmere Island, Canada. *Journal of Palaeolimnology* **16**, 169-186.

APPENDIX A: LABORATORY PROCEDURES

A.1. WET DENSITY

Wet density was measured using a $2cm^3$ capacity brass phial and a balance weighing to four decimal places. The clean phial was weighed empty, the balance then tared, and the phial carefully filled with wet sediment using a fine metal spatula. Any air bubbles were removed by lightly tapping the base of the phial on a firm surface as filling proceeded, and the surface of the sediment was levelled-off flush with the top of the phial with the spatula. The phial was then reweighed and the weight of the sediment was divided by two to arrive at a value in units of g/cm^3.

Replicate measurements were carried out on random samples to assess the consistency of the analysis and afterwards sediment was carefully returned to its sample bag for subsequent analyses, taking care to avoid contamination with other sediment samples. The phial was carefully washed and dried before measuring the next sample.

A.2. DRY WEIGHT

An empty crucible was weighed to 3 decimal places and its weight recorded. 1-2 grammes of wet sediment were added, taking care to keep sediment away from the rim of the crucible where it could be lost during handling. The full crucible was re-weighed and placed in an oven at 105°C for a minimum of 12 hours. After this time the crucibles were removed using tongs and immediately placed in a desiccator to cool. Once cooled the crucibles were reweighed.

The percentage weight remaining after drying can be calculated thus:

$$\frac{(A - B) \times 100\%}{C - B}$$

where
A = weight of dried residue + crucible (g)
B = crucible weight (g)
C = weight of wet sample + crucible (g)

The dried sample in the crucible was then used for loss-on-ignition analysis.

A.3 LOSS ON IGNITION

The dried sediment samples from the previous analysis in their crucibles were placed in a furnace and ignited at 550°C for a minimum of two hours. After this time, the crucibles were allowed to cool for a minute and then placed on an asbestos mat using long-handled tongs, cooling for a few minutes prior to being placed in a desiccator and allowed to cool fully before reweighing.

The percentage of the dry weight lost on ignition (proxy measure of organic matter loss) can be calculated thus:

$$\frac{(A - D) \times 100\%}{A - B}$$

where
A = weight of dried residue + crucible (g)
B = weight of crucible (g)
D = weight of ashed residue + crucible (g)

The remaining ash sample was retained in small self-sealing plastic bags for further analysis.

A.4. SEQUENTIAL EXTRACTION METHOD (Organic matter, biogenic silica, minerogenic material)

I. Laboratory procedure

(i) *Drying the sediment.* Approximately 1.0 g of wet sediment was weighed into a labelled 100 ml beaker of known weight (A). This was placed in an oven at 105°C overnight (minimum 8 hours) then removed and allowed to cool in a desiccator. A record was made of the weight of beaker plus dry sediment (B). The weight of dry sediment (C) was calculated as the weight difference (B-A).

(ii) *Removal of organic matter by oxidation with 30% hydrogen peroxide solution.* 50 ml of 30% H_2O_2 was added to the beaker and then placed on a hotplate at 50-60°C. As the reaction proceeded the beakers were topped-up with additional H_2O_2, washing down the sides of the beaker so as to ensure that all the sediment was subject to oxidation. Once the effervescence appeared to have ceased (usually after 2-4 hours, longer for samples with higher organic contents) the beaker was removed from the hotplate and allowed to cool. The sediment was carefully transferred to a labelled centrifuge tube, washing the beaker out with distilled water. The sample was centrifuged at 2000 r.p.m. for 5 minutes. After this time the supernatant was discarded and the pellet resuspended in distilled water. The sample was centrifuged two more times, rinsing with distilled water each time. Finally the rinsed sediment and supernatant was returned to the original beaker and placed in a drying oven at 105°C overnight. Following drying, the beaker was removed and allowed to cool in a desiccator. The weight of beaker plus sediment was recorded (D).

(iii) *Removal of biogenic silica by wet alkaline extraction.* 50 ml 0.3 M sodium hydroxide (NaOH) was added to the sediment in the beaker. The beaker was heated at 100°C on a hotplate (including heating-up time) for 2½ hours. Evaporative losses were replaced with small volumes of additional NaOH as necessary to prevent the sample from boiling dry. After this time, the beaker was removed from the hotplate and allowed to cool. The sediment suspension was transferred to a centrifuge tube, washing the beaker out with distilled water. The centrifuge procedure was repeated as in 2. The beaker was placed in a drying oven for the final time at 105° overnight, removed and allowed to cool in a desiccator. The weight of the beaker plus residue was recorded (E).

(iv) *Procedural control.* To ensure that all diatom valves had been destroyed by the alkaline digestion procedure a small volume of the suspension was isolated from the sample by pipette and examined under the light microscope at x.400 magnification.

II. Calculations

The organic matter, biogenic silica and clastic material contents of each sample were derived from the following measurements:

A = beaker weight (g)
B = beaker plus dry sediment (g)
C = dry sediment (g)
D = beaker plus dry sediment after peroxide digestion (g)
E = beaker plus dry sediment after wet alkaline digestion (g)

Values were often in thousandths of a gramme. For this Thesis all weights were recorded and calculations made using units of grammes. However, it may be more convenient to express constituent fractions in units of dry weight in milligrammes (mg).

(i) Organic matter as a percentage of dry weight

Weight of organic matter in sample:

$$OM\ (g.d.w.) = (D-A)-C$$

Organic matter as a percentage of dry weight of sediment:

$$\%OM\ g.d.w. = ((D-A-C)/C)*100\%$$

(ii) Biogenic silica as a percentage of dry weight

Weight of biogenic silica in sample:

$$BSi\ (g.d.w.) = (D-E-A)$$

Biogenic silica as a percentage of dry weight of sediment:

$$\%BSi\ (g.d.w.) = ((D-E-A)/C)*100\%$$

NB. A small amount of mineral silica is also lost from the sample by alkaline extraction.

(iii) Minerogenic material as a percentage of dry weight

Weight of clastic residue in sample:

$$clastic\ (g.d.w.) = (E-C)$$

Clastic material as a percentage of dry weight of sediment:

$$\%clastic\ (g.d.w.) = (E-C)/C*100\%$$

APPENDIX B - MINERAL MAGNETIC CONCEPTS AND TERMS

B.I. TYPES OF MAGNETIC BEHAVIOUR

All minerals exhibit some degree of magnetic behaviour arising from electron and orbital spins within the atom. By measuring the strength and direction of magnetization of samples when exposed to known magnetic field strengths and the subsequent remanence once relaxed, it is possible to identify minerals and their magnetic granulometry. There are four typical types of magnetic behaviour, described below.

(i) Ferrimagnetism

Ferrimagnetic minerals, typically oxides of iron such as magnetite (Fe_3O_4) and maghemite (γFe_2O_3), acquire a strong positive magnetic moment when a magnetic field is applied and retain at least part of this moment when removed from the field, i.e. they acquire a magnetic 'remanence'. Natural ferrimagnets are often termed 'magnetites' although they can exist with various degrees of impurity, which hampers exact mineralogical identification. Due to the strength of their response, even low concentrations of ferrimagnets may dominate a mixed assemblage of magnetic minerals.

(ii) 'Imperfect' (Canted) Anti-ferromagnetism

Haematite ($\propto Fe_2O_3$) and goethite ($\propto$ FeOOH) have a rhombohedral structure which gives rise to a different form of magnetic behaviour to ferrimagnets. The in-field magnetic moment and magnetic remanence are weaker than those of ferrimagnets but it is also retained once removed from the field. This net magnetization arises from irregularities in the crystal lattice where the two atomic sub-lattices are not exactly antiparallel in alignment.

(iii) Paramagnetism

These minerals, which include most other iron minerals, acquire an alignment in the same polarity as the field direction. This paramagnetic moment is relatively weak and it is lost when the magnetic field is removed. Paramagnetic behaviour can be significant in special circumstances but tends to be masked by the other 'stronger' forms of magnetic behaviour (above).

(iv) Diamagnetism

Diamagnetic minerals acquire alignment opposite to the applied field. This moment is very weak and is lost when removed from the field. Hence, diamagnetism is usually obscured by all the other forms of magnetic behaviour. Diamagnetic effects may be introduced by carbon, silica, calcium carbonate and plastics used in core tubes, sample holders and packing.

B.2. MAGNETIC GRAIN-SIZE

Measurements of magnetic properties can give more information than mere mineralogy because magnetic behaviour in antiferro- and ferrimagnetic minerals is also strongly dependent on variations in magnetic grain-size. Magnetic grain behaviour is not directly related to a sample's particle-size and it is important to make the distinction between the two. Coarse mineral particles or aggregates can be characterised by fine magnetic grains and their magnetic parameters will reflect the size of these, not the size of the particle. Mineral magnetic grain sizes are normally termed 'domains'.

In a large crystal there are many domains (Multi-Domain, MD, grains). They may be seen as invisible compartments separated by domain walls. The direction in which the domains become aligned is a reflection of their adjustment both to the external magnetic field and to each other to achieve the most energetically economical state. When a sample is placed in a saturating magnetic field (SIRM) the domains will become aligned in the field direction. Once removed the domains relax and the sample will lose its total magnetic moment and retain an IRM. MD grains display a roughly linear decline in remanent magnetization with the log of time, a loss known as 'viscous loss' of remanence.

As the grain-size decreases it passes a point where it is energetically advantageous for grains to divide into separate domains and each grain forms its own magnetic domain, known as stable single domain (SSD) grains. They display a maximum loss of total magnetic moment on removal from an applied magnetic field and do not exhibit any significant viscous loss of remanence.

Intermediate between MD and SSD grains are pseudo single domain (PSD) grains of poorly defined size range which behave like SSD grains but display some viscous loss like MD grains. Smaller still are superparamagnetic (SP) grains. They are too small to retain a magnetisation once removed from the applied field due to losses through thermal randomisation. However, they also have a unique characteristic: if they are magnetized in a high-frequency field some SP grains behave like SSD grains, with lower magnetic susceptibility. Between SSD and PSD grains there is a narrow range called the fine 'viscous' (FV) grains. Their response to changes in magnetic fields is delayed and they show some viscous loss of remanence like MD grains.

It is only possible to discriminate between magnetic grain-sizes of ferrimagnetic minerals. This is because most anti-ferromagnetic minerals found in natural samples are of SSD size (the MD/SSD boundary for haematite is at about 100 μm) and methods to isolate them through high-field magnetization are time-consuming and less readily available.

B.3. MAGNETIC PROPERTIES AND THEIR INTERPRETATION

(i) Magnetic susceptibility (κ)

As a magnetic field is applied to a sample there is an apparent hysteresis curve: as the field strength increases so the magnetization of the sample will correspondingly increase. The initial low-field (0.1mT) magnetization is reversible and on removal of the field the net magnetization is zero. With no induced remanence further magnetic measurements can be undertaken on the samples without repacking. The ratio of magnetisation induced to intensity of the magnetising field, known as susceptibility (κ), strongly reflects changes in the concentration of ferrimagnetic minerals (e.g. magnetite and maghemite). The magnetic susceptibility of ferrimagnets is a factor of 100-100 times that of anti-ferrous magnetic minerals, i.e. the concentration of the anti-ferromagnetic magnetite may be <1% of that of haematite for the two to contribute equally to the susceptibility.

κ is also very sensitive to changes in magnetic grain-size. At low temperature susceptibility measurements are broadly discernible but are hard to quantify (Oldfield, 1991). The susceptibility of SP grains is much greater than that of an equivalent amount of mineralogically similar SSD and small MD grains.

κ is the parameter least dependent on grain-size or shape and the least sensitive to

canted antiferromagnetic components. Therefore it is commonly used to normalize other parameters in respect of the concentration of magnetic minerals (e.g. SIRM/κ, see below).

κ is measured using a dual-frequency Bartington Instruments Susceptibility Meter and Single Sample Sensor. The procedure is as follows. The equipment is turned on and left to equilibriate with background noise for 5-10 minutes until minimal drift is attained between readings. Before sample insertion, the value on the meter is noted (A) and then inserted. The first reading after this is ignored, as the sample has just crossed the coils and the meter is measuring part sample, part air. The next two readings are noted (B and C). These should be similar. The sample is then removed, the next reading ignored and the subsequent reading (D) taken. D becomes value A for the next sample and the procedure is repeated. The overall reading for each sample is calculated as:

$$((B+C)-(A+D))/2$$

The same sample alignment is assumed and each sample measured approximately 3-5 times to increase the signal-to-noise ratio (necessary for weak samples).

Raw meter output is in 10^{-10}m3 units of total susceptibility. This is divided by sample mass (g) and multiplied by 10 to yield units of $10^{-8}m^3kg^{-1}$. Volume specific susceptibility measurements are dimensionless. To calculate these, raw meter units (10^{-10} m^3) are divided by the sample volume in cm^3 (standard styrene pots are 10cc by volume) to give 10^{-4} SI units, then multiplied by 100 to give 10^{-6} SI units.

(ii) Frequency dependent susceptibility (X_{FD})

This is the variation of κ between the two frequencies - high (4.7 kHz) and low (0.47 kHz). It gives an indication of the presence of FV grains in the sample. Significant frequency dependent susceptibility values (κfd) values denote the presence of fine 'viscous' ferrimagnetic grains close to the SP/SSD transition. In roughly isodiametric crystals this implies a diameter around 0.015-0.025 μm (Oldfield, 1991). By expressing κ as a proportion of κ (often shown as a percentage for convenience, i.e. κ%) the relative contribution of fine grain viscous grains to the total ferrimagnetic assemblage can be identified. Many contemporary and fossil soils, especially under temperate conditions of pedogenesis, have κfd% values between 8% and 15%, as do the dusts and sediments derived from them and materials affected by high temperatures, such as anthropogenic particulates from industry and fossil fuel combustion. Fine-viscous grained ferrimagnets are rare in most unweathered parent materials and rudimentary soils, giving low values for κfd and κfd%.

κfd is calculated as κlf-κhf/sample mass. Units are $10^{-8}m^3kg^{-1}$.
κfd% is (κlf-κhf/κlf)*100 and is expressed in percentage units.

(iii) Anhysteretic remanent magnetization (ARM)

ARMs are grown by subjecting a sample to a slowly decaying 100 mT peak alternating field (i.e. 0 mT→100 mT→0 mT) in the presence of a constant external DC field of 0.04 mT parallel to the axis of the generating coil. This DC field is roughly equal to the earth's present magnetic field. The sample is held stationary within the generating coil and instead of being demagnetized the sample acquires a remanence which is approximately proportional to the strength of the steady field.

ARM is sensitive to both the concentration and grain size variations of ferrimagnetic

minerals present in a sample (magnetite and maghemite). It is highly selective of true stable single domain ferrimagnetic grains, around 0.02-0.1 μm (Maher, 1988) provided ARM values are high relative to both low field and high field isothermal remanence (Maher, 1988).

Raw values for ARM are in $10^{-8}Am^2$. These are divided by the sample mass (g) to give units of $10^{-5}Am^2kg^{-1}$ mass intensity. For κ_{ARM}, raw ARM in $10^{-8}Am^2$ units is divided by mass to give units of $10^{-5}Am^2kg^{-1}$ and then divided by the biasing field strength (usually $0.4*79.6=31.84Am^{-1}$), then multiplied by 1000 to give $10^{-8}m^3kg^{-1}$ units.

(iv) Isothermal Remanent Magnetization (IRM), Saturation Isothermal Remanent Magnetization (SIRM)

Samples are magnetized in stages, typically at 20mT, 40mT, 100mT, up to the maximum forward field available (1T), known as the SIRM. When the sample is removed from the field at each stage of the magnetization sequence the induced magnetization does not return to zero but relaxes to an Isothermal Remanent Magnetization instead. This is measured using a magnetometer and the results may be plotted on an IRM acquisition curve. Further increases in the applied field take magnetization beyond the point at which magnetization is reversible, and magnetization increases non-linearly and the process is non-reversible. Finally, a point is reached where increasing field strengths produce no further magnetization. This point is Saturation Magnetization, the largest magnetization an assemblage can possess. Removal of the applied field to zero sees this magnetization relax to Saturation Isothermal Remanent Magnetization, the highest level of remanence that can be induced in a sample. This is fixed and cannot be reversed naturally. It is an expression of the combined effect of all the remanence carrying materials (Oldfield, 1991) and also responds to grain size variations. Unlike susceptibility, SIRM is a remanence and is not affected by diamagnetic or paramagnetic components of the mineral assemblage. Generally, IRM acquisition over 300mT is due to haematite constituents only.

All remanence-carrying magnetic grains will make some contribution to SIRM, though the ferrimagnetic component will dominate even in relatively low concentrations. SIRM is also grain size dependent, with coarser multidomain grains having lower values for a given concentration than stable single domain grains. The SIRM can be gradually demagnetized by subjecting the sample to a series of increasingly reverse (negative) magnetic fields. The relative ease or difficulty with which the initial magnetization can be reduced and then reversed is an indication of magnetic mineralogy and grain size. There are two characteristic types of response to demagnetization: 'hard' or 'soft', discussed below.

Raw SIRM and IRM values in $10^{-8}Am^2$ are divided by mass (g) to give units of $10^{-5}Am^2kg^{-1}$ mass intensity.

(v) ±IRM/SIRM

By plotting measurements which denote the ease or difficulty with which the SIRM can be reduced and finally reversed, by increasingly high opposed DC fields, it is possible to explore, in relative terms, the probable grain size and mineralogical component responsible for the SIRM.

The remanence at each stage of demagnetization is the reverse field-ratio, known as the S-ratio. Raw units of $10^{-8}Am^2$ are divided by sample mass (g) yielding units of $10^{-5}Am^2kg^{-1}$ mass intensity.

The remanence at each stage of demagnetization, normalised by the SIRM, is the reverse field-ratio, also known as the S-ratio. It is calculated for example, for -20mT as:

$$-20mT = ((IRM_{-20mT}*-1)/SIRM+1)/2)*100$$

and is expressed in percentage units.

(vi) 'Soft' remanence (SIRM - IRM_{-20mT})
The Soft Isothermal Remanence is that part of the original SIRM which can be demagnetized in the lowest reverse field used (-20mT). Soft behaviour indicates the presence of ferrimagnetic minerals with a high proportion of coarse MD grains. It may be expressed in mass specific (SOFT) or percentage terms (SOFT%).

SOFT is calculated as:

$$SOFT = (SIRM-IRM_{-20mT})/2$$

This value is divided by sample mass (g) to give units of $10^{-5}Am^2kg^{-1}$ mass intensity.

SOFT% is calculated as:

$$SOFT\% = ((SIRM-IRM_{-20mT})/2)/SIRM)*100\%$$

Percentage units. Note that SOFT% is the same as -20mT%.

(vii) 'Hard' remanence (SIRM + IRM_{-300mT})
That part of the original SIRM, which requires fields in excess of -300mT to be demagnetized, is termed the 'Hard' Isothermal Remanence. Such samples are relatively resistant to demagnetization in low reverse field strengths. Hard behaviour is related exclusively to the imperfect anti-ferromagnetic component and it can be seen as a rough guide to the concentration of haematite in a sample. It may be expressed as a mass-specific value (HARD) or percentage (HARD%).

For HIRM or HARD, the value is calculated thus:

$$HARD = (SIRM+IRM_{-300mT})/2$$

This value divided by sample mass gives units of $10^{-5}Am^2kg^{-1}$ mass intensity.

For HARD%, the value is:

$$HARD\% = ((SIRM+IRM_{-300mT})/2)/SIRM)*100\%$$

Percentage units.

(viii) SIRM/κ
This quotient is affected by many factors. It can be diagnostic of mineralogy and if samples are of similar mineralogies and concentrations, it can be used to identify the dominant magnetic grain-size. Contributions to κ from paramagnetic, superparamagnetic and multidomain grains will tend to reduce the value of the ratio. Contributions to SIRM from stable single domain or anti-ferromagnetic grains will tend to increase it. A low,

theoretically zero, ratio, indicates the dominance of paramagnetic minerals. By combining this with other quotients it is possible to decipher what the SIRM/κ variations are responding to. High values indicate either AF contributions or greigite. In the case of AF contributions, high values will be accompanied by a relatively high contribution to SIRM from the 'hard' remanence component, which fails to saturate in fields greater than 300 mT. Greigite, on the other hand, is not so hard and will saturate at this field strength.

SIRM $10^{-5}Am^2kg_{-1}$/Xlf $10^{-8}Am^2kg^{-1}$ results in a quotient with units of 10^3Am^{-1}.

(ix) κ_{ARM}/κ

κ_{ARM} is especially responsive to the presence of fine SSD magnetite/maghemite grains around 0.02-0.04 μm in diameter (Maher, 1988). Normalizing by κlf removes the effects of concentration, allowing diagnostics of the grain-size and/or shape.

The quotient κ_{ARM} $10^{-8}Am^2kg^{-1}$/Xlf $10^{-8}Am^2kg^{-1}$ yields a dimensionless value.

(x) SIRM/ARM

ARM is highly sensitive to fine grains so in samples with remanence characteristics dominated by ferrimagnets, this quotient is a good indicator or relative magnetic grain size variations. High ratios (>100) indicate multidomain grains; low values (<30) to dominance by stable single domain grains or the presence of grains slightly larger than SP grain sizes. The ratio declines as ARM/κ increases.

SIRM $10^{-5}Am^2kg^{-1}$/ARM $10^{-5}Am^2kg^{-1}$ yields a dimensionless value.

(xi) κ_{ARM}/SIRM

This quotient is dependent on magnetic grain size independent of paramagnetic and superparamagnetic contributions. It is only useful if the anti-ferrimagnetic contribution to SIRM is small. Under these circumstances the expressions of synthetic magnetite, summarized in Maher (1988), may be used as a guide to grain size interpretation. Bacterially-produced magnetite in the form of magnetosomes has extremely high κ_{ARM}/SIRM values, far higher than the range produced by abiotically produced synthetic materials. Presumably this reflects the biotically controlled production of magnetosomes within a narrowly-defined SSD range.

The quotient κ_{ARM} $10^{-8}Am^2kg^{-1}$/SIRM $10^{-5}Am^2kg^{-1}$ results in units of 10^3Am^{-1}.

APPENDIX C.1. SURFACE-SEDIMENT LITHOLOGY AND PARTICLE-SIZE DATA

Sample	WD	% DW	% LOI	% OM	% BSi	% Min	Median	Mean	Std	Skew
SOMB11	1.085542	23.14	9.67	9.094992	2.110936	90.90501	30.0	33.96	25.85	1.66
SOMB12	1.221285	41.4	6.11	5.707196	2.977667	94.2928	25.8	31.39	25.38	1.76
SOMB13	1.577108	23.68	14.51	12.15915	10.87924	87.84085	28.99	35.05	28.58	1.68
SOMB14	1.089157	27.11	11.09	11.02706	8.670352	88.97294	28.31	32.71	25.27	1.74
SOMB15	1.263855	10.57	11.61	5.251837	4.032981	94.74816	29.64	33.63	25.36	1.72
SOMB16	1.057028	23.54	12.79	12.85673	9.599308	87.14327	26.39	30.62	22.89	1.86
SOMB17	1.069478	19.99	10.29	7.922149	7.45614	92.07785	26.61	31.44	24.92	1.75
SOMB18	1.046185	14.21	20.32	6.108561	2.816901	93.89144	25.34	29.51	21.95	1.39
SOMB19	1.037349	13.31	13.8	13.39198	7.2663	86.60802	22.86	28.53	23.72	1.79
SOMB20	1.083936	21.09	13.92	7.7784	8.114158	92.2216	28.74	32.8	24.61	1.56
SOMB21	1.133333	28.05	8.62	9.824358	8.241652	90.17564	34.65	42.01	35.1	1.48
SOMB22	1.017269	10.96	7.73	14.18605	5.523256	85.81395	18.75	28.15	27.77	2.2
SOMB23	1.082731	17.18	4.73	8.799245	5.708894	91.20075	20.86	30.36	27.35	1.54
SOMB24	1.012048	8.83	8.84	9.615385	2.129121	90.38462	19.67	29.68	28.87	2
SOMB25	1.013253	7.46	16.39	12.82923	8.105353	87.17077	22.56	30.39	27.5	1.95
SOMB26	1.077108	19.13	4.32	1.912923	1.965652	98.08708	38.05	45.1	35.45	1.13
SOMB27	1.386747	45.79	1.82	1.926087	0.496835	98.07391	39.88	50.32	44.16	2.01
SOMB28	1.016064	11.21	17.21	7.317073	6.576655	92.68293	20.82	29.49	26.95	1.88
SOMB29	1.024096	12.06	11.24	6.640106	4.548473	93.35989	26.58	38.17	35.99	1.65
SOMB30	1.019277	5.95	1.2	13.92993	9.455466	86.07007	24.34	32.78	29.72	1.88
SOMB31	1.129317	29.94	7.38	5.403557	2.51368	94.59644	26.85	40.27	48.72	4.21

Sample	WD	% DW	% LOI	% OM	% BSi	% Min	Median	Mean	Std	Skew
SOMB32	1.019679	18.45	19.8	13.98096	8.697079	86.01904	20.91	31.21	29.96	1.98
SOMB33	1.005622	14.88	17.18	17.18321	14.59396	82.81679	22.15	30.91	27.93	1.86
SOMB34	1.039357	16.49	10.97	7.724838	8.232309	92.27516	21.71	30.37	27.47	1.86
SOMB35	1.06747	23	10.69	9.614422	5.282924	90.38558	21.62	29.7	25.31	1.31
SOMB36	1.050201	18.88	7.49	7.195888	6.910337	92.80411	23.21	32.25	28.53	1.61
SOMB37	1.361044	55.83	1.9	3.91219	1.434879	96.08781	34.87	41.92	33.52	1.25
SOMB38	1.038153	11.17	12.8	7.43721	7.26652	92.56279	22.85	33.27	31.38	1.8
SOMB39	1.05502	16.87	9.41	12.4632	8.734053	87.5368	24.71	35.79	32.66	1.35
SOMB40	1.123695	33.37	7.35	6.152692	3.995498	93.84731	34.63	46.62	43.74	2.03
SOMB41	1.264659	37.13	3.61	2.4053	2.822987	97.5947	48.7	61.65	57.49	2.28
SOMB42	1.0492	13.375	8.84	8.152174	9.730849	91.84783	17.74	26.56	26.04	2.24
SOMB43	1.12952	22.065	5.075	4.075568	2.801953	95.92443	22.99	34.93	34.2	2.37
SOMB44	1.070683	21.3	9.97	9.994138	9.290739	90.00586	25.65	34.38	30.56	1.93
SOMB45	1.016064	13.95	13.54	9.487613	9.206081	90.51239	23.38	31.91	28.73	1.83
SOMB46	1.04257	10.62	7.17	6.499702	7.215265	93.5003	26.4	35.14	31.61	1.74
HEY5	1.031325	13.63	10.45	16.90687	7.261641	83.09313	46.04	77.69	83.95	2.07
HEY6	1.1	52.25	2.95	18.22086	4.141104	81.77914	43.08	67.59	70.69	2.08
HEY7	1.017269	12.31	28.76	21.51815	9.966997	78.48185	22.11	31.11	30.69	2.06
HEY8	1.074699	14.29	23.75	23.79434	13.35193	76.20566	22.66	33.33	32.36	1.65
HEY9	1.018072	12.11	25.44	20.94415	13.96277	79.05585	25.23	34.98	33.12	2.35
HEY10	1.112048	24.03	12.49	12.84732	4.401651	87.15268	31.75	47.63	53.42	2.81
HEY11	1.038554	4.87	22.6	23.88393	11.65179	76.11607	19.71	29.3	29.2	1.88
HEY12	1.318474	33.05	7.16	5.832842	3.131172	94.16716	69.02	104.7	105.62	1.83
HEY13	1.025301	6.5	25.57	26.88889	11.61111	73.11111	22.52	32.03	31.07	1.92

Sample	WD	% DW	% LOI	% OM	% BSi	% Min	Median	Mean	Std	Skew
HEY14	1.332892	41.03	7.69	5.548805	9.315512	94.45119	38.73	56.89	66.88	3.6
HEY15	1.1551	28.56	15.58	14.67734	4.269772	85.32266	32.46	55.77	65.36	2.25
HEY16	1.054779	12.47	25.5	23.76874	11.23212	76.23126	20.39	41.02	68.6	4.37
CHAN2	1.061446	11.16	11.33	5.721224	6.868379	94.27878	25.17	30.7	24.9	2.26
CHAN3	1.033333	11.05	23.3	11.25979	9.221027	88.74021	23.01	27.96	22.53	1.94
CHAN4	0.993173	7.65	23.21	21.04008	14.36069	78.95992	22.29	27.8	22.79	1.96
CHAN5	1.011245	5.45	16.89	11.57727	16.83484	88.42273	22.32	27.07	21.76	1.93
CHAN6	0.992369	5.63	28.26	15.78427	28.72556	84.21573	19.12	23.59	18.11	1.29
CHAN7	1.018072	4.59	21.02	8.506494	8.993506	91.49351	22.59	27.62	22.22	1.9
CHAN8	1.028112	11.52	30.23	15.88465	15.20039	84.11535	23.66	29.52	24.42	1.98
CHAN9	1.011245	9.65	18.91	13.46989	10.52142	86.53011	23.82	28.77	21.61	1.47
CHAN10	1.083534	4.12	16.2	5.322842	3.587133	94.67716	24.76	28.9	22.13	1.96
CHAN11	1.017269	8.96	33.43	17.04427	11.43255	82.95573	20.92	29.25	27.2	2.08
CHAN12	1.019679	11.42	29.05	6.138807	6.021505	93.86119	26.3	31.71	26.42	1.92
CHAN13	1.602811	67.8	2.84	0.685901	0.816549	99.3141	51.7	64.95	57.1	2.61
CHAN14	1.614056	61.4	3.23	1.850793	1.337455	98.14921	54.47	69.89	62.63	2.23
MOSS3	1.022088	17.95	21.26	8.096109	6.00679	91.90389	12.24	16.01	12.41	1.37
MOSS4	1.051807	7.7	26.14	15.83072	7.335423	84.16928	23.58	28.64	22.93	1.99
MOSS5	1.05502	8.74	41.53	9.633911	12.04239	90.36609	26.89	31.21	23.48	1.92
MOSS6	1.060241	9.52	28.88	6.814044	7.048114	93.18596	21.4	26.21	19.76	1.35
MOSS7	1.042972	20.15	14.6	13.0884	11.5576	86.9116	20.65	26.18	21.39	1.88
MOSS8	1.107229	8.72	15.77	10.65302	3.821848	89.34698	22.53	27.79	22.46	1.85
MOSS9	1.202811	25.98	6.61	4.17324	3.314267	95.82676	30.3	39.05	33.44	1.63
MOSS10	1.153012	22.2	5.96	5.709877	1.099537	94.29012	25.89	33.74	29.7	1.85

MOSS11	0.984739	3.13	21.41	15.58074	19.12181	84.41926	17.65	23.44	19.75	1.49
MOSS12	0.983534	2.88	24.39	81.80301	9.51586	18.19699	18.15	24.68	21.27	1.45
MOSS13	0.98755	3.67	34.79	32.49097	20.57762	67.50903	17.4	24.29	21.42	1.38
MOSS14	0.979518	4.86	16.28	10.90674	8.87383	89.09326	24.94	31.56	26.05	1.82
MOSS15	1.010442	6.4	14.41	2.965378	2.012106	97.03462	13.2	18.49	16.35	2
MOSS16	0.996386	3.27	38.42	27.63155	39.18473	72.36845	15.64	26.88	29.65	2.25
MOSS17	0.980723	1.13	15.15	26.31579	22.63158	73.68421	16.06	22.64	20.57	1.79
MOSS18	1.0249	7.04	12.42	10.25537	10.70126	89.74463	20.25	27.05	23.96	2.14
MOSS19	0.986345	3.33	33.91	17.15564	1.243163	82.84436	16.8	22.52	19.34	1.57
MOSS20	0.985542	3.13	29.36	8.069793	24.20938	91.93021	17.59	22.83	18.95	1.72
MOSS21	1.196185	28.235	7.39	3.245973	3.823034	96.75403	14.39	18.9	14.96	1.54
KNOB1	1.158635	39.03	7.82	10.9001	5.729333	89.0999	25.72	41.71	56.51	4.14
KNOB2	1.035743	18.16	19.58	21.50198	13.12253	78.49802	16.55	25.83	26.76	2.2
KNOB3	1.333735	33.73	8.48	12.24963	7.843137	87.75037	29.74	40.94	40.85	2.42
KNOB4	1.102008	25.18	13.43	17.5134	10.36508	82.4866	23.9	30.64	26.32	1.91
KNOB5	1.153012	21.94	12.81	15.88207	6.79981	84.11793	33.82	48.84	49.38	2.07
KNOB6	1.069478	18.33	23.9	21.04108	8.247099	78.95892	23.77	32.27	29.66	1.9
KNOB7	1.126506	29.28	13.51	15.84026	8.174752	84.15974	30.03	39.27	34.4	1.35
KNOB8	1.120482	24.53	12.44	16.85215	6.597774	83.14785	32.21	42.34	39.79	2.55
KNOB9	1.610442	68.61	2.43	2.727827	2.849741	97.27217	27.09	36.85	34.01	1.96
KNOB10	1.062651	23.87	20.39	19.83881	10.44637	80.16119	32.66	42.02	37.94	2.32
KNOB11	1.291165	46.25	6.35	7.Mw311-2	6.56474	92.12689	35.61	52.54	65.14	3.74
Sample	**WD**	**DW**	**% LOI**	**% OM**	**% BSi**	**% Min**	**Median**	**Mean**	**Std**	**Skew**
PUMP1	1.047791	8.18	21.29	7.781483	5.907575	92.21852	29.96	42.3	44.3	2.87

PUMP2	1.181526	21.53	5.1	19.58142	9.059633	80.41858	40.29	98.34	131.09	1.84
PUMP3	1.079116	19.7	14.13	13.3391	7.605877	86.6609	27.37	40.93	49.04	3.52
PUMP4	0.997992	11.37	57.87	29.25089	16.11177	70.74911	21.25	27.98	25.17	1.94
PUMP5	1.05261	15.25	20.84	18.72421	9.711203	81.27579	28.52	34.59	28.46	1.83
PUMP6	1.01004	17.11	26.3	30.03319	15.76327	69.96681	24.16	32.16	29.32	1.97
PUMP7	1.04498	31.79	7.25	15.98078	8.801442	84.01922	35.99	44.25	34.36	1.23
LITE2	1.003614	3.51	34.33	55.33263	31.57339	44.66737	24.96	30.13	22.82	1.37
LITE3	0.998795	3.8	66.93	48.98551	27.43961	51.01449	20.66	24.48	18.45	1.55
LITE4	1.002008	3.44	53.12	47.75785	31.27803	52.24215	20.44	25.36	20.1	1.69
LITE5	0.98755	3.45	42.02	52.38612	34.27332	47.61388	17.28	24.27	21.07	1.78
SPIR2	1.118072	23.65	12.55	5.853659	3.830172	94.14634	28.03	34.95	31.73	4.46
SPIR3	1.159438	36.84	7.84	8.435852	6.414763	91.56415	32.5	37.12	28.25	3.25
SPIR4	1.144578	35.98	6.02	7.406733	6.951774	92.59327	36.5	46.45	41.7	3.09
SPIR5	1.04739	21.85	18.09	6.260784	8.084792	93.73922	28.59	33.53	25.72	3.54
TRAN4	1.145382	38.98	5.79	8.753085	7.751488	91.24692	34.18	38.68	30.33	1.62
TRAN5	1.166265	43.76	4.82	4.965815	10.43541	95.03418	33.92	40.48	34.29	3.04
TRAN6	1.076305	21.1	8.45	10.2381	8.639456	89.7619	29.59	34.8	27.4	1.69
TRAN7	1.087952	31.53	6.25	7.529195	9.680393	92.47081	20.47	26.98	22.6	1.88
TRAN8	1.104819	28	9.25	10.05573	10.87957	89.94427	21.37	28.29	24.07	1.87
TRAN9	1.093976	30.26	11.6	14.78914	14.44252	85.21086	21.91	29.05	25.6	2.08
TRAN10	1.034137	28.33	14.49	15.55177	14.14572	84.44823	23.03	28.09	21.43	1.59
TRAN11	1.028514	16.42	23	26.82783	13.20755	73.17217	22.55	28.27	22.77	1.84
TRAN12	1.226908	31.41	3.92	4.814682	4.00429	95.18532	34.55	43.91	40.26	3.07
TRAN13	1.184739	27.21	4.72	6.603261	8.831522	93.39674	32.66	41.99	39.23	3.35
TRAN14	1.136145	23.03	5.68	9.604044	7.898062	90.39596	29.67	35.83	29.45	2.69

TRAN15	1.116466	19.78	5.56	11.46341	7.5	88.53659	28.47	35.95	30.89	2.42
TRAN16	1.072691	15.72	6.52	21.71408	8.210299	78.28592	23.72	32.13	28.3	1.64
TRAN17	1.289157	38.54	3.63	4.781913	2.861144	95.21809	39.43	49.51	42.25	2.2
TRAN18	1.24739	35.78	3.57	2.678886	5.375397	97.32111	42.23	48.59	34.28	0.94
TRAN19	1.160241	24.66	4.56	4.747453	7.630609	95.25255	33.37	41.07	35.3	3.29
TRAN20	1.31245	40.03	4.19	3.335001	5.019176	96.665	44.28	63.41	63.34	2.68
TRAN21	1.156225	24.92	6.3	6.833542	7.659574	93.16646	34.74	43.51	38.06	2.22
TRAN22	1.158635	26.6	4.5	7.814302	12.11073	92.1857	30.7	36.91	29.63	1.81
TRAN23	1.078715	16.34	6.81	9.163229	6.511491	90.83677	28.52	36.03	30.88	1.78
TRAN24	1.10241	20.43	7.3	10.14117	8.038029	89.85883	26.55	32.55	26.87	1.93
TRAN25	1.075502	16.13	9.4	9.350649	13.65079	90.64935	23.01	28.7	23.54	2.09
Sample	**WD**	**% DW**	**% LOI**	**% OM**	**% BSi**	**% Min**	**Median**	**Mean**	**Std**	**Skew**
TRAN26	1.04739	11.39	9.42	16.72255	12.65717	83.27745	22.65	29.27	25.11	1.99
TRAN27	1.060241	13.03	13.26	16.22458	11.7153	83.77542	19.89	26.67	23.73	2.17
TRAN28	1.007631	4.5	25.43	19.28306	19.97457	80.71694	18.89	24.22	19.71	1.66
TRAN29	1.06988	14.745	8.495	10.95924	8.982182	89.04076	22.53	29.39	26.03	2.06
TRAN30	1.15161	52.51	5.355	5.156997	5.260969	94.843	34.39	41.99	33.13	1.31
AMOS3	1.00843	24.2	27.4	28.69621	9.672578	71.30379	24.02	35.41	36.39	3.26
AMOS4	1.045783	24.53	27.24	19.15199	7.905138	80.84801	34.07	57.27	71.39	2.9
AMOS5	1.134137	13.85	15.25	14.32725	11.36664	85.67275	36.03	47.68	48.72	3.97
AMOS6	1.13092	24.2	12.08	14.05602	10.65871	85.94398	43.42	72.54	86.52	2.76
AMOS7	1.392369	40.48	5.49	7.210697	4.323919	92.7893	50.31	78.93	90.53	2.64
TIOG1	1.00402	8.62	51.11	52.50737	46.60767	47.49263	19.64	24.74	20	1.74
TIOG2	1.01205	7.67	58.26	59.89305	23.12834	40.10695	20.34	28.73	24.73	1.39
TIOG3	1.00321	10.49	50.45	46.73077	24.71154	53.26923	21.43	28.01	22.73	1.3

TIOG4	1.007229	9.22	59.89	52.33711	21.67139	47.66289	23.2	30.81	25.34	1.2
EMER1	1.238554	40.81	5.71	7.9025	5.511567	92.0975	15.86	22.89	20	1.44
EMER2	1.271084	43.31	3.47	8.34121	2.835539	91.65879	17.28	24.25	20.77	1.42
EMER3	1.31044	46.13	3.66	9.863346	3.658805	90.13665	16.34	24.54	23.36	2.01
EMER4	1.2245	36.2	4.13	6.80999	5.741504	93.19001	19.61	30	31.11	2.14
EMER5	1.259438	19.68	8.74	7.606166	5.831879	92.39383	14.07	21.14	19.49	1.46
EMER6	1.24498	38.9	3.6	8.4246	5.543387	91.5754	16.16	25.17	24.76	2.1
EMER7	1.22249	43.14	4.12	8.077617	4.407341	91.92238	15.87	22.19	18.68	1.23
EMER8	1.387149	48.85	5.28	9.337045	3.327429	90.66296	14.96	22.59	21.11	1.77
EMER9	1.330522	47.37	2.61	6.657323	3.060033	93.34268	13.33	20.42	19.46	1.71
EMER10	1.240964	40.59	3.5	10.95838	2.37667	89.04162	13.04	18.96	17.47	1.84
EMER11	1.343373	44.18	2.82	10.74963	2.013423	89.25037	15.56	22.79	20.93	1.94
EMER12	1.284739	48.2	2.78	5.676993	3.113697	94.32301	14.9	22.45	21.36	1.6
EMER13	1.24257	33.22	3.78	4.035226	0.814932	95.96477	25.44	33.98	31.62	1.88
EMER14	1.253815	38.63	4.66	8.779715	3.343899	91.22029	17.51	25.68	25.2	1.88
EMER15	1.379116	39.28	2.71	7.589548	3.537874	92.41045	18.19	26.3	25.26	1.83
EMER16	1.331125	40.945	3.21	9.74383	1.567435	90.25617	14.03	20.91	20.31	2.01
EMER17	1.32	39.1	3.2	12.50997	2.210322	87.49003	13.35	20.14	20.34	2.4
EMER18	1.29	40.1	3.05	10.93243	2.459459	89.06757	12.2	18.98	20.14	2.68
EMER19	1.313655	38.63	4.13	6.491633	1.788806	93.50837	19.57	28.97	29.75	2.2
EMER20	1.406426	44.87	3.23	3.927752	5.002867	96.07225	18.48	31.1	33.95	1.87
EMER21	1.410442	43.3	1.94	9.633258	0	90.36674	15.59	24.26	25.26	2.19
EMER22	1.239759	34.7	4.12	9.380836	4.209165	90.61916	13.55	19.99	19.14	2
EMER23	1.280723	38.37	3.22	4.811683	6.471945	95.18832	13.54	19.98	19.57	2.27
Sample	**WD**	**% DW**	**% LOI**	**% OM**	**% BSi**	**% Min**	**Median**	**Mean**	**Std**	**Skew**

EMER24	1.319277	41.62	3.69	6.645401	1.169591	93.3546	28.6	44.8	51.86	3.04
EMER25	1.273494	41.61	4.1	8.128405	2.400236	91.87159	22.35	34.57	37.77	3.1
EMER26	1.256627	37.89	2.77	6.172987	2.679746	93.82701	14.3	21.8	21.87	2.18
EMER27	1.281526	38.83	4.41	7.401552	3.305548	92.59845	14.57	21.75	21.45	2.19
EMER28	1.270683	38.55	4.52	5.103858	3.635015	94.89614	13.22	20.06	19.61	1.92
EMER29	1.261446	37.23	3.13	8.123602	2.335011	91.8764	12.08	18.97	19.66	2.33
EMER30	1.401205	47.54	2.6	4.408867	1.096059	95.59113	17.95	25.45	24.01	2.14
EMER31	1.307631	39.33	3.72	7.496777	5.765334	92.50322	14.76	22.88	23.41	2.01
EMER32	1.414056	53.15	3.08	5.546995	1.056571	94.453	19.8	30.36	31.92	2.09
SIG131	1.524998	71.02	3.16	2.562604	0.331287	97.4374	35.96	41.84	30.4	1.82
SIG132	1.577108	72.03	2.18	1.458762	2.43127	98.54124	37.56	44.98	32.46	1.69
TWIS3	1.05743	8.18	15.44	10.20408	10.89482	89.79592	27.83	36.06	31.21	1.63
TWIS4	1.014056	5.29	34.39	25.13711	15.90494	74.86289	19.66	28.63	29.45	2.22
TWIS5	1.27992	10.46	14.49	5.61562	5.373568	94.38438	27.91	41.65	40.33	1.49
TWIS6	1.04257	7.6	19.22	79.93716	4.019961	20.06284	18.18	25.29	24.25	2.2
TWIS7	1.06506	13.39	12.42	15	10.26119	85	23.25	35.07	38.2	2.73
TWIS8	1.265462	19.5	4.91	3.680585	1.894102	96.31941	26.38	39.81	45.63	3.43
TWIS9	1.025703	12.2	18.73	26.69584	12.63676	73.30416	16.57	23.71	22.24	1.63
TWIS10	1.037751	9.83	19.77	22.86822	19.05685	77.13178	17.23	24.03	21.92	1.57
TWIS11	1.0751	10.37	18.71	22.69821	16.43223	77.30179	19.78	26.73	24.81	2.04
TWIS12	1.044578	18.98	11.35	17.33204	12.49594	82.66796	26.21	36.75	36.52	2.55
BOTH1	1.194378	21.1	11.25	9.902164	2.268011	90.09784	43.52	49.92	34.94	0.98
GNES2	1.060643	8.18	28.48	16.7129	13.28017	83.2871	22.49	27.14	20.16	1.63
GNES3	1.019679	9.12	20.08	29.05325	16.15385	70.94675	23.13	28.76	23.98	2.11
GNES4	1.094378	8.14	25.13	16.25639	4.667905	83.74361	23.65	27.64	19.17	1.21

GNES5	1.095181	16.36	15.66	7.961442	5.801499	92.03856	28.79	33.97	25.47	1.77
GNES6	1.138956	20.42	18.52	5.810147	6.894435	94.18985	29.14	34.52	26.03	1.7
GNES8	1.06037	5.46	19.27	13.96011	43.58974	86.03989	19.61	27.31	24.14	2.04
GNES9	1.022892	7.26	23.43	11.43519	17.82407	88.56481	21.46	28.3	24.6	1.81
GNES10	1.07751	16.95	8.97	6.007537	5.719353	93.99246	34.82	42.85	36.35	2.34
GNES11	1.088755	16.38	9.02	5.503247	1.006494	94.49675	38.14	45.2	34.37	1.21
GNES12	1.223293	34.7	4.34	12.96443	13.13205	87.03597	39.9	46.96	34.53	1.2
GNES13	1.043775	11.07	13.5	9.229535	5.718299	90.77047	27.01	33.28	26.91	2.22
GNES14	1.004819	5.79	42.07	15.51331	19.52109	84.48669	20.29	26.82	22.94	1.83
GNES15	1.017269	8.14	31.62	7.590585	4.97223	92.40942	19.67	27.51	25.2	1.98
GNES16	1.023293	8.37	16.78	13.09136	10.5632	86.90864	23.02	31.5	29.39	2.07
GNES17	0.98996	5.15	43.3	17.59024	14.84494	82.40976	19.97	29.01	28.78	2.21
Sample	**WD**	**% DW**	**% LOI**	**% OM**	**% BSi**	**% Min**	**Median**	**Mean**	**Std**	**Skew**
GNES18	1.02008	7.27	31.3	8.612735	9.104891	91.38727	33.12	38.97	31.39	1.83
GNES19	1.018474	5.57	45.43	27.02194	29.78056	72.97806	15.1	23.32	23.94	2.53
GNES20	1.008835	6.51	28.21	17.73428	23.7841	82.26572	16.88	23.9	21.64	2.08
GNES21	1.019679	7.92	21.23	15.1219	14.87338	84.8781	21.74	32.28	32.34	2.1
GNES22	1.033335	9.98	22.13	25.68915	26.62757	74.31085	21	27.86	25.02	2.26
ORWE1	1.668675	51.21	3.52	1.26932	0.440529	98.73068	44.23	58.29	48.02	1.7
ORWE2	1.716064	58.75	1.85	1.080069	0.604839	98.91993	50.44	66.69	62.83	2.86

C.2. SURFACE-SEDIMENT MINERAL MAGNETIC DATA

Sample	Mass g	xlf $10^{-8}m^3kg^{-1}$	xhf $10^{-8}m^3kg^{-1}$	xfd $10^{-8}m^3kg^{-1}$	xfd%	SIRM $10^{-5}Am^2kg^{-1}$	x_{ARM} $10^{-8}m^3kg^{-1}$	x_{ARM}/SIRM $10^{-3}mA^{-1}$	SIRM/x $10^{1}Am^{-1}$	x_{ARM}/x
SOMB11	1.8585	30.9034	30.05673	0.846668	2.739726	354.5566	820.7889	2.314973	11.47306	26.55983
SOMB12	1.8514	36.68952	35.48659	1.202935	3.278689	394.0061	561.4678	1.425023	10.73893	15.30322
SOMB13	1.6455	24.43574	23.87614	0.559597	2.290076	268.0913	365.5814	1.363645	10.97128	14.96093
SOMB14	1.7611	28.61953	27.72166	0.897868	3.137255	294.122	496.6025	1.688424	10.27697	17.35188
SOMB15	1.4945	25.11319	25.37847	-0.26528	-1.05634	241.2404	310.809	1.288379	9.606125	12.37633
SOMB16	2.0839	23.62962	23.20514	0.424484	1.796407	247.0334	266.4257	1.078501	10.4544	11.27507
SOMB17	2.0739	27.71942	27.13585	0.583567	2.105263	277.8757	325.3221	1.170747	10.02459	11.73625
SOMB18	1.5929	24.92009	26.00358	-1.08348	-4.34783	273.1797	362.4366	1.326733	10.96223	14.54395
SOMB19	1.8058	24.25748	26.91989	-2.66241	-10.9756	247.7324	273.0016	1.102002	10.21262	11.25432
SOMB20	1.7893	28.28118	26.81056	1.470622	5.2	296.2616	307.1089	1.036614	10.47557	10.85913
SOMB21	1.9201	24.7194	23.38322	1.336184	5.405405	229.0487	273.1004	1.192325	9.265949	11.04802
SOMB22	1.6641	29.58416	28.7547	0.829463	2.803738	301.0179	449.9368	1.494718	10.17497	15.2087
SOMB23	1.5488	22.29373	22.92469	-0.63095	-2.83019	200.8361	177.9027	0.88581	9.008635	7.979942
SOMB24	1.7142	28.9167	28.34125	0.575457	1.99005	294.165	330.5172	1.123578	10.17284	11.42998
SOMB25	3.0223	65.22665	60.96853	4.258119	6.52819	675.2211	643.2658	0.952674	10.35192	9.862008
SOMB26	1.0344	35.49022	33.84206	1.648152	4.643963	403.1302	310.2671	0.769645	11.35891	8.742327
SOMB27	1.2961	29.49103	28.6984	0.792623	2.687674	271.7704	218.4652	0.803859	9.215361	7.407854
SOMB28	1.8998	27.83423	27.68696	0.147271	0.529101	310.9896	327.1541	1.051978	11.17292	11.75366
SOMB29	1.9729	28.72057	28.72057	0	0	331.6796	330.7656	0.997244	11.5485	11.51668

Sample	Mass	xlf	xhf	xfd	xfd%	SIRM	x_{ARM}	x_{ARM}/SIRM	SIRM/x	x_{ARM}/x
SOMB30	1.3686	17.61243	17.8537	-0.24127	-1.36986	226.4296	240.9606	1.064174	12.85624	13.68128
SOMB31	2.1391	33.64613	33.06901	0.577121	1.715266	378.1672	325.5401	0.860836	11.23954	9.675409
SOMB32	2.1402	24.49164	24.08002	0.411624	1.680672	301.8971	369.7215	1.22466	12.32654	15.09582
SOMB33	1.6216	25.81193	24.9951	0.816833	3.164557	290.3003	326.4047	1.124369	11.24675	12.6455
SOMB34	1.9074	26.62116	26.05233	0.568828	2.136752	262.1513	328.8717	1.254511	9.847479	12.35377
SOMB35	1.6146	11.69074	11.98546	-0.29472	-2.52101	139.1354	142.9818	1.027645	11.90134	12.23035
SOMB36	2.1867	28.50352	28.08802	0.415503	1.457726	256.9585	296.0682	1.152202	9.014974	10.38707
SOMB37	1.2191	22.22778	21.95962	0.268164	1.206434	84.04625	77.96762	0.927675	3.781135	3.507665
SOMB38	1.9111	26.29756	26.01681	0.280757	1.067616	252.3775	267.8867	1.061452	9.596991	10.18675
SOMB39	2.0967	26.28697	25.80017	0.486796	1.851852	259.0139	322.9877	1.24699	9.853322	12.28699
SOMB40	1.6714	27.54993	26.99477	0.555162	2.015113	225.0026	223.2375	0.992155	8.167084	8.103015
SOMB41	1.7078	24.57354	23.98445	0.589092	2.39726	175.1455	137.8476	0.787046	7.127402	5.609595
SOMB42	1.3479	31.76053	30.54287	1.217656	3.833866	326.4746	571.9914	1.752024	10.27926	18.00951
SOMB43	1.0875	33.1675	32.35853	0.808963	2.439024	373.362	301.1239	0.80652	11.25686	9.078885
SOMB44	1.6986	26.96682	26.49783	0.468988	1.73913	267.5221	320.3398	1.197433	9.920416	11.87904
SOMB45	1.797	24.98829	25.11843	-0.13015	-0.52083	259.8672	282.7577	1.088086	10.39956	11.31561
SOMB46	2.2545	24.59843	24.96741	-0.36898	-1.5	261.6228	290.3265	1.109714	10.63575	11.80264
HEY5	1.9888	11.16355	11.41726	-0.25372	-2.27273	75.08841	76.82216	1.02309	6.726215	6.88152
HEY6	2.0879	9.728449	10.29242	-0.56397	-5.7971	49.2305	52.16464	1.0596	5.060467	5.362071
HEY7	2.1006	10.65615	10.42942	0.226727	2.12766	99.34529	226.6324	2.28126	9.322815	21.26776
HEY8	1.9497	12.27424	12.0989	0.175346	1.428571	112.5854	284.8965	2.530493	9.172491	23.21092
HEY9	2.1423	10.27221	10.6673	-0.39509	-3.84615	101.6747	266.0453	2.616633	9.898029	25.89951

Sample	Mass	xlf	xhf	xfd	xfd%	SIRM	x_{ARM}	x_{ARM}/SIRM	SIRM/x	x_{ARM}/x
HEY10	2.329	10.95551	11.43184	-0.47633	-4.34783	44.2171	49.71196	1.12427	4.03606	4.537621
HEY11	2.0189	10.62489	11.5253	-0.90041	-8.47458	95.37724	247.9814	2.600006	8.976777	23.33968
HEY12	2.3157	10.6959	10.55391	0.141981	1.327434	30.73577	42.20579	1.373181	2.873604	3.94598
HEY13	1.9872	16.28363	16.28363	0	0	211.9581	913.7282	4.31089	13.01664	56.11329
HEY14	2.186	16.88818	16.10268	0.785497	4.651163	88.43204	73.53842	0.831581	5.236328	4.354432
HEY15	1.9184	13.3185	13.14991	0.168589	1.265823	49.23779	35.54391	0.721883	3.696947	2.668763
HEY16	2.031	10.38938	10.69052	-0.30114	-2.89855	75.21017	185.9638	2.472588	7.239143	17.89942
CHAN2	2.2371	22.09972	21.6031	0.496623	2.247191	218.4843	207.8798	0.951463	9.886291	9.406442
CHAN3	1.8563	16.53993	17.39915	-0.85922	-5.19481	254.9898	425.876	1.670169	15.41662	25.74835
CHAN4	1.8406	19.45156	18.97713	0.474428	2.439024	317.0887	919.097	2.898549	16.30145	47.25055
CHAN5	2.1635	20.54955	19.96242	0.58713	2.857143	294.6161	641.0292	2.175811	14.33686	31.19431
CHAN6	1.6752	13.95622	13.95622	5.33e-15	3.82e-14	209.7878	475.5387	2.266761	15.03185	34.0736
CHAN7	1.6395	20.26883	19.91324	0.355593	1.754386	267.5349	343.0024	1.282085	13.19933	16.92266
CHAN8	2.4145	18.56436	17.87679	0.687569	3.703704	273.8265	308.6435	1.12715	14.75012	16.6256
CHAN9	2.0292	21.97699	21.66526	0.31173	1.41844	237.6391	261.633	1.100968	10.81309	11.90486
CHAN10	2.3777	25.45249	24.64447	0.808016	3.174603	269.8397	322.839	1.19641	10.6017	12.68399
CHAN11	1.9307	8.484274	8.484274	-3.6e-15	-4.2e-14	146.9865	174.8983	1.189893	17.32458	20.6144
CHAN12	1.6538	25.47724	23.93539	1.54185	6.051873	265.66	232.0313	0.873415	10.42735	9.107396
CHAN13	1.798	25.48604	24.99813	0.487908	1.914414	177.8421	135.3418	0.761022	6.97802	5.310429
CHAN14	1.513	24.57254	24.32322	0.249327	1.014656	168.8895	134.3025	0.795209	6.873098	5.465551
MOSS3	2.7932	27.38174	27.06701	0.314733	1.149425	269.0929	549.8007	2.043163	9.827459	20.0791
MOSS4	2.4048	19.83655	19.30757	0.528975	2.666667	145.1328	195.9605	1.350215	7.316436	9.88759

Sample	Mass	xlf	xhf	xfd	xfd%	SIRM	x_{ARM}	x_{ARM}/SIRM	SIRM/x	x_{ARM}/x
MOSS5	1.5797	28.39708	27.59148	0.805591	2.836879	261.3603	402.6467	1.540581	9.203774	14.17916
MOSS6	2.0818	33.92287	32.27613	1.646741	4.854369	303.0338	555.6895	1.833754	8.933024	16.38097
MOSS7	1.693	18.58974	18.33333	0.25641	1.37931	83.12723	82.60823	0.993757	4.471672	4.443753
MOSS8	1.0483	17.11423	16.89828	0.215952	1.26183	149.7765	287.2622	1.91794	8.751575	16.78499
MOSS9	1.6997	57.45039	54.72619	2.724202	4.741834	1187.609	786.2506	0.662045	20.6719	13.68573
MOSS10	3.0305	34.10389	32.57565	1.52824	4.481132	291.0668	455.0654	1.563439	8.534711	13.3435
MOSS11	2.8484	21.22177	19.70593	1.515841	7.142857	234.0829	395.0593	1.687689	11.03032	18.61576
MOSS12	1.9127	-6.29882	-12.5976	6.298816	-100	314.311	478.3534	1.521911	-49.9	-75.9434
MOSS13	1.8238	10.71289	10.06363	0.649266	6.060606	189.0036	347.9551	1.840997	17.64263	32.48003
MOSS14	2.8272	27.60706	26.23295	1.374107	4.977376	253.2366	409.5664	1.617327	9.172895	14.83557
MOSS15	1.7531	37.41856	36.03502	1.383543	3.697479	269.8064	511.8126	1.896963	7.210495	13.67804
MOSS16	1.9208	2.234887	1.676165	0.558722	25	213.3537	314.8246	1.4756	95.46512	140.8683
MOSS17	1.9991	12.42126	11.97764	0.443616	3.571429	189.5076	318.0795	1.678452	15.25672	25.60767
MOSS18	2.9997	15.80153	15.14314	0.658397	4.166667	99.44442	132.1496	1.328879	6.29334	8.363086
MOSS19	2.0169	16.621	15.34247	1.278539	7.692308	118.4407	176.0323	1.486249	7.125963	10.59095
MOSS20	2.5336	13.7679	13.01692	0.750976	5.454545	156.9679	292.8355	1.865576	11.401	21.26944
MOSS21	3.0494	35.3443	33.77731	1.566989	4.433498	272.6798	496.8952	1.822266	7.714958	14.05871
KNOB1	1.6582	15.63362	15.7358	-0.10218	-0.65359	117.1159	57.69442	0.492627	7.491282	3.690407
KNOB2	1.5622	14.69335	14.10562	0.587734	4	130.5249	101.8629	0.780409	8.883264	6.932584
KNOB3	1.4189	13.64658	13.2589	0.387687	2.840909	98.52152	53.85683	0.54665	7.2195	3.946543
KNOB4	1.6229	15.96659	15.61568	0.359014	2.197802	117.2929	56.74098	0.483754	7.346146	3.553731
KNOB5	1.1416	11.45929	11.3984	0.06945	0.606061	88.91716	37.82341	0.425378	7.759396	3.300677

Sample	Mass	xlf	xhf	xfd	xfd%	SIRM	x_{ARM}	x_{ARM}/SIRM	SIRM/x	x_{ARM}/x
KNOB6	1.8218	14.50245	14.83713	-0.33467	-2.30769	111.2005	63.61993	0.572119	7.667705	4.386839
KNOB7	1.4579	11.20401	11.10986	0.094151	0.840336	93.29358	57.22696	0.613407	8.326805	5.107723
KNOB8	1.1327	10.73632	10.86645	-0.13014	-1.21212	74.73811	38.83816	0.519657	6.961244	3.617457
KNOB9	0.8063	10.95833	10.90421	0.054115	0.493827	31.05486	21.23936	0.683931	2.833905	1.938194
KNOB10	1.6019	13.52797	14.15718	-0.62921	-4.65116	99.59479	59.70998	0.599529	7.36214	4.413818
KNOB11	1.6489	12.27614	12.228	0.048142	0.392157	39.29659	24.02453	0.611364	3.201054	1.95701
PUMP1	3.1123	15.23546	16.85134	-1.61588	-10.6061	297.1626	167.5465	0.563821	19.50467	10.99714
PUMP2	1.5369	1098.405	1058.422	39.98269	3.640068	16266.28	7006.59	0.430743	14.809	6.378876
PUMP3	1.7619	14.27634	13.98696	0.289385	2.027027	97.24418	40.89211	0.42051	6.811561	2.864327
PUMP4	1.8179	13.4675	13.7216	-0.2541	-1.88679	168.6202	86.97819	0.515823	12.52053	6.458377
PUMP5	2.2017	15.68627	15.68627	0	0	181.0464	97.71159	0.539705	11.54171	6.229114
PUMP6	1.5946	8.39046	7.676378	0.714082	8.510638	115.6422	78.74547	0.68094	13.78259	9.38512
PUMP7	1.7001	20.66713	20.37808	0.289051	1.398601	237.6171	119.968	0.504879	11.49734	5.804773
LITE2	1.7728	-3.54045	-5.31067	1.770225	-50	329.569	147.8062	0.448483	-93.0868	-41.7479
LITE3	1.883	-3.57526	-2.97938	-0.59588	16.66667	165.131	91.80766	0.555969	-46.1872	-25.6786
LITE4	1.722	-4.35161	-3.72995	-0.62166	14.28571	135.0903	52.87073	0.391373	-31.0438	-12.1497
LITE5	1.9066	-2.86205	-2.38504	-0.47701	16.66667	124.3989	31.18614	0.250695	-43.465	-10.8964
SPIR2	2.0083	23.43431	23.10518	0.329134	1.404494	168.4639	93.78514	0.556708	7.188772	4.002044
SPIR3	1.8104	17.07579	17.42251	-0.34672	-2.03046	107.5353	48.28557	0.449021	6.297527	2.827721
SPIR4	1.8421	23.91904	24.07237	-0.15333	-0.64103	149.381	81.87566	0.548099	6.245476	3.433032
SPIR5	1.7163	17.47312	17.30511	0.168011	0.961538	148.8082	68.92454	0.463177	8.516406	3.944605
TRAN4	1.1304	32.4406	31.20241	1.238191	3.816794	298.5624	232.8767	0.779994	9.203356	7.178559

Sample	Mass	xlf	xhf	xfd	xfd%	SIRM	x_{ARM}	x_{ARM}/SIRM	SIRM/x	x_{ARM}/x
TRAN5	2.503	29.80796	29.14822	0.659733	2.21328	219.0211	185.9475	0.848994	7.347738	6.238184
TRAN6	2.4138	27.84201	27.60606	0.235949	0.847458	223.0827	205.8128	0.922585	8.012451	7.392167
TRAN7	1.6671	21.01415	21.20963	-0.19548	-0.93023	107.2876	78.60699	0.732675	5.105495	3.740669
TRAN8	2.0675	22.32008	22.21954	0.100541	0.45045	176.1966	153.0988	0.868909	7.894084	6.859241
TRAN9	2.5416	19.26188	18.87665	0.385238	2	135.5678	93.0245	0.686184	7.038136	4.82946
TRAN10	1.9395	19.74193	20.35251	-0.61058	-3.09278	185.7955	153.4464	0.825889	9.41121	7.772616
TRAN11	1.7817	21.97672	22.2737	-0.29698	-1.35135	240.265	184.5711	0.768198	10.93271	8.398485
TRAN12	2.3089	29.54233	29.27619	0.266147	0.900901	213.8249	170.6909	0.798274	7.237917	5.777842
TRAN13	1.9062	28.24392	27.78542	0.458505	1.623377	201.3086	201.7215	1.002051	7.127501	7.142119
TRAN14	1.5662	26.33023	26.03355	0.296679	1.126761	164.7392	172.925	1.04969	6.256655	6.567545
TRAN15	2.4224	19.7098	19.57002	0.139786	0.70922	121.0073	88.37183	0.730302	6.139447	4.483648
TRAN16	2.2903	22.32974	22.22636	0.103378	0.462963	134.9653	130.5995	0.967652	6.044194	5.848679
TRAN17	1.6044	27.6058	27.29311	0.312687	1.132686	172.7972	134.5656	0.778749	6.259451	4.874543
TRAN18	1.6163	22.37719	21.94352	0.433666	1.937984	155.4617	181.6515	1.168465	6.94733	8.117711
TRAN19	1.6611	27.85457	27.12155	0.733015	2.631579	207.5041	184.046	0.886951	7.449555	6.60739
TRAN20	1.9207	22.50568	22.42781	0.077874	0.346021	124.1389	103.1764	0.831136	5.515891	4.584457
TRAN21	1.9009	26.15096	25.92237	0.228592	0.874126	165.9388	142.2454	0.857216	6.345419	5.439394
TRAN22	1.1831	28.38721	28.25739	0.12982	0.457317	187.0409	158.474	0.847269	6.588916	5.582586
TRAN23	1.321	29.9343	29.24879	0.685518	2.290076	211.8461	163.76	0.773014	7.077033	5.470646
TRAN24	1.9564	22.60248	21.4191	1.183376	5.235602	168.1252	150.8929	0.897503	7.438351	6.675942
TRAN25	2.9914	20.92656	20.70393	0.222623	1.06383	154.2402	175.8811	1.140307	7.370547	8.404686
TRAN26	1.1833	16.477	16.00284	0.474158	2.877698	109.2518	120.6571	1.104394	6.630565	7.322755

Sample	Mass	xlf	xhf	xfd	xfd%	SIRM	x_{ARM}	x_{ARM}/SIRM	SIRM/x	x_{ARM}/x
TRAN27	1.8724	16.18247	15.67278	0.509684	3.149606	151.6148	188.0104	1.240054	9.369076	11.61816
TRAN28	1.7088	12.54654	12.54654	8.88e-15	7.08e-14	191.3952	228.9602	1.196269	15.25482	18.24887
TRAN29	1.5686	22.63922	22.63922	-7.1e-15	-3.1e-14	140.9076	151.6873	1.076502	6.224047	6.700202
TRAN30	2.0734	20.64665	17.13613	3.510526	17.00288	79.98236	58.29378	0.728833	3.873866	2.823401
AMOS3	0.7295	9.353191	8.753627	0.599564	6.410256	56.9975	68.07298	1.194315	6.093909	7.278049
AMOS4	1.0071	12.85632	11.74802	1.108303	8.62069	64.19744	70.51855	1.098464	4.993454	5.485127
AMOS5	1.1884	16.01635	15.60213	0.414216	2.586207	68.51135	73.11141	1.067143	4.277589	4.564799
AMOS6	1.6773	15.11999	14.84256	0.277431	1.834862	55.01569	37.76885	0.686511	3.638606	2.497942
AMOS7	1.2867	15.31406	15.27199	0.042072	0.274725	53.75275	76.84692	1.429637	3.510025	5.018062
TIOG1	1.2352	10.11691	9.929556	0.18735	1.851852	443.5637	283.6557	0.639492	43.84381	28.03779
TIOG2	1.314	5.736529	5.941405	-0.20488	-3.57143	393.249	233.4972	0.593764	68.55174	40.70356
TIOG3	0.6313	8.012821	8.856275	-0.84345	-10.5263	416.4637	230.5714	0.553641	51.97467	28.77531
TIOG4	1.1726	24.5916	24.5916	-3.6e-15	-1.4e-14	1149.598	429.4375	0.373554	46.74759	17.46277
EMER1	1.1308	29.65289	29.4037	0.249184	0.840336	201.0602	85.82732	0.426874	6.780459	2.8944
EMER2	1.1538	33.8106	33.55941	0.251193	0.742942	197.3603	73.93191	0.374604	5.837232	2.186649
EMER3	1.3508	32.91612	32.97522	-0.0591	-0.17953	202.385	81.19597	0.401196	6.148506	2.466754
EMER4	1.2956	38.27547	38.1071	0.168367	0.439883	227.0994	81.05064	0.356895	5.933289	2.117561
EMER5	1.1746	32.97489	32.97489	7.11e-15	2.15e-14	189.0991	69.68952	0.368534	5.734639	2.113412
EMER6	1.3432	32.73136	33.21007	-0.4787	-1.46252	184.1311	71.94522	0.390728	5.625525	2.198051
EMER7	1.282	34.15368	34.04386	0.109819	0.321543	190.6615	77.67302	0.407387	5.582458	2.274221
EMER8	1.2227	32.01762	32.09055	-0.07293	-0.22779	205.7258	80.64329	0.391994	6.425395	2.518716
EMER9	1.3422	34.05012	34.10275	-0.05263	-0.15456	193.0951	77.54	0.401564	5.670909	2.277231

Sample	Mass	xlf	xhf	xfd	xfd%	SIRM	x_{ARM}	x_{ARM}/SIRM	SIRM/x	x_{ARM}/x
EMER10	1.3128	32.15982	32.15982	0	0	177.7132	81.90493	0.460883	5.525941	2.54681
EMER11	1.1289	32.60317	32.49265	0.110519	0.338983	193.8981	74.94119	0.386498	5.947215	2.298586
EMER12	1.50023	33.36057	33.27546	0.085103	0.255102	195.4033	78.32367	0.400831	5.857313	2.347792
EMER13	1.1442	39.66768	39.49743	0.170248	0.429185	190.1769	77.34184	0.406684	4.794253	1.949745
EMER14	1.1909	34.31598	34.23921	0.07677	0.223714	207.3178	84.48044	0.407492	6.041437	2.461839
EMER15	1.0448	34.72293	34.75714	-0.03421	-0.09852	193.077	76.72112	0.39736	5.560504	2.209523
EMER16	1.2731	32.90447	32.93808	-0.03361	-0.10215	196.0651	88.53455	0.451557	5.958615	2.690654
EMER17	1.7121	32.64521	32.54362	0.101593	0.311203	176.8564	76.00986	0.429783	5.417531	2.328362
EMER18	1.2614	33.34152	33.37873	-0.03721	-0.11161	191.6186	73.75706	0.384916	5.747146	2.212169
EMER19	1.3643	34.57393	34.47552	0.098408	0.28463	183.0155	72.52906	0.3963	5.293454	2.097796
EMER20	1.2892	34.00627	34.00627	-7.1e-15	-2.1e-14	170.3528	64.29412	0.377417	5.009452	1.890655
EMER21	1.2528	33.89312	33.89312	0	0	199.2405	72.36943	0.363226	5.878496	2.135225
EMER22	1.0009	34.70671	34.67433	0.032376	0.093284	182.6214	72.58131	0.397441	5.261848	2.091276
EMER23	0.8826	33.98792	33.93654	0.05138	0.151172	169.0974	65.8733	0.389558	4.97522	1.938139
EMER24	1.1177	36.18394	35.90825	0.275687	0.761905	182.5786	68.93008	0.377537	5.045845	1.904991
EMER25	1.1447	34.91496	34.72142	0.193542	0.554324	185.7686	68.55495	0.369034	5.320603	1.963484
EMER26	0.9281	34.40462	34.23139	0.173236	0.503525	173.7573	73.01339	0.420203	5.050405	2.122197
EMER27	0.6869	33.96267	33.88926	0.073406	0.216138	172.3976	65.66313	0.380882	5.076091	1.933391
EMER28	1.2524	34.12495	34.09189	0.033067	0.096899	182.64	71.43984	0.391151	5.352095	2.093478
EMER29	1.0808	34.06886	34.06886	0	0	180.7591	69.13365	0.382463	5.305698	2.029233
EMER30	1.3526	35.85774	35.74192	0.11582	0.322997	181.5586	55.64612	0.306491	5.063302	1.551858
EMER31	1.0963	33.79054	33.42397	0.366564	1.084813	182.3038	69.5191	0.381337	5.395114	2.057354

Sample	Mass	xlf	xhf	xfd	xfd%	SIRM	x_{ARM}	x_{ARM}/SIRM	SIRM/x	x_{ARM}/x
EMER32	1.1491	34.48505	34.31925	0.165793	0.480769	173.3605	57.35996	0.330871	5.02712	1.663329
SIG131	1.1628	23.72319	23.66698	0.056216	0.236967	71.2783	53.36648	0.748706	3.004583	2.249549
SIG132	1.6772	22.17177	22.27836	-0.1066	-0.48077	68.31136	54.97708	0.804801	3.081006	2.479598
TWIS3	5.0448	10.46558	10.84271	-0.37714	-3.6036	36.96703	21.29344	0.576012	3.53225	2.034617
TWIS4	1.3962	13.48654	14.29573	-0.80919	-6	110.6628	91.26643	0.824725	8.205427	6.767224
TWIS5	1.3093	13.0715	13.0715	-1.8e-15	-1.4e-14	51.00717	32.37897	0.634793	3.902165	2.477066
TWIS6	1.6406	17.45201	17.9653	-0.51329	-2.94118	98.70673	89.54698	0.907202	5.655896	5.131042
TWIS7	1.9431	16.03211	15.92	0.112113	0.699301	45.39257	26.06725	0.574262	2.831354	1.62594
TWIS8	2.0352	15.90102	15.95087	-0.04985	-0.31348	49.25176	19.87697	0.403579	3.097396	1.250044
TWIS9	1.236	8.988289	9.781373	-0.79308	-8.82353	76.0674	60.93396	0.801052	8.462946	6.779261
TWIS10	1.5815	11.22986	11.6171	-0.38724	-3.44828	59.31761	41.09367	0.692773	5.282131	3.65932
TWIS11	1.6951	10.21128	11.13958	-0.9283	-9.09091	47.55369	31.06834	0.653332	4.656976	3.042551
TWIS12	1.4378	22.43917	22.75821	-0.31904	-1.4218	224.8022	120.731	0.537055	10.01829	5.38037
BOTH1	1.626	18.78681	19.2496	-0.4628	-2.46341	98.79569	87.41578	0.884814	5.25878	4.653041
GNES2	2.5732	13.41211	13.92143	-0.50932	-3.79747	68.54168	86.87093	1.267417	5.110433	6.477052
GNES3	1.6415	8.719737	10.25851	-1.53878	-17.6471	50.43633	40.5482	0.803948	5.784156	4.650163
GNES4	3.0901	21.21604	21.47477	-0.25873	-1.21951	162.7983	145.938	0.896434	7.673361	6.878661
GNES5	3.1052	25.91224	26.65562	-0.74338	-2.86885	215.9302	260.5281	1.206538	8.333137	10.05425
GNES6	1.7228	31.58432	31.93623	-0.35191	-1.11421	268.8794	246.2793	0.915947	8.513067	7.797518
GNES8	3.1754	10.40769	11.48435	-1.07666	-10.3448	194.1554	416.5288	2.145337	18.65498	40.02123
GNES9	1.2481	11.5571	12.66836	-1.11126	-9.61538	92.20808	96.23607	1.043684	7.978482	8.327011
GNES10	1.8256	29.4471	29.34862	0.098485	0.334448	228.159	249.6459	1.094175	7.748095	8.477776

Sample	Mass	xlf	xhf	xfd	xfd%	SIRM	x_{ARM}	x_{ARM}/SIRM	SIRM/x	x_{ARM}/x
GNES11	2.2527	29.79956	30.36181	-0.56226	-1.88679	227.7078	208.1462	0.914093	7.641314	6.984875
GNES12	3.1163	17.96893	19.70786	-1.73893	-9.67742	158.9817	145.0254	0.912214	8.847587	8.070895
GNES13	2.4548	22.63657	22.63657	0	0	151.8777	151.6103	0.998239	6.709397	6.697584
GNES14	2.9063	12.61879	13.01313	-0.39434	-3.125	130.9669	190.7	1.456094	10.37872	15.11238
GNES15	2.9859	21.05184	21.2398	-0.18796	-0.89286	194.0255	268.6002	1.384355	9.216557	12.75899
GNES16	2.7782	17.84734	18.4575	-0.61017	-3.4188	163.1604	155.362	0.952204	9.142	8.705053
GNES17	2.382	16.37721	17.32937	-0.95216	-5.81395	255.1747	226.6197	0.888096	15.58109	13.8375
GNES18	1.6639	28.44141	28.56507	-0.12366	-0.43478	459.5958	391.0749	0.850911	16.15939	13.75019
GNES19	2.5087	6.679389	7.951654	-1.27226	-19.0476	88.24421	201.6584	2.285231	13.21142	30.19114
GNES20	2.6751	12.56144	13.47169	-0.91025	-7.24638	187.6962	222.0513	1.183036	14.94225	17.67721
GNES21	2.9035	21.16987	22.3204	-1.15054	-5.43478	263.6363	352.6768	1.33774	12.45338	16.65938
GNES22	2.7514	13.56602	12.48074	1.085281	8	100.5977	113.9369	1.132599	7.415419	8.398697
ORWE1	1.3396	18.03352	17.97837	0.055148	0.30581	90.53735	81.84488	0.90399	5.020504	4.538487
ORWE2	1.8647	11.31886	13.77457	-2.45571	-21.6958	50.85206	51.32121	1.009226	4.492685	4.534132

Sample	Mass	HARD	HARD%	SOFT	SOFT%	-40mT%	-100mT%	-300mT%	$\chi_{ARM}/\chi fd$
	g	$10^{-5}Am^2kg^{-1}$		$10^{-5}Am^2kg^{-1}$					10^1
SOMB11	1.8585	6.08708	1.716815	110.9533	45.58695	41.63215	38.03633	36.13999	969.4337
SOMB12	1.8514	6.47934	1.644477	113.5329	46.34333	43.15512	39.66469	37.51853	466.7482
MOSS11	2.8484	2.699939	1.153412	77.62185	42.91704	37.20685	31.42136	28.88642	260.6206
MOSS12	1.9127	2.10068	0.668344	122.3193	43.80921	39.89319	35.88627	34.19851	75.94338
MOSS13	1.8238	4.000292	2.116516	57.25454	41.98618	35.70063	28.11781	24.1054	535.9205
MOSS14	2.8272	5.175686	2.043814	70.68056	44.48917	39.82378	34.07901	30.65916	298.0601
MOSS15	1.7531	1.595842	0.591477	92.75589	43.62901	38.49224	33.55431	31.5778	369.9288
MOSS16	1.9208	4.535753	2.125931	62.7443	43.10802	37.68756	30.77132	27.06296	563.4731
MOSS17	1.9991	2.299348	1.213327	62.81983	41.25392	34.53382	27.37728	23.93596	717.0147
MOSS18	2.9997	3.316781	3.335312	27.99259	35.84688	26.27805	11.5437	1.39763	200.7141
MOSS19	2.0169	3.936877	3.323923	35.48495	37.35227	28.13794	16.62094	9.187969	137.6824
MOSS20	2.5336	2.737233	1.743818	52.52426	39.3412	31.57209	23.25303	18.70181	389.9397
MOSS21	3.0494	3.077879	1.128752	86.83212	44.16092	39.25689	34.11298	31.87045	317.102
KNOB1	1.6582	4.95031	4.226848	17.30596	43.69138	37.42238	23.2546	9.111797	-564.632
KNOB2	1.5622	3.961562	3.035101	34.47198	39.88305	33.01106	22.11934	12.85579	173.3146
KNOB3	1.4189	4.596069	4.665041	13.14103	43.2308	36.474	19.19254	1.617189	138.9183
KNOB4	1.6229	5.548663	4.730603	14.33909	44.78868	39.23353	24.54845	9.38826	161.6948
KNOB5	1.1416	3.903596	4.390149	11.32815	42.83596	35.75994	16.40883	-3.76344	544.6117
KNOB6	1.8218	4.868842	4.378434	17.21449	43.03934	36.63427	21.81346	7.004899	-190.096
KNOB7	1.4579	3.972404	4.257961	13.82389	42.05861	34.55245	16.6937	-1.31223	607.819
KNOB8	1.1327	3.492387	4.672833	10.1996	40.87004	32.10354	9.49305	-13.7741	-298.44

Sample	Mass	HARD	HARD%	SOFT	SOFT%	-40mT%	-100mT%	-300mT%	x_{ARM}/xfd
KNOB9	0.8063	1.425865	4.591439	6.021357	18.78198	-7.31508	-58.183	-103.613	392.4843
KNOB10	1.6019	4.184484	4.201509	16.73907	41.56222	34.22392	18.05906	1.905872	-94.8971
KNOB11	1.6489	1.509691	3.841786	7.204021	26.67427	5.132407	-36.1489	-72.3493	499.0376
PUMP1	3.1123	2.108102	0.70941	172.5861	40.22791	38.0298	35.51868	33.29356	-103.687
PUMP2	1.5369	-28.3265	-0.17414	11911.52	49.77491	49.71655	49.69641	49.69208	175.2406
PUMP3	1.7619	3.751794	3.858117	15.43888	41.83683	34.53171	17.22561	0.566769	141.3068
PUMP4	1.8179	2.995197	1.776298	62.86155	38.94558	33.55264	26.47705	20.87428	-342.294
PUMP5	2.2017	6.44479	3.559745	31.21168	45.2389	41.06335	31.80934	23.36587	0
PUMP6	1.5946	2.708494	2.342132	31.63537	38.17204	30.07436	17.49171	7.775868	110.2752
PUMP7	1.7001	3.250564	1.367984	70.3913	43.76647	39.94693	34.08038	29.2456	415.0412
LITE2	1.7728	1.807302	0.548384	221.7289	39.79297	37.123	35.50361	34.91187	83.49574
LITE3	1.883	8.08847	4.898213	87.44053	33.96661	28.48143	24.20192	21.20414	-154.072
LITE4	1.722	5.19793	3.847745	62.12348	32.9793	25.30882	18.56995	14.41186	-85.0479
LITE5	1.9066	0.000501	0.000403	65.64463	28.79024	18.33295	11.95839	9.806894	-65.3786
SPIR2	2.0083	18.15285	10.77551	23.83795	45.80023	41.86366	33.15444	23.51822	284.9455
SPIR3	1.8104	12.23643	11.37899	11.36215	45.0872	39.89487	25.54483	8.794441	-139.265
SPIR4	1.8421	19.84358	13.28387	23.78508	44.67053	40.01425	30.92494	20.97485	-533.993
SPIR5	1.7163	16.70131	11.22338	27.30869	43.8338	39.19131	30.18713	20.17078	410.2389
TRAN4	1.1304	3.887207	1.301975	121.3489	43.19331	39.36407	35.85273	33.47112	188.0782
TRAN5	2.503	9.248534	4.222669	54.54552	44.31465	39.81047	32.88681	28.13513	281.8525
TRAN6	2.4138	7.349087	3.294333	55.92093	44.3816	40.0087	32.95613	28.32516	872.2758
TRAN7	1.6671	6.457571	6.018932	31.93427	36.12837	27.57748	16.1748	6.201358	-402.122

Sample	Mass	HARD	HARD%	SOFT	SOFT%	-40mT%	-100mT%	-300mT%	x_{ARM}/xfd
TRAN8	2.0675	5.262351	2.986636	37.44918	43.96861	38.6401	29.97725	22.47014	1522.752
TRAN9	2.5416	3.801025	2.803782	45.73872	37.55654	29.74948	20.96085	14.15216	241.473
TRAN10	1.9395	12.61332	6.788822	58.42611	41.53734	35.82435	29.43024	24.91565	-251.315
TRAN11	1.7817	3.732894	1.553657	77.71663	43.26864	38.42429	32.64817	29.51296	-621.488
TRAN12	2.3089	6.493517	3.036838	60.56221	43.377	38.73899	32.14203	27.32651	641.3405
TRAN13	1.9062	4.52077	2.245691	48.3148	44.03891	38.7157	30.94193	25.72029	439.9545
TRAN14	1.5662	4.756241	2.887134	38.80128	42.85138	36.34626	26.87564	20.52527	582.8697
TRAN15	2.4224	5.101526	4.215883	33.28069	38.63579	31.32791	19.20204	10.42217	632.1944
TRAN16	2.2903	7.726616	5.724892	35.03359	40.38364	33.24463	22.83944	15.07431	1263.315
TRAN17	1.6044	6.377918	3.690985	39.57152	43.37357	37.48909	28.50542	22.13235	430.3525
TRAN18	1.6163	6.298944	4.051766	39.38528	41.85189	35.66762	26.15854	19.14088	418.8739
TRAN19	1.6611	7.28707	3.511771	50.81695	44.09901	39.21824	31.83604	26.75029	251.0808
TRAN20	1.9207	8.016844	6.457962	28.70926	40.68515	33.50021	21.94077	12.32364	1324.908
TRAN21	1.9009	6.647607	4.006059	41.42098	42.47867	36.55598	27.43765	21.0755	622.2667
TRAN22	1.1831	7.14915	3.822238	41.67629	44.04357	38.80022	30.4954	24.28965	1220.726
TRAN23	1.321	7.685673	3.627952	47.98788	44.65361	40.04229	32.59676	27.25423	238.8849
TRAN24	1.9564	5.611048	3.337423	39.7446	42.96956	36.83697	27.46629	21.2528	127.5105
TRAN25	2.9914	6.028217	3.908332	38.55764	41.89626	35.19178	25.51324	18.84999	790.0405
TRAN26	1.1833	4.177916	3.824115	28.39614	38.1048	28.71456	15.36039	5.984322	254.4657
TRAN27	1.8724	4.132378	2.725578	38.87359	41.54445	34.30995	24.08143	17.92053	368.8764
TRAN28	1.7088	4.982394	2.603197	56.06576	42.34746	36.45159	28.98782	24.55611	2.58e+16
TRAN29	1.5686	5.954161	4.225579	34.43215	41.32907	34.18996	23.65484	16.01516	-2.1e+16

Sample	Mass	HARD	HARD%	SOFT	SOFT%	-40mT%	-100mT%	-300mT%	$\chi_{ARM}/\chi fd$
TRAN30	2.0734	6.435311	8.045913	16.21843	37.32376	26.66221	8.614958	-7.48398	16.60543
AMOS3	0.7295	2.245014	3.938794	16.75227	24.21709	7.723598	-16.5759	-34.2679	113.5376
AMOS4	1.0071	2.405819	3.74753	24.23866	20.59352	6.228628	-11.3793	-24.966	63.62747
AMOS5	1.1884	3.047718	4.448486	16.66589	32.24693	18.24512	-2.8604	-19.7341	176.5056
AMOS6	1.6773	3.113504	5.659302	13.6546	27.44329	11.62781	-13.485	-35.7398	136.1378
AMOS7	1.2867	3.332324	6.199355	12.31653	28.68638	10.06258	-15.9658	-37.252	1826.574
TIOG1	1.2352	17.31323	3.903211	71.08026	48.19363	46.44627	42.7939	39.16765	1514.04
TIOG2	1.314	16.43153	4.178403	52.25741	48.31041	46.49891	42.21956	37.81668	-1139.7
TIOG3	0.6313	17.04169	4.091998	58.13158	48.32418	46.57753	42.58632	38.48543	-273.365
TIOG4	1.1726	52.614	4.57673	121.518	49.54025	48.98292	47.47822	45.84971	-1.2e+17
EMER1	1.1308	15.70647	7.811827	51.36765	43.64658	38.87625	31.38422	27.07448	344.4336
EMER2	1.1538	17.41344	8.823173	50.53634	43.51285	38.73948	31.33062	26.90092	294.323
EMER3	1.3508	17.90841	8.848688	51.74604	43.68329	39.08384	31.80486	27.48071	-1373.98
EMER4	1.2956	25.59186	11.26901	57.83278	44.39324	40.44122	34.40127	30.46429	481.3921
EMER5	1.1746	17.32737	9.163115	48.23352	43.25565	38.31774	30.64905	25.98167	9.81e+15
EMER6	1.3432	8.765268	4.76034	52.62993	42.23845	37.59379	29.33311	24.13809	-150.292
EMER7	1.282	15.56088	8.161524	47.38373	43.48262	38.55009	30.6051	25.91583	707.2828
EMER8	1.2227	16.9625	8.245195	52.77735	43.76495	39.14014	31.94816	27.69974	-1105.72
EMER9	1.3422	17.21584	8.91573	47.13362	43.6794	38.88166	31.10507	26.41467	-1473.37
EMER10	1.3128	11.98373	6.743293	44.80438	42.90666	37.49257	28.74504	23.76203	0
EMER11	1.1289	17.41436	8.981193	48.60947	43.53537	38.75054	31.10363	26.52921	678.0829
EMER12	1.50023	15.79547	8.083525	47.59575	43.76732	38.9541	31.12248	26.48031	920.3344

Sample	Mass	HARD	HARD%	SOFT	SOFT%	-40mT%	-100mT%	-300mT%	$\chi_{ARM}/\chi fd$
EMER13	1.1442	15.15132	7.96696	52.1258	42.79378	37.97676	30.37533	25.80331	454.2905
EMER14	1.1909	13.83276	6.672248	53.03258	43.83065	39.23775	31.72803	27.49163	1100.442
EMER15	1.0448	15.29425	7.921319	48.13287	43.54419	38.63154	30.80754	26.15494	-2242.67
EMER16	1.2731	13.01316	6.637164	47.70965	43.79451	38.91042	30.83214	26.19085	-2634.15
EMER17	1.7121	10.96952	6.202501	42.65432	43.18146	37.73501	28.63604	23.48202	748.1803
EMER18	1.2614	16.76253	8.747864	48.04071	43.45809	38.58148	30.80602	26.18912	-1982.1
EMER19	1.3643	15.62595	8.538049	46.8815	43.00165	37.77225	29.7917	25.01251	737.0258
EMER20	1.2892	16.5777	9.731395	42.50323	42.67693	37.19141	28.79875	23.50539	-9.0e+15
EMER21	1.2528	19.88444	9.980117	48.79718	43.85376	39.1976	31.89122	27.40925	0
EMER22	1.0009	16.2435	8.894629	44.83512	43.27821	38.0899	29.91169	25.05622	2241.848
EMER23	0.8826	15.18679	8.981095	40.65669	42.89067	37.39892	28.37516	23.08683	1282.079
EMER24	1.1177	17.24644	9.44604	47.87072	42.81974	37.67678	29.97803	25.20137	250.0301
EMER25	1.1447	18.52955	9.974533	46.54121	43.25685	38.28902	30.57433	25.76947	354.2124
EMER26	0.9281	17.04397	9.809067	42.60877	42.9436	37.57609	29.25659	24.04686	421.4683
EMER27	0.6869	16.88717	9.795477	42.22717	42.89606	37.44651	29.02899	23.83823	894.5157
EMER28	1.2524	16.74348	9.167476	44.70118	43.29965	38.14419	30.03278	25.13345	2160.469
EMER29	1.0808	15.19706	8.407356	44.09659	43.252	37.99991	29.68515	24.66444	0
EMER30	1.3526	24.92182	13.7266	45.88998	43.03928	38.28999	31.28236	26.24089	480.4553
EMER31	1.0963	16.23893	8.907622	45.28002	43.18783	38.04068	29.93032	25.01632	189.6506
EMER32	1.1491	18.88648	10.89434	42.81753	42.87653	37.65711	29.57317	24.30047	345.9724
SIG131	1.1628	2.936698	4.120045	17.89413	32.38973	18.21032	-3.24299	-17.2575	949.3097
SIG132	1.6772	2.82192	4.130967	17.90098	30.81946	16.1517	-5.82347	-20.1706	-515.756

Sample	Mass	HARD	HARD%	SOFT	SOFT%	-40mT%	-100mT%	-300mT%	x_{ARM}/xfd
TWIS3	5.0448	7.239192	19.58283	7.116646	23.96148	7.251827	-22.5172	-58.7688	-56.4606
TWIS4	1.3962	23.32144	21.07433	34.53708	35.89893	27.03245	15.87808	14.33957	-112.787
TWIS5	1.3093	14.13313	27.70812	9.000629	32.70262	21.48739	4.176041	-20.8644	-1.8e+16
TWIS6	1.6406	5.534686	5.607202	27.98507	35.6384	25.45741	12.55667	2.185227	-174.455
TWIS7	1.9431	9.173137	20.20845	11.20592	22.80758	6.679568	-13.8787	-37.8905	232.5094
TWIS8	2.0352	14.52875	29.49895	8.642167	32.18651	23.42545	6.357552	-21.5721	-398.764
TWIS9	1.236	5.877889	7.727211	20.55474	32.23829	20.60149	3.812302	-10.652	-76.8316
TWIS10	1.5815	6.74522	11.37136	12.38009	32.40755	20.19447	-1.51457	-24.7069	-106.12
TWIS11	1.6951	5.482656	11.5294	10.51034	26.76095	10.45114	-15.5879	-43.0218	-33.4681
TWIS12	1.4378	21.462	9.547061	29.66603	47.06486	44.18265	37.44795	29.88166	-378.419
BOTH1	1.626	13.13526	13.29538	21.33364	39.07154	31.02831	18.48612	6.119225	-188.886
GNES2	2.5732	5.384731	7.85614	20.24244	28.45615	14.7875	-2.72115	-17.2174	-170.562
GNES3	1.6415	5.25991	10.42881	12.22146	25.97817	10.81927	-13.5347	-38.7963	-26.3509
GNES4	3.0901	10.41845	6.399603	39.18047	42.60838	36.87587	28.11898	21.25266	-564.05
GNES5	3.1052	13.96196	6.465959	58.97244	43.67599	38.84477	32.77505	28.34161	-350.462
GNES6	1.7228	13.58264	5.051572	94.41794	43.47006	39.34113	35.53392	32.34368	-699.827
GNES8	3.1754	8.484561	4.369985	57.41333	42.38476	35.83261	29.16175	25.37281	-386.872
GNES9	1.2481	8.555821	9.278819	22.01077	37.05604	27.14931	13.03671	0.806274	-86.6009
GNES10	1.8256	13.89824	6.091475	57.54077	44.47324	40.06694	33.98297	29.42037	2534.855
GNES11	2.2527	19.90116	8.739779	55.01628	44.69475	40.57645	34.67187	29.96111	-370.198
GNES12	3.1163	16.21516	10.19939	35.87273	42.90357	37.29497	29.06443	21.75756	-83.3992
GNES13	2.4548	16.0748	10.58404	34.2534	42.57519	36.84134	28.17667	20.56317	0

Sample	Mass	HARD	HARD%	SOFT	SOFT%	-40mT%	-100mT%	-300mT%	$\chi_{ARM}/\chi fd$
GNES14	2.9063	9.814048	7.493535	38.69842	38.71919	29.98278	21.01649	14.68326	-483.596
GNES15	2.9859	8.113003	4.181411	52.63079	43.00976	37.30618	30.06183	25.30773	-1429.01
GNES16	2.7782	10.7899	6.613068	33.84134	43.64394	38.49686	29.8328	21.38185	-254.623
GNES17	2.382	4.533535	1.77664	164.0533	37.40263	33.81503	31.91762	30.7537	-238.005
GNES18	1.6639	18.1133	3.941136	90.54281	47.85675	45.87723	42.57187	39.54964	-3162.54
GNES19	2.5087	4.578688	5.188656	28.19135	31.89855	18.03785	5.033663	-3.721	-158.504
GNES20	2.6751	8.960623	4.774002	42.77263	43.92949	38.67769	30.81131	24.63295	-243.946
GNES21	2.9035	10.03555	3.806589	73.12704	44.73937	40.21742	34.93887	31.75642	-306.533
GNES22	2.7514	7.804063	7.757695	22.23541	39.01402	30.11902	16.31647	4.152879	104.9837
ORWE1	1.3396	2.904257	3.2078	19.67572	37.99824	27.24327	9.680214	-3.45429	1484.085
ORWE2	1.8647	2.021373	3.975007	11.83949	27.10789	7.986678	-21.9097	-44.416	-20.8987

C.3. CORE DATA

(i) Sombre Lake

Mean depth (cm)	% DW	Mean particle µm	% LOI	HARD%
0.50	15.40	37.76	9.66	3.03
0.75	16.59	41.55	9.61	3.00
1.25	17.78	34.23	9.55	3.00
1.50	24.97	39.46	7.54	2.97
1.75	24.97	44.69	7.54	2.70
2.25	32.15	49.58	5.53	2.43
2.50	42.40	46.30	5.15	2.21
2.75	42.40	43.01	5.15	2.21
3.25	52.64	41.29	4.77	1.98
3.50	53.09	41.29	4.78	2.39
3.75	53.09	39.56	4.78	2.39
4.25	53.54	38.83	4.78	2.80
4.50	40.01	36.47	7.32	3.26
4.75	40.01	34.11	7.32	3.26
5.25	26.47	32.10	9.85	3.72
5.50	28.19	37.27	9.15	3.96
5.75	28.19	42.43	9.15	3.96
6.25	29.90	36.70	8.44	4.20
6.50	30.21	37.50	8.43	3.99
6.75	30.21	38.30	8.43	3.99
7.25	30.51	39.12	8.41	3.99
7.50	32.44	40.98	7.60	3.79

(ii) Heywood Lake

Mean depth	% DW	Mean particle µm	% LOI	HARD%
1.25	16.53	44.38	18.3	0.71
1.50	17.96	49.31	17.21	0.85
1.75	17.96	54.24	17.21	2.54
2.25	19.39	38.48	16.11	2.54
2.50	18.33	44.95	17.57	4.22
2.75	18.33	51.41	17.57	2.28
3.25	17.27	46.58	19.02	2.28
3.50	21.71	45.52	15.16	0.33
3.75	21.71	44.46	15.17	1.21
4.25	26.15	61.03	11.31	1.21
4.50	30.81	60.98	9.38	2.09
4.75	30.81	60.93	9.38	2.71
5.25	35.46	81.62	7.44	2.71
5.50	38.49	82.04	6.72	3.33
5.75	38.49	82.45	6.72	3.695
6.25	41.51	88.19	6.00	3.695
6.50	30.47	77.67	12.11	4.06
6.75	30.47	67.14	12.11	4.31
7.25	19.43	43.46	18.22	4.31
7.50	18.41	37.55	19.13	4.55
7.75	18.41	31.63	19.13	4.44
8.25	17.39	36.03	20.04	4.44
8.50	25.18	35.11	15.28	4.32
8.75	25.18	38.58	15.28	3.42
9.25	32.96	72.57	10.51	3.42
9.50	27.91	57.25	13.97	2.51
9.75	27.91	58.31	13.97	1.84
10.25	22.85	41.92	17.43	1.84
10.50	22.57	40.52	17.15	1.16
10.75	22.57	39.12	17.15	1.90
11.25	22.28	37.93	16.87	1.90

(iii) Emerald Lake

Mean depth (cm)	% DW	Mean particle µm	% LOI
0.00	40.758	24.635	3.7403
0.375	44.76	23.66	3.53
0.625	54.45	26.7	2.86
0.875	52.43	30.4	3.37
1.125	50.79	28.56	3.10
1.375	43.58	28.91	1.66
1.625	43.10	27.85	1.85
1.875	49.27	30.34	1.70
2.125	56.55	29.31	1.30
2.375	50.23	29.76	2.68
2.625	56.15	26.76	1.93
2.875	46.15	24.58	2.71
3.125	49.38	23.93	2.98
3.375	36.82	25.58	4.77
3.625	33.22	25.92	5.14
3.875	32.89	28.61	3.50
4.125	44.07	28.94	1.78
4.438	42.80	27.99	1.81

APPENDIX D: LACUSTRINE ^{210}Pb CHRONOLOGIES[1]

D.1. SOMBRE LAKE (SOMB2)

Coring date: 1991 (V.Jones)

^{210}Pb flux = 0.35±0.01 PCI cm^{2}yr^{-1}
90% equilibrium depth = 5.4 cm or 2.46 g cm^2
99% equilibrium depth = 7.5 cm or 3.20 g cm^2

Depth *cm*	*Dry mass* *g cm^2*	*Cum.unsupp. ^{210}Pb* *PCI cm^2*	*Chronology Date* *AD*	*Age* *yr*	*SD error*	*Sedimentation* *g cm^2 yr^{-1}*	*rate* *cm yr^{-1}*	*%Std error*
0.00	0.0000	11.17	1991	0				
0.25	0.0272	10.87	1990	1	2	0.0363	0.215	3.8
1.25	0.2107	8.89	1984	7	2	0.0222	0.091	4.0
2.25	0.5128	6.55	1974	17	2	0.0481	0.124	5.7
2.75	0.7936	5.49	1968	23	2	0.0515	0.092	8.9
3.25	1.0744	4.72	1963	28	2	0.0672	0.102	9.1
3.75	1.4493	4.27	1960	31	2	0.2830	0.377	25.4
4.25	1.8243	3.91	1957	34	2	0.0785	0.119	9.9
4.75	2.1080	2.86	1947	44	2	0.0131	0.023	6.5
5.25	2.3918	1.32	1923	68	4	0.0097	0.021	11.2
5.75	2.5694	0.77	1905	86	6	0.0113	0.032	18.3
6.25	2.7470	0.42	1886	105	10	0.0071	0.020	31.0
6.75	2.9302	0.23	1867	124	17	0.0243	0.066	67.1
7.25	3.1134	0.14	1851	140	25	0.0063	0.016	73.1

D.2. HEYWOOD LAKE (HEY2)

Coring date: 1991 (V.Jones)

^{210}Pb flux = 0.11±0.01 PCI cm^{2}yr^{-1}
90% equilibrium depth = 10.5 cm or 2.98 g cm^2
99% equilibrium depth = 14.2 cm or 3.81 g cm^2

[1] CRS Model (Appleby & Oldfield, 1978)

D.2 HEYWOOD LAKE (contd.)

Depth *cm*	*Dry mass* *g cm²*	*Cum.unsupp.* *^{210}Pb* *PCI cm²*	*Chronology* *Date* *AD*	*Age* *yr*	*SD* *error*	*Sedimentation* *g cm² yr⁻¹*	*rate* *cm yr⁻¹*	*%Std* *error*
0.00	0.0000	3.40	1991	0				
0.25	0.0332	3.36	1991	0	2	0.0886	0.589	14.8
1.25	0.1878	3.16	1989	2	2	0.0752	0.403	14.1
3.25	0.5931	2.66	1983	8	2	0.0708	0.326	18.3
4.25	0.8404	2.37	1979	12	2	0.0614	0.165	13.3
6.25	1.7099	1.59	1967	24	2	0.0787	0.212	24.8
8.25	2.3237	0.93	1950	41	4	0.0179	0.061	12.6
11.25	3.1805	0.15	1892	99	14	0.0145	0.057	44.3
13.25	3.6036	0.06	1857	132	22	0.0115	0.054	49.0

D.3. TRANQUIL LAKE (TRAN1)

Coring date: 1991 (V.Jones)

Depth *cm*	*Dry mass* *g cm²*	*Cum.unsupp.* *^{210}Pb* *Bqkg⁻¹*	*Chronology* *Date* *AD*	*Age* *yr*	*SD* *error*	*Sedimentation* *g cm² yr⁻¹*	*rate* *cm yr⁻¹*	*%Std* *error*
0.00	0.00		1991	0				
0.25	0.09	10.87	1984	7	1	0.012	0.027	16.0
0.50	0.17	8.89	1976	15	2	"	"	"
0.75	0.28	6.55	1967	24	4	"	"	"
1.00	0.39	5.49	1958	33	5	"	"	"
1.25	0.50	4.72	1949	42	7	"	"	"
1.50	0.61	4.27	1940	51	8	"	"	"
1.75	0.74	3.91	1930	61	10	"	"	"
2.00	0.87	2.86	1919	72	12	"	"	"
2.25	1.00	1.32	1908	83	13	"	"	"
2.50	1.13	0.77	1897	94	15	"	"	"

D.4. EMERALD LAKE (EMER16)

Coring date: 1994 (P.Noon)

Depth *cm*	*Dry mass* *g cm²*	*Cum.unsupp.* *^{210}Pb* *Bqkg⁻¹*	*Chronology* *Date* *AD*	*Age* *yr*	*SD* *error*	*Sedimentation* *g cm² yr⁻¹*	*rate* *cm yr⁻¹*	*%Std* *error*
0.00	0.00	81.6@0.13cm	1994	0				
0.25	0.12	72.5@0.38cm	1991	3	1	0.046	0.082	23
0.50	0.28	51.5@0.63cm	1988	6	1	0.053	0.078	17
0.75	0.46		1984	10	2	0.053	0.073	18
1.00	0.64		1979	15	2	0.040	0.057	17
1.25	0.82	88.4@1.38cm	1974	20	2	0.028	0.040	15
1.50	0.99		1968	26	3	0.022	0.032	16
1.75	1.15	48.9@1.88cm	1961	33	3	0.024	0.034	20
2.00	1.33		1954	40	4	0.032	0.043	28
2.25	1.52	15.9@2.38cm	1949	45	4	0.047	0.060	42
2.50	1.72		1945	49	5	0.056	0.071	51
2.75	1.91	5.3@2.88cm	1942	52	4	0.061	0.083	56
3.00	2.09		1939	55	4	0.047	0.071	50
3.25	2.24	32.3@3.38cm	1935	59	4	0.031	0.056	33
3.50	2.37		1930	64	5	0.016	0.032	23
3.75	2.48	40.2@3.88cm	1922	72	5	0.012	0.024	23
4.00	2.59		1911	83	6	0.0087	0.018	20
4.25	2.72	18.2@4.38cm	1896	98	7	0.0081	0.018	15